MINERALOGY AND ORIGIN OF GEM CORUNDUM ASSOCIATED WITH BASALT IN THAILAND

A thesis submitted to the University of Manchester
for the degree of DOCTOR OF PHILOSOPHY
in the Faculty of Science and Engineering.

2000

Seriwat Saminpanya

Department of Earth Sciences

Contents

List of figures

List of tables

Abstract

The main aim of work reported in the thesis is to describe the corundums from Thailand in terms of their host rocks, their physical properties (surface features and cathodoluminescence), spectroscopic characteristics, trace element fingerprints and their mineral inclusions in order to establish the possible environment of formation of Thai corundums.

Petrographic and geochemical studies reveal that the continental alkali basalt host rocks of Thai corundums are rich in crustal and mantle xenocrysts (apatite, kaersutite, feldspars, nepheline, clinopyroxene, orthopyroxene, olivine, spinel, magnetite, biotite and pyrope-almandine) and xenoliths (quartzite, gabbro, feldspathic aggregates, ultramafic rock fragments). The magmas were generated in the upper mantle and ascended to the Earth's surface rapidly with minor contamination by the lithosphere, during the Miocene to Recent (ca 11 - 0.4 Ma), and picked up the corundums and other xenocrysts and xenoliths.

Almost all gem corundums (rubies and sapphires) from Thailand are recovered or mined from the secondary deposits (alluvium, elluvial, residual-soil and colluvium deposits and stream sediments) near alkali basalt outcrops. The thickness of gem-bearing layers varies from 0 - 5 m with up to 15 m overburden thickness. Surface features of corundums reveal that they experienced alkali magma etching during their ascent to the Earth's surface. Certain samples show evidence of physical weathering and chemical reaction with the soil solution in the secondary deposits.

Cathodoluminescent characteristics of corundum have been investigated. Optical spectroscopy (UV-visible) was used to investigate the transition metals in the structure of corundum and distinguish the Thai samples from Verneuil corundum samples. Using optical spectroscopy, Thai corundums can be divided into two groups. ***The first group*** includes sapphires (Blue, very strongly greenish Blue, greenish Blue, bluish Green, Green-Blue and Green colours). This group exhibits absorption spectra of the crystal field transition (d-d) for Fe^{3+} with peaks between ca 330 nm and 450 nm, a broad absorption band of the intervalence charge transfer (IVCT) for Fe^{2+}/Ti^{4+} occurs between 500 nm and 650 nm and an absorption band of Fe^{2+}/Fe^{3+} IVCT is centred between 840 nm and 900 nm. ***The second group*** includes rubies (Violet, Purple, reddish Purple, bluish Purple, bluish Violet colours) and exhibits a d-d band for Cr^{3+} centred at ca 550 nm. The band at 350 nm – 450 nm as seen in synthetic Verneuil ruby is not found but the only right shoulder of this band is seen. There are also weak peaks at 665 ± 1 nm and 692/693 nm.

Using electron probe microanalysis (EPMA) to analyse trace elements, Thai corundums show two discrete populations, rubies and sapphires. Sapphires are rich in Ga (up to 0.101 wt% Ga_2O_3), high field strength elements and poor in Cr. These data and their inclusion suite suggest that they might have crystallized in syenitic gneiss metasomatised by highly evolved fractionated magma (e.g. carbonatitic magma). Rubies are rich in Cr (up to 0.564 wt% Cr_2O_3) and poor in Ga. These data and geobarometry and geothermometry information from their inclusions suggest that rubies might have crystallized from metamorphic rocks with basic composition (e.g. ruby–garnet-clinopyroxenite or ruby-garnet-pyriclasite). Thai rubies and sapphires are always found together. This suggests that their origins are between the deep crust and upper mantle (**46-105 km depth**) at **13-30 kbar and 1000 – 1150°C** i.e. in high-pressure granulite or eclogite-facies conditions.

Declaration

No portion referred to in this thesis has been submitted in support of an application for another degree or qualification of this or any university or other institute of learning.

(Seriwat Saminpanya)

Copyright and the ownership of intellectual property rights

The Author

The Author graduated from:

the Department of Geology, Chiang Mai University, Thailand in 1982 with *B.S. (Geology),*

the Faculty of Environment and Resource Studies, Mahidol University, Thailand in 1988 with *M.Sc. (Technology of Environmental Management)*, and

the Sukhothai Thammathirat Open University Nonthaburi, Thailand in 1992 with *B.P.H. (Occupational Health and Safety).*

He holds the Diploma of:

***Graduate Gemologist (GG)* from Gemological Institute of America, in December 1992,**

***Diploma in Gemmology (FGA)* from the Gemmological Association and Gem Testing Laboratory of Great Britain in November 1999.**

His career is an Assistant Professor at the Department of General Science, Srinakharinwirot University, Bangkok, Thailand. He has been a postgraduate student in the Department of Earth Sciences, the University of Manchester, UK since the 1st April 1997.

Acknowledgements

I would like to thank my supervisors Prof. DAC Manning and Dr GTR Droop who have helped me in every aspect of my work. Academically they taught me to solve the geological and mineralogical problems that can provide new useful knowledge for me to apply in my career. They spent time proof reading several drafts of this thesis. They also helped and gave useful guidance which helped me get the best out of living in Manchester with my family throughout 3 years. They are very supportive and sincere. I also thank Professor CMB Henderson who also supervised me and gave several crucial suggestions for this thesis.

Many persons have helped me in various aspects of my work. The author wishes to thank Dr Pornsawat Wathanakul and Dr Suporn Intasopa for giving advice in this research. Dr Pornsawat also provided several useful documents for use as references in this thesis; Mr Suchat Varadi and Mr Nikhom Namwong for permission and arrangement to access the Boon Mani Mine at Bo Phloi and a corundum mine at Nong Bon respectively; Kamnan Pukkham Tamaphut for permission to access to the area of Ban Nong Nam Cho basalt; Ajarn Suraphon Sanokham, Mr Surasak Noijin, Mr Nakhon Khaokaeo, and Mr Narongsak Chuaykhum, for the donation of corundum, garnet and zircon samples; Ms Ratisa N Ranong, Ms Sorataya Inthraraksakun, Ms Bang-on Daraj for helping prepare the rock samples in some stages; Ms Supinya Wongsriruksa and Ajarn Wanchad Sumanochitraporn for providing crucial documents from Thailand; Mrs Sarah Blake and Miss Thitintharee Pavaro for great and kindly help in spectroscopy analyses; Dr H Wilkomen for photography of corundum samples; Dr M Moazzen for discussion and exchange of geological knowledge.

Thanks to Mr Paul Lythgoe who helped in analyses of basalt samples with the XRF and corundum samples with the LA-ICP-MS; Mr Dave Plant and Dr C Hayward for analysis of trace elements in corundum samples with the EPMA; Mr H Williams, Mr D Johnson, Mr S Mills, and Mr K Brown (staff in the rock-sectioning workshop), Ms S Maher (in photo lab.), Ms H Collier, Mrs R Rana, Mr S Caldwell, Mr H Lock, Ms P Collins, Mr D Wright, Mr R Hartley and Mr T Jenson (the staff in the Department of Earth Sciences) for helpfully providing the facilities and data from laboratories as well as training with certain techniques.

The author is grateful to his parents, Second Lieutenant Preeda Saminpanya and Mrs Usa Saminpanya, his 4 older brothers and 2 older sisters who have encouraged and given lots of resources for his education; his wife, Dr Pornpan Saminpanya and his son, Master Pitthayut Saminpanya (Neo), for giving a great ambition to the author. Finally, the author is in debt with the Royal Thai Government who financially supported this project.

Dedicated to my parents, Second Lieutenant Preeda Saminpanya whom I lost while I was writing this thesis and Mrs Usa Saminpanya.

CHAPTER 1
INTRODUCTION

The study area is located within the territory of Thailand. The location and physiography of Thailand will be presented first, together with a brief résumé of its geology in order to provide the geological context for this study. This will be followed by a statement of the problems that still remain to be solved in connection with the Thai corundum deposits, and a summary of the aims and objectives of this study.

1.1 Location and physiography of Thailand

Thailand is located in Southeast Asia; it lies approximately between latitudes 5°-21°N and longitudes 98° –105°E, and has a surface area of 513,115 km^2 (Figures 1.1 and 1.2, A). It is bounded by Myanmar (formerly Burma) to the west and the south, Laos to the north and the east, Cambodia to the east, and the Andaman sea, Malaysia, and Gulf of Thailand to the south. Thailand's physiography includes mountain ranges and intermontane basins in the northern, western and southern regions; in the centre is an area of low land, the Chao Praya Plain. In the north-eastern area is a plateau with a low-angle slope called the Khorat Plateau, and in the south-eastern (or eastern) part is an area whose physiography is the same as the western region. The southern region forms a peninsula known as the South Peninsula. The highest mountain in Thailand is Doi Inthanon; it is situated in the northern region and its summit is 2,565 metres above mean sea level.

1.2 Geologic setting of Thailand

The geology of Thailand, as summarized in Figure 1.1, consists of rock formations spanning periods of the geological time scale from Precambrian to Quaternary. Sedimentary, metamorphic and igneous rocks are distributed throughout the country. Recent papers synthesising general geological information about Thailand include, for example, Bunopas (1992), Dheeradilok *et al.* (1992) and Mantajit (1997).

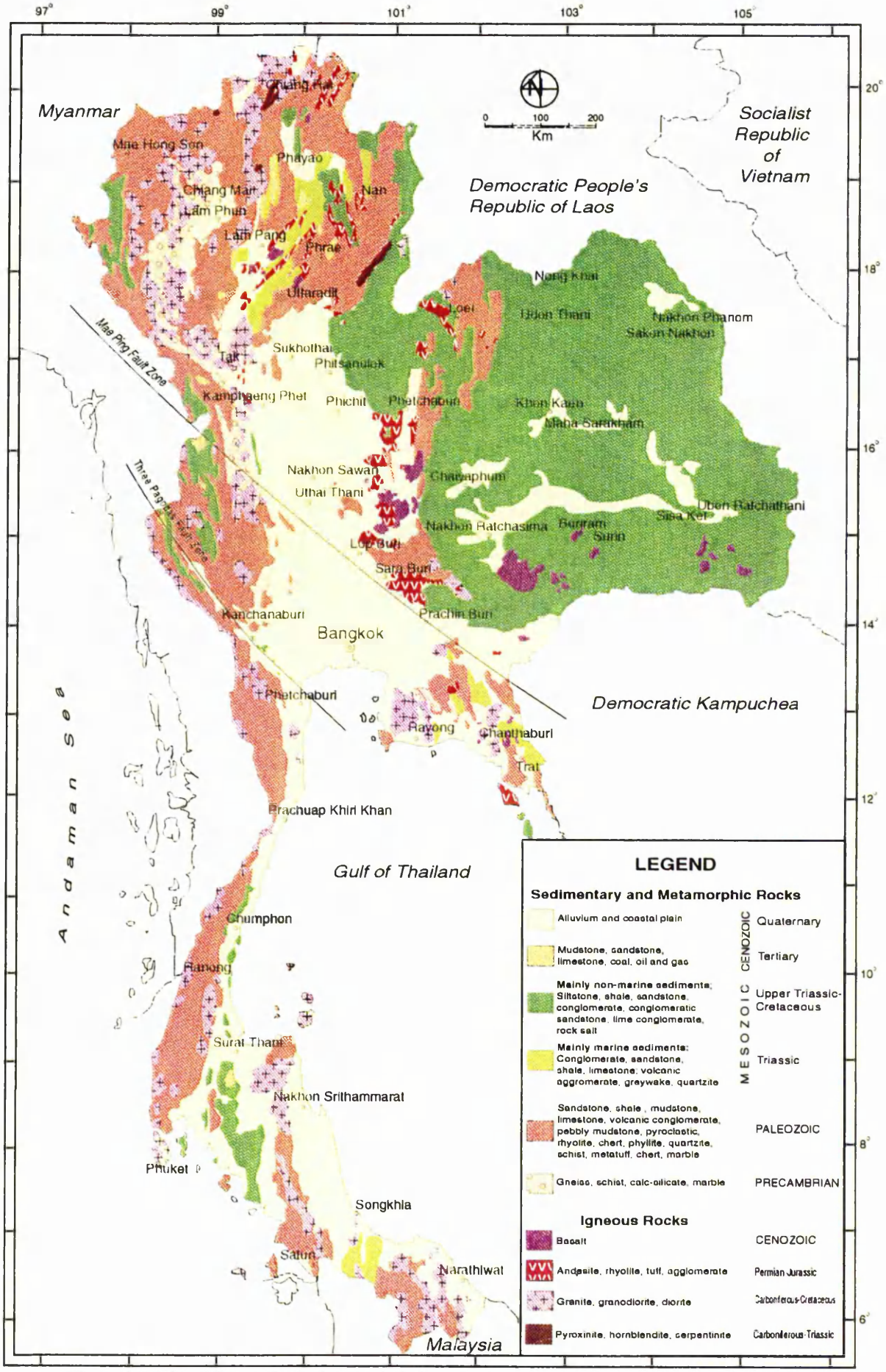

Figure 1.1 Simplified geological map of Thailand (Modified from the Geological Map of Thailand, Scale 1:2,500,000, Geological Survey Division, Department of Mineral Resources, Bangkok, 1987)

The oldest rocks (the Lan Sang Gneiss Complex) are of Precambrian age and consist of gneiss, schist, calc-silicate and marble. These rocks are exposed on the northern, western, and eastern regions of the country. The Palaeozoic era is represented by sedimentary rocks such as sandstone, shale and mudstone, and by metamorphic rocks such as phyllite and quartzite. Palaeozoic igneous activity took place from the Carboniferous period up to the Mesozoic era. The plutonic rocks include principally granite, granodiorite and diorite and the volcanic rocks are dominated by andesite and rhyolite.

The Mesozoic rocks of Thailand are classified into two major sedimentary categories, marine and non-marine groups. The marine sediments, which include conglomerate, sandstone and limestone as well as agglomerate and quartzite, are the major components of the Triassic, Lampang Group. The non-marine sediments (Khorat Group) with the age of Upper Triassic-Cretaceous comprise mainly of siltstone, shale, conglomerate and rock salt, and dominate in the Khorat Plateau.

The Cenozoic sequences are composed of mudstone, sandstone, hydrocarbon deposits (coal, oil and natural gas), unconsolidated sediments and young basalts of alkaline affinity. One of those basalts has the oldest age of 24 Ma (Intasopa, 1993). The gem corundums, which are the subject of this thesis, are found in association with alkali basalts of this suite.

1.3 Tectonic setting of Thailand

Thailand consists of two microcontinents, the Shan-Thai (Sibumasu) and Indochina blocks (Figure 1.2 A, B). They separated from Gondwanaland (in the southern hemisphere) at different times and joined up during the Late Triassic near the Eurasian continent. In between the two blocks used to be the Palaeo-Tethys ocean (Metcalfe, 1997; Hada *et al.,* 1997; Hada and Bunopas, 1997). The evidence for the former existence of this ocean are pelagic sediments and ophiolites found along two major sutures of collision, the Nan (or Nan-Uttaradit) suture and the Sa Keao (or Sa Keao-Chanthaburi) suture (Figure 1.2, B) (Bunopas and Vella, 1992; Hada and Bunopas, 1997).

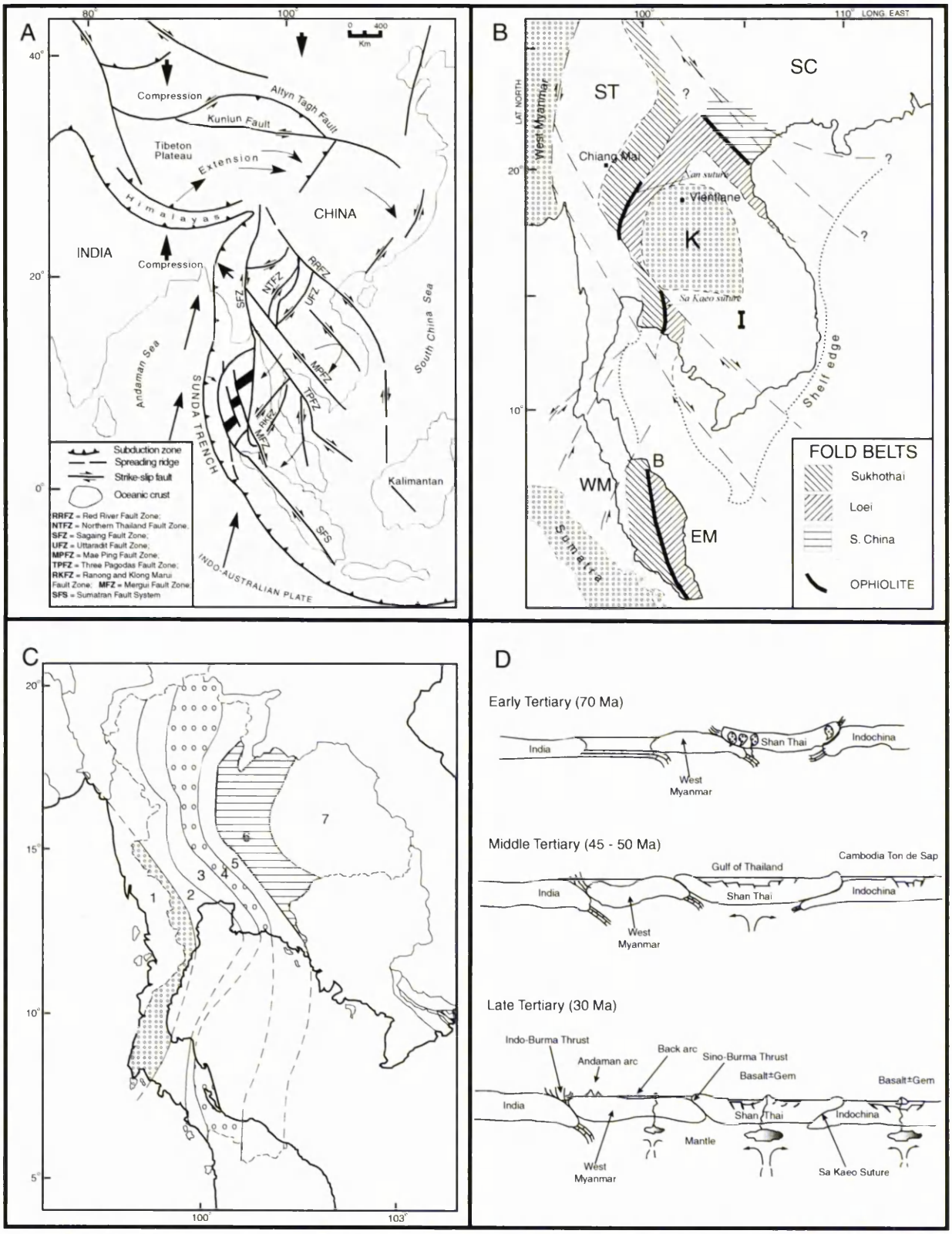

Figure 1.2 A.Tectonic map of Southeast Asia and South China showing the main fault pattern *(Modified from Polachan et al., 1991)*.
B. Ancient cratonic area composed of Shan-Thai (ST: including eastern Myanmar, western Thailand and northwestern Malay penninsular), South China (SC) and Indochina (I: including eastern Thailand); Fold belts, major faults and ophiolites are also shown. (K, Khorat Plateau; WM, West Malay Penninsula; B, Bentong Ophiolite line; EM, East Malay Penninsula) *(Modified form Bunopas, 1992)*.
C. Seven stratigraphic belts of Thailand: 1-5 on Shan-Thai and 6-7 on Indochina terranes *(Bunopas, 1992)*.
D. Plate tectonic reconstruction of the evolution of Thailand and adjacent areas during Tertiary, gem corundum bearing basalt generated in the Late Tertiary *(Modified from Charusiri et al., 1997)*.

The Shan-Thai terrane rifted away from Gondwanaland during the Middle or Late Palaeozoic (Hutchison, 1989); it is underlaind by Precambrian amphibolite-facies metamorphic rocks (Bunopas and Vella, 1992) including gneiss, quartzite, marble and micaschist. The mineral assemblage of the gneiss exposed in the Bo Phloi area is microcline, tremolite, plagioclase, strained quartz, biotite, chlorite, muscovite, apatite, zircon and sericite. The marble contains biotite, diopside and sphene (Bunopas and Bunjitradulya, 1975). The Indochina terrane is probably underlain by Precambrian amphibolite-facies rocks as well, which originated in Gondwanaland along the eastern margin of the Australian plate and rifted away by Early Carboniferous times (Metcalfe, 1988; Bunopas and Vella, 1992). The moderately to strongly deformed Palaeozoic sediments are widely distributed over the Indochina terrane but the relatively stable Mesozoic sediments (Khorat Group) are the dominant covers on the terrane (Richter and Fuller, 1996).

The Indian plate originally formed part of Gonwanaland and separated from the African plate during the Late Cretaceous (Tapponnier *et al.*, 1986), moved to the north and collided with the Eurasian plate at 50 – 43.5 Ma. (Eocene) (Longsley, 1997). Since that time, The Indian plate has continued to converge with Eurasia, and the present-day convergence rate is still ca. 5 $cm \cdot yr^{-1}$ with the angle of convergence of about 12 degrees from north (Lee and Lawver, 1995). The collision created the Himalayan orogeny and the strain of collision has been absorbed mainly in substantial crustal thickening. It has been suggested that some of the strain has been responsible for extension of the Tibetan Plateau (Dewey *et al.*, 1989) and/or the extrusion (escaping) of Southeast Asia for as much as 1000 km from the Indian craton along major strike-slip faults (Peltzer and Tapponnier, 1988). The collision also caused the clockwise rotation of Southeast Asia. Movement on the strike-slip faults was associated with development of Cenozoic basins in this region (Polachan *et al.*, 1991). The major strike slip fault zones in Thailand include the Mae Ping Fault Zone (MPFZ), Three Pagodas Fault Zone (TPFZ) and Ranong and Khlong Marui Fault Zone (Figure 1.2, A). Topographically and on a landsat imagery, the first two fault zones are seen clearly as having large sinistral displacements; the latter is dextral. These movements formed originally during the Late Permian to Middle Triassic due to the collision of the Shan-Thai and Indochina blocks (e.g. Tapponnier *et al.*, 1982). However, during the collision of the Indian and Eurasian plates, during the Late Cretaceous to Early Tertiary, the faults were reactivated and

changed their sense of movement but built up smaller displacements than before (Polachan *et al.*, 1991).

Bunopas (1992) has also shown the fold belts in Figure 1.2, B and has divided Thailand into 7 stratigraphic belts running approximately north-south of the country (Figure 1.2, C). The stratigraphic belts 1-5 are on the Shan-Thai terrane and belts 6 and 7 are on the Indochina terrane and mainly covered by the Mesozoic Khorat Group. The main cratonic areas underlain by the Precambrian basement complexes are within belts 3 and 7. The Lower Palaeozoic strata are confined to within belts 2 and 3 and the west most margin of belt 4. Belt 5 and the east of belt 4 contain the active Mid-Palaeozoic volcanic arc-trench system, which developed certain periods before the final continental collision. Belts 4 and 5 are called the Sukhothai Fold-Belt and belt 6 is called the Loei Fold-Belt. Belts 1 and 2 used to be the basins between the Mid-Palaeozoic and the Mid-Mesozoic, which have advanced towards the west and now they are composed of the sedimentary rocks of Silurian, Triassic and Jurassic ages (Bunopas, 1992; Bunopas and Vella, 1992).

Several major basins, especially in the Gulf of Thailand, developed during the Oligocene by rifting (Cole and Crittenden, 1997). The development of these basins was the result of the transference of the stress of the Indian–Eurasian collision to the major strike-slip faults together with the clockwise rotation of the crust leading to formation of pull-apart basins (extension along an east-west direction) and horst-graben basins in Thailand. There are over 60 Cenozoic basins in Thailand with the sediment thickness up to 8 km. principally originated in non-marine environment (Polachan *et al.*, 1991). From drilling data, the basement of the basins comprise Mesozoic-Palaeozoic rocks, for example clastic, carbonate, volcani-clastic, granites and metamorphic rocks (Polachan *et al.*, 1991; Pradidtan & Dook, 1992). There is no detailed information on the nature of the deep crust under the basins.

The origin of the Neogene basalts in Southeast Asia (including Vietnam, China, Thailand and Malaysia) is still unclear from a tectonic point of view. Mukasa *et al.* (1994) believe that they are rift-related but Barr and Macdonald (1979) suggested that the basalts in Southeast Asia are not clear in tectonic setting, unlike the rift-related

continental basalts in for example the East African rift and the Rhine Graben. The subduction zone at the Sunda trench, southwest Sumatra, is not likely to be related to the eruption of the alkali basalts centred in Vietnam about 1,000 km further away to the northeast. Note that the Indian plate combined with the Australian plate in Middle Eocene (45 Ma) due to the spreading of the ridges from the southern boundary of Australia causing the Australian plate to move northwards to the Indian plate. These two plates have moved north-northwestward contributing to the subduction of the oceanic crust at the Sunda trench. The subduction (Figure 1.2, A) started in the Middle Eocene (42–46 Ma) (Gordon and Jurdy, 1986; Polachan *et al.*, 1991).

Barr and Macdonald, (1979) suggested that the development of the China Basin in the Late Mesozoic–Cenozoic may have caused the alkali igneous activity in Southeast Asia. The eruption of basalts in Indochina may have been related to downwarps in this area (e.g. the Hanoi Downwarp having been formed since early Palaeocene until the present and the Mekhong Downwarp). The downwarps are accompanied by crustal thinning (from 35-40 km to 30-35 km) and mantle upwelling, as described by Isayev and Kkhoan (1976). Mitchell and Garson (1981) suggest that the alkali basalts and associated gemstones could be related to northwestward migration of the lithosphere over an underlying hot spot or mantle plume. Charusiri *et al.* (1997) present a brief plate tectonic model of the Thai gem corundums erupted to the Earth's surface during the Late Tertiary (Figure 1.2, D).

1.4 Problems on the origin of corundums associated with alkali basalt

Corundum in Thailand is found in association with alkali basalt (e.g. Vichit *et al.*, 1978; Levinson and Cook, 1994). Many studies have been undertaken on the corundum-related basalt throughout the country. However, most of these studies emphasise the petrography and geochemistry of the basalt (e.g. Vichit *et al.*, 1978; Barr and MacDonald, 1978, 1981; Jungyusuk and Sirinawin, 1983; Barr and Dostal, 1986). The relationship between the genesis of corundum and the basalt host rock is still problematic. Vichit *et al.* (1978) state that corundum in the basalts of Thailand might crystallise in the later stage mantle at a depth of approximately 65 - 95 km. However, Levinson and Cook (1994) argue that corundum is formed when alumina-rich rocks are subducted to a depth of about 50 km where metamorphism converts the aluminous

minerals into corundum. Subsequently, alkali basalt from a deeper level carries corundum to the surface. Coenraads *et al.* (1990, 1995) state that the corundums crystallised from alkaline felsic melts at upper mantle depths. Guo *et al.*, (1996a) proposed that the corundum formed before becoming involved with the host magma by the interaction between carbonatitic (or Si-poor) magmas and a silicic component (felsic system) giving rise to corundum-bearing lenses in the crust at about 10 - 20 km depth; later, the alkali basalt erupted from the upper mantle brought the lenses, incorporated as crustal fragments, up to the Earth's surface.

Petrographically, the corundum-related basalts of Thailand contain megacrysts (e.g. clinopyroxene, olivine, ilmenite, spinel, and garnet), crustal xenoliths, and ultramafic nodules. In general, the basalts are undersaturated rocks (nepheline hawaiite, basanite, and nephelinite). They are Cenozoic (with an age range of 0.44±0.11 to 11.03±0.03 Ma) (e.g. Barr and MacDonald 1978, 1981; Barr and Dostal, 1986; Yaemniyom, 1982).

The corundum (sapphires and rubies) and related minerals (e.g. zircon, garnet, spinel, and magnetite) are mined in alluvium near the basalt outcrops. These minerals are strongly believed to have come from those basalt bodies by weathering and transportation. Very few samples have been found of corundum embedded in basalt (Vichit, 1992).

From the information above, radically different genetic models have been proposed to explain the occurrence of corundums (ruby and sapphire) in alkali basalt. Many questions concerning the genesis of the corundum in relation to the host Tertiary alkali basaltic rocks therefore need to be addressed. In particular, the petrogenetic origin of the corundums and their host rocks need to be investigated carefully by means of host-rock petrography, geochemistry and mineralogy as well as geochemistry and spectroscopy of the corundums and associated minerals. The results will provide geological data which should lead towards an understanding of the origin of the corundum associated with alkali basalt, which, in turn, might lead eventually to the discovery of new gem-corundum deposits.

1.5 Aims and objectives

The main aims of this study are to describe the corundums from Thailand in terms of their host rocks, their physical properties (surface features and cathodoluminescence),

spectroscopic characteristics, trace element fingerprint and their mineral inclusions in order to establish the possible environment of formation for Thai corundums.

The objectives of this study are:

1) To describe and classify the rock types in terms of petrography and geochemistry of major and trace elements. The petrography has been done using the optical microscope. The bulk chemical compositions of the rock samples, in terms of major and trace elements, has been investigated using X-ray fluorescence (XRF) spectrometry and certain wet-chemical techniques. The mineral chemistry and groundmass chemistry of basalts have been obtained by use of the scanning electron microscope equipped with an energy-dispersive spectrometer (SEM-EDS) and the Geoscan electron microprobe fitted with an energy-dispersive spectrometer. Certain heavy minerals from the gem-bearing gravels were analysed by the SEM-EDS to identify possible host basalt sources of the corundums.
2) To describe the characters of the alluvial deposit of the corundums from Thailand using the information from previous work and the available data from field work.
3) To describe the physical and optical characteristics of corundum in terms of surface features and cathodoluminescent effects. These characteristics are established by the unaided eye, scanning electron microscopy (SEM) and cathodoluminescence microscopy respectively.
4) To obtain spectroscopic information for corundum by means of UV-visible spectrophotometry, infrared spectroscopy and Raman spectroscopy and to combine this with chemical information of corundum.
5) To determine the chemical composition of corundums in terms of trace elements. Electron-probe microanalysis (EPMA) and laser ablation-inductively coupled plasma-mass spectrometry (LA-ICP-MS) are employed for this. The investigation is done with various corundums from different geological environments throughout the world. Information on Thai corundums will be presented by matching the results obtained from them with those obtained from well-characterised corundums of known origin from other well-documented localities to reflect the formation environment for Thai corundums.
6) To identify the mineral inclusions in Thai corundums in order to support the information of their environment of formation. The chemical compositions of

inclusions have been used to estimate their pressure (P) and temperature (T) limits of formation, which are applied to be the formation condition of the corundum host. The technique used is the SEM-EDS, with which it is possible to analyse the inclusions exposed at the surface of the polished sections of corundum. The THERMOCALC computer programme has been used to calculate the P-T conditions of inclusion formation.

1.6 Thesis layout

This thesis is presented in 10 chapters. Chapter 1 is about the geological background, the statements of problem, aims and objectives. Chapters 2, 3 and 4 deal with useful background information. Chapter 2 presents the geographic distribution, ages, lithology, petrography, geochemistry (major and trace elements) of basaltic rocks in Thailand. Moreover, in Chapter 2, groundmass analyses of basalts obtained by using the SEM-EDS will also be presented with the comparison to the results from the XRF. Mineral chemistry of basalts from Thailand and the chemical composition of certain heavy minerals from gem gravel deposits are discussed in Chapter 3. Gem corundum occurrences in Thailand together with the characteristics of the alluvial deposits are given in Chapter 4.

Chapters 5-9 are the main parts of the study. Chapter 5 describes the surface features of Thai corundums. Chapter 6 describes the cathodoluminescence of Thai corundums as well as of certain corundums from other localities outside Thailand. Chapter 7 covers the investigation of corundum by means of spectroscopy (UV-visible, infrared and Raman spectroscopy). Trace elements in corundums are presented in Chapter 8. This chapter also contains the results of trace elements obtained by LA-ICP-MS and EPMA. In Chapter 9, the mineral inclusions in corundums have been identified and the pressure and temperature obtained from the mineral inclusions have been used to suggest the environment of formation for corundums from Thailand. The discussion and conclusion are left to the end of the thesis, in Chapter 10. Note that for the clarity of this thesis the local terms frequently used are given in Appendix 1-1.

CHAPTER 2
CORUNDUM-RELATED BASALTS IN THAILAND

2.1 Introduction

This chapter is regarded as the description and classification of corundum-related basalts in Thailand in terms of lithology, petrography and geochemistry of major and trace elements. The first part is a literature review for the distribution and ages of all basalts found in Thailand. The followed parts were accomplished in this study including lithology, petrography, whole rock geochemistry, and groundmass geochemistry of corundum-related basalts in Thailand. At the end of this chapter, groundmass geochemistry will be compared to whole rock geochemistry in order to examine whether or not other rocks contaminated the magma of the rock samples. This is because the samples prepared for the whole rock geochemistry may not be free from the contamination materials (e.g. xenocrysts, xenoliths and alteration products).

2.2 Distribution, general characteristics and ages of basalts in Thailand

Thai basalts occur as small bodies along the southern margin of the Khorat Plateau, as well as in the northern, western, and eastern regions of Thailand. Jungyusuk and Sirinawin (1983) described the distribution of Thai basalts by the use of geographic names as shown in Figure 2.1. They concluded that Thai Cenozoic basalts are mostly alkaline which can be divided into basanitoid basalts and hawaiitic basalts. The locations and types of Thai basalts are summarized in Table 2.1.

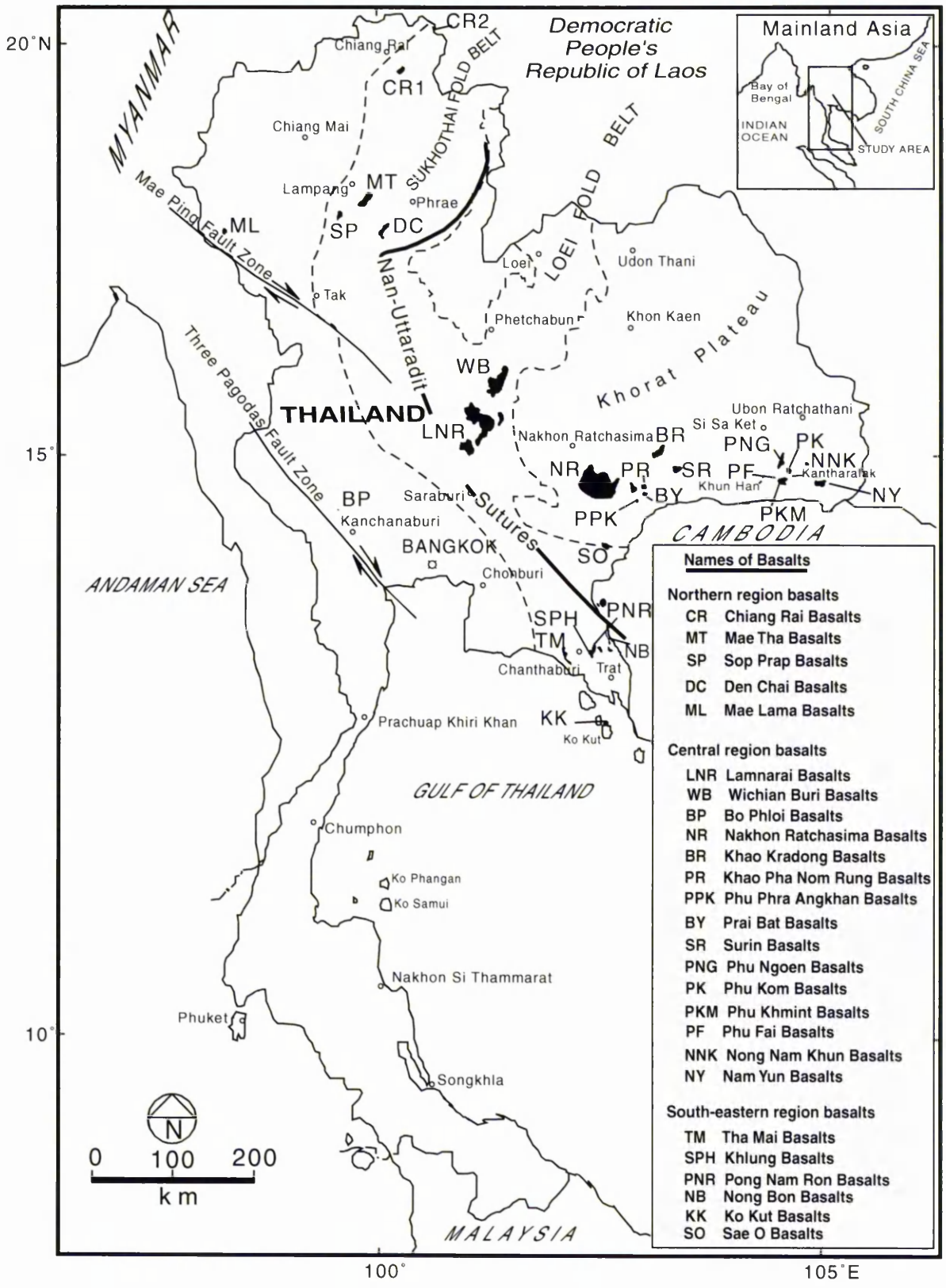

Figure 2.1 Map of Thailand showing distribution of basalts. (Basalts locations from Jungyusuk and Sirinawin, 1983; and Vichit, 1992; Structure boundaries after Polachan *et al.*, 1991 and Bunopas, 1992).

Table 2.1 Locations and types of Thai basalts. *(Modified from Jungyusuk and Sirinawin, 1983).*

Geographic names	Outcrops		Types	S/R*
	Locations	Covered areas (km^2)		
Northern region basalts				
Chiang Rai Basalts: **CR**	1) At Mae Khong river bank, south-east of Chiang Khong: **CR2 (CK** in this study).	-	Alkali olivine basalt[a] Basanite[e]	S
	2) At Ban Chiang Khian, about 30 km west of Amphoe Thoeng: **CR1**.	50	Tholeiite[a, f]	-
Lampang Basalts Mae Tha basalt: **MT**	At about 12 km south-east of Lampang, along the road from Ban Mae Tha to Ban Mae Mo	200	Basanite[a]	-
Sop Prap basalt: **SP (SP, BN** in this study)	At 33.3 km south-east of Lampang, along the Lampang-Sop Prap highway	90	Hawaiite[a], Basaltic andesite of calc-alkali affinities[d]	S
Den Chai basalt: **DC**	At the south of Amphoe Den Chai, Phrae province.	70	Transition hawaiite (flow 1-4), hawaiite (flow5-6), and basanite (flow 7)[a]; Basaltic andesite of calc-alkali affinities[d]	S
Mae Lama basalt: **ML**	At Mae La Ma, Mae Hong Son province in the north-west of Thailand	small outcrop	Tholeiite[a]	-
Central region basalts				
Lam Narai basalt: **LNR**	Extending from Amphoe Khok Samrong and Amphoe Chai Badan in Lop Buri province.	700	Alkali olivine basalt, Hawaiite[a]	-
Wichian Buri basalt: **WB (KS** in this study)	At about 50 km north of Lam Narai basalt	200		S
Bo Phloi basalt: **BP**	At Ban Bo Phloi of Kanchanaburi province, about 145 km west of Bangkok.	1.5	Nepheline hawaiite[a], Basanitoid[d]	S
The Khorat Plateau basalts Nakhon Ratchasima basalt: **NR**	In south-east of Nakhon Ratchasima province	1,400	Hawaiite[a]	-
Buri Ram basalts	1) Khao Kradong basalt: **BR**, at 7 km south of Buriram.	30	Hawaiite	-
	2) Khao Pha Nom Rung basalt: **PR**, at about 50 km south of Khao Kradong.	17.5	Hawaiite[a]	-
	3) Phu Phra Angkhan basalt: **PPK**, at the west of Khao Pha Nom Rung.	35	Hawaiite	-
	4) Khao Prai Bat basalt: **BY**, at 2 km south of Khao Pha Nom Rung.	12	Hawaiite	-
Surin basalt: **SR**	At Khao Pha Nom Sawai, 20 km south of Surin province.	55	Hawaiite	-
Si Sa Ket basalts:	1) Phu Ngoen basalt: **PNG** in the north-west of Amphoe Kantharalak.	75	Nepheline hawaiite	-
	2) Phu Kom basalt: **PK**, at about 3 km north of Amphoe Kantharalak.	25	Alkali olivine basalt	-
	3) Phu Khmint basalt: **PKM**, at south west of Amphoe Kantharalak.	120	Hawaiite	-
	4) Phu Fai diabase: **PF** at about 10 km east of Amphoe Khun Han.	0.5	Diabase	-
Ubon Ratchathani basalts	At southern part of Ubon Ratchathani province. 1) Ban Nong Nam Khun basalt: **NNK**.	80	Hawaiite	-
	2) Nam Yun Basalt: **NY** at Khao Noi Keeribunpot, about 8 km north of Amphoe Nam Yun.	70	Alkali olivine basalt	S, R
South-eastern region basalts	Confined mainly in Chanthaburi and Trat provinces, about 350 km southeast of Bangkok.			-
Chanthaburi basalts Tha Mai basalts: **TM**	1) Khao Phloi Waen basalt, at the western part of Chanthaburi township (**PW** in this study).	small hill	Nephelinite[a], Basanite[d]	S
	2) Khao Woa basalt, at the western part of Chanthaburi township.	small hill	Basanitoid[d]	-
	3) Khlong Song Phi Nong basalt, at Khao Phloi Waen basalt.	-		-

[a] Barr and MacDonald (1978); [b] Vichit *et al.* (1978); [c] Sirinawin (1981), [d] Panjasawatwong (1983); [e] Panjasawatwong and Youngsnong (1995); [f] Sriprasert (1997).; *S = sapphire / R = ruby.

Table 2.1 (Continued).

Geographic names	Outcrops		Types	S/R*
	Locations	Covered areas (km^2)		
Khlung basalt: **SPH**	On the eastern part of Chanthaburi township, about 30 km further north of Amphoe Khlung e.g.-Ban We Lu, Ban Ang Et, Ban I Ram, and Khlong I Tak (**TP** in this study). -Saphan Hin		Basanitoid[b] Alkali olivine basalt[b], Hawaiite[c]	S. R
Pong Nam Ron basalts: **PNR**	At about 20 km east-southeast of Amphoe Pong Nam Ron.	-	Basanite[a]	-
Trat basalts (Nong Bon basalt: **NB**)	At about 20 km north of Amphoe Bo Rai, Trat province, distribute from Ban Nong Bon towards the south and spread over the flat area of Bo Rai. e.g.- Ban Na Yai, Amphoe Bo Rai.		Nephelinite[a], Olivine: nephelinite[b] Basanitoid[b]	R
Ko Kut basalt: **KK**	On Kut Island, south of Trat province, in the Gulf of Thailand.	-		-
Sae O basalt: **SO**	At Ban Sae O, Prachinburi province on the southern margin of Khorat Plateau	10	Hawaiite	-

[a] Barr and MacDonald (1978); [b] Vichit *et al.* (1978); [c] Sirinawin (1981), [d] Panjasawatwong (1983); [e]Panjasawatwong and Youngsnong (1995); [f] Sriprasert (1997).: *S = sapphire / R = ruby.

Vichit *et al.* (1978) classified Thai basalts into two broad categories, namely corundum-related basalts and corundum-free basalts. The corundum-related basalts include the Chiang Rai basalts (CR2), Lampang basalt (SP), Den Chai basalts (DC), Wichian Buri basalts (WB), Bo Phloi basalt (BP), Ubon Ratchathani basalts (NY), and Chanthaburi-Trat basalts (TM, SPH and NB).

Basalts in Southeast Asia are Cenozoic in age (Barr and MacDonald, 1981). The ages of most basalts in Thailand have their range from Late Tertiary (Miocene) to Early Quaternary. However there are also basalts of Jurassic age (San Kamphaeng and Ban Mae Koha) as reported in Jungyusuk and Khositanont (1992). The ages of corundum-related basalts range from 11.03 Ma (Wichian Buri basalt) – 0.44 Ma (Khao Phloi Waen basalt). Several authors have obtained ages for the basalts in Thailand, for example, Carbonnel *et al.* (1972, cited in Jungyusuk and Sirinawin, 1983), Barr *et al.* (1976), Bignell and Snelling (1977), Barr and MacDonald (1979 and 1981), Intasopha, (1993) and Sutthirat *et al* (1994). The ages of Thai basalts are summarized in Table 2.2.

Table 2.2 Ages (Ma) of basalts in Thailand. Note: shaded cells are the oldest and the youngest Cenozoic basalts.

Geographic name of basalt	Method of investigation				Corundum associated
	K/Ar	Fission track	$^{40}Ar/^{39}Ar$	Palaeomag-netic	
1. Chiang Khong basalt	1.74±0.18[e]	-	-	-	Sapphire
2. Ban Chiang Khian basalt (Chiang Rai)	1.69±1.25[e]	-	-	-	-
3. Mae Tha basalt (Lampang)	0.80±0.3[f], 0.60±0.2[f]	<1.7[b]	0.59±0.05[h]	0.69-0.95[b]	-
4. Den Chai basalt	5.64±0.28[d]	-	-	5.62-6.06[d]	Sapphire
5. Lam Narai	11.29±0.64[e]	-	18.10±0.7[g], 24.10±1.0[g]	-	-
6. Wichian Buri (Phetchabun)	-	-	9.08±0.29[g], 8.82±0.09[h], 11.03±0.03[h]	-	Sapphire
7. Bo Phloi basalt	3.14±0.17[e]	-	4.17±0.11[h]	-	Sapphire
8. Khao Kradong (Buri Ram)	0.92±0.30[e]	-	-	-	-
9. Phu Fai (Si Sa Ket)	3.28±0.48[e]	-	-	-	-
10. East Chanthaburi	-	2.57±0.20[a]	-	-	Sapphire
11. Khao Wua (Chanthaburi)	-	-	3.00±0.19[h]	-	Sapphire
12. Khao Phloi Waen (Chanthaburi)	0.44±0.11[e]	-	-	-	Sapphire
13. Nong Bon (Trat)	1.13±0.17[e]	-	2.38±0.16[h]	-	Ruby/Sapphire
14. Ko Kut	8.5±1.0[e]	-	-	-	-
15 San Kamphaeng, Chiang Mai	206±10[i]	-	-	-	-
16 Ban Mae Koha, San Kamphaeng, Chiang Mai	190±10[i]	-	-	-	-

a = Carbonnel *et al.* (1972); b =Barr *et al.* (1976); c = Bignell and Snelling (1977); d = Barr and MacDonald (1979) e = Barr and MacDonald, (1981). f = Sasada *et al.* (1987), g = Intasopha, S.B. (1993), h = Sutthirat *et al* (1994) and i = cited in Jungyusuk and Khositanont (1992).

2.3 Sample collection and sample identification

In this study basalt samples were collected from the outcrops throughout the country (Figure 2.2). The collection was focussed on the basalts regarded as the host rocks of corundum. They are the Chiang Khong basalt: CK, Ban Nong Nam Cho (called shortly as Ban Nong) basalt: BN, Den Chai basalt: DC, Bo Phloi basalt: BP, Wichian Buri basalt (collected from Ban Khok Samran): KS, Nam Yun basalt: NY, and Chanthaburi-Trat basalts (PW, TP, NB). In the area of Chanthaburi-Trat, fresh outcrops are very rare; only the three freshest basalts (Phloi Waen basalt: PW, Tok Phrom basalt: TP, and Nong Bon basalt: NB) were chosen as the represented localities for the Chanthaburi-Trat basalts.

Samples were collected from the outcrops, which are assumed to represent the source of corundum, i.e. from basalt outcrops closest to the corundum deposits. For example for

the Wichian Buri basalt, the samples were collected from Ban Khok Samran where corundum is found in the residual soil on top of the outcrop. Most outcrops of Thai basalts are in mountain areas with dense vegetation and are not well exposed because of the effects of weathering in a tropical climate. In those areas, therefore, the sampling was made in the freshest outcrops and those easiest to access.

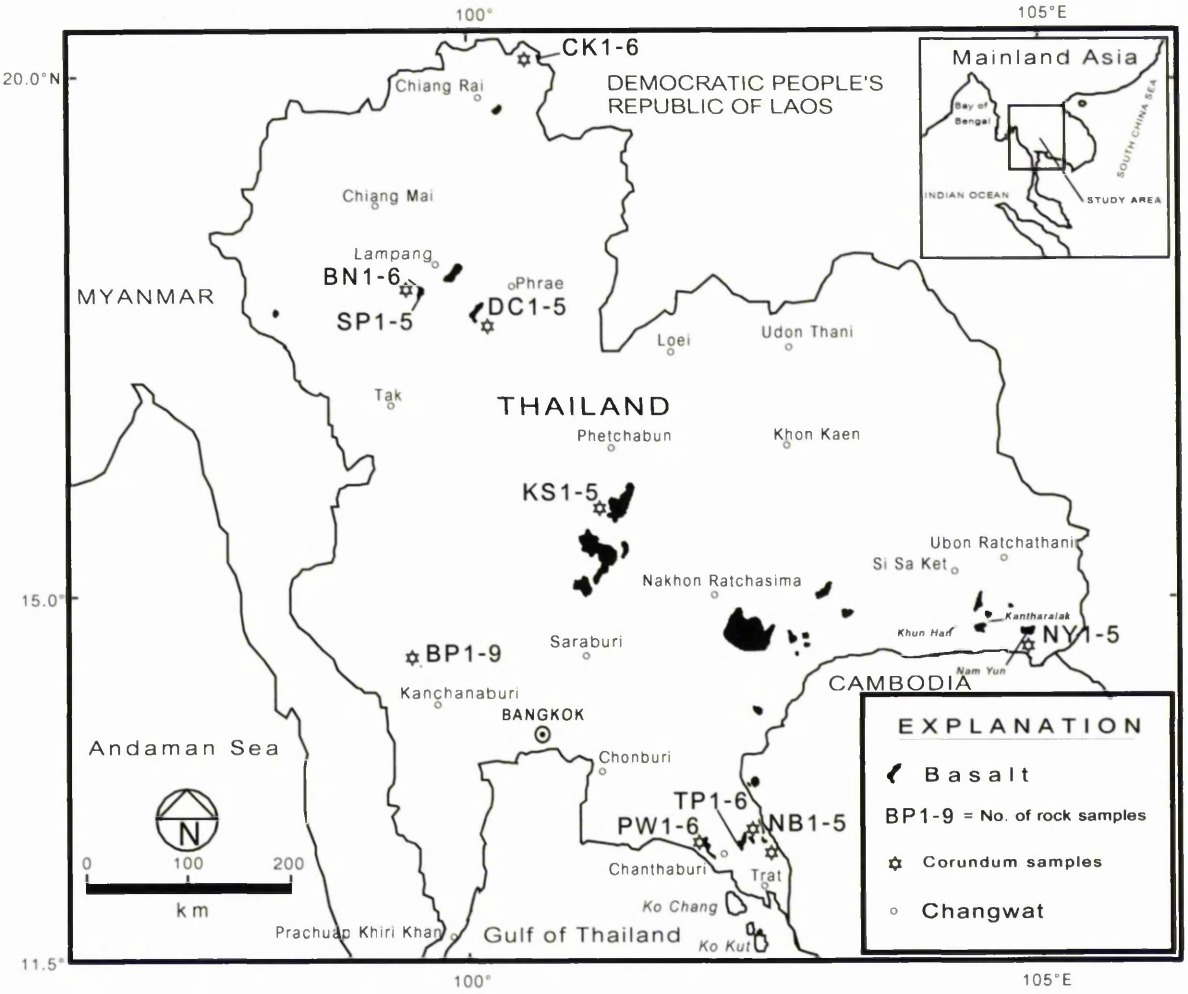

Figure 2.2 Localities of basalt samples. Localities of corundum samples are also given. (Distribution of basalts modified from Vichit, 1992).

Sixty-one basalt samples were collected, and the descriptions of their locations and lithologies are shown in Table 2.3. The appearances of the rocks in outcrop at certain localities are shown in Figures 2.3 – 2.10.

Table 2.3 Description of basalt samples collected from Thailand for this study.

Area name	Sample No.	Location	Outcrop characteristic at sample collection area	Lithology
1. Chiang Khong, Chiang Rai province	**CK1-6**	Pha Than, Mae Khong river bank, Wat (temple) Luang pier, near Chiang Khong Customs House	Sub-circular shape, covering area app. 200 m^2, well-developed columnar joints, partly weathered from the surface	Greyish black colour, very fine grained and dense texture, containing abundant megacrysts of black spinel, some ultramafic xenoliths, white mineral filled in the vesicles
2. Lampang province	**SP1-5**	1) Road cut, km 568-9 of Phahol Yothin Rd. (A1), Amphoe Sop Prap, 33 km south-west of Lampang township	At least 5 layers of basalt flow, pahoehoe and block lava type	Vesicular to dense basalt, greyish brown colour, white mineral filling in the vesicles
	BN1-6	2) Pha Kon Sao, Ban Nong, Tambon Nam Cho, Amphoe Mae Tha	Forms as hills and covered with soil weathered from basalt	Dense and grey colour, very fine grained texture, containing ultramafic xenolith and megacrysts of olivine, pyroxene, and black spinel
3. Den Chai, Phrae province	**DC1-3**	-Road cut, km 86 of Den Chai - Si Satchanalai road (No. 101)	Columnar joints	Dense, dark grey colour, containing abundant of large ultramafic nodules
	DC4-5	-Road cut, km 85 of the same route	Small outcrop	Dense and very fine grained texture, dark green coloured rock: serpentinite (?)
4. Wichian Buri, Petchabun province	**KS1-5**	Ban Khok Samran, Tambon Nam Ron, Amphoe Wichian Buri	Basaltic terrain, covered by thin layer of reddish brown soil weathered from basalt	Hard and dense rock, greyish black colour, look like stressed rock, fine grained texture
5. Bo Phloi, Kanchanaburi province	**BP1-9**	Khao Lan Thom, 300 m east of Bo Phloi township	Small plug-liked body, forming as low hills with columnar joints, covering 1.5 km^2 of area	Dense, fine-grained and porphyritic texture, greyish black colour, containing numerous lherzolite nodules; megacrysts of clinopyroxene, spinel, sanidine, and olivine; and xenolith of gneiss
6. Nam Yun, Ubon Ratchathani province	**NY1-5**	Road cut of route No. 2214, 500 m north of Amphoe Nam Yun township	Overlain by yellowish brown soil weathered from basalt	Greyish black colour, fine grained texture, some vesicles filled with white mineral
7. Chanthaburi province	**PW1-6**	1) Khao Phloi Waen, Amphoe Tha Mai: **PW**	Small hill, mostly weathered	Vesicular to dense basalt, reddish brown to greyish brown colours, containing spinel and pyroxene xenocrysts
	TP1-6	2) Mining area of Ban Tok Phrom, Amphoe Khlung: **TP**	Floated rock on alluvial sediments weathered from basalt	Greyish black colour, partly weathered, very fine grained texture, embedded with a crystal of green conchoidal fracture mineral
8. Trat province	**NB1-5**	Ban Nong Bon, Amphoe Bo Rai: **NB**	Pebble from mine	Partly weathered sample, containing spinel and pyroxene xenocrysts, greyish black colour,

Figure 2.3 Outcrop of Chiang Khong basalt (**CK**) at Pha Than, the Mae Khong river bank, near the pier of Wat (temple) Luang and Chiang Customs House.

Figure 2.4 Sop Prap basalt (**SP**) exposes at the road cut, km 568-9 of Phahol Yothin Road. (A1), Amphoe Sop Prap, 33 km south-west of Lampang township. The rock shows elongate vesicles indicating the flow of lava. No xenocrysts or xenoliths are found in this rock.

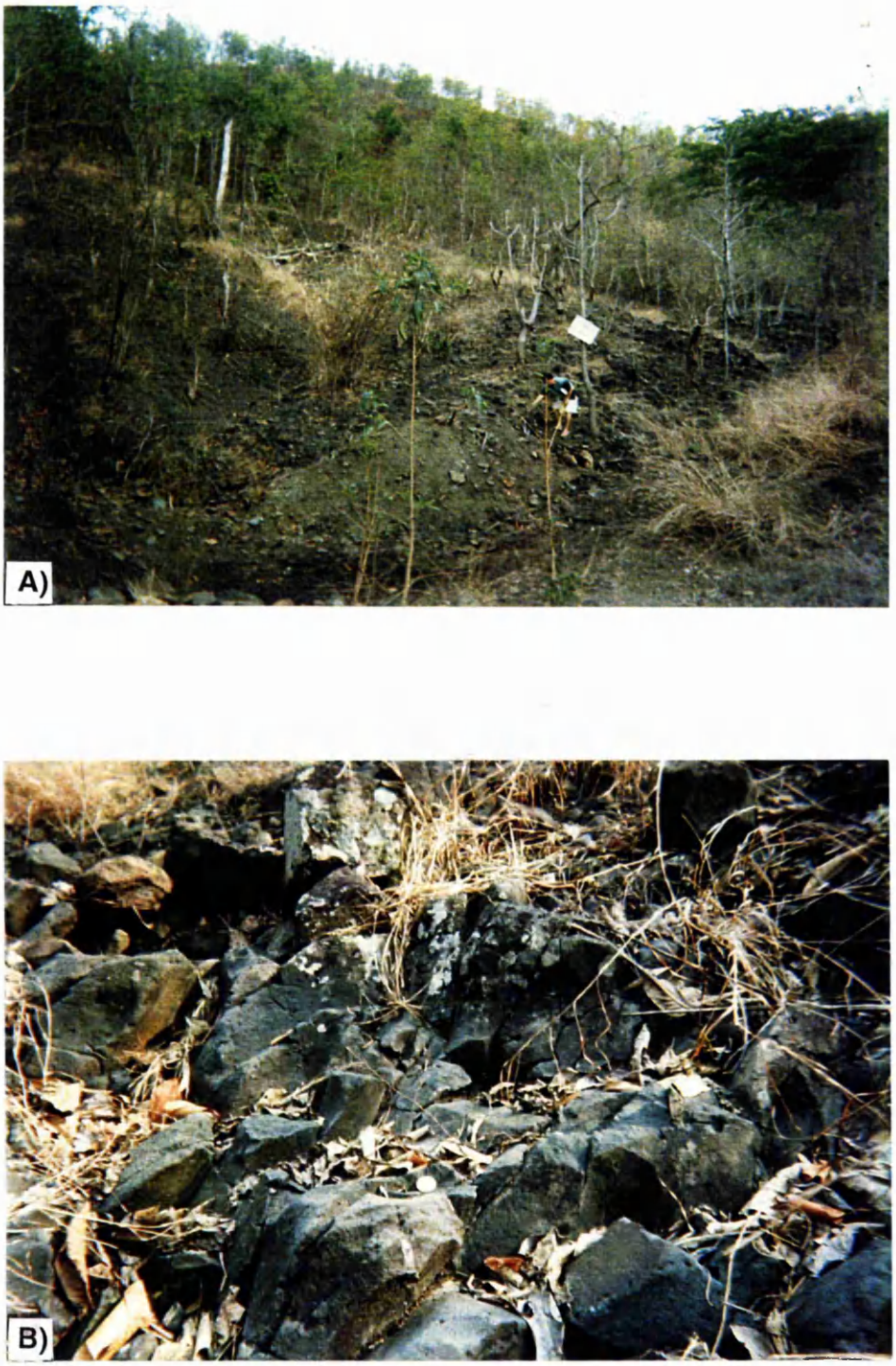

Figure 2.5 Ban Nong basalt (**BN**). **A)** Outcrop at the roadside to the Phra That Doi Kaew, at Tambon Nam Cho, Amphoe Mae Tha, Lampang. **B)** The appearance of the outcrop in A when looking close-up.

Figure 2.6 Outcrop of Den Chai basalt (**DC**) exposed at the road cut, km 86 of Den Chai - Si Satchanalai road (No. 101). The basalt shows flow layers.

Figure 2.7 Outcrop of Khok Samran basalt (**KS**). The basalt body is overlain by weathered soil derived from the basalt. Boulders of basalt are left on the ground.

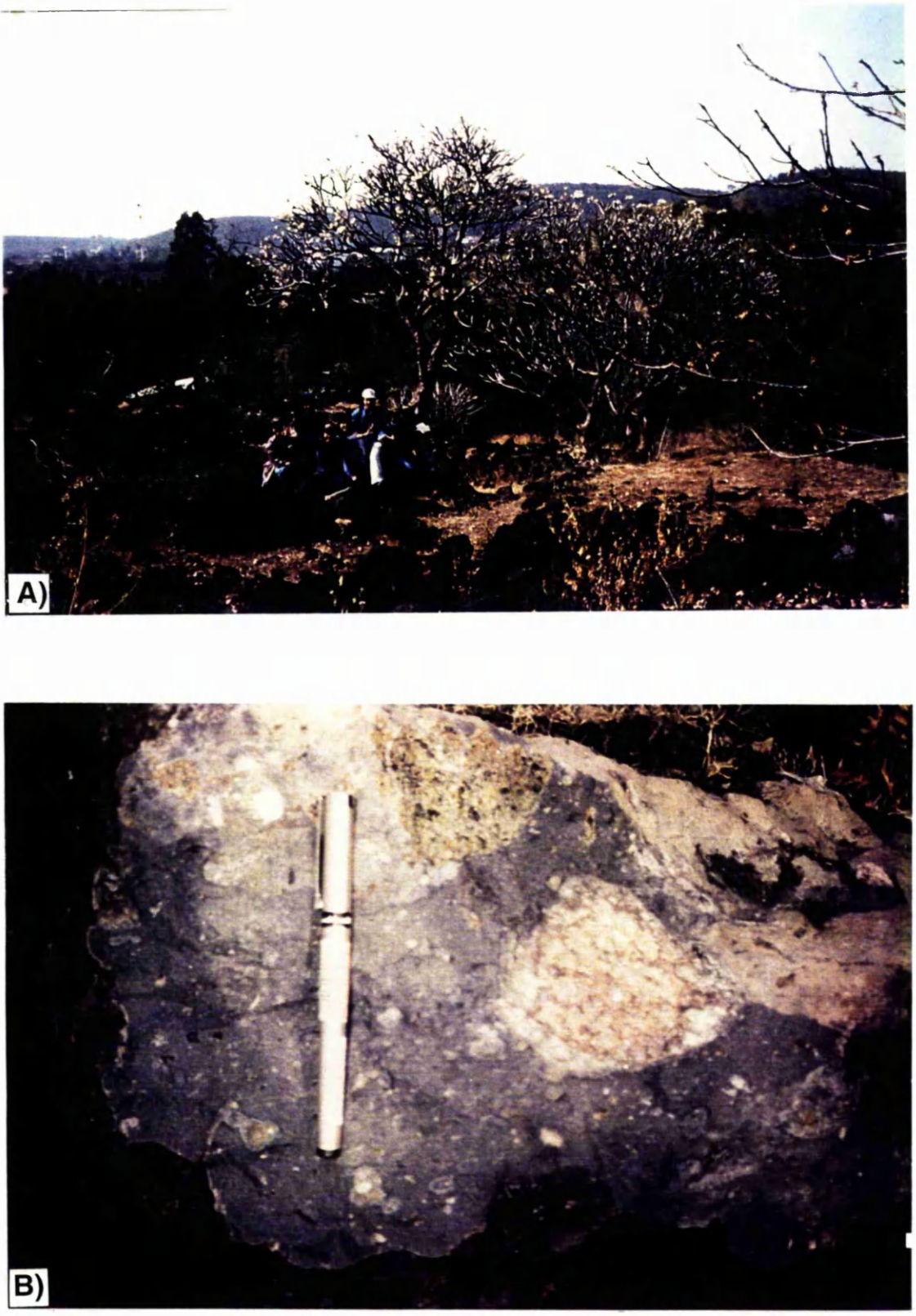

Figure 2.8 Bo Phloi basalt (**BP**). **A)** Landscape of Khao (hill) Lan Thom, 300 m east of Bo Phloi township where the basalt outcrops, seen as black rocks at the foreground of the picture, is exposed. **B)** Abundant xenocrysts and xenoliths are seen clearly when looking close-up to the fresh surface of Bo Phloi basalt, ultramafic xenolith (top centre), feldspathic xenolith (centre right).

Figure 2.9 Nam Yun basalt (**NY**), the outcrop at the roadside of the route No. 2214, 500 m north of Amphoe Nam Yun township.

Figure 2.10 Phloi Waen basalt (**PW**) at the top of Khao (hill) Phloi Waen, Amphoe Tha Mai, Chanthaburi province. The rock shows black clinopyroxene xenocrysts (centre left).

2.4 Petrography

A number of authors have studied the lithology and petrography of corundum-related basalts in Thailand. They are, for example, Aranyakanon *et al.* (1970), Bunopas and Bunjitradulya (1975), Vichit (1976), Sivabovorn *et al.* (1976), Vichit *et al.* (1978), Barr and Macdonald (1978, 1979, 1981), Sirinawin (1981), Yaemniyom (1982), Jungyusuk and Sirinawin (1983), Barr and Dostal (1986), Thannasuthipitak and Sirinawin (1986), Barr and James (1990), Panjasawatwong and Youngsnong (1995), Sutthirat *et al.* (1995) and Sriprasert (1997).

Apart from archiving the characteristics of the rocks, petrography can bring further benefit in helping to interpret their geochemistry. In this study, 62 polished sections were made from 61 basalt samples. Polished sections were prepared by cutting each rock sample into 3 - 4 slabs 1 cm thick, and one or two slabs for each rock sample were chosen. The chosen slabs were cut into 20 mm x 25 mm rectangles and then attached to 26 mm x 46 mm x 1.25 mm glass slides and polished until 0.03 mm thick (e.g. Phillips, 1971: 232-236). The remaining slabs were saved for geochemical analysis

Polished sections of rock samples were examined by the use of the polarizing microscope. The identification for certain minerals (e.g. ulvöspinel-magnetite, apatite, nepheline, leucite, and zeolite) was confirmed by the SEM-EDS analysis. Typical appearances of polished sections under the polarizing microscope from all localities are shown in Figures 2.11 - 2.22. Information for each polished section includes phenocrysts, groundmass, xenocrysts, xenoliths, amygdales, texture, and degree of alteration. The mineral constituents are given in mode percentage with the range of grain size. Rock name and preliminary interpretation (crystallization history, magma type, and origin of xenocrysts and xenoliths) were also determined.

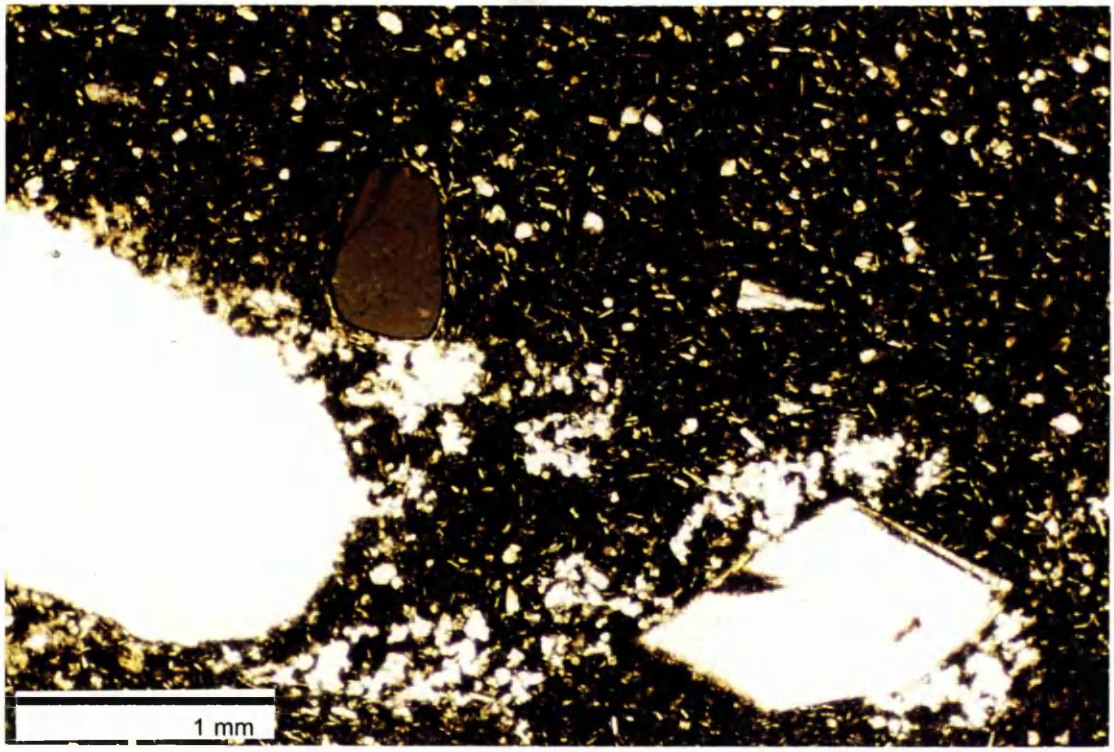

Figure 2.11 The appearance of Chaing Khong Basalt (sample **CK5**) in thin section, showing a green-brown spinel xenocryst (centre left), an olivine phenocryst (bottom right), and a rounded amygdale filled with calcite (left centre). The groundmass contains olivine granules, plagioclase feldspar laths and ulvö spinel-magnetite and glass (indistinguishable in this magnification). PPL.

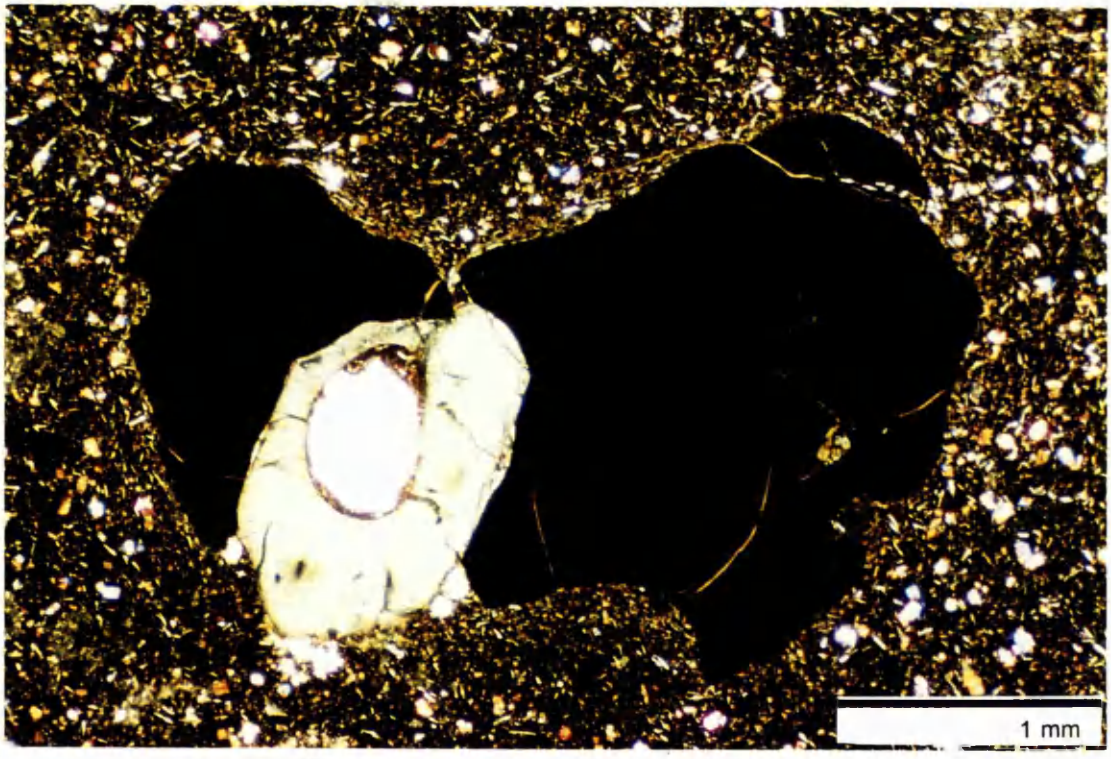

Figure 2.12 Xenolith of ulvöspinel-magnetite (black) + apatite (pale green) + calcite (white, rounded, in apatite) embedded in groundmass of sample from Chiang Khong (**CK2**). The minerals in the groundmass are similar to those of sample CK5. XPL.

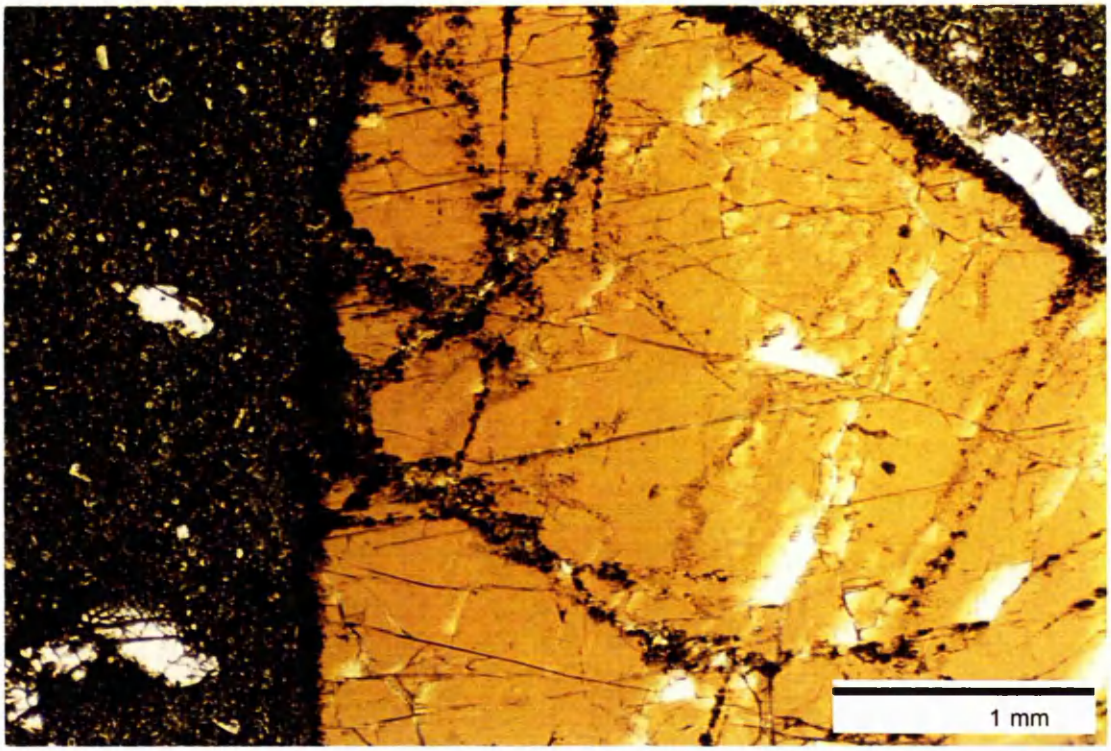

Figure 2.13 Sample from Ban Nong (**BN3**) shows xenocryst of brown-yellow amphibole, variety kaersutite, in very fine-grained groundmass of olivine, clinopyroxene, plagioclase, ulvöspinel-magnetite and glass. Minerals in groundmass cannot be distinguished in this magnification. Olivine microphenocrysts are present at the left centre and bottom left of the photo. PPL.

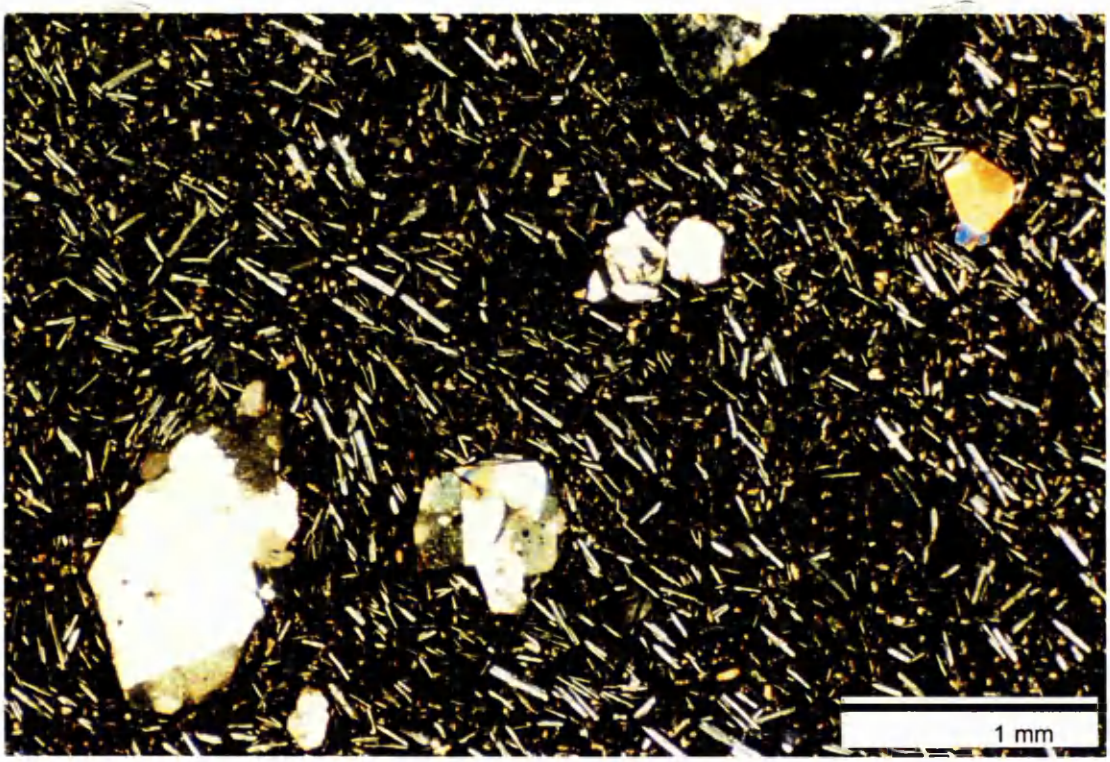

Figure 2.14 Xenocryst and xenolith-free basalt, sample from Sop Prap (**SP2**) shows olivine phenocrysts replaced by calcite except the yellow interference colour grain on the top right. Plagioclase laths in groundmass show the arrangement known as trachytic texture. Tiny granules and laths of clinopyroxene and olivine in groundmass exhibits yellow interference colour. Rounded black with yellow material at the top right of photo is clay mineral filling in amygdale. The black area in groundmass is composed of ulvöspinel-magnetite and glass, which cannot be distinguished in this magnification. XPL.

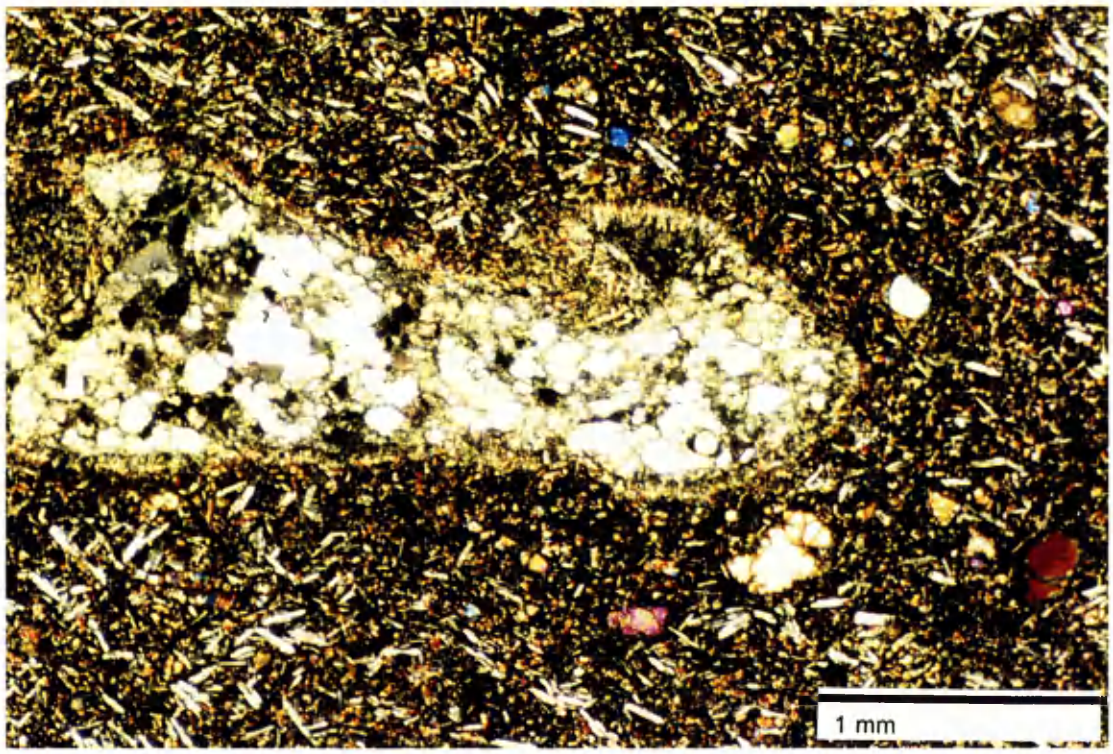

Figure 2.15 Sample from Den Chai (**DC1**) shows a xenolith of quartzite, in the middle of the photo, with tiny laths of clinopyroxene-reaction rim. Olivine microphenocrysts are set in the groundmass of olivine granules, Ti-augite laths, plagioclase feldspar laths as well as ulvöspinel-magnetite and glass that are indistinguishable in this magnification. XPL.

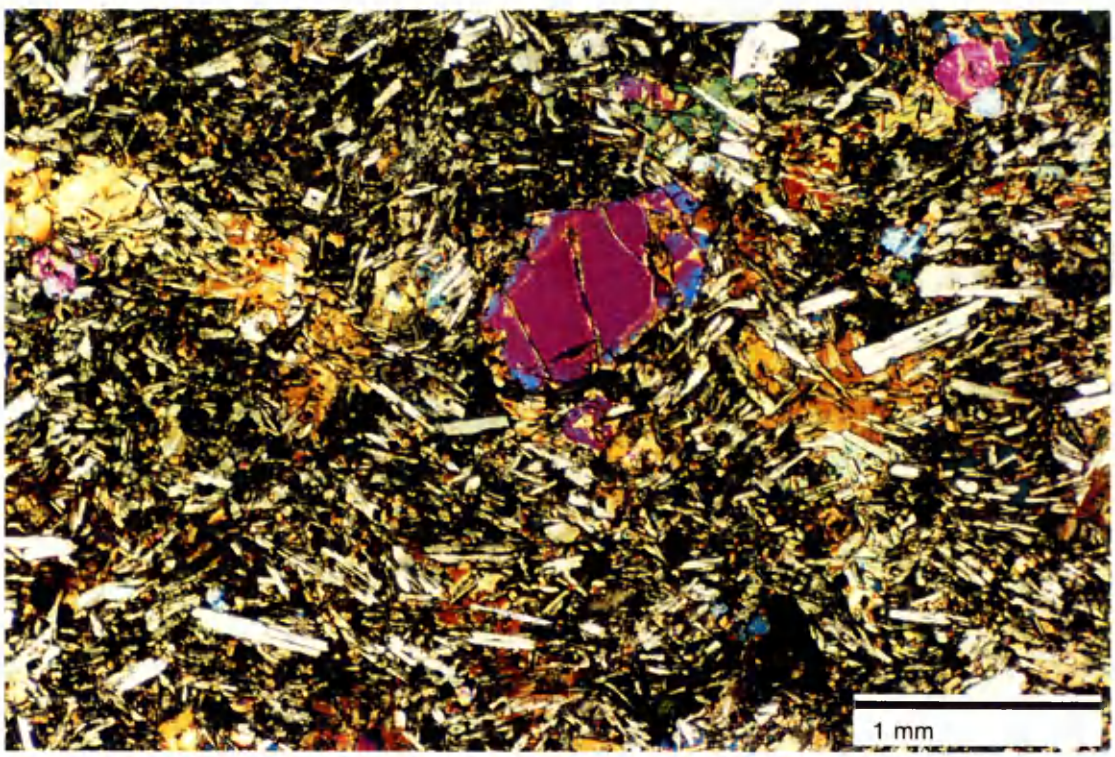

Figure 2.16 A xenocryst and xenolith-free sample from Khok Samran (**KS5**) exhibits ophimottled texture in groundmass by clinopyroxene (orange, brown or green interference colours) acting as the oikocrysts enclosing the chadacrysts of plagioclase laths. Olivine phenocrysts with blue (rim) and purple (core) interference colours are present at the centre and top right of the photo. Ulvöspinel-magnetite granules appear throughout the section as seen in black. XPL.

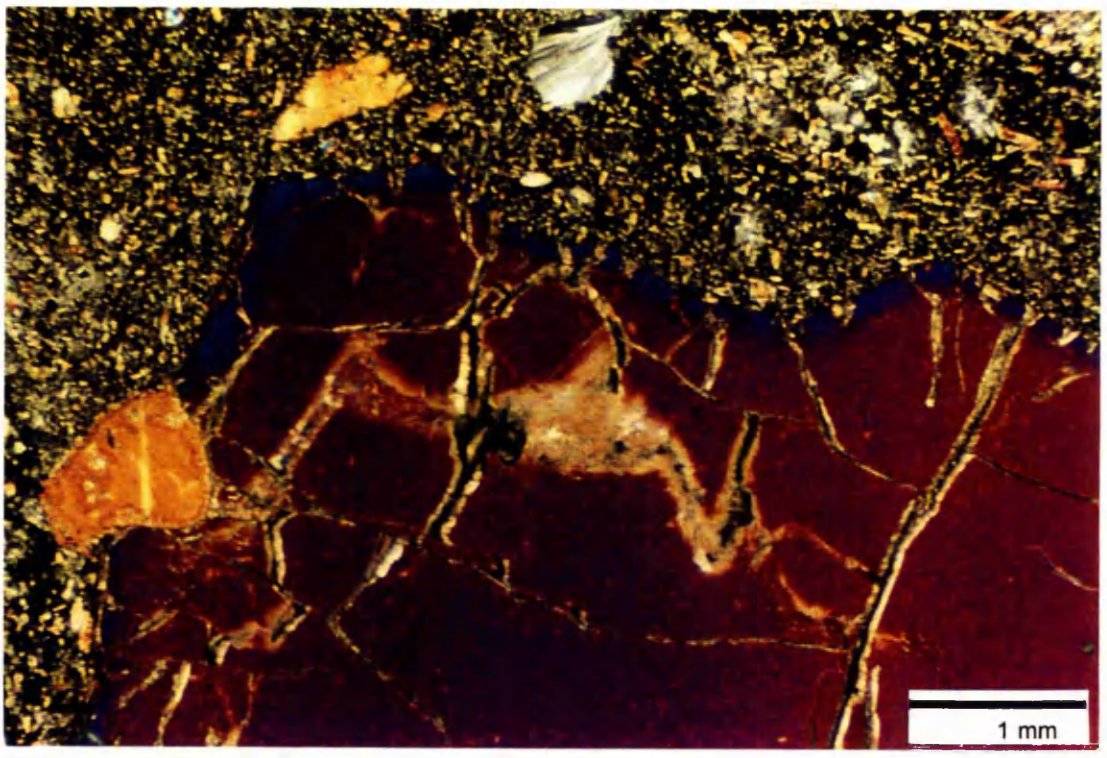

Figure 2.17 Sample from Bo Phloi (**BP9**) shows a xenolith of olivine (yellow interference colour) + clinopyroxene (purple and blue interference colours). An olivine microphenocryst is present at the top left of the photo. A rounded amygdale filled with zeolite (first order interference colour) is present at top centre. Groundmass consists of olivine granules (yellow interference colour, not clearly seen), tiny laths of Ti-augite (orange to brown interference colours) and a mixture of alkali feldspar, leucite and zeolite (seen as first order interference colour of ophimottled texture at top right of the photo). XPL.

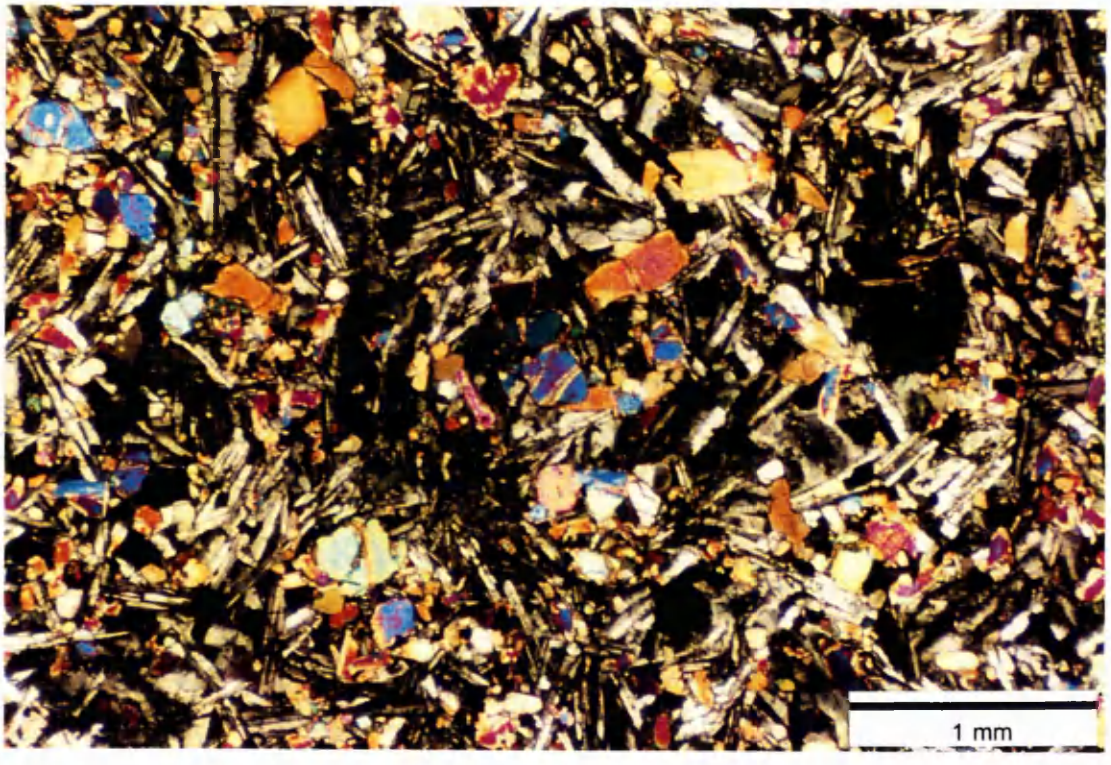

Figure 2.18 Sample from Nam Yun (**NY1**) is relatively coarse grained with no xenocrysts or xenoliths. Olivine phenocrysts have stubby shapes whereas Ti-augite phenocrysts appear prismatic. The plagioclase laths and ulvöspinel-magnetite (opaque) are set in the consertal ?zeolite. XPL.

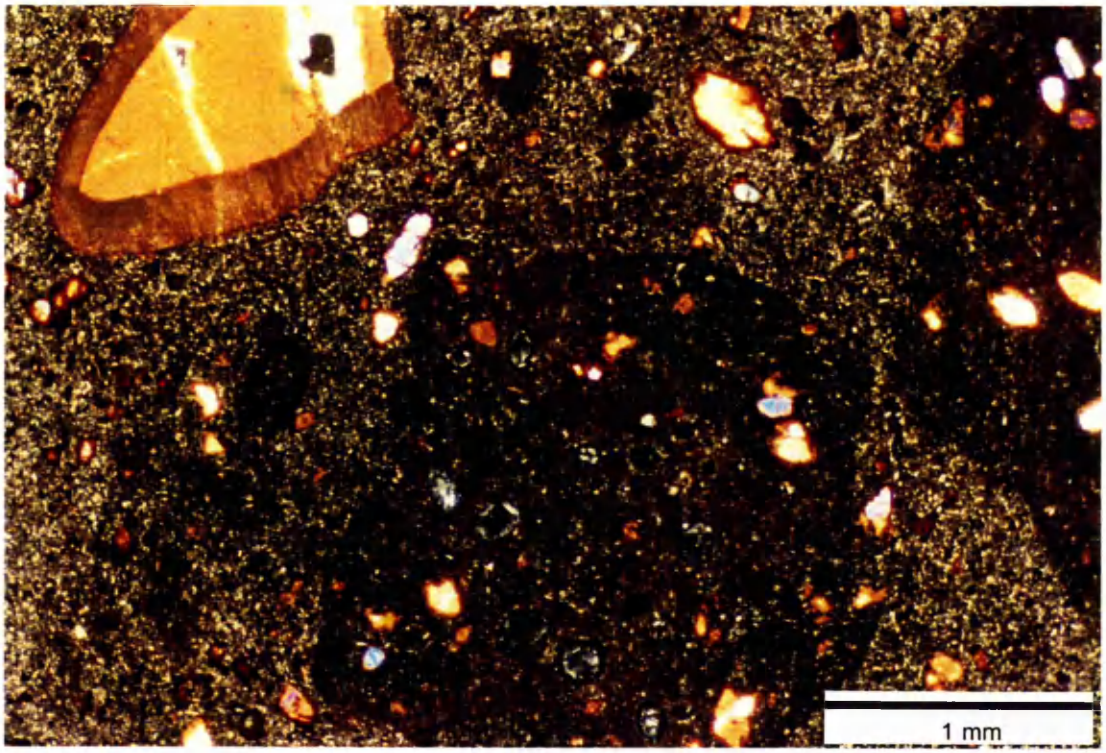

Figure 2.19 A sample with a certain degree of alteration from Khao (hill) Phloi Waen (shortly called Phloi Waen), **PW2**, shows two basalt xenoliths at the centre bottom and right of the photo. A clinopyroxene xenolith (yellow interference colour) is present at the top left. Microphenocrysts of olivine with red-brown alteration rim are set in a groundmass of ulvöspinel-magnetite granules (opaque) and the phases, which cannot be distinguished in this magnification, include olivine, clinopyroxene and glass. XPL.

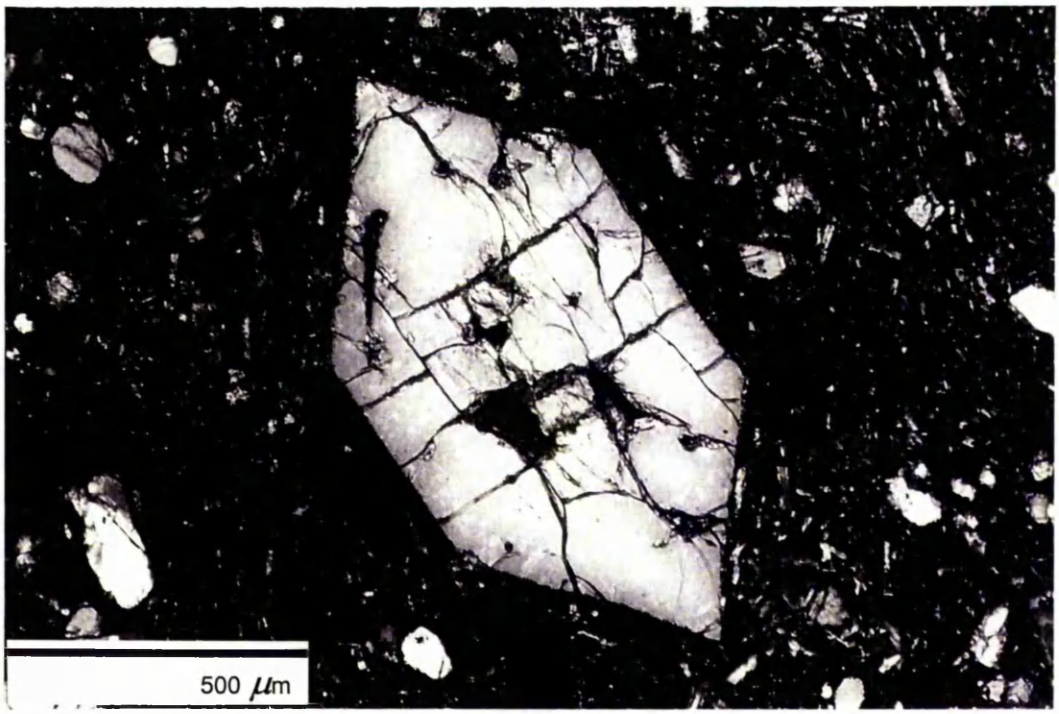

Figure 2.20 A stunning euhedral olivine phenocryst appears in the sample from Tok Phrom, **TP1/2**. Certain olivine microphenocrysts are set in a groundmass of olivine granules, clinopyroxene laths and the phases which are indistinguishable in this magnification include ulvöspinel-magnetite and glass. XPL.

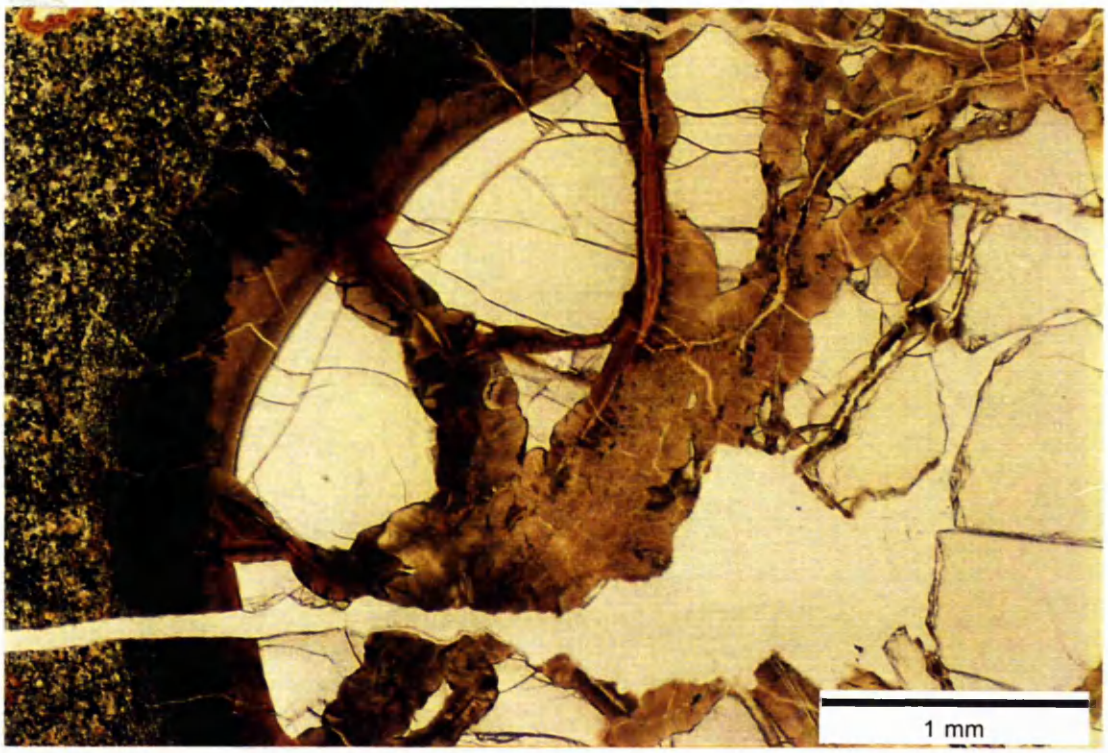

Figure 2.21 Garnet (variety almandine-pyrope) xenocryst (clean domains with cracks) embedded in a sample from Nong Bon (**NB5/2**). The garnet has altered borders (black and brown) indicating disequilibrium with the host melt. Groundmass contains olivine granules (red altered rim), ulvöspinel-magnetite (opaque) and the phases which are indistinguishable in this magnification include clinopyroxene and glass. PPL.

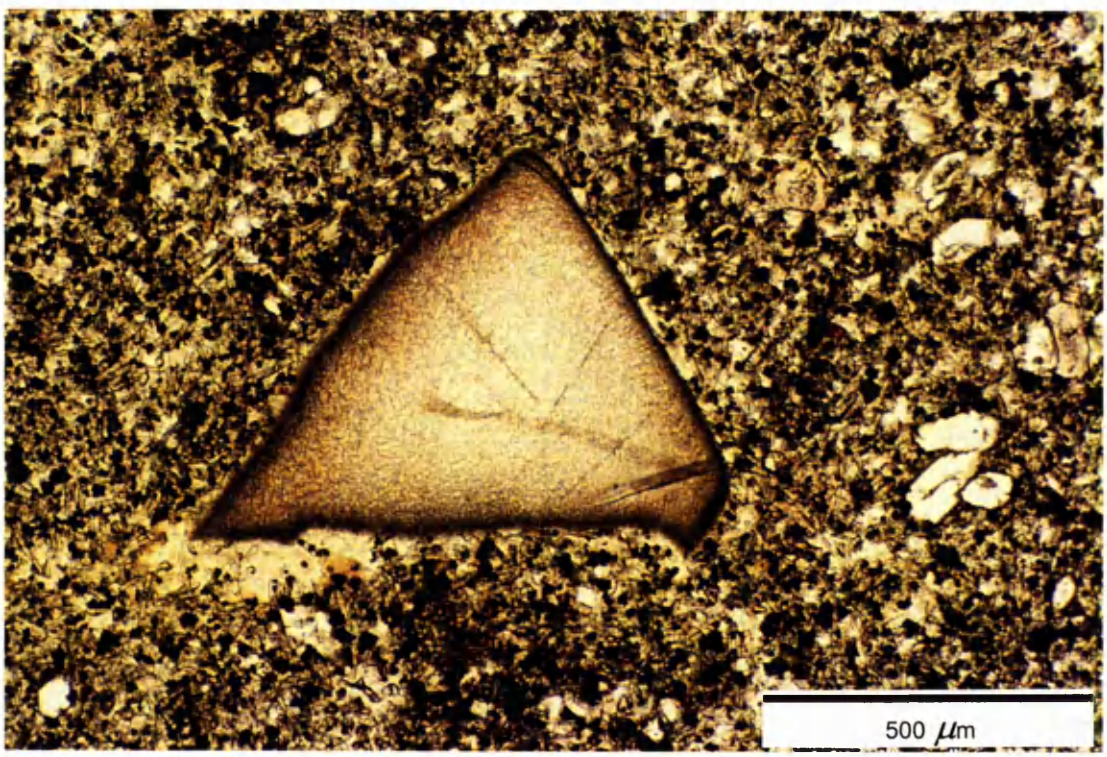

Figure 2.22 A brown apatite xenocryst is set in the groundmass of a sample from Nong Bon (**NB5/2**). Clean olivine microphenocrysts are present near the bottom right. Spongy-core clinopyroxene microphenocrysts are seen near the centre top and at the right centre of the photo. Groundmass consists of brown clinopyroxene laths, opaque ulvöspinel-magnetite and brown glass. PPL.

Summarized petrography for representative polished sections is presented in Table 2.4. Full description for all polished sections are given in Appendix 2-1.

Table 2.4 Summarized petrography for representative basalt samples.

Locality /Sample	Phenocryst	Xenocryst	Xenolith	Groundmass	Amygdale	Name
Chiang Khong CK5	Olivine <1%, Clinopyroxene <1%.	Olivine, ?Melted clinopyroxene, Spinel, Apatite, Unknown minerals, Brown aggregate (Melted amphibole), Plagioclase, Ulvö spinel-magnetites. Mode ~5%.	Spinel + Olivine, Ulvö spinel-magnetite + Apatite, Quartzite. Mode ~1%.	Plagioclase 15%, Olivine 15%, Ulvö spinel-magnetite 25%, Glass ~43%.	Calcite. Mode ~1%.	Olivine-Phyric Basalt with Xenocrysts and Xenoliths.
Ban Nong BN3	Olivine <1%, Clinopyroxene <<<1%.	Amphibole (kaersutite), Spinel, Olivine, Ulvöspinel-magnetite, Clinopyroxene, Orthopyroxene, Biotite. Mode 2%.	?Volcanic rock xenoliths, Quartzite. ~2%.	Olivine 7%, Clinopyroxene 20%, Ulvö spinel-magnetite 20%, Plagioclase <1%, Glass 46%.	Calcite, Brown / yellow / black colloform unknown minerals. Mode <1%.	Olivine-Phyric Basalt with Xenocrysts and Xenoliths.
Sop Prap SP1	Olivine 10%.	-	-	Olivine 2%, Clinopyroxene 7%, Plagioclase 25% (trachytic texture), Ulvö spinel-magnetite 7%, Glass 34%.	Calcite, Aragonite, Colloform and drusy unknown minerals. Mode ~15%.	Amygdaloidal Olivine-Phyric Basalt.
Den Chai DC2	Olivine ~1%, Ti-augite <<<1%.	Orthopyroxene <1%.	Quartzite with apatite (∅ 20μm) at margin, Spinel-lherzolite (3 cm across). Mode 70%.	Plagioclase 5% (trachytic texture), Olivine 4%, Clinopyroxene 4%, Ulvöspinel-magnetite 2%, Glass 12%.	Zeolite. Colloform mineral. Mode ~1%.	Olivine-Phyric Basalt with Xenocrysts and Xenoliths.
Khok Samran KS1	Plagioclase ~2%, Olivine ~1%.	-	-	Plagioclase 20% (trachytic texture), Olivine 10%, Clinopyroxene 5%, Ulvöspinel-magnetite 7%, Apatite (∅ 20 μm) <<<1%, Glass 44%.	Zeolite <<1%.	Olivine-Plagioclase-Phyric Basalt.

Table 2.4 (Continued).

Locality /Sample	Phenocryst	Xenocryst	Xenolith	Groundmass	Amygdale	Name
Bo Phloi BP9	Clinopyroxene ~1%, Olivine ~1%, Plagioclase <<1% (ophitic texture).	Clinopyroxene, Olivine, Alkali feldspar, Nepheline, Leucite. Mode 5%.	Olivine + Clinopyroxene, Alkali feldspar + Plagioclase + Clinopyroxene + Biaxial Apatite + Zircon + Calcite. Mode 10%.	Olivine ~5%, Ti-augite 10%, Magnetite 10%, Alkali feldspar 5% (ophimottled texture), Zeolite, Leucite interstice <<< 1%, Apatite <<< 1%, Glass 51%.	-	-
Nam Yun NY1	Olivine 7%, clinopyroxene <<<1%.	-	-	Olivine 7%, Ti-augite 20%, Ulvöspinel-magnetite 5%, Plagioclase 20% Alkali feldspar 5%, Zeolite (consertal texture) 34%.	Zeolite, Calcite. Mode <1%.	Olivine-Phyric Basalt ?
Phloi Waen PW3	Olivine ~7%, Clinopyroxene <<<1%.	Spinel, Clinopyroxene, Orthopyroxene, Olivine, Plagioclase, Mode 2%.	Aggregate, Lherzolite, Orthopyroxene + Clinopyroxene + Olivine, Olivine + Spinel. Mode 3%.	Olivine 2%, Clinopyroxene 20%, Ulvö spinel-magnetite 20%, Alkali feldspar in interstice <<<1 %, Glass 36%.	Vesicles. Mode 10%.	Vesicular Olivine-Phyric Basalt with Xenocrysts and Xenoliths.
Tok Phrom TP1	Olivine ~2%, Ti-augite with leucite at rim ~1%, Ulvö spinel-magnetite <<<1%.	Olivine, Clinopyroxene, Brown aggregate. Mode 2%.	Peridotite nodule 2%.	Olivine ~10%, Ti-augite 10%, Ulvöspinel-magnetite 15%, Plagioclase feldspar 10% (ophimottled texture and poikilitic texture), Glass 48%.	Zeolite. Mode <1%.	Olivine-Phyric Basalt with Xenocrysts and Xenoliths.
Nong Bon NB5/2	Olivine 5%, Clinopyroxene 1%.	Garnet, Clinopyroxene, Biotite, Ulvö spinel-magnetite aggregate, Apatite. Mode 7%.	Pyroxenite <<<1%.	Olivine 10%, Clinopyroxene 25%, Ulvö spinel-magnetite 20%, Glass 32 %.	Globular Fe-oxides. Mode <1%.	Olivine-Phyric Basalt with Xenocrysts and Xenoliths.

In summary, most rock samples are olivine-phyric basalt with xenocrysts and xenoliths.

Phenocrysts are mainly olivine and clinopyroxene with a combined mode of <10%. Clinopyroxene phenocrysts in most localities show "hour-glass" sector zoning with Ti-rich resorption rim (brown rim and pale green-brown core).

The groundmass, up to 90%, is composed of olivine, clinopyroxene, plagioclase feldspar, ulvöspinel-magnetite and glass. Accessory minerals in the groundmass include apatite, alkali feldspar, nepheline, leucite and zeolite found up to 1% in total.

Xenocrysts (combined mode up to 7%) include clinopyroxene, olivine, spinel, amphibole, orthopyroxene, plagioclase feldspar, alkali feldspar, nepheline, apatite, garnet, ulvöspinel-magnetite, and quartz. Xenoliths (<10%) include ultramafic nodules (e.g. pyroxenite, lherzolite, peridotite), quartzite, ?melted crustal material, gabbro, and gneiss. Xenocrysts and xenoliths are not found in the samples from three localities (Sop Prap: SP, Khok Samran: KS and Nam Yun: NY). Samples from Bo Phloi contain the most abundant inclusions (e.g. xenoliths of ?melted crustal material and gabbro, and xenocrysts of alkali feldspar and nepheline). Apatite xenocrysts are found in samples from two localities (Chiang Khong: CK and Nong Bon: NB). Garnet xenocrysts are found in samples from only one locality (Nong Bon: NB). Samples from Sop Prap (SP), Khok Samran (KS) and Nam Yun (NY) are xenocryst- and xenolith- free. Secondary phases forming in amygdales are calcite, aragonite, zeolites and clay minerals.

Alteration products are iddingsite and chlorite. Certain samples show a high degree of alteration (e.g. DC4, and DC5). Calcite pseudomorphs after olivine phenocrysts are abundant in Sop Prap basalt (SP). Den Chai basalt samples (DC4 and DC5) show chlorite-alteration throughout the rocks and their textures are different from DC1-3.

2.5 Whole-rock geochemistry

As with the petrography, several authors have studied the geochemistry of Thai basalts, for example Vichit *et al.* (1978), Barr and Macdonald (1978, 1979, 1981), Jungyusuk and Sirinawin (1983), Thannasuthipitak and Sirinawin (1986), Barr and James (1990), Yamamoto (1991), Panjasawatwong and Youngsnong (1995), Mukasa *et al.* (1996) and Zhou and Mukasa (1997).

In this study, bulk chemical composition of the rock samples in terms of major and trace elements are investigated using X-ray fluorescence (XRF) spectrometry and wet

chemical techniques (only for loss on ignition and ferrous oxide). Groundmass geochemistry was obtained by the use of the SEM-EDS.

2.5.1 Samples and techniques

For chemical analysis (XRF and wet chemical), slabs of basalt were hammered into 2–3 cm chips. Visible xenocrysts, xenoliths, and alteration products were picked out. Then the chips were ground in a swing mill (made of tungsten carbide) to the consistency of flour (absence of gritty particles when rubbed between the fingers before grinding (Ramsey, 1997)). The powder samples were packed in plastic bags.

XRF analysis

The XRF spectrometry (Philips, PW 1450) was employed for this work. The standard rocks (W-1 and NIMN, Govindaraju, 1989) were used to run for checking the accuracy of the machine. Overall, the XRF results are in high accuracy compared to the results published in the literature (see Appendix 2-2 for more detail). Principles of the technique can be found in e.g. Potts (1987) and Fitton (1997).

Sample pellets were prepared by mixing the 2 grams of rock powder with binder flakes (boric acid) to stop the sample crumbling and compressing the mixture between platens in a die at a suitable pressure (Potts, 1987) (e.g. 6 tons/inch^2). The pressed-powder method was the only sample preparation method available to the author. Smaller errors might have been possible using the fusion-bead technique (Potts, 1987) but this was not available at Manchester.

Major-element results of the samples obtained by XRF spectrometry were selected on the basis of the following criteria:

1) The results from the quadratic calibrations were used as the standards give a better fit;
2) Checking to see if all the sample compositions lie within the range of the calibration standard rock suite used;
3) If the sample compositions are within the range and the totals are in between 99 - 101 wt%, the results are likely to be reliable;
4) If the sample compositions are outside the calibration range, select an alternative, more suitable calibration and recompute the results. Then check 2) and 3) above; and

5) If the sample composition results do not match the criteria above, there may be certain errors and they should be solved.

The Fe_2O_3 values from the XRF were treated and the ratio of Fe_2O_3/FeO is adjusted for normative mineral calculation based on the method suggested by Middlemost (1989) (details in Appendix 2-3).

An important criterion for choosing the results for trace elements analyzed by XRF spectrometry is only to use a value for a particular element if that value falls in the range of its calibration value. If the results are outside the range, choose the closest one, otherwise the data recorded in the computer may be recomputed with a couple of other standard rock suites that give values covering the values of samples.

Wet chemical analysis for ferrous oxide and loss on ignition (LOI)

Because XRF analysis cannot distinguish between iron in different oxidation states (Fe^{2+} and Fe^{3+}), iron oxide concentrations obtained by XRF are normally written as Fe_2O_3. True FeO and Fe_2O_3 therefore needed to be determined. True FeO can be determined by wet chemical analysis and subtracted from the Fe_2O_3 from the XRF result [True Fe_2O_3 = (total Fe_2O_3 from XRF) - 1.111344 x (true FeO from wet chem.)].

FeO was determined by indirect titration as outlined by Rowland (1997). Sample powder is mixed with NH_4VO_3 (ammonium metavanadate) and digested in cold 48% HF in a covered plastic beaker for a few days to digest the silicate materials. The excess HF is neutralized with boric acid and the excess metavanadate is titrated against ferrous ammonium sulfate. Barium diphenylamine sulphate is used as an indicator.

To determine the degree of alteration of rock samples, volatile components were analyzed. Adsorbed water (H_2O^-) was determined by heating the samples at 110°C and weighing the samples before and after heating. The volatile components (e.g. OH^-, CO_3^{2-}, F^-, Cl^-) is then determined, after the adsorbed water is found, by igniting the same samples in the furnace at 1000-1200°C for 30 minutes, cooling, and weighing (Rowland, 1997). The results for total volatile content will be presented in the form of LOI (loss on ignition) which is corrected by addition with the ferrous FeO interference factor. That is (actual LOI) = (observed LOI) + C, where C = [1.111344x%FeO - %FeO] (Lechler and Desilets, 1987).

Groundmass analysis by the SEM-EDS

The samples used were the same polished sections as used for the petrography. The polished sections needed to be coated with carbon film (20 nm of thickness) to prevent charging during an electron bombardment (Reed, 1996). A fresh and apparently homogeneous area (ca 300 μm x 300 μm or 150 μm x 150 μm) in the groundmass of each sample was chosen using SEM-BSE imaging and then the electron beam was controlled to raster on it. The analytical conditions of the SEM-EDS were set at 15 kV for accelerating voltage, 1.5 nA for probe current, and 39 mm for working distance. Cobalt was used for calibration before analysing the samples. Link System ZAF-4/FLS software was used to convert the X-ray spectra obtained from the specimen into chemical analyses. The standards used for SEM-EDS analysis are listed in Table 2.5.

Table 2.5 Standards used for SEM-EDS analysis.

Element	Standard (Mineral/Synthetic)	Ideal composition
F	Fluorite	CaF_2
Na	Jadeite	$NaAlSi_2O_6$
Mg	Periclase	MgO
Al	Corundum	Al_2O_3
Si, Ca	Wollastonite	$CaSiO_3$
P	Apatite	$Ca_5(PO_4)_3(F,Cl,OH)$
S	Pyrite	FeS_2
Cl	Halite	NaCl
K	Orthoclase	$KAlSi_3O_8$
Ti	Rutile	TiO_2
Mn	Tephroite	Mn_2SiO_4
Fe	Fayalite	Fe_2SiO_4
Ba	Baryte	$BaSO_4$
Cr, Ni, Cu, Zn, Zr	Metal	Cr, Ni, Cu, Zn, Zr

2.5.2 Results

The major oxides were recalculated into CIPW (Cross, Iddings, Pirsson and Washington) normative minerals. Representative results are presented in Table 2.6. All data are given in Appendix 2-4. Note that the XRF data are reported on an anhydrous, volatile free basis. The ignition loss values are reported and are high (up to 5%). No correction for this has been made because of uncertainties in interpretation of the LOI values (which include CO_2, H_2O, SO_2 and effected by oxidation during ignition of Fe^{2+}). There is no effect on the use of these data.

Major elements

All rock samples were chemically classified based on the diagram of total alkalis (wt% of Na_2O+K_2O) plotted against silica (wt % of SiO_2) as shown in Figure 2.23. Most rock samples plot in the field of the alkaline series. The Chiang Khong basalt (CK) samples fall in two fields, basanite (normative olivine >10%) and trachybasalt. The Ban Nong basalt (BN), Tok Phrom basalt (TP) and Nong Bon basalt (NB) samples are classified as basanite. The Sop Prap basalt (SP) samples fall in two fields, trachybasalt and basaltic andesite. The Den Chai basalt (DC1-3) samples are classified as trachybasalt. The Khok Samran basalt (KS) samples fall in the trachybasalt and basalt fields. The Bo Phloi basalt (BP) samples are classified as phonotephrite. The Nam Yun basalt (NY) samples fall in the trachybasalt field. All the Khao Phloi Waen basalt (simply called Phloi Waen, PW) samples fall in the basanite field except one (PW4) which falls in the basalt field.

Weight per cents of oxides are plotted against SiO_2 (wt%) and MgO (wt%) as shown in Figures 2.24 and 2.25 respectively. Average M' value [atomic $Mg/(Mg+Fe^{2+})$] for all samples is 0.78 and the range is 0.52 – 0.96. Ni and Cr contents in most cases are lower in general than primary magma. [Note: primary magmas are generally thought to contain Ni 400-500 ppm, Cr >1000 ppm, SiO_2 ≤50%, Mg' >0.7, Wilson (1989: 22)]. This suggests that the magmas of the samples were not themselves primary magmas produced by partial melting in the mantle but were fractionated (Riddle, 1993: 389).

Table 2.6 Chemical composition and CIPW normative mineral composition of representative rock samples.

Sample No	CK5	BN3	SP1	DC2	KS1	BP9	NY1	PW3	TP1	NB5
Major oxides (wt%)										
SiO_2	44.80	46.64	48.84	45.50	47.06	47.33	48.54	42.64	43.43	42.67
Al_2O_3	15.04	13.80	15.66	13.69	16.65	13.57	15.69	12.33	12.64	12.56
Fe_2O_3	8.44	7.36	6.86	7.11	6.22	6.29	4.81	13.51	6.54	10.11
FeO	3.06	4.17	1.78	2.61	3.65	2.53	5.62	0.88	5.41	3.61
MgO	6.32	6.85	4.85	12.83	6.36	8.68	5.98	8.82	10.15	7.54
CaO	10.24	9.83	9.04	7.83	9.25	8.46	8.23	10.11	9.39	10.34
Na_2O	2.14	4.95	2.16	3.70	3.42	4.03	2.91	3.00	3.64	3.81
K_2O	3.00	1.21	3.01	1.34	1.85	3.85	2.09	1.07	2.45	2.09
TiO_2	2.82	2.38	2.05	2.02	2.02	1.75	1.89	2.93	2.96	3.23
MnO	0.18	0.18	0.20	0.20	0.20	0.21	0.18	0.22	0.25	0.21
P_2O_5	0.83	0.59	0.65	0.61	1.09	0.85	0.65	1.07	0.92	1.22
LOI	3.14	2.04	4.90	2.58	2.24	2.44	3.41	3.41	2.21	2.61
Total	100	100	100	100	100	100	100	100	100	100
Mg' [Mg/ $(Mg+Fe^{2+})$]	0.79	0.75	0.83	0.90	0.76	0.86	0.65	0.95	0.77	0.79
Nat. Fe_2O_3/FeO	2.76	1.76	3.85	2.73	1.71	2.49	0.86	15.31	1.21	2.80
H_2O^-	0.72	1.00	1.43	0.62	0.37	0.61	0.59	2.09	0.43	1.20
Trace elements (ppm)										
Nb	119	111	125	80	46	150	65	168	128	178
Zr	386	379	632	273	358	405	228	540	430	543
Y	57	55	49	45	51	56	42	60	49	62
Sr	870	979	3325	647	1748	1112	631	1558	1076	1407
Rb	49	66	110	50	19	286	26	227	63	257
Zn	82	85	64	59	81	78	98	139	112	146
Cu	53	50	43	53	51	51	80	61	68	66
Ni	71	105	115	566	33	215	188	249	211	140
Cr	73	184	145	574	50	241	192	185	178	90
Ce	111	105	109	88	156	153	67	181	130	179
Nd	47	38	31	30	65	45	24	75	45	91
V	286	281	200	220	231	200	193	315	308	341
La	34	35	43	27	48	57	23	61	49	62
Ba	321	1009	541	292	458	489	65	594	499	635
Sc	25	31	16	23	29	14	17	27	22	23
CIPW Normative minerals (%)										
Q			0.39							
Or	18.44	7.33	18.79	8.16	11.23	23.40	12.82	6.68	14.83	12.77
Ab	11.88	20.64	19.38	19.45	25.66	9.18	25.56	16.26	6.55	8.90
An	23.38	12.16	25.47	17.32	25.30	7.78	24.44	17.74	11.20	11.37
Ne	3.78	12.11		6.97	2.19	14.05		5.63	13.59	13.24
Di	19.30	27.58	14.15	14.88	11.78	23.78	11.00	22.37	24.46	27.24
Hy			13.22				9.83			
Ol	11.87	10.34		24.65	14.05	13.08	7.50	19.55	17.40	12.74
Mt	3.78	3.80	2.88	3.17	3.25	3.25	3.54	3.36	3.97	4.49
Il	5.56	4.63	4.12	3.95	3.95	3.44	3.72	5.81	5.77	6.34
Ap	1.99	1.41	1.60	1.44	2.59	2.04	1.58	2.62	2.20	2.92
Total	99.98	100.00	100.00	99.99	100.00	100.00	99.99	100.02	99.97	100.01

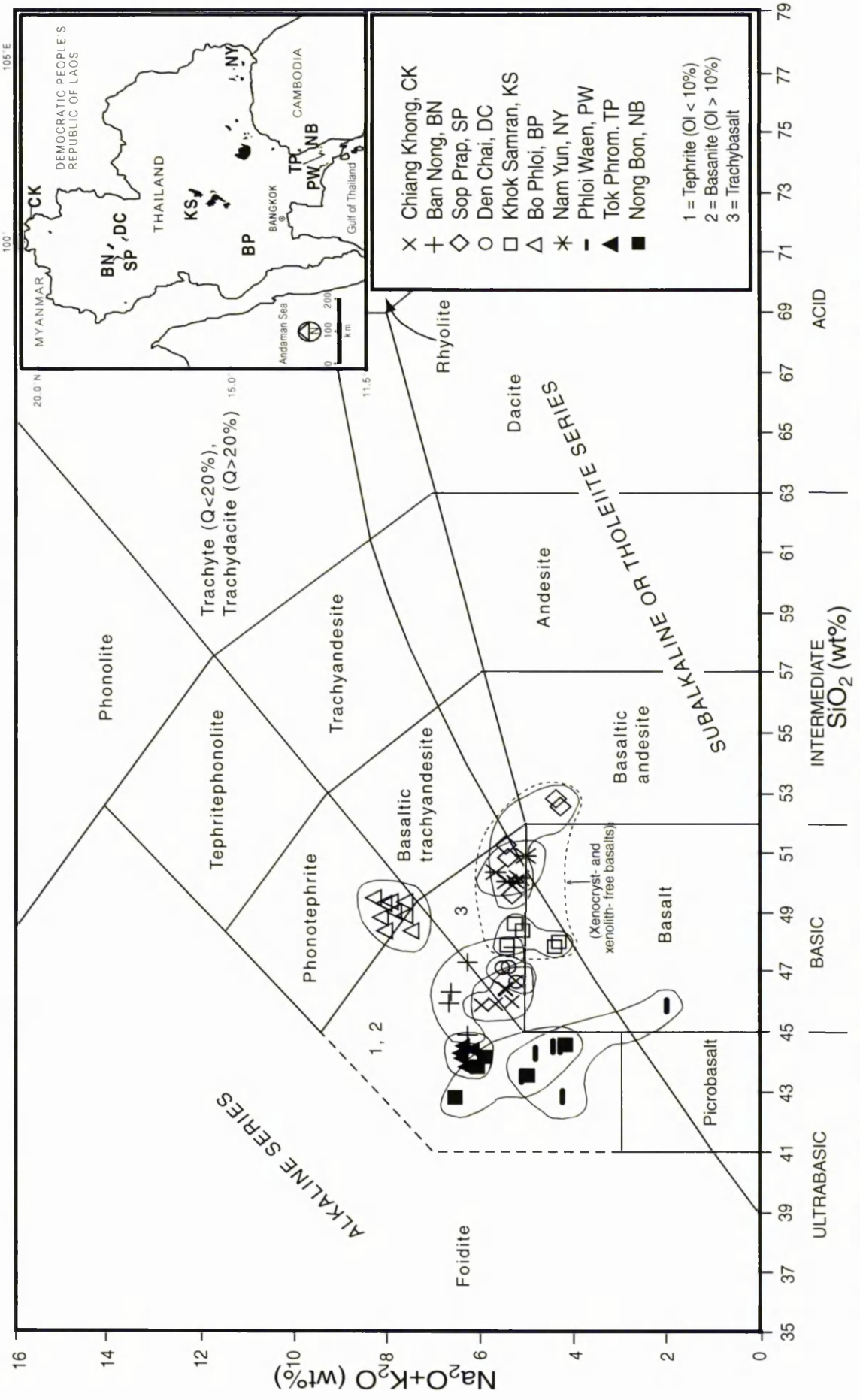

Figure 2.23 Chemical classification and nomenclature of rock samples, using the total alkalis versus silica (TAS) diagram of Le Maitre *et al.* (1989), curved line after Irvine and Baragar (1971).

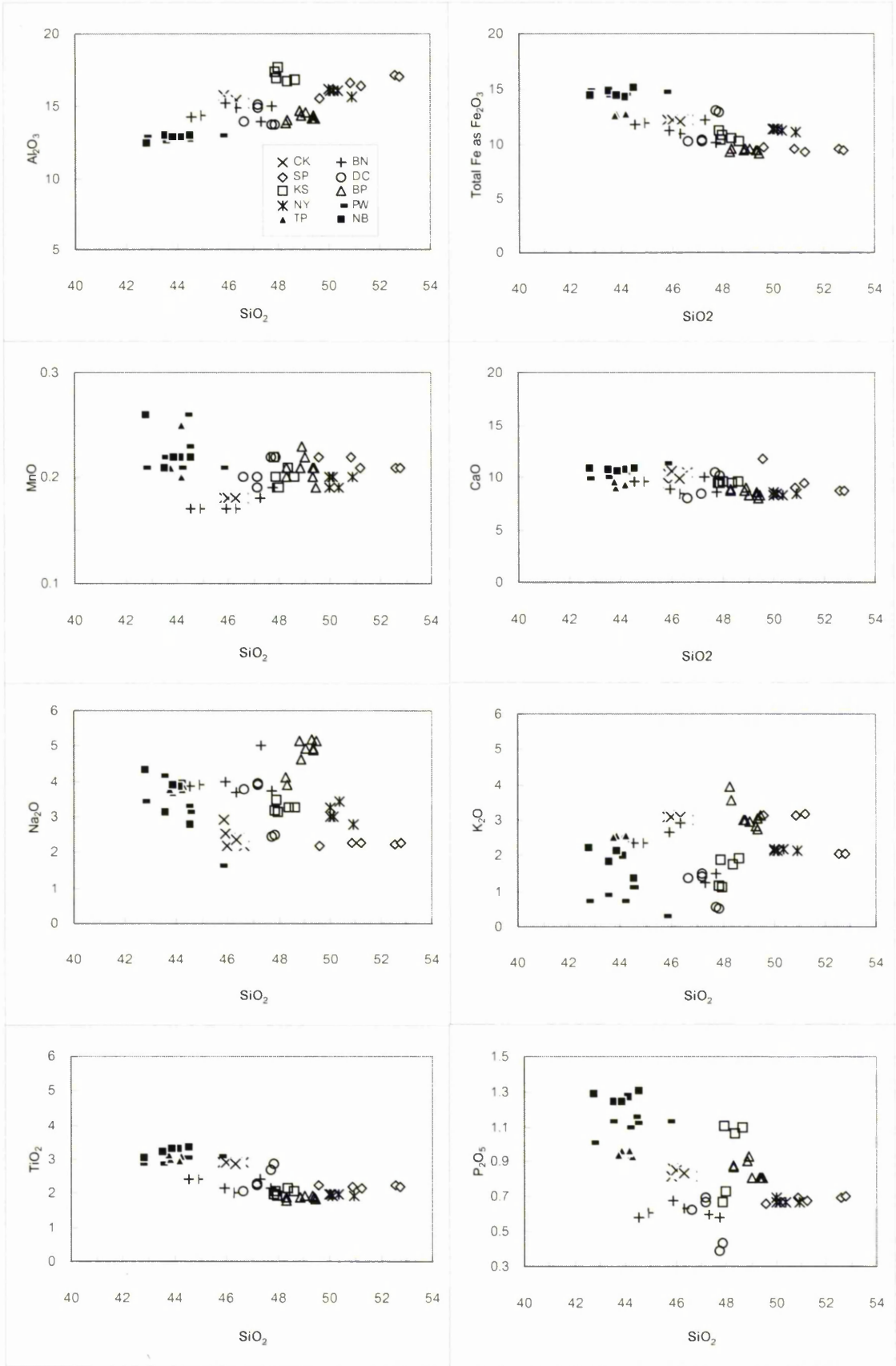

Figure 2.24 Weight per cent of oxides plotted against SiO_2 (wt%) for all rock samples.

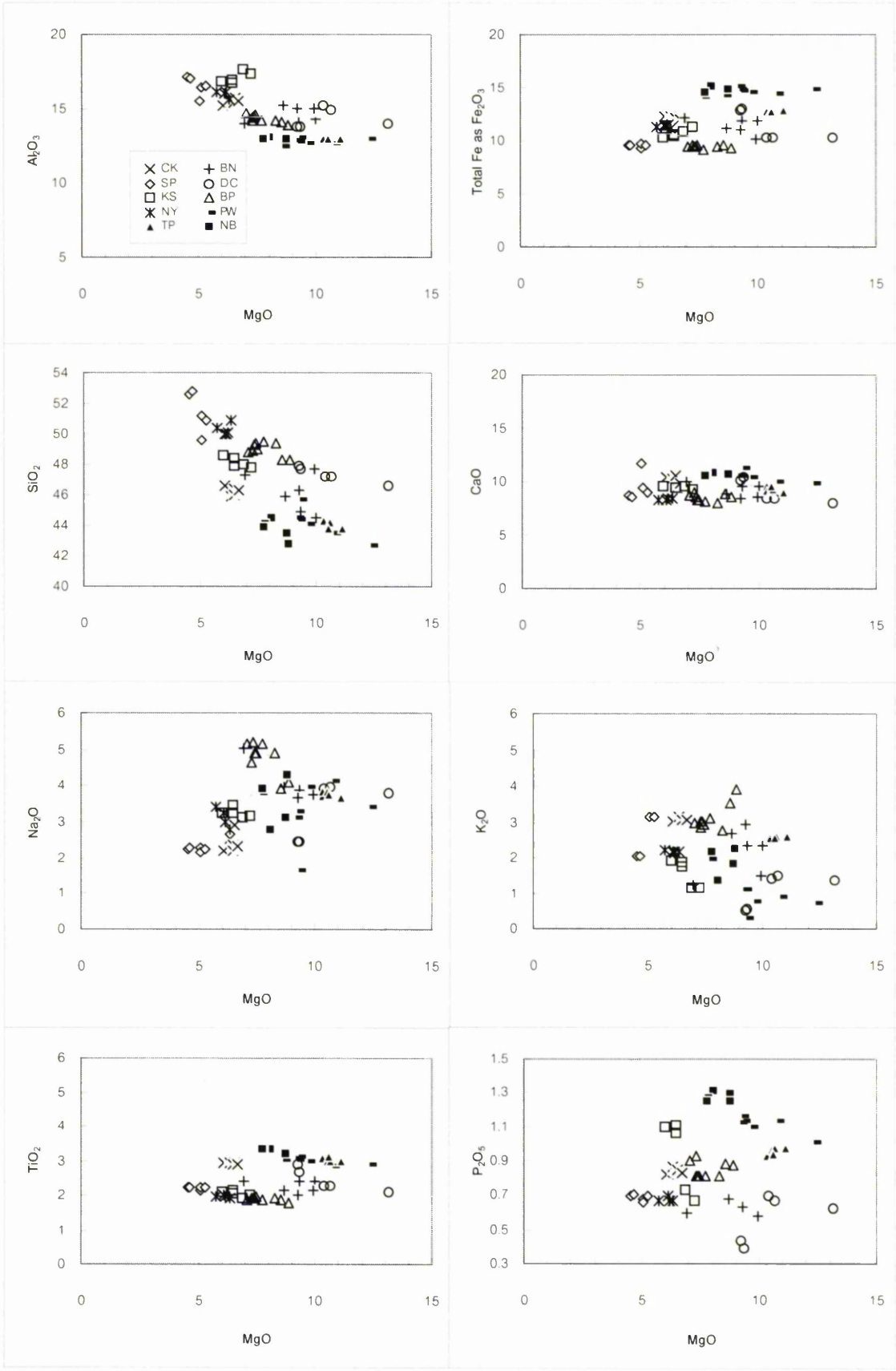

Figure 2.25 Weight per cent of oxides plotted against MgO (wt%) for all rock samples.

From Figure 2.25, the negative correlation between Al_2O_3, SiO_2 and MgO and the positive correlation between Fe_2O_3 and MgO indicate fractionation. This is confirmed by Figure 2.26. However K_2O, Na_2O, and P_2O_5 show no correlation with MgO, suggesting that these elements were mobile during alteration. CaO and TiO_2 remain nearly constant while MgO decreases. This suggests that minimum plagioclase and ulvöspinel-magnetite were removed from the magma during fractionation.

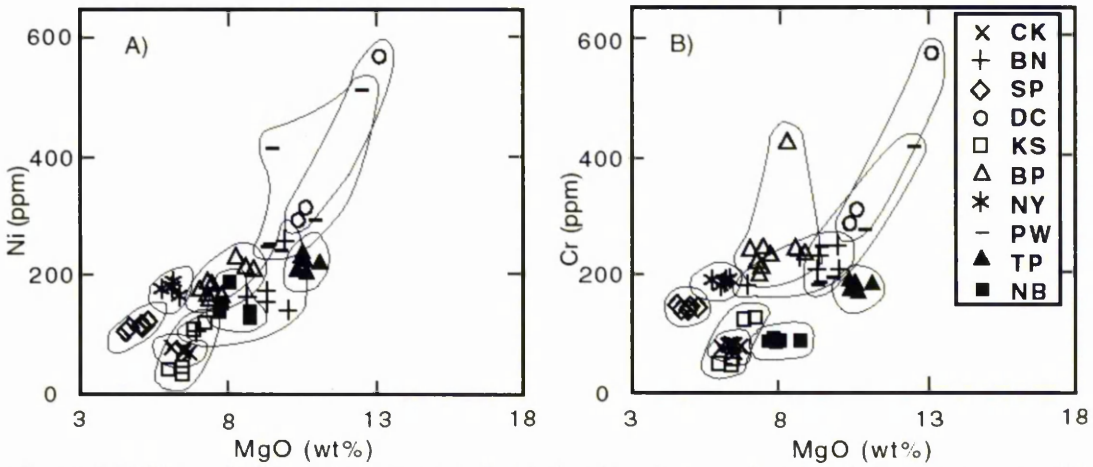

Figure 2.26 Plots of Ni and Cr against MgO, **A)** showing clear positive correlations at most localities, indicating olivine fractionation. **B)** shows a similar pattern as in A); it is possible that olivine and Cr-spinel fractionated. Certain localities show very narrow range of Ni-Cr contents indicating that there was very limited fractionation in their magmas.

The Bo Phloi basalt samples contain higher Na_2O+K_2O (average 7.90 wt%) than the other samples. This is confirmed petrographically by the observation that alkali feldspar is abundant in the groundmass. The rock samples are plotted on a K_2O versus Na_2O diagram and they fall in the K and Na sub-series of magmas (Figure 2.27).

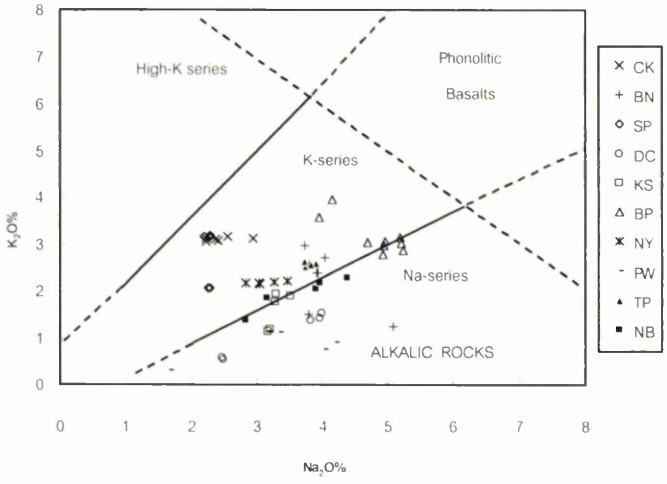

Figure 2.27 Analysed rock samples plotted on a diagram of K_2O versus Na_2O (wt%). The subdivision of the alkalic magma series into high-K, K and Na sub-series is shown (fields from Middlemost, 1975).

Figure 2.28 indicates that the tectonic environment of the rock samples is likely to be continental basalt.

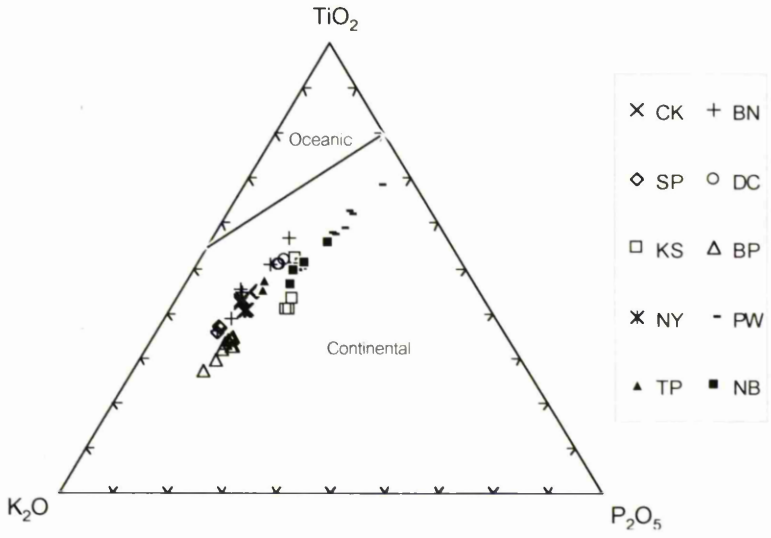

Figure 2.28 The TiO_2-K_2O-P_2O_5 discrimination diagram for basalts showing that the rock samples are continental basalts (fields from Pearce *et al.*, 1975).

Trace elements

Trace element analyses of representative rock samples are given in Table 2.6. Sr in samples from Sop Prap (SP) has very high values (up to 3325 ppm in sample SP1) and most Sr results were previously out of the calibration range. They were recomputed using the high Sr standard rock suite to obtain new values that fall within the range of the standards. The higher values for Sr in SP are probably due to Sr substitution for Ca in plagioclase and secondary calcite (confirmed by petrography).

Nb, Zr and Y contents of all samples are plotted on Meschede (1986) discrimination diagram (Figure 2.29), giving the tectonic environment as within-plate alkali basalts, which agrees well with the major-element plot (Figure 2.28). KS samples are obviously different from the other samples as they fall in the field of within-plate alkali basalts and within-plate tholeiites.

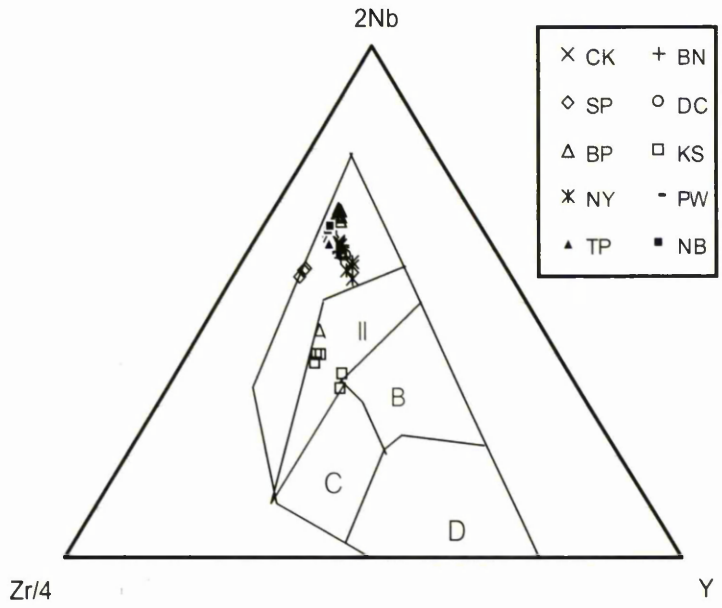

Figure 2.29 Analysed samples plotted on the Zr-Nb-Y discrimination diagram for basalts (fields after Meschede, 1986), AI = within-plate alkali basalts; AII = within-plate alkali basalts and within-plate tholeiites, B =E-type MORB; C = within-plate tholeiites and volcanic-arc basalts; D = N-type MORB and volcanic-arc basalts.

Normalized incompatible elements are plotted in Figure 2.30. Overall, the samples show similar patterns except for the samples from Khok Samran (KS) and Nam Yun (NY). Most samples are enriched in incompatible elements and show a typical basaltic pattern of decreasing enrichment with increasing incompatibility (Wilson, 1989: 271-273). The K trough and the Rb and Nb peaks suggest that the rocks were derived from low-K, and Rb- and Nb- enriched mantle with a small degree of partial melting (which is also indicated by low SiO_2). The SiO_2 content is dependent on the pressure; the higher pressure the less SiO_2 (Zhou and Mukasa, 1997). The K depletion suggests that the rocks have experienced little contamination by crustal materials (as K is enriched in granitic rocks). The La/Ba versus La/Nb diagram (Figure 2.31) clarifies this argument. In addition, Mukasa *et al.* (1996) studied isotopic signatures of alkali basalts from Thailand and found that the crustal contamination was minimal. The magma of the basalt samples containing ultramafic xenocrysts or xenoliths probably originates from the depth greater than 80 km (implied from the depth of mantle xenoliths studied by Sutthirat *et al.*, 1999).

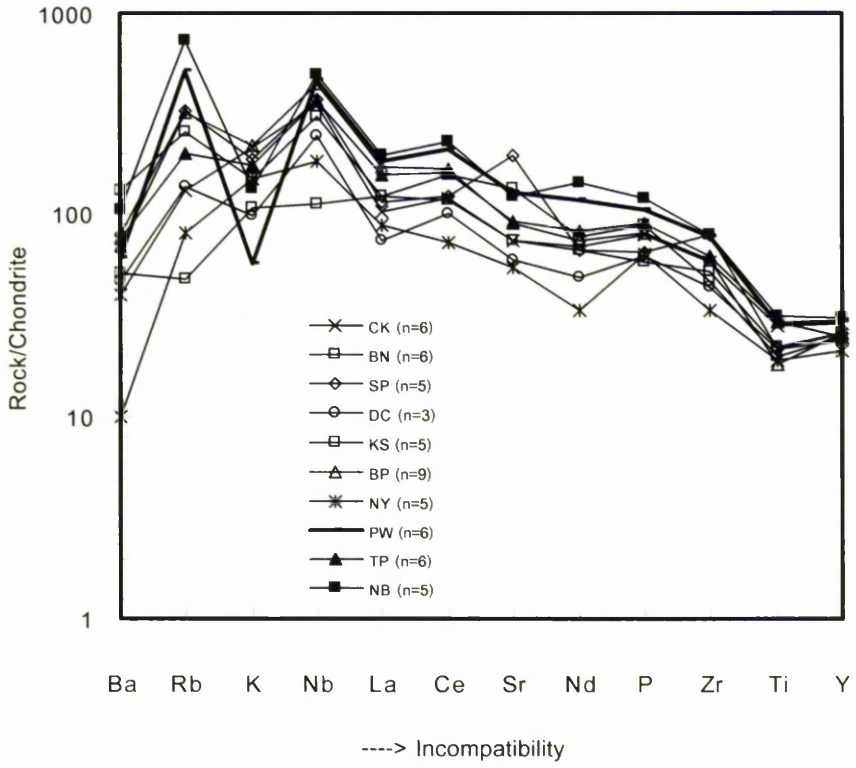

Figure 2.30 Chondrite-normalized abundances of incompatible elements in averages of n samples for basalts from different localities in Thailand. (Normalizing values from Thomson, 1982).

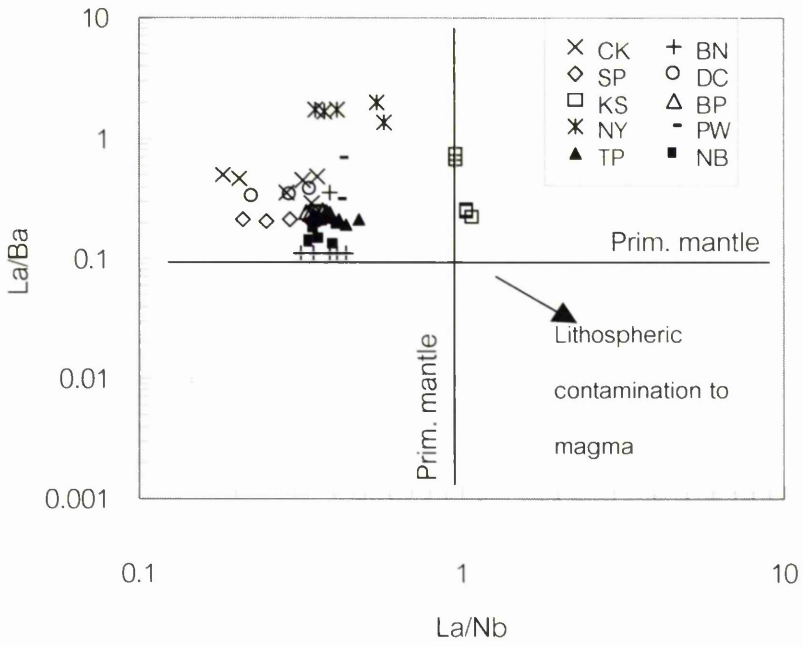

Figure 2.31 La/Nb vs. La/Ba diagram for alkali basalts from Thailand; the trend towards high La/Nb and low La/Ba reflects increasing input to magmas from the continental lithospheric mantle or crust. This diagram suggests that there is no evidence of contamination of basalt samples. (Fields from Kent *et al.*, 1996).

2.6 Whole rock geochemistry versus groundmass geochemistry

Comparison of the results between those from the XRF and from the SEM-EDS for the same samples is performed in this section. Homogeneous areas in the groundmasses (Figure 2.32, as for example) of basalt samples were analyzed with the SEM-EDS by rastering the electron beam on it. The results of rastering are given in Table 2.7 together with the XRF analyses. The results from the SEM-EDS contain no volatile analyses. Therefore the XRF results used for comparison were treated by subtracting the volatile contents (H_2O^- + LOI) from the total and normalising to 100%.

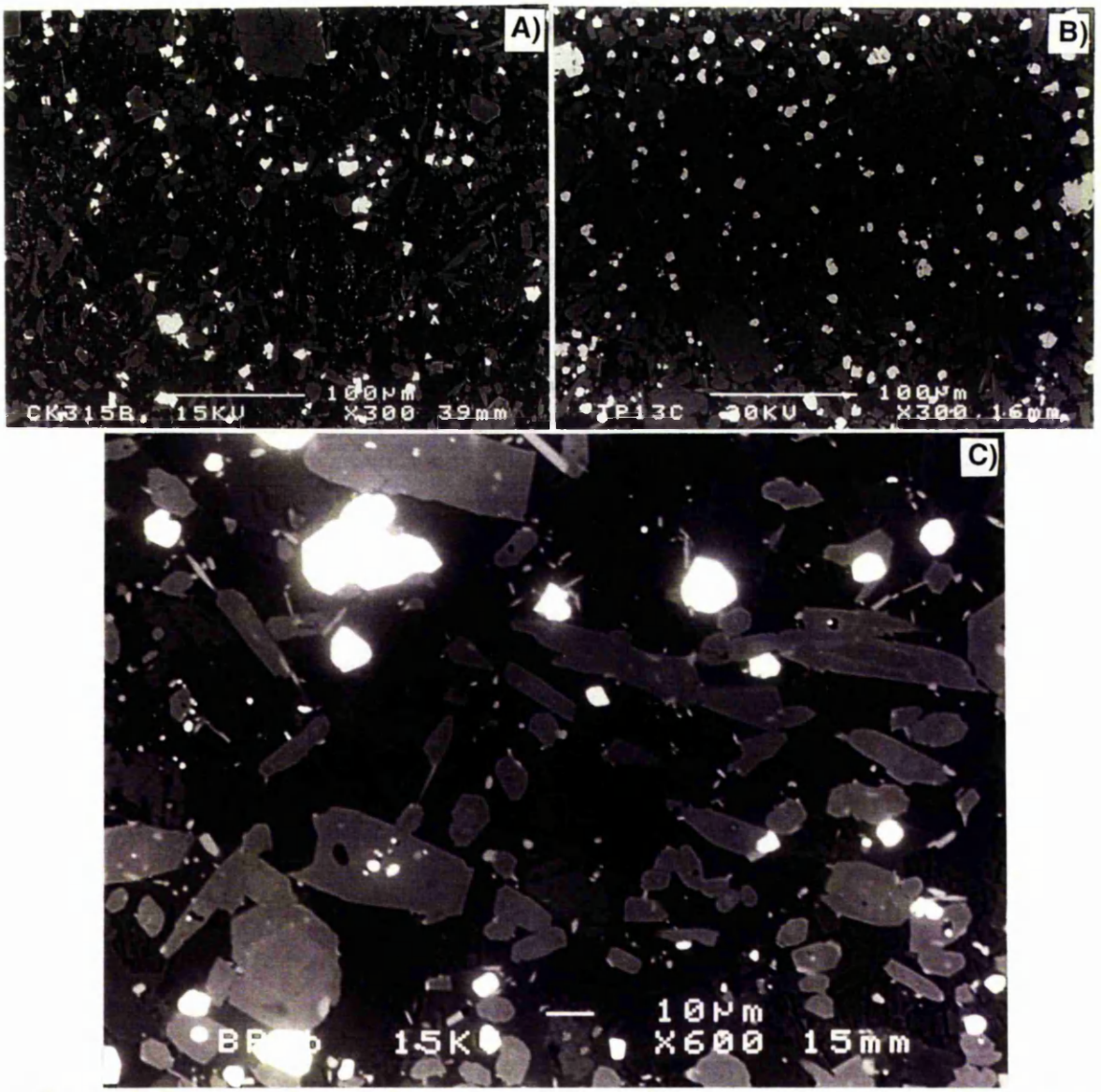

Figure 2.32 Backscattered electron images for groundmass of samples CK3, TP1 and BP9. The images were taken in the areas analyzed by the SEM-EDS. The analysis numbers in the images correspond to the analysis results in Table 2.7. **A)** is for analysis CK315B; Olivine is present as stubby crystals (e.g. at the top centre of the image). Clinopyroxene laths are seen as grey or the same tone of olivine. The brightest granules are ulvöspinel-magnetite. Plagioclase feldspar laths are difficult to see but with careful observation, they exhibit the darkest domains. **B)** is for analysis TP13C; the largest crystals are olivine present (top left and bottom left) while smaller clinopyroxene laths are abundant in the whole area. Ulvö spinel-magnetite granules are very obvious due to their brightness. **C)** is for analysis BP9b, showing obvious grey clinopyroxene laths with zoning, bright ulvöspinel-magnetite and tiny apatite needles. These phases are set in alkali feldspar and glass (dark), which occur between the grains.

Table 2.7 Chemical composition (wt%) for major elements of basalt samples for whole rock analyses by the XRF and groundmass analyses by the SEM-EDS.

No. of rock sample	CK3			BN6			SP1			DC3			KS3			BP9			NY1			PW2			TP1			NB5		
Equipment used	XRF	SEM-EDS	Difference	XRF	SEM-EDS	Difference	XRF	SEM-EDS	Difference	XRF	SEM-EDS	Difference	XRF	SEM-EDS	Difference	XRF	SEM-EDS	Difference	XRF	SEM-EDS	Difference	XRF	SEM-EDS	Difference	XRF	SEM-EDS	Difference	XRF	SEM-EDS	Difference
SiO_2	46.31	48.34	-2.02	45.78	49.39	-3.61	50.94	52.59	-1.66	47.40	49.19	-1.80	48.54	51.68	-3.14	48.40	49.40	-1.00	49.56	53.04	-3.47	44.42	43.07	1.36	44.46	45.97	-1.51	42.57	43.78	-1.21
Al_2O_3	15.43	18.67	-3.24	15.50	19.79	-4.29	16.79	20.29	-3.50	15.67	17.47	-1.80	16.83	20.44	-3.60	14.46	17.54	-3.08	16.39	17.55	-1.16	11.90	14.86	-2.96	13.09	15.88	-2.79	13.37	15.09	-1.72
$Fe_2O_3^*$	12.22	9.36	2.87	11.23	6.39	4.85	9.27	5.85	3.42	10.36	8.18	2.19	10.34	5.98	4.37	9.34	7.28	2.07	11.41	7.94	3.47	14.51	12.79	1.72	12.76	9.44	3.32	14.43	11.94	2.49
MgO	6.48	4.48	2.00	8.87	4.20	4.67	5.08	2.25	2.83	9.60	5.22	4.38	5.99	2.78	3.21	8.32	5.02	3.29	6.12	4.47	1.65	9.12	5.64	3.48	9.50	6.10	3.41	7.48	6.73	0.75
CaO	10.06	7.66	2.40	8.91	8.31	0.60	9.49	7.20	2.29	8.39	9.10	-0.70	9.71	9.36	0.35	8.67	8.23	0.44	8.54	8.14	0.39	10.65	10.06	0.59	9.60	9.61	-0.01	10.79	9.55	1.24
Na_2O	2.41	3.24	-0.83	4.10	6.91	-2.81	2.32	3.73	-1.41	3.94	7.22	-3.28	3.24	4.79	-1.54	4.16	5.93	-1.77	2.97	3.87	-0.91	4.07	6.71	-2.64	3.70	5.35	-1.65	3.99	4.86	-0.87
K_2O	3.05	3.95	-0.90	2.70	2.52	0.18	3.21	4.43	-1.22	1.44	0.39	1.05	1.94	2.27	-0.33	3.79	3.71	0.08	2.18	2.53	-0.35	0.76	1.60	-0.85	2.47	2.47	-0.01	2.16	2.75	-0.59
TiO_2	3.01	2.68	0.34	2.05	1.53	0.53	2.07	2.17	-0.10	2.33	2.53	-0.20	2.10	1.54	0.56	1.80	1.65	0.15	1.97	1.49	0.48	3.27	3.51	-0.24	3.28	3.21	0.08	3.77	3.39	0.38
MnO	0.15	0.17	-0.02	0.15	0.00	0.15	0.11	0.21	-0.10	0.21	0.00	0.21	0.21	0.00	0.21	0.21	0.00	0.21	0.20	0.00	0.20	0.22	0.00	0.22	0.23	0.00	0.23	0.22	0.00	0.22
P_2O_5	0.87	1.46	-0.59	0.71	0.97	-0.26	0.72	1.27	-0.55	0.65	0.70	-0.04	1.08	1.17	-0.09	0.83	1.23	-0.40	0.64	0.96	-0.32	1.08	1.76	-0.69	0.90	1.97	-1.07	1.23	1.92	-0.69
Total	100.00	100.00	0.00	100.00	100.00	0.00	100.00	100.00	0.00	100.00	100.00	0.00	100.00	100.00	0.00	100.00	100.00	0.00	100.00	100.00	0.00	100.00	100.00	0.00	100.00	100.00	0.00	100.00	100.00	0.00
Total before normalizing to 100%	95.63	98.10	-2.47	97.29	100.13	-2.84	93.66	95.01	-1.35	96.26	95.33	0.93	96.98	96.19	0.79	96.37	97.27	-0.90	95.79	96.37	-0.58	95.06	95.71	-0.65	97.52	98.71	-1.19	96.76	97.44	-0.68

*Total Fe as Fe_2O_3; Note: Adjusted to 100%, volatile free for XRF results (due to the results from SEM-EDS containing no volatile).

Weight per cent oxides from both techniques are plotted in variation diagrams (Figure 2.33). The plots indicate that the results for whole-rock analyses (by the XRF) and for groundmass analyses (by the SEM-EDS) are significantly different (see also Table 2.7). In most cases, SiO_2, Al_2O_3, Na_2O, K_2O, and P_2O_5 obtained from the SEM-EDS are greater than those from the XRF. Fe_2O_3 and MgO of all samples obtained from the XRF are greater than those from the SEM-EDS. CaO, TiO_2 and MnO contents of most samples are higher in the results obtained by the XRF. Other graphical comparisons were made to show the differences of results between the two techniques (Figures 2.34).

The higher values of MgO, Fe_2O_3 and MnO in whole-rock analyses (XRF results) indicate that the olivine phenocrysts were analysed. Fe_2O_3 content in whole-rock analyses is probably controlled by the clinopyroxene phenocrysts as well. The higher CaO contents in the whole-rock analyses imply that clinopyroxene phenocrysts or calcite in amygdales were analysed. SiO_2, Al_2O_3, K_2O and Na_2O are the major components of late-stage minerals such as feldspars, feldspathoid in groundmass, and therefore these oxides show higher concentrations in the groundmass analyses than in the whole-rock analyses. TiO_2 is still not clear in this study whether or not the ulvö spinel-magnetite mainly existing in groundmass control the TiO_2 contents obtained by both methods of analysis. The higher TiO_2 contents in most whole-rock analyses may be possibly controlled by the phenocrysts of titanaugite clinopyroxene. P_2O_5 clearly shows higher contents in the groundmass analysis of every case, as it is a major component of apatite found as the tiny needles under a high magnification (i.e. SEM).

Although SEM-EDS is one of the choices for analysing fine-grained rocks like basalt, providing results in a short time, the result is still not representative of the whole-rock composition. XRF still plays a major role in whole-rock analysis.

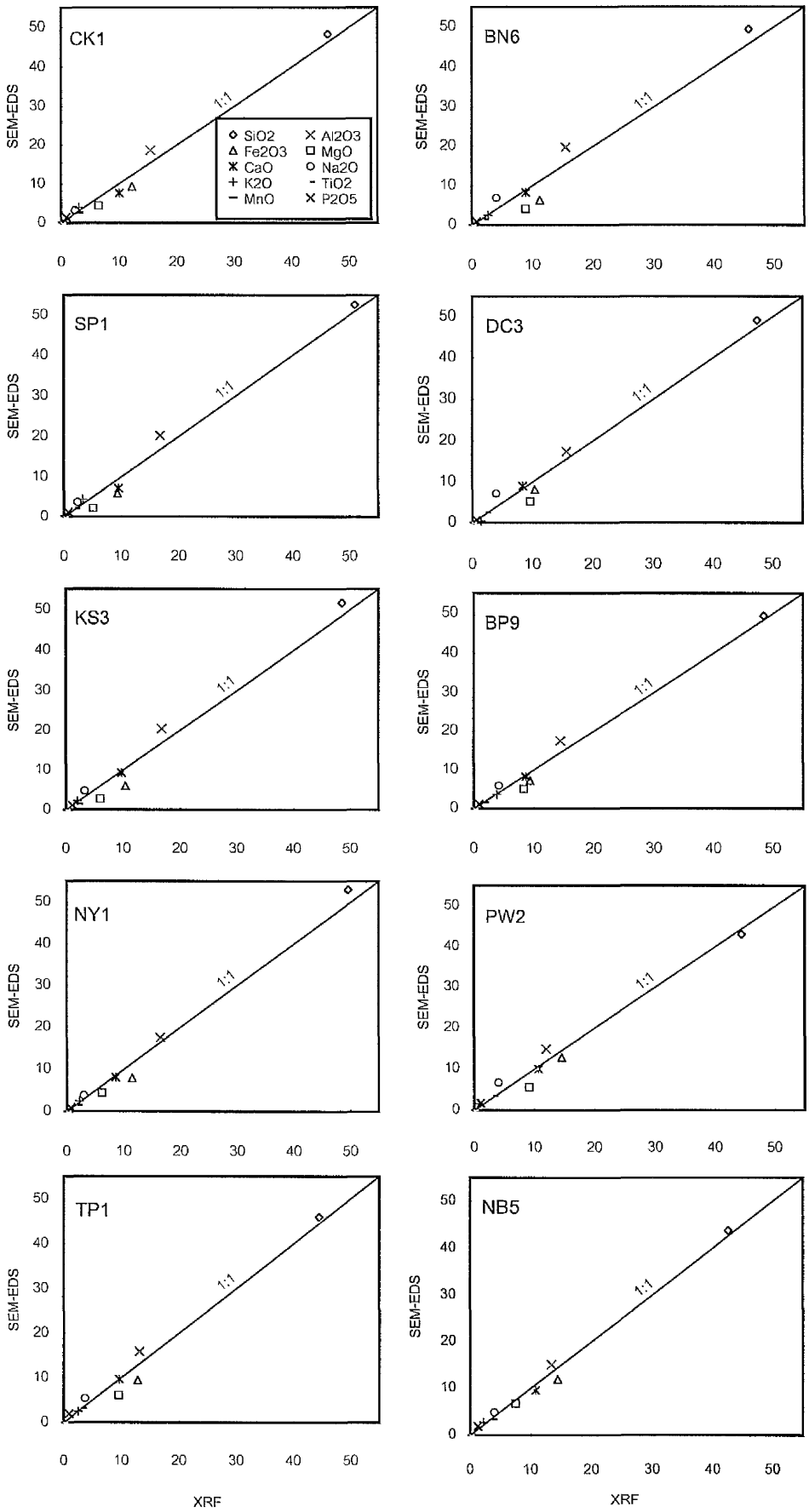

Figure 2.33 Plots of weight per cent of major oxides analysed by XRF against by SEM-EDS for basalt samples from Thailand.

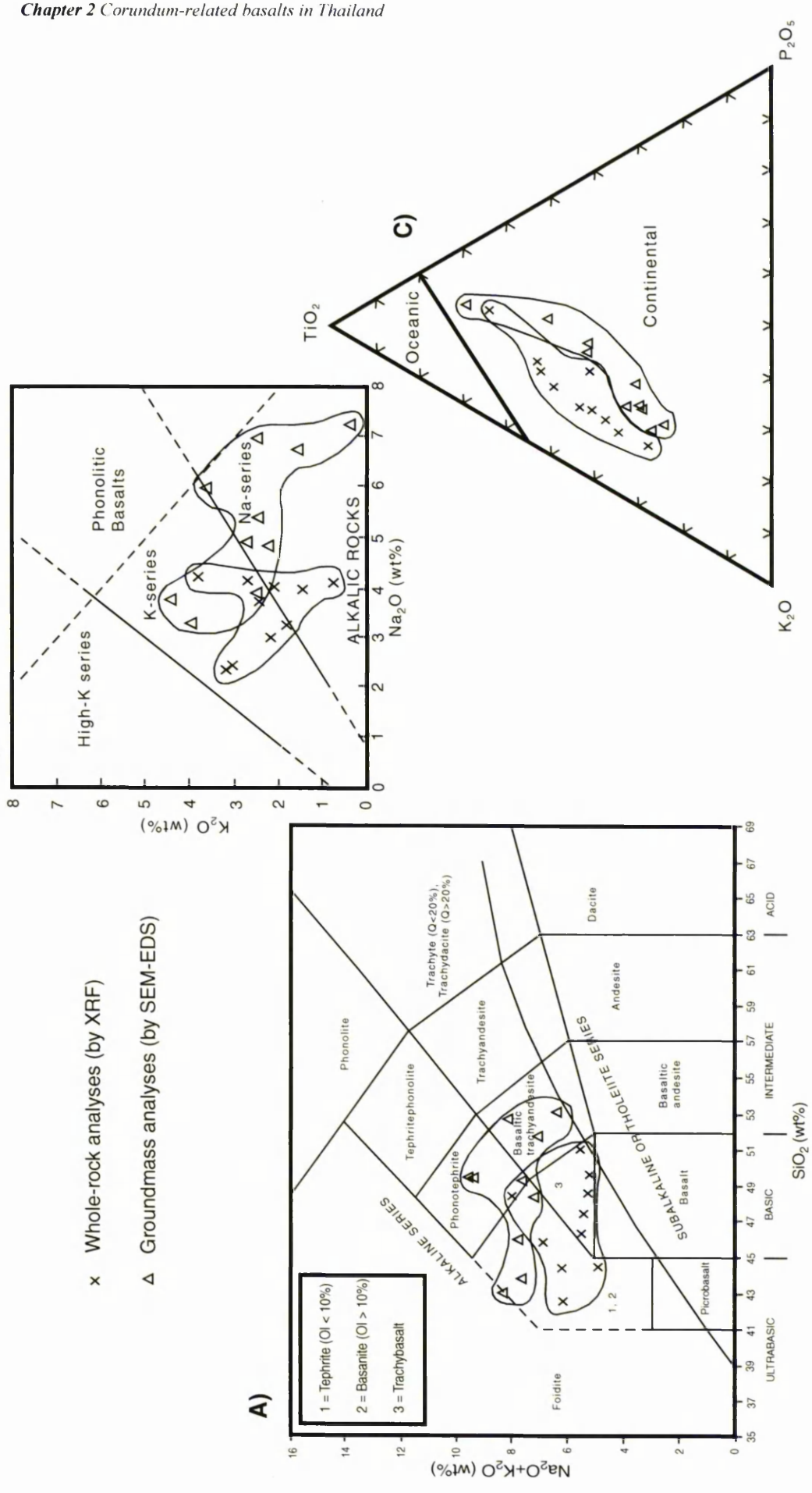

Figure 2.34 Variation diagrams of chemical composition for rock samples, between whole-rock analyses (obtained by XRF) and groundmass analyses (obtained by SEM-EDS); **A)** on the total alkalis-silica diagram (fields after Le Maitre *et al.*, 1989, curve line after Irvine and Baragar, 1971); **B)** on the K_2O (wt%) versus Na_2O (wt%) diagram (fields after Middlemost, 1975); **C)** on the TiO_2- K_2O-P_2O_5 discrimination diagram (fields after Pearce *et al.*, 1975).

Information in this section does not show the clear evidence of contamination of the rock samples by the xenocrysts or xenoliths. If the rock samples were highly contaminated for example by crustal materials, then the SiO_2 contents from the XRF analyses would have been higher than those from the SEM-EDS analyses. The higher percentages of MgO, Fe_2O_3, CaO, TiO_2 and MnO in the whole-rock analyses, compared to the results frrom the groundmass analyses, do not indicate that ultramafic xenocrysts and xenoliths have contaminated the rock samples during sample preparation. This is because the xenocryst- and xenolith- free rocks (SP1, KS3 and NY1) behave in an identical way as the other samples, in terms of the comparison of the chemical compositions obtained by both techniques.

2.7 Summary

Geochemical information obtained in this study implies that the basaltic magmas of the samples were most probably derived from the same reservoir at a depth > 80 km, as the evidence is of the same tectonic environment. However they experienced slight differences in their ascent histories due to inhomogeneous lithosphere, different geographic positions. All magmas were evolved by fractionation from the partial-melted mantle. The MgO graphic plots indicate that olivine plays the dominant role of fractionation. The xenocrysts and xenoliths did not act as major contaminants changing the magma composition because they did not completely melt and mix with the host magmas. Therefore the host magmas still retain the composition of the melts derived from the mantle. In other words, the magmas generally experienced minimal contamination. In exceptional cases, however, for example Bo Phloi, the basalts show a higher degree of crustal contamination, as reflected in the slightly higher K contents but it is not a major effect.

CHAPTER 3
MINERAL CHEMISTRY OF BASALTS AND CERTAIN MINERALS IN GEM GRAVEL DEPOSITS

3.1 Introduction

The purpose of this chapter is two-fold. First, it sets out to reveal the chemical characteristics of primary minerals in the corundum-associated basalts from Thailand. The major primary minerals (crystallized from basalt melt) in basalts of this study are olivine, clinopyroxene, feldspars and ulvöspinel-magnetite. The accessory minerals include apatite, nepheline, leucite and zeolite. Secondly, the chapter aims to compare the compositions of the minerals in xenocrysts and xenoliths in basalts and inclusions in corundum with those of the same mineral species recovered from secondary corundum-bearing deposits. The minerals serving this purpose are clinopyroxene and spinel. The comparisons are being made to investigate whether or not these minerals originated from the same environment.

3.2 Methods and techniques

The representative polished sections prepared for petrography in Chapter 2 were chosen on the basis of least alteration. Rough grains of minerals associated with corundum in the secondary deposits were chosen to be cut and polished. The polished sections were coated with a 20 nm carbon film. Then they were analysed at the Department of Earth Sciences, University of Manchester with a scanning electron microscope equipped with an energy-dispersive spectrometer (SEM-EDS) and a Geoscan electron microprobe fitted with an energy-dispersive spectrometer (Dunham and Wilkinson, 1978).

The SEM-EDS (JEOL JSM 6400) was set to the following conditions for analysis: an accelerating voltage of 15 kV, a probe current of 1.5 nA, a working distance of 39 mm and a beam diameter of ca 1 μm. The Geoscan (Cambridge Instruments GEOSCAN Microprobe) was set to an accelerating voltage of 15 kV, a probe current of 15 nA and a beam diameter of ca 5-10 μm. Both machines are equipped with Link System ZAF-4/FLS software for converting the X-ray spectra obtained from the specimen into chemical analyses. The detection limit is about 0.2 wt% (Clapsopoulos, 1991: 221). The results from these two machines were very similar.

3.3 Primary minerals

3.3.1 Major phases

Olivine

Olivine exists as phenocrysts, microphenocrysts and tiny crystals in the groundmass. Representative analyses are shown in Table 3.1, and all data are given in Appendix 3-1. Minor components (<1 wt%) are MnO, CaO and NiO. Average FeO-content tends to be lower in phenocrysts and higher in groundmass, while in turn, the average MgO-content behaves in the opposite of the average FeO content. Forsterite (Fo%) contents (atomic proportions: $Mgx100/(Mg+Fe^{2+})$) vary from $Fo_{49.2}$ in olivine of groundmass from the Nam Yun basalt to $Fo_{89.9}$ in olivine phenocrysts from the Den Chai and Phloi Waen basalts. The forsterite content, Fo% has been used as the differentiation index to assess the variation of minor elements when the magma becomes more evolved (Kerr, 1998). This indicates that magma of the Nam Yun basalt is most evolved, due to the lowest value Fo contents (49.2 - 71.1%). The weight % of MnO and CaO are plotted against Fo% in Figures 3.1 and 3.2 and these two oxides are enriched in groundmasses with respect to phenocrysts.

MnO contents in olivines from most localities show a vague negative correlation with Fo content except in Sop Prap and Phloi Waen. Simkin and Smith (1970) suggested that the distribution of Mn in olivine was dependent upon the bulk composition of magma, and whether or not Fe-Ti oxide was a co-precipitating phase. Olivine from Bo Phloi shows the highest manganese contents (ca 0.4 – 1.0 wt% of MnO) which are correlated with a high degree of undersaturation, indicated by the basalt from Bo Phloi containing normative nepheline (up to 14.81 %, in sample BP5). This evidence agrees with Brown, 1982, but no explanation for the correlation was given.

The variation patterns of CaO against Fo% are very similar to those of MnO and Fo%. Jurewicz and Watson (1988) proposed that the Ca content of olivine depends on the CaO and FeO contents of the melt. In other words, high FeO in the melt gives rise to high CaO in olivine.

In many cases the phenocrysts have a more primitive composition than groundmass olivine. In other cases, e.g. SP, DC, PW, CK the two variations have similar compositions. This may reflect difficulties in distinguishing the two texturally. However, high scatter plots, for example, KS, and to a lesser extend PW suggest that a single generation of olivine is present.

Table 3.1 Representative olivine compositions for basalt samples from different localities in Thailand.

Locality	CHIANG KHONG		BAN NONG, NAM CHO			SOP PRAP		DEN CHAI			KHOK SAMRAN		BO PHLOI		NAM YUN		PHLOI WAEN		TOK PHROM		NONG BON		
Occurrence	Phenocryst	Groundmass	Phenocryst	Micro-phenocryst	Groundmass	Phenocryst	Groundmass	Phenocryst	Micro-phenocryst	Groundmass	Phenocryst	Groundmass	Phenocryst	Groundmass	Phenocryst	Groundmass	Phenocryst	Micro-phenocryst	Phenocryst	Groundmass	Phenocryst	Micro-phenocryst	Groundmass
Analysis No	CK14-OL2	CK13-OL6	BN134-O15	BN326-OL4	BN133-OL9	SP155-OL37	SP155-OL61	DC162-OL5	DC161-OL15	DC157-OL5	KS211-OL11	KS214-OL4	BP924-OL1	BP82-OL7	NY131-OL2	NY131-L10	PW321-OL1	PW14-OL7	TP1319-OL2	TP1317-OL5	NB51OP-L1/1	NB51OM-L1	NB5238A-L12
SiO_2	40.00	38.76	38.61	39.90	37.69	39.89	39.64	40.24	38.83	38.83	37.88	39.72	38.13	37.83	37.52	36.12	39.79	39.73	38.93	38.02	39.45	39.97	39.39
TiO_2																							
Al_2O_3					0.26														0.44				
FeO	15.97	22.51	22.41	16.63	25.30	16.02	16.81	14.33	21.82	22.37	26.83	17.91	25.46	26.15	28.60	34.21	15.98	16.26	18.63	24.44	17.84	16.89	16.68
MnO	0.21	0.50	0.43	0.28	0.62	0.24	0.24	0.19	0.48	0.30	0.27	0.37	0.78	0.99	0.32	0.41	0.23		0.25	0.62		0.19	0.35
MgO	43.60	37.91	38.22	43.02	35.30	43.60	42.74	45.08	38.54	38.12	34.75	41.78	35.38	34.74	33.35	28.74	43.77	43.53	40.95	36.49	42.20	42.73	43.18
CaO	0.31	0.38	0.30	0.20	0.30	0.26	0.28	0.25	0.40	0.41	0.31	0.19	0.35	0.34	0.29	0.42	0.24	0.18	0.19	0.43	0.18	0.24	0.20
Na_2O					0.36		0.32												0.32				
NiO																		0.32					
Cr_2O_3																							
Total	100.10	100.06	99.97	100.02	100.02	100.01	100.02	100.09	100.07	100.03	100.04	99.97	100.09	100.04	100.09	99.91	100.01	100.02	99.99	100.00	99.66	100.01	100.07
Numbers of atoms on the basis of 4 O																							
Si	1.007	1.009	1.005	1.008	0.997	1.006	1.004	1.005	1.007	1.009	1.01	1.011	1.008	1.005	1.005	1.000	1.003	1.003	0.994	1.001	1.006	1.011	0.996
Ti	0	0	0	0	0	0	0	0	0	0	0	0	0	0	0	0	0	0	0	0	0	0	0
Al	0	0	0	0	0.008	0	0	0	0	0	0	0	0	0	0	0	0	0	0.013	0	0	0	0
Fe^{2+}	0.336	0.490	0.488	0.351	0.560	0.338	0.356	0.299	0.473	0.486	0.60	0.381	0.563	0.581	0.641	0.792	0.337	0.343	0.398	0.538	0.380	0.357	0.353
Mn	0.004	0.011	0.010	0.006	0.014	0.005	0.005	0.004	0.011	0.007	0.01	0.008	0.017	0.022	0.007	0.010	0.005	0	0.005	0.014	0	0.004	0.008
Mg	1.637	1.471	1.484	1.621	1.392	1.639	1.614	1.679	1.490	1.477	1.38	1.585	1.394	1.376	1.332	1.186	1.645	1.639	1.559	1.433	1.604	1.611	1.628
Ca	0.008	0.011	0.008	0.005	0.009	0.007	0.008	0.007	0.011	0.011	0.01	0.005	0.010	0.010	0.008	0.013	0.006	0.005	0.005	0.012	0.005	0.006	0.005
Na	0	0	0	0	0.019	0	0.016	0	0	0	0	0	0	0	0	0	0	0	0.016	0	0	0	0
Ni	0	0	0	0	0	0	0	0	0	0	0	0	0	0	0	0	0	0.007	0	0	0	0	0
Cr	0	0	0	0	0	0	0	0	0	0	0	0	0	0	0	0	0	0	0	0	0	0	0
Total	2.993	2.991	2.995	2.992	3.002	2.994	3.003	2.995	2.993	2.991	2.99	2.989	2.992	2.995	2.995	3.000	2.997	2.997	2.997	2.999	2.994	2.989	2.995
Fo%	83.0	75.0	75.3	82.2	71.3	82.9	81.9	84.9	75.9	75.2	69.8	80.6	71.2	70.3	67.5	60.0	83.0	82.7	79.7	72.7	80.8	81.9	82.2

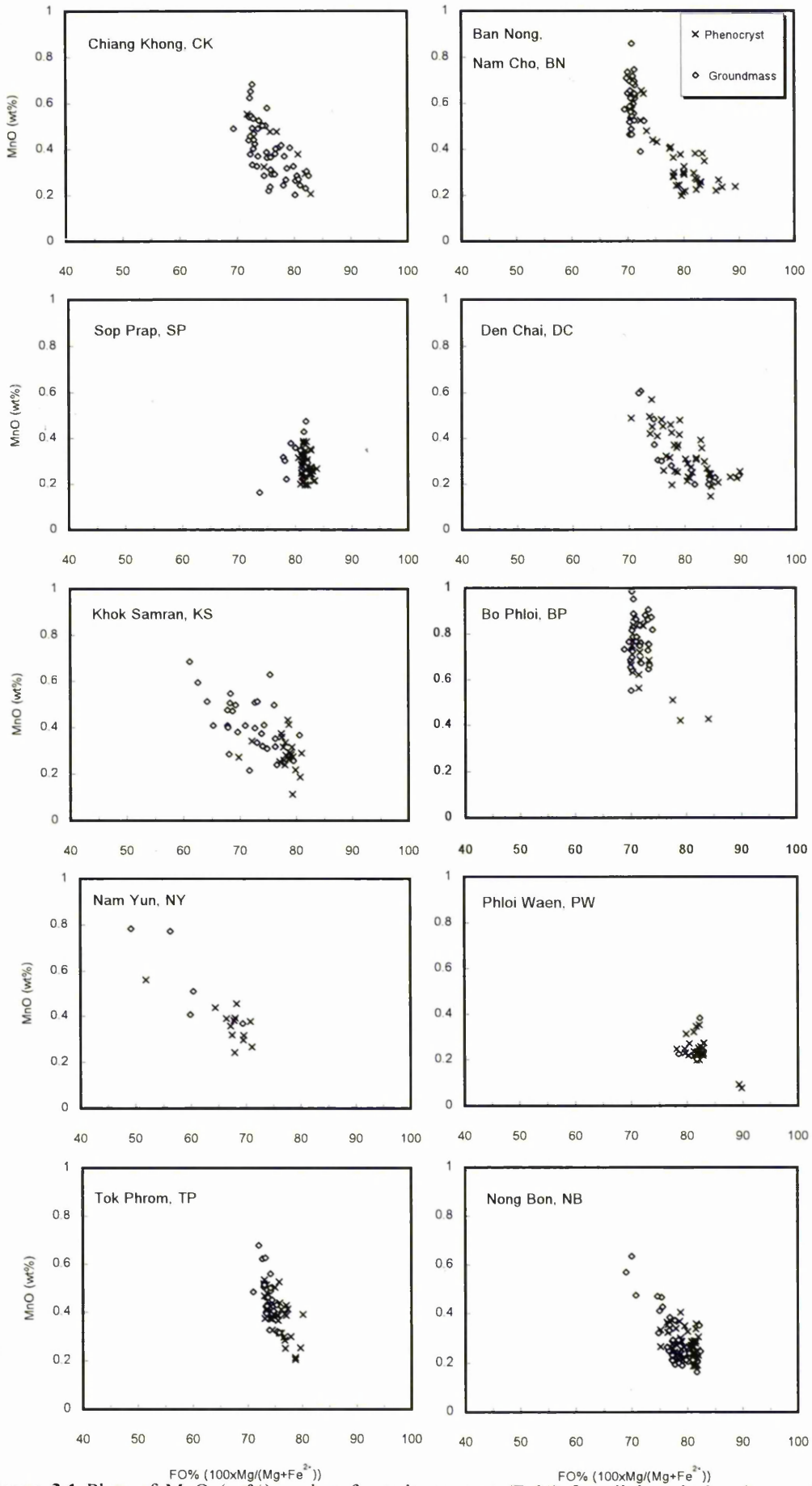

Figure 3.1 Plots of MnO (wt%) against forsterite content (Fo%) for olivines in basalt samples from different localities in Thailand.

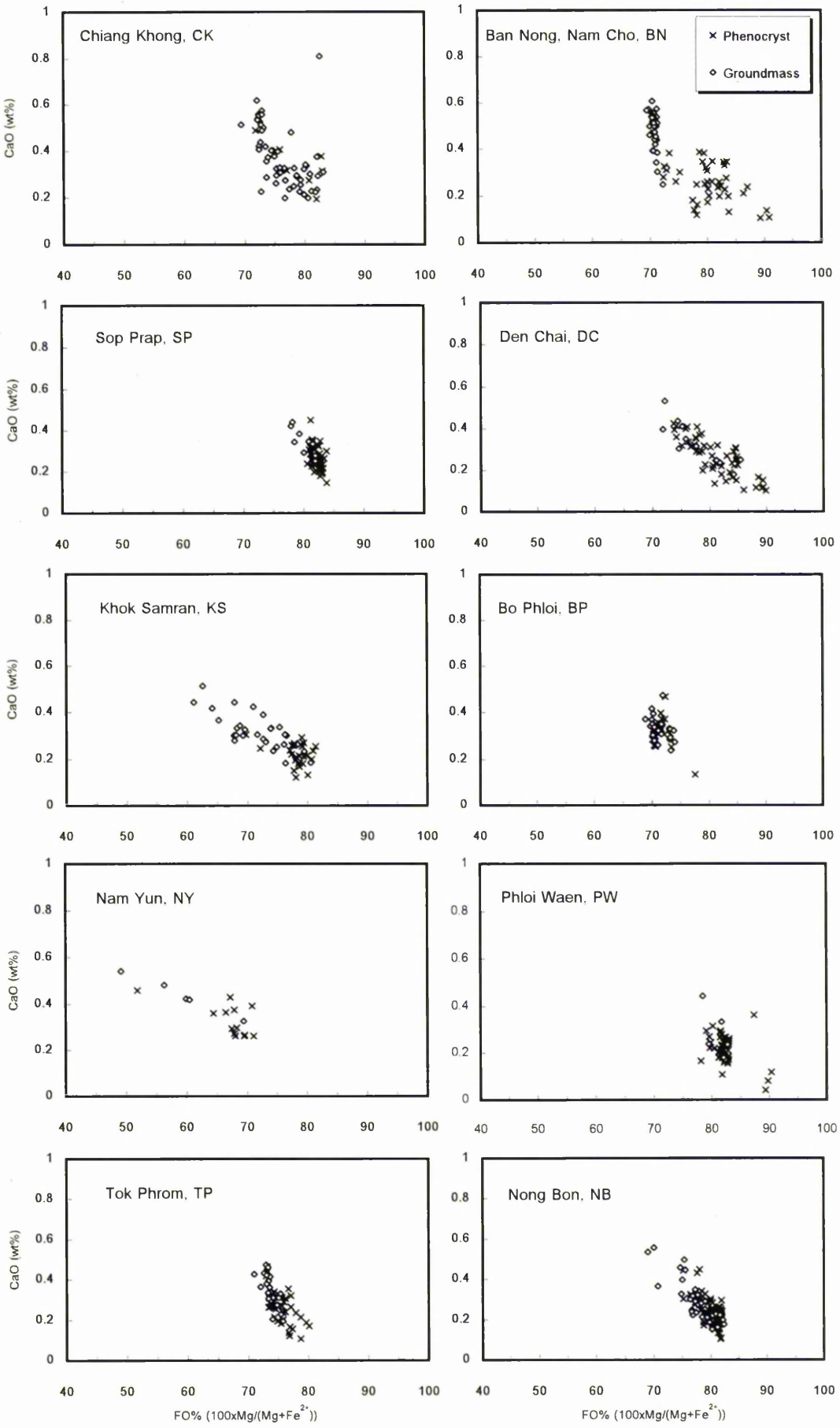

Figure 3.2 Plots of CaO (wt%) against forsterite content (Fo%) for olivines in basalt samples from different localities in Thailand.

Clinopyroxene

Clinopyroxene occurs as phenocrysts, microphenocrysts, tiny laths and oikocrysts with ophimottled texture in groundmass (MacKenzie *et al.*, 1997). Representative compositions are given in Table 3.2, and all data are given in Appendix 3-2. Major compositions in atomic per cent are plotted in the quadrilateral diagram (Morimoto, 1988), (Figure 3.3). Most analyses fall in the area of $Wo_{45-55}En_{30-45}Fs_{10-20}$ which belongs to the titanaugite field, according to Deer *et al.* (1997: 16). Exceptions are the compositions in the cores of clinopyroxene phenocrysts from Phloi Waen, which have lower Fs (<5% - 12%) contents. In most cases, phenocryst and groundmass clinopyroxenes have similar composition.

The ophimottled pyroxene in the groundmass from Khok Samran was analysed and found to contain significantly higher TiO_2, Al_2O_3, Fe_2O_3 contents and significantly lower SiO_2 and MgO contents than clinopyroxene laths in the groundmass (Table 3.2). This indicates that the ophimottled clinopyroxene crystallized from a more evolved magma than the laths. The compositions of clinopyroxene cores and rims at certain localities were analysed and it was found that the rims show slightly higher Ca contents especially in the samples from Nam Yun and Phloi Waen. Ti contents in the rim are higher than in the core but SiO_2 in the rim is less than the core. TiO_2 and Al_2O_3 are higher in groundmass clinopyroxenes than in clinopyroxene phenocrysts.

One of the coupled substitutions of cations in octahedral and tetrahedral sites can be expressed as $(Mg, Fe)^{VI} + 2Si^{IV} \rightarrow Ti^{VI} + 2Al^{IV}$ (Kerr, 1998). This is confirmed by the plot in Figure 3.4. Ti and Al behave in a similar way as differentiation increases (lower Mg, Fe). The plot suggests that this substitution is strongly related to major element fractionation. The relative crystallization temperature of clinopyroxene from the melt at every locality of this study is shown in Figure 3.5 (Kerr, 1998).

Table 3.2 Representative clinopyroxene compositions for basalt samples from different localities in Thailand. (Note: ΣFe = Fe^{2+}+Fe^{3+}+Mn; mg*=100xMg/(Mg+Fe^{2+}+Fe^{3+}+Mn).

Locality	CHIANG KHONG			BAN NONG, NAM CHO			SOP PRAP	DEN CHAI		KHOK SAMRAN		BO PHLOI		NAM YUN			PHLOI WAEN		TOK PHROM				NONG BON			
Occurrencec	Phenocryst	Microphenocryst	Groundmass	Phenocryst (Core)	Phenocryst (Rim)	Groundmass	Groundmass	Microphenocryst	Groundmass	Groundmass	Ophimottled texture in groundmass	Phenocryst	Groundmass	Phenocryst (core)	Microphenocryst	Microphenocryst (Rim)	Phenocryst (Core)	Phenocryst (Rim)	Phenocryst	Phenocryst (Spongy core)	Phenocryst (Clean rim)	Groundmass	Phenocryst (Core)	Phenocryst (Rim)	Microphenocryst	Groundmass
Analysis No	CK18-CPX2	CK13-CPX2	CK315B-CPX1	BN446-CPX5	BN446-CPX5	BN447-CPX1	SP1A-CPX2	DC264-CPX5	DC160-CPX1	KS1X-CPX4	KS211-CPX8	BP734-CPX2	BP82A-CPX9	NY132-CPX13	NY131-CPX6	NY132-CPX6	PW15-CPX3	PW15-CPX2	TP1320-CPX5	TP1330-CPX14	TP1330-CPX17	TP324a-CPX2	NB132-CPX9	NB132-CPX11	NB131-CPX7	NB5238A-CPX25
SiO_2	43.79	46.90	46.45	49.76	45.81	44.23	43.87	45.96	44.05	49.83	47.52	53.18	50.35	49.58	51.00	49.10	51.29	48.53	45.64	51.05	46.31	46.23	51.83	49.34	50.80	48.44
TiO_2	4.30	2.74	3.57	0.92	2.99	3.49	4.59	2.85	4.10	1.62	2.90	0.53	1.82	2.01	1.42	2.56	0.76	2.39	3.84	1.31	3.36	3.68	0.68	2.24	1.63	2.69
Al_2O_3	9.03	8.36	6.08	4.91	7.53	8.64	8.36	8.11	8.45	2.73	4.56	0.77	3.67	3.78	2.50	3.39	5.45	5.11	7.14	7.60	6.55	6.84	4.30	4.14	3.14	4.14
Fe_2O_3	3.19	2.56	2.91	2.29	2.22	4.85	3.55	2.70	4.88	2.38	4.23	2.17	2.32	1.90	2.27	2.74	0.39	2.78	3.46	0.00	3.78	1.80	1.45	2.43	1.73	3.23
FeO	5.09	4.45	5.23	8.77	5.95	3.42	4.09	4.31	4.18	5.97	5.36	5.81	4.91	6.38	6.55	8.06	6.46	4.18	3.87	4.52	3.56	6.26	3.96	4.18	5.68	3.77
MnO	0.25	0.19	0.20	0.38	0	0	0	0	0	0.225	0.299	0.47	0	0	0	0.22	0	0	0	0	0	0	0	0	0	0.20
MgO	10.87	12.71	12.60	12.13	11.39	11.68	11.49	12.19	11.39	13.52	12.68	14.35	13.75	13.42	14.06	11.99	12.85	13.09	11.83	13.74	12.43	11.54	14.87	13.25	13.04	13.45
CaO	22.64	20.78	21.78	19.98	22.13	22.37	21.74	22.79	22.59	21.67	21.63	21.61	21.91	22.17	21.50	20.83	21.53	23.18	23.13	19.75	22.68	22.36	22.08	23.61	22.77	23.03
Na_2O	0.54	0.92	0.64	0.86	0.80	0.80	0.90	0.49	0.64	0.79	0.75	0.97	1.04	0.52	0.67	1.01	1.09	0.64	0.68	1.35	0.78	0.87	0.83	0.64	0.89	0.77
Cr_2O_3	0	0	0	0	0	0.27	0.22	0.70	0	0	0	0	0	0.30	0	0	0	0	0	0.95	0.49	0	0	0	0	0
Total	99.70	99.99	99.45	99.99	99.26	100.00	98.81	100.10	100.26	99.06	99.92	99.87	100.01	100.06	99.97	99.89	99.83	99.90	99.89	100.28	99.93	100.04	100.00	99.81	99.69	100.03
Numbers of atoms on the basis of 6 O																										
Si	1.652	1.738	1.747	1.865	1.725	1.655	1.662	1.712	1.652	1.873	1.785	1.973	1.863	1.848	1.898	1.850	1.894	1.805	1.710	1.860	1.729	1.730	1.898	1.836	1.893	1.801
Ti	0.122	0.076	0.101	0.026	0.085	0.098	0.131	0.080	0.116	0.046	0.082	0.015	0.051	0.056	0.040	0.072	0.021	0.067	0.108	0.036	0.094	0.104	0.019	0.063	0.046	0.075
Al	0.402	0.365	0.269	0.217	0.334	0.381	0.373	0.356	0.374	0.121	0.202	0.033	0.160	0.166	0.109	0.150	0.237	0.224	0.315	0.326	0.288	0.302	0.185	0.182	0.138	0.181
Fe^{3+}	0.090	0.071	0.082	0.065	0.063	0.136	0.101	0.076	0.138	0.067	0.119	0.061	0.064	0.053	0.064	0.078	0.011	0.078	0.098	0	0.106	0.051	0.040	0.068	0.048	0.090
Fe^{2+}	0.161	0.138	0.164	0.275	0.187	0.107	0.130	0.134	0.131	0.188	0.168	0.180	0.152	0.199	0.204	0.254	0.199	0.130	0.121	0.138	0.111	0.196	0.121	0.130	0.177	0.117
Mn	0.008	0.006	0.006	0.012	0	0	0	0	0	0.007	0.010	0.015	0	0	0	0.007	0	0	0	0	0	0	0	0	0	0.006
Mg	0.611	0.702	0.706	0.677	0.640	0.651	0.649	0.677	0.637	0.758	0.710	0.794	0.759	0.746	0.780	0.674	0.707	0.726	0.661	0.746	0.692	0.644	0.812	0.735	0.725	0.746
Ca	0.915	0.825	0.877	0.802	0.893	0.897	0.882	0.910	0.907	0.873	0.870	0.859	0.869	0.885	0.857	0.841	0.852	0.924	0.928	0.771	0.908	0.896	0.866	0.941	0.909	0.917
Na	0.039	0.066	0.047	0.062	0.059	0.058	0.066	0.036	0.046	0.058	0.054	0.070	0.075	0.037	0.048	0.073	0.078	0.046	0.049	0.095	0.056	0.063	0.059	0.046	0.064	0.055
Cr	0	0	0	0	0	0.008	0.007	0.021	0	0	0	0	0	0.009	0	0	0	0	0	0.027	0.014	0	0	0	0	0
Total	4.000	4.000	4.000	4.000	4.000	4.000	4.000	4.000	4.000	4.000	4.000	4.000	4.000	4.000	4.000	4.000	4.000	4.000	4.000	4.000	4.000	4.000	4.000	4.000	4.000	4.000
Ca%(Wo%)	51.2	47.4	47.8	43.8	50.1	50.1	50.1	50.6	50.1	46.1	46.4	45.0	47.1	47.0	45.0	45.4	48.1	49.7	51.3	46.6	49.9	50.2	47.1	50.2	48.9	48.9
Mg%(En%)	34.2	40.3	38.5	37.0	35.9	36.4	36.8	37.7	35.1	40.0	37.8	41.6	41.1	39.6	41.0	36.3	40.0	39.1	36.6	45.1	38.1	36.0	44.1	39.2	39.0	39.7
ΣFe%(Fs%)	14.5	12.3	13.8	19.2	14.0	13.6	13.1	11.7	14.8	13.8	15.8	13.4	11.7	13.4	14.0	18.3	11.9	11.2	12.1	8.3	12.0	13.8	8.8	10.6	12.1	11.4
mg*	70.2	76.6	73.6	65.8	71.9	72.8	73.8	76.3	70.3	74.3	70.5	75.6	77.8	74.7	74.5	66.5	77.1	77.7	75.1	84.4	76.1	72.3	83.4	78.8	76.3	77.7

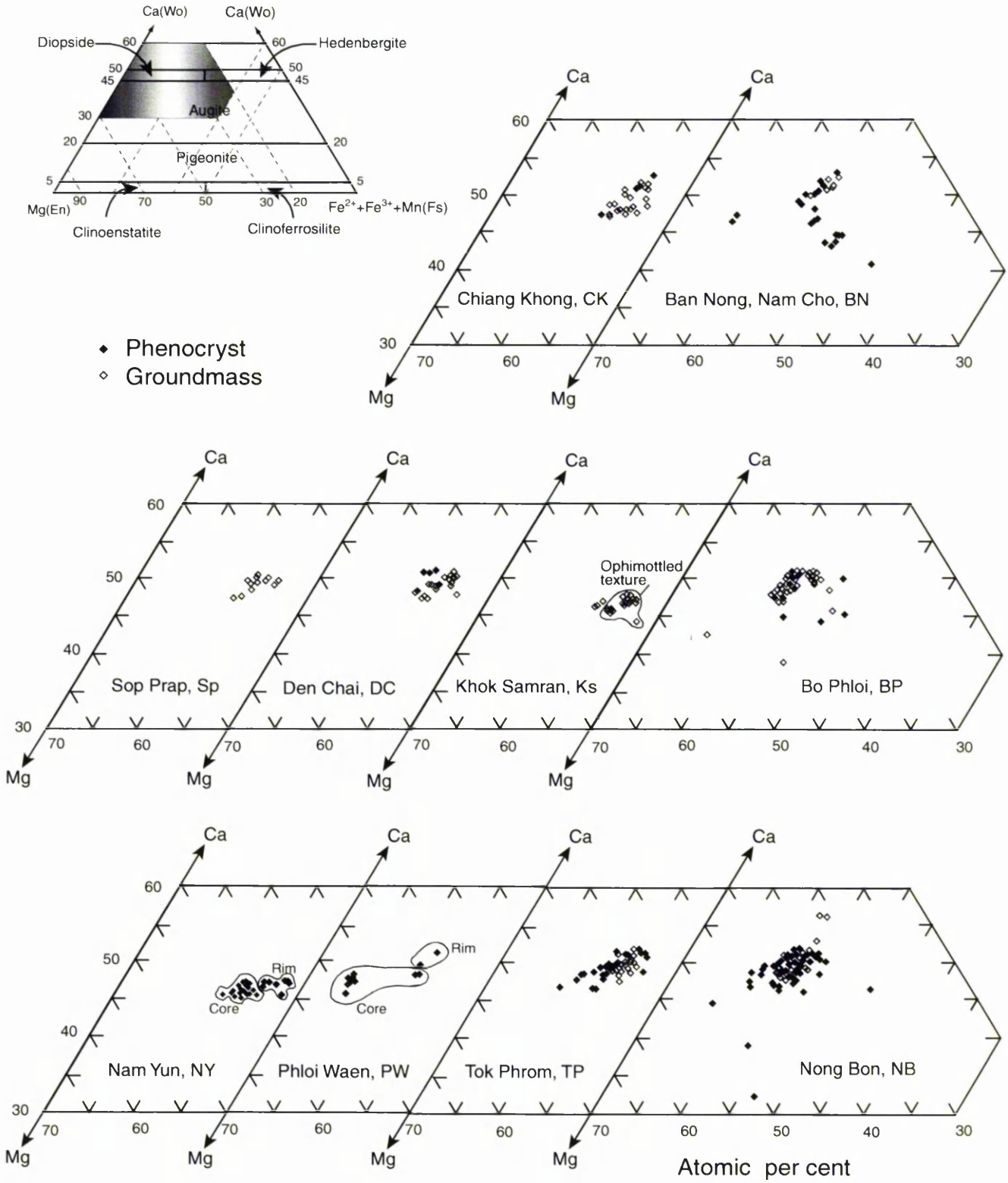

Figure 3.3 Clinopyroxenes in basalts from Thailand plotted in the Ca-Mg-Fe^{2+}+Fe^{3+}+Mn quadrilateral diagram (Wo-En-Fs). The fields (inset) are from Morimoto *et al.*, 1988.

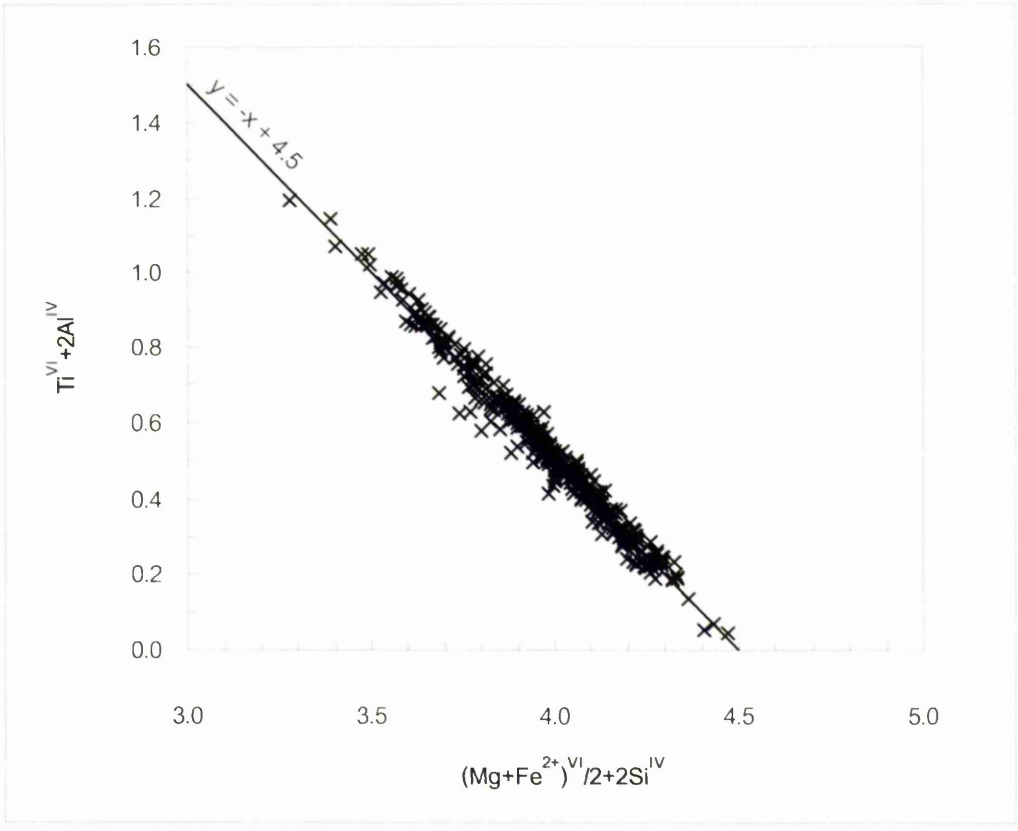

Figure 3.4 Plot of $Ti^{VI}+2Al^{IV}$ against $(Mg+Fe^{2+})^{VI}/2+2Si^{IV}$ for clinopyroxene in alkali basalts from Thailand. The strong negative correlation indicates coupled substitution. Note, the division factor (2) of $Mg+Fe^{2+}$ is for compensation of charge balance.

Feldspars

Feldspar in this study includes plagioclase feldspar and alkali feldspar. Representative compositions of feldspars are shown in Table 3.3 and the range of An-Ab-Or content for each locality is given in Table 3.6. All data are presented in Appendix 3-3. Most plagioclase feldspars exist as tiny laths in groundmass and classified as labradorite (Figure 3.6). Feldspars in basalts from Bo Phloi, Nam Yun and Tok Phrom vary from labradorite to alkali feldspar (sanidine composition). The basalt from Phloi Waen contains alkali feldspar (sanidine composition) in the groundmass. Plagioclase phenocrysts exist in basalt from Khok Samran and Bo Phloi. The basalt from Tok Phrom also has plagioclase in the form of a poikilitic texture in the groundmass in which plagioclase encloses clinopyroxene. Alkali feldspar exists interstitially in the groundmass of the samples from Bo Phloi, Phloi Waen and Tok Phrom.

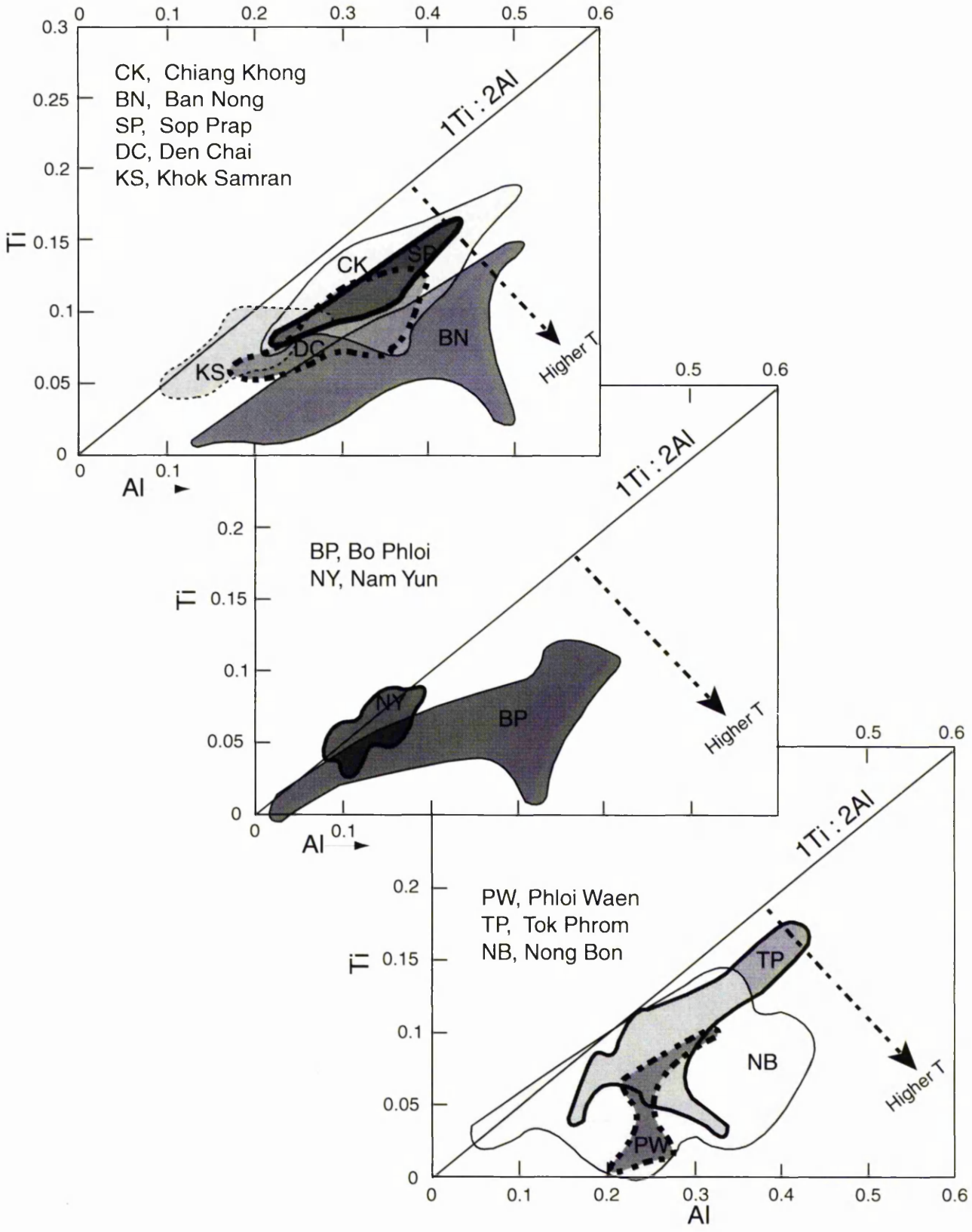

Figure 3.5 Atomic plots of Ti against Al (on the basis of 6 O) of clinopyroxenes in basalts from different localities in Thailand, showing the relative temperature conditions of crystallization. The pyroxenes from the lower temperature evolved magma generally plot close to the line Ti : 2Al than those from higher temperature melts (Kerr, 1998).

Table 3.3 Representative feldspar compositions for basalt samples from different localities in Thailand.

Locality	CHIANG KHONG	BAN NONG, NAM CHO	SOP PRAP	DEN CHAI	KHOK SAMRAN		BO PHLOI		NAM YUN	PHLOI WAEN	TOK PHROM	
Occurrence	Groundmass	Groundmass	Groundmass	Groundmass	Phenocryst	Groundmass	Phenocryst	Interstice in groundmass	Groundmass	Interstice in groundmass	Interstice in groundmass	Poikilitic texture in groundmass
Analysis No	CK315A-PL6	BN6-PL5	SP155-PL6	DC264-PL8	KS110-P23	KS110-P32	BP81-PL1	BP734-AF5	NY131-PL3	PW318-AF2	TP324b-AF1	TP324b-PL3
SiO_2	52.96	53.79	53.61	52.96	54.30	52.59	52.73	65.00	54.46	65.92	65.38	55.66
TiO_2	0.32	0	0.28	0	0	0	0	0	0	0	0.36	0.31
Al_2O_3	29.10	29.06	28.08	29.09	28.43	29.36	29.49	19.36	28.58	18.22	19.47	27.12
$Fe_2O_3^*$	0.90	0.56	0.83	0.82	0.44	0.81	0.59	0.45	0.66	0.33	0.76	0.77
MgO	0.29	0	0	0	0	0	0	0	0	0	0.22	0.38
CaO	12.10	12.14	11.33	12.21	11.28	12.87	12.64	1.05	11.52	0	0.93	9.09
Na_2O	4.10	4.45	4.56	4.25	4.89	4.03	4.33	5.94	4.76	3.33	5.89	5.87
K_2O	0.71	0.29	0.69	0.43	0.42	0.31	0.30	7.28	0.44	12.22	7.24	0.46
BaO	0	0	0	0.28	0	0	0	0.31	0	0	0	0
Total	100.66	100.29	99.38	100.04	99.77	99.97	100.08	99.39	100.42	100.02	100.25	99.66
Numbers of ions on the basis of 32 O												
Si	9.570	9.720	9.791	9.637	9.847	9.568	9.577	11.794	9.823	12.023	11.708	10.069
Ti	0.044	0	0.038	0	0	0	0	0	0	0	0.048	0.043
Al	6.197	6.189	6.044	6.239	6.077	6.294	6.313	4.139	6.074	3.917	4.108	5.782
Fe^{3+}	0.122	0.076	0.114	0.112	0.060	0.111	0.080	0.061	0.090	0.046	0.102	0.105
Mg	0.077	0	0	0	0	0	0	0	0	0	0.059	0.102
Ca	2.342	2.351	2.217	2.380	2.192	2.509	2.460	0.204	2.225	0	0.179	1.762
Na	1.436	1.557	1.616	1.500	1.720	1.423	1.523	2.088	1.663	1.176	2.044	2.059
K	0.163	0.067	0.160	0.100	0.096	0.073	0.070	1.684	0.102	2.843	1.654	0.105
Ba	0	0	0	0.020	0	0	0	0.022	0	0	0	0
Total	19.981	19.960	19.980	19.988	19.992	19.977	20.024	19.992	19.978	20.005	19.936	20.027
An	59.4	59.1	55.5	59.8	54.7	62.7	60.7	5.1	55.8	0.0	4.6	44.9
Ab	36.4	39.2	40.5	37.7	42.9	35.5	37.6	52.5	41.7	29.3	52.7	52.4
Or	4.1	1.7	4.0	2.5	2.4	1.8	1.7	42.4	2.6	70.7	42.7	2.7

* Total Fe as Fe_2O_3

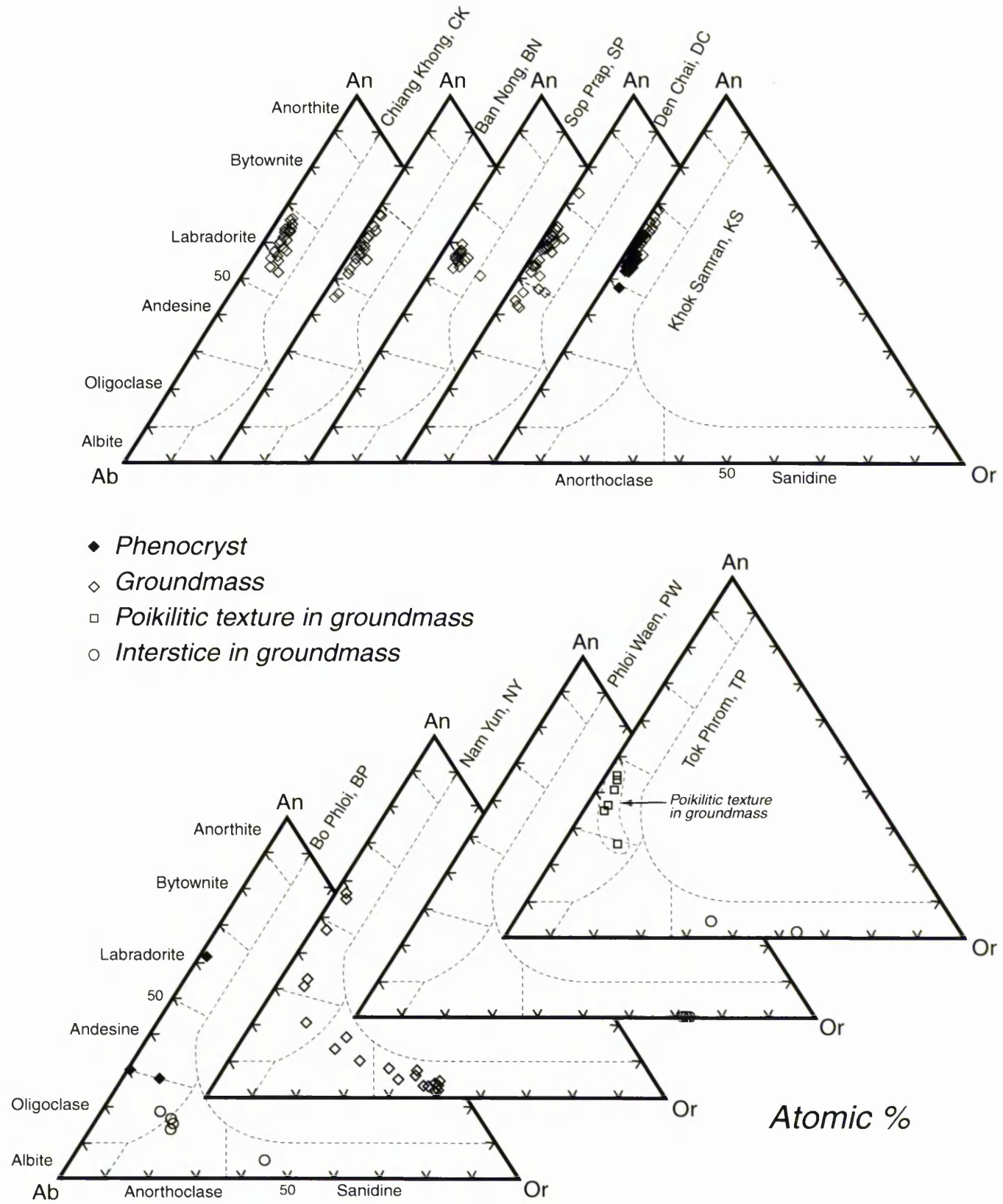

Figure 3.6 Plots of feldspars in alkali basalts from Thailand.

Ulvöspinel-Magnetite

Ulvöspinel-magnetite solid solution occurs as tiny granules in the groundmass of all basalt samples. It is opaque under the optical microscope. Representative compositions of this mineral are given in Table 3.4, and all data are presented in Appendix 3-4. The plots of mole % for TiO_2-FeO-Fe_2O_3 are shown in Figure 3.7

Table 3.4 Representative compositions of ulvöspinel-magnetite in groundmass of basalt samples from different localities in Thailand.

Locality	CHIANG KHONG	BAN NONG, NAM CHO	SOP PRAP	DEN CHAI	KHOK SAMRAN	BO PHLOI	NAM YUN	PHLOI WAEN	TOK PHROM	NONG BON
Analysis No	CK519B -MT7	BN6-MT1	SP1B-MT10	DC264-MT6	KS211-MT8	BP81-MT3	NY132-MT5	PW2-MT3	TP324a -MT1	NB132-MT1
SiO_2	0.31	0.48	0.20	0.41	0.33	0.18	0.23	0.28	0.23	5.30
TiO_2	23.77	21.57	21.82	19.04	27.13	20.62	28.52	0.75	23.08	19.79
Al_2O_3	3.85	3.02	4.27	5.10	1.68	1.84	1.34	0.52	2.72	2.57
Fe_2O_3	19.14	25.00	21.71	22.78	15.48	28.54	12.92	64.05	24.26	16.73
FeO	45.59	46.41	42.71	42.01	52.34	43.98	54.50	25.55	45.07	45.46
MnO	0.63	0.61	0.59	0.71	0.61	0.79	0.65	0.53	0.53	0.70
MgO	3.25	2.45	3.78	4.88	2.68	3.78	1.94	2.83	3.82	4.36
CaO	0.48	0	0.22	0.06	0	0.12	0	0.17	0.18	2.87
Na_2O	0.39	0.37	0.42	0	0	0	0	0	0.39	0
K_2O	0	0	0	0	0	0	0	0	0	0
NiO	0	0	0	0	0	0	0	0	0	0
Cr_2O_3	0.20	0.39	0.52	5.15	0	0	0	0.34	0	0
ZnO	0	0	0	0.02	0	0	0	0	0	0
Total	97.61	100.30	96.24	100.16	100.25	99.85	100.10	95.02	100.28	97.78
Numbers of ions on the basis of 32 O										
Si	0.091	0.140	0.059	0.116	0.096	0.053	0.066	0.088	0.065	1.514
Ti	5.228	4.687	4.847	4.042	5.926	4.509	6.280	0.177	4.970	4.254
Al	1.326	1.029	1.486	1.697	0.574	0.631	0.461	0.192	0.919	0.867
Fe^{3+}	4.211	5.433	4.822	4.837	3.383	6.244	2.847	15.194	5.227	3.597
Fe^{2+}	11.150	11.211	10.544	9.913	12.709	10.693	13.341	6.735	10.791	10.862
Mn	0.156	0.150	0.148	0.170	0.151	0.195	0.161	0.141	0.128	0.170
Mg	1.417	1.056	1.664	2.054	1.162	1.638	0.844	1.331	1.630	1.858
Ca	0.151	0	0.069	0.017	0	0.036	0	0.058	0.055	0.878
Na	0.222	0.205	0.240	0	0	0	0	0	0.215	0
K	0	0	0	0	0	0	0	0	0	0
Ni	0	0	0	0	0	0	0	0	0	0
Cr	0.047	0.088	0.121	1.150	0	0	0	0.085	0	0
Zn	0	0	0	0.004	0	0	0	0	0	0
Total	24.000	24.000	24.000	24.000	24.000	24.000	24.000	24.000	24.000	24.000
%End-Members										
Spinel	18.8	13.8	21.8	26.1	14.7	20.7	10.6	16.9	21.3	33.1
Hercynite	0	0	0	0	0	0	0	0	0	0
Gahnite	0	0	0	0	0	0	0	0	0	0
Galaxite	2.1	2.0	1.9	2.2	1.9	2.5	2.0	1.8	1.7	3.0
Magnetite	22.6	30.7	25.1	24.6	18.5	31.4	16.1	79.0	26.6	19.0
Chromite	0.3	0.5	0.6	5.9	0	0.0	0	0.4	0	0
Ulvö spinel	56.2	53.0	50.5	41.2	64.9	45.4	71.2	1.8	50.5	44.9
Total	100.0	100.0	100.0	100.0	100.0	100.0	100.0	100.0	100.0	100.0

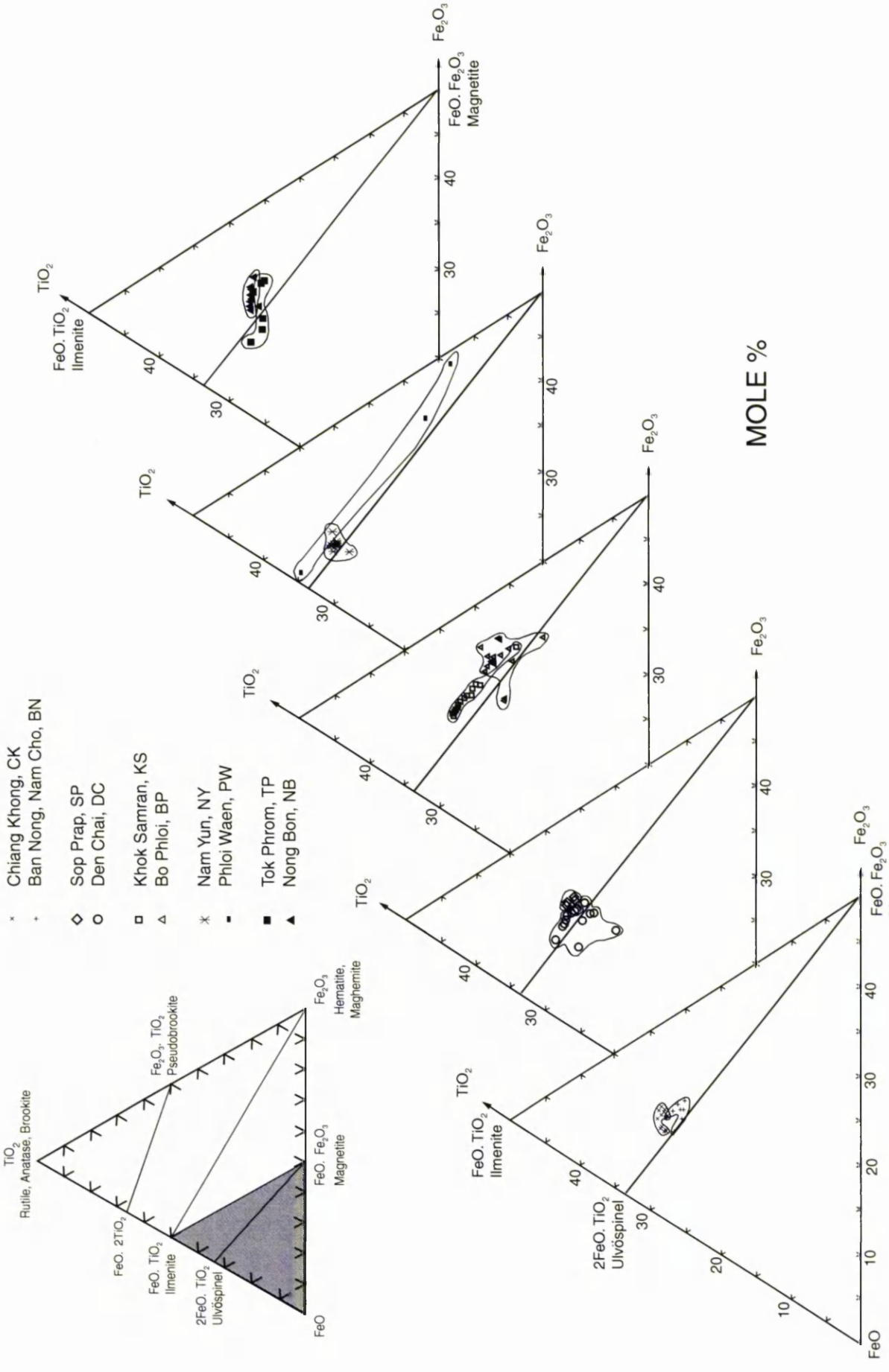

Figure 3.7 Ulvöspinel-magnetite in groundmass of basalts form Thailand plotted on the diagram of TiO_2-FeO-Fe_2O_3.

Samples from Den Chai (DC) have the highest value of chromium contents (up to 18.36 wt% Cr_2O_3, analysis DC157-MT1). TiO_2 contents in samples from Phloi Waen are very low (down to 0.75 wt%, Table 3.4). Petrographically, ulvöspinel-magnetite grains from this locality are heavily altered and this leads to the poor analyses as seen in Table 3.4. Most ulvöspinel-magnetite analyses in this study are plotted near the ulvöspinel end member (Figure 3.7). The analyses of samples from Bo Phloi are plotted in the middle of the ulvöspinel-magnetite end members. The analyses of samples from Phloi Waen are plotted in a wider range between the two end members.

3.3.2 Accessory minerals

Accessory minerals, including apatite, nepheline, leucite and zeolite, are found in the groundmass of many basalt samples. Apatite was found as tiny granules, laths or needles in the samples from Bo Phloi and Khok Samran. Nepheline ($Ne_{76.7-80.8}Ks_{14.3-16.0}Q_{3.7-8.3}$) is found in the samples from Nong Bon as groundmass oikocrysts. Leucite is found as an anhedral phase in interstices in the groundmass of basalts from Ban Nong, Bo Phloi, and Tok Phrom. Zeolite is found interstitially in the groundmass for samples from Ban Nong and Bo Phloi. Representative compositions of accessory minerals are presented in Table 3.5. All data are presented in Appendix 3-5 (Apatite), Appendix 3-6 (Nepheline, leucite and zelolite).

Table 3.5 Representative compositions of accessory minerals in basalt samples from Thailand.

Mineral	Apatite		Nepheline[a]	Leucite			Zeolite	
Locality	BO PHLOI	KHOK SAMRAN	NONG BON	BAN NONG, NAM CHO	BO PHLOI	TOK PHROM	BAN NONG, NAM CHO	BO PHLOI
Occurrence	Groundmass	Groundmass	Oikocryst of Poikilitic texture in groundmass	Interstice In groundmass	Interstice In groundmass	Interstice In groundmass	Interstice In groundmass	Interstice In groundmass
Analysis No	BP921A-AP2	KS1-AP1	NB131-NE5	BN6-LEU6	BP924A-LEU3	TP324c-LEU1	BN446-ZE1	BP924A-ZE4
SiO_2	0	0.60	43.47	55.47	55.61	55.23	54.70	53.02
TiO_2	0	0	0	0	0	0.18	0	0
Al_2O_3	0	0	32.48	22.87	22.75	23.19	25.06	27.57
Fe_2O_3*	0	0	1.23	0.52	0.67	0.74	0.77	1.01
FeO**	0.35	0.32	0	0	0	0	0	0
MgO	0	0.35	0	0	0	0.32	0.36	0.60
CaO	52.11	53.02	0.39	0	0	0	0.61	0
Na_2O	0.34	0	17.07	0.26	0.32	0.22	11.95	15.53
K_2O	0.12	0.16	4.32	20.87	20.30	20.32	4.75	1.55
P_2O_5	41.10	40.27	0	0	0	0	0	0
Cl	0.40	0	0	0	0	0	0	0
Original. Total	94.42	94.72	0	0	0	0	0	0
-O=Cl	0.09	0	0	0	0	0	0	0
Total	94.33	94.72	98.96	99.99	99.65	100.20	98.20	99.28
Numbers of ions								
O	12.5	12.5	32	6	6	6	80	80
Si	0	0.052	8.407	2.011	2.017	1.994	25.683	24.541
Ti	0	0	0	0	0	0.005	0	0
Al	0	0	7.403	0.977	0.972	0.987	13.869	15.037
Fe^{3+}	0	0	0.179	0.014	0.018	0.020	0.271	0.352
Fe^{2+}	0.025	0.023	0	0	0	0	-	-
Mg	0	0.045	0	0	0	0.017	0.254	0.411
Ca	4.851	4.926	0.080	0	0	0	0.308	0
Na	0.058	0	6.399	0.018	0.022	0.015	10.877	13.932
K	0.014	0.018	1.066	0.965	0.939	0.936	2.844	0.916
P	3.023	2.957	0	0	0	0	0	0
Cl	0.030	0	0	0	0	0	0	0
Total	8.001	8.021	23.535	3.985	3.969	3.974	54.107	55.189

* Total Fe as Fe_2O_3 for nepheline, leucite and zeolite; ** Apatite: total Fe as FeO, H_2O was not analysed;
[a] $Ne_{80.8}Ks_{15.0}Q_{4.2}$

3.3.3 Summary

The characteristics in terms of end members of the primary minerals in basalts from Thailand are summarized in Table 3.6.

From all analyses of alkali basalt samples, olivine has an average range of Fo of 68 – 84%. Clinopyroxene has an average range of end member of $Wo_{51-44}En_{45-34}Fs_{18-9}$. Average ulvöspinel-magnetite end member is $Sp_{24-14}Her_0Gah_{0.1}Gal_{3-2}Mag_{34-18}Chro_{3-0.2}Ulvö_{62-41}$. Feldspar has a wide range of end members, $An_{0-73}Ab_{0-70}Or_{0-72}$. Nepheline has an average end member (n=6) of $Ne_{80}Ks_{15}Q_5$.

Table 3.6 Summary of characteristics for primary minerals in basalt samples from different localities in Thailand.

Locality	Major minerals				Accessory minerals
	Olivine	Clinopyroxene	Feldspar	Ulvöspinel-Magnetite	
Chiang Khong	$Fo_{83.1\text{-}69.4}$	$Wo_{52.4\text{-}47.3}En_{40.3\text{-}32.0}Fs_{16.9\text{-}12.3}$	$An_{66.0\text{-}35.4}Ab_{45.1\text{-}30.9}Or_{19.6\text{-}3.1}$	$Sp_{23.5\text{-}16.9}Her_0Gah_0Gal_{2.2\text{-}1.4}Mag_{22.8\text{-}19.2}Chro_{0.6\text{-}0.2}Ulvö_{59.7\text{-}52.0}$	-
Ban Nong	$Fo_{90.9\text{-}69.5}$	$Wo_{53.1\text{-}40.7}En_{46.5\text{-}32.0}Fs_{24.9\text{-}6.9}$	$An_{68.6\text{-}45.4}Ab_{51.7\text{-}30.3}Or_{4.4\text{-}1.1}$	$Sp_{31.0\text{-}7.9}Her_0Gah_0Gal_{2.9\text{-}1.9}Mag_{30.7\text{-}18.7}Chro_{1.1\text{-}0.3}Ulvö_{60.1\text{-}46.4}$	Leucite, Zeolite
Sop Prap	$Fo_{83.8\text{-}73.7}$	$Wo_{50.1\text{-}47.3}En_{41.0\text{-}34.9}Fs_{15.7\text{-}11.7}$	$An_{58.3\text{-}49.7}Ab_{43.4\text{-}38.2}Or_{11.6\text{-}3.5}$	$Sp_{21.8\text{-}16.4}Her_0Gah_0Gal_{2.1\text{-}1.9}Mag_{28.7\text{-}24.7}Chro_{0.6\text{-}0.3}Ulvö_{52.6\text{-}50.5}$	-
Den Chai	$Fo_{89.9\text{-}70.5}$	$Wo_{51.0\text{-}47.1}En_{40.5\text{-}34.9}Fs_{16.1\text{-}11.0}$	$An_{73.0\text{-}42.2}Ab_{53.6\text{-}25.4}Or_{7.7\text{-}1.1}$	$Sp_{26.1\text{-}18.9}Her_0Gah_{0.9\text{-}0.0}Gal_{2.8\text{-}1.8}Mag_{24.6\text{-}17.3}Chro_{22.6\text{-}0.6}Ulvö_{58.3\text{-}29.0}$	-
Khok Samran	$Fo_{81.4\text{-}61.2}$	$Wo_{47.7\text{-}45.3}En_{41.2\text{-}36.4}Fs_{16.7\text{-}12.6}$	$An_{68.9\text{-}0.0}Ab_{48.9\text{-}0.0}Or_{3.4\text{-}0.0}$	$Sp_{17.9\text{-}11.9}Her_0Gah_0Gal_{2.9\text{-}1.0}Mag_{40.8\text{-}18.2}Chro_{0.6\text{-}0.0}Ulvö_{65.5\text{-}40.2}$	Apatite
Bo Phloi	$Fo_{84.0\text{-}69.0}$	$Wo_{50.9\text{-}39.0}En_{51.0\text{-}32.5}Fs_{20.1\text{-}6.5}$	$An_{60.7\text{-}5.1}Ab_{70.1\text{-}37.6}Or_{42.4\text{-}0.0}$	$Sp_{24.1\text{-}14.0}Her_0Gah_0Gal_{2.9\text{-}1.8}Mag_{40.0\text{-}27.3}Chro_{6.1\text{-}0.0}Ulvö_{51.9\text{-}29.0}$	Apatite, Leucite, Zeolite
Nam Yun	$Fo_{71.1\text{-}49.2}$	$Wo_{47.3\text{-}45.0}En_{42.7\text{-}34.5}Fs_{18.4\text{-}11.9}$	$An_{56.4\text{-}2.8}Ab_{68.0\text{-}41.4}Or_{48.7\text{-}2.2}$	$Sp_{12.6\text{-}9.9}Her_0Gah_0Gal_{2.1\text{-}1.3}Mag_{18.3\text{-}14.3}Chro_0Ulvö_{73.2\text{-}68.2}$	-
Phloi Waen	$Fo_{90.5\text{-}78.2}$	$Wo_{51.2\text{-}45.6}En_{49.3\text{-}36.5}Fs_{12.4\text{-}4.6}$	$An_{0.0\text{-}0.0}Ab_{29.3\text{-}27.6}Or_{72.4\text{-}70.7}$	$Sp_{20.2\text{-}15.3}Her_0Gah_0Gal_{3.0\text{-}1.4}Mag_{79.0\text{-}1.9}Chro_{0.4\text{-}0.0}Ulvö_{79.4\text{-}1.8}$	-
Tok Phrom	$Fo_{80.1\text{-}71.0}$	$Wo_{51.8\text{-}46.2}En_{45.1\text{-}33.5}Fs_{16.3\text{-}8.3}$	$An_{44.9\text{-}1.6}Ab_{62.2\text{-}35.5}Or_{62.9\text{-}2.7}$	$SP_{25.5\text{-}11.2}Her_0Gah_0Gal_{2.8\text{-}1.7}Mag_{28.5\text{-}23.4}Chro_{0.4\text{-}0.0}Ulvö_{58.8\text{-}48.4}$	Apatite, Leucite
Nong Bon	$Fo_{82.4\text{-}69.1}$	$Wo_{56.4\text{-}32.3}En_{51.2\text{-}31.0}Fs_{22.4\text{-}5.9}$	-	$Sp_{33.1\text{-}16.1}Her_0Gah_0Gal_{3.0\text{-}2.0}Mag_{29.9\text{-}19.0}Chro_0Ulvö_{60.8\text{-}44.9}$	Nepheline
Average	$Fo_{83.7\text{-}68.1}$	$Wo_{51.2\text{-}43.6}En_{44.9\text{-}33.8}Fs_{18.0\text{-}9.2}$	-	$Sp_{23.6\text{-}13.9}Her_0Gah_{0.1\text{-}0.0}Gal_{2.7\text{-}1.6}Mag_{34.3\text{-}18.4}Chro_{3.2\text{-}0.2}Ulvö_{62.0\text{-}41.0}$	-

3.4 Comparison of compositions of minerals from basalt and alluvium

Clinopyroxene and spinel are used for comparison in this study. The representative compositions of clinopyroxene and spinel used for comparison are given in Table 3.7. All data are presented in Appendix 3-7 (CPX in alluvium, xenocryst and xenolith) and Appendix 3-8 (Spinel in alluvium, xenocryst, xenolith and corundum). The compositions of these two minerals are plotted in Figures 3.8 and 3.9.

Gravel clinopyroxene samples recovered from alluviums of Den Chai and Bo Phloi are more Fe-rich than those from xenocrysts and xenoliths in basalts (Figure 3.8). All clinopyroxene samples from Den Chai probably originated in different environments. Clinopyroxene samples recovered from alluvium of Bo Phloi probably originated in the same environment as the phenocryst and groundmass clinopyroxenes in basalt.

Gravel-spinel samples from Den Chai are Cr-free, whereas basaltic spinels are ≥10% of 100xCr/(Cr+Al). Spinel samples from xenocrysts and xenoliths in basalt from Den Chai originated from the similar environments, which are different from those of gravel spinels (Figure 3.9, A). Gravel spinels, spinel xenocrysts and spinel xenoliths in basalt from Bo Phloi possibly originated from the similar environments but they crystallized in different environment from the spinel inclusion in corundum (Figure 3.9, B). Gravel spinel and certain spinel xenocrysts have no Cr content, but are distinguished on the basis of 100xMg/(Mg+Fe).

Table 3.7 Representative compositions of clinopyroxene and spinel in alluvium, in xenocrysts and xenoliths in basalts and in corundum from Thailand. (Note: $\Sigma Fe=Fe^{2+}+Fe^{3+}+Mn$; mg*=100xMg/ $Mg+Fe^{2+}+Fe^{3+}+Mn$).

Mineral	Clinopyroxene					Spinel						
Locality	DEN CHAI		BO PHLOI			DEN CHAI			BO PHLOI			
Occurrence	Gravel in alluvium	Spinel-Lherzolite xenolith	Gravel in alluvium	Xenocryst	Xenolith (Olivine + CPX)	Gravel in alluvium	Xenocryst	Spinel lherzolite xenolith	Gravel in alluvium	Xenocryst	Xenolith (Spinel+ Olivine)	Inclusion in corundum
Analysis No	DCCPX 4-1	DC271-CPX2	BPCPX1 -4	BP924-CPX18	BP9-CPX5	DCSP8-3	DC376A -SP1 (Core)	DC269-SP1	BPSP1-3	BP81-SP7	BP82-SP3	BPEP13-SP2
SiO_2	48.55	51.30	47.19	47.89	51.76	0.35	0	0.21	0.30	0.45	0.26	0.39
TiO_2	1.28	0.62	2.04	2.01	0.54	0.65	0.54	0	0.56	0.69	1.18	0.29
Al_2O_3	9.17	4.75	9.42	9.07	7.10	59.23	51.46	58.26	59.10	60.14	41.15	56.41
Fe_2O_3	3.75	0.37	3.39	2.61	0.65	8.80	7.93	2.45	8.22	5.82	14.08	6.04
FeO	3.08	2.95	4.11	4.29	2.64	10.51	14.35	9.24	11.65	13.55	23.19	29.79
MnO	0.23	0	0.20	0	0	0	0	0	0	0	0.48	0.55
MgO	13.98	16.02	11.55	12.38	15.61	19.01	15.40	20.77	18.95	19.03	10.31	6.70
CaO	18.23	22.87	20.37	20.43	19.16	0	0	0	0	0	0	0
Na_2O	1.64	0	1.57	1.41	1.59	0.50	0.62	0	0.31	0	0	0.35
K_2O	0	0.36	0	0	0	0	0	0	0	0	0	0
NiO	0	0	0	0	0	0	0	0.51	0	0	0	0
Cr_2O_3	0	0.87	0	0	0.97	0	9.75	8.66	0.28	0.33	8.44	0.81
ZnO	0	0	0	0	0	0.49	0	0	0	0	0	0
Total	99.91	100.11	99.84	100.09	100.02	99.5	100.05	100.09	99.38	100.01	99.09	101.33
Numbers ions												
O	6					32						
Si	1.774	1.872	1.747	1.762	1.867	0.073	0	0.042	0.063	0.093	0.061	0.087
Ti	0.035	0.017	0.057	0.056	0.015	0.101	0.088	0	0.088	0.107	0.209	0.048
Al	0.395	0.204	0.411	0.393	0.302	14.478	13.127	14.126	14.489	14.642	11.402	14.730
Fe^{3+}	0.103	0.010	0.094	0.072	0.018	1.374	1.292	0.380	1.286	0.904	2.491	1.007
Fe^{2+}	0.094	0.090	0.127	0.132	0.080	1.822	2.597	1.589	2.027	2.341	4.560	5.519
Mn	0.007	0	0.006	0	0	0	0	0	0	0	0.096	0.104
Mg	0.762	0.871	0.637	0.679	0.840	5.877	4.968	6.370	5.877	5.859	3.614	2.214
Ca	0.714	0.894	0.808	0.805	0.741	0	0	0	0	0	0	0
Na	0.116	0	0.112	0.101	0.111	0.199	0.261	0	0.124	0	0	0.149
K	0	0.017	0	0	0	0	0	0	0	0	0	0
Ni	0	0	0	0	0	0	0	0.084	0	0	0	0
Cr	0	0.025	0	0	0.028	0	1.667	1.409	0.046	0.053	1.568	0.142
Zn	0	0	0	0	0	0.075	0	0	0	0	0	0
Total	4.000	4.000	4.000	4.000	4.000	24.000	24.000	24.000	24.000	24.000	24.000	24.000
%END MEMBER												
Ca(Wo)	42.5	47.9	48.3	47.7	44.1	-	-	-	-	-	-	-
Mg(En)	45.3	46.7	38.1	40.2	50.1	-	-	-	-	-	-	-
ΣFe(Fs)	12.2	5.4	13.6	12.1	5.8	-	-	-	-	-	-	-
mg*	78.9	89.7	73.7	76.9	89.6	-	-	-	-	-	-	-
Spinel	-	-	-	-	-	76.0	64.2	80.9	75.2	74.1	45.5	28.5
Hercynite	-	-	-	-	-	13.1	16.2	7.9	15.4	18.6	25.3	62.4
Gahnite	-	-	-	-	-	1.0	0	0	0	0	0	0
Galaxite	-	-	-	-	-	0	0	0	0	0	1.2	1.3
Magnetite	-	-	-	-	-	8.6	8.1	2.4	8.0	5.7	15.6	6.3
Chromite						0	10.4	8.8	0.3	0.3	9.8	0.9
Ulvöspinel	-	-	-	-	-	1.3	1.1	0	1.1	1.3	2.6	0.6
Total	-	-	-	-	-	100.0	100.0	100.0	100.0	100.0	100.0	100.0

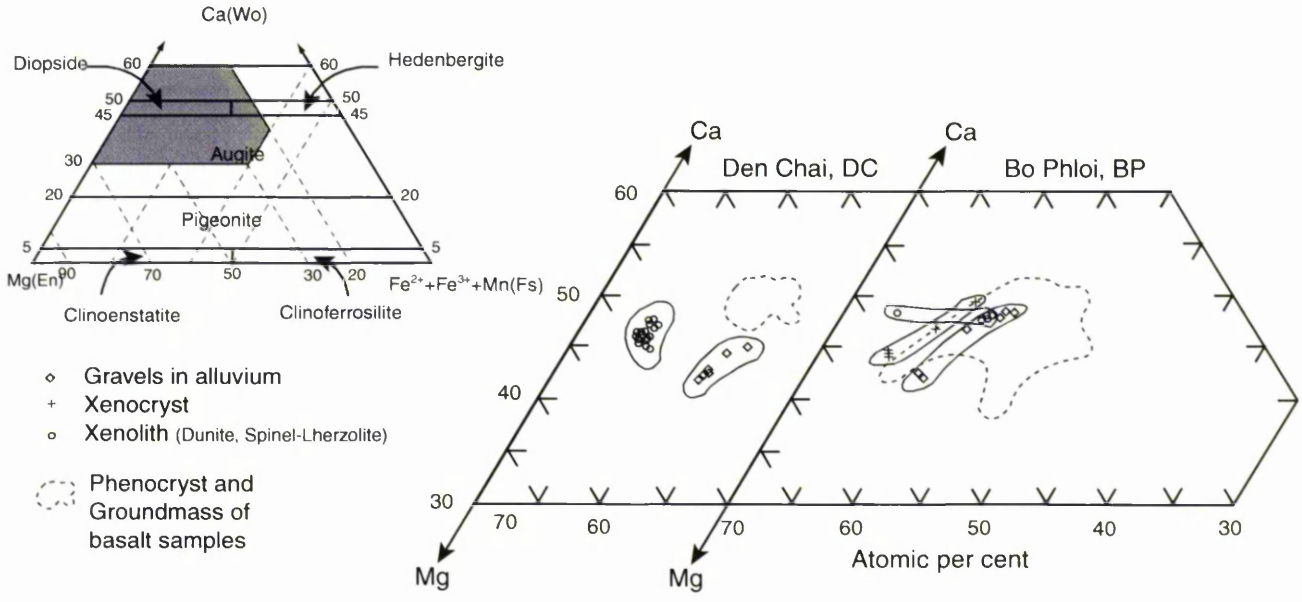

Figure 3.8 Clinopyroxenes of different provenance from the same locality are plotted in the Ca-Mg-Fe^{2+}+Fe^{3+}+Mn quadrilateral diagram (Wo-En-Fs). The fields (inset) are from Morimoto *et al.*, 1988.

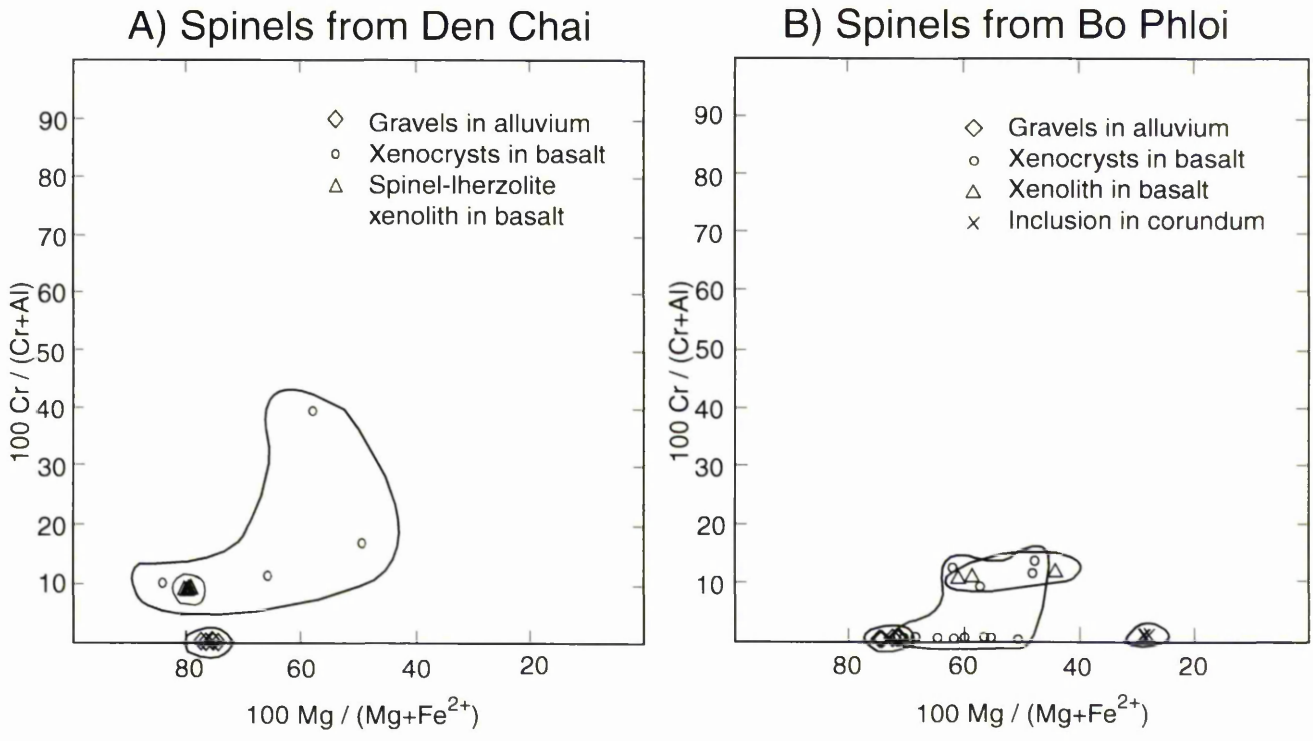

Figure 3.9 Atomic plots of spinels of different provenance from the same locality.

CHAPTER 4
THAI CORUNDUM OCCURRENCES AND CHARACTERISTIC OF SECONDARY DEPOSITS

4.1 Introduction

This chapter describes the characteristics of the secondary deposits of corundums (rubies and sapphires) from Thailand using the information from the literature and data from the preliminary fieldwork of this study. The following sections will present the occurrence and distribution of corundum together with the depositional characteristics of different localities (from north to south) in Thailand. This will form important background information to the other chapters.

4.2 Corundum occurrences in Thailand

All corundum deposits in Thailand are found as secondary deposits, i.e. in eluvial or alluvial placers and residual soil associated with alkali basalt. It has long been considered that the sources of rubies and sapphires in Thailand are basalt. Rubies and sapphires are found as a product of weathering and erosion in or near basaltic terrain, but rubies and sapphires in fresh basaltic rocks are extremely rare (Vichit, 1987). Vichit *et al.* (1978) and Vichit (1987) claimed that the 4 basalt samples in which sapphires are embedded were collected from Bang Kacha, Chanthaburi province and Bo Phloi, Kanchanaburi province. However the author has not seen them. The distributions of basalts and of ruby and sapphire occurrences are shown in Figure 4.1.

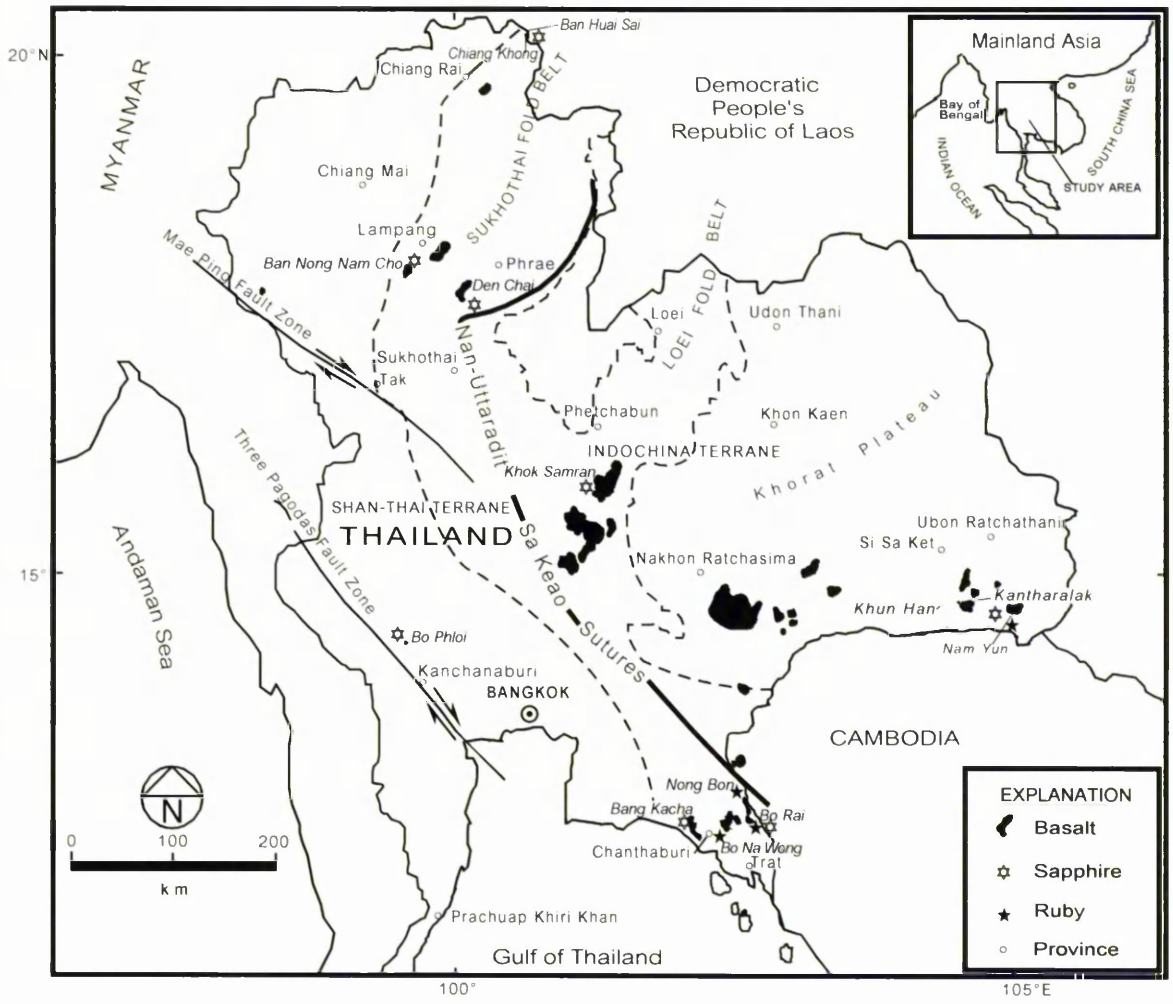

Figure 4.1 Locations of corundum (ruby and sapphire) deposits and distribution of basalts in Thailand. (Corundum and basalt localities after Vichit, 1992; structures and boundaries after Polachan *et al.*, 1991 and Bunopas, 1992).

The Thai corundum samples chosen for this study come from Ban Nong Nam Cho, Den Chai, Khok Samran, Bo Phloi, Nam Yun, Bang Kacha, Bo Na Wong, Bo Rai and Nong Bon. Samples from Ban Huai Sai, Democratic People's Republic of Laos are included in this group as they are said to be derived from the same outcrop of Chiang Khong Basalt. Examples of the corundum grains are shown in Figure 4.2.

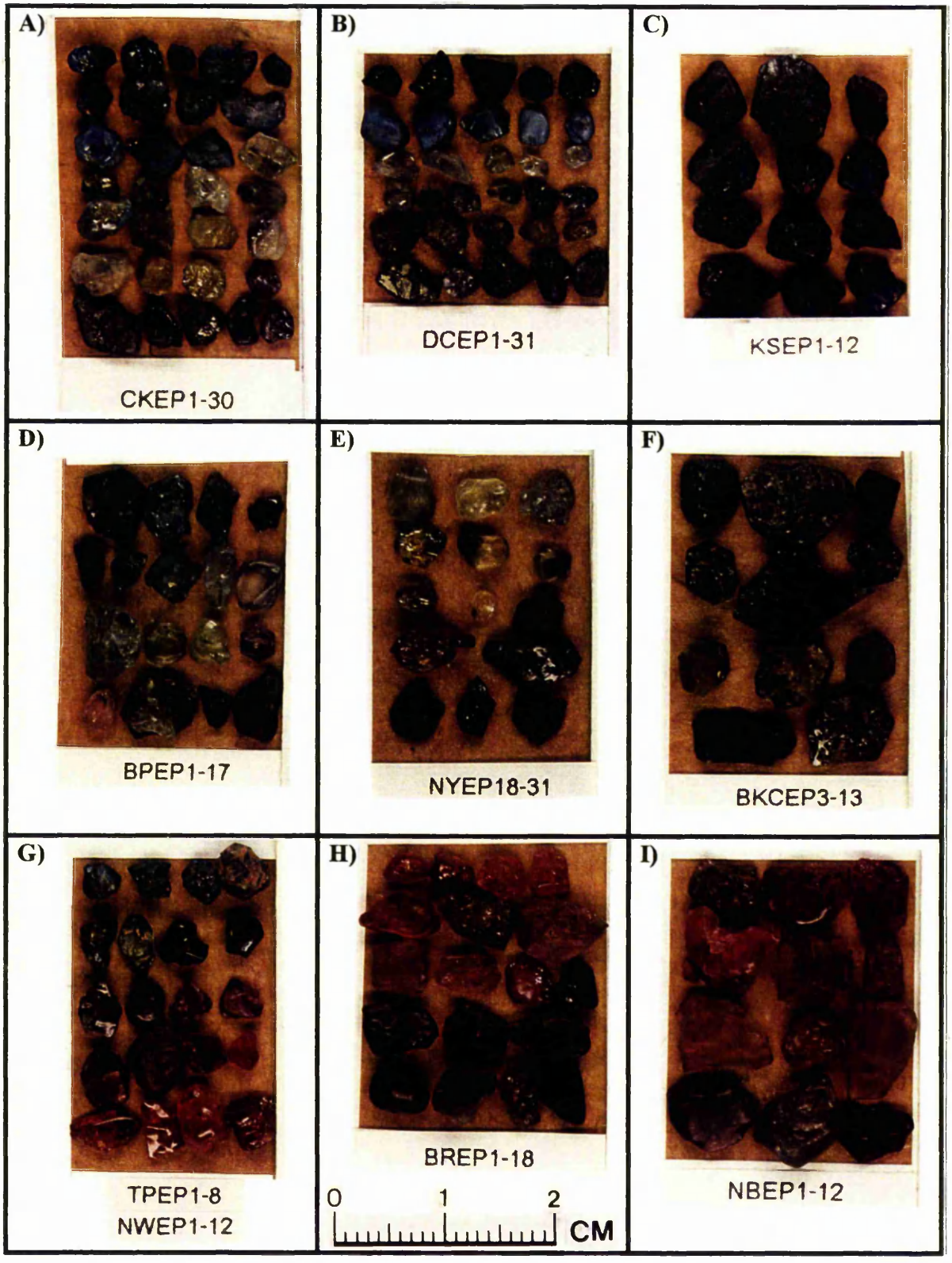

Figure 4.2 The appearance of corundum samples from secondary deposits of various localities in Thailand and Democratic People's Republic of Laos. **A)** Ban Huai Sai (in Democratic People's Republic of Laos), **B)** Den Chai, **C)** Ban Khok Samran, **D)** Bo Phloi, **E)** Nam Yun, **F)** Bang Kacha, **G)** Tok Phrom (Blue, 2 upper rows) and Bo Na Wong (purple and red, 3 lower rows), **H)** Bo Rai and **I)** Nong Bon. Note that all sets were prepared as shown for making polished sections.

4.3 Characteristics of the deposits of corundums

4.3.1 Ban Huai Sai near Chiang Khong

Sapphire and zircon have been mined from the soil weathered from basalts (simply called lateritic soil) as well as from the gravel deposits close to basalt outcrop. The mines are still active in Ban Huai Sai, Khwaeng Bo Kaew, in the Democratic People's Republic of Laos. Light to dark blue sapphires, many noticeably colour-zoned and mainly ≤ one carat per grain (1 carat = 0.2 gram), have been mined from this area. The basalt occurs mainly on the Laotian side. The outcrop in Laos extends across to the Thai side of the Mae Khong River, the boundary between Thailand and Laos, near Chiang Khong Customs House, in Amphoe Chiang Khong, Chiang Rai province. The outcrop on the Thai side is very small, 50 m. in diameter (Panjasawatwong and Youngsnong, 1995; Kammerling, 1995).

The information acquired by the author from the local people at Amphoe Chiang Khong shows that in the past native people could extract sapphires from the sand and gravel bed of the Mae Khong river near the basalt outcrop by a primitive method. They used a pan or sieve to sluice sapphires from sand and gravel with river water.

4.3.2 Ban Nong Nam Cho and Sop Prap, Lampang

The Lampang basalt includes the Mae Tha basalt and Sop Prap basalt outcrops. It was not until 1978 that the Lampang basalt was reported to have sapphires associated with it (Thanasuthipitak, 1978) but it was not explored in detail. The Sop Prap basalt, which is located in the southern part of Lanpang province, was investigated by Sutthirat *et al.* (1995) who found that corundum-associated basalts occur in the areas of Tambon Nam Cho, Amphoe Mae Tha; and Amphoe Sop Prap. Basalts are underlain by the Permian and Permo-Triassic rocks (quartzite, sandstone, shale, conglomerate, rhyolite, andesite, tuff and agglomerate). Sapphires were found in residual and alluvial soils as well as in stream channels flowing from a nearby volcanic crater. These deposits are located in the areas of Amphoe Mae Tha at Ban Nong, Tambon Nam Cho; Ban Tao Poon and Ban Mae Hi, Tambon Nasaeng. The sapphire grains range from 1-5 mm of diameter and are coloured blue, dark blue, greenish blue or dark brown. Some brown sapphires show asterism. Sapphires have accumulated at levels 0 - 2.2 m from the surface in layers that range in thickness from 0.2 to 1.3 m. The distribution of basalt outcrop and sapphire localities in these areas is shown in Figure 4.3.

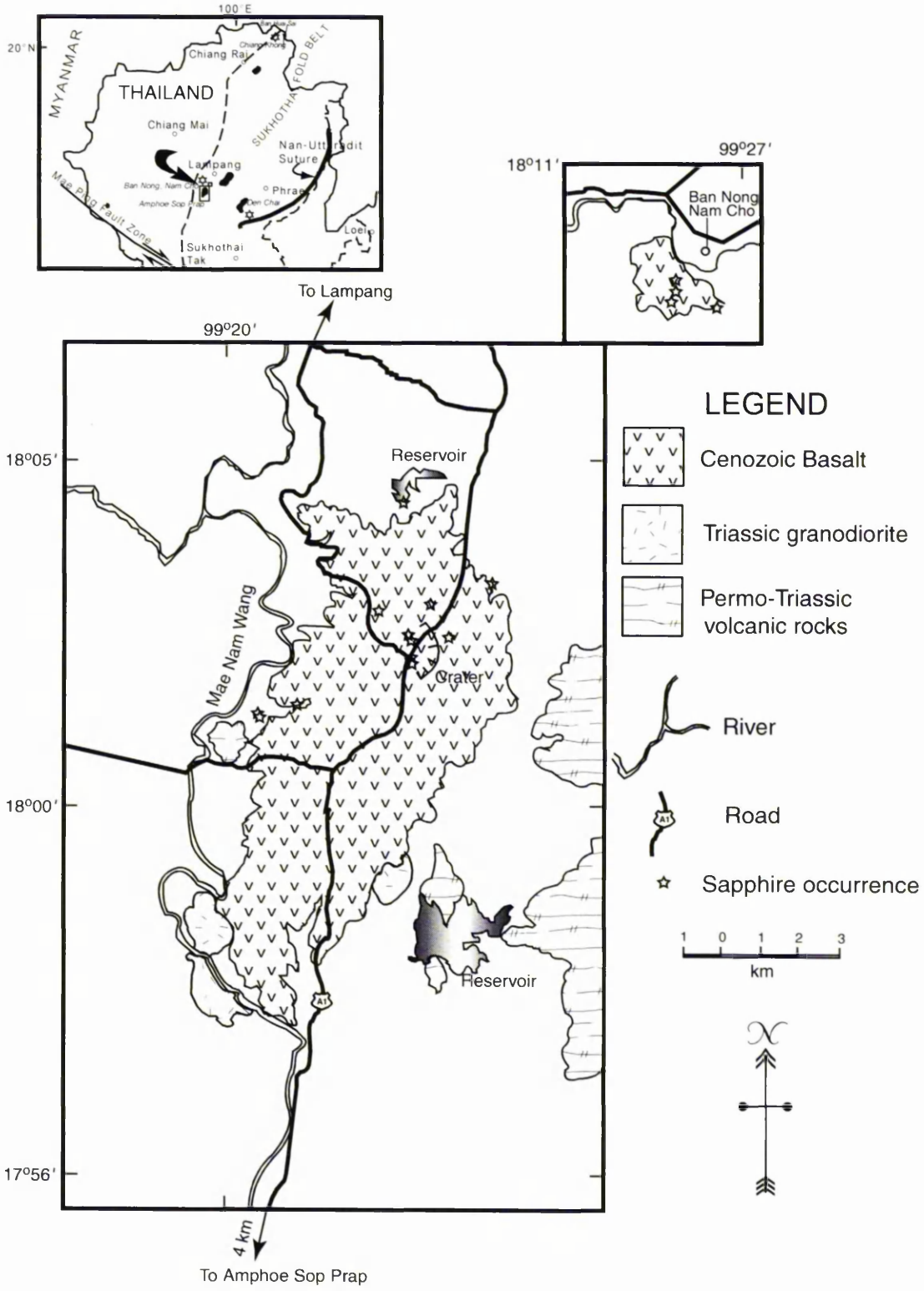

Figure 4.3 Sop Prap basalt and sapphire occurrences in the areas of Amphoe Mae Tha and Amphoe Sop Prap, Lampang province. (Modified from Sutthirat *et al.*, 1995).

4.3.3 Phrae and Sukhothai

In the area of Amphoe Den Chai, Phrae province, sapphires occur in recent alluvial deposits in streams, e.g. at Huai Si-Siat, Huai Wua Dang, Huai Mae Kanung, and Huai Mae Sung. Other deposits are located at Ban Thung Laeng and Ban Hat Pha Khan in Amphoe Long, Phrae province. The thickness of the corundum-bearing layers varies from 30 cm to 1 m. The overburden is from 1 to 7 metres thick. The sapphires are coloured generally in shades of blue but a small quantity of green, yellow and star sapphires also occurs. The sapphires are usually flawed, and generally milky. Rubies have been found only in trace amounts. The average grain size of these corundums is 3-5 mm in diameter, and no grains greater than 1 cm across have ever been found. The corundums are found associated with ilmenite, olivine, black spinel, black pyroxene, zircon, quartz and flakes of gold (Vichit, 1992). Seven flows of the Den Chai basalt have been recognised; the lowest is underlain by Permian-Carboniferous rocks, mainly sandstone, limestone, conglomerate, chert and shale (Charoenprawat, 1968; Piyasin, 1975).

Sapphire deposits are also found at Amphoe Si Satchanalai, Sukhothai province, 25 km south-west of the outcrop of Den Chai basalt. They occur at Ban Huai Po, Ban Satho, Ban Na Pla Kang, Ban Pak Sin, Ban Sam Saen and elsewhere. The sapphire deposits are in the form of gravel terraces of the Yom River. Sapphires are found at depths ranging from 20 cm to 2 m. The gem-bearing gravels are between 0.3 to 1 m thick. The Permian-Carboniferous bedrock is composed of shale, tuffaceous sandstone, phyllitic shale, and slate (Charoenprawat, 1968; Piyasin, 1975). The colours of the sapphires from this locality are similar to those from the Den Chai deposit but in addition black star sapphires may be found in this area. These sapphires range in diameter from 1 mm to 5 mm. Only a small remnant of basalt occurs, found at ca 6.5 km west of Ban Satho. Elsewhere, the basalt has been completely eroded away. Black spinel is the most common associated mineral; others include zircon, quartz, pyrite and gold (Vichit *et al.*, 1978; Vichit, 1992). Figure 4.4 shows the localities of sapphire deposits and basalt outcrops in the Phrae and Sukhothai provinces.

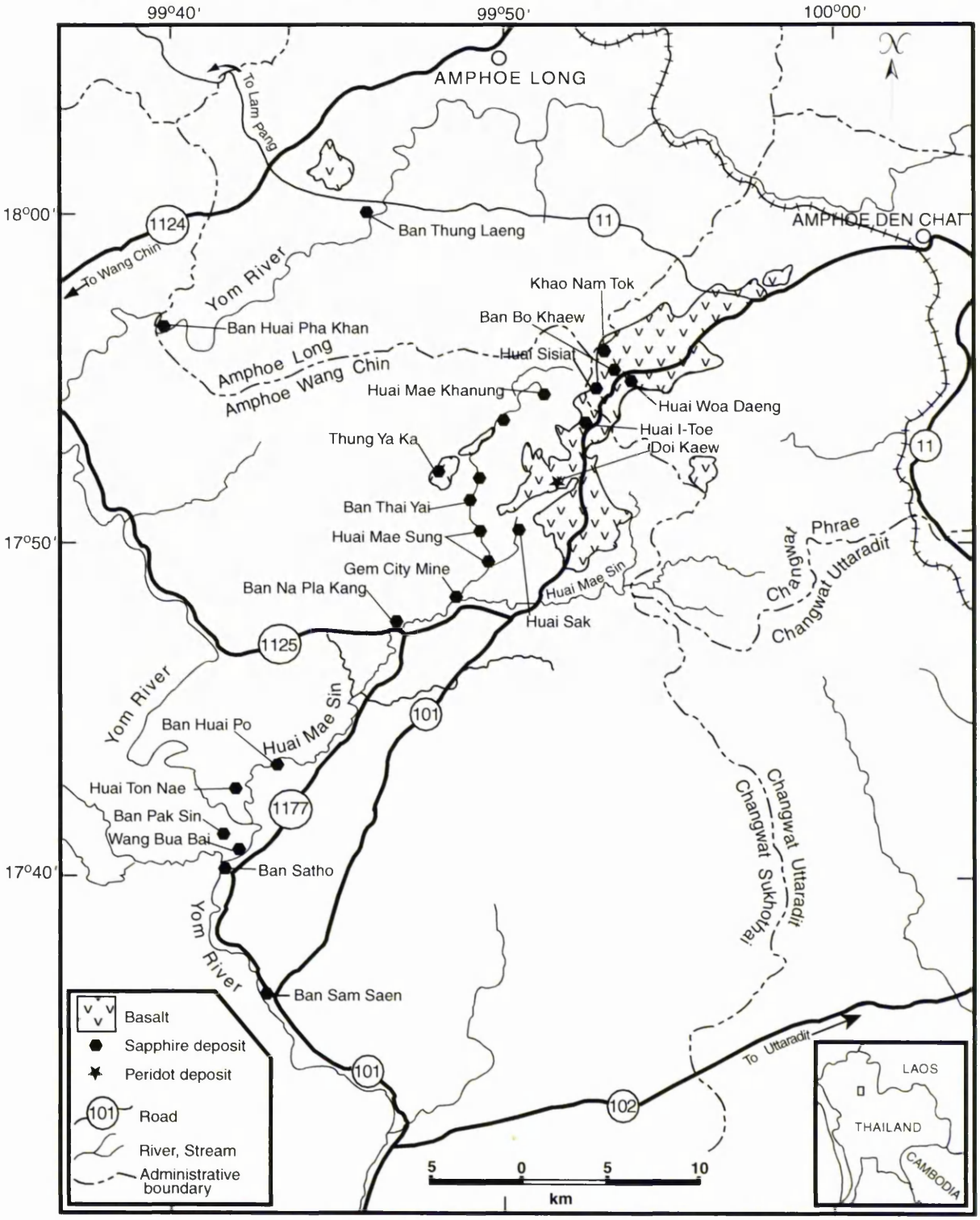

Figure 4.4 Map showing locations of sapphire deposits and basalt in Phrae and Sukhothai provinces. (After Vichit 1992).

4.3.4 Wichian Buri, Phetchabun

Sapphire deposits occur at Ban Khok Samran and Ban Marp Samo, 10 km north-east of Amphoe Wichian Buri, Phetchabun province. Basalts overlie Permian sedimentary rocks (limestone, shale, slaty shale and sandstone) and Triassic acid volcanic rocks.

The sapphires are found in residual soils weathered from basalt; sediment in streams cutting through the basaltic flow; eluvium; colluvium, channel-filling sediment and alluvium. Sapphires are generally found in the uppermost 2 m of the soil. Sapphire reserves estimated from a pitting survey are 15.4 tonnes in an area of 42 km^2. Most of the sapphires are blue or greenish blue, but they are generally of poor quality due to an opaque or very dark tone. Yellow sapphires occur very rarely. 90% of the sapphires have grain sizes in the range 2 mm x 3 mm to 1 mm x 2.5 mm. The larger grains are up to 1.5 cm in diameter. Black spinel, black amphibole (kaersutite), zircon, feldspar and garnet are found as associated minerals (Vichit, 1987; Vichit, *et al.*, 1988; Vichit, 1992). The sapphire deposits and distribution of basalts in this area are shown in Figure 4.5.

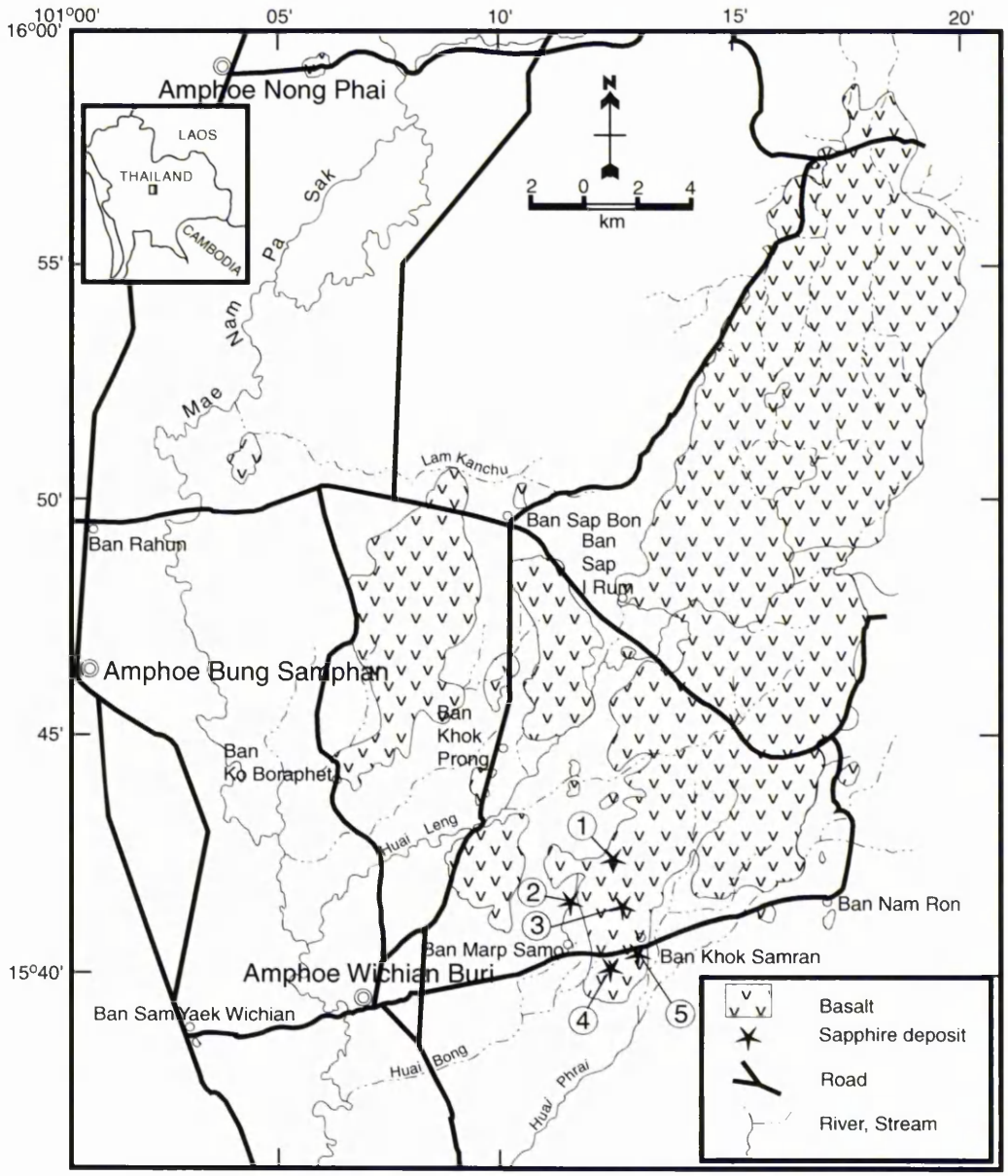

Figure 4.5 Locations of sapphire deposits and distribution of basalts in Wichian Buri, Phetchabun province. (**1**. Khlong Yang-Khlong Prak Mu, **2**. Nong Hoi Khong, **3**. Khlong Khaton, **4**. Ban Kutta Bong, **5**. Ban Khok Samran) (After Vichit, 1992).

4.3.5 Bo Phloi, Kanchanaburi

The Kanchanaburi corundum deposits are located in the area of Amphoe Bo Phloi, Kanchanaburi province, about 25 km north from Kanchanaburi town centre. The potential sapphire-bearing zone is approximately 10 km long and 1 to 3 km wide (Figure 4.6). The deposits extend from Ban Chong Dan, north of the area to Ban Nong Yang Chang, south of the area. The area expected to contain sapphire deposits extends southbound along Huai Lam Taphoen from Ban Chong Dan to Khao Hin Lap and Khao Chon Kai (out of the map). The annual production from this locality is about 4 million carats (800 kg). The deposits were one of the major sources for supplying gem corundum into the market in the past (Vichit, 1987). Sapphires are found in residual basaltic soils (Figure 4.7), colluvium, talus, and placer (eluvial and alluvial deposits) (Chuwong *et al.*, 1995; Hansawek and Pattamalai, 1997). The latter type of deposits is mined with heavy equipment (Figure 4.8).

Sapphire-bearing layer, 5 metres thick on average, lies at a depth that varies from 3 to 15 metres. The stratigraphic succession of the sediments descending from topsoil is given in Figure 4.9 (Limsuwan, 1999). The sapphires have various shades of blue, ranging from pale to dark blue colours. Samples with colour zoning, different pale colours are common. Sheen, yellow and purple sapphires and ruby are also found but they are rare. The diameters of sapphire grains range from <1 mm to 2 cm. A large piece, 10 cm x 9 cm x 3 cm (2,250 carats), has been reported. The associated minerals include black spinel, black pyroxene, magnetite, zircon and sanidine (Vichit, 1992).

The well-known basalt outcrop at Khao Lan Thom, east of Bo Phloi town centre, forms a low hill covering an area of approximately 0.5 km^2 and overlies quartzite of Silurian-Devonian age (Bunopas and Bunjitadulya, 1975). Other small outcrops of basalt are found at Huai Nam Phu, 3 km southeast of Ban Chong Dan and at Huai Maka in the area of Ban Chong Dan (Vichit, 1992; Hansawek and Pattamalai, 1997).

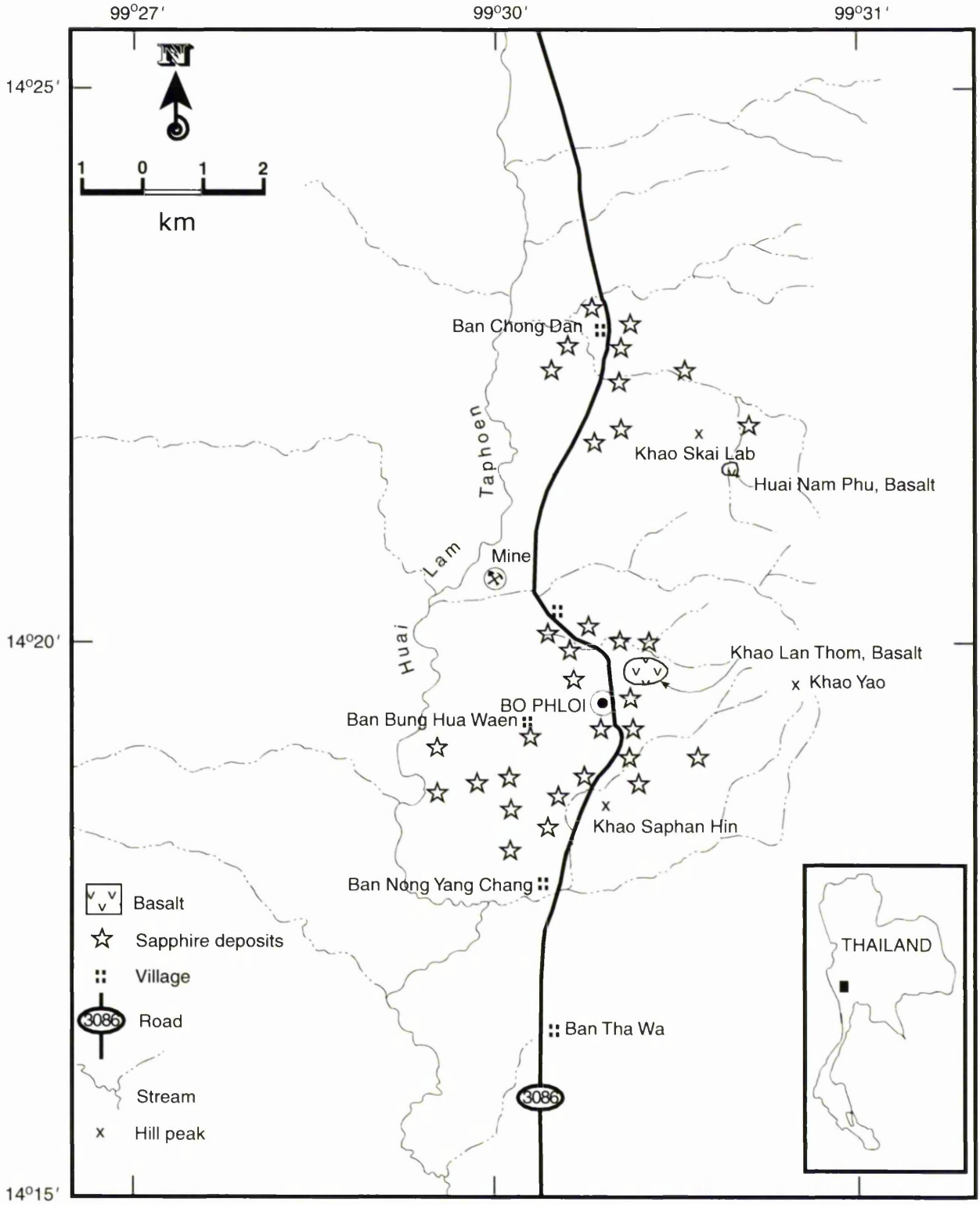

Figure 4.6 Locations of sapphire deposits and basalts in Amphoe Bo Phloi, Kanchanaburi province, West-Central Thailand (Vichit, 1992).

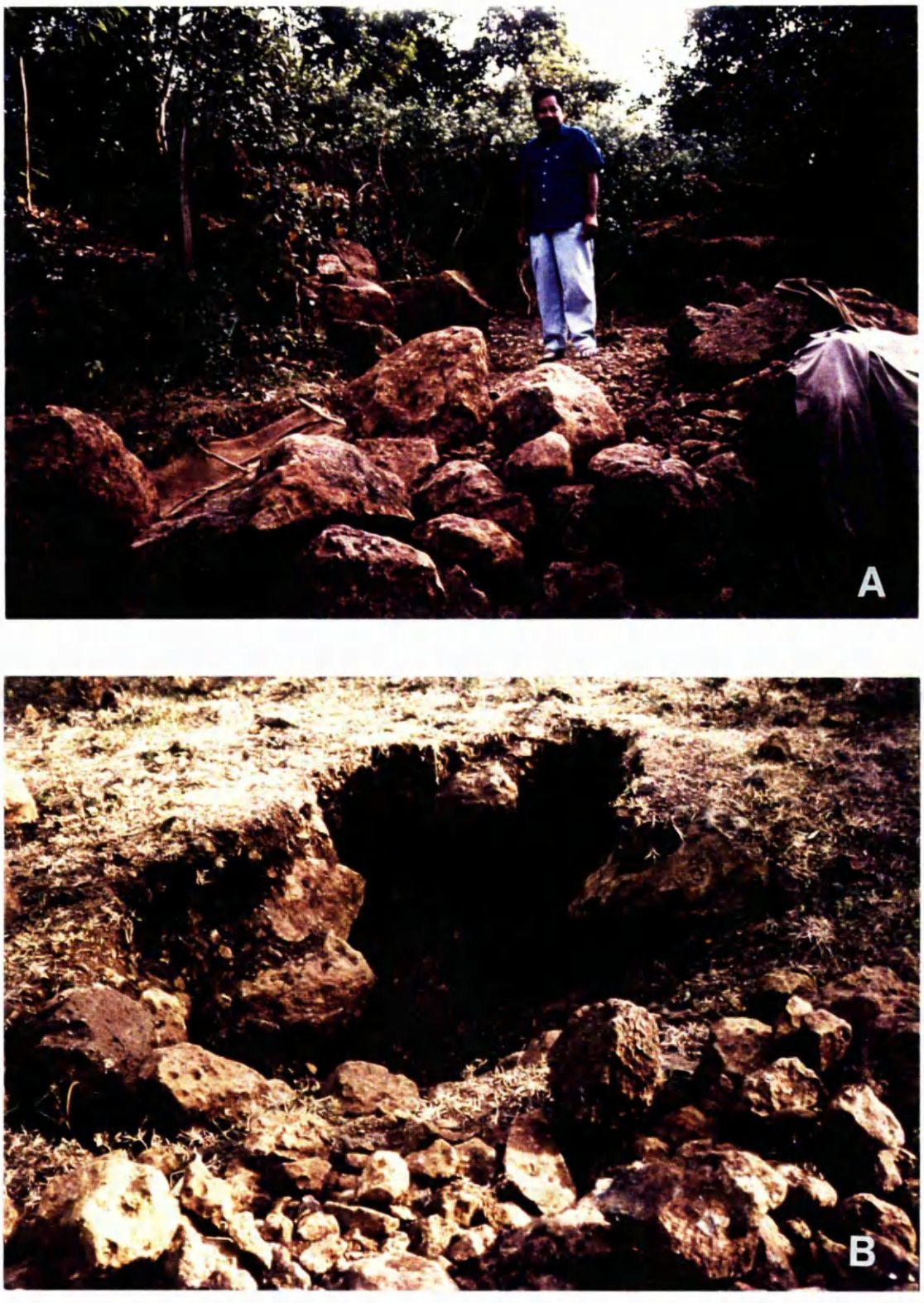

Figure 4.7 The residual soil and gravels on top of the basalt outcrop at Khao Lan Thom, Bo Phloi were dug out to wash for the corundum by the miner standing on the pit **A)**, and the boulders of basalts and a hole were left on the ground **B).**

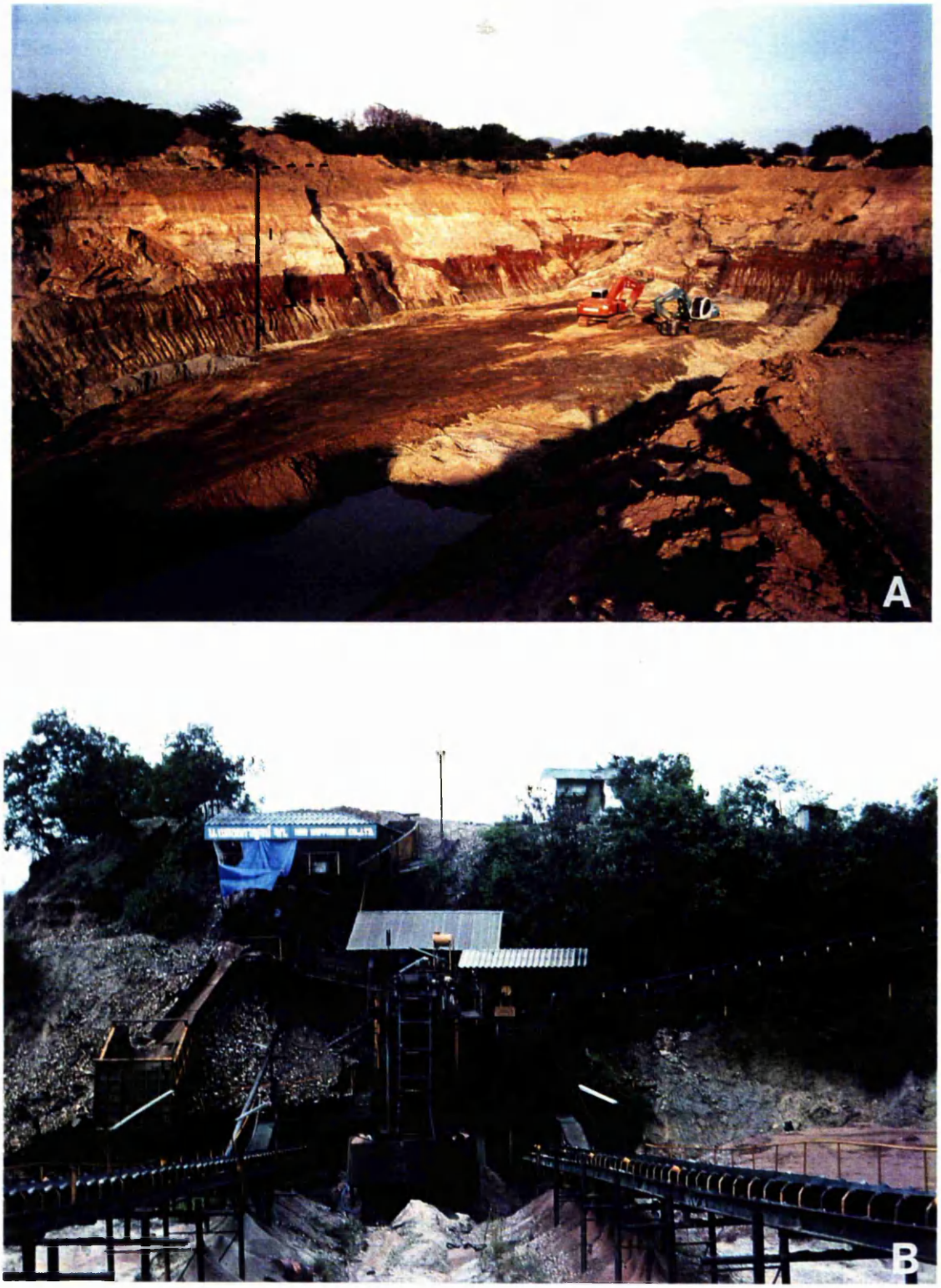

Figure 4.8 A) The open-cast, Bunmani Mine, at Bo Phloi, Kanchanaburi showing the sedimentation sequences of the placer deposit on the east bank of Huai Lam Taphoen. **I**-Overburden, **II**-Gem-bearing gravel bed. The wood in the centre left of the figure is probably more than 35,600±4,200 years old, the age obtained by C-14 dating of other pieces (Hansawek and Pattamalai, 1997). **B)** The gem-bearing gravels from the open-cast in A) were loaded by the lorries, transported and dumped into the trommel through the palong and jig for separating corundums from the gravels

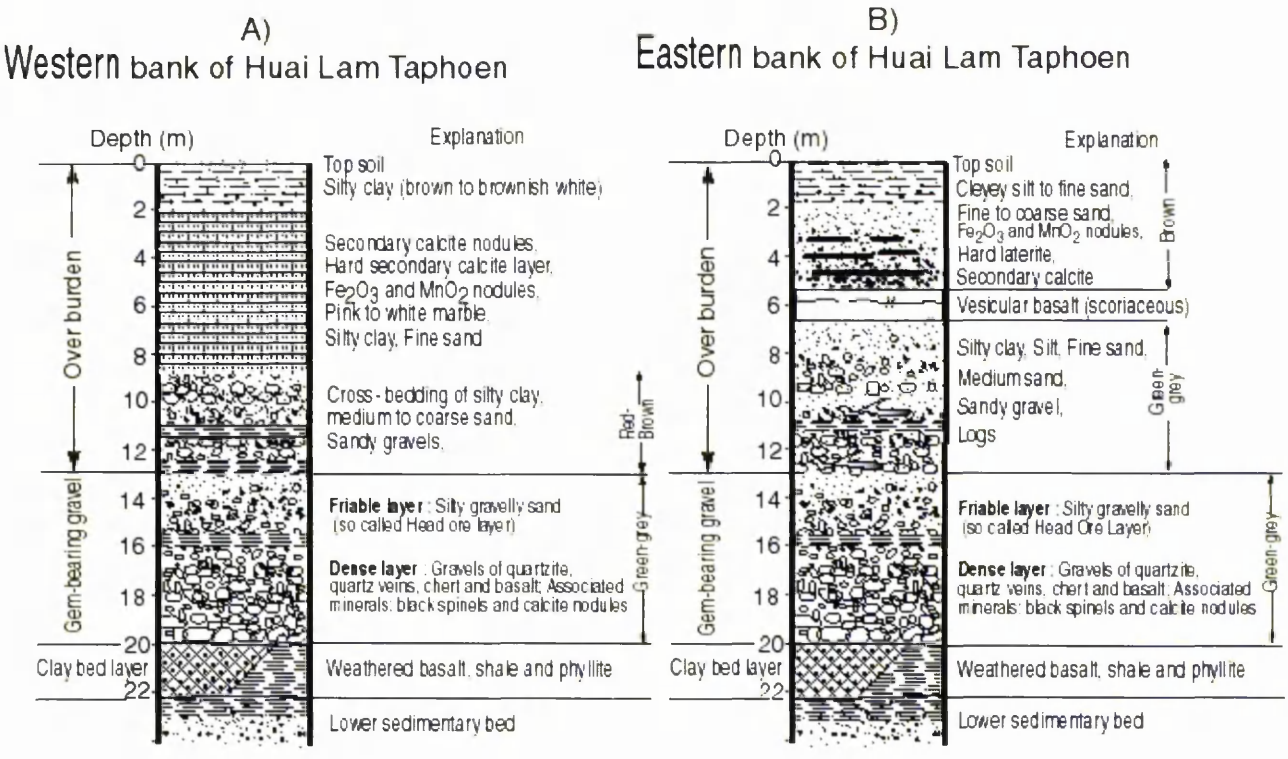

Figure 4.9 Cross-sections of gem corundum deposits in alluvium of Bo Phloi area, **A)** western bank of Huai Lam Taphoen and **B)** eastern bank of Huai Lam Taphoen. Details of sections compiled from the data of open-cast and drilling holes at Ban Chong Dan (Limsuwan, 1999).

4.3.6 Ubon Ratchathani - Si Sa Ket

Corundum deposits occur at Amphoe Nam Yun, Ubon Ratchathani province and Amphoe Kantharalak, Si Sa Ket province. The gem field has an area of ca 18 x 20 km^2. Corundums are found at many localities such as Huai Ta Aek and Plan Thung Yao (at Amphoe Kantharalak) and at Ban Non Yang and Ban Ta Koi (at Amphoe Nam Yun) as shown in Figure 4.10. The corundum deposits are mined from alluvial gravel, along the banks of the stream, and from laterite. A 0.5 – 3 m thick overburden of gravel, fine to coarse sand, silt and clay as well as laterite covers the 10 - 50 cm gem-bearing layer. Associated minerals are zircon, garnet, magnetite, clinopyroxene, ilmenite, black spinel and olivine. Petrified wood and tektites are commonly found associated with gravels in the overburden layer. Corundums found in these areas are mainly blue and green, whereas rubies are also found in trace amounts. No basalt outcrop is found under the sapphire deposits (Vichit, 1992). The nearest basaltic outcrop (<1 km away) to this sapphire occurrence is the Nam Yun Basalt, which rests on the Middle-Upper Cretaceous rocks (siltstone, sandstone, and conglomerate) called the Khok Kruat Formation, Khorat Group.

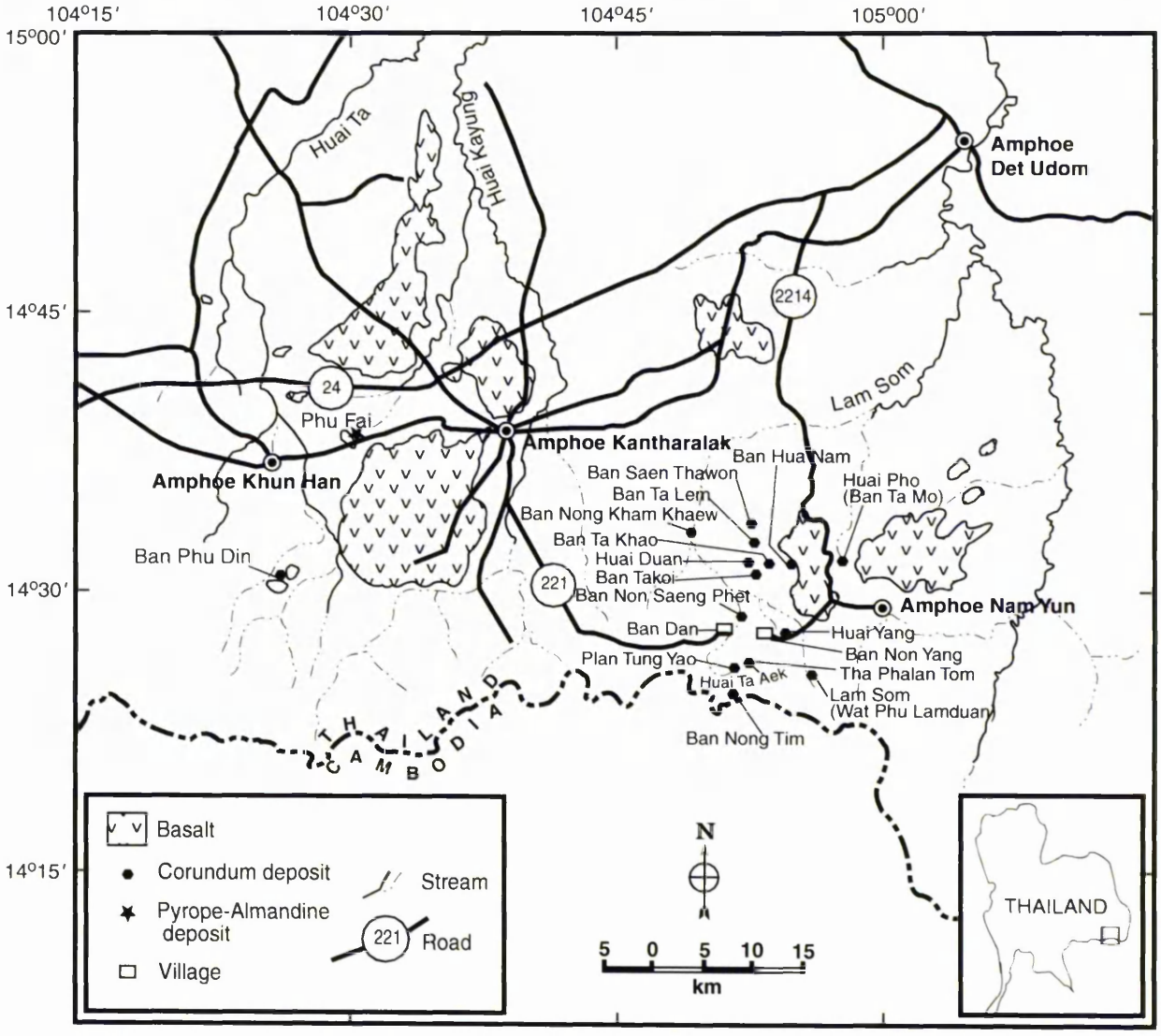

Figure 4.10 Map of southeast quadrant of the Khorat Plateau showing the distribution of basalts, corundum and garnet localities (Vichit *et al.*, 1992).

4.3.7 Chanthaburi - Trat

The Chanthaburi-Trat corundum deposit is the most significant ruby-sapphire concentration associated with basalt in Thailand. There is a variation of corundum colours across the region, with colours apparently segregated in three geographic zones; blue-green-yellow sapphires characterise the western part of the region (Chanthaburi province), blue-green sapphires and rubies characterise the area between Chanthaburi and Trat provinces, and rubies characterise the eastern area (Trat province). The localities of the gem deposit and the three zones are shown in Figure 4.11. The proportion of sapphires and ruby found in each location of the three zones are given in Table 4.1 (Vichit, 1992). Each zone is described respectively as follows.

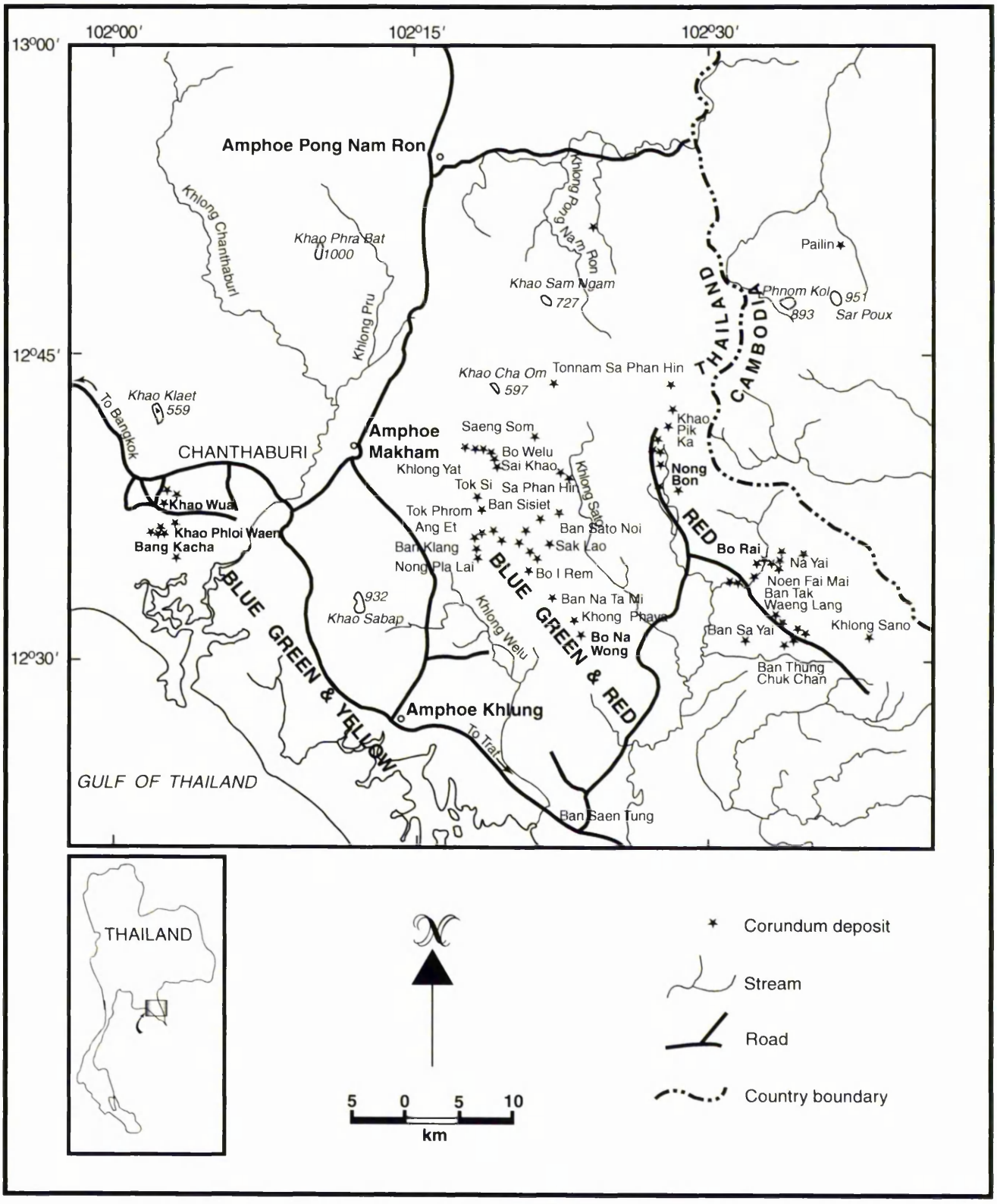

Figure 4.11 Gemstone localities and zones of BLUE-GREEN-YELLOW SAPPHIRES, BLUE-GREEN SAPPHIRES-RED (RUBY), and RED (RUBY) of eastern Thailand (After Vichit, 1992).

Table 4.1 Estimated proportion of sapphires and ruby in three zones of Chanthaburi-Trat area.

Zone	Location	%	
		Sapphires	**Ruby**
Western region of Chanthaburi province	Khao Woa, Khao Phloi Waen and Bang Kacha	≈100	-
Between Chanthaburi and Trat provinces	Ban Klang	90-95	5-10
	Tok Phrom	80-90	10-20
	Bo I Rem	≈100	-
	Ban Tok Si, Ban Sisiat	60-70	30-40
	Nong Pla Lai	80-90	10-20
	Bo Welu, Ban Sai Khao, Ban Takhian	30-40	60-70
	Ban Saeng Som	80-90	10-20
	Ban Saeng Daeng	10-20	80-90
	Ban Chak Lao	80-90	10-20
	Ban Sato Noi	70-80	20-30
	Ban Saphan Hin	10-20	80-90
	Ban Na Ta Mi, Bo Na Wong, Khong Phaya	-	≈100
Trat province	Bo Rai, Nong Bon, Ban Sua Dao, Noen Tak Daet, Khao Pik Ka, Ban Ta Ngam, Noen Chali, Ban Tak Waeng, Ban Sa Yai, Ban Noen Si, Ban Wai Kai, Ban Ta Bad, Ban Muan Dan	-	≈100

Source: Modified from Vichit, 1992.

The Zone of Western Region of Chanthaburi Province

This zone is located in the Amphoe Tha Mai area, Chanthaburi province, about 6 km west of Chanthaburi town centre. Sapphires occur around Khao Wua, Khao Phloi Waen, and at Bang Kacha. The locations of these sapphire deposits are shown in Figure 4.12. Few mines are active at present.

Khao Wua and Khao Phloi Waen are small hills with heights of 85 m and 129 m above mean sea level respectively. Sapphires are found in deeply weathered basalt at a depth of approximately 3 - 8 m in the areas surrounding these hills. The average thickness of

the gem-bearing layer is 30 cm – 1 m. The bedrock under the basalt in this area consists of Carboniferous rocks (phyllitic shale, shale, sandstone, siltstone and chert) (Sivabovorn *et al*, 1976).

At Bang Kacha, sapphires are mined in the swamp which is less than 1 - 1.5 km away from the edge of basalt outcrop. The thickness of the mineral-bearing layer is 10 - 80 cm and this is overlain by a 2 – 4 m layer of silty and sandy clays with buried wood and shell fragments. ^{14}C dating gave an age of 5,070±120 years for a wood sample from this layer. (Atomic Energy for Peace, Thailand). The gem-bearing layer is composed of subangular and subrounded pebbles, cobbles, and boulders of basalt. The bedrock underlying the gem deposit consists of grey and yellow-brown clay, siltstone, sandstone, laterite and vein quartz.

Sapphires found in this zone are blue, green, and yellow as well as a combination of these colours. Star and green sapphires are the most common. The associated minerals are pyrope-almandine garnet, pyroxene, phlogopite (?), zircon, and black spinel (Vichit, 1992).

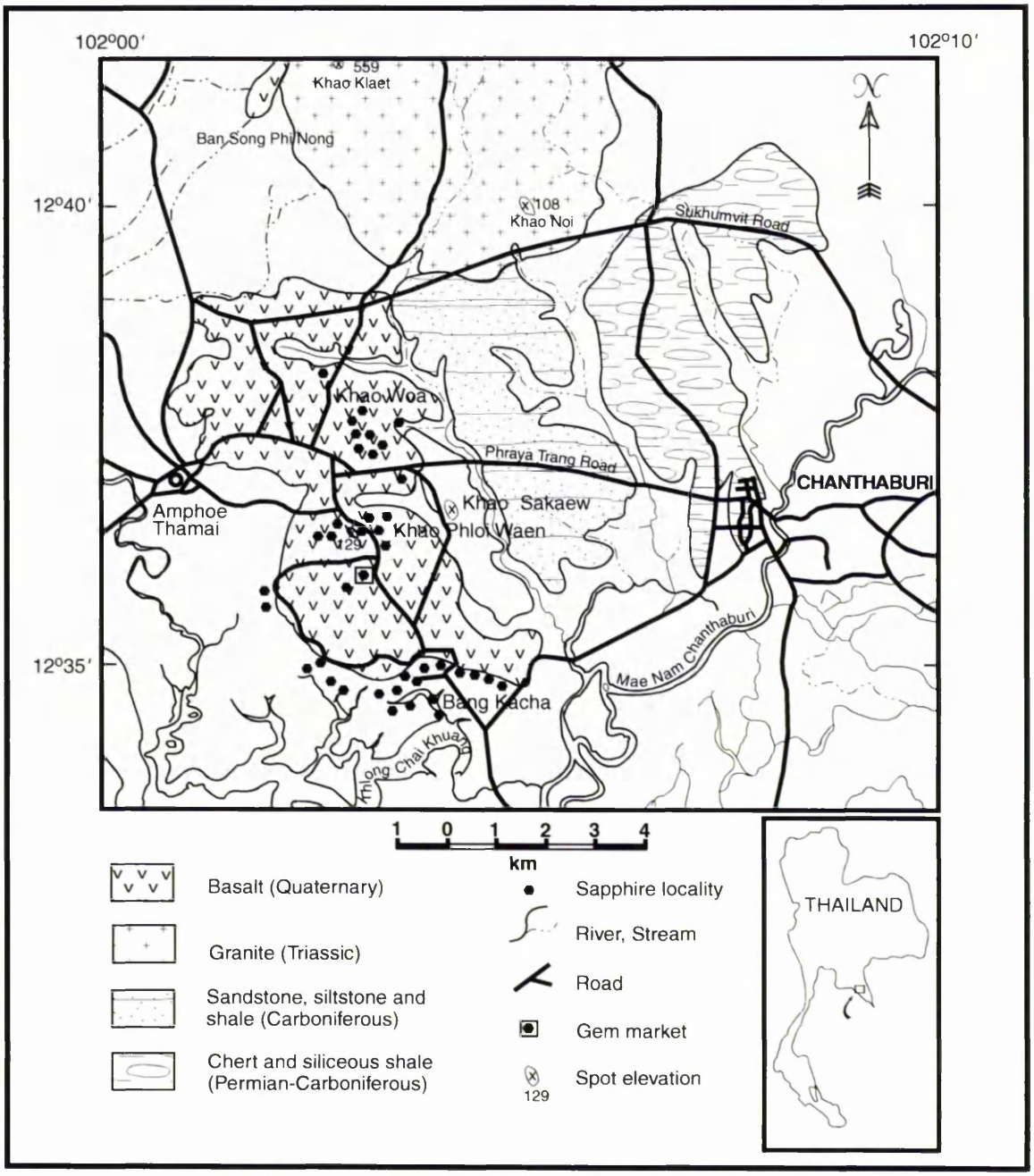

Figure 4.12 Geological map showing locations of sapphire deposits in the first zone (zone of western region of Chanthaburi province) (After Vichit, 1992; geological map modified from Tansathien *et al.*, 1976).

The Zone between Chanthaburi and Trat Provinces

This zone is in the area of Amphoe Khlung, Chanthaburi province and Amphoe Khao Saming, Trat province (Figure 4.13). Corundum deposits occur at many localities such as Bo Welu, Ban Sai Khao, Tok Phrom, Ang Et, Ban Chak Lao (Sak Lao) and Khao Noi (at Amphoe Khlung) and at Bo I Rem, Na Ta Mi, Khong Phaya and Bo Na Wong (at Amphoe Khao Saming). Most of these corundum deposits are confined to or near alkali basalt flows; however, on the south of the zone no basalt flow remains except at Wat (Temple) Muang Kao Saen Tum at Bo Na Wong where there is a plug-like body of basalt with well developed columnar jointing. In addition to basalt, Permian-

Carboniferous rocks (tuffaceous sandstone, shale, and siltstone) outcrop in the northern part of this zone, while Carboniferous rocks (shale, siltstone, and chert) outcrop at Khong Phaya and Bo Na Wong to the south (Sivabovorn *et al*, 1976).

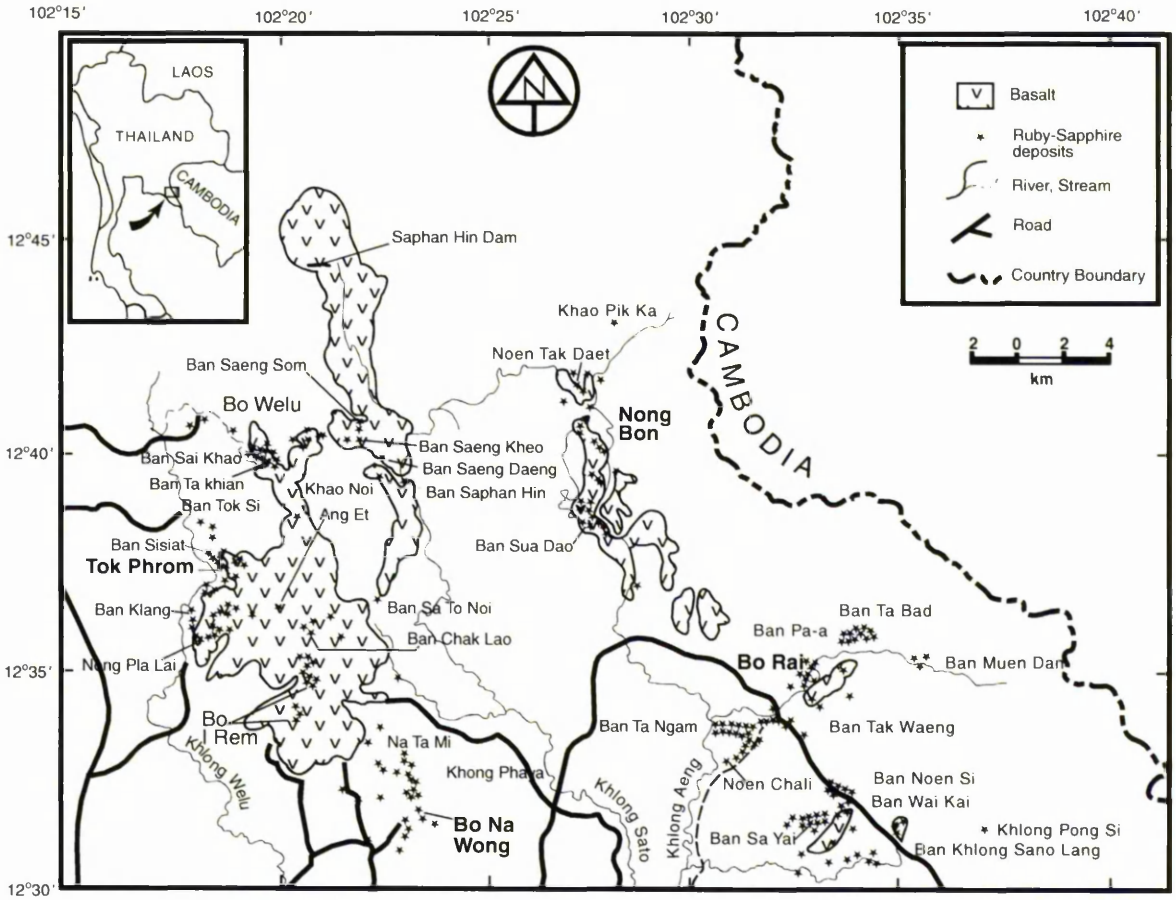

Figure 4.13 Map showing locations of ruby and sapphire deposits and distribution of basalts in the zone between Chanthaburi and Trat provinces and the zone of Trat province (After Vichit, 1992).

The corundums found in this zone include blue and green sapphires as well as rubies. The proportion of ruby and sapphire in each area varies according to the location. For instance Bo I Rem yields almost 100 % blue and green sapphires; Na Ta Mi, Khong Phaya and Bo Na Wong yield about 100% of rubies; Bo Welu and Ban Sai Khao yield 60-70% of rubies and 30-40% of sapphires. The corundums in this zone are generally found in the soil of weathered basalt or are associated with stream gravels. They can be found from the surface to a depth of about 10 m. In a few areas corundums can be found at a depth of up to 40 m. The thickness of the mineral layer is approximately 30 cm. to 1 m. Associated minerals are zircon, ilmenite, magnetite and (very rare) garnet (Vichit, 1992).

The Zone of Trat Province

This zone is situated in the areas of Bo Rai and Nong Bon, Trat province. The locations of the gem deposits in Trat are shown in Figure 4.13. The basalts crop out in an area of Triassic rocks (siltstone, mudstone, tuffaceous sandstone, agglomerate and conglomerate lenses) (Sivabovorn *et al.*, 1976). Ruby deposits at Bo Rai, 35 km north to north-west of Trat, occur at Ban Ta Bad, Ban Ta Ngam, Ban Noen Chali, Ban Sa Yai, Ban Noen Si, Ban Wai Kai and elsewhere. Vichit (1987) stated that the Bo Rai area, basalt outcrops occur at Bo Rai village (from Ban Khlong Yo to Ban Na Yai), Ban Sa Yai and Ban Wai Kai (or Ban Thung Chuk Chan). The outcrops are generally low hills, about 40-60 m above mean sea level. Almost all of basalts have weathered to reddish brown or lateritic soil, but well-developed columnar joints in basalt can be observed at Chedi Sano, 700 m north-east of Ban Khlong Sano Lang. The rubies and small amount of sapphires of the Bo Rai area are found in eluvium, alluvium, and residual basaltic soil. The depth of mineral layer varies from place to place. In general, rubies are recovered from depths of between 2 m and 10 m.

The ruby deposits of Nong Bon, 40 km east of Chanthaburi, occur at Khao Pik Ka, Noen Tak Daet, Nong Bon, and Ban Sua Dao. The rubies are found in residual basaltic or lateritic soil and alluvial gravels in the present stream, which is developed in the nearby basaltic terrain. The mineral layer is at depths ranging from 3 to7 m and never greater than 10 m. The associated minerals are ilmenite, magnetite, pyrope-almandine garnet, and pyroxene. Garnet and pyroxene are also found as the xenocrysts embedded in basalt.

The colours of rubies in this zone are generally pinkish red, rose red, and intense red but rubies from Nong Bon have rather dark, purple red colour. The rubies from Bo Rai may contain fractures enabling themselves to be classed as the lower quality rubies called "Lai Thai". Associated minerals found in this area are quartz (rock crystal), ilmenite, magnetite, garnet, and pyroxene, whereas zircon occurs rarely (Vichit, 1987; Vichit, 1992).

4.3.8 Summary

The thickness of overburden and corundum-bearing layers and corundum varieties found at each locality are summarized in Table 4.2.

Table 4.2 Thickness of overburden and corundum-bearing layers and corundum varieties found in alluvial deposits in Thailand and Democratic People's Republic of Laos.

Locality		Overburden (m)	Gem-bearing layer (m)	Corundum variety
Ban Huai Sai near Chiang Khong		na	na	Light and dark blue
Ban Nong, Nam Cho and Sop Prap, Lampang		0 - 2.2	0.2 - 1.3	blue, dark blue, greenish blue or dark brown, brown with asterism
Phrae and Sukhothai	Phrae	1.0 – 7.0	0.3 – 1.0	various shades of blue with small quantity of green, yellow and star sapphires
	Sukhothai	0.2 - 2.0	0.3 – 1.0	
Wichian Buri, Phetchabun		0	0 - 2.0	blue and greenish blue, (dark tone), Yellow
Bo Phloi, Kanchanaburi		3.0 – 15.0	5.0	various shades of blue, near colourless of different colours, sheen, yellow and purple sapphires, and ruby
Ubon Ratchathani - Si Sa Ket		0.5 – 3.0	0.1 - 0.5	mainly blue and green, rubies in trace amount
The zone of western region of Chanthaburi province	Khao Wua, Khao Phloi Waen	3.0 – 8.0	0.3 – 1.0	blue, green, and yellow as well as a combination of these colours, star sapphires
	Bang Kacha	2.0 – 4.0	0.1 – 0.8	
The zone between Chanthaburi and Trat provinces		0 - 10.0	0.3 - 1.0	blue and green sapphires as well as rubies
The Zone of Trat province	Bo Rai	2.0 – 3.0 or 6.0 - 10.0	na	rubies, blue sapphires in trace amount
	Nong Bon	3.0 – 7.0	na	rubies

na = not available

CHAPTER 5
SURFACE FEATURES OF THAI CORUNDUM

5.1 Introduction

Surface feature is a physical property investigated for corundum samples in this study in addition to colour, size and crystal morphology which are given in Appendices 7-1 and 8-1. Surface features can be used to help interpret the history of transit of corundum from its origin to the deposit from which it has been mined.

The surface features of a corundum grain reflect processes at two stages in its history:
(i) corrosion by disequilibrium resorption or chemical etching by the enclosing basaltic magma during transport of the grain from the Earth's interior to the surface, and
(ii) sedimentary reworking processes in the alluvium after the corundum was freed from its basalt host by the chemical weathering and physical disaggregation of the latter.

According to Coenraads (1992) and Krzemnicki *et al.* (1996), surface features of corundum caused by interaction with the magma include, for example, triangular etch features, hillocks, spongy features, and randomly oriented needle-like patterns. Abrasion and fracturing of the surface indicates that mechanical impact processes operated during erosion of the basalt and subsequent transport of the corundum grain into the alluvium deposit.

5.2 Method and technique

Rough corundum samples (ca 0.5 cm across) were selected from Ban Huai Sai, Democratic People's Republic of Laos and several localities in Thailand. They were washed in clean water, and glued on to stubs, and left to dry prior to coating with gold using the sputter-coating process. Gold, with its high atomic number (Z=79), yields secondary electrons efficiently resulting in a sharp secondary electron image (SEI) of the sample surface. Being a good electrical conductor, it also enables the charges that would otherwise built up on the sample due to electron bombardment to drain off to earth (Trewin, 1989; Reed, 1996: 181-182).

The JEOL JSM 6400 SEM (scanning electron microscope) was used to view the surface features of the samples. To obtain the secondary electron image, the SEM was set up with an accelerating voltage of 15 or 20 kV, a probe current of <0.5 nA and a working

distance of 13-25 mm. Note that the ideal working distance for SEI is 15 mm, (suitable for a thin section) but in this study several values of working distance were used depending on the height of the samples. The working distance is the distance between the top of the sample holder and the lens. If too small a value of working distance is used for a thick sample, the lens can be damaged by the sample and the image may not be clear. A single-lens reflex camera connected to the SEM was used for taking photographs of the images.

5.3 Results

Not all samples of corundum show clear evidence of their transportation history. Most of them have smooth and unaltered crystal faces or parting surfaces. Representative surface features are shown in this section. Surface features found in this study that can be attributed to etching by basaltic magma include triangular surface features, hillock and needle-like patterns. Surface features, after the release of the corundum by the disintegration of the enclosing host rock, attributable to:

i) the abrasion and collision include smooth surfaces, scratch, abraded surfaces and conchoidal fractures, and

ii) the reaction with the soil solution includes spongy appearance which has the products of clay mineral and quartz grains left on the surface. Images and descriptions of these surface features are presented in Figures 5.1-5.8.

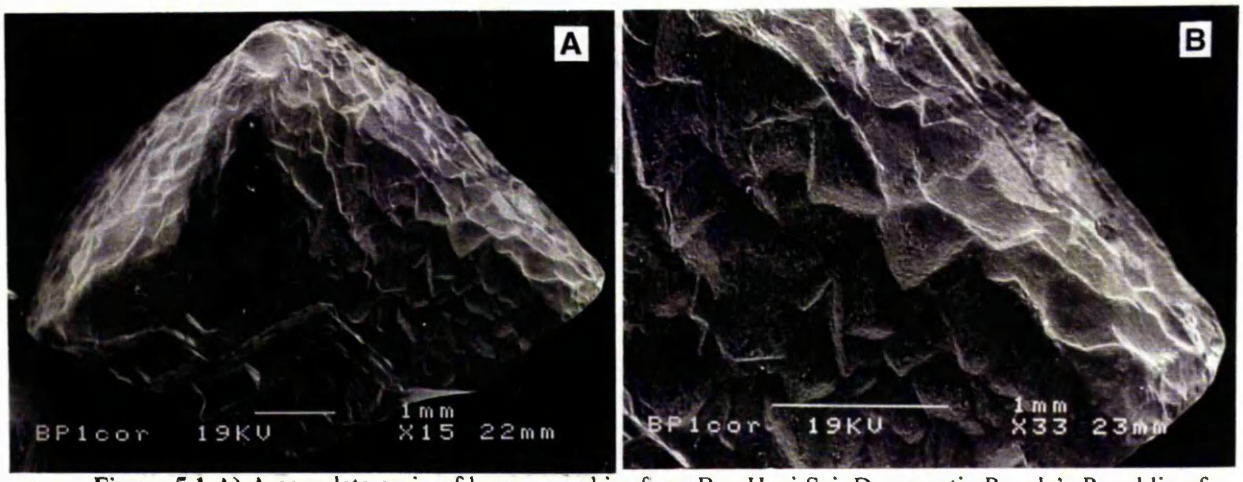

Figure 5.1 A) A complete grain of brown sapphire from Ban Huai Sai, Democratic People's Republic of Laos showing the indented triangular features caused by etching by the magma during transportation to the Earth's surface. **B)** Detail of the triangular pits reveals the trigonal symmetry of the grain.

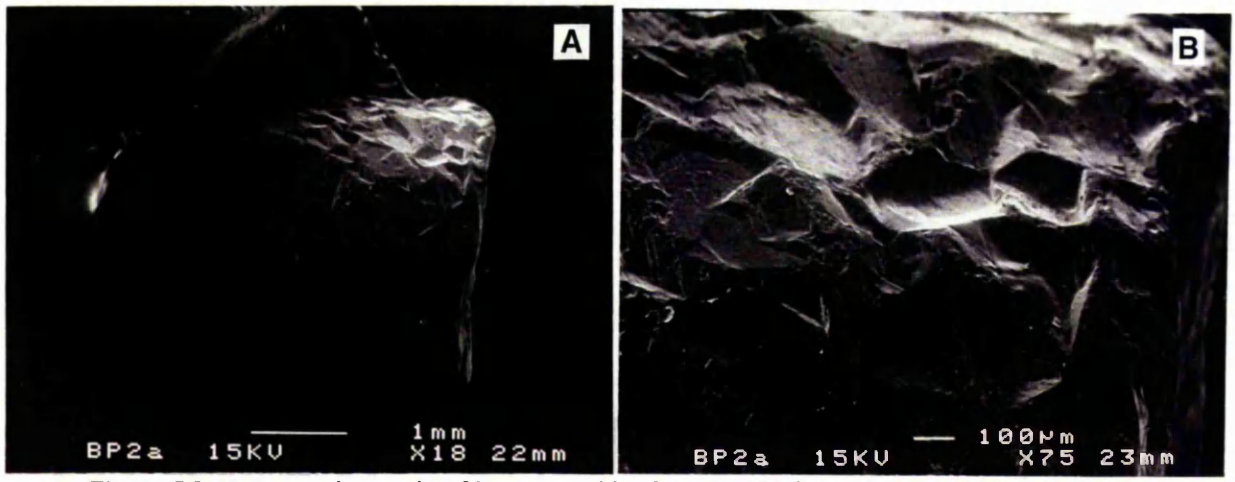

Figure 5.2 A) A complete grain of brown sapphire from Bo Phloi showing indented triangular features caused by etching by the basaltic magma. **B)** Detail of triangular pits reveals the trigonal symmetry of the grain; scratches due to abrasion in the alluvium can be seen at the centre top and left centre of the image.

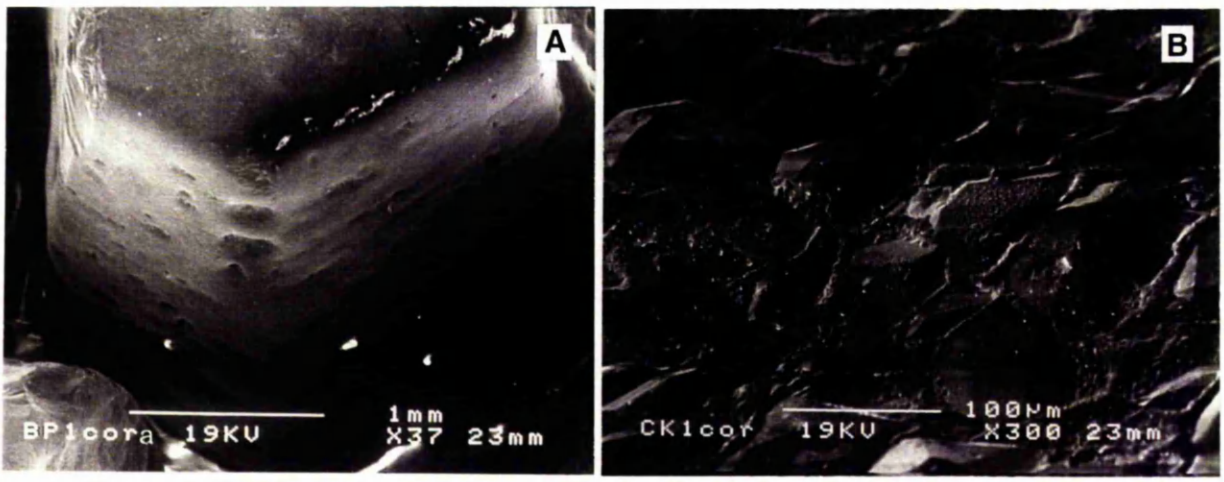

Figure 5.3 A) Oblique view of a brown sapphire from Bo Phloi showing hillocks on the pyramid faces, caused by etching by the basaltic magma. **B)** Roof-like hillocks on the surface of a blue sapphire from Ban Huai Sai, Democratic People's Republic of Laos.

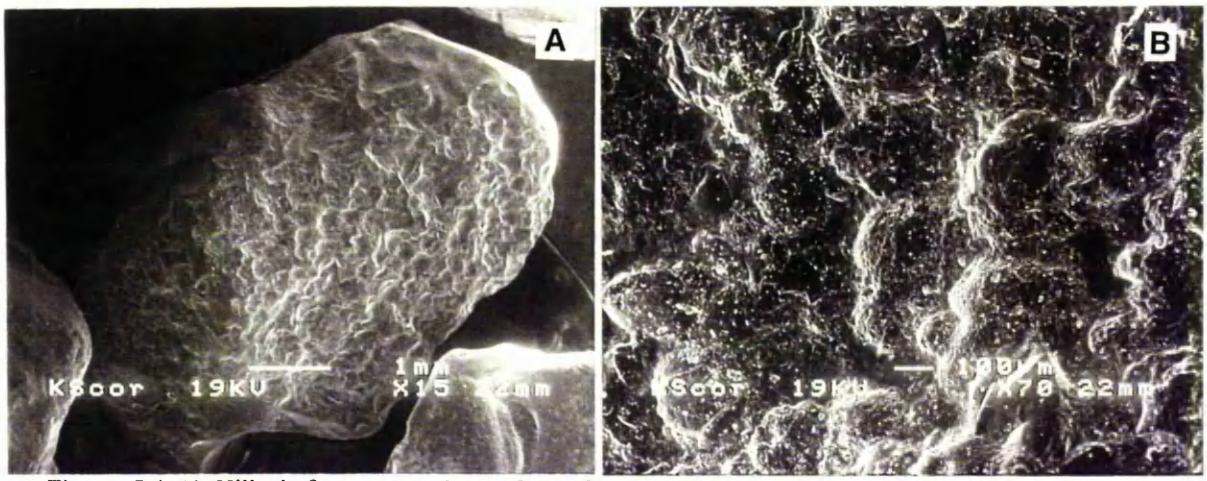

Figure 5.4 A) Hillock features on the surface of a dark blue sapphire sample from Khok Sam Ran showing wavy channel-like depressions. **B)** Detail of the feature in A) showing tiny terrace patterns on the slopes of the hillocks.

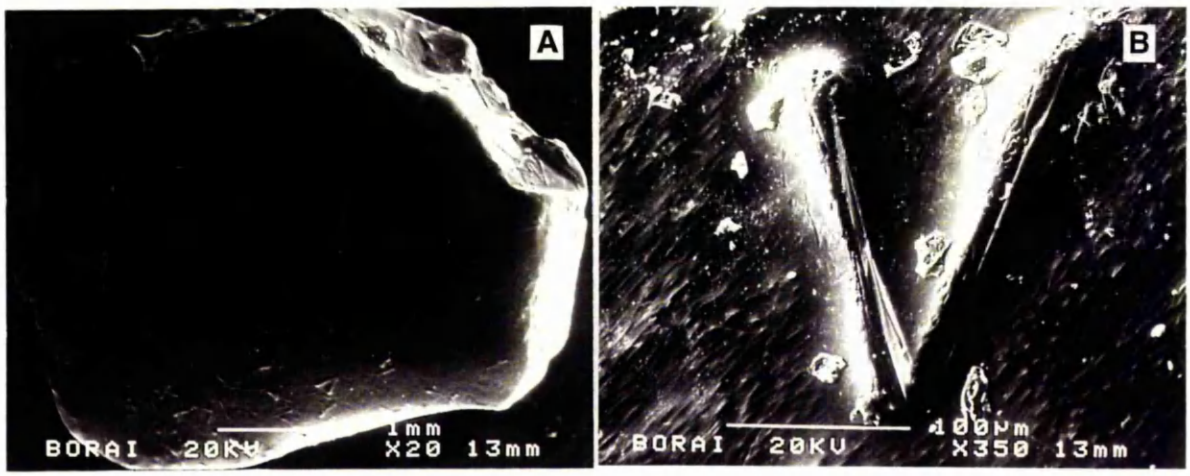

Figure 5.5 A) Ruby from Bo Rai showing a randomly oriented needle-like pattern on its surface. **B)** A part of the area of A), showing the plagioclase-like laths rising above the surface.

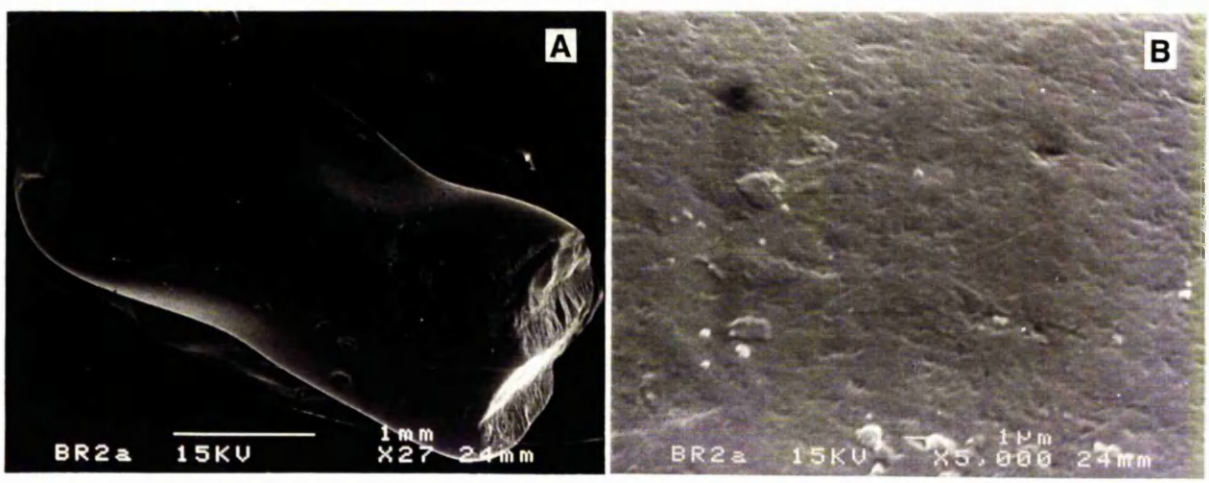

Figure 5.6 A) Ruby from Bo Rai showing a generally smooth surface, conchoidal fracture (top left), scratches and a broken end caused by abrasion and impact after physical separation from the enclosing basalt. **B)** Detail of the surface in A).

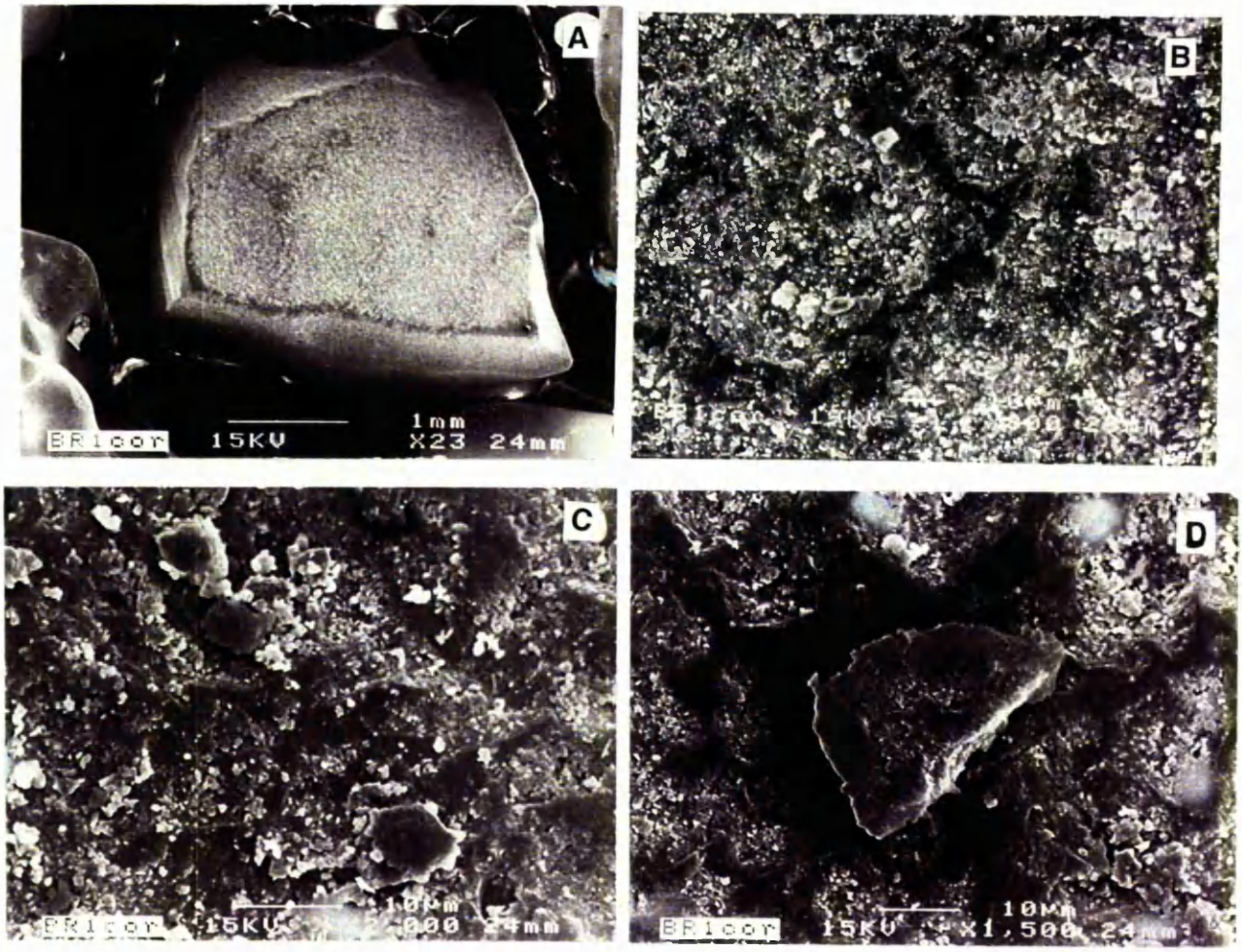

Figure 5.7 A) A complete grain of a blue-purple sapphire sample (BR1cor) from Bo Rai. **B)** Detail of the spongy surface. **C)** The tiny platy grains of Si-Al rich mineral (?clay mineral) originated by the reaction between corundum and soil solution during the corundum was in alluvium. **D)** One of the quartz grains on the surface of corundum sample BR1cor.

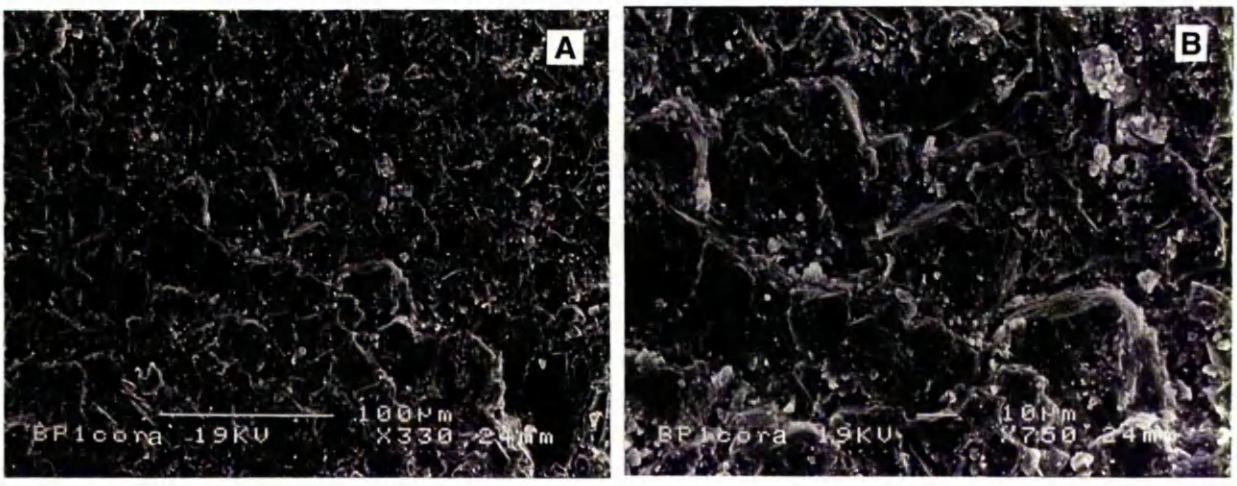

Figure 5.8 A) Spongy appearance in association with cracks and triangular hillocks with a sharkskin-like pattern on the surface of a blue-green sapphire from Bo Phloi. **B)** Detail of the features in A).

Triangular indented features are found on the surfaces of the brown sapphire samples from Bo Phloi (BP1cor, BP2a) (Figures 5.1 and 5.2). The size range of the triangular pits is in the order of 200-500 μm across. According to Coenraads (1992), these triangular features are typical of etched surfaces at a low angle to the [0001] axis of corundum.

Hillocks are found on the surface of the brown sapphire sample from Bo Phloi (BP1cora), the blue sapphire sample fron Ban Huai Sai (CK1cor) and the dark blue sapphire sample from Khok Sam Ran (KScor) (Figures 5.3, A, B and 5.4 respectively). Sample BP1cora has a euhedral form showing pinacoid and hexagonal pyramid faces. The hillocks exist on the hexagonal pyramid faces. Sample CK1cor shows sub-triangular hillocks with pockmarks in certain areas (e.g. centre of the image). Sample KScor shows depression channels with a wavy appearance indicating heavy dissolution. The slope of the depressions are tiny terraces revealing the growth layers of the corundum.

A randomly oriented needle-like pattern is found on the surface of the ruby sample BORAI from Bo Rai (Figure 5.5). The long prismatic needles measure about 10x100 μ m. This sculpture-like feature comprises needles rising up above the corundum surface. The needles occur in pairs or groups showing a 'V' or 'X' arrangement. Whereas the corundum surface contains numerous tiny lineaments aligned in one direction (Figure 5.5, B). This feature can be compared to a similar feature found on the surface of a sapphire from Cyangugu district, Rwanda (Krzemnicki, *et al.*, 1996). One possible interpretion of this is that plagioclase feldspar laths covered the surface of the corundum in the ascending alkali basalt, protecting the corundum partly from corrosion; the plagioclase laths were later eroded leaving their scars as casts on the surface of the corundum.

Surface features of corundum caused by abrasion and impact during sedimentary processes after release of the corundum from the enclosing basalt are found in several samples. For example scratches are found in BP2a (Figure 5.2, B, centre top and left centre) and the abraded crests of the triangular pits in this sample can be seen in the centre of the image. Conchoidal fractures are found in the bottom right of KScor (Figure 5.4, B) and top left of BR2a (Figure 5.6, A).

A spongy appearance characterises the surfaces of the blue-purple sample BR1cor from Bo Rai and the blue-green sapphire sample BP1cora from Bo Phloi (Figures 5.7 and 5.8). This feature is always associated with cracks. The spongy appearance in this study is not the effect of the interaction between the magma and corundum surface. It was the chemical weathering whilst the corundums were in the alluvium, giving the products of Si-Al mineral platelets (? clay minerals) and quartz grains left on the corundum surface (Figure 5.7, C and D). Note that the SEM-EDS was used to identify these two minerals. The Sample BP1cora has spongy appearance associated with cracks and triangular hillocks. The hillocks have a sharkskin-like pattern (Figure 5.8).

The surface features found in this study for different localities are summarized in Table 5.1.

Table 5.1 Summary of surface features found in Thai corundums.

Locality \ Feature	1. interaction with magma			2.interaction with other materials in alluvium		1+2
	Triangular pit	Hillock	needle-like pattern	Water worn	Spongy	Spongy + Hillock
Ban Huai Sai	√	√		√	√	
Den Chai				√		
Khok Sam Ran		√		√		
Bo Phloi	√	√		√		√
Bang Khacha				√		
Bo Rai			√	√	√	
Nong Bon				√		

5.4 Conclusion

Surface features of corundums in this study (triangular, hillock and needle-like patterns) suggest that Thai corundums originated from the environment other than the environment of origin of their basalt host. Corundums were transported to the Earth's surface by the magma of their basalt host.

CHAPTER 6
CATHODOLUMINESCENCE OF CORUNDUM

6.1 Introduction

Cathodoluminescence can be used to indicate qualitatively the characteristics of corundum in terms of its trace element impurities. The principles and techniques used to characterise this property of corundum, and the results obtained will be discussed.

6.2 Principles of cathodoluminescence of minerals

Cathodoluminescence (CL) is the process whereby emission of visible radiation (light) from the surface of certain substances occurs when they are bombarded by energetic electrons. Cathodoluminescence is a form of luminescence, which is categorized into several forms, according to the nature of the primary excitation. The basic process of luminescence involves the excitation of the electrons of certain atoms in a substance to a state of higher energy. The external energy is supplied by electron impact (for CL), by photons, by X-rays or by other forms of energy. The electron remains in the excited level only briefly and then returns to a state of lower energy, emitting a photon in the process. The electron may return directly to the ground state or else may return via one or more intermediate states (Marshall, 1988: 1-4).

From Marshall (1988) and Miller (1989) the luminescence centre can be outlined as follows. There are two general forms of luminescence centre (the domain in the material where the luminescence occurs): intrinsic and extrinsic centres. ***Intrinsic centres*** include lattice imperfections (e.g. poorly ordered structure, radiation-damaged structure). Intrinsic CL requires detailed crystallographic and solid state physical investigation and is not discussed in detail in this study. ***Extrinsic centres*** are related to the parent medium during crystallization such as impurities in surfaces, regular lattice and interstitial sites, or compositional variation between different parts of a crystal. The *extrinsic centre* responds to electron excitation in three different ways:

-***Activator centre (Activator)***, which shows high luminescence when its electron returns to the ground state, e.g. Mn^{2+} in calcite.

-***Trap centre***, in which the electron (of the centre) trapped in the level between the ground state and excited state requires additional energy to raise it to the excited state and produces luminescence on returning to the ground state,

-***Quencher centre***, in which little or no luminescence is emitted when the electron returns to the ground state (e.g. Fe^{2+} in calcite). If a quencher centre is present in the substance, it causes new closely spaced energy levels to be set up so that the electron can easily return to the ground state with the emission of a succession of low-energy photons (infrared) or by losing energy to the lattice as heat.

6.3 Method and technique

Samples used in this study include 232 corundum grains and 19 polished sections of the corundum-bearing rocks from Thailand and from elsewhere of the world. They were chosen from the polished sections prepared for electron microprobe analysis (Chapter 8). Details of sample preparation are described in full in section 8.3.2. Unlike the samples for the electron microprobe, the samples were not coated with carbon for CL analysis.

A cold cathode luminescence stage (CITL, Model 8200 mk3) mounted on an optical microscope with an attached camera, was used to study the CL of the corundum samples. A polished section is placed on a glass slide supported on an X-Y stage. The polished section can be moved any direction across the microscope stage. The electron beam from a cold cathode electron gun bombards the sample obliquely. The stage is connected to a CL-electronic control unit for controlling the gun voltage, gun current and vacuum system. Viewing may be transmitted light, CL, or a combination of the two, observed through a lead glass window, which absorbs X-radiation. The equipment was used in a darkened room (Miller, 1989).

The observation conditions used in this study include a gun voltage of 19 kV to 25 kV, a gun current of 200 μA to 300 μA, a pressure of 0.16 Torr to 0.20 Torr (1Torr = 10^{-5} bars).

6.4 Cathodoluminescence characteristics of corundum

Several previous studies have been published on the CL characteristics of corundum. Crookes (1879, cited in Marshall, 1988) found that ruby glowed red CL and sapphires showed bluish-grey light. Leverenze (1968) reported that Cr is the activator in corundum. Chinner *et al.* (1969) saw red CL in natural corundum. Dudley (1976) also saw red CL in some samples. Gaal (1976-77) studied CL in gemstones such as ruby and

diamond. Ponahlo and Koroschetz (1985, cited in Marshall, 1988) found that the natural rubies showed a relatively small increase in CL intensity with electron beam power, whereas synthetic rubies showed much greater increase.

The Cr^{3+} in corundum gives two red bands of CL at about 694 and 692 nm and synthetic corundum displays a signal about ten times more intense than that shown by the natural gem (Leverenze, 1968; Solomonov, *et al.*, 1996).

The CL results of this study are displayed in Figures 6.1-6.7. The description for each sample is given with each figure.

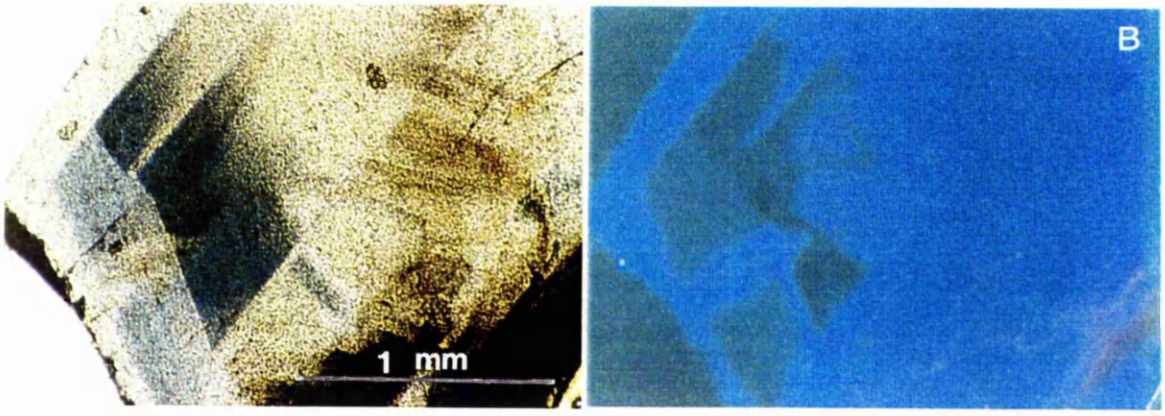

Figure 6.1 A) Polished section of a greenish blue sample of sapphire from Ban Huai Sai, Democratic People's Republic of Laos (CKEP40) showing blue colour patches under ordinary transmitted light. **B)** Sample in A under the CL microscope, showing dull blue luminescence in general but nonluminescence in the area of the blue patches, indicating that the patches contain higher Fe^{2+}. [Conditions for CL: 19 kV, 300 μA, 0.2 Torr, Kodak film, ISO 400, 5 minutes of exposure time].

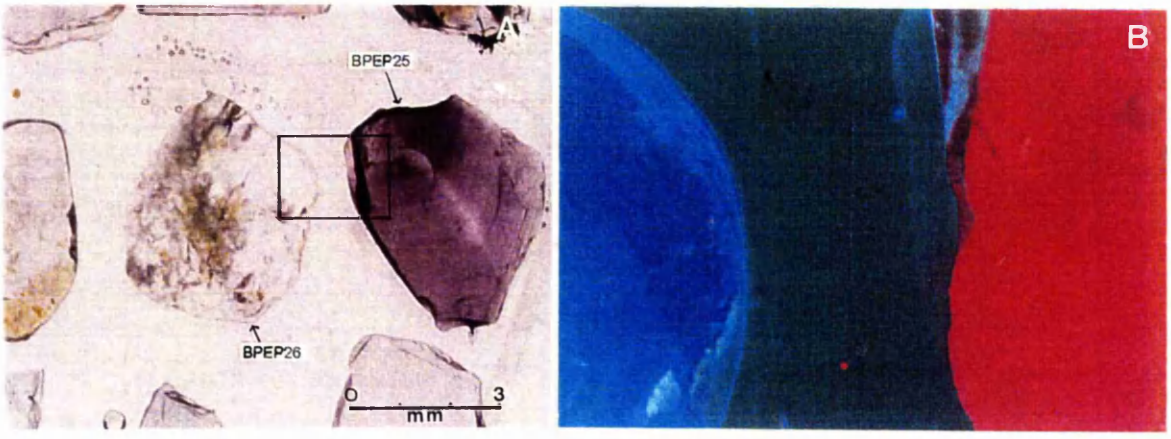

Figure 6.2 A) Polished section of corundum samples from Bo Phloi; sample BPEP25 has a brown-violet appearance in its rough grain and sample BPEP26 is pale orange-yellow in its rough grain. **Note**, the rectangular window indicates the field of view for B. **B)** The CL appearance of samples in A, indicating that sample BPEP25 contains high Cr^{3+}content, sample BPEP26 showing dull blue luminescence. [Conditions for CL: 19 kV, 300 μA, 0.2 Torr, Kodak film, ISO 400, 4 minutes of exposure time].

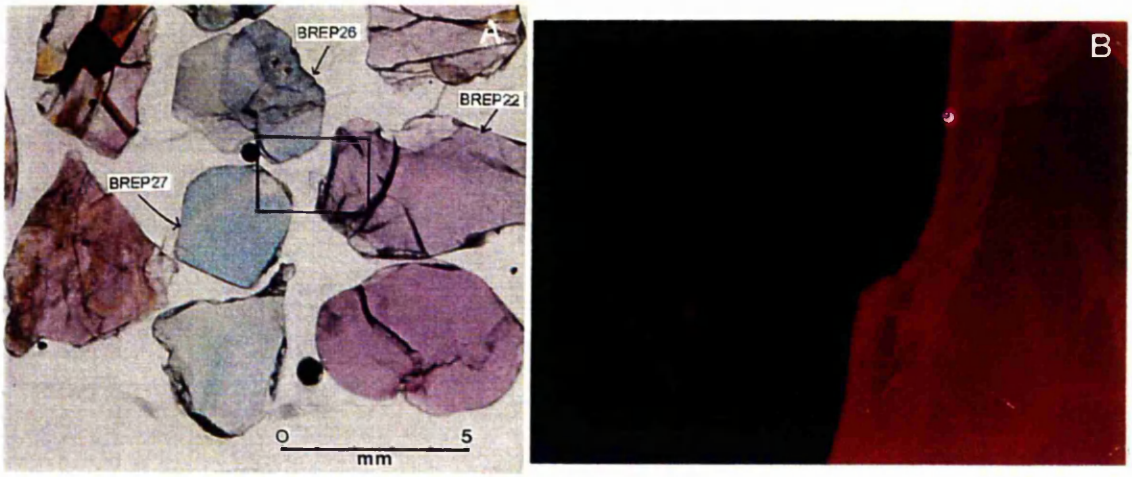

Figure 6.3 A) Polished section of corundum samples from Bo Rai showing their natural colour under an overhead light source. **Note**, the rectangular window indicates field of view for B. **B)** Blue sapphire samples (BREP26 and BREP27) show nonluminescence indicating higher contents of Fe^{2+} whereas ruby sample BREP22 shows bright red luminescence indicating its higher content of Cr^{3+}. [Conditions for CL: 25 kV, 140 μA, 0.16 Torr, Kodak Ektachrome, ISO 400, automatic exposure].

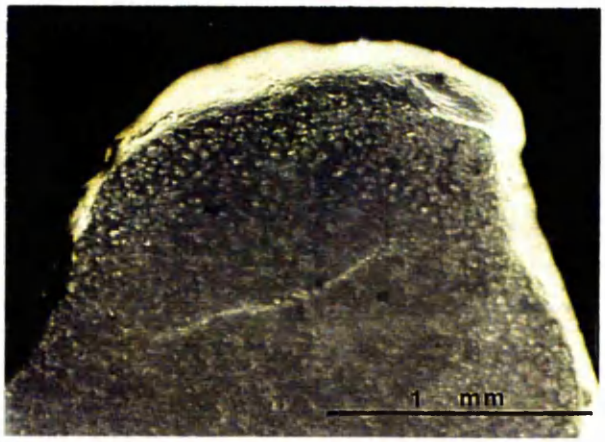

Figure 6.4 Polished section of a yellow sapphire sample from Nam Yun (NYEP24) showing yellow-green luminescence of CL. [Conditions for CL: 19 kV, 300 μA, 0.16 Torr, Kodak Ektachrome, ISO 400, automatic exposure].

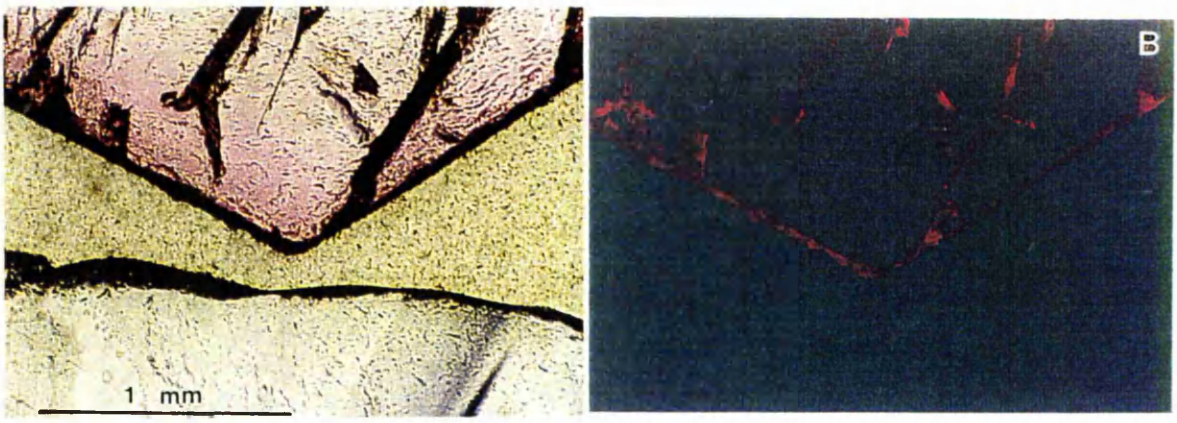

Figure 6.5 A) Polished section of a ruby sample from Mong Hsu, Myanmar (MSEP6, top) and a blue-green sapphire sample from Bang Kacha, Thailand (BKCEP15, bottom) under ordinary transmitted light. **B)** The CL appearance of samples in A); MSEP6 shows faint red luminescence, whereas BKCEP15 shows nonluminescence indicating a high Fe^{2+} content. [Conditions for CL: 15 kV, 380 μA, 0.2 Torr, Kodak film, ISO 400, automatic exposure].

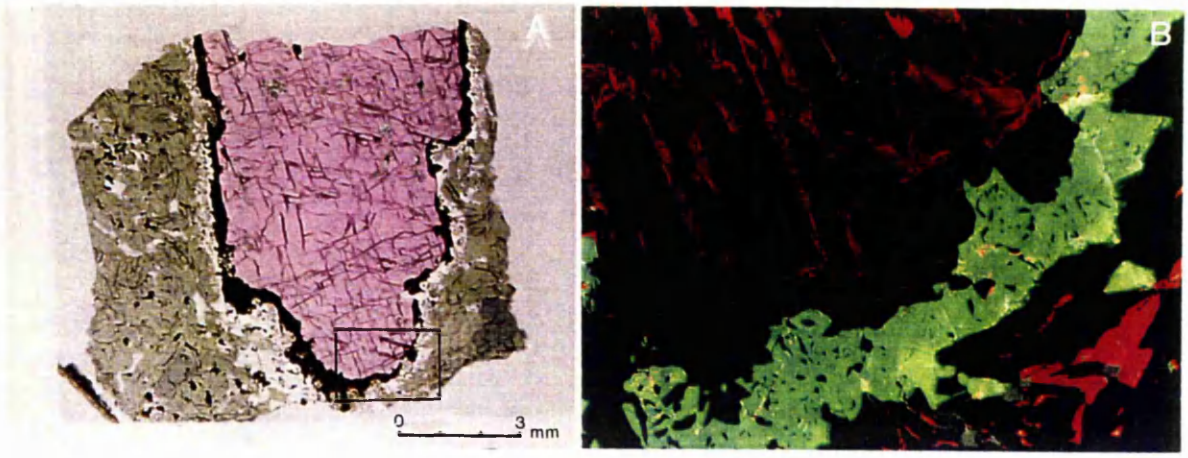

Figure 6.6 A) Polished section of ruby (seen as purple colour in photo) in ultramafic rock from South India (Δ793) under an overhead light source. **Note**, the rectangular window indicates field of view for B. **B)** CL appearance of a part of an area in A); ruby shows weak red luminescence except in the areas of cracks and partings, which are bright red luminescent. [Conditions for CL: 19 kV, 320 μA, 0.2 Torr, Kodak film, ISO 400, 3.20 minutes of exposure time].

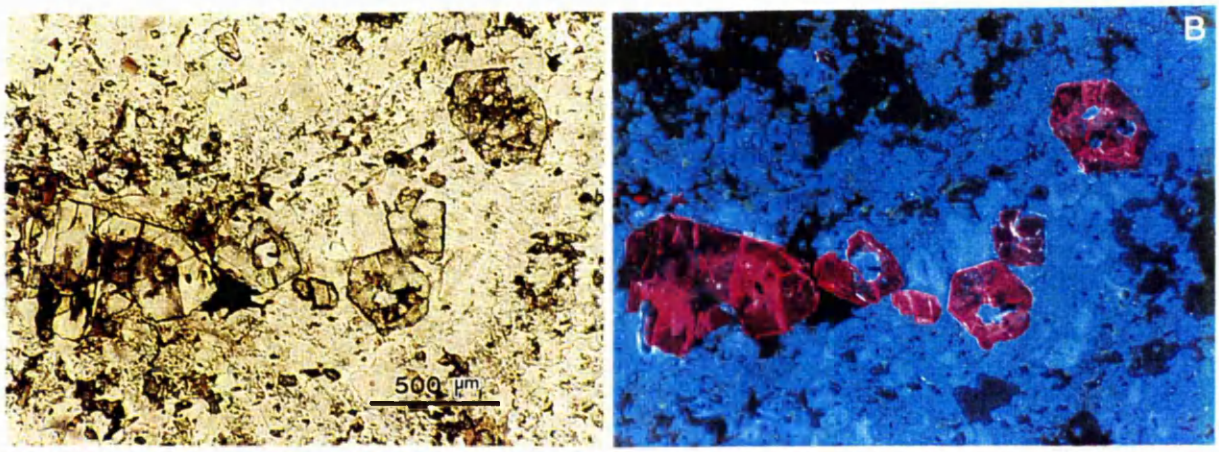

Figure 6.7 A) Crystals of corundum (large high-relief, euhedral colourless grains) in pelitic-hornfels from Belhelvie, Scotland (Δ1192) set in mainly cordierite (colourless) and biotite (reddish brown), under ordinary transmitted light. **B)** The CL appearance of the corundum crystals in A) is bright red luminescent. This indicates that the crystals contain relatively high Cr^{3+} contents. [Conditions for CL: 19 kV, 320 μA, 0.2 Torr, Kodak film, ISO 400, automatic exposure].

6.5 Summary

Most rubies show bright red CL luminescence due to the Cr^{3+} activator. Certain rubies show faint or weak red CL luminescence probably due to the extrinsic impurities (that is not only Cr but also other cations occurring in the structure). The Fe^{2+} in rubies could serve as a quench centre causing the ruby to show less strong luminescence.

Blue sapphire shows dull blue CL luminescence. Some blue sapphires are nonluminescent. The main cause of the CL appearance of sapphires is likely to be a quench centre, Fe^{2+}, in their structure. Yellow sapphire can exhibit yellow-green luminescence (for example sample NYEP24, Figure 6.4) and the reason for this is not known.

6.6 Conclusion

Cathodoluminescence of corundum can be used to qualitatively estimate contents of certain trace elements in corundum. For example, the samples showing very bright red luminescence contain relatively high Cr^{3+}. In sapphires, the higher Fe^{2+} contents lead to darker luminescence.

CHAPTER 7
SPECTROSCOPY OF CORUNDUM

7.1 Introduction

Spectroscopic methods used to investigate the corundum samples in this study include optical, infrared and Raman spectroscopy. Optical (ultraviolet and visible) spectroscopy gives the information about the electron transitions in the electronic field as well as the electron transitions between trace element impurities in corundum. Infrared and Raman spectra are related to the phenomena of molecular vibration. The main aim of this chapter is to find out whether there are any characteristics (fingerprints) of corundum samples in terms of their spectra. The phenomena investigated in this chapter are related to the parts of electromagnetic spectrum given in Figure 7.1. The optical spectroscopy is discussed first and followed by the infrared and Raman techniques. In each case, the theory of the technique is summarised and spectra are given for Thai sapphires and rubies.

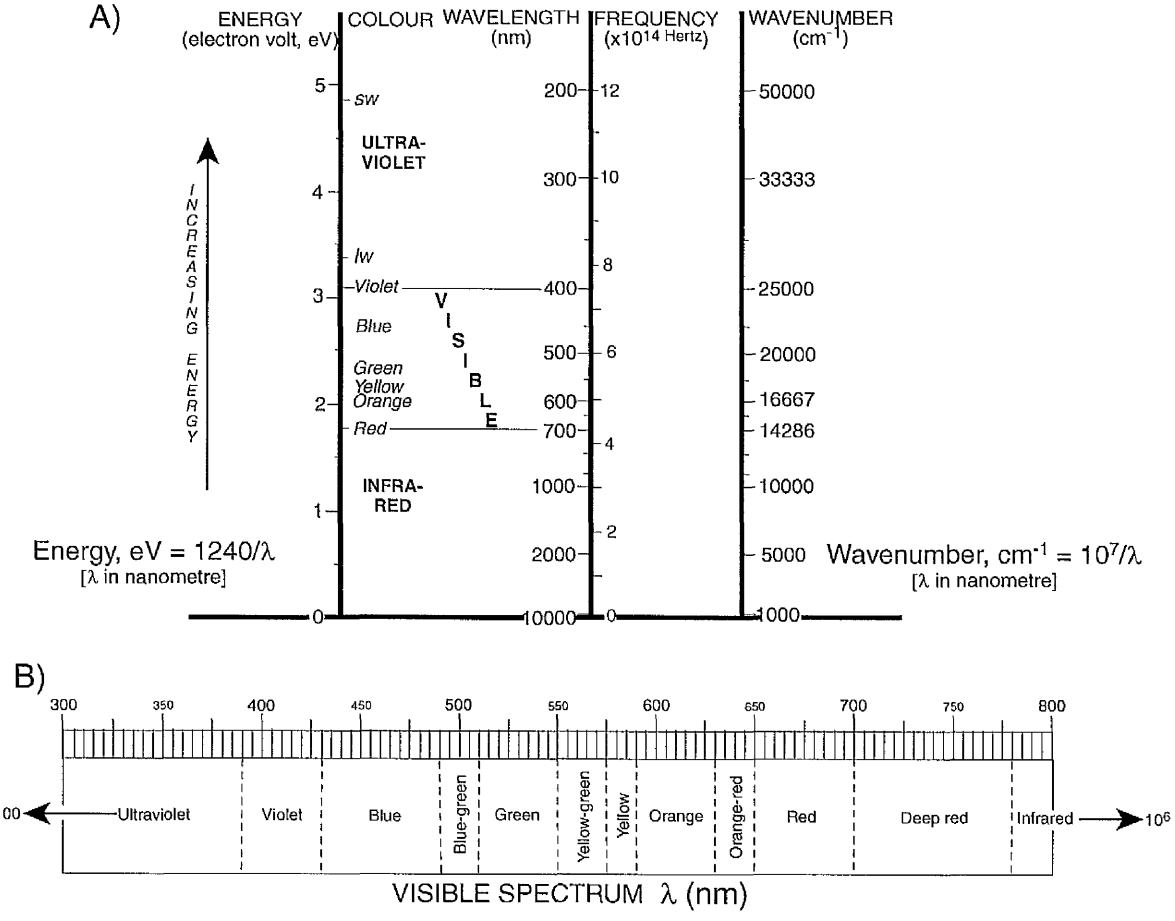

Figure 7.1 A) Portion of electromagnetic spectrum in the range of ultraviolet, visible and infrared wavelengths with different units for describing the spectrum (Nassau, 1983). B) Visible spectrum with wavelength (λ) scaled in nanometre (nm). Sharp boundaries between the colours cannot be observed and there are no sharp cut-offs at the violet and red ends (Webster, 1998).

7.2 Optical spectroscopy

Chemically, corundum is made up of AlO_6 complexes, with a structure shown in Figure 7.2. The oxygen atoms are approximately in the arrangement of hexagonal close packing. Between the oxygen atoms there are sites for cations octahedrally co-ordinated by six oxygen ions, but only two-thirds of the available positions are filled. A group of three oxygen atoms form a common face of two neighbouring octahedra and thus the groups are linked to a pair of Al ions (Deer *et al.*, 1996: 536).

When the Al^{3+} in corundum is substituted by a transition ion, for example Cr^{3+}, Fe^{2+} or Ti^{4+} as the trace elements, the resulting complexes are often coloured as the transition ions have unpaired electrons in their 3*d* shell. The transition elements have a partly filled *d* or *f* electron shell (Burns, 1970: 9). The production of colour in corundum by trace element impurities has been explained by two theories, crystal field (ligand field) theory, and charge transfer transition theory. A variety of unstable colour centres of unknown structure is another cause of colour in certain yellow sapphires (Schmetzer and Bank, 1981). The colour of corundum is determined by the residual spectrum transmitted to the eyes of the observer after certain wavelengths of white light are absorbed by the mechanism of excitation of the electron of the transition element ions in the corundum structure. Pure (colourless) corundum absorbs no wavelength of white light. The spectrum fingerprint of an individual corundum sample reflects the energy used to excite the electron of the transition ions in the corundum structure. The energy (eV) of the absorbed spectra can be observed in form of the UV-visible spectra.

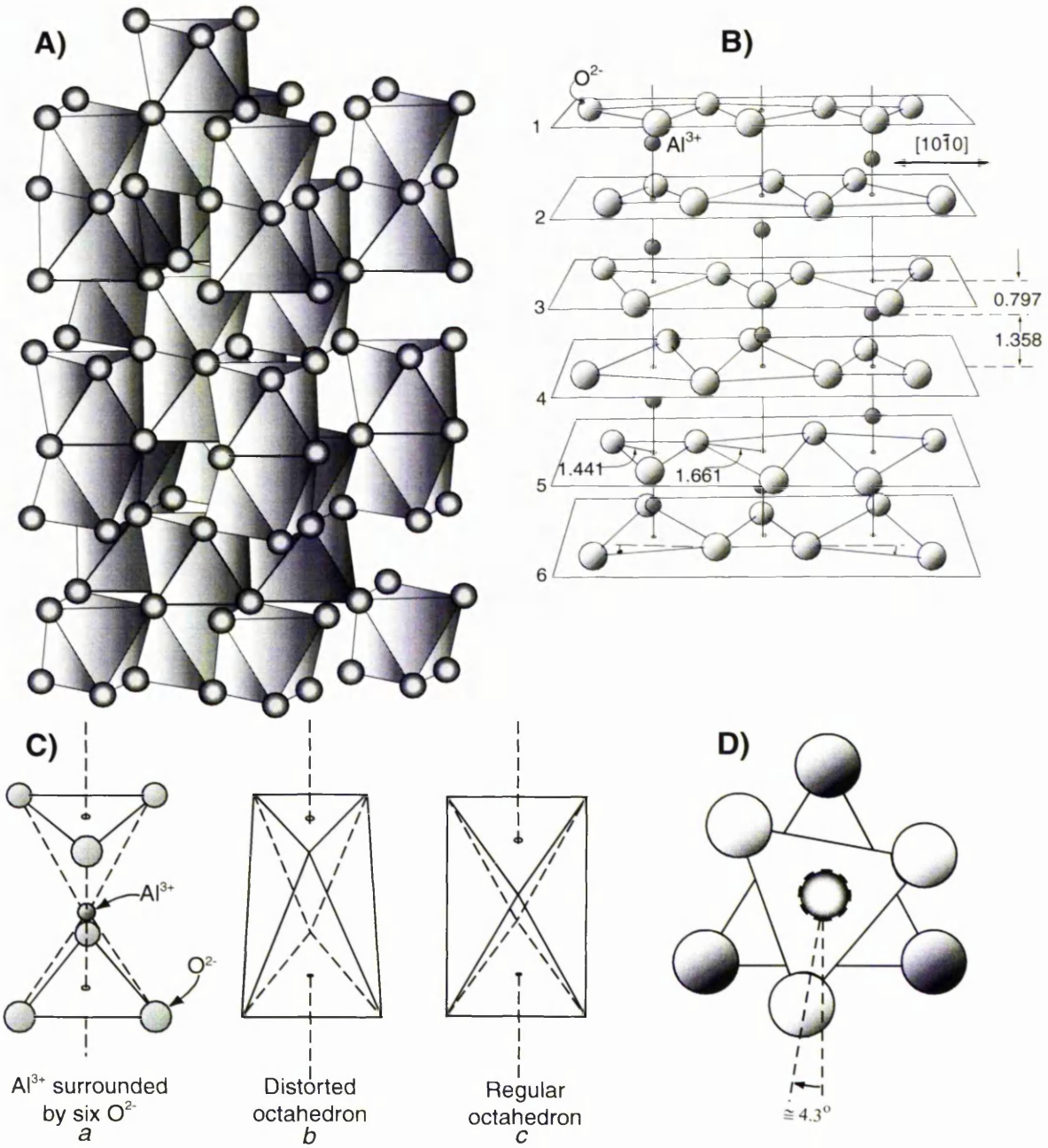

Figure 7.2 The structure of corundum (Al_2O_3) is approximately one of hexagonal close packing of oxygens. **A)** Polyhedral representation of octahedral co-ordination of O^{2-} ions (small spheres) about Al^{3+} (not seen in this model). Pairs of octahedra share faces (face-sharing octahedra) i.e. two neighboring AlO_6-octahedra share a common face forming "groups" of 2Al and 9O atoms. Two thirds of the octahedral coordinated interstices are filled with cations. The oxygen ions are coordinated by distorted tetrahedra of four cations (Beran, 1991; O'Keeffe and Hyde, 1996: 222). **B)** Portion of corundum lattice. Oxygen ions are found on the equally spaced planes but aluminium ions are between the planes. Aluminium ions occur at sites about one thirds or two third of the distance between two planes of oxygen ions. Certain distances in structure are given in Å (Geschwind & Remeika, 1961). The Al-O distances are 3x1.97Å and 3x1.86Å (Newnham and De Haan, 1962). **C)** Distorted octahedral oxygen ligand environment around an Al ion shown in two different ways (*a* and *b*) compared to the regular octahedron, *c* (Nassau, 1983: 80). **D)** Cr^{3+} ion (centre) is surrounded by six neighbouring oxygen ions in ruby. Three oxygen ions in the upper layer rotated ca 4.3° from a regular position, viewed along trigonal crystal axis (optic axis) (Shinada *et al.*, 1966 in Henderson and Imbusch, 1989: 421).

7.2.1 Crystal field theory and colour in ruby

The theory is applied to ruby in terms of the distribution of 3*d* electrons of Cr^{3+} in the octahedral field of ruby. However, V^{3+} or Fe^{3+} ions in octahedral co-ordination can be the colour agents in ruby but they make only a minor contribution (Schmetzer and Bank, 1981; Fritsch and Rossman, 1988). The 6 oxygen ions (at the octahedral corners) surrounding the Cr^{3+} are called ligands (ions directly attached to a metal ion, which are regarded as bonded to it); (Orgel, 1966:14). The ligands create an electrical field about the central transition ion, so called the *ligand field* or *crystal field* (Figure 7.3).

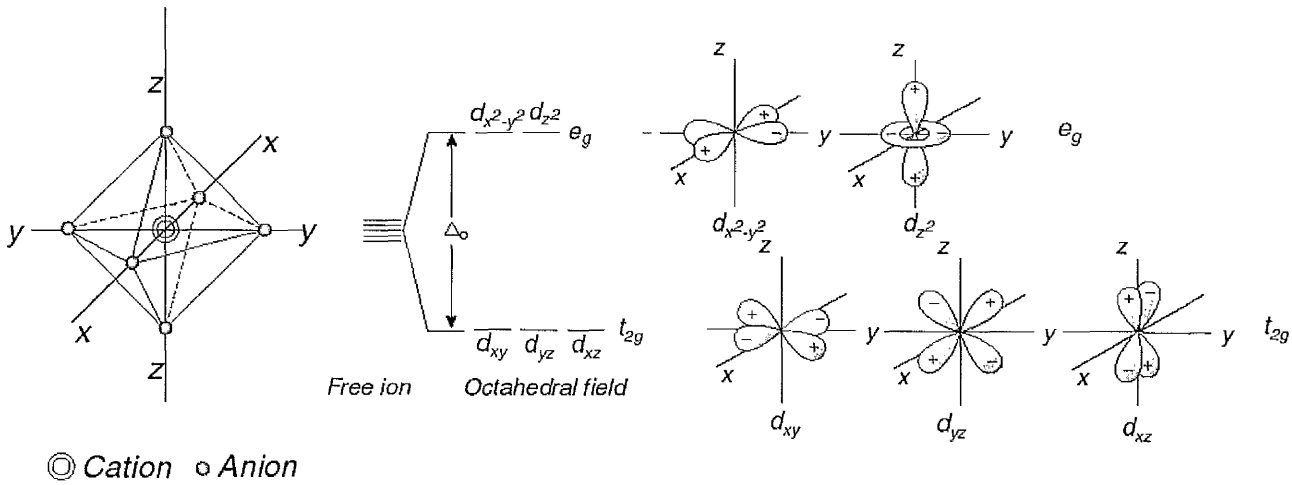

Figure 7.3 Energy level diagram showing the crystal field splitting of the 3*d* orbitals of a transition metal ion in the octahedral crystal field of oxygen ions. There are two main groups of energy separation (t_{2g} and e_g) occur and each of them may be separated into additional energy levels in a distorted co-ordination site. Such separation corresponds to visible and infrared spectra (Burns, 1983).

The five d-electron probability 'clouds' (d orbitals) within each electron 'shell' of an atom (each of which can accommodate a maximum of two electrons of opposite spin) are designated d_{xy}, d_{yz}, d_{xz}, $d_{x^2-y^2}$ and d_{z^2} and have the geometries shown in Figure 7.3. When the atom is in octahedral coordination, these five orbitals are not all at the same energy level. The five orbitals are classified into two different categories (t_{2g} and e_g) according to their different energy levels; this is called a splitting pattern. The electrons in the t_{2g} orbital are at a lower energy level and therefore more stable than those in e_g. The electrons in the e_g orbitals pointing towards negatively charged oxygen ions suffer more repulsion and have higher energy than the electrons in the t_{2g} orbitals which are further away from the oxygen ions (Loeffler and Burns, 1976). The size of the energy

gap Δ_0 ('crystal-field splitting parameter', $_0$ signifies an octahedral crystal field) between the t_{2g} and e_g levels can be measured by recording the UV-visible spectrum of the complex (Burns, 1970: 17-19; Lee, 1977: 429). Corundum has 63% ionic character, which means that the electron pairs making up the bonds spend more of the time near the oxygen ions than they do near the aluminium or chromium ions. The distribution of the electronic charge gives rise to a comparatively strong electric field, which is called the crystal field or ligand field. The colour of ruby results from the substitution of chromium ions (Cr^{3+}). Each chromium ion has three unpaired electrons. The electronic configuration of a neutral Cr atom is $1s^2$, $2s^2$, $2p^6$, $3s^2$, $3p^6$, $3d^5$, $4s^1$. If Cr donates 3 electrons to oxygen ions, then three electrons will be left in the d shell, written as $3d^3$. Cr^{3+} has inner shells of electrons (Nassau, 1983). The lowest possible energy of these three unpaired electrons is in a ground state designated as $^4A_2$ and they lodge in the t_{2g} orbitals (d_{xy}, d_{yz} and d_{zx}) (Burns, 1970:19). When a chromium ion is immersed in a crystal field, three excited states of its unpaired electrons absorb energies in the visible range. There is a complicated spectrum of excited states. Five excited states are designated ^2E, $^4T_2$, $^4T_1$, $^2T_2$, $^2T_1$. These symbols as well as $^4A_2$ are the symmetry labels from group theory, which are used to described the behaviour of wave functions when subjected to these symmetry operation (Kettle, 1969: 56; Shriver and Atkins, 1999).

The spin-allowed $^4A_2 \rightarrow {}^4T_2$ and $^4A_2 \rightarrow {}^4T_1$ transitions for octahedrally co-ordinated Cr^{3+} give peaks at 18000 cm^{-1} (555 nm) and 25000 cm^{-1} (400 nm) (Figure 7.4). The weak peaks at 14430 cm^{-1} (693nm) and 15110 cm^{-1} (662 nm) originate from spin-forbidden transitions $^4A_2 \rightarrow {}^2E$ and $^4A_2 \rightarrow {}^2T_1$ (Burns, 1985; Henderson and Imbusch, 1989).

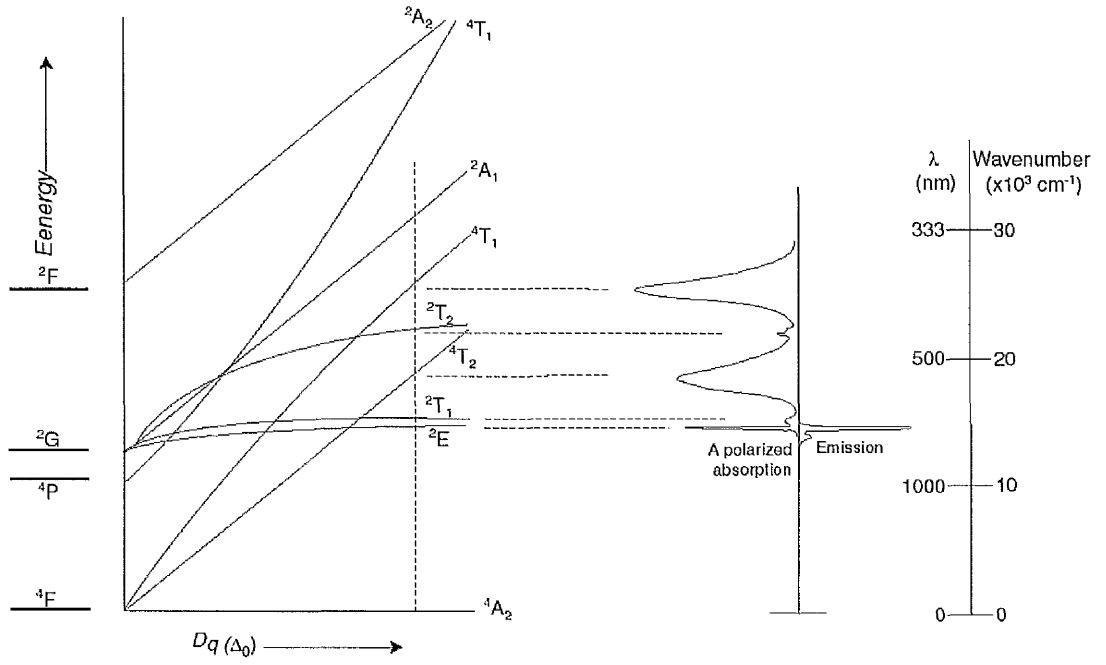

Figure 7.4 Simplified diagram plotted of energy against Dq or Δ_0. The vertical broken line represents Cr^{3+} in the octahedral crystal field of corundum. The absorption spectrum of ruby due to the transition of electron from $^4A_2$ to higher energy levels is shown on the right. The luminescence due to the electron turns down from ^2E to $^4A_2$ is also shown as emission peak (Henderson and Imbusch, 1989: 413). **Note**: terms ^{2}G, ^{4}P and ^{4}F are represented free atom (free ions) terms, which split to the molecular terms (spectroscopic terms) when electrons are in crystal field. For example ^{4}F splits into $^4T_1 + {}^4T_2 + {}^4A_2$. The superscript 4 is for 3 unpaired electrons. The spectrum is averaged from o-ray and e-ray spectra.

In fact, each of the ^4T energy levels splits into two sub-levels ($^4A_1$ and ^4E for $^4T_1$; $^4A_2$ and ^4E for $^4T_2$) due to the trigonally distorted octahedral site symmetry of the chromium environment. If the ruby is examined with polarized light the colour will change as the ruby is rotated. This phenomenon is called pleochroism. When the plane of vibration ($\vec{E}$ or electric vector) of the polarized light is parallel to the optic axis of ruby, the extraordinary ray (e-ray) will be seen as an orange-red colour. This is because of the transitions $^4A_2 \rightarrow {}^4A_2$ (of the $^4T_2$) and $^4A_2 \rightarrow {}^4A_1$ (of the $^4T_1$). They peak at 18300 cm^{-1} (546 nm) and 24800 cm^{-1} (403 nm) respectively. On the other hand, the ordinary ray (o-ray) with a purple–red colour will be seen if $\vec{E}$ is perpendicular to the optic axis. This is in accordance with the transitions $^4A_2 \rightarrow {}^4E$ (of $^4T_2$) and $^4A_2 \rightarrow {}^4E$ (of $^4T_1$). They peak at 18100 cm^{-1} (553 nm) and 24500 cm^{-1} (408 nm) respectively (Nassau, 1983: 85-87; Burns, 1985:85) (Figure 7.5).

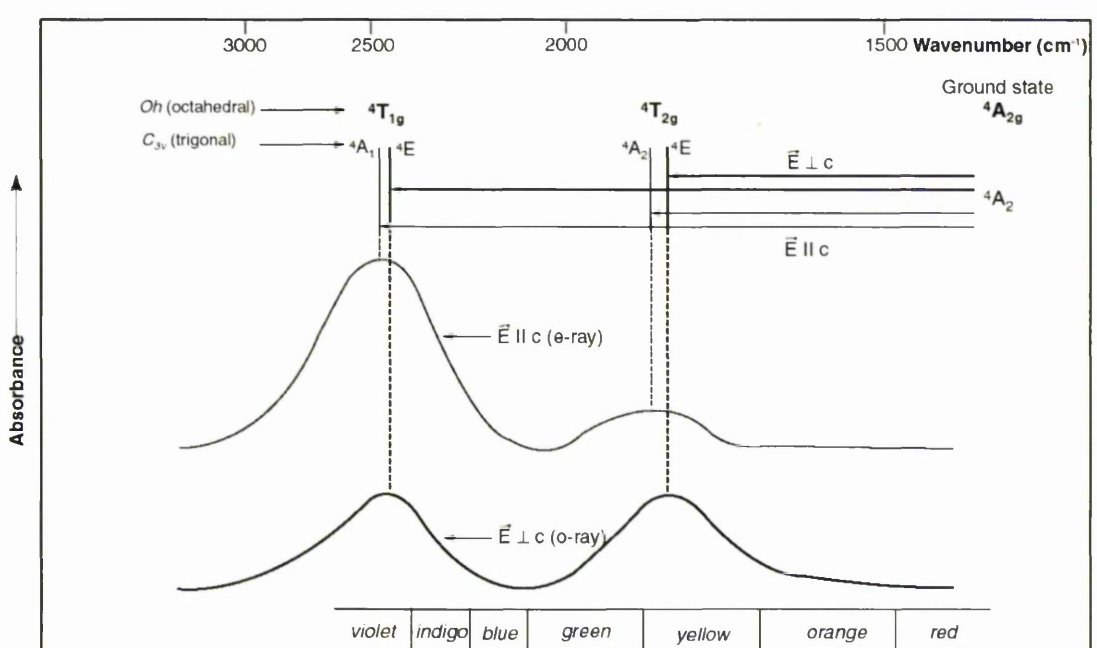

Figure 7.5 Absorption spectra of ruby. The spectra originate from crystal field transitions within Cr^{3+} replacing Al^{3+} in corundum. The spectra differ slightly for polarized light ($\vec{E}$ ||c and $\vec{E}$ ⊥c), observed as pleochroism, due to splitting of additional energy levels in trigonal symmetry. Peaks corresponding to the transitions ${}^4A_2 \rightarrow {}^2T$ and ${}^4A_2 \rightarrow {}^2E$ are not shown (Modified from Burns, 1983).

According to Nassau (1980) selection rules forbid a direct transition from the ground state to the ${}^2E$ level, but two of the ${}^4T$ levels can be entered from the ground state. The energies associated with these transitions correspond to wavelengths in the violet and in yellow-green regions of the spectrum. The levels are not sharp lines; broad bands of wavelengths can be absorbed. When white light passes through a ruby, the violet and yellow-green components are absent but all reds are transmitted with some blue giving ruby a deep red colour with a slightly purple cast. The amount of Cr impurity required for an intense red ruby is as high as 1– 3 % due to the forbidden transition resulting in a weak crystal field.

Because of the selection rules, electrons can return from the excited ${}^4T$ levels to the ${}^4A_2$ ground state only through the intermediate ${}^2E$ level. The initial transitions from ${}^4T$ to ${}^2E$ release small amounts of energy corresponding to infrared wavelengths (${}^4T_1 \rightarrow {}^2E$ releases 1.2 eV; ${}^4T_2 \rightarrow {}^2E$ releases 0.4 eV) (Figure 7.1). However, the drop from ${}^2E$ to the ground state gives rise to strong emission of red light. This phenomenon is called luminescence (e.g. fluorescence or cathodoluminescence). The luminescence consists of two very closely spaced lines, called R_1 and R_2 at 1.788 eV and 1.791 eV (693.5 nm

and 692.3 nm) respectively, due to a very fine-scale splitting of the ^2E level by distortions from octahedral symmetry (Nassau, 1983: 85) (Figure 7.4). This can be used to explain the cathodoluminescent phenomena in ruby in § 6.4.

In addition to the major peaks associated with Cr, Webster (1998: 80) stated that Cr^{3+} in corundum can give narrow peaks at 468.5 nm, 475 nm, 476.5 nm, 659.2 nm and 668 nm.

7.2.2 Charge transfer and crystal field transition in sapphires

Charge transfer (intervalence charge transfer, IVCT) is the motion of an electron from one transition-metal ion to adjacent sites and results in a temporary change in the valence state of both ions. This is produced by the absorption of light energy. In blue sapphire, there are two kinds of intervalence charge transfer. They are ***heteronuclear*** and ***homonuclear***.

Heteronuclear charge transfer involves two different transition-metal ions. Considering two adjacent face-shared octahedra in corundum (Figure 7.6, A), in the lower or ground state, iron and titanium exist as Fe^{2+} and Ti^{4+} and occupy the octahedra in substitution for $2Al^{3+}$ ($Fe^{2+}+Ti^{4+}\Leftrightarrow 2Al^{3+}$). When a Fe+Ti-bearing corundum is subjected to light, an electron of Fe^{2+} is excited and transfers to Ti^{4+} as the equation:

$$Fe^{2+} + Ti^{4+} \rightarrow Fe^{3+} + Ti^{3+}$$

The right-hand side has a higher energy than the left-hand side. The process consumes energy from the light of about 2 eV (Figure 7.6, B) by absorbing yellow and red light (Figure 7.7, A). This reaction can reverse when the excitation stops and the energy is released in form of heat. The absorption is the broad band from 17800 cm^{-1} (562 nm) to 14200cm^{-1} (704 nm) and the band is centred at 17000 cm^{-1} (588 nm) for $\vec{E} \perp c$. Green, blue and violet are blended and transmitted to the eye of the observer. The amount of Ti and Fe impurities required for a deep blue sapphire is as low as 0.01 (1/100) percent because this electronic transition is allowed by quantum considerations, giving rise to a strong energy of transition.

The Fe^{2+}-Ti^{4+} distance is 2.65 Å along the c axis direction (optic axis) but 2.79 Å along the direction perpendicular to the c axis, so pleochroism can be observed. When the plane of vibration ($\vec{E}$ or electric vector) of the polarized light is parallel to the optic axis

of blue sapphire, the extraordinary ray (e-ray) will be seen as a blue-green colour. Conversely, the blue or o-ray will be seen when $\vec{E}$ is perpendicular to the optic axis.

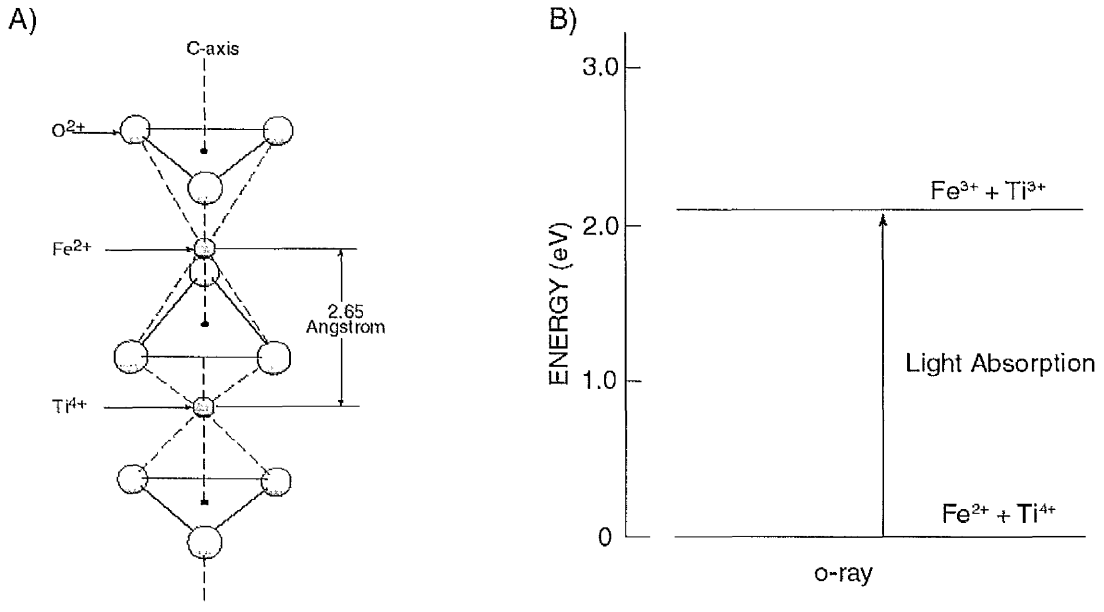

Figure 7.6 A) Two adjacent octahedral sites in corundum structure, containing Fe^{2+} and Ti^{4+} in blue sapphire. **B)** Transition of an electron from ground state to the excited state in blue sapphire, so-called intervalence charge transfer (IVCT) (Nassau, 1987).

Homonuclear charge transfer is relevant to one metal with two different states in two adjacent octahedral sites. In blue sapphire, iron can exist in two forms, Fe^{2+} and Fe^{3+}. An electron of Fe^{2+} in one site transfers to Fe^{3+} in another site, hence the sites are written as A and B respectively, as follows:

$$Fe_A^{2+} + Fe_B^{3+} \rightarrow Fe_A^{3+} + Fe_B^{2+}$$

The right-hand side has a higher energy than the left-hand side. This mechanism absorbs the energy from the electromagnetic spectrum in the near-infrared region at 11500 cm^{-1} (870 nm) (Figure 7.7, A).

In the ultraviolet region, the crystal field transition (d-d) of Fe^{3+} also occurs in blue sapphire. The peaks of Fe^{3+} in crystal field transition are near 26000 cm^{-1} or between 375 nm and 387 nm ($^6A_1 \rightarrow {}^4T_1(G)$) and 22200 cm^{-1} or 450 nm ($^6A_1 \rightarrow {}^4T_2(G)$) (Figure 7.7, B).

According to Webster (1998: 81), Fe peaks in corundum may be found at 460 nm and 470 nm in addition to the peaks mentioned above.

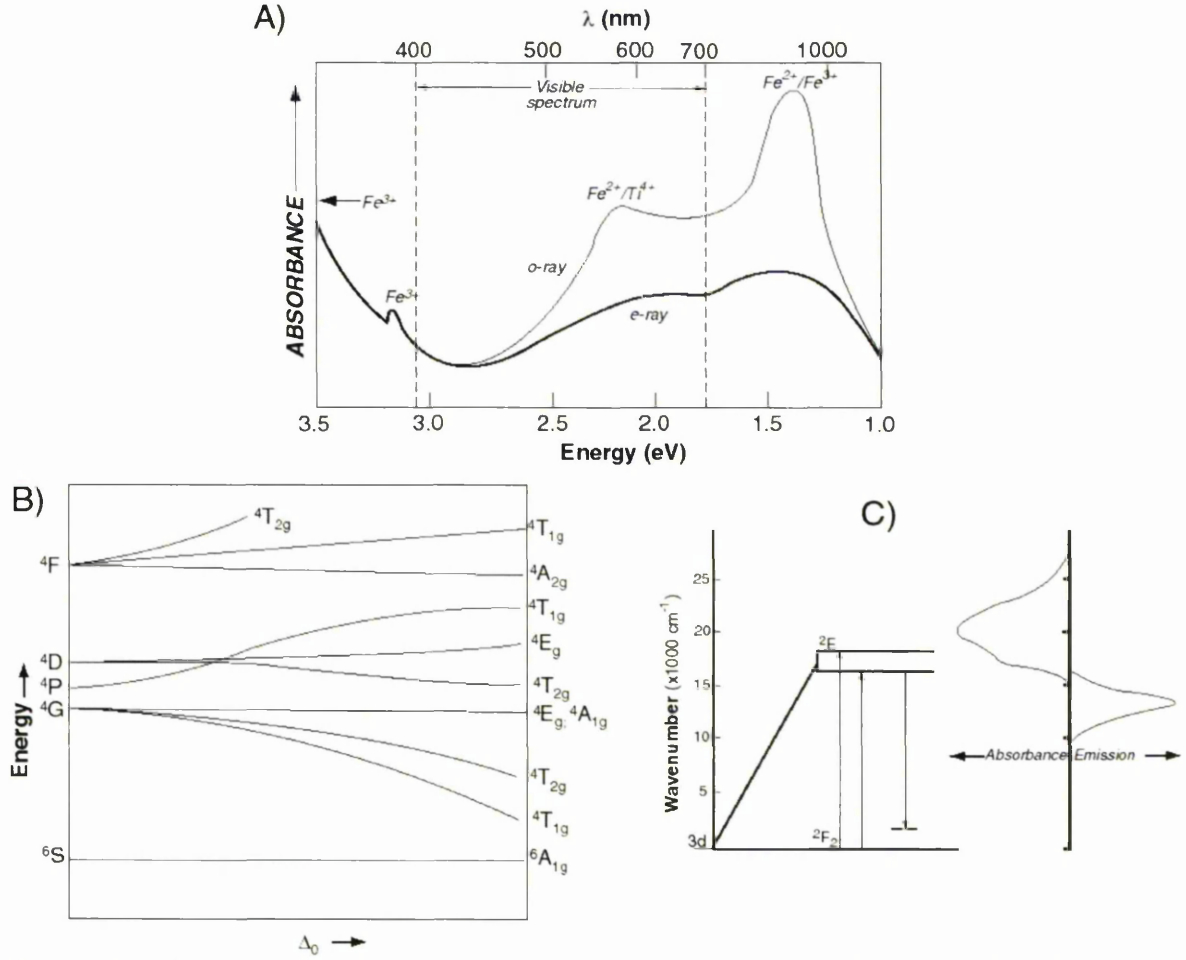

Figure 7.7 A) Spectra of blue sapphire showing the causes of absorption including crystal field transition of Fe^{3+} below 400 nm (in ultraviolet region), intervalence charge transfer (IVCT) of Fe^{2+}/Ti^{4+} in the visible region and IVCT of Fe^{2+}/Fe^{3+} in the near infrared region. Blue sapphire has dichroism blue (o-ray) and blue-green (e-ray) due to the different absorption in between 500 nm and 700 nm of the two rays (modified from Nassau, 1987). **B)** Diagram used to explain the energy levels of Fe^{3+} in corundum for electron transition in crystal field, $^6A_{1g} \rightarrow {}^4T_{1g}(^4G)$ and $^6A_{1g} \rightarrow {}^4T_{2g}(^4G)$ (see text) (Burns, 1985). **C)** The splitting of energy levels in the octahedral crystal field for Ti^{3+} in corundum. The corresponding absorption and emission (luminescence) spectra are also given (Henderson and Imbusch, 1989: 434).

7.2.3 UV-visible and near infrared spectra of corundum from previous work

The absorption bands in the UV-visible region of corundum samples were summarized by Schmetzer and Bank (1981) in Table 7.1 and the bands of corundums other than those mentioned above can be found from this table. For example, yellow sapphire has an absorption pattern similar to blue sapphire but the band of $Fe^{2+} \rightarrow Ti^{4+}$ IVCT is very weak due to a deficiency of Ti^{4+}. An exception is a yellow sapphire from Sri Lanka which has point defects (hole colour-centres), each of which has one missing electron or one extra electron. This may be caused by irradiation. These unpaired electrons may then become excited and absorb visible light (Hughes, 1997: 74). It should be noted that there are several trace elements present in natural corundums, so superposition of

bands may be encountered in a single sample. The centre position of the bands for any given trace element may vary from sample to sample.

Table 7.1 Absorption bands of natural corundum and their causes of colours (*Schmetzer and Bank, 1981*).

PART A: Absorption bands			
Notation	**Absorption band in cm^{-1} (*nm*)**	**Polarization ($\vec{E}$)**	**Assignment**
a	14500(*690*), 22200(*450*) 25800(*388*), 26600(*376*)	$\|c \approx \perp c$	Fe^{3+}crystal-field transition (d-d) and/or Fe^{3+}-pairs*
b	17880(*559*) 14300(*699*)	$\perp c > \|c$ $\|c \approx \perp c$	Fe^{2+}/Ti^{4+}-pairs
c	11500(*870*)	$\perp c > \|c$	Fe^{2+}-pairs or Fe^{2+}/Fe^{3+}-pairs
d	18450(*542*), 20300(*493*) 20500(*488*), 20620(*485*)**	$\|c > \perp c$ -	Ti^{3+} (d-d), $^2T_2 \rightarrow {}^2E$
e	18000(*555*) 18450(*542*)	$\perp c$ $\|c$	Cr^{3+} (d-d), $^4A_2 \rightarrow {}^4T_2$
	24400(*410*) 25200(*397*)	$\perp c$ $\|c$	Cr^{3+} (d-d), $^4A_2 \rightarrow {}^4T_1$
f	17420(*574*) 17510(*571*)	$\perp c$ $\|c$	V^{3+} (d-d), $^3T_1 \rightarrow {}^3T_2$
	24930(*401*) 25310(*395*)	$\|c$ $\perp c$	V^{3+} (d-d), $^3T_1 \rightarrow {}^3T_1$
g	Continuous increase of the absorption from red to violet	$\|c \approx \perp c$	Lattice imperfections caused by irradiation
PART B: Causes of colour			
General colour	**Colour $\vec{E} \parallel c$**	**Colour $\vec{E} \perp c$**	**Cause of colour (from PART A)**
Yellow sapphire*** (from Sri Lanka)	yellowish	yellowish	g±a
Ruby	Yellowish-red	Reddish-violet	e±f
Green to yellowish-green sapphire***	Green to yellowish green	Green to yellowish green	a
Blue sapphire	Light blue	Dark blue to violet	b±c
Rose coloured sapphire	(not observed)	(not observed)	d
Padparadschah (orange-pink sapphire)	Yellowish-orange	Brownish orange	g+e
Reddish-brown to reddish-violet sapphire	Light yellow to yellowish green	Dark reddish brown to reddish violet	a+e
Bluish violet sapphire	Light violet to light blue	Dark violet to reddish violet	e+b±c
Green to bluish green sapphire	Green to bluish green	Bluish green to blue	a+b±c±e±d
Golden yellow sapphire (e.g. from Thailand)	Light yellow	Dark yellow	a±d
Green to yellowish green sapphire (	Yellish green	Bluish green	a+c+d±b

* term '**pairs**' implies intervalence charge transfer (IVCT); ** McClue (1962) and Johnson, *et al.*, (1995); *** weak pleochroism;

Moreover, Nassau (1983:100) argued that the colour of padparadschah sapphire (orange-pink sapphire) is caused by the substitution of $Cr^{4+} + Mg^{2+} \Leftrightarrow 2Al^{3+}$ in octahedra. Schmetzer *et al.* (1980) gave the absorption spectra of an alexandrite-like

corundum and it is explained by the superposition of absorption bands for d-d transitions of Cr^{3+}, (V^{3+}), Fe^{3+} as well as IVCT of Fe^{2+}/Ti^{4+} and Fe^{2+}/Fe^{3+}.

7.2.4 Samples and techniques

Seventy rough and faceted corundum samples from Thailand and outside Thailand were used to investigate corundum spectra in this study. The samples were chosen on the basis of having few inclusions and a suitable size (>0.5 cm across). Synthetic corundum samples (produced by the Verneuil process) were used to calibrate the bands and to compare the bands of natural corundum samples. A Hitachi UV-VIS-NIR spectrophotometer (Model U-4001), controlled by personal computer software, was used to examine the samples. The experiments were carried out at the Gem and Jewelry Institute of Thailand. The machine has double beams. In other words, a beam of light is switched between a reference path and a sample path, which are recombined at the detector, which thus compares the two beams. The signal from the reference path is subtracted from that of the sample path to give a spectrum of the sample with no effect of the ambient spectrum.

The absorbance (A) in most instruments is from the relation of (Rossman, 1988):

$$A = -\log_{10}(I_I/I_0)$$

where I_0 is the intensity of the incident light and I_I is the intensity of light passing through the sample. I_I/I_0 is the transmittance (T).

Range of T: 100% 30% 10% 1% 0.1%(=10^{-3})...0%.

Range of A: 0 0.5 1 2 3 ...∞.

As the sample did not fit in the cell holder, a piece black cardboard (5 cm x 5 cm) with a slit (0.5 mm diameter) in the middle was then used with a piece of Blu® Tack for holding the sample at the right position to the beam. The other advantage is to reduce the scattering from the surface of the sample and the leakage of the beam to the detector. The sample with the black cardboard was placed in the cell holder of the equipment and oriented in order to separate as much as possible the vibrations of the ordinary (o) and extraordinary (e) rays. Two polarizing filters (one for the sample path, other for the reference path) were placed between the beam source and the sample. To obtain the o-ray and e-ray, the sample is placed in the direction as shown in Figure 7.8. The faceted samples were searched for the optic axis (c-axis) by the aid of a polariscope

(polarimeter) as the optic figure under the polariscope marks the optic axis direction. It may be difficult to find the optic figure using the polariscope. Observation with the aid of a polarizing filter can also be used to roughly mark the optic axis direction.

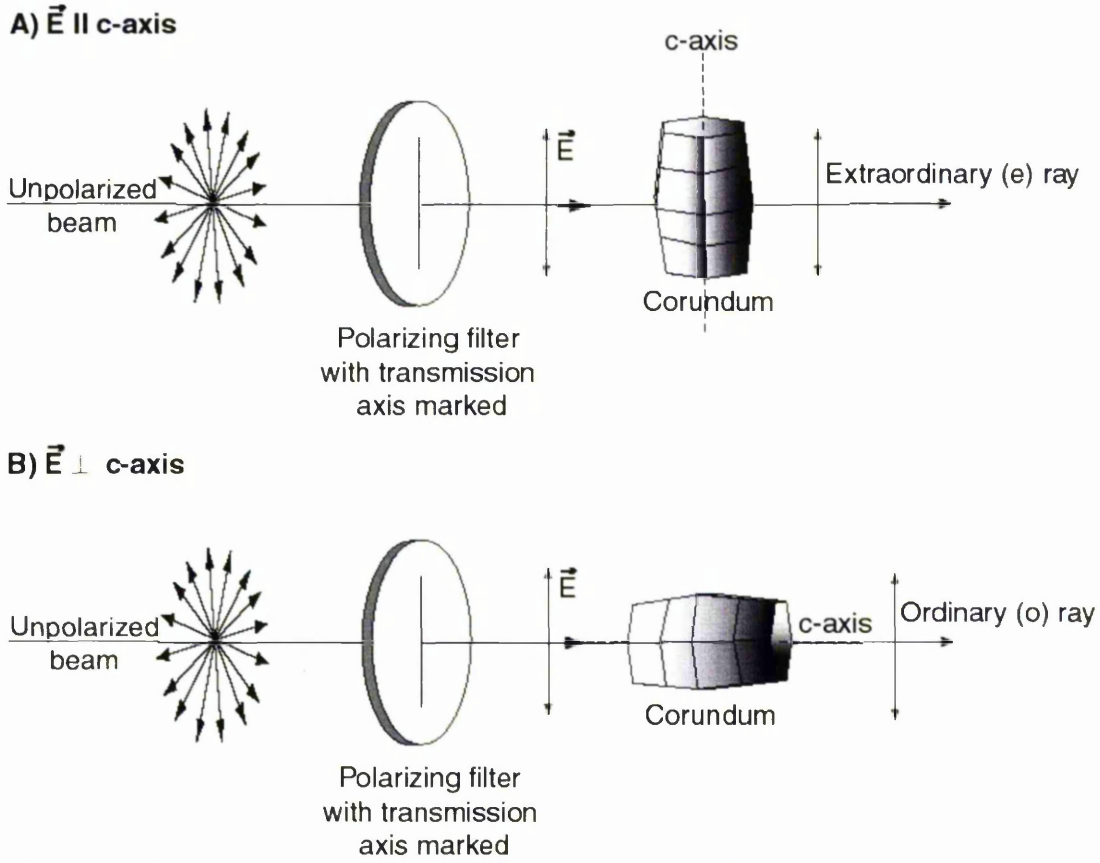

Figure 7.8 Corundum sample (not to scale) is subjected to the beam of UV-visible light in a spectrophotometer to ideally obtain the extraordinary (e) ray as in **A)** and ordinary (o) ray as in **B)**. Note that in practice, the ray obtained could be a mixture of the two rays because manual orientation may not be perfect. For example samples that are too thin, too small or anhedral could possibly lead to inaccurate orientation.

The equipment was set to scan the spectrum from 250 nm to 1500 nm, with a spectral resolution of 2 nm and duration time of ca 3 minutes per run. Each sample was run twice, one for the e spectrum and another for the o spectrum. A baseline was run before the samples without lodging the sample in the cell holder. Baselines were recalibrated after finishing ten to twelve samples.

7.2.5 Results

The results are presented in forms of graphic spectra with vertical absorbance scale and horizontal wavelength scale. As not all samples gave good output, certain spectra are chosen to show in this report (Figures 7.9 to 7.15). Wavelength (λ) scale in nanometre (nm) can be converted to the wave number (cm^{-1}) by $\mathbf{cm^{-1} = 10^7/\lambda(nm)}$.

Other than the causes of spectrum, the colour notation in terms of ***hue, tone*** and ***saturation*** are also given in each diagram. For example in Figure 7.9, A, CKD: very slightly greenish Blue, 6/4 means sample number: CKD, hue: very slightly greenish Blue, tone: 6 and saturation: 4. ***Hue*** is the pure spectral sensation. ***Tone*** is the lightness or darkness of the hue; the higher number the darker tone (scale 0-10). ***Saturation*** *(intensity)* is the strength and purity of the hue; the higher number the stronger the hue (scale 1-6). More details are given in the Appendix 7-1.

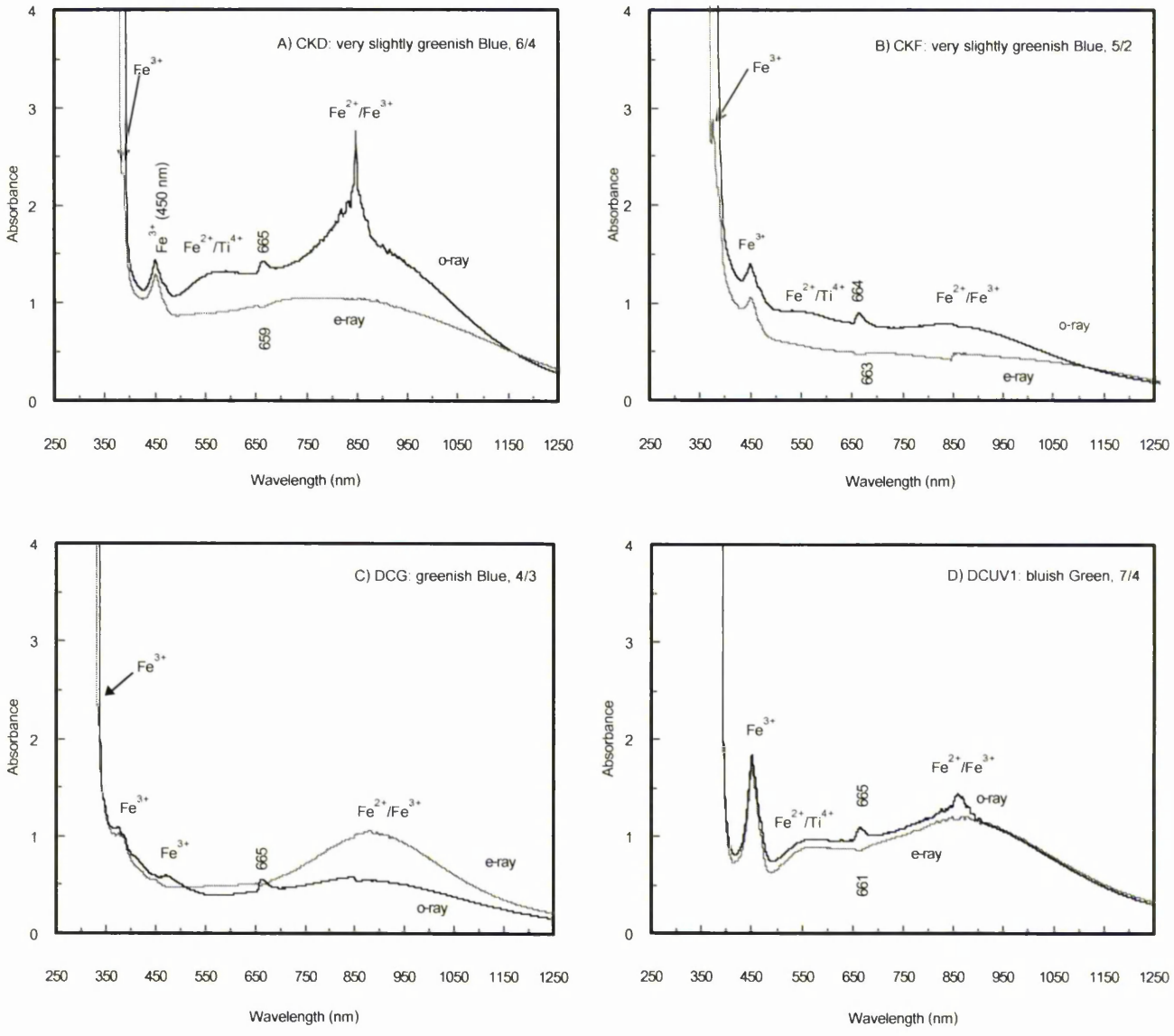

Figure 7.9 Spectra of corundum samples: **A)** CKD, very slightly greenish Blue sapphire, from Ban Huai Sai Democratic People's Republic of Laos showing peaks of the crystal field transition (d-d) for Fe^{3+} at 387 nm and 450 nm; bands of intervalence charge transfer (IVCT) for Fe^{2+}/Ti^{4+} are centred at 592 nm and for Fe^{2+}/Fe^{3+} (peaked at 848 nm). A weak peak at 665 nm (o-ray) and a valley at 659 nm (e-ray) are the positions of the absorption and fluorescence respectively as found in ruby due to Cr^{3+}. **B)** CKF, very slightly greenish Blue sapphire, from the same locality as in A) showing peaks of d-d for Fe^{3+} at 371 nm (e-ray) and 450 nm (o-ray). Bands of IVCT for Fe^{2+}/Ti^{4+} (centred at 557 nm) and Fe^{2+}/Fe^{3+} (cetred at 848 nm) are not strong as in A). A weak peak at 664 nm (o-ray) and a valley at 663 nm (e-ray) are the positions of the absorption and fluorescence respectively as found in ruby due to Cr^{3+}. **C)** DCG, greenish Blue sapphire, from Den Chai showing peaks and shoulder of d-d for Fe^{3+} at 337 nm and 375 nm and 471 nm, broad band of IVCT for Fe^{2+}/Fe^{3+} (centred at 881 nm, e-ray). **D)** DCUV1: bluish Green sapphire from Den Chai shows the peak of d-d for Fe^{3+} at 451 nm and the band of IVCT for Fe^{2+}/Fe^{3+} peaks at 859 nm. The band of IVCT for Fe^{2+}/Ti^{4+} is centred at ca 550. The weak peak at 665 nm and the valley at 661 nm are explained as in B).

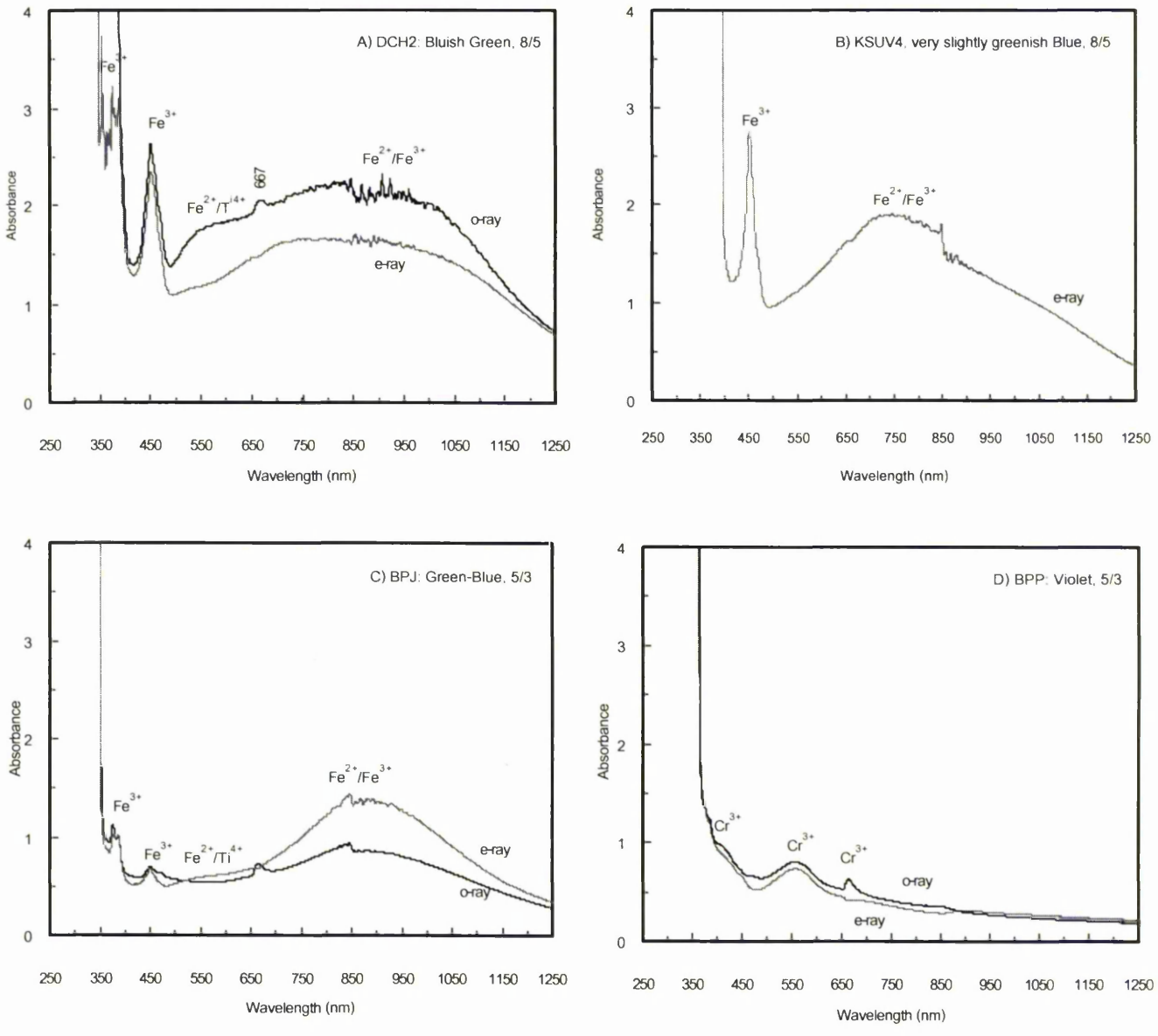

Figure 7.10 Spectra of corundum samples: **A)** DCH2, bluish Green sapphire from Den Chai showing many absorption peaks below 400 nm. The peak of d-d for Fe^{3+} appears at 451 nm for o-ray and 452 nm for e-ray and the band of IVCT for Fe^{2+}/Fe^{3+} is centred at 855 nm. The band of IVCT for Fe^{2+}/Ti^{4+} shows only in o-ray (centred at ca 570). The weak peak at 667 nm is probably due to Cr^{3+}. **B)** KSUV4, very slightly greenish Blue sapphire (simply called: *dark blue sapphire*) from Khok Sam Ran, showing absorption peak of d-d for Fe^{3+} (452 nm) and absorption band of IVCT for Fe^{2+}/Fe^{3+} (centred at 848 nm). **C)** BPJ, Green-Blue sapphire from Bo Phloi shows peaks of d-d for Fe^{3+} at 376 nm, 386 nm and 450 nm. The IVCT band for Fe^{2+}/Fe^{3+} is peaked at 846 nm associated with cut off. The band of IVCT for Fe^{2+}/Ti^{4+} is not prominent. The weak peak at 665 nm is probably due to Cr^{3+}. **D)** BPP, Violet sapphire from Bo Phloi showing shoulder, strong band and peak of d-d for Cr^{3+} centred at 415 nm, 555 nm and 664 nm respectively (o-ray).

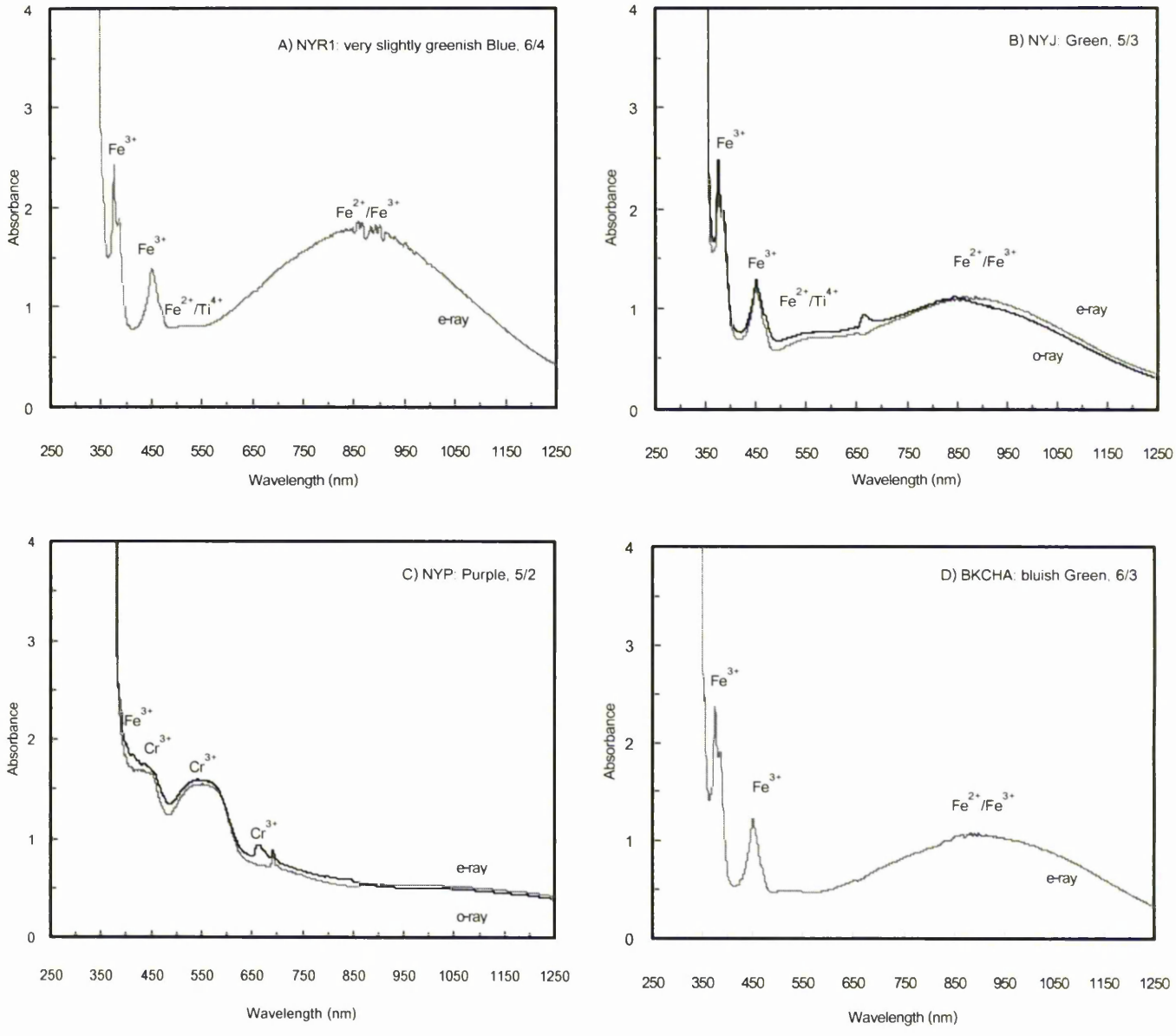

Figure 7.11 Spectra of corundum samples: **A)** NYR1, very slightly greenish Blue sapphire from Nam Yun showing peaks of d-d for Fe^{3+} at 376 nm, 387 nm and 450 nm. The centre of IVCT band for Fe^{2+}/Fe^{3+} is positioned at 874 nm. The band of IVCT for Fe^{2+}/Ti^{4+} is not prominent. **B)** NYJ, Green sapphire from Nam Yun showing d-d peaks for Fe^{3+} (376 nm 385 nm and 451 nm) for Cr^{3+} (665 nm) (o-ray); bands of IVCT for Fe^{2+}/Fe^{3+} (centred at 845 nm) (o-ray). **C)** NYP, Purple sapphire (may be called ruby), from Nam Yun showing bands of d-d for Cr^{3+} centred at ca 450 nm, 541 nm and weak peaks of 666 nm and 692 nm. Note that the first band probably superimposes on the d-d peaks of Fe^{3+}. **D)** BKCHA, bluish Green sapphire from Bang Kacha showing the d-d peaks for Fe^{3+} (349 nm, 376 nm and 451 nm); bands of IVCT for Fe^{2+}/Fe^{3+} (centred at ca 893 nm).

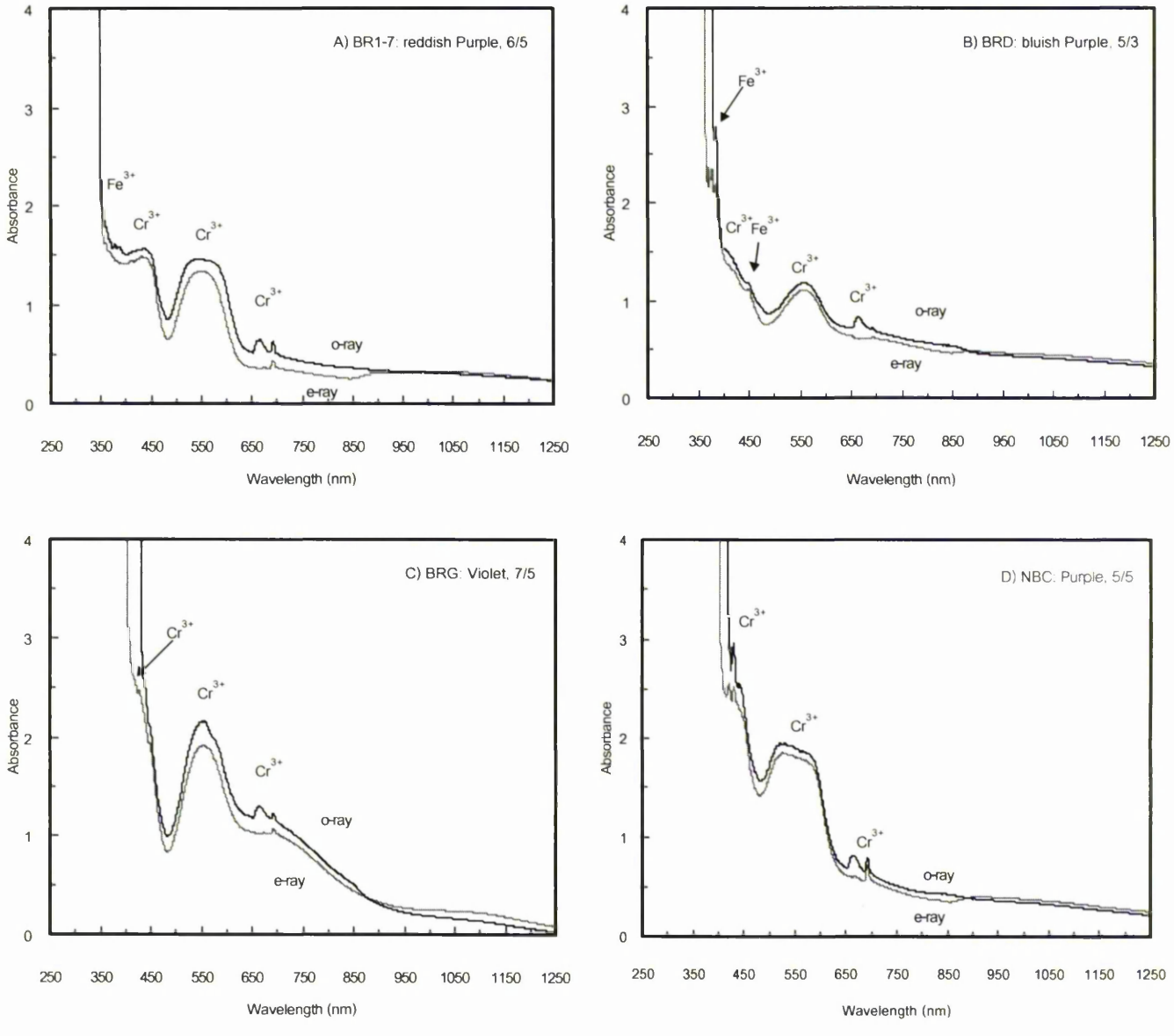

Figure 7.12 Spectra of corundum samples: **A)** BR1-7, ruby from Bo Rai shows peaks and bands very similar to NYP, ruby from Nam Yun. The o-ray shows bands of d-d for Cr^{3+} centred at ca 450 nm, 542 nm and weak peaks of 666 nm and 693 nm. Note that the first band superimposes on the d-d peaks of Fe^{3+} which are seen as two tiny peaks at 378 nm and 386 nm. **B)** BRD, bluish Purple corundum from Bo Rai showing the bands and peaks of d-d for Cr^{3+}; the first position of Cr^{3+} seen as shoulder at ca 410 nm; the second band peaks at 557 nm; the weak peaks at 665 nm and 692 nm (o-ray) are associated with the fluorescent line seen as valley in the e-ray. The Fe^{3+} peaks are also present at 387 nm and 449 nm (o-ray). **C)** BRG, Violet corundum from Bo Rai showing the shoulder and peaks of d-d for Cr^{3+} at 428 nm (e-ray), 551 nm, 665 nm and 692 nm (o-ray). The peaks of Fe^{3+} probably superimpose the position of Cr^{3+} band near 400 nm. **D)** NBC, Purple corundum (simply called ruby) fron Nong Bon showing the peaks, shoulder and band of d-d for Cr^{3+} at 431 nm, 552 nm, 666 nm and 693 nm. The shoulder between 400 nm and 450 nm is probably associated with the Fe^{3+} peaks (e.g. 441 nm).

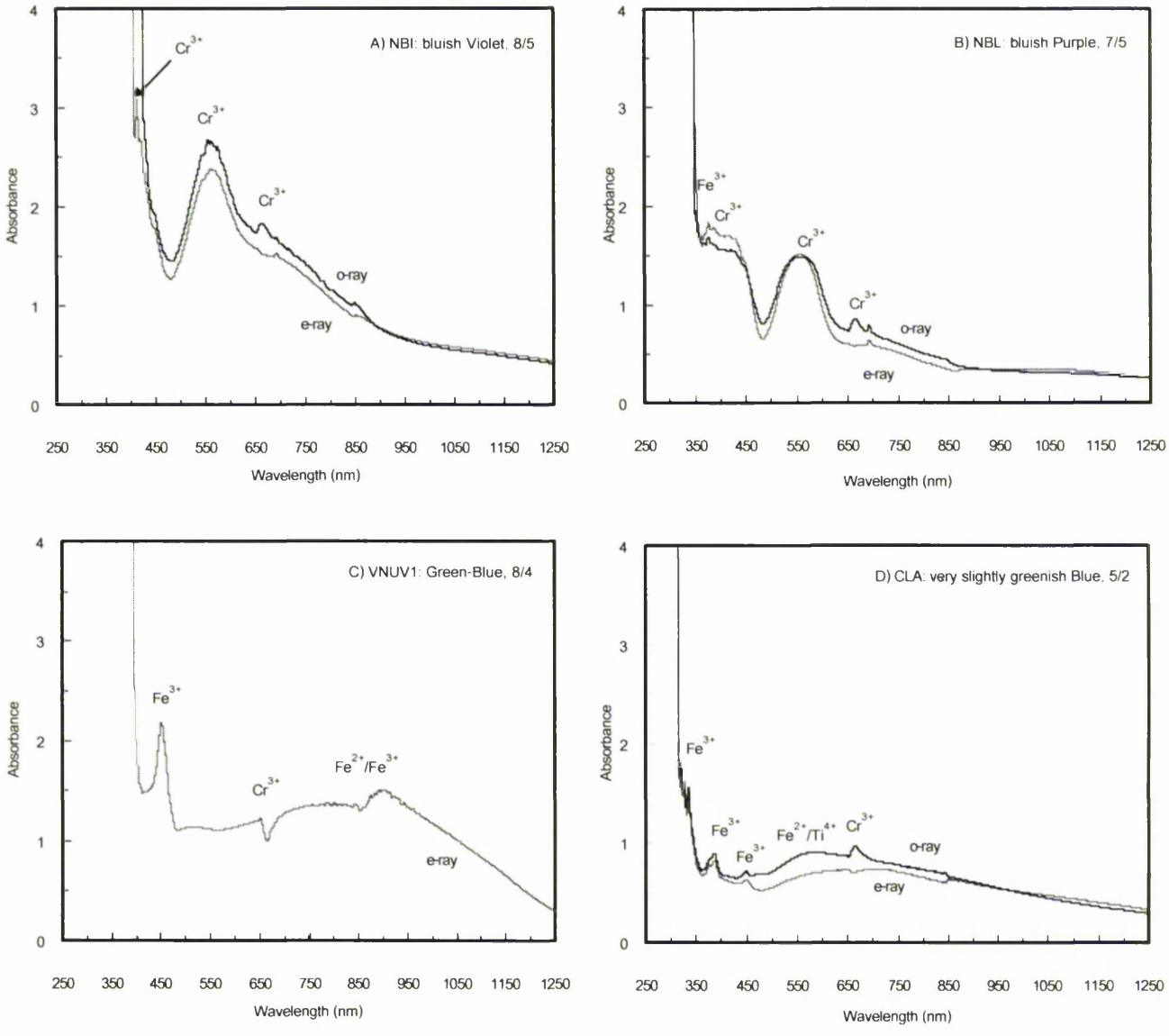

Figure 7.13 Spectra of corundum samples: **A)** NBI, bluish Violet corundum from Nong Bon showing the peaks in similar shape as in BRG (Figure 7.12). The shoulder and peaks of d-d for Cr^{3+} are present at 413 nm (e-ray), 555 nm, 663 nm and 693 nm (o-ray). The peaks of Fe^{3+} probably superimpose the position of Cr^{3+} band near 400 nm. The weak peak at 848 nm is probably due to IVCT of Fe^{2+}/Fe^{3+}. **B)** NBL, bluish purple corundum showing the d-d bands and peaks for Cr^{3+} at ca 400 nm, 553 nm, 666 nm and 692 nm. The peak of d-d for Fe^{3+} is present at 377 nm. **C)** VNUV1, Green-Blue sapphire from Viet Nam showing peaks of d-d for Fe^{3+} at 452 nm, broad band of IVCT for Fe^{2+}/Fe^{3+} (maximum at 893 nm). The peak and valley due to Cr^{3+} are present at 651 nm and 664 respectively. **D)** CLA, very slightly greenish Blue sapphire from Sri Lanka showing d-d peaks for Fe^{3+} at 321, nm 335 nm, 386 nm, and 449 nm; band of IVCT for Fe^{2+}/Ti^{4+} (centred at ca 580 nm). The weak peak at 665 nm is probably due to Cr^{3+}. The band of IVCT for Fe^{2+}/Fe^{3+} is absent.

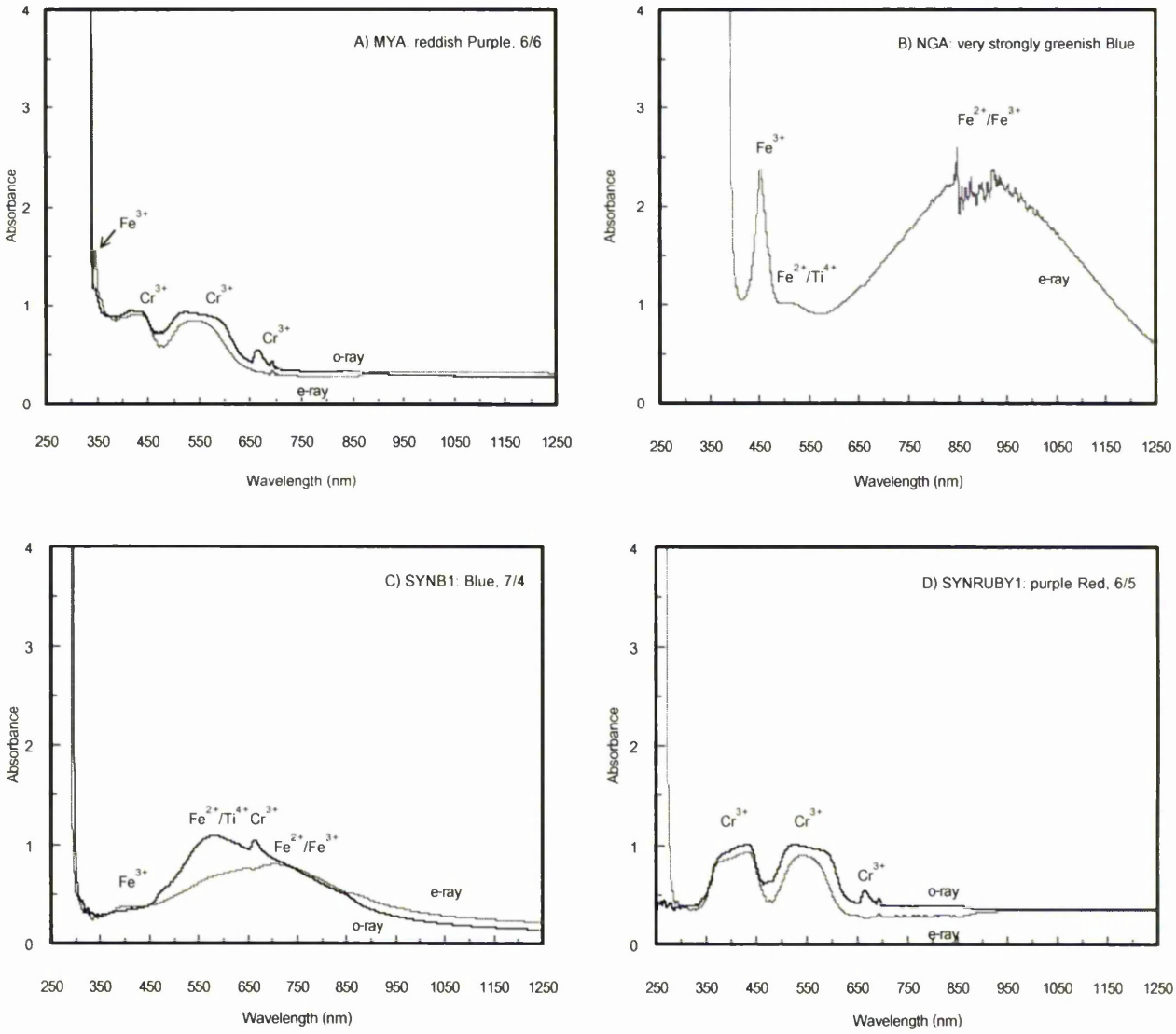

Figure 7.14 Spectra of corundum samples: **A)** MYA, ruby from Mong Hsu, Myanmar showing d-d bands and peaks for Cr^{3+} centred at 420 nm, 540 nm, 666 nm and 693 nm. The peak for Fe^{3+} is present at 346 nm. **B)** NGA, very slightly greenish Blue corundum from Nigeria shows the peak of d-d for Fe^{3+} at 452 nm; band of IVCT for Fe^{2+}/Ti^{4+} (centred at ca 510 nm); band of IVCT for Fe^{2+}/Fe^{3+} (centred at ca 870 nm). **C)** SYNB1, synthetic Verneuil Blue sapphire shows d-d peak for Fe^{3+} (centred at 400 nm) and band of IVCT for Fe^{2+}/Ti^{4+} (centred at 581 nm). The peak at 664 nm is probably due to Cr^{3+}. **D)** SYNRUBY1, synthetic Verneuil ruby shows the typical bands and peaks of d-d Cr^{3+} centred at ca 400 nm, 546 nm, 666 nm and 693 nm.

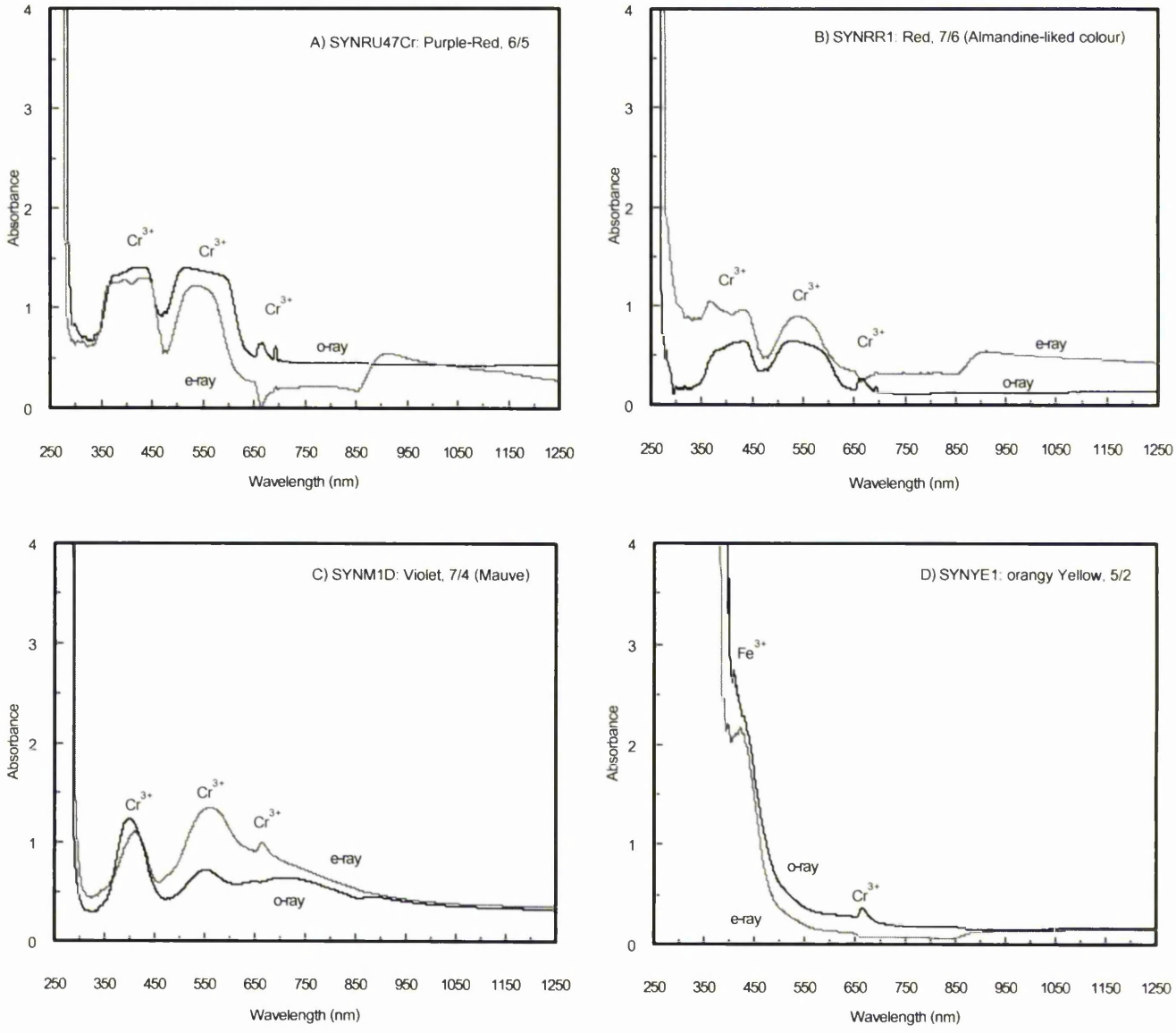

Figure 7.15 Spectra of synthetic corundum samples (produced by the Verneuil method): **A)** SYNRU47Cr, ruby (with 0.47% Cr content) shows the typical bands and peaks of d-d Cr^{3+} as seen in C). Bands and peaks of d-d Cr^{3+} centred at ca 400 nm, 537 nm, 667 nm and 693 nm. The fluorescent line at 665 nm seen as valley in e-ray. **B)** SYNRR1, ruby shows two d-d bands for Cr^{3+} (centred at ca 400 nm and 540 nm) and two weak d-d peaks of Cr^{3+} (667 nm and 693 nm). The band centred ca 900 is probably due to Fe^{2+}/Fe^{3+}. **C)** SYNM1D, Violet sapphire shows d-d peaks for Cr^{3+} at 412 nm, 563 nm and 664 nm (e-ray). **D)** SYNYE1, orangy Yellow sapphire shows d-d peaks for Fe^{3+} at 410 nm (o-ray) 389 nm, 398 nm and 423 nm (e-ray) and for Cr^{3+} at 664 nm (o-ray).

7.2.6 Discussion

Corundum samples from Thailand can be divided into two groups according to their optical spectra. The first group includes sapphires with very slightly greenish Blue, very strongly greenish Blue, greenish Blue, bluish Green, Green-Blue and Green colours. The samples in this group exhibit absorption spectra of the crystal field transition (d-d) for Fe^{3+} (peaks between ca 330 nm and 450 nm). They also show the two broad absorption bands of the intervalence charge transfer (IVCT) for Fe^{2+}/Ti^{4+} (between 500 nm and 650 nm but the band is weak in some samples e.g. DCG. This is prominent in o-ray ($\vec{E} \perp$ c axis) and in most cases, it rarely exists in e-ray. The band of Fe^{2+}/Fe^{3+} IVCT is centred between 840 nm and 900 nm.

The second group includes corundums that warrant the name *ruby,* i.e. corundum samples with Violet, Purple, reddish Purple, bluish Purple, bluish Violet colours. The samples in this group dominantly exhibit the d-d band for Cr^{3+} (centred at ca 550 nm). The band of 350 nm – 450 nm, as seen in synthetic Verneuil ruby, is not found but the right shoulder of this band is found in the natural samples. This is due to Fe impurity in natural samples causing the band to be superimposed by the peaks of d-d for Fe^{3+}. There are also weak peaks at 665±1 nm and 692/693 nm.

A pale blue sapphire sample from Sri Lanka (CLA) does not show the band of Fe^{2+}/Fe^{3+} that is characteristic of most sapphires of metamorphic origin (Kashmir, India; Mogok, Myamar; Umba Valley, Tanzania) reported by Schmetzer and Kiefert (1990). An exception is for blue sapphires from Andranondambo, Madagascar (skarn type) which shows an Fe^{2+}/Fe^{3+} band (Schwarz *et al.,* 1996). On the other hand, sapphires derived from alkali basalt, including sapphires from Thailand, Viet Nam and Nigeria in this study, show an Fe^{2+}/Fe^{3+} band (Schmetzer and Kiefert, 1990).

The Fe^{2+}/Fe^{3+} band in synthetic blue sapphire is absent and the d-d for Fe^{3+} is not prominent. Synthetic rubies including purple Red, Purple-Red, Red samples show spectra typical of ruby (bands and peaks for Cr^{3+}) except for the synthetic violet (mauve) sample which shows narrower bands. Synthetic orangy Yellow sapphire exhibits d-d peaks for Fe^{3+} and for Cr^{3+}.

Not only does absorption differ in terms of directional structure (o-ray or e-ray), the level of absorbance for each of the samples also depends on other factors. For example, sample thickness is one such factor; if the beam passes through a relatively thick portion of a sample, the light will be absorbed much more than with a thinner portion. Hue, tone and saturation of corundum also affect the intensity of the spectrum. These cause certain samples in present study to be obtained only one spectrum (o-ray or e-ray) as shown in Figures 7.10B, 7.11A & D, 7.13C and 7.14B. The overall peaks and bands observed in this study are summarized in Table 7.2.

Table 7.2 Summary of centred positions (nm) of absorption spectra (o-ray and e-ray) for corundum samples in this study and causes of absorption.

Locality/Sample No		Colour (hue, tone/saturation)	Crystal field transition (d-d)								IVCT	
			Cr^{3+}					Fe^{3+}			Fe^{2+}/Ti^{4+}	Fe^{2+}/Fe^{3+}
			1st band (400 nm)	2st band (555 nm)	Peaks (ca 660-700 nm)	Lines 692, 693 nm	Fluorescent line	Peaks between ca 375 and 387 nm		Peak 450 nm	Centred at	Centred at
Ban Huai Sai	CKD	very slightly greenish Blue, 6/4	-	-	665	-	659*	387	-	450	592	848
	CKF	very slightly greenish Blue, 5/2	-	-	664	-	663*	371	-	450	557	848
Den Chai	DCG	greenish Blue, 4/3	-	-	665	-	-	337	375	471	-	881*
	DCUV1	bluish Green, 7/4	-	-	665	-	661*	-	-	451	550	859
	DCH2	bluish Green, 8/5	-	-	667		-	374*	388*	451	570	855
Khok Sam Ran	KSUV4	very slightly greenish Blue, 8/5	-	-	-	-	-	-	-	452*	-	848*
Bo Phloi	BPJ	Green-Blue, 5/3	-	-	665	-	-	376	386	450	560*	846
	BPP	Violet, 5/3	415	555	664	-	668*	-	-	-	-	-
Nam Yun	NYR1	very slightly greenish Blue, 6/4	-	-	-	-	-	376*	387*	450*	-	874*
	NYJ	Green, 5/3	-	-	665	-	659*	376	385	451	550	845
	NYP	Purple, 5/2	450	541	666	692	-	-	-	-	-	-
Bang Kacha	BKCHA	bluish Green, 6/4	-	-	-	-	-	349*	376*	451*	-	893*
Bo Rai	BR1-7	reddish Purple, 6/5	450	542	666	693	-	378	386	-	-	-
	BRD	bluish Purple, 5/3	410	557	665	692	665*	387	-	449	-	-
	BRG	Violet, 7/5	428*	551	665	692	665*	-	-	-	-	-

Table 7.2 (Continued).

Locality/Sample No		Colour (hue, tone/saturation)	Crystal field transition (d-d)								IVCT	
			Cr^{3+}					Fe^{3+}			Fe^{2+}/Ti^{4+}	Fe^{2+}/Fe^{3+}
			1st band (400 nm)	2st band (555 nm)	Peaks (ca 660-700 nm)	Lines 692, 693 nm	Fluorescent line	Peaks between ca 375 and 387 nm		Peak 450 nm	Centred at	Centred at
Nong Bon	NBC	Purple, 5/5	431	552	666	693	-	-	-	441	-	-
	NBI	bluish Violet, 8/5	413*	555	663	693	-	-	-	-	-	848
	NBL	bluish Purple, 7/5	400	553	666	692	-	377	-	-	-	-
Viet Nam	VNUV1	Green-Blue, 8/4	-	-	651*	-	664*	-	-	452*	-	893*
Sri Lanka	CLA	very slightly greenish Blue, 5/2	-	-	-	-	665*	321, 335	386	449	580	-
Mong Hsu	MYA	reddish Purple, 6/6	420	540	666	693	-	346	-	-	-	-
Nigeria	NGA	very strongly greenish Blue, 8/4	-	-	-	-	-	-	-	452*	510*	870*
Synthetic Verneuil corundum	SYNB1	Blue, 7/4	-	-	-	-	664	-	-	400	581	-
	SYNRUBY1	purple Red, 6/5	400	546	666	693	664*	-	-	-	-	-
	SYNRU47Cr	Purple-Red, 6/5	400	537	667	693	665*	-	-	-	-	-
	SYNRR1	Red , 7/6 (almandine-liked colour)	400	540	665	693	-	-	-	-	-	900?
	SYNM1D	Violet , 7/4 (mauve)	412	563	664	-	-	-	-	-	-	-
	SYNYE1	orangy Yellow, 5/2	-	-	664	-	668*	389*, 398*	410, 423*	-	-	-

* e-ray.

7.3 Infrared and Raman spectroscopy of corundum

Infrared and Raman spectra can be of great value in structural studies, providing information on the bonding and reactivity of protons in minerals. They can serve as fingerprints to give proof of identity without recourse to any other analytical method (Farmer, 1974; Estep-Barnes, 1977). Infrared and Raman techniques depend on the

interaction of electromagnetic radiation with matter or the vibrational frequency of molecules, but the physical bases are fundamentally different; infrared: absorption, Raman: scattering. Fadini and Schnepel (1989) have differentiated the basic principles of both techniques. However, to obtain the complete picture it is best to use the two techniques together.

This section presents some basic principles of infrared and Raman techniques and their application to corundum including sample preparation and the observation of corundum spectra.

7.3.1 Infrared (IR) spectroscopy

An infrared absorption spectrum yields information on both the structure and bonding of a substance and can be used to identify certain kinds of unknown mineral specimens (Jones, 1987). Two types of infrared spectra can be recorded: 1) a transmission spectrum and 2) a reflectance spectrum.

For a transmission spectrum, the sample is transparent to the beam and the absorption spectra can be recorded (Martin, *et al.*, 1989). Reflection methods are of three types (Russell, 1974): diffuse reflection, specular (mirror-like) reflection, and internal reflection or attenuated total reflection (ATR).

Diffuse reflectance is the radiation which penetrates into the samples and then emerges. Diffuse reflectance is from powdered material, but results are difficult to interpret as they are partly due to transmission and reflection, and also depend upon particle size. This technique can also be used to recognize the spectra of clay minerals and hydrous metal oxides (e.g. Smith, 1995).

Specular reflectance is the radiation which reflects directly off the sample surface. The intensity of the reflectance of IR radiation from a highly polished surface of the specimen is measured.

For ***internal reflection***, the sample is placed on both sides of a plate made of a dense, transparent, crystalline material of high refractive index (for example, thallium bromide mixed with thallium iodide). The beam is radiated into the plate with the proper

incident angle and undergoes multiple internal reflections before passing the plate to the detector. The absorptions take place while the radiation beam penetrates the sample (Skoog, *et al.*, 1998). This method has proved highly successful with liquids and powders (Russell, 1974).

Sample preparation for the infrared technique

-Destructive method (Estep-Barnes, 1977; Jones, 1987)

1) The particle size should be less than the wavelength of the incident infrared radiation (near-IR = 0.78-2.5 μm; mid-IR = 2.5-50 μm; far-IR = 50-1000 μm, Skoog *et al.*, 1998) in order to minimize losses due to scattering and reflection effects. In other words, the optimum particle size is about 2 μm or less. The large amount of grinding needed to produce such small particles can result in the generation of local high temperatures and unexpected changes in structure of the mineral. Therefore, wet-grinding should be done to minimize the formation of local hot-spots. If water-soluble minerals are thought to be present then the specimen should be ground in alcohol.

2) The crushed sample is suspended in a material (mounting matrix) of similar refractive index to avoid distorted and shifted bands. The matrix should be transparent to infrared radiation in the spectral range of interest. Potassium bromide (KBr) or caesium iodide (CsI) is used as the matrix as they are chemically stable and they need only low sintering pressure to form a pellet.

The pellets are prepared using about 1 mg (modern developments using about 10 μg) of ground mineral in about 300-400 mg of alkali halide. The mixture is pressed to form a firm pellet. The pellet should be heated at 80-100°C overnight to eliminate any adsorbed water.

-Non-destructive method

This method is used to measure the external reflectance on the surface of the specimen for an area as small as 100 μm x 100 μm. Corundum has been analysed in the form of cut or polished crystals. Generally, at least one polished surface is required to be placed on the reflectance device (Martin, *et al.*, 1989; Rydzak and Cannon, 1989). The latter authors annealed the samples at 1650°C to get rid of the surface strain caused by polishing. Martin *et al.* (1989) investigated the effects of polarization, for example in

beryl and quartz, by arranging the beam incident to the different vibration directions of the crystals. They found that the spectra differ slightly according to the position of the samples, but overall they are still within the spectral range of those species. In corundum, Barker (1963) measured the reflectivity of IR from the synthetic corundum in two independent measurements: parallel to the c-axis and anywhere in the plane perpendicular to the c-axis. In most cases, the corundums are prepared by polishing two parallel faces approximately perpendicular or parallel to the c-axis (e.g. Cook and Perkowitz, 1985; Rydzak and Cannon, 1989; Rossman, 1990). Smith (1995) investigated OH in corundum by the non-destructive diffuse reflectance technique and the samples were analysed in two directions, perpendicular and parallel to the c-axes. The results for both orientations are identical, but differ in their intensities, which are weaker for the vibrational path perpendicular to the c-axis.

Infrared spectra of corundum

Corundum has absorption bands in the extended mid- and far-infrared regions (<800 cm^{-1}) due to Al-O stretching or lattice vibrations (Estep-Barnes, 1977). For corundum from Ceylon, Boldyrev and Povarennykh (1968; cited in Liese, 1975) show strong infrared absorption in the ranges of 607-595 cm^{-1} and 460-450 cm^{-1} (1078m, 775w, 635w, 595s, 453s, 378w, 355sh; Note: m = medium, w = weak, s = strong, sh = shoulder). Dorsey (1968) found the absorption bands of Al-O-Al linkages at 638, 583, 487, 445, and 386 cm^{-1}. Wafers and Bell (1972) reported absorption at about 760, 642, 602 and 450 cm^{-1}. In hydrothermal synthetic ruby, the very high absorbance resulting from Al-O stretch frequencies and lattice absorption takes place near 1700 cm^{-1} (Belt, 1967). The typical spectrum of powdered corundum is given in Figure 7.16.

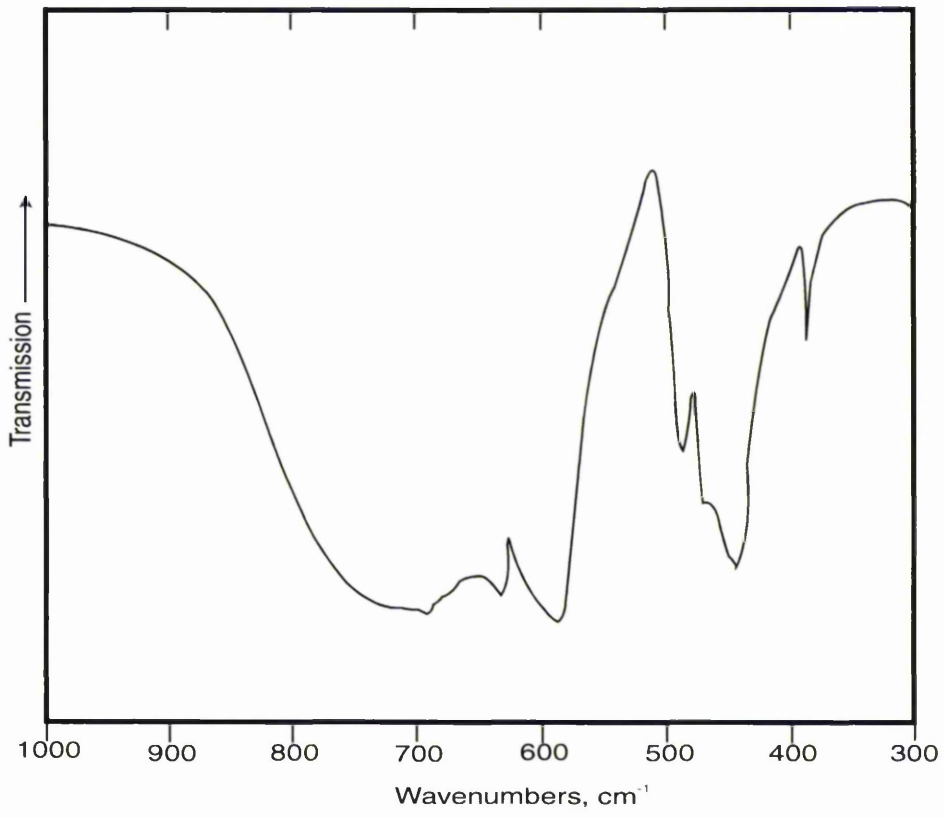

Figure 7.16 Typical infrared spectrum of powdered corundum (Phillippi, 1970).

Volynet *et al.* (1972) found that the OH-group absorption bands (between 3160 and 3418 cm^{-1}) in synthetic corundum grown in an oxygen-hydrogen flame (Verneuil's method) are similar to other materials grown by the same method. They stated that the vibration of the OH group is perpendicular to the optical axis of corundum. Also Smith (1995) interpreted a series of absorption bands in the mid-infrared range (1900 to 3400 cm^{-1}) in rubies as being due to the OH in diaspore (α–AlOOH) occurring as their veins penetrating and traversing the stones, and coating the surface of the crystals. In heat-treated rubies, the peaks at 3310, 3232, 3187, and 3368 cm^{-1} are for the OH bond of diaspore inclusions (whitish clouds) formed during heat-treatment. Smith (op. cit.) also shows absorption peaks for OH groups bonded with the corundum lattice between 3100 and 3600 cm^{-1} for various corundums from different sources.

Hydrogen atoms are incorporated in the structure of corundum as a charge compensation mechanism for transitional metal ions, occupying the interstitial site between two oxygen atoms or trapped by cation vacancies (Eigenmann and Günthard, 1971; Beran, 1991). The structural OH groups caused by Ti, V or Fe bonds are much more typically recorded in blue sapphires from basaltic terrains (for example Thailand, Cambodia,

southern Vietnam, Australia, etc) than for rubies or sapphires from metamorphic provinces (Smith, 1995; Rossman and Smyth, 1990). The absorption features of the OH bonding of hydrothermal synthetic corundum are stronger than other natural and synthetic counterparts (Smith, 1995).

In this study, certain corundum samples were analysed with the diffuse reflectance technique. The instrument used is the ATI Mattson Genesis Series FTIR and the standard used is KBr powder. The machine was run with the spectral resolution of 2 cm^{-1}. The investigation was done at the Department of Chemistry, the University of Manchester. The spectra for sapphires from Khok Sam Ran (KSR1), Nong Bon (NB1-6), Nam Yun (NYR1), and synthetic Verneuil ruby (SYNRU47Cr) are shown in Figure 7.17.

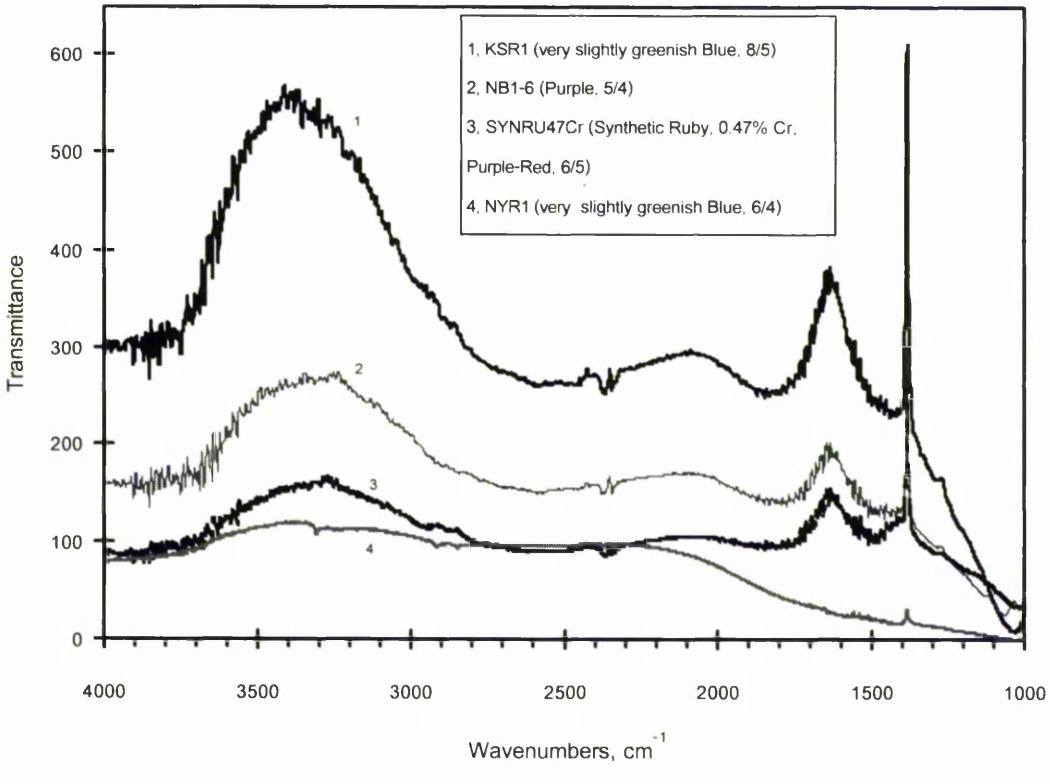

Figure 7.17 Infrared spectra for rough corundum samples from Khok Sam Ran (KSR1), Nong Bon (NB1-6), Verneuil synthetic ruby with 0.47% Cr (SYNRU47Cr), and Nam Yun (NYR1). The numbers following the colours of the stones are tone/saturation scales.

The spectra in Figure 7.17 are selected from the region greater than 1000 cm^{-1} (the region less than 1000 cm^{-1} has very high reflectivity, not shown). Spectral interferences include artefact peaks such as atmospheric water (peaks about 1400 to 2000 cm^{-1}) and atmospheric carbon dioxide (peaks between 2300 and 2400 cm^{-1}; Smith, 1974; Smith, 1995). The region between 3000 and 4000 cm^{-1} would be expected for the OH bond in

the structure of corundum. Most spectra are masked by a spurious broad band of reflection in this region that could be due to the high reflectance from the surfaces of the samples. This feature is clearly observed with the sample from Khok Sam Ran (KSR1) which is nearly opaque and, of all the samples studied, least transparent to the beam. However, the single spectrum for the Nam Yun sapphire sample (NYR1) shows a weak absorption peak at 3309 cm^{-1}, which agrees with the OH peak of basaltic corundum referred to by Smith (1995). This is consistent with the possibility that the alluvial sapphire from Nam Yun is derived from a basaltic terrain.

7.3.2 Raman spectroscopy

For the purpose of this work, the results obtained using the Raman technique can be interpreted without detailed theory. Gas or mixed gas lasers have been used for non-destructive studies of single crystals a few millimetres in size or of very small quantities ($\leq$ 2 mg) of powdered mineral (Griffith, 1974). The Raman microscope (microprobe) technique in conjunction with laser excitation is suitable for studying surface areas down to 10 μm x 10 μm or less (Griffith, 1978).

When a mineral is irradiated with intense light of a frequency which the mineral cannot absorb, a small part of the incident radiation is scattered in all directions. Additional frequencies are observed in the spectrum of the scattered light, called the Raman spectrum (Fadini and Schnepel, 1989). Raman light is very weak, only $1/100000^{th}$ part of the incident radiation. The Raman frequencies are discrete and both higher and lower than the frequency of the exciting radiation (ν). The frequency differences between ν and the new lines correspond to some vibrational, rotational or lattice mode characteristics of the mineral being studied. The new frequencies in the scattered light are called Raman shifts or Raman bands. The frequencies lower than ν are called Stokes lines; these are stronger than the higher frequencies, which are called anti-Stokes lines. In Raman spectroscopy, only the Stokes lines are measured (Griffith, 1974).

The Raman microprobe has been widely used in gemmology recently as this technique is usually non-destructive, and allows not only the host gemstones but also inclusions to be identified. For example, Nassau (1981) used Raman spectra to identify various gemstones and concluded that the spectra reflect the chemical composition and crystal structure (but not for different colours or origins). Dele-Dubois and Schbnell (1987)

used the Raman microprobe to identify inclusions in ruby and emerald. Hänni *et al.* (1997) gave examples of the application of the Raman microprobe and identified various gem materials such as tremolite, emerald with fractures filled by organic fillers, solid and liquid inclusions in gemstones, and mounted gemstones.

Sample preparation for the Raman technique

The single crystals can be less than a millimetre in diameter, but for easy operation, a well-formed crystal of the order of 5 mm or greater is better. The examination should be done in a number of orientations relative to the laser beam. Goniometers or X-ray techniques can help for this purpose. As the exciting lines are absorbed by the sample, red samples are best examined with red or yellow sources, blue and green samples by blue and green sources. The samples must be transparent to the exciting beam. Fluorescence more likely occurs with a high frequency Argon laser (blue end, λ = 488.0 or 415.5 nm) than a low frequency Helium/Neon laser (red end, λ = 632.8 nm; Griffith, 1974; Skoog, *et al.*, 1998).

In gemmology, in addition to the above mentioned, the samples may be tested without special preparation. The host gems have to be transparent to the beam and the beam can be focused directly onto the area to be identified. Focusing the beam through a cut facet into the inclusion can identify inclusions. Hänni *et al.* (1997) suggest that analysis of inclusions not reaching the surface is possible down to a depth of 5 mm, but best results are obtained when the inclusion is close to the surface of the host. The resulting spectra of the unknown materials will normally be compared to the reference spectra of the database to match the peaks.

Raman scattering in corundum

Porto and Krishnan (1967) studied spectra of corundum crystals in different orientations obtained by the X-ray diffractometer and found that the spectra vary between 300-800 cm^{-1} (Figure 7.18). White (1975) reported that the spectral peaks of powdered corundum occur at 378, 418, 432, 451, 578, 645, and 751 cm^{-1}. Watson *et al.* (1981) also show the spectrum of sapphire which has peaks at 378.7, 417.4, 430.2, 448.7, 576.7, 644.6, and 750 cm^{-1}.

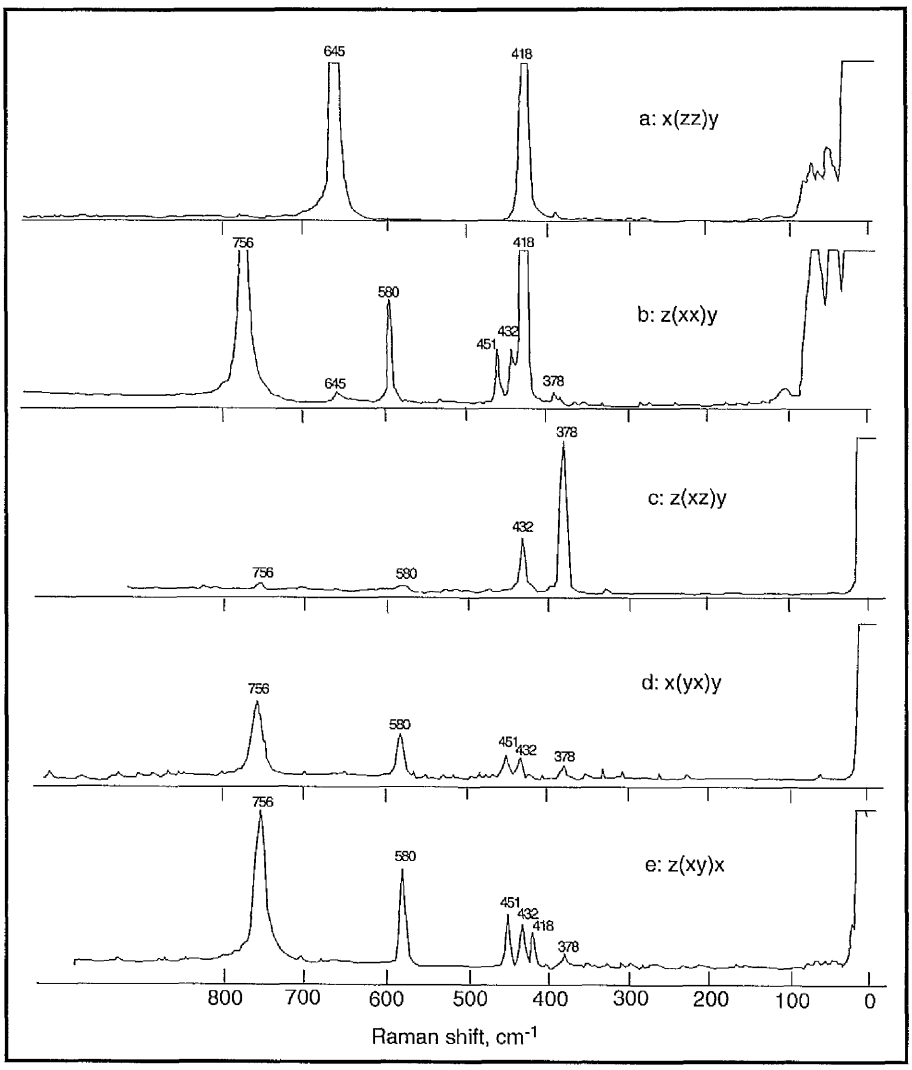

Figure 7.18 Raman spectra collected from different crystal orientations of a synthetic corundum, for example x(zz)y spectrum, which means that the light entered the x axis of the crystal polarized in the z direction and scattered light polarized parallel to the z axis was collected along the y axis (Porto and Krishnan, 1967).

Attempts have been made here to analyse ruby and sapphire samples by the use of the Renishaw Raman Microprobe, which has a spectral resolution of 1 cm^{-1}. The experiment was done at the Materials Science Centre, at the University of Manchester Institute of Science and Technology (UMIST). The laser beam was generated from a He/Ne source (red beam). An example of the type of spectrum is presented in Figure 7.19. It was found that the samples were fluorescent, giving broad jagged bands.

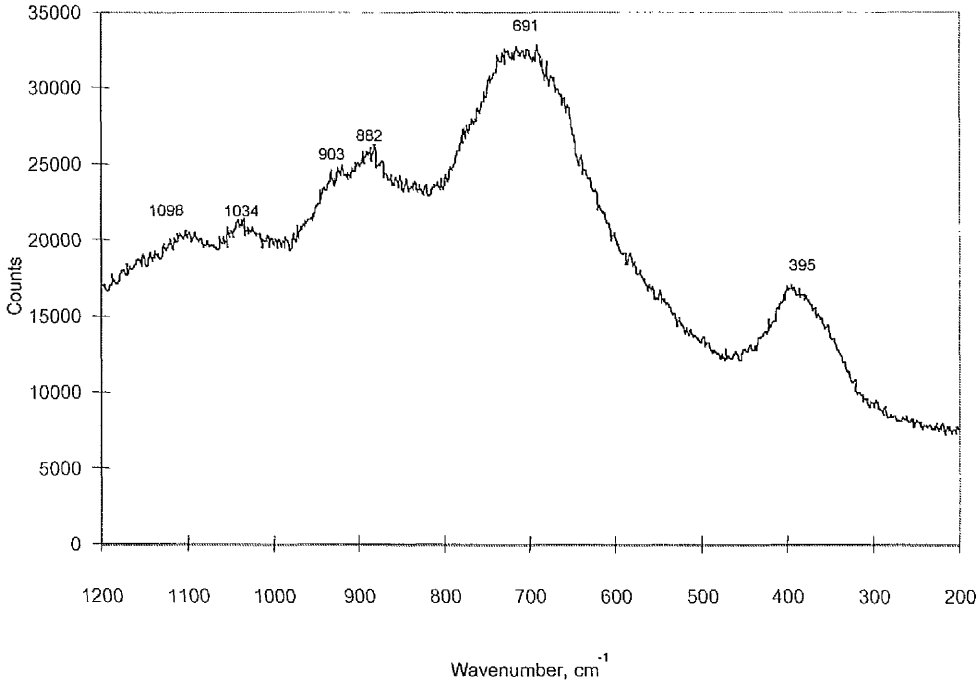

Figure 7.19 Raman spectrum of purple corundum (ruby) from Nong Bon (NB1-6).

The Raman spectrum of purple corundum sample NB1-6 from Nong Bon shows peaks at 1098, 1034, 903, 882, 691, and 395 cm^{-1}. These peaks and others (not shown) do not agree with the peaks from Porto and Krishnan, (1967) (Figure 7.18). This could be the result of fluorescence of the sample.

7.3.3 Summary

The infrared and Raman techniques can be used in complementary ways to identify corundum in terms of its vibrations of atoms in the structure and chemical impurities. The Raman microscope can be used to identify inclusions in corundum. However unlike the infrared spectra the Raman spectra could not differentiate between corundums of different colours and origins. The minerals to be tested by infrared spectroscopy must be available either as fine powders or thin slabs with approximately parallel faces. Thus it is not convenient for gemstone testing, except for the reflectance technique that uses the highly reflective surface of a gemstone. The Raman technique can be carried out without special sample preparation. The results of this study yield artefact peaks due to high reflectance of the samples under infrared irradiation and high fluorescence in the Raman microprobe, giving rise to unsatisfactory results.

CHAPTER 8
TRACE ELEMENTS IN CORUNDUMS

8.1 Introduction

Trace element geochemistry in corundum has been studied both to distinguish natural from synthetic corundums (e.g. Stern and Hänni, 1982; Tang *et al.*, 1989; Muhlmeister *et al.*, 1998) and to differentiate rubies from different localities (e.g. Tang *et al.*, 1988; Osipowicz *et al.*, 1995; Sanchez *et al.*, 1997). However Sutherland *et al.* (1998b) were able to classify corundums derived from basaltic terrains into a metamorphic suite and a basaltic suite by the use of trace element characteristics with the aid of their metamorphic and magmatic mineral inclusions (previously studied by Sutherland and Coenraads, 1996; Sutherland and Schwarz, 1997). The trace element 'fingerprints' of corundums from Thailand can be compared with those of other corundums from well-characterised geological environments as one of the approaches that can be used to deduce the origin.

Several techniques have been used to obtain trace-element concentrations in corundum: energy dispersive X-ray fluorescence (ED-XRF), proton-induced X-ray emission (PIXE), and neutron activation analysis (NAA) (e.g. Stern and Hänni, 1982; Tang *et al.*, 1989; Muhlmeister *et al.*, 1998). However, laser ablation - inductively coupled plasma - mass spectrometry (LA-ICP-MS) and electron probe microanalysis - wavelength dispersive spectrometry (EPMA-WDS) have been employed in this work as they have relatively low detection limits, easy sample preparation and are suitable for a large number of samples.

8.2 Laser ablation - inductively coupled plasma - mass spectrometry (LA-ICP-MS) for trace elements analysis in corundums

Laser ablation - inductively coupled plasma - mass spectrometry (LA-ICP-MS) can be used to analyse almost all elements in the periodic table at the level of parts-per-million in solid samples with a spatial resolution of about 20 μm (Perkins and Pearce, 1995). The equipment is very easy to use and takes a short time for an analysis with an extremely low detection limit (< 50 ng g^{-1} or <0.05 ppm) (Jarvis, 1997). This technique has been used for analysing trace elements in certain minerals (Jackson *et al.*, 1992), basalts and olivine phenocrysts (Jeffries, *et al.*, 1995) and scheelite (Sylvester and

Ghaderi, 1997). Christensen *et al.* (1995) used this technique to investigate Sr isotopes in marine gastropod shells and feldspars.

Corundum is a refractory mineral whose hardness is nine in Mohs' scale and which has a melting point of about 2030 to 2050°C (Hughes, 1997). It is difficult to dissolve for solution analysis by, for example, atomic absorption spectrometry (AAS) or inductively coupled plasma - atomic emission spectroscopy (ICP-AES). LA-ICP-MS overcomes this difficulty. The following sections of this chapter present the principle of LA-ICP-MS in general, details of sample preparation, instrument operating conditions and results and discussion, respectively.

8. 2.1 Principle of LA-ICP-MS

There are two main parts of the system: laser probe and ICP-MS.

The laser probe

The laser is used to remove the material from corundum sample by firing the laser on the analysed area giving an ablated vapour/particulate mixture, which can then be transported by carrier gas to the ICP-MS. This part is mainly composed of laser bench, microscope, mirror box, and ablation cell (Figure 8.1).

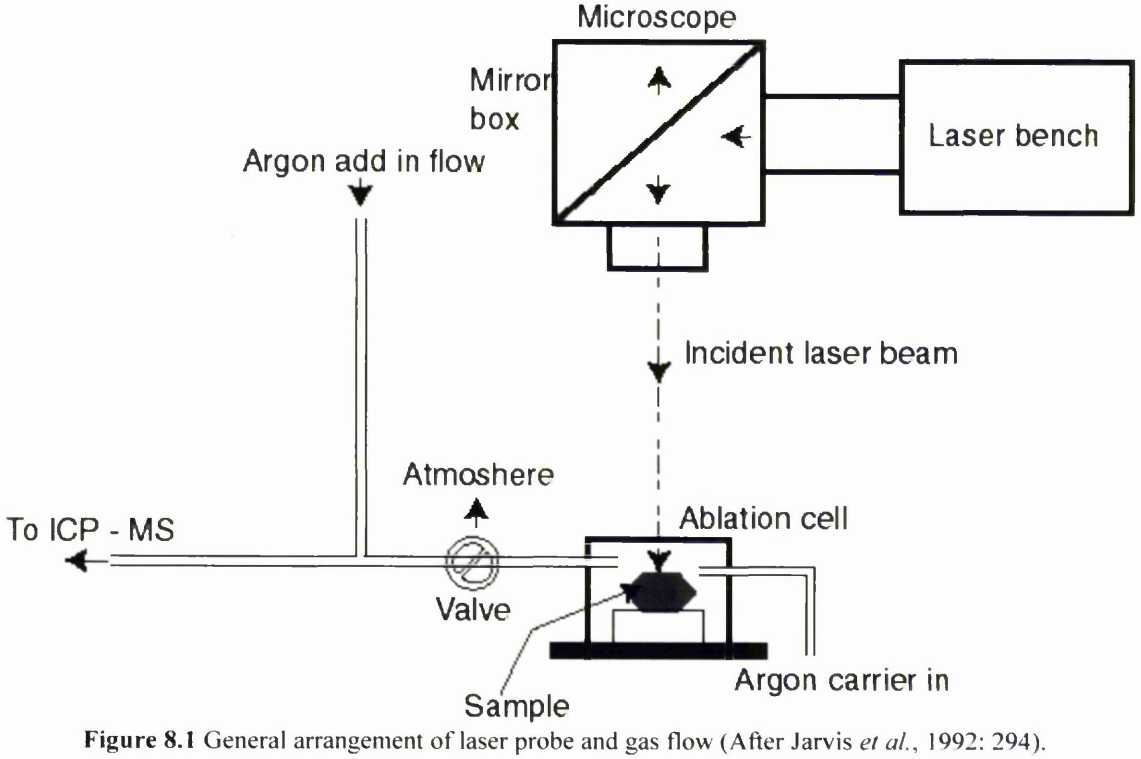

Figure 8.1 General arrangement of laser probe and gas flow (After Jarvis *et al.*, 1992: 294).

The laser beam is emitted by a rod of Nd:YAG (Neodymium:Yttrium aluminium garnet, $Y_3Al_5O_{12}$ doped with approximately 3 wt% Nd_2O_3), which is situated on the laser bench. The atoms of Nd are excited by the energy from a xenon flash lamp into a high energy level. The laser emission takes place when the excited atoms of Nd fall back to the lower energy level (Perkins and Pearce, 1995). The beam size is approximately 10 μm in diameter and the laser has a wavelength of 1066 nm in the near-infrared region (Mattey, 1997). Certain workers quadruple the frequency of the beam to gain a wavelength in the UV region, 266 nm (Jackson *et al.*, 1992; Chenery and Cook, 1993). The ablation temperature varies depending on the material ablated, and for example in fused glass is up to 39,800 K (Fedorovich *et al.*, 1993).

The output laser beam is arranged to reflect at the mirror in the mirror box and is directed onto the sample in the ablation cell which is placed on the stage of the reflected light microscope. The stage is controlled to move along x-y-z directions by the computer joystick. The image of the sample appears on the monitor through a video camera connected to the microscope. The sample is enclosed in an ablation cell, which is made of fused silica, through which argon gas is passed. The argon transports the micro-particulate sample produced during ablation to the plasma torch of ICP-MS directly.

The ICP-MS instrument (Jarvis, 1997)

This part of the apparatus is composed of plasma torch, lens supplies, quadrupole mass filter (mass analyser), electron multiplier and computer (Figure 8.2).

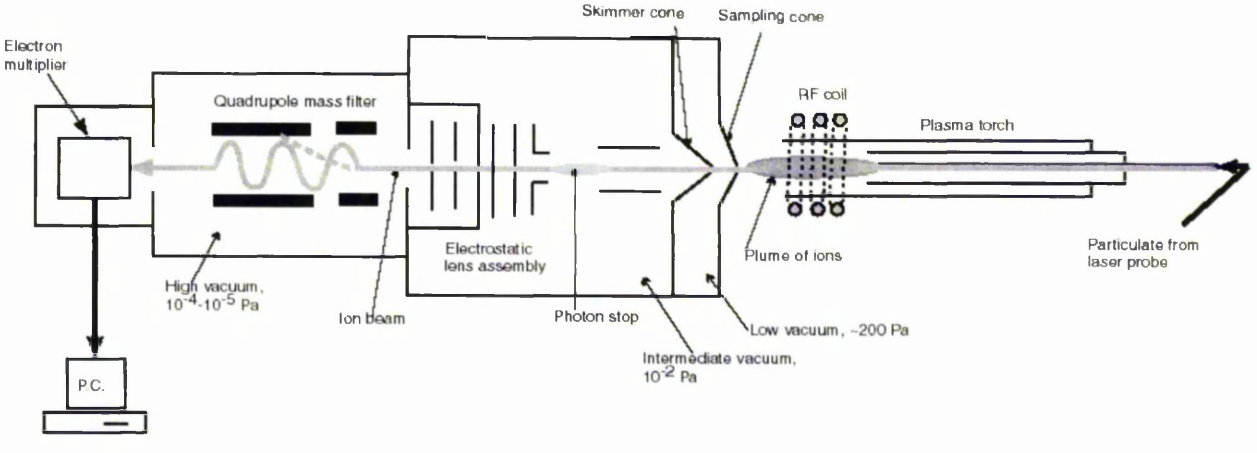

Figure 8.2 The overview of ICP-MS (Modified from Jarvis, 1997).

The particulate sample from the laser probe is introduced to the torch through the injector tube where it is heated by the RF coil and converted into a plume of ions and plasma (temperatures 6,000 to 10,000 K (Walsh, 1977)). The plume of ions then passes through nickel apertures, a sampling cone and a skimmer cone, because of the different pressures between the later components of the apparatus (which are evacuated) and the atmospheric plasma. The ions form the beam and pass through a physical obstruction called the 'photon stop' placed directly in the ion beam path to prevent light reaching the ion detector, reducing the background signal. The electrostatic lens assembly focuses the beam and lets it continue its passage into the mass analyser (quadrupole mass filter).

The quadrupole mass filter has the function of mass separation by electric field. The filter allows ions of only one mass/charge ratio (*m/z*) through to the detector for each combination of potential applied to opposing pairs of stainless steel or molybdenum rods. The mass resolution power of the analyser is electronically controlled by the ratio of peak amplitude of a radiofrequency (RF) to the dc potential. The dc potential is the power supplied to the rods to let the *m/z* range of interest pass through the detector. The electron multiplier is usually used as a detector. A personal computer (P.C.) is connected to monitor and controls the instrument functions such as RF power level, gas flow rates, cooling water flow and instrument start-up and shut-down.

8.2.2 Sample preparation

Analyses of minerals have been made from a range of mineral groups using samples prepared in a variety of ways. The only restriction on the size of a sample is that it fits in the sample chamber, with its top, which should be fairly flat, a minimum distance below the top of the sample cell. No polishing of the sample is required, unless desired in order to observe textures more clearly (Christensen *et al.*, 1995). Jackson *et al.* (1992) used 30 μm polished thin sections, Pearce *et al.* (1992) used sawn and ground blocks as well as single grain mounts, and Jeffries *et al.* (1995) used a block of samples to fit the sample chamber (53 mm in diameter, 35 mm in height). Sylvester *et al.* (1997) mounted the mineral samples in epoxy, cut to expose a fresh surface, polished, and cleaned with methanol. For whole-rock samples, Fedorowich *et al.* (1993) fused the powder (grain size <50 μm) in a tungsten strip furnace (temperature 1650 to 1890°C) to

obtain a glass bead. Jarvis and Williams (1993) used powder pellets of silicate rocks pressed in a die at 10 tons. Binder (for example, polyvinyl alcohol, Elvansite 2013 or Mowiol) is added (in ratio of 4:1, binder to sample) to give mechanical strength to the pellet (Jarvis *et al.*, 1992: 296).

In this study, corundum samples, in forms of polished thick section (~100 μm), rough and gem-faceted samples (measured less than a centimetre across) were analysed. These dimensions of the samples do not cause a problem. However it is difficult to find a flat and fresh surface of the rough samples to be ablated. Jeffries *et al.* (1995) noted that polished surfaces can cause an undesirable reflectance of the laser light, which results in an initial signal reduction.

8.2.3 Instrument operating conditions

The analyses were carried out using the VG Plasma Quad Fisons Instrument ICP-MS and LUV266X Merchantek™ EO Laser at Department of Earth Sciences, University of Manchester. The laser ablation system was run under Q-switched mode (the lasing operation is delayed and pulse is emitted of high power and short duration; sampling is rather shallow but over a broad surface and material is removed almost entirely as vapour (Jarvis, *et al.*, 1992: 292; Jarvis *et al.*, 1993)). The data set was acquired within 60 minutes by scanning the mass range 7 to 238 (Li to Pb). The other instrument operating conditions are given in Table 8.1.

Table 8.1 LA-ICP-MS operating conditions for corundum analysis.

ICP-MS-Instrument operating conditions	
Instrument	VG Plasma Quad™ (PQZ)
Forward power	1.35 kW
Reflected power	<1 W
Plasma gas	argon
Flow rate:	
coolant gas	13.5 $lmin^{-1}$
carrier gas	0.95 $lmin^{-1}$
auxiliary gas	1.00 $lmin^{-1}$
ICP-MS-Data aquisition parameters	
Dwell time	320 μs
Channels per AMU (*m/z*)	19
Multielement: element range for scan	Li to U
Laser	
Laser type	Nd: YAG, maximum output 600 mJ
Wavelength	266 nm (UV laser)
Laser mode	Q-switched
Laser energy	800 V
Shot repetition rate (pulse/sec)	8 Hz
Shots per site	10
Sampling scheme	(10x10)x2, i.e. 100 sites per analysis, being done as 2 rasters of each analysed area, totally 2000 shots per analysis.

8.2.4 Results and discussion

The analyses in this study have been done semi-quantitatively without using an internal standard (an element of known concentration within the sample). Analysis has been carried out in comparison with a glass standard, NIST610 (National Institute Standards and Technology, in USA). In this case, a blank and NIST610 were run at intervals during analysis of the samples. The blank was simply a measurement of counts in the absence of the laser ablation. The NIST610 standard is a synthetic glass containing a range of elements from across the mass range (Li to U). The machine is set to run in the scan mode in which the whole mass range is being scanned and thus the dwell time on each isotope peak is short. The results are inevitably less precise as the instrument is scanned across a large mass range giving fewer counts for each analyte reaching the detector. The detection limit will be higher than with a smaller mass range (Perkins and Pearce, 1995), as in single-ion monitoring mode.

The samples were analysed to obtain trace element concentrations by the equation below:

$$\text{Conc El}_{sam} = (\text{ACPS El}_{sam} - \text{ACPS El}_{Blank}) \times \text{Conc El}_{NIST610} / (\text{ACPS El}_{NIST610} - \text{ACPS El}_{Blank})$$

where **Conc** = Concentration; **El** = Analysed element; sam = sample; **ACPS** = Area counts per second; **NIST610** = reference glass standard.

ACPS values for the blanks were obtained as plasma blank without the laser being fired (Perkins and Pearce, 1995). As no internal standard for natural corundum was available, the concentration of trace elements was obtained by comparison with the glass standard only. Nevertheless, Perkins and Pearce (1995) argued that it is not possible to calibrate results directly by comparing the ACPS for analyte with signal from a calibration reference material. Despite the semi-quantitative analysis a single internal standard should be used. The concentration of an element selected as an internal standard contained in sample is possibly achieved by electron-probe microanalysis (EPMA). The results of this study are given in Table 8.2. In this table, results are presented in the sequence of analysis to show the effects of instrument drift (gradual change of the analyte sensitivity or instrument parameters with time).

Table 8.2 Trace element concentration (ppm) in NIST610 and corundum samples analysed by LA-ICP-MS.

Sample No	NIST610	SYNRUBY1*	SYNB1*	SYNRR1*	SYNYE1*	CKF	DCG	KSA	BPJ	NYJ	BKCHA	BRD	NBC	R27*	CKEP9	CKEP8	CKEP7	CKEP13	CKEP12	CKEP11	CKEP17
Time	-	12:38:06	12:41:54	12:59:51	13:05:50	13:14:35	13:21:35	13:27:57	13:37:20	14:06:20	14:12:18	14:18:19	14:21:25	14:24:46	14:44:20	14:46:32	14:48:55	14:50:35	14:52:07	14:57:10	14:58:34
^{7}Li	482						8		5	10	10			<1						<1	
^{9}Be	461		1	<1	<1	8	1	1	1	<1	1	<1	<1	<1	4		1	1	<1	5	2
^{11}B	358	26	26	20	18	52	122	18	271	230	206	1	6	8	4	2	2	1	2	19	4
^{24}Mg	465	1	2	3	3	160	3122	78	2456	2988	3117	50	30	66	41	1	<1	2		9	<1
^{31}P	343	19	20	12	24	72	553	42	415	444	728	21	28	39	101	4	2	1	4	11	4
^{39}K	463	22		46	60	364	458	130	331	381	474			96							
^{45}Sc	112						2	<1	2	1	2	<1									
^{47}Ti	433	5	16	3	<1	1931	41980	814	33938	40657	45869	103	59	77	64	270	22	7	27	557	1
^{51}V	440	<1	2		<1	4	12	6	6	7	9	5	3	1	1	1	<1	<1	<1	9	<1
^{52}Cr	388	185	2	88	4	10	40	29	33	30	53	59	401	764	14	1	<1	1	1	<1	3
^{55}Mn	436	<1		<1	<1	10	609	7	431	515	666	6	3	10	2	1	<1		<1	1	<1
^{56}Fe	453	32	25	14	8	2502	846	2439	682	905	1108	659	336	112	168	224	100	75	213	1085	194
^{59}Co	401					<1	4	1	3	4	5	2	2	2	3	1	1	1	1	1	1
^{60}Ni	439			2	3	19	54		26	79	89					13					
^{63}Cu	433	3	3	1	2	99	83	6	51	335	135	4	3	17	22	80	85	13	33		7
^{66}Zn	429	<1	1	5	<1	34	65	8	54	171	131	8	2	16	7	16	<1	<1	1	1	1
^{69}Ga	438	<1			<1	224	5	42	3	3	4	4	3	1	20	18	10	7	15	186	16
^{72}Ge	431				<1	3		1	<1	<1	<1	<1	<1	<1	1	<1		<1		1	
^{75}As	318	49	42	52	47	80	56	48	52	29	32	4	7	11	2						
^{78}Se	112	5	5	6	4	5	13	11	11	4	3	7	8	6							
^{85}Rb	430					1	8	<1	6	5	8										
^{88}Sr	505	<1		<1	<1	3	1554	<1	1166	1403	1494	4	1	2	1	<1			<1	<1	<1
^{89}Y	453			<1		1	15		13	13	18	<1	<1	1	1					<1	
^{90}Zr	440	<1	1	1	<1	21	21	7	16	24	27	4	2	1	604	1	1	1	<1	2	4
^{93}Nb	382	<1	<1		<1	152	244	3	190	230	284	<1	<1	<1	1	16	22	12	1	176	11
^{95}Mo	396	<1	<1	<1	<1	1	2	<1	1	2	2	1	1	1	1	<1	<1	<1	<1	<1	<1
^{109}Ag	241	<1	<1	<1	<1	4	12	<1	14	1	7		<1	1	<1					<1	
^{111}Cd	261	2	1	4		4	9	1	27	871	327	1	4	6	<1	<1		1	1	<1	1
^{115}In	440					<1	<1	<1	1	<1	1	<1	<1	<1	<1	<1	<1		<1	<1	
^{118}Sn	390	1	1		<1	61	9	1	8	37	34	1	4	2	<1	2	2	1	11	12	7
^{121}Sb	388	1	1	<1	<1	1	1	<1	2	2	3	<1	<1	1							
^{133}Cs	351						2		<1	1	1										
^{137}Ba	416	1	1			34	130	3	174	134	175	2	<1	16	2		<1		77	<1	1
^{139}La	437	<1	<1		<1	1	15	<1	12	15	17	<1	<1	1	1		<1			1	
^{140}Ce	443	<1	<1	<1	<1	3	13	<1	13	13	19	<1	<1	71	2	<1	<1		<1	3	<1
^{141}Pr	431					<1	3		2	2	3	<1	<1	1	<1	<1		<1		<1	<1
^{146}Nd	430	1		<1	<1	1	10	<1	60	11	14	<1	<1	4	1	1	<1	<1		<1	<1
^{147}Sm	451	1		<1			4		3	3	4	<1	<1	<1	<1			1	<1		<1
^{153}Eu	430	<1	<1		<1	<1	2	<1	1	<1	1		<1	<1		<1	<1			<1	<1
^{157}Gd	423					<1	3		4	3	2			<1						<1	
^{159}Tb	446	<1		<1		<1	1	<1	1	<1	<1	<1	<1	<1	<1	<1	<1	<1	<1	<1	<1
^{163}Dy	435			<1			2		2	2	2		<1	1			<1			<1	
^{165}Ho	453	<1	<1				<1	<1	<1	<1	1	<1	<1	<1		<1		<1	<1	<1	<1
^{166}Er	435			<1	<1	<1	2	<1	1	2	2	<1	<1	<1	<1	<1	1		<1	<1	<1
^{169}Tm	423	<1	<1		<1	<1	<1	<1	<1	<1	<1		<1	<1	<1	<1			<1	<1	<1
^{172}Yb	463		<1	<1			1	<1	2	<1	2	<1	2	<1	<1		<1	<1		<1	<1
^{175}Lu	433					<1	<1		<1	<1	<1		<1	<1	<1						
^{178}Hf	411	<1	<1		<1	4	1	1	<1	1	2	1	1	1	8	<1	<1	<1	1	1	<1
^{181}Ta	361		<1	<1	<1	257	22	2	16	20	24			<1	1	12	17	39	6	179	45
^{182}W	435	<1				1	13		11	15	19			3			<1	<1		3	
^{185}Re	122	<1	<1	1	<1	<1						<1									
^{197}Au	23	<1		<1		1	1	<1	4	<1	<1	<1	<1	<1	<1	<1	<1	<1	<1	<1	<1
^{205}Tl	61	<1	<1	<1	<1	<1	<1	<1		<1	<1					<1			<1		
^{208}Pb	419	1	1	1	1	11	49	4	29	46	62	1	1	6	2	1			<1	1	<1
^{209}Bi	374	<1	<1	<1	<1	<1	1	<1	1	1	1	<1	<1	<1	<1	<1	<1		<1	<1	<1
^{232}Th	463		<1		<1	7	1	<1	1	1	2	<1		<1	<1	1	<1	<1	<1	9	<1
^{238}U	463	<1	<1	<1		<1	1	<1	1	1	1	<1	<1	<1	<1	<1	<1		<1	<1	

*Synthetic Verneuil corundums; Prefix: CK = Ban Huai Sai, DC = Den Chai, KS = Khok Samran, BP = Bo Phloi, NY = Nam Yun, BR = Bo Rai, NB = Nong Bon, CRM/ZOI = corundum in zoisite from Tanzania.

Table 8.2 (Continued).

Sample No	CKEP16	CKEP15	BPEP12	BPEP11	BPEP10	BPEP8	BPEP7	BPEP6	BPEP5	NYEP13	NYEP12	NYEP10	NYEP9	NYEP8	BREP40	BREP39	BREP37	BREP35	BREP34	BREP33	BREP31	BREP30	BREP29	CRM/ZOI-2
Time	15:00:45	15:02:57	15:12:06	15:13:49	15:15:30	15:17:12	15:18:54	15:20:34	15:22:13	15:47:14	15:48:56	15:50:42	15:52:25	15:54:01	16:20:33	16:22:21	16:24:08	16:25:45	16:27:28	16:29:10	16:30:47	16:32:29	16:34:05	16:45:54
^{7}Li																								2
^{9}Be	<1	<1	<1	<1							<1			<1										
^{11}B	5	17	1	1	1	1	1	1	2					1	7	4	<1				<1	1	1	2
^{24}Mg		2	<1		1	<1	1	1	<1	<1	1	5	2	2	4	4	6	5	3	4	4	4	4	845
^{31}P	4	8	16	9	4	6	4	5	4	32	16	15	5	7	87	77	41	19	7	6	3	9	1	7
^{39}K																								10
^{45}Sc																								
^{47}Ti	4	33	1		1		<1	4		3	1	13	10	19			1	8	3	1	3		1	5
^{51}V	<1	<1	<1	<1	<1	<1	<1	1	<1	<1	1	<1	2	3	<1	<1	1	<1	<1	<1	1	1	<1	1
^{52}Cr	1	1	1	1	1	<1	1	1	<1	<1	1	1	1	1	78	41	72	30	19	25	34	90	17	614
^{55}Mn		2	1	<1	<1					1	<1	<1	<1	<1	1	<1		<1	<1			<1		7
^{56}Fe	55	486	39	31	33	34	32	27	37	116	98	54	170	704	26	51	57	41	34	40	25	151	24	63
^{59}Co	<1	<1	<1	<1	<1	<1	<1	<1													<1	<1	<1	<1
^{60}Ni					5	5	26	5	48			4						7		15	2	15	3	14
^{63}Cu	78		21	10	70	98	172	47	194	35	62	101	<1	41	70	43	56	77		37	1	50	13	68
^{66}Zn	1	1	<1	1	<1	<1	<1	<1	1	<1	1	1	1	2		<1	3	2	<1		<1	1		2
^{69}Ga	5	47	2	2	1	2	3	2	4	4	8	3	11	32		<1	2	1	1	1	1	1	<1	3
^{72}Ge	<1	1	<1			1	<1		<1		<1	<1	<1											
^{75}As																								
^{78}Se																								
^{85}Rb																								
^{88}Sr	<1	<1	<1	<1	<1	<1	<1			<1	<1	<1	<1	<1	<1	<1	<1	<1	<1	<1	<1	1		2
^{89}Y											<1		<1	<1		<1	<1	<1	<1		<1			
^{90}Zr	<1	1	<1							<1						<1	<1		<1	1				<1
^{93}Nb	<1	3		<1	<1		<1	<1	<1	<1	<1	<1		<1			<1			<1	<1	<1		<1
^{95}Mo	<1	<1	<1	<1	1	1		1		1		<1	<1	1					<1				<1	
^{109}Ag								35				<1	<1		<1		40		<1		<1	<1	8	<1
^{111}Cd		1	1	1	1		1	1	1	1	1	1	2	<1		1	<1	2	<1	<1	<1	1		1
^{115}In		<1				<1	<1	<1	<1	<1	<1	<1		<1		<1	<1		<1			<1		<1
^{118}Sn	<1	14	<1		<1	<1	<1	<1		<1		<1	<1	<1			<1						<1	
^{121}Sb												<1												<1
^{133}Cs												<1		<1										
^{137}Ba			<1	<1	1	<1	<1	<1			1	1		1		<1		1				<1	<1	40
^{139}La																	<1	<1		<1		<1		<1
^{140}Ce	4	<1	<1						<1				<1	<1			<1	<1	<1	<1	<1	1		<1
^{141}Pr	<1	<1	<1		<1	<1		<1		<1				<1		<1	<1	<1	<1	<1	<1	<1		
^{146}Nd	1	<1		1	<1	<1	<1	1	<1		<1	1	<1	<1		<1	<1	<1	<1	1	1	<1	<1	
^{147}Sm	1	1	<1	1	1	<1	<1	2	<1	2	<1	1	<1	<1		<1	<1	1	1	<1	1	<1	<1	<1
^{153}Eu	<1	<1	<1		<1	<1	<1	<1	<1	<1	<1	<1	<1	<1			<1	<1	<1	<1	<1	<1	<1	<1
^{157}Gd																								
^{159}Tb	<1		<1	<1	<1	<1	<1	<1	<1	<1	<1	<1	<1	<1		<1	<1	<1	<1		<1		<1	<1
^{163}Dy		<1			<1						<1		<1	<1				1		<1		<1		<1
^{165}Ho	<1	<1	<1	<1	<1	<1	<1	<1		<1	<1	<1	<1	<1			<1	<1	<1		<1	<1	<1	<1
^{166}Er		<1	<1	<1	<1	<1	<1	<1		<1	<1	<1	<1	<1	<1		<1	<1	<1	1			<1	
^{169}Tm		<1	<1	<1						<1			<1	<1		<1	<1	<1	<1	<1	<1	<1	<1	<1
^{172}Yb	<1			<1		<1		<1	<1	1		<1		1			<1	<1		<1	<1		<1	<1
^{175}Lu	<1						<1		<1	<1				<1					<1	<1	<1	<1	<1	
^{178}Hf	<1	<1	<1	1	1	<1	1	1	1	<1	<1	<1	<1	<1			<1			<1		<1	<1	<1
^{181}Ta	1	8	<1	<1	<1	<1		<1		<1	<1	<1	<1	<1		<1	<1	<1	<1	<1	<1	<1	<1	<1
^{182}W													<1								<1			<1
^{185}Re							<1				<1						<1	<1	1		<1	<1	<1	
^{197}Au	<1	<1	1	<1	<1	<1		<1		<1				<1			<1	<1						<1
^{205}Tl			<1	<1	<1	<1	<1		<1	<1	<1	<1	<1	<1		<1	<1		<1	<1	<1		<1	
^{208}Pb	<1	<1	<1	<1		<1				<1	<1	<1	<1	<1	1		1	<1		<1	<1	<1	1	<1
^{209}Bi	<1	<1	<1	<1	<1	<1	<1	<1	<1	<1	<1	<1	<1	<1	<1	<1	<1	<1	<1	<1	<1	<1	<1	<1
^{232}Th		1	<1	<1	<1	<1	<1		<1	<1	<1	<1	<1			<1	<1	<1		<1	<1	<1		<1
^{238}U			<1	<1	<1				<1	<1	<1									<1		<1	<1	

*Synthetic Verneuil corundums; **Prefix**: CK = Ban Huai Sai, DC = Den Chai, KS = Khok Samran, BP = Bo Phloi, NY = Nam Yun, BR = Bo Rai, NB = Nong Bon, CRM/ZOI = corundum in zoisite from Tanzania.

Element concentrations in most cases seem to decrease with time. For example ^{47}Ti content of sample from Bo Phloi analysed at 13:37:20 is 33938 ppm (BPJ) as compared to the very low values (down to 0 ppm) of ^{47}Ti content analysed later on the same day between 15:12:06 and 15:22:13 (samples with prefix BP).

Noticeably, the corundum samples from Ban Huai Sai (prefix CK) consistently show high anomalous concentrations of ^{181}Ta compared to corundum from other localities. For example, sample CKF has ^{181}Ta content up to 257 ppm (Table 8.2). The Ta concentration in Ban Huai Sai corundum is high in some samples and it is suspected that this is due to analysis of inhomogeneous samples. Areas of rutile (TiO_2) as inclusions might have been ablated, which could have resulted in anomalous Ta and Nb signals. In this case sample CKF has the ^{47}Ti content of 1931 ppm. This is because some of the Ti in rutile could be substituted by Ta and Nb owing to the closeness in the ionic radii of Ti^{4+} (60.5 pm), Ta^{5+} (64 pm) and Nb^{5+} (64 pm) (Deer *et al.*, 1996). That is why Nb concentration increases with Ta concentration in some cases. Tantalum and niobium usually occur in the minerals associated with cassiterite in tin deposits. These three elements would be expected to have certain correlation in the corundum samples from this locality.

Instrument drift is probably the cause of decrease in element contents with time. This could be the result of undissociated material being deposited in the sampling cone orifice (only 1mm wide) causing signal drift (loss) and reduction in precision (Jarvis, 1997). Moreover an internal standard for corundum is not available in this study.

However the Ta anomaly may be genuine and other elements (including Ti, V, Cr, Mn, Fe, Cu, Ga, Nb, Sn, and W) could have lodged in the corundum structure in trace amounts. All of them need to be confirmed by the EPMA technique.

8.3 Electron probe microanalysis technique for trace elements in corundums

8.3.1 Sample identifications

Corundum samples from Thailand

The corundum samples from Thailand as well as Ban Huai Sai, in the Democratic People's Republic of Laos were purchased from, or donated by, mine operators at the localities as shown in Figure 8.3. Brief descriptions of corundum samples used in this

study, from Thailand are given in Table 8.3 and full description including locality, sample number, colour, dimension and morphology are given in Appendix 8-1.

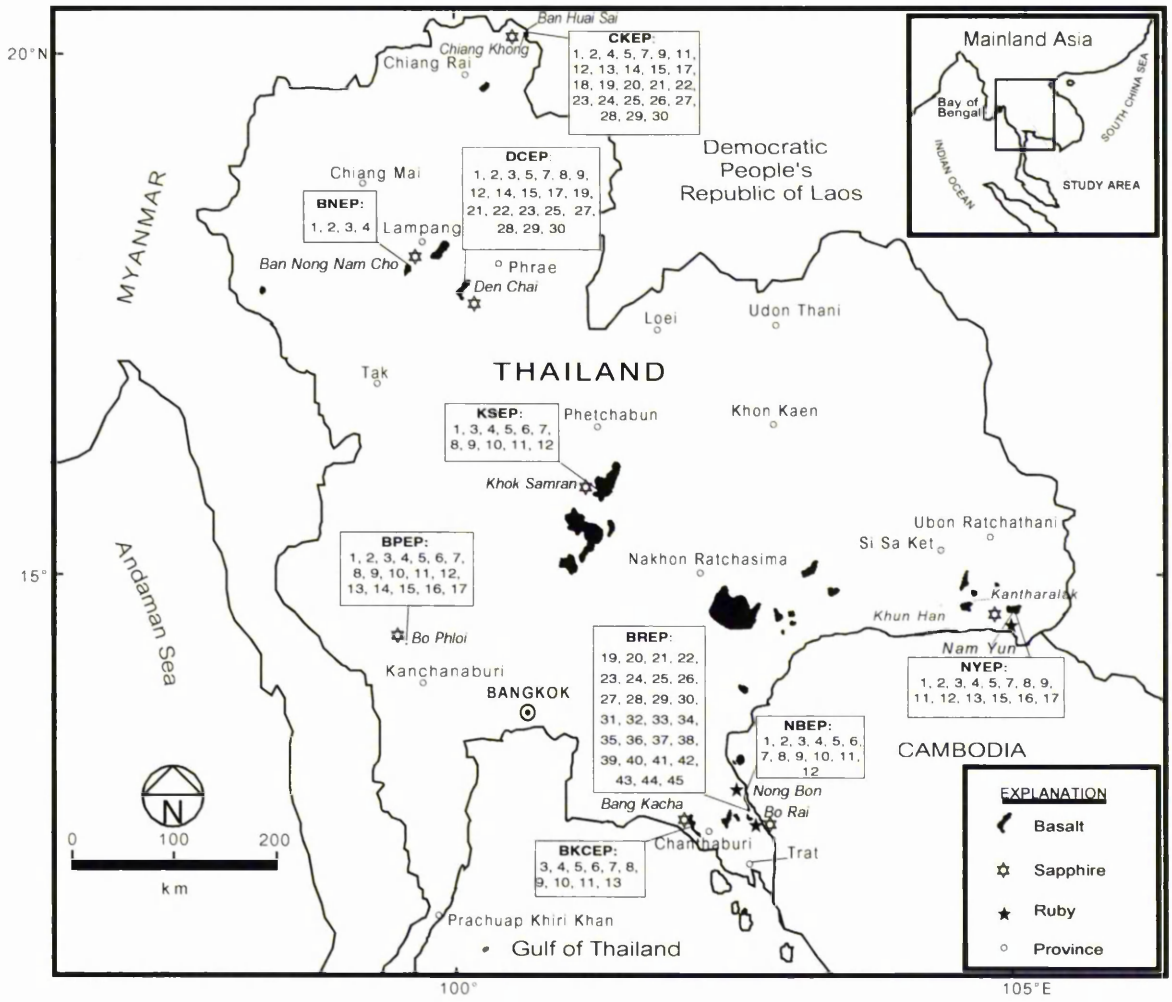

Figure 8.3 Map of Thailand showing the localities of corundum samples (rubies & sapphires) and the distribution of basalts (Modified from Vichit *et al.*, 1992). The sample numbers are given in boxes.

Table 8.3 Corundum samples from Thailand and adjacent area analysed by the EPMA-WDS.

Locality	Sample number	Description*
1. Ban Huai Sai, near Chiang Khong	**CKEP**: 1, 2, 4, 5, 7, 9, 11, 12, 13, 14, 15, 17, 18, 19, 20, 21, 22, 23, 24, 25, 26, 27, 28, 29, 30	Sapphires
2. Ban Nong Nam Cho	**BNEP**: 1, 2, 3, 4	Sapphires
3. Den Chai	**DCEP**: 1, 2, 3, 5, 7, 8, 9, 12, 14, 15, 17, 19, 21, 22, 23, 25, 27, 28, 29, 30	Sapphires
4. Khok Samran	**KSEP**: 1, 2, 3, 4, 5, 6, 7, 8, 9, 10, 11, 12	Sapphires
5. Bo Phloi	**BPEP**: 1, 2, 3, 4, 5, 6, 7, 8, 9, 10, 11, 12, 13, 14, 15, 16, 17	Sapphires
6. Nam Yun	**NYEP**: 1, 2, 3, 4, 5, 7, 8, 9, 11, 12, 13, 15, 16, 17	Sapphires
7. Bang Kacha	**BKCEP**: 3, 4, 5, 6, 7, 8, 9, 10, 11, 13	Sapphires
8. Bo Rai	**BREP**: 19, 20, 21, 22, 23, 24, 25, 26, 27, 28, 29, 30, 31, 32, 33, 34, 35, 36, 37, 38, 39, 40, 41, 42, 43, 44, 45	Ruby and sapphires
9. Nong Bon	**NBEP**: 1, 2, 3, 4, 5, 6, 7, 8, 9, 10, 11, 12	Ruby

*Colours presented in this section are simply grouped into two categories, ruby (red, pink and purple) and sapphires (other colours than ruby). See Appendix 7-1 for more details.

Corundum samples from elsewhere in the world

Corundum samples from well-characterised geological environments elsewhere in the world were chosen to compare with Thai corundum samples. They range from igneous rock (pegmatitic plumasite), pelite xenoliths in dolerite and gabbro, metamorphosed igneous rocks, and metasedimentary rocks. They include 10 types of host-rock composition and are subdivided into 16 different rock types, for example plumasite, buchite, hornfels, gneiss, schist, granulite etc. The descriptions of these rocks including rock-type, locality, mineral assemblage, sample number, geological setting, reference and variety of corundum are given in Table 8.4. The information on samples of corundums of unknown origin is also given in Table 8.4. The descriptions of colour, dimension and morphology of the corundums are given in Appendix 8-1.

Table 8.4 Corundum samples from outside Thailand.

Col. No. in Tab. 8.7	Host – rock bulk composition	Rock type	Locality	Assemblage	Sample No.	Geological setting	Reference	Corundum variety
A. IGNEOUS CORUNDUM : (crystallized directly from magma)								
1	Al-rich "diorite"	Pegmatitic plumasite	?Natal, S. Africa	CRM+PL (+BT)	Δ1556	Intrusive (details unknown)	Du Toit, 1918	Sapphire (grey)
B. CORUNDUM IN SMALL (<10 cm diameter) **PELITE XENOLITHS IN MAFIC MAGMA:** (pelitic compositions ?modified by diffusive interaction with mafic magma)								
2	Al-rich pelitic (restite)	Corundum - mullite - buchite	Mull, Scotland, UK	CRM+PL+SP+MULL+GLASS + (Interstitial basalt: PL+OPQ+Altered PIG)	SVI/I	Very high-grade contact metamorphism, Xenoliths in a dolerite sill	Thomas, 1922, 1930; Brearley, 1986; Schairer& Yagi, 1952	Sapphire (blue)
		Corundum – plagioclase - hornfels	Bushveld intrusion, S. Africa	CRM+PL±SP+ (SER+RU)	18058	Very high-grade contact metamorphism, Xenoliths in Bushveld gabbro intrusion	Willemse and Viljoen, 1970	Ruby (purple)
C. METAMORPHIC CORUNDUM IN ROCKS OF IGNEOUS ORIGIN:								
3	(i) Ultramafic	Actinolite - gneiss	S. India (Kodaikanal)	CRM+ACT (Ca-Amphibole)+ SP+PL	Δ793	Granulite – facies, regional metamorphism		Ruby (purple)
4	(ii) Syenitic	Syenite - gneiss	Bancroft, Ontario, Canada	CRM+SCAP+KSF+BT+MU+SP+PL+NE (+CAL)	BC21	High – grade, regional metamorphism	Moyd, 1949	Sapphire (grey)
D. METAMORPHIC CORUNDUM IN ROCKS OF SEDIMENTARY ORIGIN:								
5	(i) 'Normal pelitic'	Corundum – biotite - hornfels	Loch Awe, Etive, Scotland	CRM+MU+KSP+QZ+BT	MM125A	Contact metamorphic aureole, Medium – grade CM. (600°C, 2 kbar)	Droop & Treloar, 1981, Moazzen, 1999	Sapphire (blue)
		Corundum – sillimanite – cordierite – hornfels	Belhelvie, Scotland	CRM+SP+SILL+CRD+BT+KFS+(ILL+ZIR+RU)	Δ1192	High – grade CM. (800°C, 4.5 kbar)	Droop & Charnley, 1985	Colourless in thin section
		Corundum – staurolite – muscovite - schist	Stoer, NW. Scotland	CRM+MU+STAUR+(+ZIR+OPQ)	Δ1636	High – grade RM. migmatitic	Cartwright & Barnicoat, 1986	Ruby (pink)

ACT=Actinolite; BT=Biotite; CAL=Calcite; CM=Contact metamorphism; CRD=Cordierite; Cr-HBL=Chromian ornblende; CRM=Corundum; Cr-ZOI=Chromian Zoisite; CTD=Chloritoid; DIAS=Diaspore; GED=Gedrite; GRT=Garnet; ILL=Ilmenite; KFS=K-Feldspar; KORN=Kornerupine; KY=Kyanite; MU=Muscovite; NE=Nepheline; OPQ=Opaque mineral; PIG=Pigeonite; PL=Plagioclase; QZ=Quartz; RM=Regional metamorphism; RU=Rutile; SCAP=Scapolite; SER=Sericite; SILL=Sillimanite; SP=Spinel; SPR=Sapphirine; STAUR=Staurolite; ZIR=Zircon

Table 8.4 (Continued).

Col. No. in Tab. 8.7	Host – rock bulk composition	Rock type	Locality	Assemblage	Sample No.	Geological setting	Reference	Corundum variety
6	(ii) Al, Mg – rich pelitic (? restitic)	Corundum – cordierite gneiss	Baffin Island, Canada	CRM+SPR+ CRD+GED+ (RU+ZIR+BT+MU+ HBL)	Δ440	Al, Mg – rich granulite, Granulite facies, RM.		Colourless in thin section
		Corundum – biotite schist	Limpopo Belt, Zimbabwe	CRM+BT+SILL+CRD	BB14A	Al, Mg – rich granulite, Granulite facies, RM. (850° C, 10 kbar)	Droop, 1989	Ruby (purple)
		Garnet – sapphirine - granulite	Limpopo Belt, Zimbabwe	CRM+GRT+SPR+BT+K ORN+GED+SP+ CRD+PL	BB29F	Granulite facies, RM. (850° C, 10 kbar)	Droop, 1989; Horrocks, 1983	Colourless in thin section
7	(iii) Bauxitic	Chloritoid – corundum - rock	Cape Emerion, Naxos, Greece	CTD+DIAS+CRM+ OPQ	Δ577	Emery, Greenschist facies, RM.	Feenstra, 1985	Colourless in thin section
		Spinel – biotite – plagioclase granulite	Limpopo Belt, Zimbabwe	CRM+SP+PL+BT	BB19	Granulite facies, RM.	Droop, 1989	
	(iv) Al – rich pelite (restite)	Corundum – spinel – hornfels (Emery)	Sithean Sluain, Scotland	CRM+PL+SP	Δ1378	Very high – grade CM., within 3 m of contact of dolerite plug	Smith, 1969	
8	(v) Calcareous	Corundum - marble	Mong Hsu, Myanmar	CRM+CAL	TYEP1, 2, 3; MSEP1 to 8	High grade RM.	Peretti *et al.*, 1995; 1996	Ruby (purple)
	(vi) Marly (Al, Ca, Si – rich)	Corundum – zoisite rock	Tanzania	CRM+Cr-ZOI+?Cr-HBL	CRM/ZOI	High grade RM.	Game, 1954; Dirlam, *et al.*, 1992.	
E. UNKNOWN ORIGIN:								
9		Vietnam			VNEP1, 2, 3			Sapphire (blue)
		Nigeria, Africa			NAEP1, 2, 3			
10		North Vietnam			NVEP1, 2, 3			Ruby (purple)
		Africa			AFEP1, 2, 3			

ACT=Actinolite; BT=Biotite; CAL=Calcite; CM=Contact metamorphism; CRD=Cordierite; Cr-HBL=Chromian ornblende; CRM=Corundum; Cr-ZOI=Chromian Zoisite; CTD=Chloritoid; DIAS=Diaspore; GED=Gedrite; GRT=Garnet; ILL=Ilmenite; KFS=K-Feldspar; KORN=Kornerupine; KY=Kyanite; MU=Muscovite; NE=Nepheline; OPQ=Opaque mineral; PIG=Pigeonite; PL=Plagioclase; QZ=Quartz; RM=Regional metamorphism; RU=Rutile; SCAP=Scapolite; SER=Sericite; SILL=Sillimanite; SP=Spinel: SPR=Sapphirine; STAUR=Staurolite; ZIR=Zircon

8.3.2 Sample preparation

Single grains (average diameter is about 5 mm) were handpicked on the basis of colour, low abundance of cracks, and minimum degree of tarnishing and staining. The individual grains of gem corundum were placed, in an array, on a piece of sticky tape in order to be able to recognise them (Figure 8.4, A). They were then embedded in the epoxy resin, cut, polished and made into sections without a cover glass as shown for example in Figure 8.4, B. The sections are approximately 100 μm thick due to the high hardness of corundum. The thicker section seems to adhere to the glass slide better than a thinner one, which may shatter and loosen from the glass slide while being polished. The samples of corundum-bearing rocks from outside Thailand were cut and polished in the ordinary way to a thickness of about 30 μm. All sections before analyses were coated with carbon by the carbon-arc technique to provide a conducting path for the probe current and thus prevent build-up of charge (Reed, 1996; Reed, 1997).

8.3.3 Methodology

The polished sections were analysed with the CAMECA SX-100 electron microprobe. Clean areas in the samples, without visible inclusions, were chosen for analysis. The computer software, SXRAY, was set to automatically run the machine under the 'trace analysis programme' (without collecting the count rates of Al and O) for collecting the count rates of 15 trace elements (V, Ni, Ga, Fe, Mn, Cr, La, Ti, Sn, Si, Y, Ta, Nb, W and Cu).

Transition group elements (V, Ni, Fe, Mn, Cr, and Ti) are expected to substitute in the structure of corundum and some of them are known to cause body colour. For example Cr is responsible for the red colour of ruby, Ti and Fe for the blue colour of sapphire (Nassau, 1983) and V, Cr, Ti and Fe for colour change sapphire (purple-red colour under incandescent light, blue-green colour under fluorescent light) (Schmetzer and Bank, 1980). Gallium is akin to Al and it uses the Al as a camouflage due to the closeness of their atomic radii (0.620 Å for Ga^{VI} and 0.535 Å for Al^{VI}) and charge, 3+ (Frye, 1974, p. 39-40; Krauskopf and Bird, 1995: 542-545). Lanthanum, a rare earth element, and yttrium, which has a similar size to lanthanum, were investigated in this study. Sn, Ta, Nb, W and Cu were examined in order to confirm the results reported by LA-ICP-MS. Although Si prefers to substitute for Al in minerals with IV co-ordinated sites, VI co-ordinated Si is possible, and thus it was analysed for experimentally in corundum in this work. Moreover Si may be controlled by the presence of divalent cations e.g. Fe^{2+} and Mg (Schmetzer and Bank, 1980).

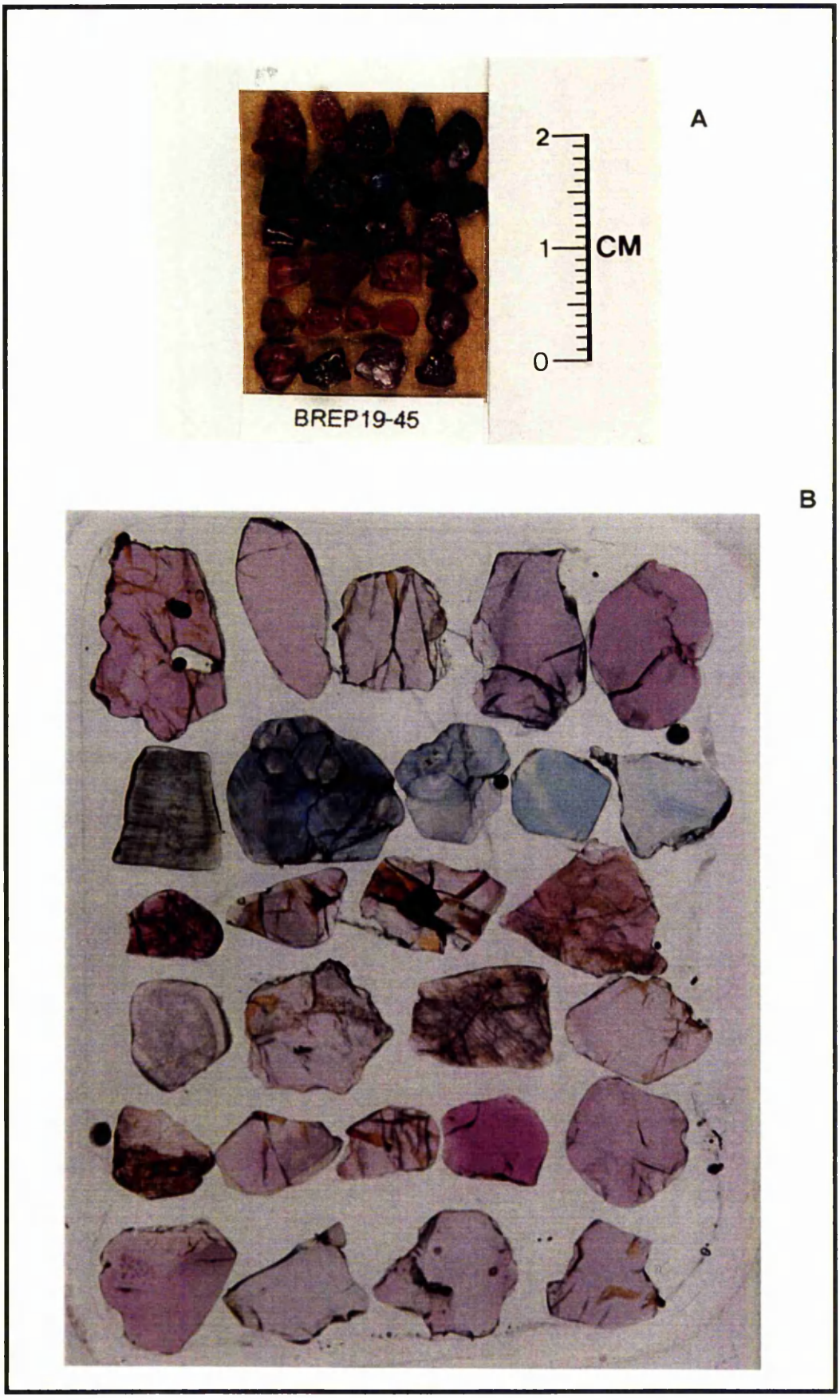

Figure 8.4 A, Corundum samples from Bo Rai, Thailand (sample numbers BREP 19-45, from left to right and top to bottom), being prepared to cut and polish and turn into the polished section as in **B**.

Five spectrometers were used to collect the counts; the other conditions designated are summarised in Table 8.5. The running time for one analysis was 12 minutes.

Note that the samples from Ban Huai Sai (CKEP1-30) and from Bo Phloi (BPEP1-17) were analysed twice, the second time in order to examine whether or not the Ta, Nb, W and Cu contents are genuine. The machine was run under conditions of 25 kV and 200 nA for this occasion.

Table 8.5 Summary of the EPMA-WDS condition for analysis of corundums.

Element	Crystal	Spectrometer No.	Standard used	Line of electron transition between atomic shells
V	LLIF (Large lithium fluoride)	1	V_2O_5	Kα
Ni	"	1	NiO	Kα
Ga	"	1	GaAs	Kα
Fe	LIF (lithium fluoride)	2	Fe_2O_3	Kα
Mn	"	2	Tephroite (Mn_2SiO_4)	Kα
Cr	"	2	Cr_2O_3	Kα
La	LPET (Large pentaerythritol)	3	Lanthanum-glass	Lα
Ti	"	3	Rutile (TiO_2)	Kα
Sn	"	3	Cassiterite (SnO_2)	Lα
Si	TAP (Thallium acid phthalate)	4	Quartz (SiO_2)	Kα
Y	"	5	Praseodymium-glass	Lα
Ta	LIF (lithium fluoride)	1	Tantalum	Lα
Nb	LPET (Large pentaerythritol)	3	Pyrochlore $(Ca,Na)_2Nb_2O_6(O,OH,F)$	Lα
W	LIF (lithium fluoride)	2	Tungsten	Lα
Cu	"	2	Copper	Kα

Al was not analysed due to a technical problem. Initially, Al was analysed at 15 kV (acceleration voltage) and 10 nA (beam current), while trace elements were analysed at 15 kV and 40 nA. This caused the machine to stop running unexpectedly on several occasions. The 'trace analysis programme' (assuming Al = 52.4 wt% and O=46.6 wt%)

was then applied at 30 kV and 60 nA or at 25 kV and 200 nA to avoid the problem and with the higher beam voltage, the count rate was more efficiently collected. Altogether, 491 analyses were collected (307 analyses from Thai-Laos corundum samples and 184 analyses from world corundum samples).

8.3.4 Results

The weight per cent for each cation is converted to weight per cent (wt%) of oxide. Ranges of the concentration of each oxide in each analysed sample are given in Tables 8.6 and 8.7 while the full set of analyses is presented in Appendices 8-2 and 8-3. Due to the high sensitivity of the machine, three decimal places are reported. The results (except zero values) are plotted in the diagrams of Figures 8.5 and 8.6.

Table 8.6 Range of trace element concentrations in corundum samples from Thailand and the Democratic People's Republic of Laos.

Locality (prefix)	Ban Huai Sai (CKEP)		Ban Nong Nam Cho (BNEP)		Den Chai (DCEP)		Bo Phloi (BPEP)		Khok Samran (KSEP)		Bang Kacha (BKCEP)		Nam Yun (NYEP)		Bo Rai (BREP)				Nong Bon (NBEP)	
Variety	Sapphires		Sapphires		Sapphires		Sapphires		Sapphires		Sapphires		Sapphires		Sapphires		Ruby		Ruby	
Wt%	*Min.*	*Max.*	*Min.*	*Max.*	*Min.*	*Max.*	*Min.*	*Max.*	*Min.*	*Max.*	*Min.*	*Max.*	*Min.*	*Max.*	*Min.*	*Max.*	*Min.*	*Max.*	*Min.*	*Max.*
V_2O_5	0	0.014	0.001	0.008	0	0.013	0	0.032	0	0.004	0	0.007	0	0.006	0	0.004	0	0.011	0.002	0.007
NiO	0	0	0	0	0	0	0	0	0	0	0	0	0	0	0	0	0	0	0	0
Ga_2O_3	0.013	0.101	0.007	0.017	0.015	0.040	0.011	0.030	0.011	0.019	0.014	0.034	0.020	0.047	0.018	0.034	0	0.009	0.002	0.007
Fe_2O_3	0.296	1.458	0.478	1.114	0.300	1.966	0.302	0.931	1.367	1.833	0.705	3.334	0.795	1.684	0.559	1.195	0.349	0.882	0.360	0.692
MnO	0	0.001	0	0	0	0	0	0.001	0	0.003	0	0.007	0	0	0	0	0	0.004	0	0.003
Cr_2O_3	0	0.042	0	0.011	0	0.018	0	0.053	0	0.007	0	0.007	0	0.010	0	0.003	0.086	0.564	0.028	0.355
La_2O_3	0	0.003	0	0.003	0	0.002	0	0.003	0	0.002	0	0.005	0	0.003	0	0.002	0	0.002	0	0.004
TiO_2	0.002	0.554	0.022	0.067	0.007	0.242	0.003	0.264	0.008	0.182	0.003	0.375	0.004	0.037	0.009	0.089	0.007	0.073	0.017	0.062
SnO_2	0	0.075	0	0.001	0	0.004	0	0.004	0	0.004	0	0.005	0	0.003	0	0.001	0	0.005	0	0.003
SiO_2	0	0.009	0	0.003	0	0.013	0	0.007	0	0.002	0	0	0	0.007	0	0.024	0.002	0.049	0	0.024
Y_2O_3	0	0.005	0	0.004	0	0.004	0	0.004	0	0.001	0	0.004	0	0.004	0	0.001	0	0.007	0	0.006
Ta_2O_5	0	0.271	na	na	na	na	0	0.006	na	na	na	na	na	na	na	na	na	na	na	na
Nb_2O_5	0	0.382	na	na	na	na	0	0.003	na	na	na	na	na	na	na	na	na	na	na	na
WO_3	0	0.023	na	na	na	na	0	0.093	na	na	na	na	na	na	na	na	na	na	na	na
CuO	0	0.004	na	na	na	na	0	0.006	na	na	na	na	na	na	na	na	na	na	na	na

Note: The shaded cells contain the maximum values; na = not analysed

Table 8.7 Range of trace elements in corundum samples outside Thailand.

	1		2		3		4		5		6		7		8		9		10	
Locality (Sample No)	**Natal (Λ1556)**		**Mull (SVI/1) & Bushveld (18058)**		**S. India (Λ793)**		**Bancroft (BC21)**		**Etive (MM125A), Behelvie (Λ1192) & Stoer (Λ16136)**		**Baffin (Λ440), Limpopo (BB14A) & Limpopo (BB29F)**		**Naxos (Λ577), Limpopo (BB19) & Sithean Sluain (Λ1378)**		**Mong Hsu (TYEP, MSEP) & Tanzania (CRM/ ZOI-1)**		**Vietnam (VNEP) & Nigeria (NAEP)**		**N. Vietnam (NVEP) & Africa (AFEP)**	
Variety*	Sapphire		Sapphir/ Ruby		Ruby		Sapphire		Sapphire /CL/ Ruby		CL/ Ruby /CL		CL/CL/CL		Ruby / Ruby		Sapphire/ Sapphire		Ruby / Ruby	
Wt%	*Min.*	*Max.*	*Min.*	*Max.*	*Min.*	*Max.*	*Min.*	*Max.*	*Min.*	*Max.*	*Min.*	*Max.*	*Min.*	*Max.*	*Min.*	*Max.*	*Min.*	*Max.*	*Min.*	*Max.*
V_2O_5	0	0.005	0.046	0.196	0.002	0.004	0	0.002	0.001	0.046	0.002	0.009	0	0.045	0	0.102	0.001	0.012	0	0.047
NiO	0	0	0	0	0	0	0	0	0	0	0	0	0	0	0	0	0	0	0	0
Ga_2O_3	0.017	0.024	0.006	0.015	0	0.004	0.006	0.014	0.004	0.033	0.002	0.013	0	0.016	0	0.015	0.023	0.054	0.001	0.006
Fe_2O_3	1.191	1.467	0.150	0.451	0.497	0.521	0.209	0.354	0.098	0.257	0.129	0.653	0.383	4.895	0	0.216	0.247	1.431	0.001	0.281
MnO	0	0	0	0.001	0	0.001	0	0.000	0	0.004	0	0.001	0	0	0	0.001	0	0	0	0
Cr_2O_3	0.001	0.003	0.089	0.674	1.252	1.466	0	0.004	0.007	0.196	0	0.037	0.002	0.279	0.332	1.700	0	0.004	0.311	1.218
La_2O_3	0	0.002	0	0.002	0	0.000	0	0.004	0	0.003	0	0.002	0	0.004	0	0.003	0	0.002	0	0.001
TiO_2	0.007	0.043	0.095	0.600	0.005	0.007	0.002	0.060	0.005	0.915	0.007	0.030	0.004	0.469	0.003	0.502	0.008	0.047	0.009	0.188
SnO_2	0	0.004	0.000	0.004	0	0.001	0	0.003	0	0.003	0	0.005	0	0.004	0	0.003	0	0.002	0	0.001
SiO_2	0	0.097	0	0.040	0	0	0	0	0	0.098	0	0.053	0	0.256	0	0.044	0	0.016	0	0
Y_2O_3	0	0.325	0	0.006	0	0.397	0	0.001	0	0.006	0	0.003	0	0.009	0	0.003	0	0.004	0	0.004

* Purple and pink colours can be generally called ruby and the other colours are called sapphires. CL = Colourless in thin section. The shaded cells contain the maximum values.

Note that the limit of detection is the concentration of background at $\bar{x}+3\sigma$ of its signal distribution (Potts, 1987: 16; Walsh, 1997). The limit of detection for this study is averaged from all analyses and listed in Table 8.8.

Table 8.8 The limit of detection for trace elements in corundum samples.

wt% oxide	Av.	Max.	Min.	Mode	σ	RSD%	n
V_2O_5	0.0026	0.0027	0.0021	0.0027	0.0002	6.8	264
NiO	nd	nd	nd	nd	nd	-	-
Ga_2O_3	0.0019	0.0020	0.0016	0.0020	0.0001	6.5	308
Fe_2O_3	0.0047	0.0051	0.0037	0.0049	0.0003	6.3	309
MnO	0.0043	0.0045	0.0036	0.0044	0.0002	4.8	19
Cr_2O_3	0.0047	0.0051	0.0039	0.0048	0.0003	6.7	252
La_2O_3	0.0016	0.0018	0.0014	0.0016	0.0001	5.3	128
TiO_2	0.0003	0.0005	0.0003	0.0003	0.00001	2.8	313
SnO_2	0.0033	0.0317	0.0025	0.0032	0.0023	70.2	157
SiO_2	0.0059	0.0090	0.0030	0.0030	0.0027	44.9	97
Y_2O_3	0.0112	0.0118	0.0093	0.0116	0.0006	5.5	81
Ta_2O_5	0.0018	0.0018	0.0017	0.0018	0.0001	3.5	68
Nb_2O_5	0.0012	0.0013	0.0011	0.0011	0.0001	5.9	63
WO_3	0.0103	0.0106	0.0101	0.0102	0.0001	1.2	64
CuO	0.0037	0.0038	0.0036	0.0036	0.0001	1.4	36

Av. = Mean; σ = standard deviation; RSD = relative standard deviation; n = number of analysis; nd = not detectable

Cr^{3+} can substitute directly for Al^{3+}, but other possibilities for Cr^{3+} substitution also exist, for example, $(Fe,V)^{3+} \leftrightarrow Cr^{3+}$ and $Ti^{4+}+Fe^{2+} \leftrightarrow 2Cr^{3+}$. However an attempt has been made to find out whether or not there is any substitution among the cations other than Al in the structure of corundum by plotting the graphs of cation percent, for example of Cr against Ga (Figure 8.5). However no linear correlation was found and it is still unclear how the cations are accommodated in the corundum structure (substitution or interstitial).

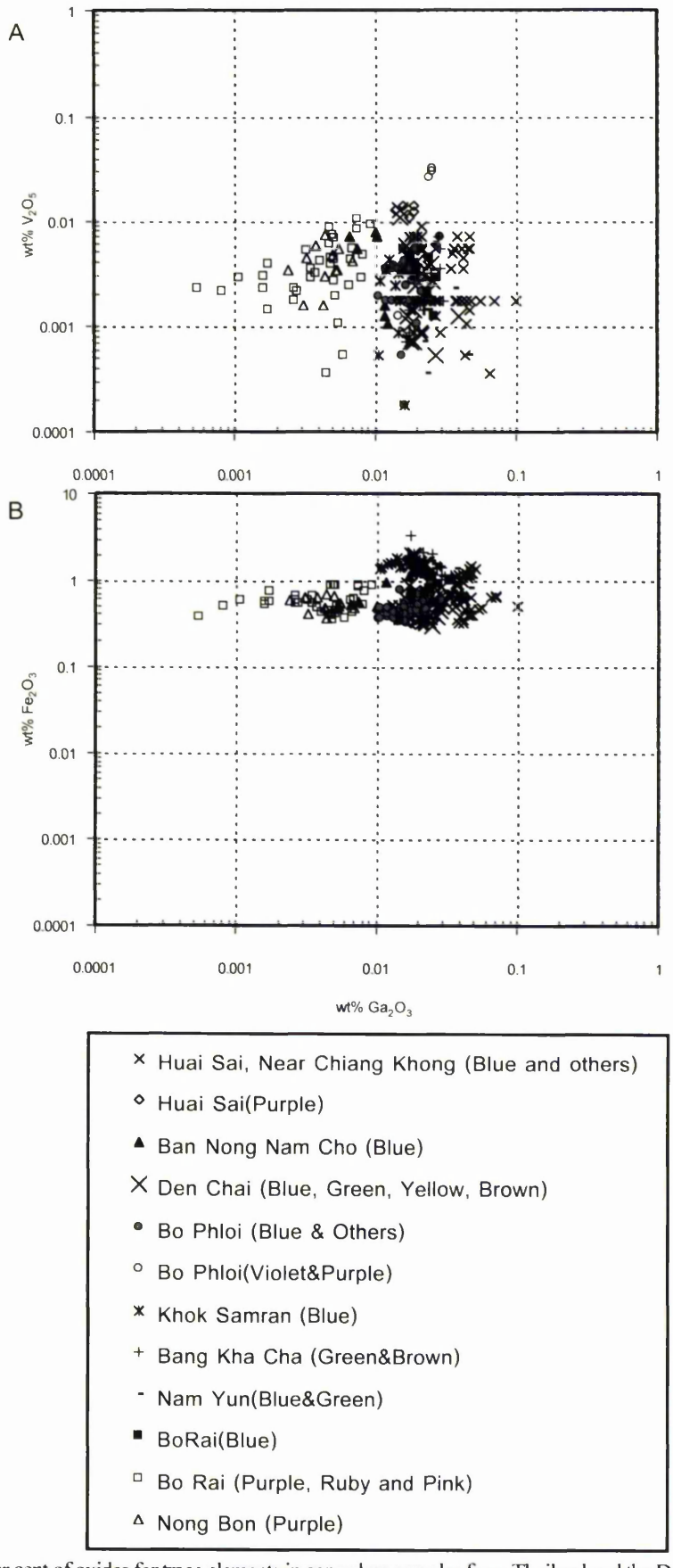

Figure 8.5 Weight per cent of oxides for trace elements in corundum samples from Thailand and the Democratic People's Republic of Laos (Ban Huai Sai), V_2O_5, Fe_2O_3, Cr_2O_3, La_2O_3, TiO_2, SnO_2, SiO_2, Ta_2O_5, Nb_2O_5, WO_3 and CuO plotted against Ga_2O_3.

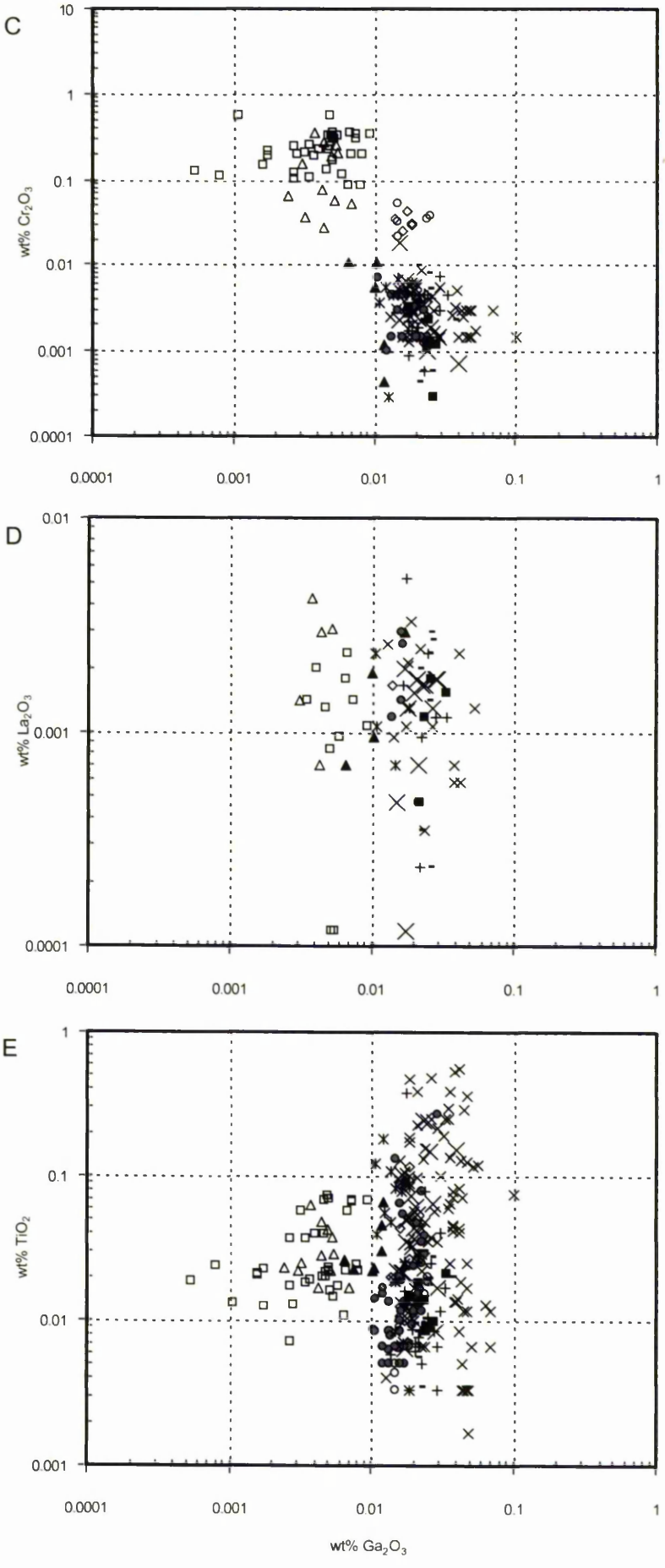

Figure 8.5 (Continued).

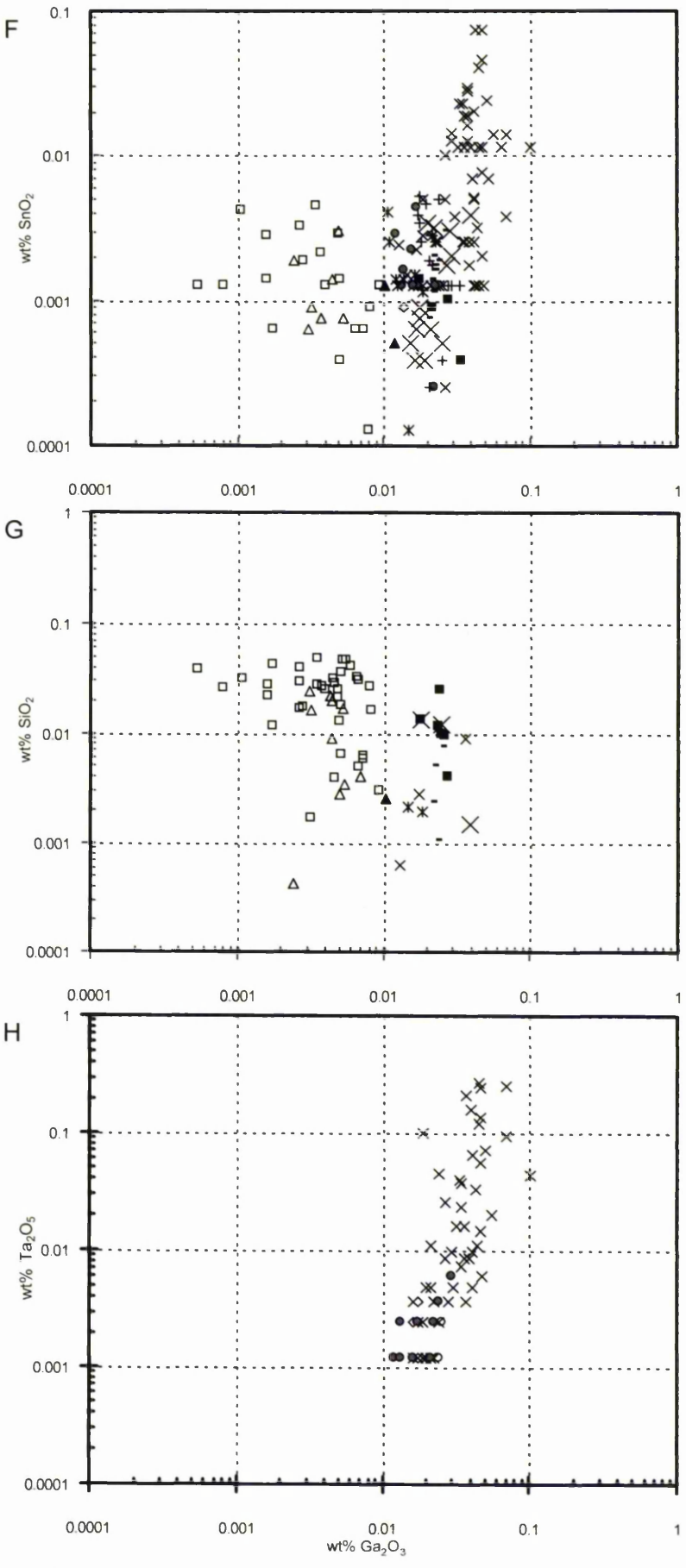

Figure 8.5 (Continued).

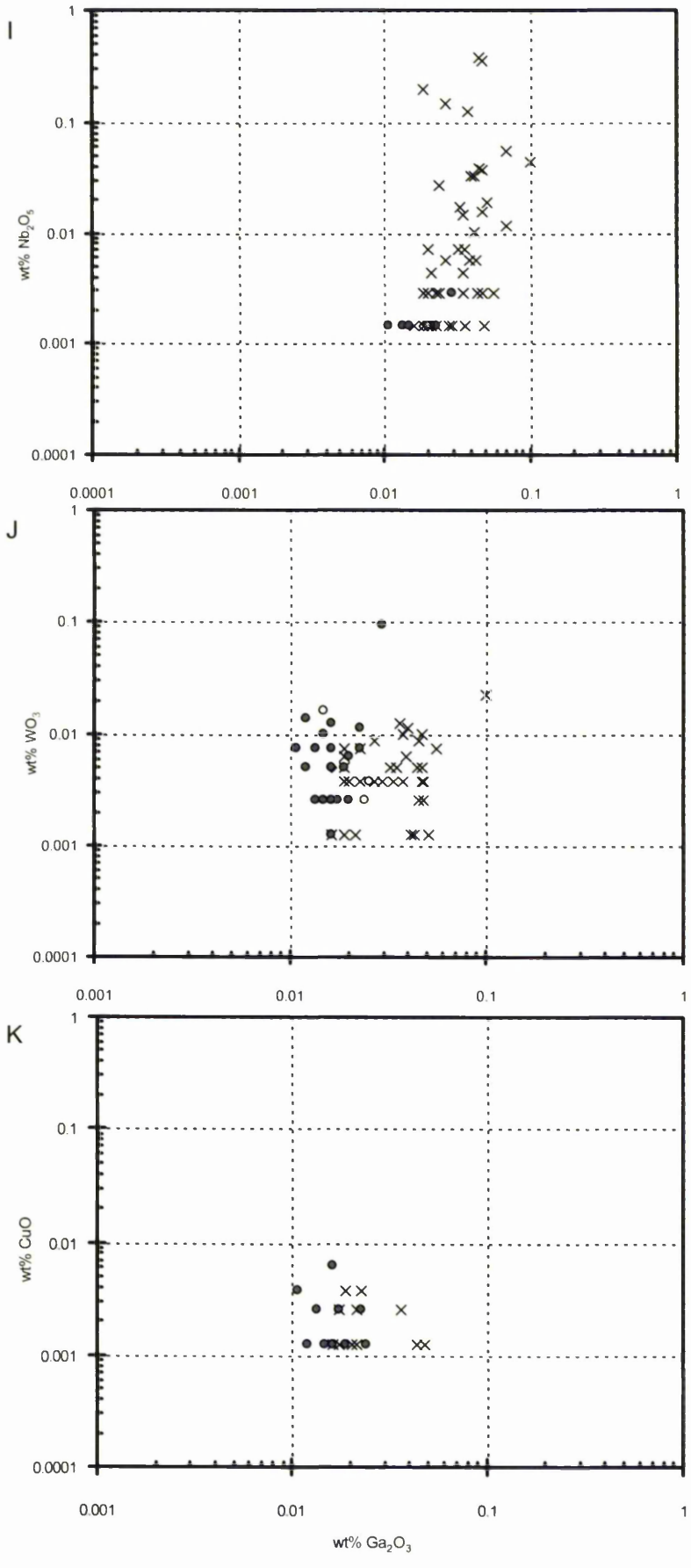

Figure 8.5 (Continued).

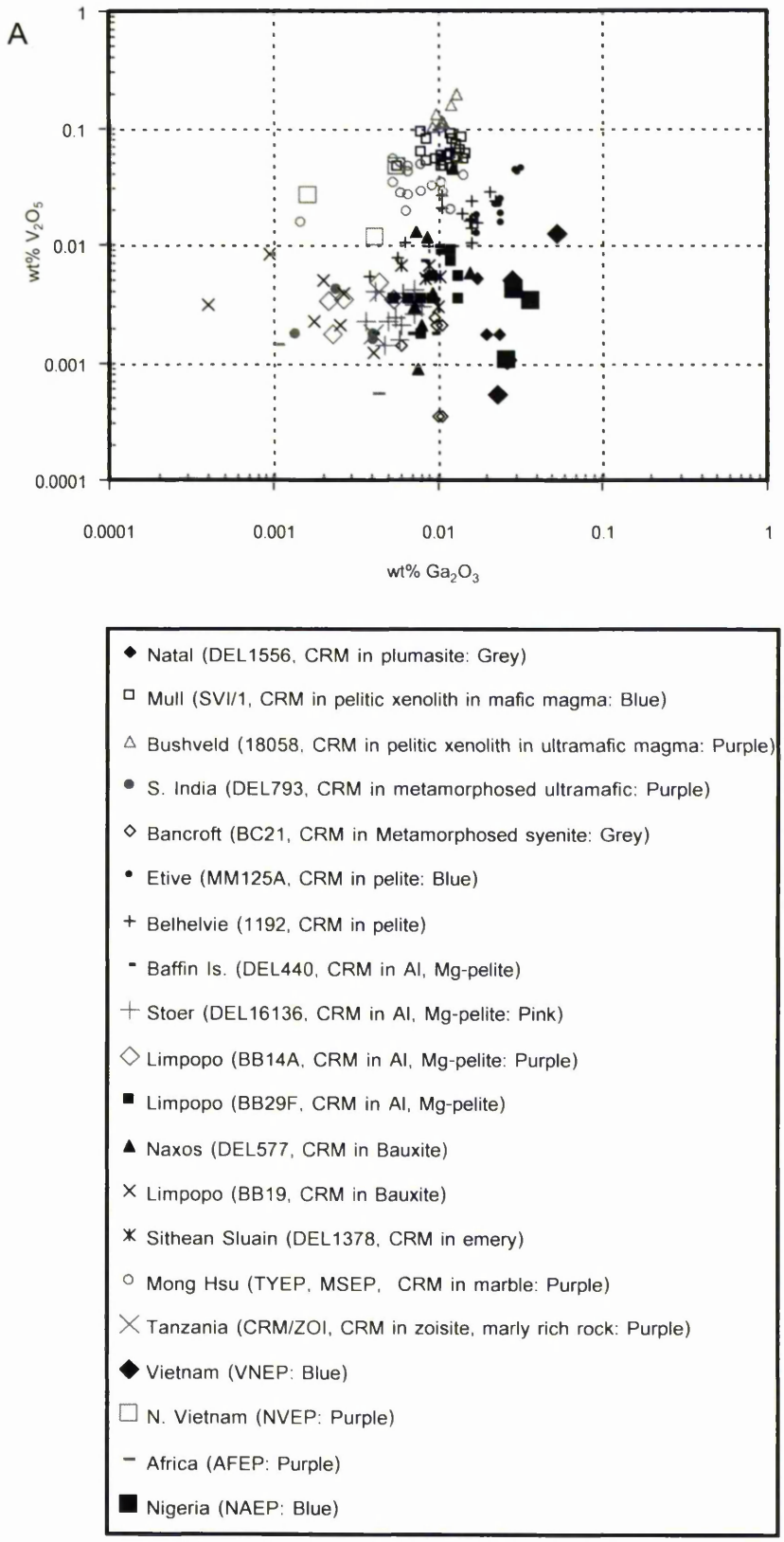

Figure 8.6 Weight per cent of oxides for trace elements in corundum samples from outside Thailand, V_2O_5, Fe_2O_3, Cr_2O_3, La_2O_3, TiO_2, SnO_2 and SiO_2, plotted against Ga_2O_3.

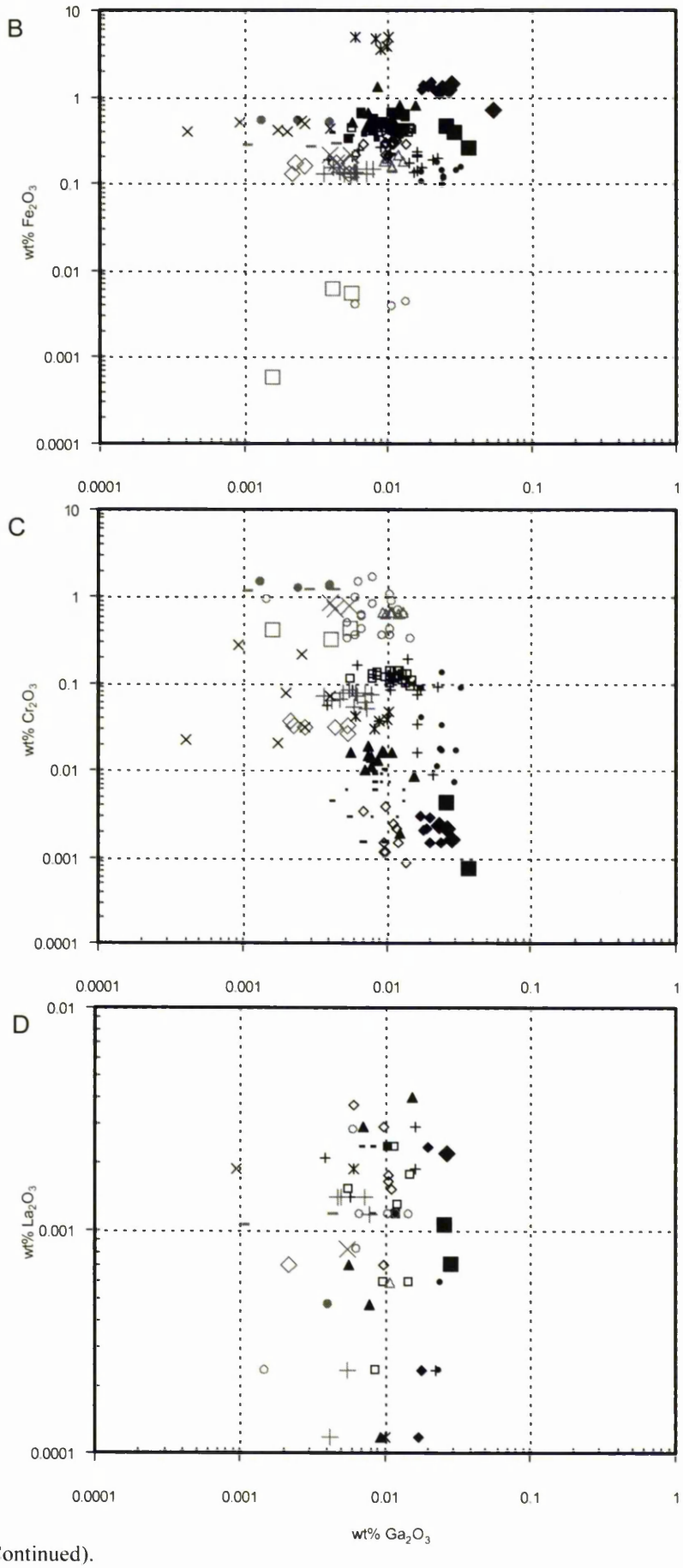

Figure 8.6 (Continued).

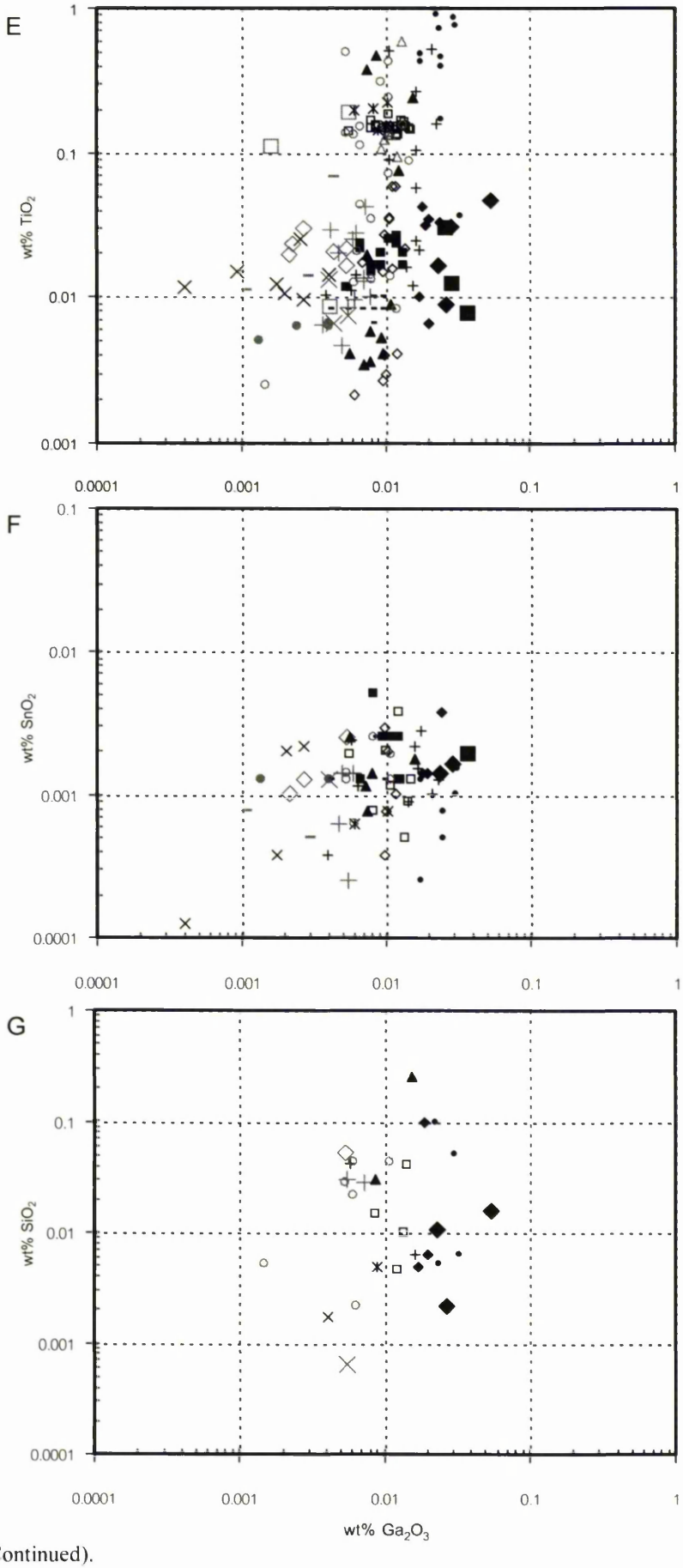

Figure 8.6 (Continued).

All analysed elements are described as follows (the results of the corundum samples from Ban Huai Sai are grouped with the Thai corundum samples).

Vanadium

Thai corundum samples have vanadium contents of less than 0.032 wt% V_2O_5. The highest value (0.032 wt%) belongs to a violet sample from Bo Phloi (Figure 8.5, A). The vanadium content in Thai corundum samples is relatively low. In most samples vanadium is below the limit of detection (0.0026 wt% of V_2O_5), shown by the zero value of the results (Table 8.6). The values of V_2O_5 mainly fall between 0.003 and 0.010 wt% (Figure 8.5, A).

Corundum samples from outside Thailand contain higher concentrations of vanadium, between 0.001 and ca 0.200 wt% V_2O_5, compared to Thai corundum samples. The corundum samples from Mull and Bushveld show relatively high vanadium contents, and the highest value (0.196 wt%) is from Bushveld sample 18058-2 (analysis number 5).

Nickel and Manganese

Nickel in corundum is not detectable, probably due to the extremely low or zero concentration. Manganese is also very low in concentration but the EPMA can detect manganese in 17 samples. However, of these, only two analyses show significant MnO concentrations, i.e. higher than the limit of detection; BKCEP9: 0.0070 wt% and BREP22: 0.0044 wt%.

Gallium

Gallium, like titanium and iron, is present in almost all samples. The plots of Ga_2O_3 for Thai corundum samples show a bimodal distribution (Figure 8.5). Most ruby samples (in purple, red and pink) contain Ga_2O_3 between 0.001 and 0.010 wt%. Most sapphire samples (in blue, green, yellow and brown) contain Ga_2O_3 between 0.010 and 0.100 wt%.

The corundum samples from outside Thailand contain Ga_2O_3 from 0.001 to 0.054 wt%. A sample from Vietnam (VNEP) contains the highest Ga_2O_3 (0.054 wt%).

Iron

Thai corundum samples contain relatively high iron contents compared to the samples from other parts of the world. The Fe_2O_3 content of Thai corundum samples is mainly restricted to a narrow window, between ca. 0.300 and 3.000 wt% (in the graph, Figure 8.5, B), than in samples from outside Thailand. The sample BKCEP9 contains the highest value (3.334 wt% of Fe_2O_3) beyond the major range. The Fe_2O_3 values of the samples with high iron content (BKCEP and NYEP) match those of the igneous corundum sample from Natal (Δ1556), Figures 8.5, B and 8.6, B. They contain the Fe_2O_3 more than 1.000 wt%.

The Fe_2O_3 contents of corundum samples from outside Thailand are mainly between 0.100 and 2.000 wt%. Exceptionally, the restitic emery samples from Sithean Sluain (Δ 1378) have high values of Fe_2O_3 and the highest value (4.895 wt%) belongs to analysis number 14 (Appendix 8-3). In contrast, the ruby samples from Mong Hsu (TYEP, MSEP) and North Vietnam (NVEP) have very low iron contents (less than 0.010 wt%).

Chromium

Chromium contents in the corundum samples from Thailand also show a bimodal distribution in the graph, like Gallium (Figure 8.5, C). The ruby samples have Cr_2O_3 values between 0.028 and 0.564 wt%, while the sapphire samples have lower values of Cr_2O_3 from 0.053 wt% down to below the limit of detection (0.0047 wt%).

The Cr_2O_3 contents in the corundum samples from outside Thailand are up to 1.700 wt%. The highest value belongs to a sample from Mong Hsu (MSEP4). The Cr_2O_3 contents of the igneous corundum from Natal (Δ1556), the corundum in the meta-syenite–gneiss from Bancroft (BC21), and the corundums of unknown origin from Vietnam (VNEP) and Nigeria (NAEP) are well below the limit of detection (0.0047 wt%).

Lanthanum

Thai corundum samples contain very low concentrations of lanthanum compared to V, Ga, Fe, Cr and Ti. In most samples, analysed La_2O_3 is below the limit of detection (0.0016 wt%). Sample BKCEP9, analysis number 10, contains the highest La_2O_3 (0.0053 wt%).

Corundum samples from outside Thailand contain La_2O_3 from 0.004 wt% (corundum in metabauxite from Naxos, Δ577, analysis number 14) down to below the limit of detection (0.0016 wt%). Most corundum samples contain La_2O_3 below the limit of detection.

Titanium

Titanium has a lower limit of detection (0.0003 wt% for TiO_2, Table 8.6) compared with the other elements analysed in this study. Thai ruby samples have TiO_2 contents mainly between 0.007 and 0.073 wt%. Thai sapphire samples have a wider range of TiO_2 contents, from 0.003 to 0.554 wt% (Figure 8.5, E). The sapphire samples from Ban Huai Sai (CKEP) dominate this range.

Titanium in the corundum samples from outside Thailand shows no distinction in the diagram E of Figure 8.6. A sample of corundum from a pelitic hornfels from Etive (MM125A, analysis number 7) has the highest value of TiO_2 (0.915 wt%), whereas a meta-syenitic corundum from Bancroft has the lowest value (0.002 wt%).

Tin

Tin is one of the granitophile metals (Sn, Nb, Ta, W, Be, Li) derived from crustal sources (Smirnov, 1968). The limit of detection of this element is relatively high (max. 0.0317 wt% SnO_2) compared to those of the other elements and the RSD is worst (70.2%) (Table 8.6). However a blue sapphire sample from Ban Huai Sai contains the highest value of SnO_2 (0.075 wt%). Most samples from Ban Huai Sai have high Sn contents, which are generally above the limit of detection (0.025 wt% of SnO_2). This agrees with the results analysed by the LA-ICP-MS.

The corundum samples from outside Thailand show very low concentrations of Tin and most of them have SnO_2 values below the limit of detection.

Silicon

Like tin, silicon has a very high detection limit and low precision in measurements of background.

In Thai corundum, silicon is more abundant in the ruby samples than in the sapphire samples. Moreover most SiO_2 values in the ruby samples are higher than the limit of detection. Sample BREP37 has the highest value of SiO_2 (0.049 wt%).

Most corundum samples from outside Thailand contain SiO_2 below the limit of detection (0.0059 wt%). A sample in a meta-bauxite from Naxos (Δ577, analysis number 14) has an anomalously high SiO_2 value (0.256 wt%).

Yttrium

All values of Y_2O_3 for Thai corundum samples are lower than the mean of the limit of detection. The results of the samples from outside Thailand are also lower than the limit of detection except for the corundum in plumasite from Natal (sample Δ1556-3, analysis number 3.1) which shows the highest Y_2O_3 value (0.325 wt%).

Tantalum

The tantalum content in samples from Ban Huai Sai is highest (up to 0.271 wt% of Ta_2O_5), whereas in samples from Bo Phloi it is very low. The maximum value of Ta_2O_5 in Bo Phloi samples is only 0.006 wt% (Figure 8.5, H).

Niobium

Niobium behaves in similar way to tantalum. It is highest in samples from Ban Huai Sai up to 0.382 wt% of Nb_2O_5, whereas the sample from Bo Phloi has the Nb_2O_5 content less than 0.003 wt% (Figure 8.5, I).

Tungsten

Tungsten in corundum samples from Bo Phloi is higher than in the samples from Ban Huai Sai (Figure 8.5, J). The maximum value in Bo Phloi samples is 0.093 wt% of WO_3, whereas the maximum value in the sample from Ban Huai Sai is 0.023 wt% WO_3.

Copper

The copper content in corundum samples is very low, with maximum values as 0.004 wt% and 0.006 wt% of CuO in the samples from Ban Huai Sai and Bo Phloi respectively. Most of the values are below the limit of detection (Figure 8.5, K).

8.4 Comparison of the results from LA-ICP-MS with those from EPMA

The results of the same samples from Ban Huai Sai and Bo Phloi analysed by both LA-ICP-MS and EPMA are presented in Table 8.9. The data in the table show that the same samples give different results when analysed by the different techniques. For most elements except Cu, the EPMA results are greater than the LA-ICP-MS results. For example, the Ga result for sample BPEP12 obtained by EPMA is up to 73 times higher than that obtained by LA-ICP-MS. The Cr result obtained by EPMA in sample BPEP5 is up to 194 times higher than that obtained by LA-ICP-MS. The V content in sample BPEP7 is 906 times higher than obtained by LA-ICP-MS.

Figure 8.7 shows the plots of concentration of trace elements obtained by LA-ICP-MS against the respective concentrations obtained by EPMA. All graphs in the figure show poor agreement between the results from the two instruments. This indicates a systematic error in one or both instruments. In this case the instrument drift of LA-ICP-MS caused its results to be less reliable than the results of EPMA.

Table 8.9 Concentration (ppm) of trace elements for corundum samples analysed by the LA-ICP-MS and EPMA. The results of EPMA were averaged from n analyses in one sample.

Sample No	CKEP7	CKEP8	CKEP9	CKEP11	CKEP12	CKEP13	CKEP15	CKEP16	CKEP17	BPEP5	BPEP6	BPEP7	BPEP8	BPEP10	BPEP11	BPEP12
Results from LA-ICP-MS:																
^{47}Ti	22	270	64	557	27	7	33	4	1	<1	4	<1		1		1
^{51}V	<1	1	1	9	<1	<1	<1	<1	<1	<1	1	<1	<1	<1	<1	<1
^{52}Cr	<1	1	14	<1	1	1	1	1	3	<1	1	1	<1	1	1	1
^{56}Fe	100	224	168	1085	213	75	486	55	194	37	27	32	34	33	31	39
^{63}Cu	85	80	22		33	13		78	7	194	47	172	98	70	10	21
^{69}Ga	10	18	20	186	15	7	47	5	16	4	2	3	2	1	2	2
^{93}Nb	22	16	1	176	1	12	3	<1	11	<1	<1	<1		<1	<1	
^{118}Sn	2	2	<1	12	11	1	14	<1	7		<1	<1	<1	<1		<1
^{181}Ta	17	12	1	179	6	39	8	1	45		<1		<1	<1	<1	<1
^{182}W	<1			3		<1										
Results from EPMA:																
n	2	4	3	4	2	3	3	3	2	2	2	2	2	2	11	12
Ti	150	1390	397	1100	220	1107	220	253	390	75	90	35	50	45	33	45
V	10	10	10	25	10		10			10	20	10	10	10	10	10
Cr		20	15					10	10	20		20	20		20	10
Fe	2645	3418	3200	3760	7915	4820	6650	3797	9155	3085	2685	3275	3050	3335	2887	3130
Cu	25		10		20		20					10	20	30		
Ga	165	158	510	290	290	257	287	180	365	170	95	135	100	85	110	125
Nb	20	618	165	85	10	83			75				10	10		
Sn	10	40	70	15	85	127	133	15	390	10					10	10
Ta	50	360	187	248	70	270	35	30	355		20	20			10	
W		30	87	10		35	65		45	60	65	30	60	50	60	10
EPMA / LA-ICP-MS:																
Ti	6.9	5.2	6.2	2.0	8.3	150.8	6.7	60.6	**539.4**	-	21.0	151.7	-	46.9	-	56.3
V	20.4	15.6	14.3	2.9	54.9	-	44.2	-	-	36.0	36.2	**906.0**	35.0	66.6	35.2	29.1
Cr	-	19.5	1.1	-	-	-	-	13.0	3.3	**193.8**	-	16.3	41.3	-	21.8	18.4
Fe	26.4	15.3	19.0	3.5	37.2	64.4	13.7	69.0	47.1	82.8	100.8	101.0	90.9	**101.3**	92.8	80.6
Cu	0.3	-	0.5	-	**0.6**	-	-	-	-	-	-	0.1	0.2	0.4	-	-
Ga	16.0	8.7	24.9	1.6	19.3	37.1	6.1	38.2	22.3	38.1	57.0	53.0	47.1	69.0	60.5	**72.9**
Nb	0.9	39.6	**299.6**	0.5	8.0	7.0	-	-	6.9	-	-	-	-	52.5	-	-
Sn	5.9	20.6	**267.2**	1.3	7.8	169.8	9.8	52.4	57.3	-	-	-	-	-	-	119.3
Ta	3.0	29.6	**343.8**	1.4	11.3	6.9	4.1	31.7	7.9	-	233.1	-	-	-	76.9	-
W	-	-	-	4.0	-	**721.3**	-	-	-	-	-	-	-	-	-	-

Note: The shaded cells contain the maximum values.

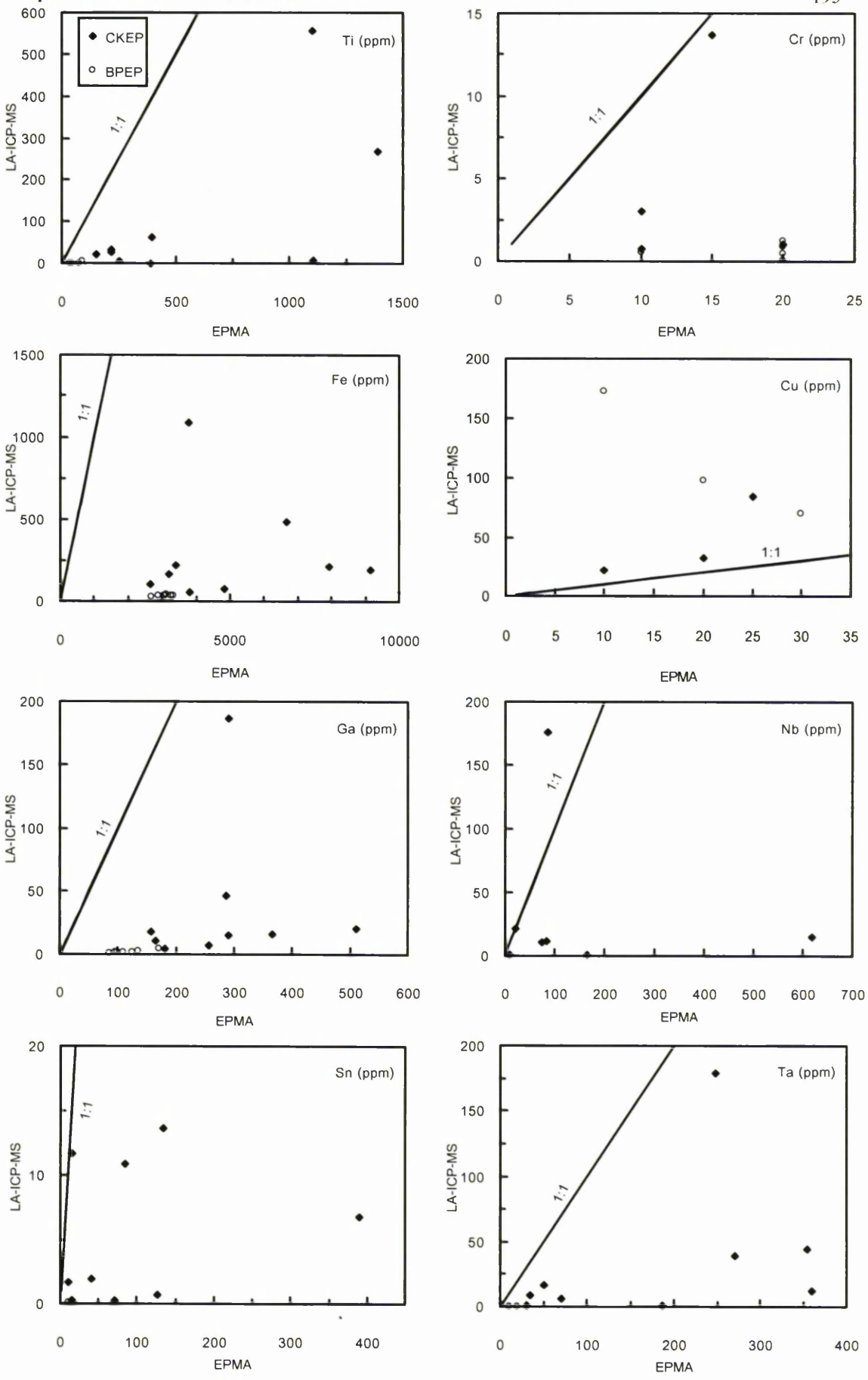

Figure 8.7 Comparison of element concentrations analysed by LA-ICP-MS and EPMA.

A comparison of other aspects of these two techniques is summarised in Table 8.10.

Table 8.10 Comparison of the performances between the LA-ICP-MS and the EPMA used for investigating the trace elements in corundum samples in this work.

Performance	LA-ICP-MS	EPMA
Sample preparation	Only clean and fresh area on the sample needed	Polished section
Time used per one analysis	2 minutes	12 minutes
Elements analysed	Wider range of elements; from ^{7}Li to ^{238}U	Number of the elements depending on the available standards, hence, 15 elements V, Ni, Ga, Fe, Mn, Cr, La, Ti, Sn, Si, Y, Ta, Nb, W and Cu
Sample loading	Not complicated	Required trained operator
Result	-Not reliable due to drift of the equipment -Not fully quantitative	-More reliable, the limit of detection down to 0.0003 of wt% oxide -Fully quantitative
Technical problem	Not found	The machine always stops running unexpectedly, as the voltage is higher than the ordinary run.

8.5 Origin of the high Ta and Nb contents

The results of Sn, Ta, Nb, W and Cu detected by the LA-ICP-MS were confirmed by using EPMA that corundum samples contain these trace elements. Plots of Sn-Ta-Nb (Figure 8.8) show that Ta-Nb contents fall near the field of columbite-tantalite {(Fe,Mn) Nb_2O_6-(Fe,Mn)Ta_2O_6} solid solution and Sn content falls near the end member of cassiterite (SnO_2). It is suspected that the Sn, Ta and Nb contents were from these inclusions in corundum. The inclusions probably exist as very tiny particles invisible to the unaided eye. The Sn, Ta and Nb contents in brown corundum samples (with abundant rutile or Fe-Ti inclusions) obtained by EPMA are very low, which indicates that these three elements do not substitute in rutile in this kind of corundum sample.

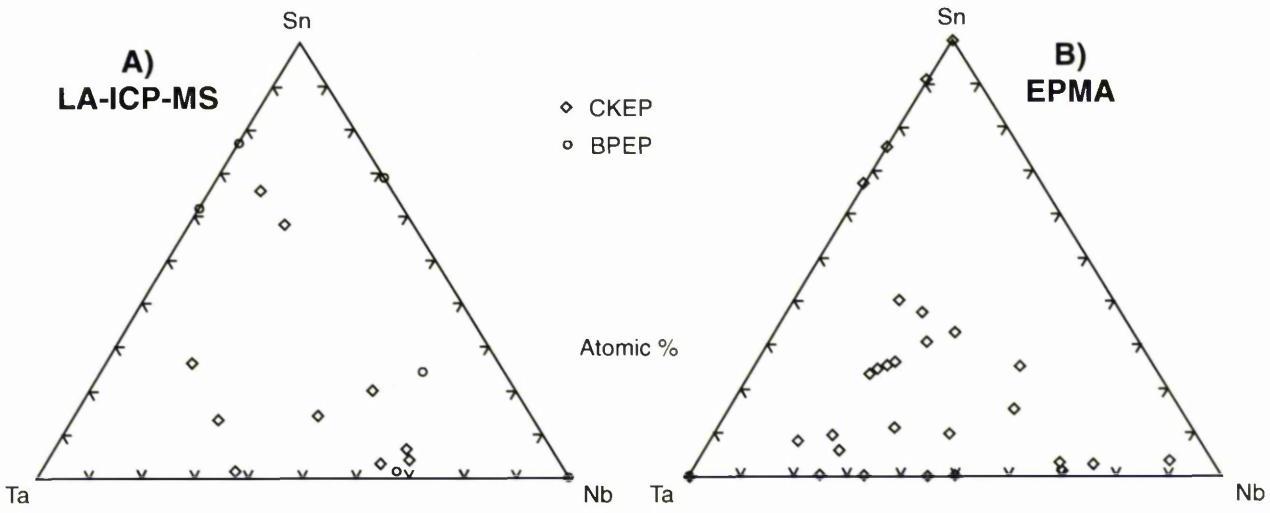

Figure 8.8 Plots of Sn-Ta-Nb in triangular diagrams using the results from LA-ICP-MS and EPMA for the corundum samples from Ban Huai Sai (CKEP) and Bo Phloi (BPEP).

However the plots of Nb, Sn, Fe against Ta or Fe against Nb (Figure 8.9) do not show any clear correlation indicating the substitution between the pair of these elements. Thus Ta, Nb and Sn do not come from mineral inclusions as mentioned above but they may occur in corundum structure in some way. The differences in diameter (Al = 1.08 Å c.f. Ta = 1.48, Nb = 1.44, Sn = 1.38 Å) and charge (3+ c.f. 5+, 5+ and 4+ respectively) do not allow Ta, Nb, and Sn to substitute for Al in the corundum structure. They are probably housed in the voids, for example the cavities between the layers (i.e. empty octahedra, see Figure 7.2, A and B) because the diameters of Ta, Nb and Sn are less than the gap between the layers (ca 2 Å along c-axis). More research on this subject is needed.

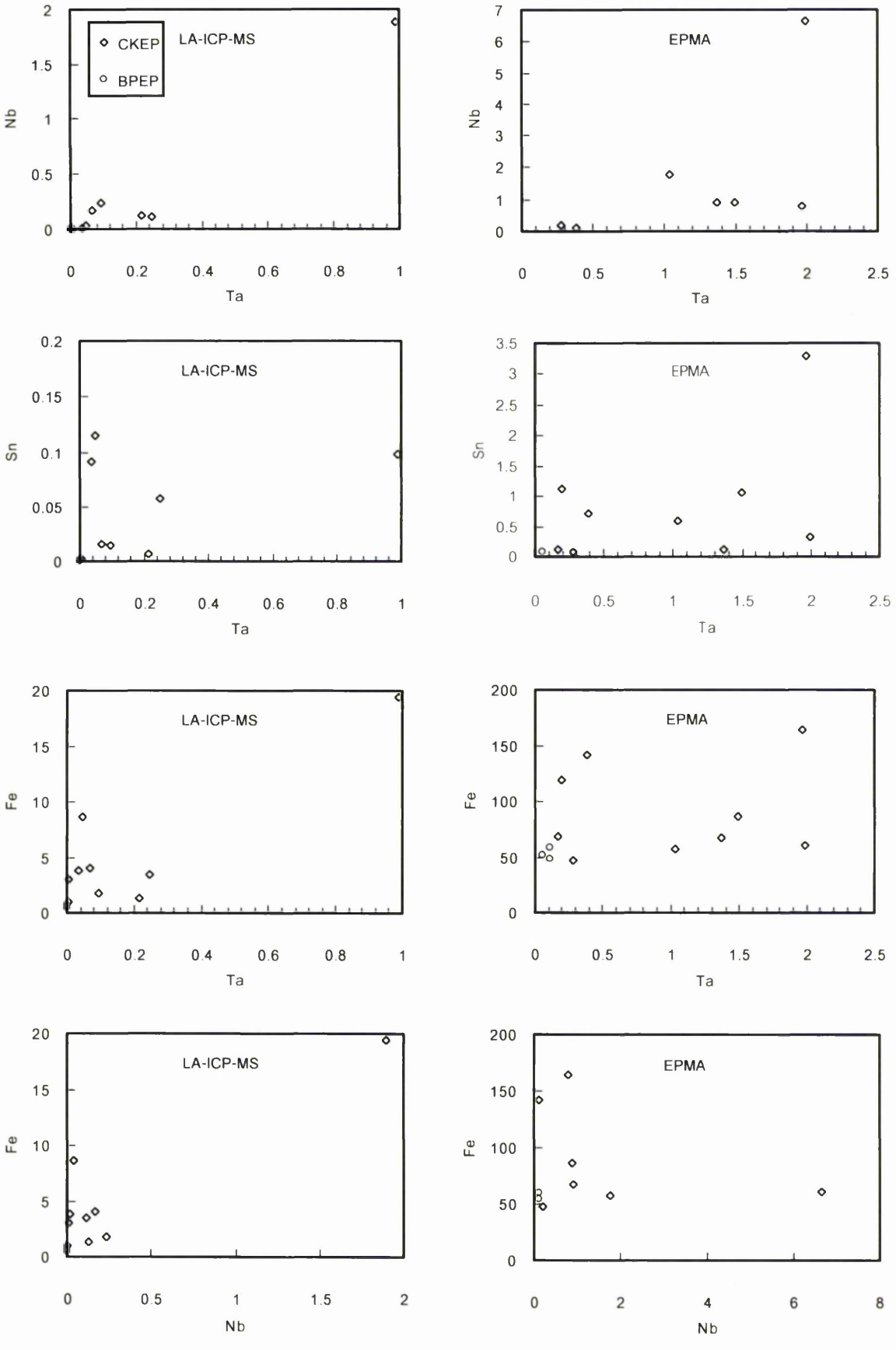

Figure 8.9 Plots of atomic proportion (concentration in ppm/atomic mass) for Nb, Sn and Fe against Ta and for Fe against Nb of the results, of the same samples from Ban Huai Sai (CKEP) and Bo Phloi (BPEP), analysed by LA-ICP-MS and EPMA.

CHAPTER 9
MINERAL INCLUSIONS IN CORUNDUM

9.1 Introduction

In gemmology the term 'inclusion', used here in the sense of Koivula (1991), is any irregularity observable in corundum by the unaided eye or using certain tools such as a hand lens or microscope. The term 'irregularity' may be a substance, for example mineral crystal, glass, fluid, cavity, and fracture or growth pattern.

Gübelin and Koivula (1986), used three terms for inclusions in gemstones:

Pre-existing (*protogenetic*) inclusions especially crystals formed before the host crystal began to form. These crystals may appear as either heavily etched or corroded individuals, which formed long before the host, or as well-formed crystals, which developed just prior to the host (e.g. solid particles, small crystals).

Contemporary (*syngenetic*) inclusions formed at the same time as the host crystal. They include euhedral crystals and primary cavities (possibly as negative crystals; filled with liquid or gas, liquid+gas, or liquid+gas+solid), primary twinning, colour zoning and healed fractures (feather or fingerprint).

It is not always easy to distinguish between pre-existing and contemporary inclusions. Guo *et al.* (1996a) group these categories together as primary inclusions.

Post-contemporary (*epigenetic*) inclusions occurred after the host crystal stopped growing (e.g. various types of fissure, exsolved crystal, transformation twin, and slip or glide twin). Note that fissures and twins are not counted as inclusions in a petrological sense.

Roedder (1984) classified fluid inclusions, on the basis of their origin, into 3 categories:
-*primary* inclusions: formed during the growth of the host,
-*secondary* inclusions: formed after the growth of the host, and
-*pseudosecondary* inclusions: appear secondary but formed during the growth of the host crystal (e.g. by forming fracture-cavity fillings).

This study focuses on the identification and characterisation of protogenetic and syngenetic mineral inclusions exposed at the surface of the polished sections of corundum samples. Coexisting minerals found with corundum are also taken into account. The aim of this study is to use the results to provide supporting information on

the environment of formation of corundum samples from Thailand. Constraints on origin including information on P-T stability limits of minerals and mineral assemblages will be obtained in this study.

9.2 Previous work

Many studies deal with the inclusions in corundum, but few authors discuss the origin of corundum with reference to the inclusions in corundum. Guo *et al.* (1996a) identified mineral inclusions in corundum samples associated with alkali basalt and classified them into two environmental suites. They are the alkali felsic suite: feldspar, zircon, $ZrSiO_4$, uraninite, UO_2, ilmenorutile, $(Ti,Nb,Ta,Fe^{3+},Fe^{2+})O_2$ and Fe-Cu sulphides and the carbonatitic suite: titaniferous columbite, uranpyrochlore, $(U,Ca,Ce)_2(Nb,Ta)_2O_6(OH)$ and fersmite, $(Ca,Ce,Na)(Nb,Ti)_2(O,OH,F)_6$. From the inclusion data, they proposed a model of corundum genesis in which corundum formed by the hybridisation of alkali and carbonatite magmas at mid-crustal level. Dao *et al.* (1997) identified diamond inclusions (accompanied by graphite and lonsdaleite) in seven rubies from Vietnam. Also Wilcock and Bosshart (1997) analysed diamond inclusions (accompanied by graphite) in sapphires from Ban Huai Sai. However there are no conclusions regarding diamond inclusions in corundum at this stage. Sutherland and Schwarz (1997) and Sutherland (1998) found that the corundums from basaltic terrains comprise two distinctive suites based on trace elements and mineral inclusions in the corundums. Firstly, corundums of magmatic origin (blue-green-yellow suite) contain primary mineral inclusions of feldspars, zircon, Fe-Ti oxides, Nb-Ta oxides, U-Th oxides and rare-earth phosphates. Secondly, corundums of metamorphic origin (sapphire-ruby suite) contain primary mineral inclusions of Mg-rich spinel, sapphirine, and fassaite.

9.3 Methods and techniques

The mineral inclusions are observed in the polished sections of corundum prepared for the analysis for trace elements in chapter 8. The preparation of the samples has been described in section 8.3.2. The mineral inclusions encountered in the sections were first observed by the use of an optical microscope to record their appearance. The inclusions exposed at the surface of the polished sections were then analysed by SEM-EDS (scanning electron microscope equipped with the energy dispersive spectrometry).

The SEM-EDS (JEOL JSM 6400 with Link Energy Dispersive X-ray Analysis System) is employed for chemical analysis and providing backscattered electron images (BSE)

and secondary electron images (SEI) of the mineral inclusions. The machine conditions for analysis include an accelerating voltage of 15 kV, a probe current of 1.5 nA and a working distance of 39 mm.

9.4 Results

The corundum samples from Thailand contain all three types of inclusions (protogenetic, syngenetic and epigenetic inclusions). Inclusions of known composition are presented in Figures 9.1-9.6. They are garnet, fassaite, sapphirine, alkali feldspar (sanidine composition), nepheline, zircon and spinels (hercynite-spinel and magnetite-hercynite series). Representative chemical compositions and mineral names of analysed inclusions are given in Table 9.1, followed by a description of each one. All analyses are reported fully in Appendix 9-1. Note that some poor analyses are reported. This is probably due to contamination of host corundum as the inclusion sizes are small.

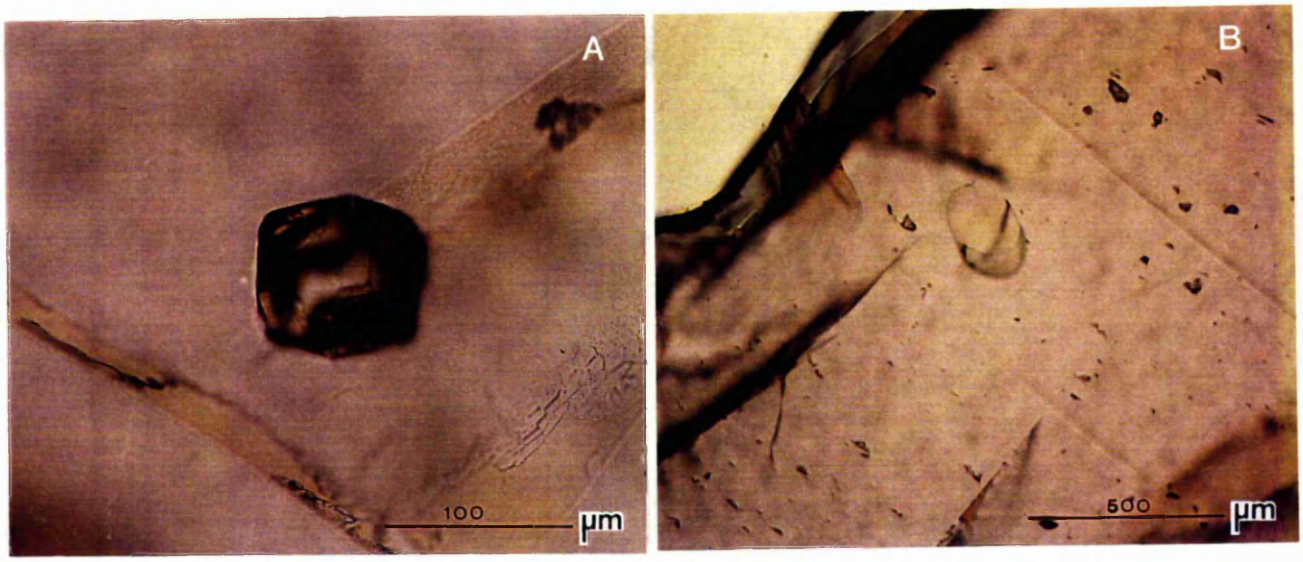

Figure 9.1 A) Garnet inclusion in ruby from Bo Rai (BREP1) shows a euhedral, probably icositetrahedral form. [Transmitted light with PPL]. **B)** Garnet inclusion in ruby from Bo Rai (BREP45) shows a somewhat distorted crystal form. It is exposed at the surface of the polished section. [Transmitted light with PPL].

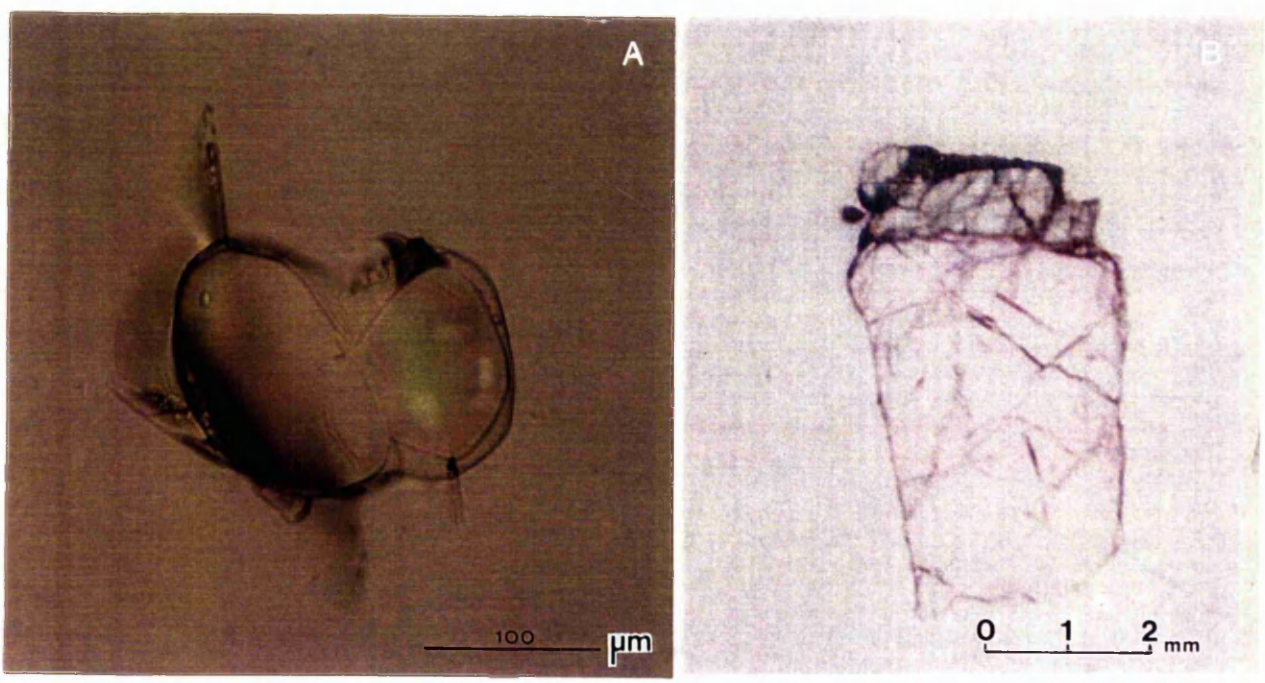

Figure 9.2 A) Two fassaite inclusions in ruby from Bo Rai (BREP43), the smaller crystal shows high interference colours. The crystals are surrounded by stress cracks. [Transmitted light with PPL]. **B)** Fassaite (green part, top) coexists with ruby (pink colour, bottom) from Bo Rai (BRJ). [Overhead illumination].

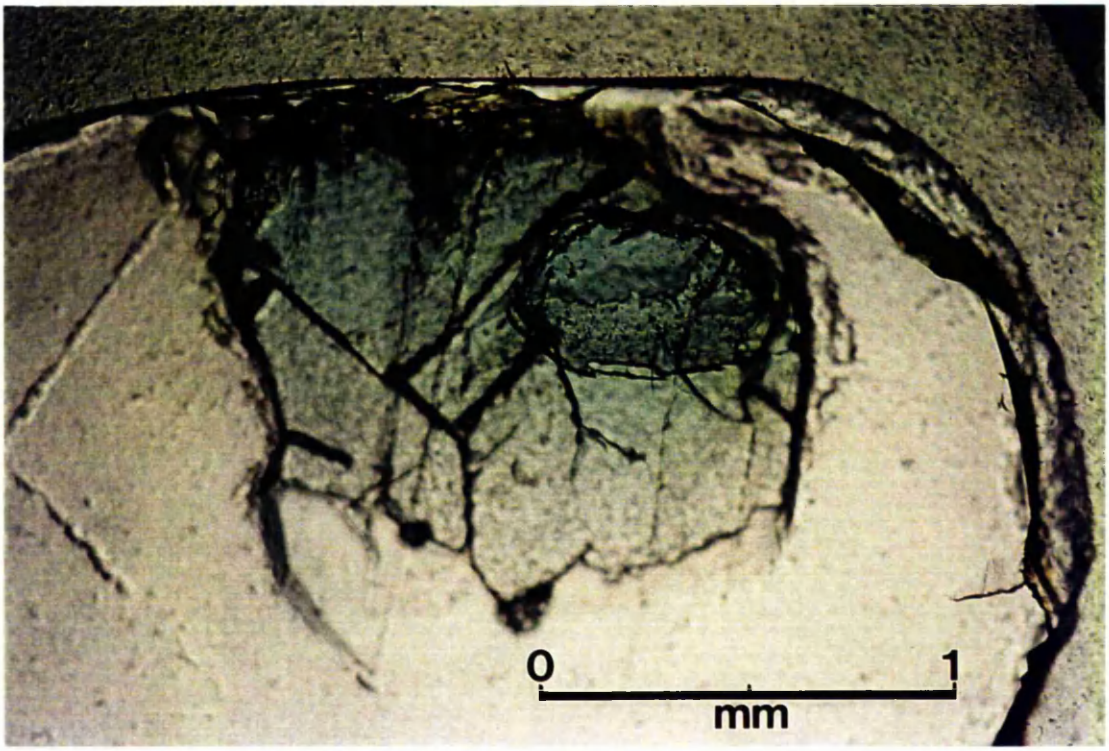

Figure 9.3 Sapphirine inclusion in ruby from Bo Na Wong (NWEP9) showing deep blue-green colour. [Transmitted light].

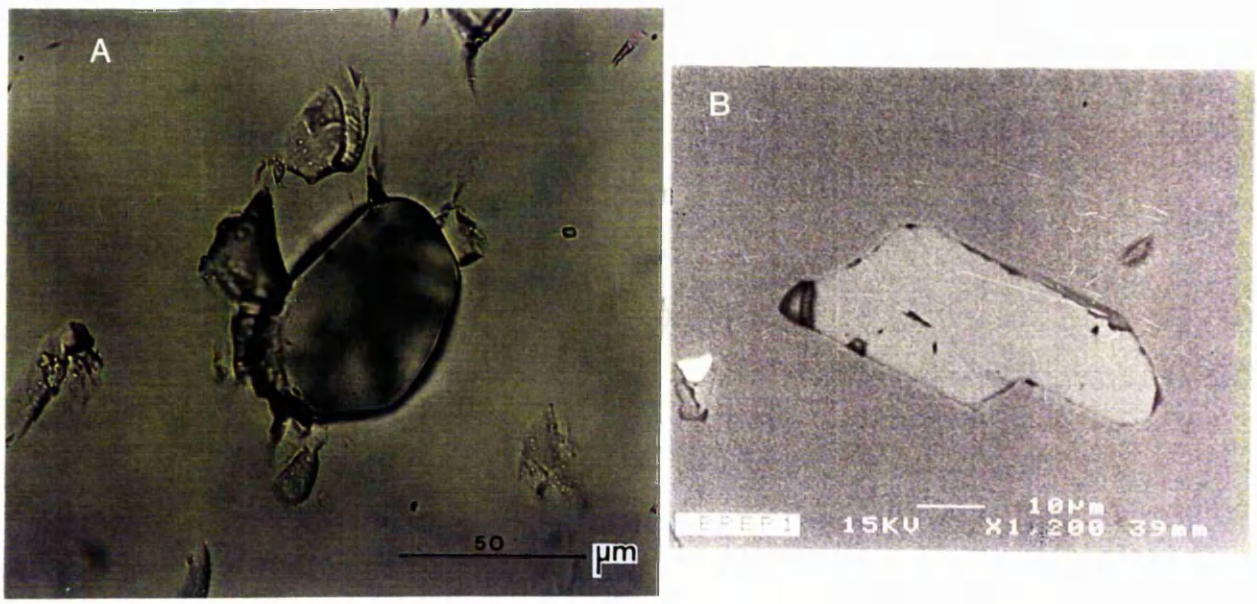

Figure 9.4 A) Sanidine inclusion in sapphire from Den Chai (DCEP16), exposed at the surface of the section; the crystal shape is nearly oval, surrounded by stress cracks. [Transmitted light]. **B)** Nepheline inclusion in sapphire from Bo Phloi, exposed at the surface of polished section, shows a prismatic subhedral outline with a broken end. [Backscattered electron image].

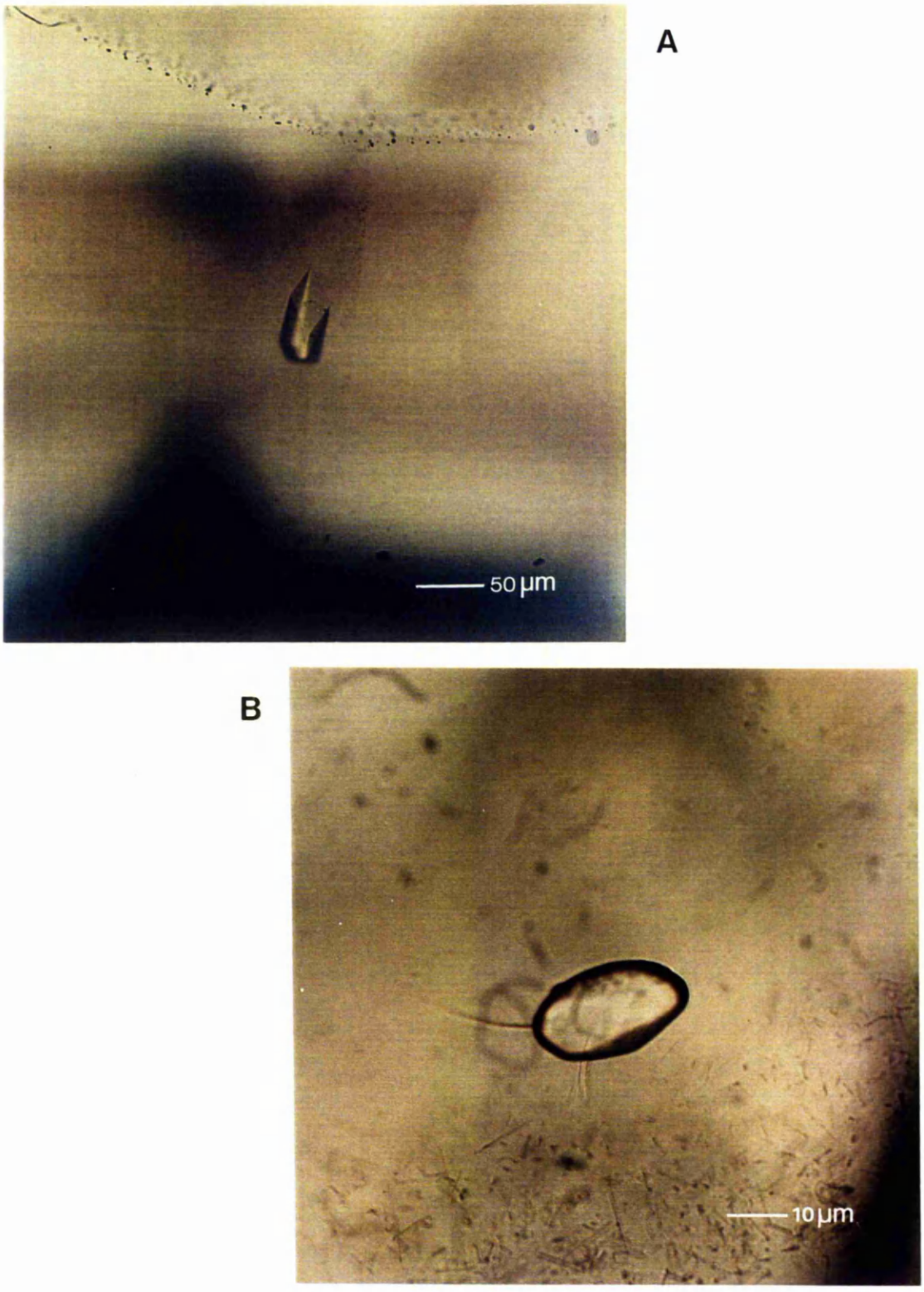

Figure 9.5 A) Zircon inclusion in sapphire from Ban Huai Sai (CKEP10) exposed at the surface of the section. The inclusion shows a euhedral prismatic habit with tetragonal prism form {110}. [Transmitted light]. **B)** Zircon inclusion in sapphire from Bo Phloi (BPEP14) shows an oval outline and is associated with two visible stress cracks. [Transmitted light with PPL)

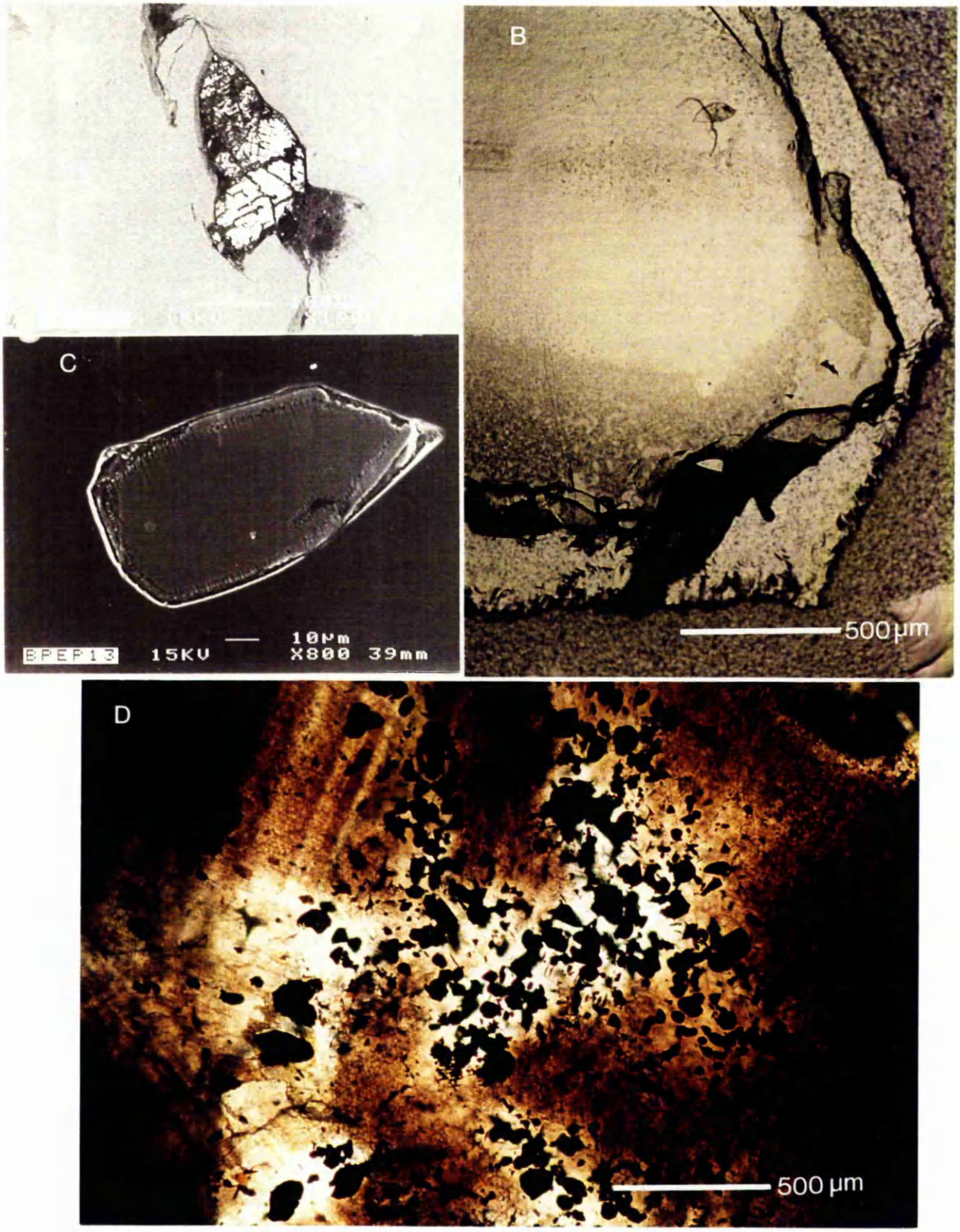

Figure 9.6 A) Hercynite-spinel inclusion in sapphire from Ban Huai Sai shows irregular outline. [Backscattered electron image]. **B)** Hercynite-spinel (black remnant, bottom of the picture) coexists with sapphire (upper left) from Ban Nong Nam Cho (BNEP4). [Transmitted light with PPL]. **C)** Hercynite-spinel inclusion in sapphire from Bo Phloi exposed at the surface of the polished section. The inclusion is euhedral with an alteration rim. [Secondary electron image]. **D)** Black platelets of magnetite-hercynite associated with yellow brown needles in star sapphire from Bang Kacha (BKCEP4), the needles accumulate along the hexagonal growth zoning of the sapphire. The picture is viewed parallel to [0001]. [Transmitted light with PPL].

Table 9.1 Representative chemical compositions (wt% oxides and number of ions) of mineral inclusions and coexisting minerals found with corundum samples from Thailand.

Mineral	Garnet		Fassaite		Sapphirine		Alkali feldspar	Nepheline	Spinel			
Sample No. of Corundum - Analysis No.	BREP1-GRT1[A]	BREP45-GRT1[B]	BREP43-FS1	BRJ-FS3 (coexisting min.)	NWEP9-SPR3	NWEP11-SPR3 (coexisting min.)	DCEP16-AF2[C]	BPEP1-NE1[D]	CKEP30-SP3	BNEP4-SP1	BPEP13-SP1	BKCEP4-SP2
SiO_2	41.90	41.67	46.80	46.77	13.79	14.10	65.35	43.02	-	-	0.39	-
TiO_2	-	-	0.92	0.23	-	-	-	-	0.24	0.31	-	1.84
Al_2O_3	23.42	23.57	14.23	15.92	62.91	63.13	21.54	33.48	55.30	53.27	56.67	30.53
Fe_2O_3*	0.90	0.95	2.70	-	0.80	0.43	-	0.32	5.06	6.92	4.69	31.21
FeO	6.65	9.04	0.94	2.98	2.27	2.86	-	-	33.81	27.78	30.63	33.58
MnO	0.23	-	-	-	0.21	-	-	-	0.65	0.68	0.86	1.48
MgO	18.18	15.77	11.55	10.19	18.99	19.19	-	0.40	4.03	6.20	6.65	0.45
CaO	8.43	9.90	21.81	22.29	0.11	-	2.63	-	-	-	-	-
Na_2O	-	-	1.58	1.32	-	-	6.51	14.68	-	0.29	-	0.52
K_2O	-	-	-	-	-	-	5.59	8.26	-	-	-	-
P_2O_5	-	-	-	-	-	-	0.38	-	-	-	-	-
NiO	-	-	-	-	0.47	0.30	-	-	-	-	-	-
Cr_2O_3	-	-	-	0.35	0.24	-	-	-	-	-	0.77	-
Total	99.71	100.90	100.54	100.05	99.79	100.01	102.00	100.16	99.09	95.45	100.66	99.61
Number of ions												
O	24	24	6	6	20	20	32	32	32	32	32	32
Si	5.982	5.962	1.691	1.699	1.614	1.644	11.473	8.310	-	-	0.087	-
Al	0.018	0.038	0.309	0.301	4.386	4.356	4.457	7.620	15.040	14.796	14.902	9.401
Al	3.922	3.936	0.296	0.381	4.293	4.319						
Cr	0	-	-	0.010	0.022	-	-	-	-	-	0.137	-
Fe^{3+}	0.096	0.103	0.073	-	0.071	0.038	-	0.047	0.879	1.227	0.787	6.136
Ti	0	-	0.025	0.006	-	-	-	-	0.041	0.055	-	0.362
Mg	3.870	3.363	0.622	0.552	3.314	3.336	-	0.114	1.388	2.177	2.211	0.176
Fe^{2+}	0.794	1.082	0.029	0.091	0.222	0.279	-	-	6.524	5.475	5.715	7.336
Mn	0.028	-	-	-	0.020	-	-	-	0.129	0.136	0.162	0.328
Ca	1.290	1.517	0.844	0.867	0.013	-	0.494	-	-	-	-	-
Na	-	-	0.110	0.093	-	-	2.216	5.498	-	0.133	-	0.261
K	-	-	-	-	-	-	1.251	2.035	-	-	-	-
P	-	-	-	-	-	-	0.057	-	-	-	-	-
Ni	-	-	-	-	0.045	0.029	-	-	-	-	-	-
Total cations	16.000	16.000	4.000	4.000	14.000	14.000	19.947	23.623	24.000	24.000	24.000	24.000

* Fe_2O_3 estimated by stoichiometric criteria of Droop (1987); except in alkali feldspar and nepheline, the total Fe as Fe_2O_3.

The end members: [A] $py_{64.7}alm_{13.3}gro_{19.2}and_{2.4}uv_0sp_{0.5}$, [B] $py_{56.4}alm_{18.1}gro_{22.9}and_{2.5}uv_0sp_0$, [C] $Or_{31.6}Ab_{55.9}An_{12.5}$, [D] $Ne_{67.9}Ks_{28.0}Q_{4.1}$.

9.4.1 Garnet

Garnet has a general formula $^{VIII}(Mg, Fe^{2+}, Mn, Ca)_3\ ^{VI}(Al,Fe^{3+},Cr,Ti)_2\ ^{IV}(Si,Al)_3O_{12}$.

Many garnet inclusions are found in the ruby samples from Bo Rai (samples BREP1 and BREP45). The typical appearance of the garnet inclusions is equidimensional or nearly rounded in shape (e.g. in Figure 9.1, A). Certain crystals have a euhedral form, probably icositetrahedron (trapezohedron), and are surrounded by healed fractures (in gemmology called "fingerprints"). Certain crystals are somewhat distorted, as they look ellipsoidal, probably due to different growth rate compared with the host (Figure 9.1, B). This may cause confusion with the other minerals in identification. Their size ranges from 130x130 to 180x280 μm. Their colour is not obviously distinguishable from that of the host.

All garnet inclusions are pyrope rich with high grossular and almandine components. Their compositions range from $py_{56}\ gro_{23}\ alm_{18}\ and_{03}\ sps_0\ uv_0$ to $py_{67}\ gro_{18}\ alm_{11}\ and_{03}\ sps_{0.5}\ uv_{0.5}$. Their average end members are present in Table 9.2. $Mg/(Mg+Fe^{2+})$ values range from 0.76 to 0.86. The inclusion in sample BREP1 has slightly lower Ca and Fe and higher Mg than those in BREP45 (Table 9.1). The average proportion of cations in their octahedral sites are $X^{VI}_{Al} = 0.977$, $X^{VI}_{Fe^{3+}} = 0.022$, $X^{VI}_{Cr} = 0.001$ and in their cubic sites are $X^{VIII}_{Mg} = 0.634$, $X^{VIII}_{Fe^{2+}} = 0.138$, $X^{VIII}_{Mn} = 0.004$, $X^{VIII}_{Ca} = 0.224$ (Table 9.2).

Deer *et al.* (1997a: 525) report that pyrope can be found in kimberlites and eclogites. MacGetchin and Silver (1970) showed that the Cr-poor pyrope is related to eclogite xenoliths. All garnet samples from this study contain very low Cr-contents, so their compositions can be plotted in the triangular diagram for eclogite classification according to Coleman *et al.* (1965) (Figure 9.7). The plots show that the compositions of all samples fall in the field of group A eclogites (i.e. >55% of pyrope content). Group A is designated for the garnet in the inclusions in kimberlites, basalts, or layers in ultramafic rocks.

The compositions of the red garnet xenocrysts in alkali basalt samples (NB5/1 and NB5/2) and the samples of gem-quality red garnet associated with corundum in alluvium from Bang Kacha, BoRai and Nong Bon together with garnets from other geological environments are also plotted in the same diagram. The compositions of the garnet inclusions in corundum are different from the garnet xenocrysts in basalt and the

gem garnet samples in alluvium, see also Table 9.2. The garnet inclusions in corundums have higher grossular (Ca) contents than the other garnets in the table and are Ti-free.

Garnet samples from alluvium and xenocrysts in basalts in this study have very similar compositions possibly called pyrope-almandine garnet, whereas garnet inclusions are possibly called pyrope-grossular garnet. The similarity in composition of garnet samples from alluvium and xenocrysts suggests that they crystallized in a similar condition. Barr and Dostal (1986) suggested that they are either high-pressure cognate phenocrysts or the remains of the disintegration of coarse-grained mafic rocks.

Table 9.2 Average proportion of atoms in octahedral and cubic sites and end members for garnets of different provenance.

Locality	**BO RAI**		**BANG KACHA**	**NONG BON**	
Provenance	**Inclusion in corundum**	**In alluvium**	**In alluvium**	**Xenocryst in basalt**	**In alluvium**
Number of analysis	**5**	**3**	**3**	**41**	**12**
Octahedral site					
X^{VI}_{Al}	0.977	0.970	0.954	0.969	0.960
$X^{VI}_{Fe^{3+}}$	0.022	0.018	0.032	0.015	0.027
X^{VI}_{Cr}	0.001	-	-	-	-
X^{VI}_{Ti}	-	0.012	0.014	0.017	0.012
Cubic site					
X^{VIII}_{Mg}	0.634	0.636	0.626	0.584	0.629
$X^{VIII}_{Fe^{2+}}$	0.138	0.233	0.238	0.271	0.235
X^{VIII}_{Mn}	0.004	0.004	0.008	0.008	0.007
X^{VIII}_{Ca}	0.224	0.127	0.128	0.137	0.129
End members					
Pyrope	63.4	63.6	62.7	58.4	62.9
Grossular	20.1	10.9	9.6	12.3	10.2
Almandine	13.8	23.3	23.8	27.1	23.5
Andradrite	2.2	1.8	3.2	1.5	2.7
Spessartine	0.4	0.4	0.7	0.7	0.7
Uvarovite	0.1	-	-	-	-

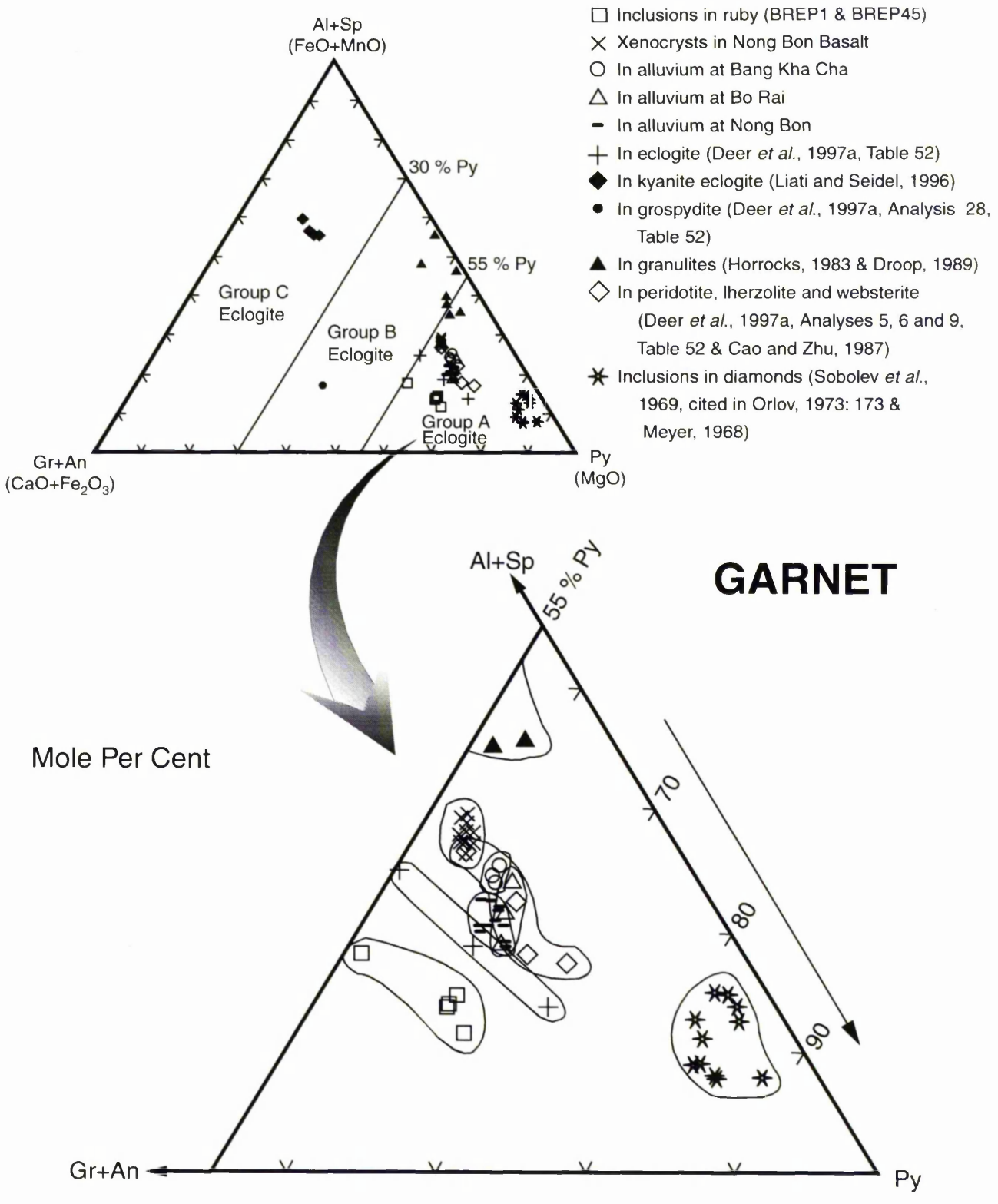

Figure 9.7 Plot of compositions for garnet inclusions in ruby samples (BREP1 and BREP45) in the diagram of eclogite garnets after Coleman, *et al.* (1965), garnets in other provenances are plotted for comparison. [**Group C eclogite**: garnets from amphibolite, charnockites and granulites; **Group B eclogite**: garnets from eclogites occurring in gneissic or migmatite metamorphic terrains, charnockites and granulites; **Group A eclogite**: garnets from eclogites associated in kimberlite pipes, eclogites within ultramafic rocks such as dunite and peridotite as well as inclusions in basalts, or layers in ultramafic rocks].

Ruby has been found in eclogite xenoliths (grospydite) in kimberlites; it is associated with orange garnet (pyrope-grossular: py_{44} gro_{42} al_{14}) (Sobolev, 1965) which is more calcic and less magnesian than the garnet inclusions in this study (average: py_{65} gro_{21} al_{14}). Ruby is also found as inclusions in eclogitic diamond. This suggests that it formed in the mantle (Meyer and Gübelin, 1981, Hall *et al.*, 1994). The pyropes from ultramafic nodules generally have lower Ca and/or higher Cr than the Bo Rai inclusions, whilst those from grospydites have much higher Ca (e.g. Sobolev *et al.*, 1968). Of the chemical categories identified by Dawson and Stephens (1975) in their statistical classification of garnets from kimberlite and associated xenoliths, the Bo Rai inclusions correspond most closely to cluster 6, which is dominated by eclogites with or without kyanite or corundum.

The moderate Ca content of the Thai garnet inclusions in corundum of this study suggests a different origin from the above. They possibly crystallized in such as basic composition rock since the compositions of garnet are close to the garnets in the fassaite-'eclogite' xenoliths in the Delegate pipe (which are ca py_{65} gro_{15} alm_{18} and_{02}) (Lovering and White, 1969).

9.4.2 Fassaite

Fassaite (high-alumina augite), $Ca(Mg,Fe^{2+}, Fe^{3+}Al)[(Si,Al)_2O_6]$, is a variety of Al-rich calcic pyroxene. It is found as inclusions within and as a co-existing mineral with, ruby samples from Bo Rai. Two crystal inclusions in sample BREP43 are euhedral in shape with a stubby prismatic habit and are surrounded by stress cracks (Figure 9.2, A). The colour of the crystals is dominated by the purple tint of the corundum, but the inclusions show high interference colours. The sizes of two crystals are 100x165 μm and 120x200 μm respectively.

The second fassaite is found as a brown green grain occurring at the rim of the ruby grain (BRJ) (Figure 9.2, B). The fassaite grain is heavily decorated with healed fractures. It has an irregular outline, green colour and strong pleochroism (green to blue-green) under the microscope in thick section.

Fassaites in this study have $Mg/(Mg+Fe^{2+})$ values ranging from 0.86 to 0.97. Their average composition (from 6 analyses) written by cell formula is $(Mg_{0.04}Fe^{2+}_{0.01}Ca_{0.85}Na_{0.10})^{M2}(Al_{0.33}Fe^{3+}_{0.04}Ti_{0.02}Cr_{0.01}Mg_{0.55}Fe^{2+}_{0.05})^{M1}(Si_{1.70}Al_{0.30})^{IV}{}_2O_6$.

Based on 6 oxygens, the Al content is very high (0.66 atoms) and the Al occupies both tetrahedral and octahedral (M1) sites. The distorted 8-fold (M2) site is largely filled with Ca ($X_{Ca} = 0.85$) but also contains appreciable Na ($X_{Na} = 0.10$).

Fassaite is commonly found in metamorphosed limestones and dolomites; however it has also been found in eclogitic inclusions in kimberlite and in meteorites (Deer *et al.*, 1997b: 399). Six analyses of fassaite from this study were plotted on the pyroxene quadrilateral diagram together with the compositions of fassaite from other localities (published in Deer *et al.*, 1997b: Table 40, pp 403-406). It is found that the compositions of fassaite in this study fall reasonably well in the field of fassaite of metamorphic origin (Figure 9.8).

Fassaites in this study do not closely resemble the clinopyroxenes from corundum-eclogite nodules from kimberlite pipes, which are generally omphacites, having much higher Na and Al^{IV} and lower Ca and Al^{IV} (Stephens and Dawson, 1977; Deer *et al.*, 1978b). On the other hand, they do correspond closely to those from ruby-garnet-clinopyroxenites from Beni Bousera, Morocco (Kornprobst *et al.*, 1990). The Mg/ $(Mg+Fe^{2+})$ values range from 0.85 to 0.97. Their average composition (from 10 analyses) written by cell formula is $(Mg_{0.04}Fe^{2+}_{0.00}Ca_{0.81}Na_{0.14})^{M2}$ $(Al_{0.45}Fe^{3+}_{0.03}Ti_{0.01}Cr_{0.00}Mg_{0.48}Fe^{2+}_{0.04})^{M1}$ $(Si_{1.66}Al_{0.34})^{IV}{}_2O_6$. The plots of Beni Bousera fassaite compositions in quadrilateral diagram (Figure 9.8) fall in the same field of fassaite of this study. The other fassaites which show a close match in composition are such as the fassaite-'eclogites' of Knockormal, S. Scotland (Bloxam and Allen, 1960) and the fassaite-'eclogite' nodules in the Delegate pipe, Australia (Lovering and White, 1969). Both these fassaites are characterised by high Al^{VI} and Al^{IV} (totalling ca 0.6 p.f.u.) with $Al^{VI}>Al^{IV}$, but the Delegate fassaites have higher Na (ca 0.13 p.f.u.) and are a closer match.

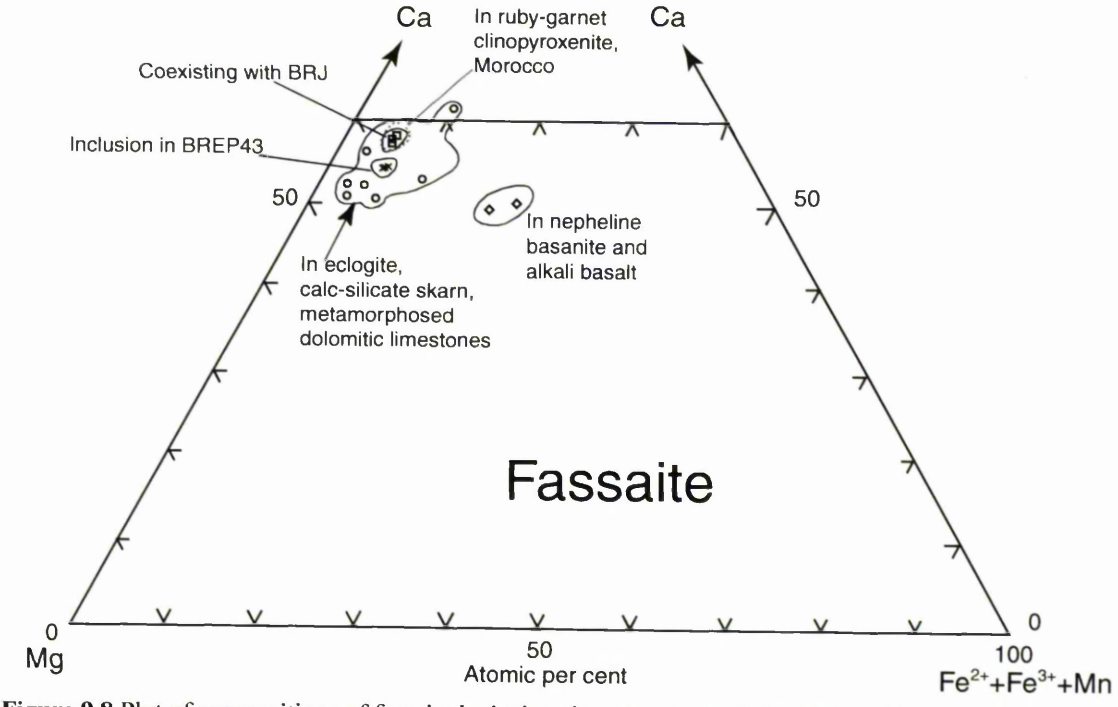

Figure 9.8 Plot of compositions of fassaite inclusions in ruby sample (BREP43) and fassaite occurring as a coexisting mineral with ruby sample (BRJ) in quadrilateral diagram of pyroxene, together with those of fassaite from metamorphic and igneous origins.

9.4.3 Sapphirine

Sapphirine, $(Mg,Fe^{2+},Fe^{3+}Al)_8O_2[(Al,Si)_6O_{18}]$, is found in the ruby sample from Bo Na Wong (NWEP9) and also as a coexisting mineral with ruby sample (NWEP11) from the same locality. The latter is though to be a remnant (size 1.9x0.4 mm) of the mineral assemblage of the parent rock of corundum. The grains of sapphirine are blue-green in colour with strong pleochroism (blue-green to deep blue-green) under microscope in thick section. The included grain (size 1.3x1.8 mm) in ruby sample NWEP9 is anhedral and contains several fractures, which suggest that it is a protogenetic inclusion (Figure 9.3).

Sapphirine has been reported as an inclusion in the ruby from Bo Rai (Koivula, 1987). It is a rare mineral, which typically occurs in Al-rich, Si-poor granulite and hornblende

granulite facies (high-grade metamorphic rocks) (Deer *et al.*, 1997b: 614). Sutherland and Coenraads (1996) found samples of ruby or pink sapphire existing in assemblages with sapphirine and spinel in basaltic terrain. According to Sutherland and Coenraads (1996), the aggregates suggested a crystallisation temperature of 780-940°C and reacted with the host magma at a temperature of over 1000°C. The compositions of sapphirines from this study are plotted on the SiO_2-Al_2O_3+Fe_2O_3-MgO+FeO triangular diagram together with the compositions of sapphirine from other localities (Figure 9.9). The compositions of sapphirine inclusions in this study conform well to those of granulite facies. The compositions are intermediate in composition between 2:2:1 and 7:9:3 (MgO+FeO : Al_2O_3+Fe_2O_3 : SiO_2) end members. The average atomic proportion (from 7 analyses) for $Mg/(Mg+Fe^{2+})$ is 0.93, and for $Fe^{3+}/(Fe^{2+}+Fe^{3+})$ is 0.16.

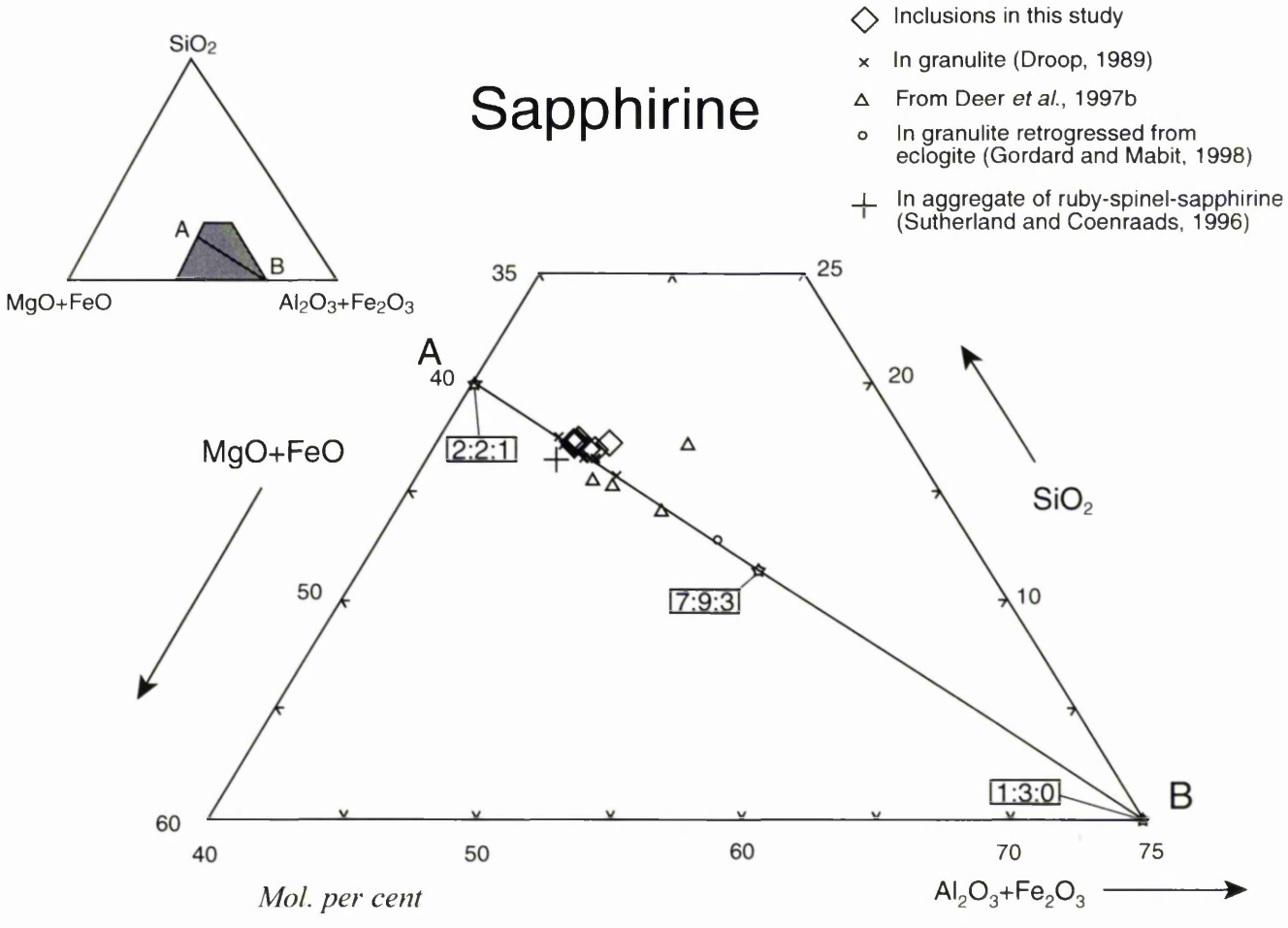

Figure 9.9 Compositions of sapphirine inclusion and sapphirine coexisting with ruby from this study plotted with sapphirine compositions from other localities. Note that sapphirines from Deer *et al.*, 1997b (Table 64, pp. 618-620) are associated with corundum; sapphirine compositions from Gordard and Mabit, 1998 and Sutherland and Coenraads, 1996 are the average values).

9.4.4 Alkali feldspar

Alkali feldspar inclusion found in this study is identified as sanidine. The sanidine inclusion exists in sapphire sample (DCEP16) from Den Chai. It is colourless and rounded. The size of the inclusion is 44x66 μm (Figure 9.4, A). This alkali feldspar contains a relatively high Ca content (i.e. $An_{12\text{-}13}$) rendering it a ternary feldspar. The overall composition averaged from 3 analyses is $Or_{31.2}Ab_{56.0}An_{12.8}$.

The compositions of the feldspar inclusion are plotted on the diagram of Figure 9.10. The isothermal lines indicate that the minimum temperature for the crystallization of sanidine inclusion in the corundum is ca 1000°C. Note that the isotherms on the feldspar triangle give a minimum temperature of crystallization because homogeneous ternary feldspars are only stable above the solvus.

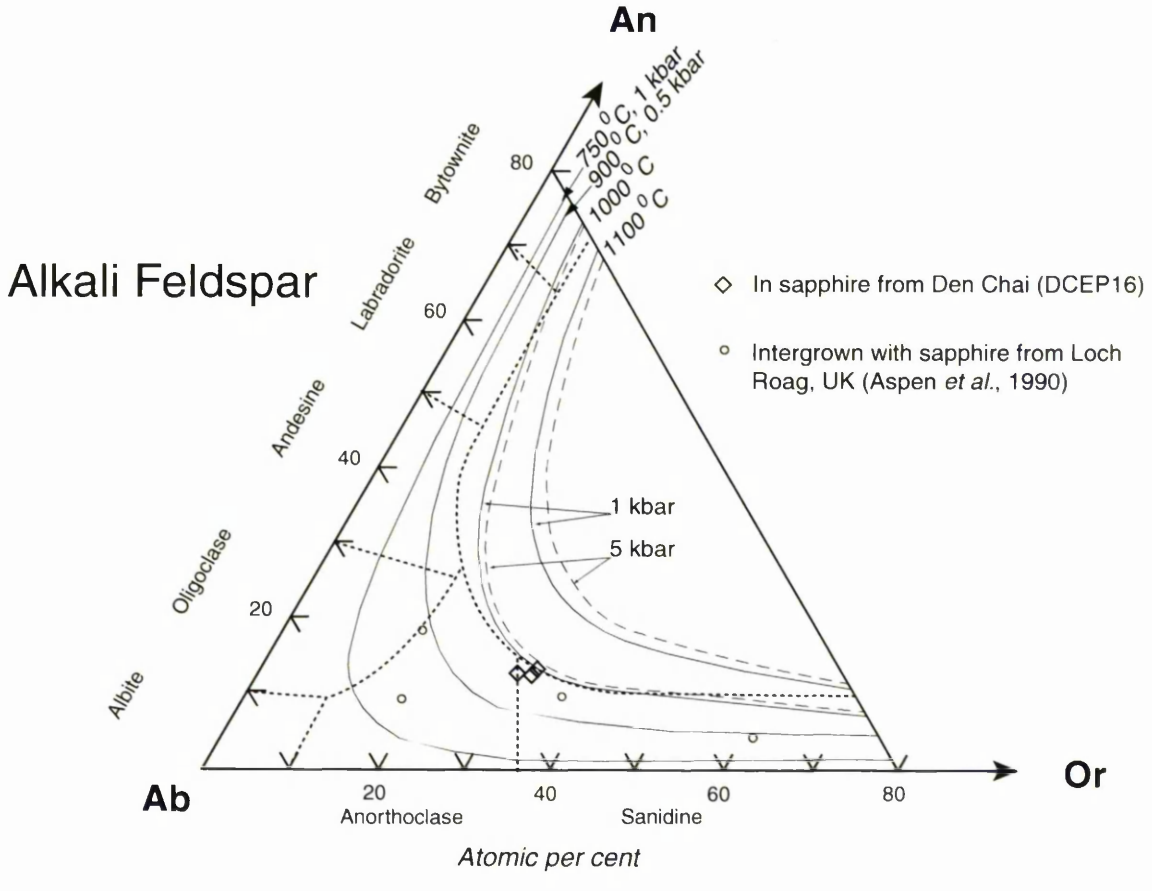

Figure 9.10 Compositions of an alkali feldspar inclusion in sapphires from Den Chai (DCEP16) are plotted in the triangular diagram together with the compositions of alkali feldspar intergrown with sapphire in xenoliths found in alkali basalt from Loch Roag, UK. Isotherms (of solvus) taken from Fuhrman and Lindsley (1988).

Sanidine and anorthoclase crystals intergrown with sapphires have been found as the xenoliths in alkali basalt at Ruddon's Point and Loch Roag of Scotland and Hoy Province, Queensland of Australia (Aspen *et al.*, 1990; Upton, *et al.*, 1983; Coenraads *et al.*, 1990). These authors suggest that they are fragments of high-pressure syenitic veins crystallized from trachytic magma in the upper mantle, probably <75 km (Aspen *et al.*, 1990).

9.4.5 Nepheline

Nepheline, $(Na,K)AlSiO_4$, is found in the sapphire sample from Bo Phloi (BPEP1). It shows a subhedral, prismatic habit with broken ends, and is 21x55 μm in size. This suggests that it is a protogenetic inclusion (Figure 9.4, B). The overall composition averaged from 4 analyses is $Ne_{68.3}Ks_{28.6}Q_{3.0}$. The Si/Al ratio is 1.009 and Ca substitution in structure is 0.032 p.f.u on the basis of 32 O. An ideal unit cell formula of the nepheline inclusion in this study can be written as $Na_{5.38}K_{2.02}Ca_{0.03}\square_{0.57}Al_{7.47}Si_{8.53}O_{32}$.

Nepheline coexisting with sapphire is found in syenitic–gneiss rock in Bancroft, Canada (Moyd, 1949), syenitic rock and nepheline-aegerine intrusive rock (urtite) in Mogok, Myanmar (Waltham, 1999). In Khibina alkali complex, Russia, corundum is found associated with nepheline in fenite at the zone of albitized trachytic nepheline syenite called foyaite (Barkov, *et al.*, 1997; Barkov, *et al.*, 2000). This suggests that sapphire from Bo Phloi could possibly crystallize in an environment of syenitic rocks which are rich in alkali (Na and K) and poor silica contents and probably related to the carbonatite intrusion.

9.4.6 Zircon

Zircon is found as inclusions in sapphire samples from three localities, Ban Huai Sai near Chiang Khong (CKEP10), Ban Nong (BNEP1) and Bo Phloi (BPEP14). The inclusion in the sapphire sample from Ban Huai Sai is euhedral, of prismatic habit and clearly showing the {010} prism form (Figure 9.5, A). The shape of the zircon inclusions from the other localities is stubby, oval and showing bipyramidal form. The crystal in sapphire from Bo Phloi is associated with stress cracks (Figure 9.5, B). The sizes of the three inclusions are 35x37μm for CKEP10, 22x32 μm for BNEP1 and 38x65 μm for BPEP14. The zircon inclusion in the sapphire sample from Ban Nong

Nam Cho (BNEP1), for example, has a composition 69.54 wt% ZrO_2 and 31.45 wt% SiO_2.

Zircon is a common accessory mineral of igneous rocks, particularly plutonic rocks that are relatively rich in sodium. Zircon is also found in sedimentary and metamorphic rocks (Deer *et al.*, 1997a: 433-435). Zircon is found intergrown with sapphire and magnetite at Khao Wua near Bang Kacha, Thailand (Coenraads *et al.*, 1995). Guo *et al.* (1996a) found that the zircon inclusions in sapphire from Australia and Asia contain high Hf, U, Th, Y and REEs similar to those of zircon found intergrown with corundum from Scotland (Aspen *et al.*, 1990). Coenraads *et al.* (1990) and Guo *et al.* (1996b) studied the zircon inclusions in blue and yellow sapphires from basaltic terrains and suggested that the corundum host must have crystallised from alkaline and highly evolved melts under very reducing conditions, not from the host basaltic magma.

9.4.7 Spinel

Spinel is found as inclusions in sapphire samples from three localities, Ban Huai Sai (CKEP30), Bo Phloi (BPEP13) and Bang Kacha (BKCEP) (Figure 9.6, A, C, D). The sapphire sample from Ban Nong Nam Cho (BNEP4) coexists with black spinel (size 280x660 μm) (Figure 9.6, B).

The spinel inclusions have many shapes, for example irregular shape (Figure 9.6, A) suggesting that it is protogenetic. The spinel inclusion in the sapphire sample from Bo Phloi has a distorted euhedral shape (Figure 9.6, C).

Brown sapphire samples from Bang Kacha that show chatoyancy or star effects contain an abundance of spinel inclusions. The inclusions in these sapphire samples are in the form of black platelets (max. 0.10x0.22 mm) associated with brown needles (max. ca 140 μm in length) (Figure 9.6, D). They were reported as hematite plates associated with the hematite needles by Hughes (1997: 447-449). Unfortunately, the chemical compositions of the hematite and rutile were not given in that book. The SEM-EDS from this study indicates that the platelets are magnetite-hercynite solid solutions (analyses of inclusions in sample BKCEP4). One of the needles was also analysed in this study but the result is not reliable because the width of needle was too small (ca 1 μ m) for analysis by the beam. The analysis result (in wt% oxide) for the needle obtained is thought to be contaminated by the alumina from the host corundum (TiO_2=3.04,

Al_2O_3=87.92, FeO=9.22, Na_2O=0.27, Total=100.45). This could imply that the needles are not pure hematite or rutile. They may be ilmenite or ilmenite-hematite solid solution, according to Moon and Phillips (1984).

The compositions of spinel inclusions in this study are hercynite-spinel and magnetite-hercynite (Table 9.1 and Figure 9.11). Their compositions in terms of end members are given in Table 9.3. Their compositions are also plotted on the diagram of Figure 9.12 to estimate the temperature of crystallization. The minimum crystallization temperature obtained from a non-exsolved spinel inclusion from Bang Kacha is 860°C.

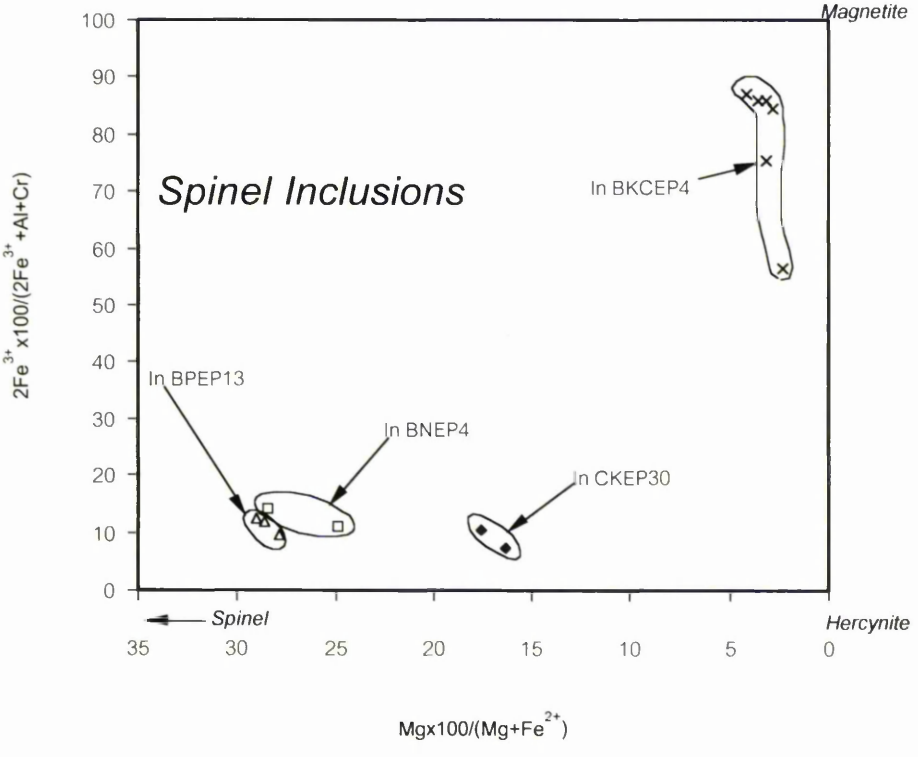

Figure 9.11 Spinel compositions in sapphires from Ban Huai Sai (CKEP30), Ban Nong Nam Cho (BNEP4), Bo Phloi (BPEP13) and Bang Kacha (BKCEP4) are plotted on the Spinel-Hercynite-Magnetite diagram (from Haggerty, 1991).

Table 9.3 Average per cent of end members for spinel inclusions in corundums of this study.

Locality	Chiang Khong	Ban Nong	Bo Phloi	Bang Kacha
No of analysis	2	2	3	6
Spinel	16.8	26.1	28.4	3.0
Hercynite	76.5	64.6	62.7	21.0
Gahnite	0.0	0.0	0.0	0.3
Galaxite	1.5	1.8	1.7	5.8
Magnetite	4.7	6.8	5.9	64.7
Chromite	0.0	0.0	0.9	0.0
Ulvöspinel	0.5	0.7	0.4	5.1

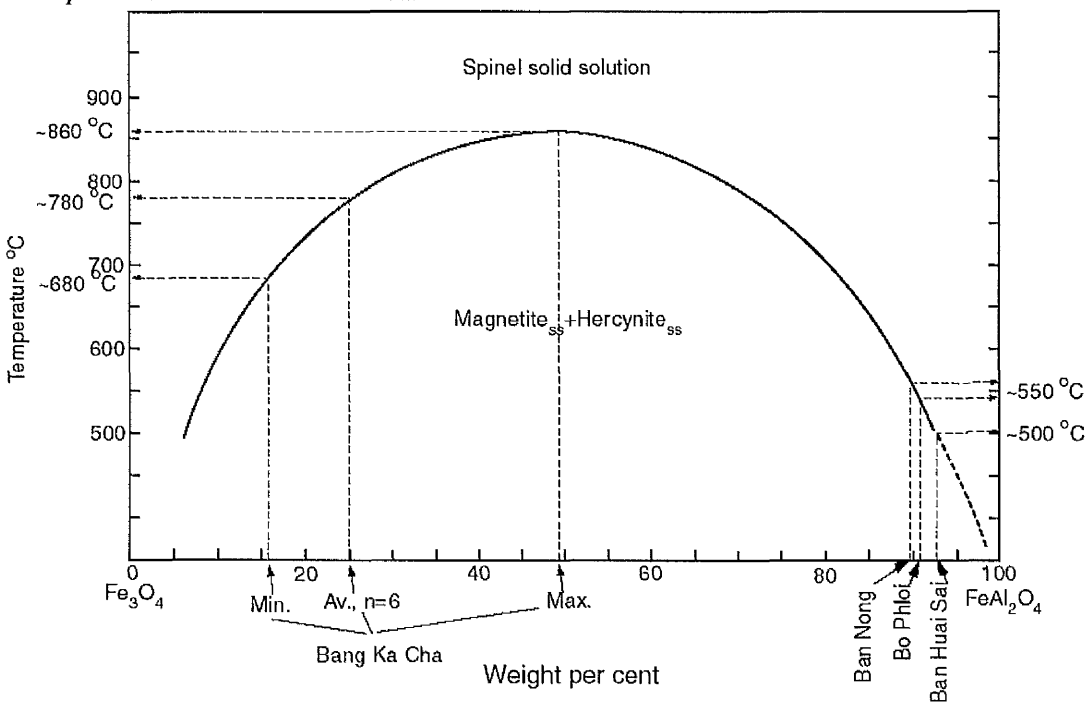

Figure 9.12 Graphical estimation of temperature limit of crystallization for inclusions of magnetite-hercynite solid solution from Bang Kacha. The minimum possible temperature of crystallization is 860 C. The solvus (at 2 kbar) is taken from Turnock and Eugster (1962).

The spinel intergrown with ruby and sapphirine at Barrington, Australia is a Cr-pleonaste (1.05-8.51 wt% of Cr_2O_3), whereas the spinel inclusion in sapphire from New South Wales, Australia is Cr-poor (0.00-0.01 wt% of Cr_2O_3) (Sutherland and Coenraads, 1996). Spinel inclusions found in this study have low Cr_2O_3 content (0.00-0.81 wt%). Hercynite was also found as exolution lamellae in magnetite of a xenolith comprising sapphire, zircon and magnetite found at Khao Wua, Thailand (Coenraads *et al.*, 1995).

9.4.8 Summary

Inclusions and coexisting minerals found with corundum in this study can be categorised into two suites, the ruby suite and the sapphire suite. They are summarised in Table 9.4.

Table 9.4 Summary of inclusions and coexisting minerals found with corundum from Thailand.

Sample No \Corundum	Ruby suite	Sapphire suite
BREP1, BREP45	Garnet	-
BREP43, BRJ	Fassaite	-
NWEP9, NWEP11	Sapphirine	-
DCEP16	-	Sanidine
BPEP1	-	Nepheline
CKEP10, BNEP1, BPEP14	-	Zircon
CKEP30, BNEP4, BPEP13	-	Hercynite-spinel series
BKCEP4	-	Magnetite-hercynite series

9.5 Geothermometry and geobarometry of mineral inclusions and coexisting minerals of corundums

Sapphirine, fassaite and garnet occurring as inclusions coexisting with corundum from this study were used for estimating of the pressure and temperature (P-T) of crystallization. If a balanced chemical reaction can be written among end-member components present in a set of mineral phases that crystallized together in equilibrium, then, in principle, the P-T location of the equilibrium curve can be used to constrain the P-T conditions of crystallization. If two or more independent equilibria can be written, then the intersection of the equilibrium curves on a P-T plot can be used to fix P and T. If one or more components from one of the reactions are absent from the equilibrium assemblage, then the equilibrium curve can only be used as a stability limit.

Provided that high-quality thermodynamic data are available for all the end-member components involved in an equilibrium, the P-T position of a curve can be calculated using standard equilibrium thermodynamics (e.g. Wood and Fraser, 1977). The data required for each end-member include standard state molar enthalpy of formation from the elements ($\Delta_f H°$), standard-state molar entropy (S°), standard-state molar volume (V°), molar heat capacity polynomial coefficients (a, b, c, d, and e), and coefficients of volume expansivity (α) and compressibility (β). Also required is the activities (a_M^W) of each end-member component M in its respective mineral phase W, which is its effective concentration and is a function of the composition of the host phase. For a balanced chemical reaction of the form

$$\mathrm{mM + nN = pP + qQ}$$

the net effect of dilution of end members in solid solutions on the position of the equilibrium curve is controlled by the activity product or equilibrium constant, K, which is given by

$$K = \frac{(a_P)^p \cdot (a_Q)^q}{(a_M)^m \cdot (a_N)^n}.$$

For a balanced reaction involving no fluids at equilibrium, the following equation holds true (Powell and Holland, 1985):

$$0 = \Delta G^{\circ}_{(r)1,T} + (P-1)(\Delta V^{\circ}_{(r)} + \Delta(\alpha V)(T-298) - \Delta(\beta V)\tfrac{P}{2}) + RT\ln K$$

$$\text{where} \quad \Delta G^{\circ}_{(r)1,T} = \Delta H^{\circ}_{(r)1,298} + \int_{298}^{T} \Delta C_P dT - T(\Delta S^{\circ}_{(r)} + \int_{298}^{T} \frac{\Delta C_P}{T} dT)$$

$$\text{and} \quad \Delta C_P = \Delta a + \Delta b T + \Delta c T^{-2} + \Delta d T^{-0.5} + \Delta e T^2.$$

$(\Delta S^{\circ}_{(r)} = \sum S^{\circ}$(reactants) for a balanced reaction;

$\Delta V^{\circ}_{(r)} = \sum V^{\circ}$(reactants) for a balanced reaction; etc.)

G is molar Gibbs free energy, C_p is molar heat capacity at constant pressure, R is the gas constant, P is pressure (bars), and T is absolute temperature.

Powell and Holland (1985) and Holland and Powell (1985, 1990, 1998) have devised an extensive self-consistent set of thermodynamic data for end-member minerals, and have written a computer program (THERMOCALC) for solving the above equation (Powell and Holland, 1988). This program solves the equation for T at given values of P. The latest version of THERMOCALC, v 2.75, is available at http://rubens.its.unimelb.EDU.AU /~RPOWELL/THERMOCALC.

The compositions of the relevant mineral end-members are shown on chemographic diagrams in Figure 9.13. Potentially useful univariant reactions that can be written between these end-members are listed in Table 9.5. The procedures for obtaining the activity values for each mineral end-member and the results of P-T are given in the next section.

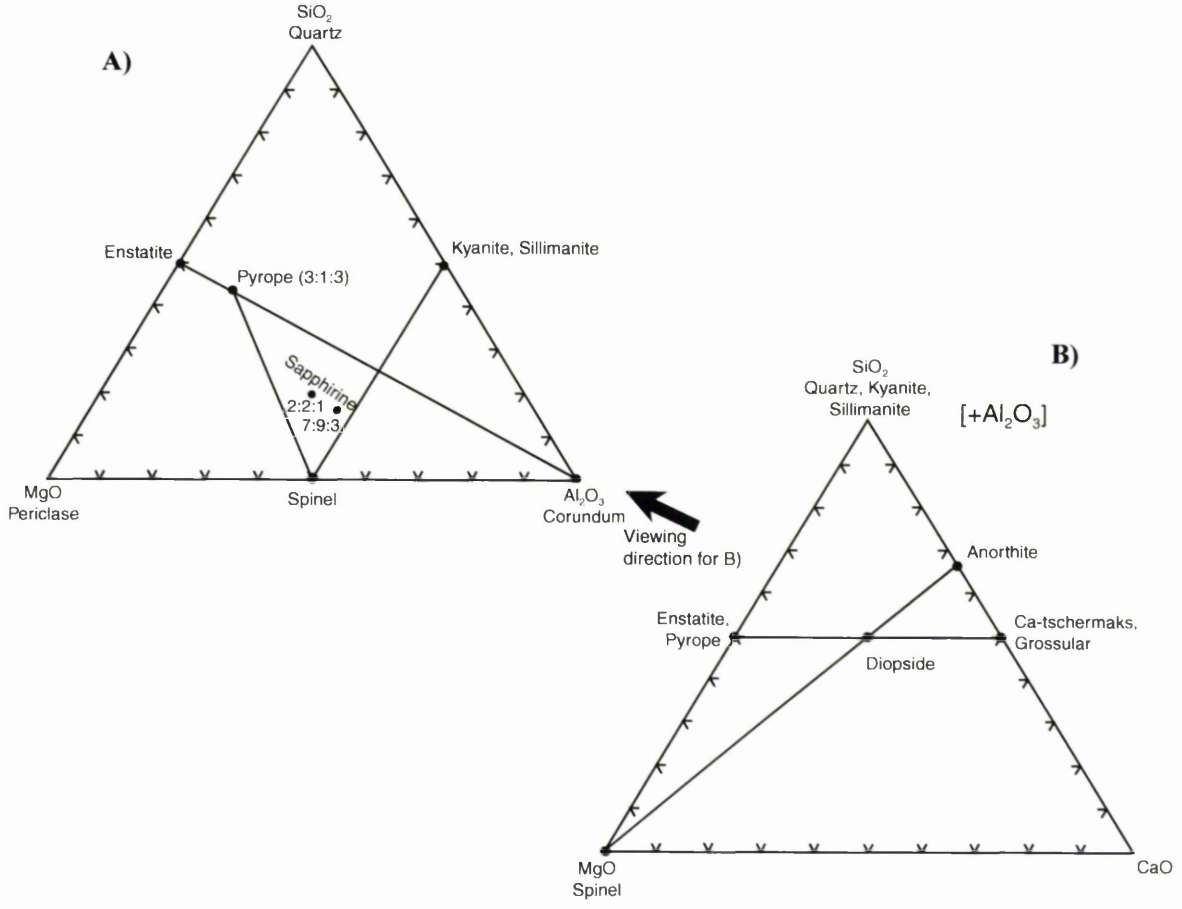

Figure 9.13 Chemographic relations amongst mineral end-members associated with corundum-inclusion assemblages, plotted on **(A)** a MgO-Al_2O_3-SiO_2 diagram, and **(B)** a CaO-MgO-SiO_2 projection from corundum.

Table 9.5 Potentially useful univariant reactions amongst end-members of mineral inclusions and minerals coexisting with corundum, and equations for calculating activities. Note: all symbols are given in the next section.

Mineral inclusion/Locality	Reaction*	Activity	Reference
Sapphirine/Na Wong	1. 4**Corundum** + 2*Pyrope*+6*Spinel*+ = 3**Sapphirine4** ; 2. *4Spinel* + *2Kyanite* = **Sapphirine4** + 2**Corundum**	$a_{2:2:1spr} = 89.9 \cdot \left[R^3 \cdot \left(X_{Mg}^{M5678}\right)^1 \cdot \left(X_{Al}^{M5678}\right)^3 \cdot \left(X_{Al}^{T3456}\right)^3 \cdot \left(X_{Si}^{T3456}\right)^1 \right]$	Holland and Powell (1998)
Fassaite/Bo Rai	3. **2Ca-tschermaks** + **Enstatite** = 2**Corundum** + 2**Diopside**; 4. **Diopside** + 2**Corundum** = *Anorthite* + *Spinel*	$a_{di}^{cpx} = X_{Ca}^{M2} \cdot X_{Mg}^{M1} \cdot \left(X_{Si}^{T}\right)^2 \cdot 1.49$	Wood (1979)
		$a_{cats}^{cpx} = 4 \cdot \left(X_{Ca}^{M2} \cdot X_{Al}^{M1} \cdot X_{Al}^{T} \cdot X_{Si}^{T}\right)^{cpx_{ss}} \cdot \overline{\gamma}_{cats}^{cpx}$	
		$a_{en}^{cpx} = X_{Mg}^{M2} \cdot \gamma_{Mg}^{M2} \cdot X_{Mg}^{M1} \cdot \left(X_{Si}^{T}\right)^2$	Carlson and Lindsley (1988)
Garnet/Bo Rai	5. *3Ca-Tschermaks* = **Grossular** + 2**Corundum**; 6. 2**Corundum** + *3Enstatite* = 2**Pyrope**	-	Berman (1990)

*Italic-typed phases are absent. Reactions involving absent phases can only be used as stability limits.

9.5.1 Activity calculations for P-T limits from minerals coexisting with corundum from Thailand

1) The Sapphirine+Corundum assemblage

Reactions: . 4**Corundum** + *2Pyrope* + *6Spinel* = 3**Sapphirine4**.....1)

4Spinel + *2Kyanite* = **Sapphirine4** + 2**Corundum**.....2)

(Note: Italic type phases are absent)

These two reactions can only be used as stability limits, since in each case there is a complete set of end-members for only one side of the reaction.

Table 9.6 Structural sites of sapphirine.

Site	Octahedral (M)	Tetrahedral (T)	Number of Oxygen
spr4 ($Mg_4Al_8Si_2O_{20}$), 2:2:1	Mg_4Al_4	Al_4Si_2	O_{20}
spr7 ($Mg_{3.5}Al_9Si_{1.5}O_{20}$), 7:9:3	$Mg_{3.5}Al_{4.5}$	$Al_{4.5}Si_{1.5}$	O_{20}

Octahedral site (M):

1	Only Al
2	Only Mg & Fe^{2+}
3	
4	
5	Mg, Fe^{2+}, Fe^{3+}, Al, Ti Cr, Ni and etc.
6	
7	
8	

Tetrahedral sites (T)

1	Only Si
2	Only Al
3	Al **or** Si
4	
5	
6	

$$a_{2:2:1spr} = \frac{(\text{Probability of finding an entire } Mg_4Al_8Si_2O_{20} \text{ molecule in 1 unit cell of impure } SPR_{ss})}{(\text{Probability of finding an entire } Mg_4Al_8Si_2O_{20} \text{ molecule in 1 unit cell of pure } SPR_{ss})}$$

Table 9.7 List of cations in M and T sites of sapphirine structure.

Octahedral (M)								Tetrahedral (T)					
8	7	6	5	4	3	2	1	6	5	4	3	2	1
Mg	Al	Al	Al	**Mg**	**Mg**	**Mg**	**Al**	Al	Al	Al	Si	**Al**	**Si**

(Shaded cells contain only the element shown. Substitution is only possible in the non-shaded cells.)

$$R = \left(\frac{Mg}{Mg + Fe^{2+}}\right)$$

$$a_{2:2:1spr} = \frac{\left(X_{Mg}^{M5678} \cdot X_{Al}^{M5678} \cdot X_{Al}^{M5678} \cdot X_{Al}^{M5678} \cdot R \cdot R \cdot R \cdot 1\right) \cdot \left(X_{Al}^{T3456} \cdot X_{Al}^{T3456} \cdot X_{Al}^{T3456} \cdot X_{Si}^{T3456} \cdot 1 \cdot 1\right)}{\left[\frac{1}{4} \cdot \frac{3}{4} \cdot \frac{3}{4} \cdot \frac{3}{4} \cdot 1 \cdot 1 \cdot 1 \cdot 1\right] \cdot \left[\frac{3}{4} \cdot \frac{3}{4} \cdot \frac{3}{4} \cdot \frac{1}{4} \cdot 1 \cdot 1\right]}$$

$$a_{2:2:1spr} = \left[\frac{\left(X_{Mg}^{M5678}\right)^1 \cdot \left(X_{Al}^{M5678}\right)^3 \cdot R^3 \cdot \left(X_{Al}^{T3456}\right)^3 \cdot \left(X_{Si}^{T3456}\right)^1}{0.0111} \right]$$

$$a_{2:2:1spr} = 89.9 \cdot \left[R^3 \cdot \left(X_{Mg}^{M5678}\right)^1 \cdot \left(X_{Al}^{M5678}\right)^3 \cdot \left(X_{Al}^{T3456}\right)^3 \cdot \left(X_{Si}^{T3456}\right)^1 \right]$$

From the average composition of 7 sapphirine analyses from the EPMA (Appendix 9-1):

$$R = \left(\frac{Mg}{Mg + Fe^{2+}} \right) = 0.927$$

$$X_{Si}^{T3456} = \left(\frac{Si_{Total\ per\ 20(O)} - 1}{4} \right) = 0.160$$

$$X_{Al}^{T3456} = \left(\frac{6 - Si_{per\ 20(O)} - 1}{4} \right) = \left(\frac{5 - Si_{per\ 20(O)}}{4} \right) = 0.840$$

$$X_{Al}^{M5678} = \left(\frac{Al_{Total} + Si_{Total} - 6 - 1}{4} \right) = \left(\frac{\left(Al_{Total} + Si_{Total\ per\ 20(O)}\right) - 7}{4} \right) = 0.830$$

$$X_{Mg}^{M5678} = \left(\frac{Mg_{Total\ \ per\ \ 20(O)} - 3R}{4} \right) = 0.132$$

$$a_{2:2:1spr} = 0.513$$

The activities of the absent end members in reactions 1) and 2) above are set at 1.0. Corundum is virtually pure Al_2O_3, so its activity is equal to 1.0. The results are given in Table 9.14.

2) The Fassaite+Corundum assemblage

Reaction **2Ca-Tschermaks + Enstatite = 2Corundum + 2Diopside**.....3)

$2CaAl_2SiO_6 + Mg_2Si_2O_6 = 2Al_2O_3 + 2CaMgSi_2O_6$

This reaction can be used as a P-T indicator because all four end-members are present within the mineral assemblage. Ca-Tschermaks pyroxene, enstatite and diopside are all components present within the fassaite.

2.1) Diopside-Ca-Tschermaks solid solution: Assume Al&Si disorder on T sites (Wood, 1979).

$$a_{cats}^{cpx} = \overline{X}_{cats}^{cpx} \cdot \overline{\gamma}_{cats}^{cpx}$$

$\overline{X}_{cats}^{cpx}$ = Ideal activity assuming Al&Si mix randomly on T sites.

$$= \left[\frac{Probability\ of\ finding\ 1\ entire\ CaAlAlSiO_6\ molecule\ in\ 1\ unitcell\ of\ cpx_{ss}}{Probability\ of\ finding\ 1\ entire\ CaAlAlSiO_6\ molecule\ in\ 1\ unitcell\ of\ pure\ cats} \right]$$

$$= \left[\frac{\left(X_{Ca}^{M2} \cdot X_{Al}^{M1} \cdot X_{Al}^{T} \cdot X_{Si}^{T} \right)^{impure\ cpx_{ss}}}{\left(X_{Ca}^{M2} \cdot X_{Al}^{M1} \cdot X_{Al}^{T} \cdot X_{Si}^{T} \right)^{pure\ cats}} \right]$$

$$= \left[\frac{\left(X_{Ca}^{M2} \cdot X_{Al}^{M1} \cdot X_{Al}^{T} \cdot X_{Si}^{T} \right)^{impure\ cpx_{ss}}}{\left(1 \cdot 1 \cdot 0.5 \cdot 0.5 \right)} \right]$$

$$= 4 X_{Ca}^{M2} \cdot X_{Al}^{M1} \cdot X_{Al}^{T} \cdot X_{Si}^{T}$$

$\overline{\gamma}_{cats}^{CPX} = activity\ coefficient$

(Note: γ_A^B=Activity coefficient of component A in phase B. Defined as $\frac{a_A^B}{X_A^B}$ for one site solution)

$$a_{cats}^{cpx} = 4 \cdot \left(X_{Ca}^{M2} \cdot X_{Al}^{M1} \cdot X_{Al}^{T} \cdot X_{Si}^{T} \right)^{cpx_{ss}} \cdot \overline{\gamma}_{cats}^{cpx}$$

Table 9.8 End-members and structural sites in fassaite.

End member\Site	M2	M1	T	Oxygen
Diopside (di)	Ca	Mg	Si Si	O_6
Hedenbergite (hed)	Ca	Fe^{2+}	Si Si	O_6
Ca-Tshermaks (cats)	Ca	Al	Al Si	O_6
Enstatite (en)	Mg	Mg	Si Si	O_6

Due to high $\frac{Mg}{Mg + Fe^{2+}}$, the fassaite approximates to a di-cats binary solid solution.

1100°C data: $\bar{\gamma}_{cats}$ in $di_{70}\ cats_{30} = 1.86$

$di_{63}\ cats_{37} = 1.5$ (Wood, 1979, see Figure 9.14)

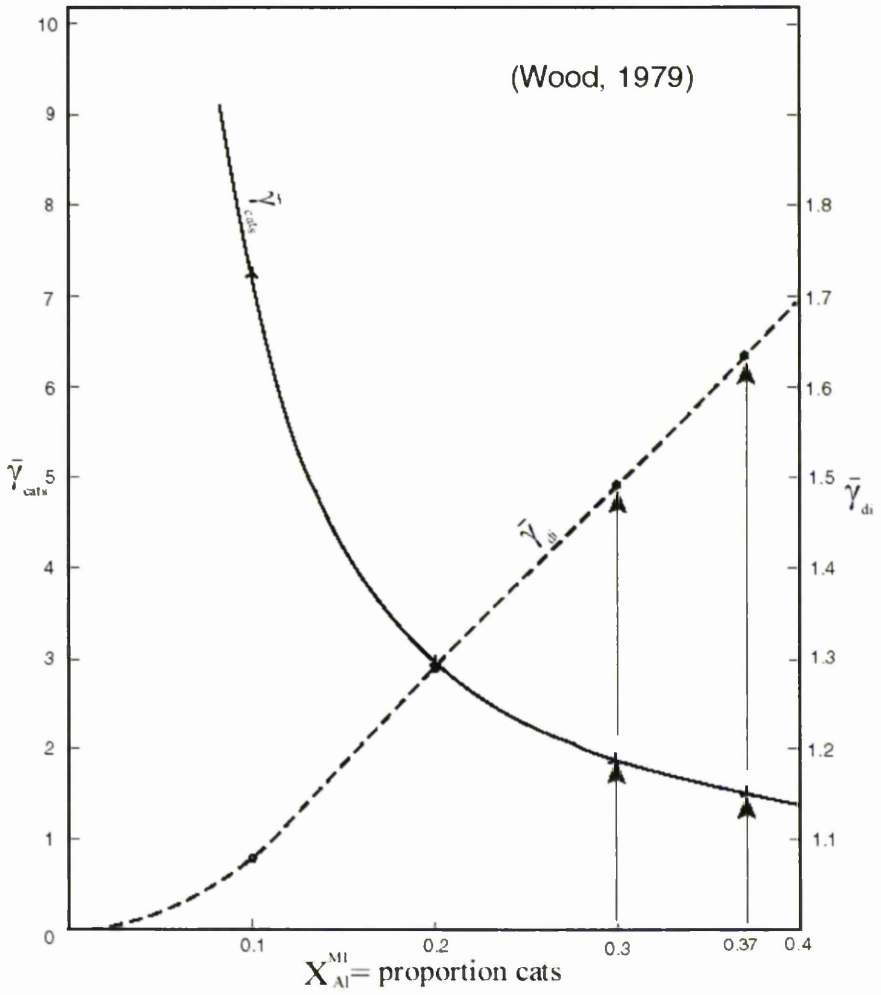

Figure 9.14 Graph for estimation the activity coefficients of cats and diopside.

Table 9.9 Activities of cats end-member in fassaite.

Analysis No\Activity	$a_{cats}^{cpx} = 4 \cdot \left(X_{Ca}^{M2} \cdot X_{Al}^{M1} \cdot X_{Al}^{T} \cdot X_{Si}^{T}\right)^{impure\ cpx_{ss}} \cdot 1.86$	
BREP43-FS1	7.44x0.844x0.296x0.155x0.845	0.243
BREP43-FS2	7.44x0.839x0.299x0.156x0.844	0.246
BREP43-FS3	7.44x0.849x0.300x0.158x0.842	0.252
Average		**0.247**
BRJ-FS1	6.0x0.869x0.363x0.146x0.854	0.235
BRJ-FS2	6.0x0.859x0.367x0.142x0.858	0.230
BRJ-FS3	6.0x0.867x0.381x0.150x0.850	0.253
Average		**0.240**

Reaction **Diopside** + 2**Corundum** = *Anorthite* + *Spinel* .....4)

$$a_{di}^{cpx} = \overline{X}_{di} \cdot \overline{\gamma}_{di}$$

$$\overline{X}_{di}^{cpx} = X_{Ca}^{M2} \cdot X_{Mg}^{M1} \cdot \left(X_{Si}^{T}\right)^2$$

$\overline{\gamma}_{di}^{cpx}$ in $di_{70}\ cats_{30} = 1.49$

$di_{63}\ cats_{37} = 1.63$ (1100°C data, Wood (1979), see graph in Figure 9.14).

Table 9.10 Activities of diopside end-member in fassaite.

Analysis No\Activity	$a_{di}^{cpx} = X_{Ca}^{M2} \cdot X_{Mg}^{M1} \cdot \left(X_{Si}^{T}\right)^2 \cdot 1.49$	
BREP43-FS1	$0.844 \times 0.579 \times 0.845^2 \times 1.49$	0.520
BREP43-FS2	$0.839 \times 0.572 \times 0.844^2 \times 1.49$	0.510
BREP43-FS3	$0.849 \times 0.579 \times 0.842^2 \times 1.49$	0.518
Average		**0.516**
BRJ-FS1	$0.869 \times 0.535 \times 0.854^2 \times 1.63$	0.552
BRJ-FS2	$0.859 \times 0.526 \times 0.858^2 \times 1.63$	0.542
BRJ-FS3	$0.867 \times 0.518 \times 0.850^2 \times 1.63$	0.529
Average		**0.541**

2.2) Enstatite, assume non-ideal mixing (Carlson and Lindsley, 1988).

$$a_{en}^{cpx} = X_{Mg}^{M2} \cdot \gamma_{Mg}^{M2} \cdot X_{Mg}^{M1} \cdot \left(X_{Si}^{T}\right)^2$$

$$\gamma_{Mg}^{M2} = \gamma_1$$

$$\gamma_{Mg}^{M2} = \exp\left[\frac{(X_2)^2[W_{G1} + 2(W_{G2} - W_{G1})X_1]}{RT}\right]$$

$$G_{XS}^{cpx} = \left(W_{U1}^{cpx} + PW_{V1}^{cpx} - TW_{S1}^{cpx}\right)\cdot\left(X_1^{cpx}\right)\cdot\left(X_2^{cpx}\right)^2 + \left(W_{U2}^{cpx} + PW_{V2}^{cpx} - TW_{S2}^{cpx}\right)\cdot\left(X_2^{cpx}\right)\cdot\left(X_1^{cpx}\right)^2$$

$$W_{G1} = W_{U1} + PW_{V1} - TW_{S1}$$
$$W_{G2} = W_{U2} + PW_{V2} - TW_{S2}$$

1 = $Mg_2Si_2O_6$ component
2 = $CaMgSi_2O_6$ component

$$\mu_1^i = \mu_1^0 + RT\ln X_1^{di}\cdot\gamma_1^{di}$$
$$G_{XS}^{cpx} = W_{G1}^{cpx}\left(X_1^{cpx}\right)\cdot\left(X_2^{cpx}\right)^2 + W_{G2}^{cpx}\cdot\left(X_2^{cpx}\right)\cdot\left(X_1^{cpx}\right)^2$$

$$RT\ln\gamma_1^{di} = (X_2)^2[W_{G1} + 2(W_{G2} - W_{G1})X_1]$$

$$X_1 = \left(\frac{X_{Mg}^{M2}}{X_{Mg}^{M2} + X_{Ca}^{M2}}\right) \qquad X_2 = \left[\frac{X_{Ca}^{M2}}{X_{Mg}^{M2} + X_{Ca}^{M2}}\right]$$

At 1273°K (1000°C), 10 kbar (T in K, P in kbar)

$$W_{G1} = W_{U1} + PW_{V1} - TW_{S1}$$
= 26.23+(10x-0.02229)-(1273x0)
=26.007 $kJmol^{-1}$

$$W_{G2} = W_{U2} + PW_{V2} - TW_{S2}$$
= 32.44+(10x-0.08646)-(1273x0)
= 31.575 $kJmol^{-1}$

$$\gamma_{Mg}^{M2} = \exp\left(\frac{(X_2)^2[26.007 + 2(31.575 - 26.007)X_1]}{0.0083143x1273}\right)$$

Table 9.11 Activities of enstatite end-member in fassaite

Analysis No\Activity	$a_{en}^{cpx} = X_{Mg}^{M2}\cdot\gamma_{Mg}^{M2}\cdot X_{Mg}^{M1}\cdot\left(X_{Si}^{T}\right)^2$	
BREP43-FS1	0.043x9.67x0.579x0.846^2	0.174
BREP43-FS2	0.047x9.51x0.572x0.845^2	0.183
BREP43-FS3	0.042x9.73x0.579x0.842^2	0.168
Average		**0.175**
BRJ-FS1	0.033x10.12x0.535x0.854^2	0.132
BRJ-FS2	0.043x9.73x0.526x0.858^2	0.161
BRJ-FS3	0.034x10.10x0.518x0.850^2	0.128
Average		**0.140**

Table 9.12 Activities of all components in the reactions 3) and 4) of fassaite inclusions were used to obtain the P-T coordinates of the equilibrium from THERMOCALC.

Component\Sample	BREP43	BRJ
Corundum (cor)	1	1
Diopside (di)	0.516	0.541
Ca-Tschermaks (cats)	0.247	0.240
Enstatite (en)	0.175	0.140

3) The Garnet+Corundum assemblage

Reactions: *3Ca-Tschermaks* = **Grossular** + 2**Corundum**.....5)

2**Corundum** + *3Enstatite* = 2**Pyrope**.....6)

As with reactions 1 and 2, these two reactions can only be used as stability limits, as a full set of end-members is only present for one side of the reaction in each case. As before, the activities of the absent end-members Ca-Tschermaks, and enstatite are set to 1.0. Corundum, being virtually pure, has an activity of 1.0. Activities for garnet inclusions were calculated using the formula of Berman (1990). The equations are too complicated to be shown here. The calculation was established by the computer program ACTIV developed by Dr GTR Droop (pers. comm.).

The compositions of garnet inclusions in Appendix 9-1 were used for the activity computation at a temperature of 1000°C. The results are given in Table 9.13.

Table 9.13 Activities for garnet inclusions at 1000°C (Berman, 1990).

Analysis No	CORXXI-BREP45-GRT1	BREP1				
		GRT1	GRT2	GRT3	GRT4	Average (n=4)
$a_{Grossular}$	0.058810	0.053594	0.055002	0.053478	0.055198	0.0543
a_{Pyrope}	0.309963	0.407626	0.418476	0.406272	0.438656	0.4178
$a_{Almandine}$	0.003867	0.001443	0.001698	0.001331	0.000760	0.0013

Note: Activities in shaded cells were used for THERMOCALC.

4) Summary

Table 9.14 shows pressure (range from 1-50 kbar) and temperature (°C) values obtained by running THERMOCALC v2.75, displayed according to the minerals coexisting with corundum and corresponding reactions.

Table 9.14 Pressures and temperatures obtained by the THERMOCALC for plotting on the P-T graph.

Mineral inclusion or coexisting Mineral		Sapphirine		Fassaite				garnet			
Reaction No		1	2	3		4		5		6	
Reaction		4cor+ 2py+ 6sp = 3spr4	4sp + 2ky = spr4 + 2cor	2cats + en = 2cor + 2di		di + 2cor = an + sp		3cats = gr+2cor		2cor + 3en = 2py	
Sample No, Number of analysis		NWEP9 &11, n=7	NWEP9 ,11, n=7	BREP4 3, n=3	BRJ, n=3	BREP4 3, n=3	BRJ, n=3	BREP 45, n=1	BREP1, n=4	BREP 45, n=1	BREP1, n=4
Calculated activity		0.513 (spr4)	0.513 (spr4)	0.247 (cats), 0.175 (en), 0.516 (di)	0.240 (cats), 0.140 (en), 0.541 (di)	0.516 (di)	0.541 (di)	0.0588 (gr)	0.0543 (gr)	0.3099 (py)	0.4178 (py)
PRESSURE (1-50 kbar)	1					395	387	1554	1579	730	859
	2		166	812	749						
	3							1617	1643		
	5	117						1679	1705		
	6					728	717			591	692
	7							1740	1768		
	8		195								
	9							1801	1830		
	10	271									
	11					1035	1021	1862	1891	464	545
	12			915	849						
	13							1922	1952		
	14		222								
	15	455						1981			
	16					1317	1301			348	413
	20	674	247								
	21					1578	1560			240	291
	22			1006	937						
	25	936									
	26		269			1818	1799			136	177
	30	1255				1997	1977			55	88
	32		288	1085	1014						
	35	1684									
	38		304								
	40			1141	1069						
	44		317								
	50		327								
Standard dev. for T		136	24	82	76	27	24	116	123	30	37
Standard dev. for P		2.4	6.9	9.7	9.3	0.5	0.46	3.8	4	1.4	1.5

9.5.2 Pressure-temperature limits from sapphirine, fassaite, garnet and sanidine in corundum

Pressures and temperatures from THERMOCALC for corundum + sapphirine, corundum + fassaite and corundum + garnet assemblages are plotted on a P-T graph in Figure 9.15 together with the temperature limits of alkali feldspar and spinel solid solution inclusions (from section 9.4). The graph indicates that the ruby samples from Bo Na Wong, and Bo Rai crystallized at pressures between 4-30 kbar (14 – 105 km depth) and temperatures between 700 - 1150°C, i.e. in either the eclogite or granulite facies. Sapphires from Den Chai crystallized under higher temperature (>1000°C, known previously from Figure 9.10). If the minimum temperature limit of sanidine in sample DCEP16 (from Figure 9.10) is plotted on Figure 9.15, then it makes the P-T field of corundum crystallization narrower. It implies that corundum from Thailand crystallized under high-pressure granulite-facies or eclogite-facies conditions, 13-30 kbar and 1000 – 1150°C. The pressure corresponds to a depth range of 46-105 km which implies crystallization either at the base of a very thick continental crust or within the upper mantle. This must be on the assumption that all Thai corundums originated in the same environments.

If, on the other hand, the sapphires formed in a different environment from the rubies (as argued by Sutherland and Schwarz, 1997 and Sutherland, 1998) then it is not valid to amalgamate the P-T estimates. From Figure 9.12, the spinel inclusion from Bang Kacha indicates the minimum temperature of crystallization of corundum of >860°C which is lower than those of corundum from Den Chai (>1000°C). Nevertheless the depth or pressure cannot be indicated for the sapphire formation in this study.

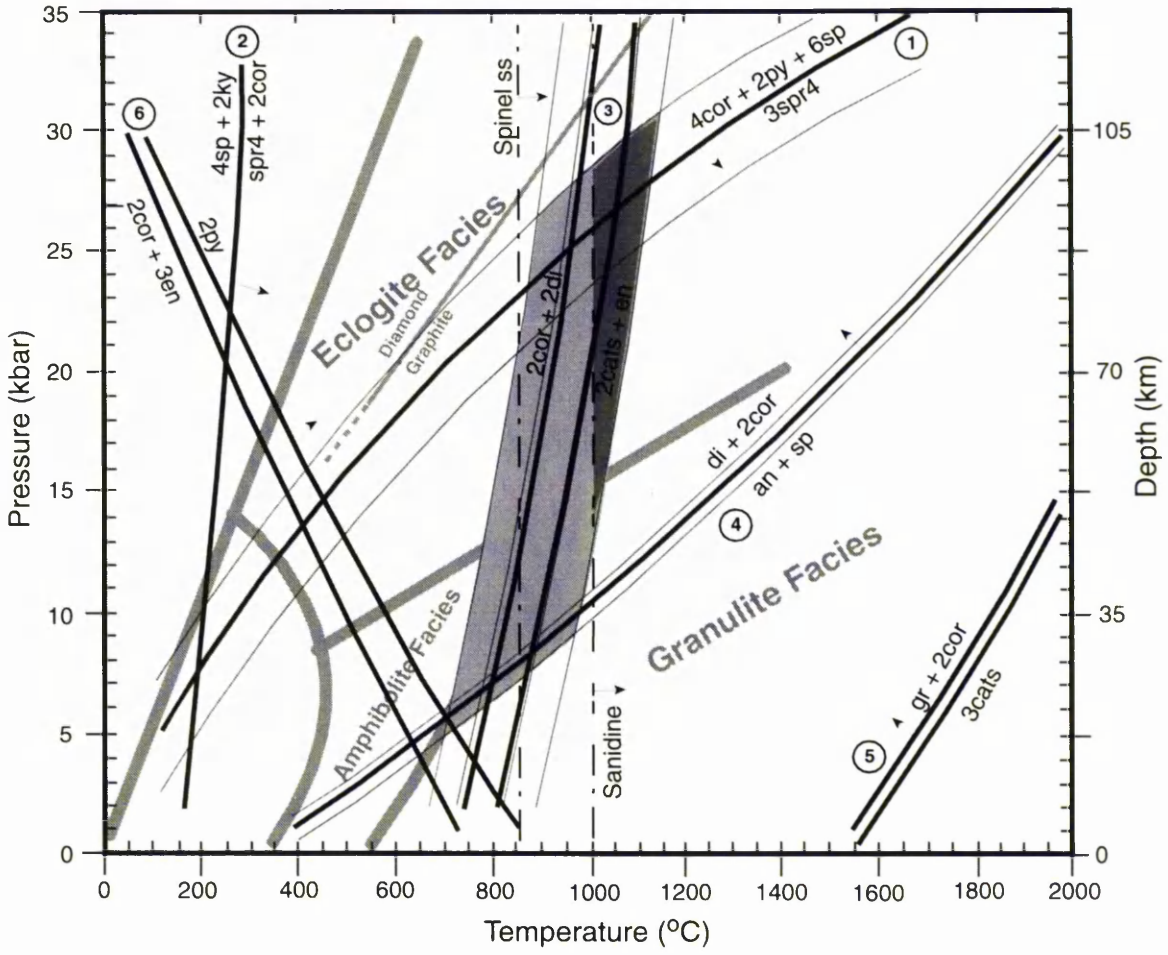

Figure 9.15 Pressure-temperature diagram showing the results of geothermometry and geobarometry for corundums from Thailand and their mineral inclusions. The whole shaded area indicates the P-T conditions for ruby crystallization as derived from inclusions associated with rubies only. When the temperature from sanidine inclusion in sapphire (DCEP 16) is included (dashes), the P-T limit is restricted to the darker shaded area at the upper right corner. Note, the thinner lines represent the limits of uncertainty (±1 standard deviation); number in a circle is an equation number.

CHAPTER 10
DISCUSSION AND RECOMMENDATION

The main aim of this thesis is to establish the origin of gem corundum associated with alkali basalt from Thailand. The strategy employed was to study the whole rock petrography, geochemistry and mineral chemistry of the alkali basalts, and the mineralogy and gemmology of gem corundums in terms of their placer deposit, surface features, cathodoluminescent characteristics, spectroscopy, trace element geochemistry and mineral inclusions. This chapter will discuss the characteristics of corundum followed by constraints on the origin of corundum and finally recommendations for future work will be made.

10.1 Characteristics of corundums from Thailand

Occurrences, surface features, cathodoluminescence and spectroscopy

A study of the Thai corundum occurrences has found that corundums embedded in basalt are very rare. This indicates that the ratio between the ore to the rock mass is extremely low. Corundums are commonly found in secondary deposits (alluvium, elluvial, residual-soil and colluvium deposits as well as stream sediments) with the thickness of the gem-bearing layer varying from 0 - 5 m and the thickness of the overburden ranging up to 15 m.

A study of surface features of corundums under a scanning electron microscope has been made. Triangular etch features, hillocks and randomly oriented needle-like patterns reveal that Thai corundums interacted with the magma while they were ascending to the Earth's surface. This information supports the view that the corundum samples recovered from the secondary deposits were derived from the alkali basalts. The results confirm previous work, for example Coenraads (1992) and Krzemnicki *et al.* (1996), except that the spongy appearance caused by magma etching reported by these authors has not been found in this study. The clay mineral and quartz deposited on the spongy surfaces of some corundums also reveal that these corundum grains experienced chemical weathering or reacted with the soil solution while they were in the alluvium.

Cathodoluminescence study indicates that Thai blue sapphires, having yellow or green colour tints, exhibit dull blue luminescence. Blue to dark blue domains in the samples

or blue sapphires containing Fe^{2+} show non-luminescence. The yellow sapphire sample (NYEP24) shows yellow-green luminescence, which has not been explained in any literature. The bright red luminescence in corundum reflects a high Cr^{3+} content that is always exhibited by the ruby, pink, violet and purple sapphires. Certain rubies may exhibit dull red because of the quencher Fe. For example, ruby sample Δ793 from South India contains Cr_2O_3 up to 1.47 wt% and Fe_2O_3 of 0.52 wt% and shows dull red, incontrast to the bright red luminescence of sample BREP22 from Bo Rai which contains 0.21 wt% Cr_2O_3 and 0.62 wt% Fe_2O_3. The ratio between the amount of activator to quencher in corundum is still unclear.

Spectroscopy was used to investigate the characteristics of Thai corundum samples and corundum from other sources. Optical spectroscopy (UV-visible) can be used to investigate the transition metals in the structure of corundum and help distinguish the Thai samples from the corundums from other origins such as Verneuil synthetic corundum.

Using the UV-visible spectra Thai corundums can be divided into two groups. ***The first group*** includes green-blue sapphires (including colour notations of very slightly greenish Blue, very strongly greenish Blue, greenish Blue, bluish Green, Green-Blue and Green), which shows absorption spectra of the crystal field transition (d-d) for Fe^{3+} between 330 nm and 450 nm. The broad absorption bands of the intervalence charge transfer (IVCT) for Fe^{2+}/Ti^{4+} appear between 500 nm and 650 nm. The band of Fe^{2+}/Fe^{3+} IVCT is centred between 840 nm and 900 nm.

A pale blue sapphire sample from Sri Lanka (CLA) in this study does not show the band of Fe^{2+}/Fe^{3+}, which is characteristic of most sapphires from metamorphic origin (Kashmir, India; Mogok, Myamar; Umba Valley, Tanzania) reported by Schmetzer and Kiefert (1990). An exception is for blue sapphires from Andranondambo, Madagascar (skarn type) which shows an Fe^{2+}/Fe^{3+} band (Schwarz *et al.*, 1996). On the other hand, sapphires derived from alkali basalt, including sapphires from Thailand, Viet Nam and Nigeria in this study show an Fe^{2+}/Fe^{3+} band (Schmetzer and Kiefert, 1990).

The ***second group*** includes corundums that warrant the name *ruby,* i.e. corundum samples with Violet, Purple, reddish Purple, bluish Purple, bluish Violet colours. The samples in this group dominantly exhibit a d-d band for Cr^{3+} (centred at ca 550 nm).

The band of 350 nm – 450 nm as seen in synthetic Verneuil ruby is not found although the right shoulder of this band is found in the natural samples. This is due to Fe impurity in natural samples causing the band to be superimposed by the peaks of d-d for Fe^{3+}. There are also weak peaks at 665±1 nm and 692/693 nm. Some samples show the fluorescent line at 664/665 nm (e-ray).

Thai rubies contain certain amounts of Fe_2O_3 (e.g. up to 0.88 wt% in sample from Bo Rai). This is indicated by the noise that interferes with the spectrum for the d-d of Cr^{3+} between 350 nm and 450 nm, compared to a smooth band for a synthetic ruby doped with 0.47% Cr only, or for a ruby from Mong Hsu, Myanmar containing up to 1.70 wt% Cr_2O_3 and 0 wt% Fe_2O_3. The Fe content causes Thai rubies to display a pink or purple tint, which is not regarded as a very good colour for ruby. This can be observed clearly by the spectrum of the d-d for Fe^{3+} as mentioned above. Moreover, the violet and purple sapphires (e.g. BRD, NBC, Figure 6.12, B & D) containing much higher Fe contents will show more pronounced Fe^{3+} peak (ca 450 nm).

The Fe^{2+}/Fe^{3+} band for the o-ray in synthetic blue sapphire is absent and the d-d for Fe^{3+} is not prominent. Synthetic rubies including purple Red, Purple-Red, Red samples show spectra typical of ruby (bands and peaks for Cr^{3+}) except for the synthetic violet (mauve) sample which shows narrower bands. Synthetic orangy Yellow sapphire exhibits d-d peaks for Fe^{3+} and for Cr^{3+}.

The spectroscopy results could possibly be used to characterize corundums from different geological environments as well as distinguish the natural from synthetic corundums.

10.2 Constraints on the origin of corundums in association with alkali basalt

Tectonic models for basalt origin in Thailand and Southeast Asia

Thai corundums occur in two microcontinental plates, the Shan-Thai (Sibumasu) and Indochina blocks (Figures 1.2 and 2.1). These plates separated from Gondwanaland in the southern hemisphere during the Middle or Late Palaeozoic in the case of the Shan-Thai terrain (Hutchison, 1989) and the Early Carboniferous in the case of the Indochina terrain (Metcalfe, 1988; Bunopas and Vella, 1992); they are composed of high-grade Precambrian metamorphic rocks (gneiss, quartzite, marble and micaschist).

The alkali basaltic magma ascended to the Earth's surface very rapidly, as indicated by the fact that the basalts contain abundant mantle xenocrysts and xenoliths. The ages of the alkali-basalt host rocks are young and the eruptions were restricted to a short period of the geological time scale (0.44 to 11 Ma: Pleistocene to Miocene). This episode took place after the Shan-Thai and Indochina blocks were amalgamated (Late Triassic). The origin of the alkali basalts in Thailand and Southeast Asia is not as clear. They may be: i) related to crustal thinning and mantle upwelling in a nearby area (China basin in the Late Mesozoic-Cenozoic) (Barr and Macdonald, 1979; Isayev and Kkhoan, 1976), ii) rift-related (developed in the Oligocene: 23 – 36 Ma) (Mukasa *et al.*, 1994; Cole and Crittenden, 1997), iii) Sunda subduction-related (Middle Eocene: 42 - 46 Ma to Recent) (Gordon and Jurdy, 1986; Polachan *et al.*, 1991), or iv) related to northwestward migration of the lithosphere over an underlying hot spot or mantle plume (Michell and Garson, 1981). In model number iii), it is difficult to accept that the subduction zone can be responsible for volcanism 1000 km behind the active calc-alkaline volcanism, although this might be a factor in occurrences of alkaline basalt in Malaysia (Barr and MacDonald, 1978). The last model is probably impossible, as there is no evidence of an age series for the basalts running through the northwest to southeast of Thailand.

The two models that are more consistent and extensively referred to are the crustal-thinning and mantle-upwelling model and the rift-related model. The crustal-thinning and mantle-upwelling model (Barr and Macdonald, 1979; Isayev and Kkhoan, 1976) initiated with the migration of Southeast Asia towards the South-Southeast (Rodolfo, 1969). Part of this migration is revealed by the development of marginal basins, mainly in the eastern half of the region. The China basin, for example, was opened by north-south extension in either the Late Jurassic to Early Cretaceous or Late Cretaceous to Early/Middle Tertiary (Ben-Avraham and Uyeda, 1973). Lithospheric thinning must have been involved and it affected the Indochinese peninsula to the west. The effects include block faulting and alkalic magmatism. On the basis of gravity data, Isayev and Kkhoan (1976) described two downwarps (Hanoi Downwarp and Maekhong Downwarp) as examples of the crustal thinning and the crustal thickness apparently decreases from 35-40 km to 30-35 km. The Hanoi Downwarp was formed at least as early as Palaeocene and has undergone continuous sinking to the present time.

In the rift-related model (eg. McCabe, *et al.*, 1988; Polachan *et al.*, 1991; Bunopas and Vella, 1992), rifting is initiated from the collision of the Indian and Eurasian plates at 50

– 43.5 Ma (Eocene) (Longsley, 1997), causing clockwise rotation of Southeast Asia and movements on the strike-slip faults resulting in formation of associated Cenozoic basins in this region. The north-south trending normal faults (nearly parallel to the Sunda trench) were developed. The clockwise rotation of the Southeast Asia stopped, causing this region to relax and extensional faulting to commence. The small but widespread field of late Tertiary basalts in Thailand and Indochina probably indicates the climax of the extensional faulting.

The crustal-thinning and mantle-upwelling model and the rift-related model are likely to be the same. In general rifting is always associated with the crustal thinning because the crust is pulled apart and the asthenosphere upwells (e.g. Moores and Twiss, 1995: 93).

Charateristics of basalt host rocks of corundums

The characteristics of the alkali basalts in this study show that they originated in a within-plate setting from the upper mantle beneath the Shan-Thai and Indochina continent blocks. The basalt samples can be classified into two groups: xenocryst- and xenolith- free basalts (include Sop Prap, Khok Samran and Nam Yun basalts) and xenocryst- and xenolith- bearing basalts (include Ckiang Khong, Ban Nong Nam Cho, Den Chai, Bo Phloi, Nam Yun, Bang Kacha, Tok Phrom and Nong Bon basalts).

The xenocryst- and xenolith- free basalts have a relatively low temperature of crystallization indicated, for example, from the plot of 1Ti:2Al in clinopyroxene (Figure 3.5). This suggests that they came from a shallower level than the other group. They also crystallized from more evolved magmas, which is indicated by the samples containing lower alkalis, higher silica contents (Figure 2.23) and lower MgO contents (Figure 2.25). This group is not regarded as the host of corundum but it occurs in the same place as the corundum-bearing basalt outcrops. The latters were probably completely removed by weathering a long time ago.

The second basalt group (xenocryst- and xenolith- bearing basalts) crystallized from more primitive magmas than those of the first group. This group contains higher alkali and lower silica contents (Figure 2.23) and higher MgO contents (Figure 2.25). It came from a relatively deep level and crystallized under higher temperatures than the first group, suggested by the crystallization of clinopyroxene (Figure 3.5). The magmas of this group ascended to the Earth's surface rapidly from depths greater than 80 km and

picked up the mantle xenocrysts and xenoliths which originated at the depth of ca 40 to 80 km (Sutthirat *et al.*, 1999). The xenocrysts are for example nepheline, garnet, clinopyroxene, spinel, olivine, apatite, amphibole, feldspar etc. The xenoliths are for example ultramafic nodules, quartzite, gabbro, feldspathic aggregate etc. Basalts in this group also picked up and carried the corundum xenocrysts to the Earth's surface. The corundum xenocrysts originated between 46 and 105 km depth beneath Thailand; this will be discussed later.

Origin of corundums

Several models for the origin of the corundum in basaltic terrains have been generated. Most models involve plutonic crystallization from melt, although regional metamorphism of Al-rich rocks subducted below the continental crust has been proposed by Levinson and Cook (1994). This model has the argument as mentioned above that the subduction zone (Sunda trench, west of Myanmar and Indonesia) is too far away (>1000 km) from the basalt outcrops. Corundum-bearing basalts also occur in Cambodia, Viet Nam and China, having a similar age range as in Thailand. They do not seem to be related to a subduction zone. Several models invoke alkaline Si- and Al-rich melts, either evolved from basaltic magmas (Coenraads *et al.*, 1990; Coenraads, 1992a) or derived from melting of amphibolitised mantle (Sutherland, 1996). A more complex melt origin was proposed by Guo *et al.* (1996a), who claimed that mineral inclusions in the corundums reflect the reaction between Si-rich and carbonatitic magmas under relatively low temperatures around 400°C at mid-crustal levels around 10-20 km. This model is consistent only with the origin of sapphires but rubies are not clearly explained by this model. Sutherland *et al.* (1998a) proposed the means of generating basaltic-type gem corundum and favour melting of mantle source-rocks containing amphibole at depths of 35-40 km near the crust-mantle boundary; such melting could produce a final Si- and Al- rich rock with over 5 wt% corundum. Moreover the different metamorphic or pegmatitic sources and assemblages (e.g. corundum-sapphirine-spinel assemblage) must exist under basaltic regions. Using trace-element and inclusion approaches, Sutherland *et al.* (1998b) and Sutherland (1998) classify corundum in basaltic terrains into metamorphic corundum (including ruby) and basaltic-type (including blue, green, yellow, brown, white, grey, opaque and black corundums). These models still need more explanation and research. Most of the models explained only the genesis of sapphires but rubies are not yet explained in detail.

The trace element variation diagram using data from this study (Figure 10.1, B) shows that Thai corundums have a bimodal distribution based on the Cr and Ga contents. The ruby, purple and pink samples (simply called rubies) contain high chromium (up to 0.57 wt% Cr_2O_3 but low gallium (<0.01 wt% Ga_2O_3). The samples with blue, green, brown and violet colours (simply called sapphires) contain high gallium (up to 0.10 wt% Ga_2O_3) but low chromium (<0.05 wt% Cr_2O_3). This evidence agrees well with the results obtained by Sutherland *et al.* (1998b) who designated the ruby group as having a metamorphic origin and the sapphire group as having an igneous origin. Thus the origin of sapphires and rubies in Thailand should be discussed separately.

1) Sapphire genesis

Both Ga and Cr substitute readily for Al in corundum, which can be explained by the simple rules of similar ionic charge and radius (Ga^{3+} = 0.620 Å, Cr^{3+} = 0.615 Å and Al^{3+} = 0.535 Å; 6-coordinate). Moreover Ga has chemical properties similar to Al and it is always present with Al. Ga is enriched in felsic and intermediate rocks, whereas Cr is enriched in ultramafic and mafic rocks (Krauskopf and Bird, 1995: 542-545).

Figure 10.1 shows that the plots of Thai sapphire samples superimpose on the fields of corundums in syenitic gneiss from Bancroft (field 4), in pegmatitic plumasite from Natal (field 1), in Al, Mg-pelite from Baffin Island and Limpopo (part of field 6). An aggregate (corundum + sillimanite + minor zircon + trace hercynite) of a high-grade metamorphic rock found in alluvium of a corundum mine in Bo Phloi is believed to be derived from the same source of corundums brought to the Earth's surface by alkali basalt (Pisutha-Arnond, *et al.*, 1999). Hercynite is also found as the inclusions in sapphires of this study. If this is true then the crystallization of sapphires from Thailand in magma of pegmatitic plumasite or directly from the magma will be ruled out. A metamorphic related origin is more likely.

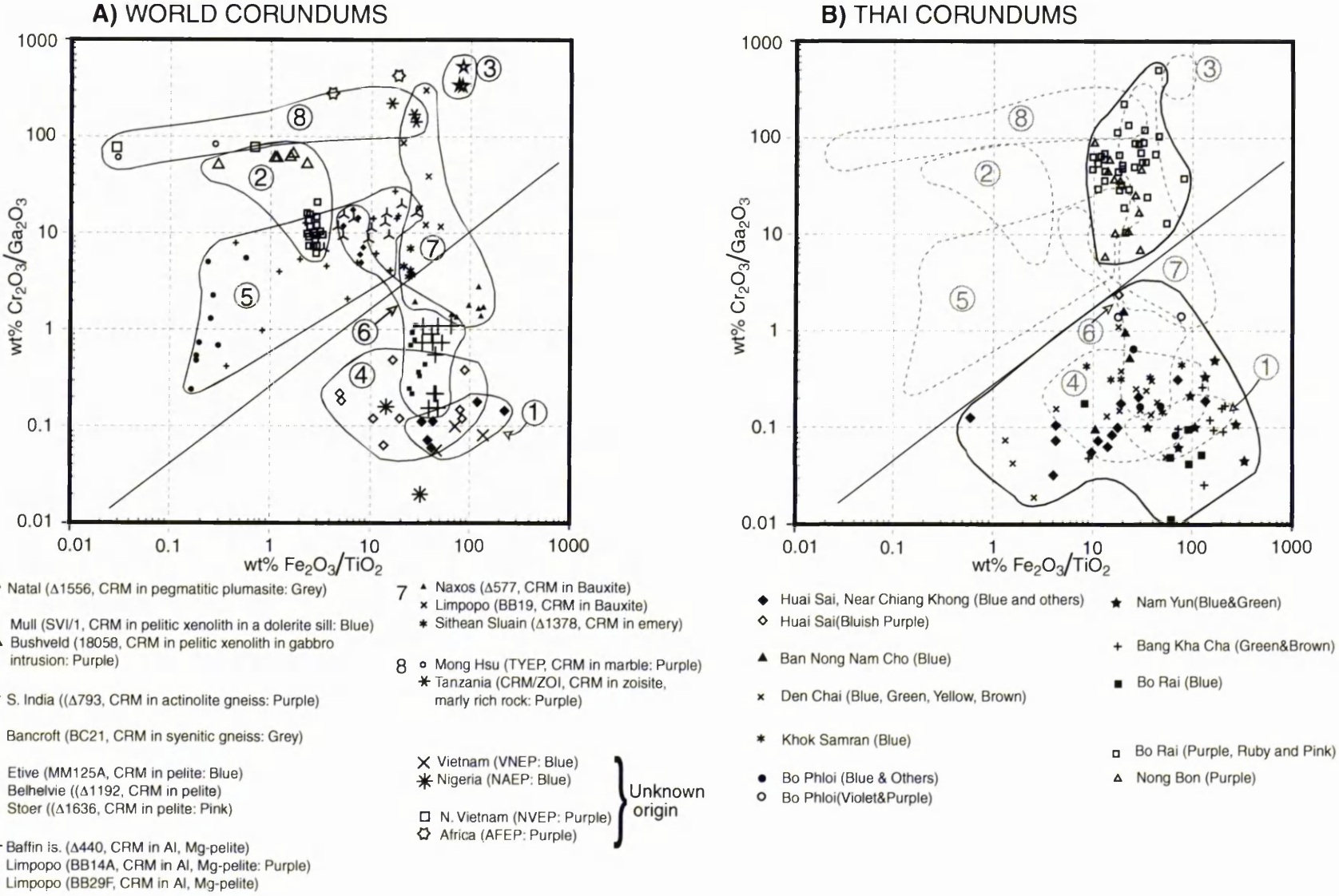

Figure 10.1 A) Plot of wt% Cr_2O_3/Ga_2O_3 against wt% Fe_2O_3/TiO_2 for the world corundums, well characterized corundums which are categorized into 8 groups. **B)** Plot of Thai corundums on the similar axes of A) in order to compare with the well characterized origin of the world corundums in A). Thai corundums can be categorized into two groups: group I), high Cr and low Ga contents (ruby) and group II), high Ga and low Cr contents (mainly blue sapphires and other colours).

However the study of fluid inclusions in sapphires from Bo Phloi (Srithai and Rankin, 1999) suggested a magmatic source. Moreover the U-Pb dating of zircon inclusions in sapphires from New South Wales and a zircon associated with sapphire from Chanthaburi (Coenraads *et al.*, 1990; Coenraads *et al.*, 1995) suggested sapphires that have a genetic link to alkali basalt. Guo *et al.* (1996) suggested that at the high temperatures of basaltic magmas, the U-Pb in zircons can be reset within the time of the magma's eruption and cooling due to Pb diffusion so that the results could then give the same age as the basalt and not the true age of sapphire. In any case, failed experimental attempts to grow corundum from a corundum-bearing basaltic composition under different pressure, temperature and hydrous conditions have been reported (e.g. Green *et al.*, 1978). The surface features of sapphires in this study indicate that the sapphires were not in equilibrium with the magma of basalt host rock. Sapphires crystallized elsewhere and the alkali basaltic magma picked them up and carried them to the Earth's surface.

In Figure 10.1, Thai sapphires plot mostly in the field of syenitic gneiss from Bancroft. The pre-existing rock of the corundum-bearing syenitic gneiss from Bancroft is the Precambrian dark paragneiss of the Grenville series (Gummer, 1946). According to Gummer (1946) and Moyd (1949), emanated hydrothermal materials are more likely to have been released from alkaline magmas into the dark paragneiss, converting this into a nepheline-corundum syenitic gneiss. The emanations lost some silica but gained carbon dioxide. The emanations, thus enriched in alumina and alkalis, continued to react with the dark gneisses, converting calcic feldspar to alkali feldspar and nepheline. By analogy to the syenitic gneiss of the Bancroft area, Canada, Thai sapphires could have originated from Precambrian paragneiss that experienced metasomatism by emanations from felsic magma (enriched in gallium and incompatible elements) or carbonatite (enriched in Nb-Ta) at deep levels beneath Thailand. Note that the main source of Nb-Ta is granitic pegmatites, carbonatite or peralkaline granite (Möller *et al*, 1989). In this case the carbonatite magma might have intruded the gneiss source rock and created the high alkali rock called fenite (syenitic composition). In addition to Bancroft, another corundum-bearing fenite has been reported from the Khibina alkaline complex, Russia (Barkov *et al.*, 1997; Barkov *et al.*, 2000). However, as Thai sapphires occur over extensive areas throughout the country, any such process or metasomatism should have taken place over a large area and perhaps not at a single intrusive complex. The process introduced in this study is slightly different from Guo *et al.* (1996a) who

said that the carbonatite reacted with the pegmatitic magma giving corundum-bearing lens in the mid-crustal levels.

The abundances of Ga, Ti and Fe, incompatible elements (e.g. Ta, Nb, Sn) and mineral inclusions in sapphires (zircon, alkali feldspar, nepheline and spinel) suggest that the sapphires might have formed in a highly evolved melt of peralkaline syenitic or granitic composition. This agrees well with the studies of some authors e.g. Aspen *et al.*, (1990) and Upton *et al.* (1999) but it is different from those of Sutherland *et al.* (1998a) who maintain that sapphires crystallized when amphibole-bearing mantle underwent partial melting because of an advancing thermal aureole.

Nb, Ta and Sn could possibly have been carried to the country rocks by the felsic or carbonatitic magma. Then the gneissic country rock was metamorphosed to the syenitic gneiss as in the Bancroft area. Nepheline is found as an inclusion in corundum and as xenocrysts in basalt from Bo Phloi of this study. This is consistent with their source being probably from the nepheline-corundum syenitic gneiss. The minimum temperatures of crystallization of sapphires obtained from a sanidine inclusion in corundum from Den Chai (Figure 9.10) and a spinel inclusion in corundum from Bang Kacha (Figure 9.12) are between 860 and 1000°C. Nevertheless, the pressure conditions for crystallization of sapphires in this study are still unclear but the sapphires may have crystallized in the lower crust where the gneissic rocks exist.

The lower crust beneath Thailand is thought to be composed of Precambrian-metamorphic granulite-facies rocks (Bunopas, 1992). The graph in Figure 9.1, B shows that the plots of sapphires also overlap the field of corundum from Al, Mg-rich pelites from Baffin Island, Canada and Limpopo, Zimbabwe. This suggests that the parent rocks could have been the Precambrian paragneiss of Thailand, which originated from the marine (flysch) sediments of a continental margin (of the Gonwanaland) and were deeply buried and metamorphosed (Bunopas, 1992).

2) Ruby genesis

The ruby group, including the red, pink and purple corundum is confined to the areas of Bo Rai and Nong Bon. They plot close to the field of corundum of bauxitic origin (e.g. BB19 from the Limpopo belt; field 7 in Figure 10.1). However not all analyses fall in this field; some analyses fall in the gap between field 8 (corundums in marble) and field

5 (corundums in normal pelitic rocks). This suggests that Thai rubies probably crystallized in a different environment from these rocks. Geothermometry and geobarometry of mineral inclusions and coexisting minerals (fassaite, sapphirine and garnet) with rubies from Bo Na Wong and Bo Rai (Figure 9.15) suggest the pressure and temperature of crystallization. Fassaite inclusions in Bo Rai rubies give the lower limit of pressure (4 kbar) and temperature (700°C). Assuming that all inclusions in rubies are crystallized in the same environment (as their localities are about 50 km far from each other), then sapphirine inclusions in Bo Na Wong rubies can give the upper limit of the pressure and temperature of crystallization. From the graph in Figure 9.15, it can be estimated that the range of crystallization pressures is between 4 and 30 kbar (14 – 105 km depth) and temperatures is between 700 and 1150°C for rubies in the eastern region of Thailand. The inclusion suite found in rubies also suggests that Thai rubies have a metamorphic origin (e.g. fassaite, Figure 9.8 and sapphirine, Figure 9.9); sapphirine analyses are plotted and match the sapphirines in granulite facies rocks. In general, corundum can crystallize in pelitic, mafic, calc-silicate and anorthositic grospyditic rocks but it can not crystallize with olivine.

The inclusions in ruby provide some clues as to the nature of the rocks in which the ruby originally crystallized. The samples show that some of the ruby-bearing source rocks contained fassaite, some contained pyropic garnet, and some contained sapphirine. An important issue is how many of these silicates coexisted with one another.

Although pyropic garnet, clinopyroxene and sapphire can each coexist with olivine, corundum apparently cannot. There are no records of corundum coexisting in stable equilibrium associated with olivine. The assemblage olivine + corundum is precluded in general by the stability of sapphirine, and also in the granulite facies by the coexistence of orthopyroxene + spinel and in the eclogite facies by the coexistence of garnet + spinel. A peridotitic source rock is thus ruled out. A high-grade pelitic or lateritic source rock, as advocated by Levinson and Cook (1995) and Barron *et al.* (1996), could have yielded the sapphirine + corundum assemblage, but is unlikely to have crystallized either clinopyroxene or a garnet as calcic as the ones observed.

The most likely candidate for a source rock (at least one containing clinopyroxene + garnet + ruby) is one of basic composition, i.e. a ruby-garnet-pyriclasite or ruby–garnet-

clinopyroxenite. Note that pyriclasite is a metamorphic rock containing mainly garnet, clinopyroxene and plagioclase. Garnet-clinopyroxenites containing minerals that correspond closely to those coexisting with ruby are known from localities outside Thailand (e.g. Bloxam and Allen, 1960; Lovering and White, 1969; Kornprobst *et al.*, 1990). That corundum can coexist with garnet + clinopyroxene at high pressure has been demonstrated experimentally by Boyd (1970) who showed that the grossular-pyrope join in the $CaSiO_3$-$MgSiO_3$-Al_2O_3 system is broken by clinopyroxene-corundum tie-lines at 30 kbar. Kornprobst *et al.* (1990) found ruby with 0.16 wt% Cr_2O_3 and 0.03 wt% TiO_2 (c.f. 0.028 – 0.564 wt% Cr_2O_3 and 0.007 - 0.073 wt% TiO_2 of this study) in the garnet – clinopyroxenite sheet associated with garnet-spinel-bearing peridotite at Beni Bousera, Morocco. They suggest that the rocks could have recrystallized from the anorthite –rich protoliths i.e. basaltic or gabbroic dykes intruding into the surrounding peridotite. This suggests that Thai rubies could have crystallized in a similar way in the peridotite zone of the upper mantle.

Sapphirine + clinopyroxene + garnet + plagioclase assemblages are known from high-pressure granulites of troctolitic composition in the Ivrea Zone, N. Italy (Lensch, 1971; Sills *et al.*, 1983), suggesting that sapphirine could have coexisted with garnet + clinopyroxene in a mafic source rock. Using thermobarometric data the limits on the depths at which ruby crystallized in its source rocks can be determined. Assuming that a lithostatic pressure of 1 kbar corresponds to a depth of 3.5 km (i.e. assuming an average overburden density of 2.9 g cm^{-3}), the data imply that the fassaite + sapphirine + garnet + ruby crystallised at a depth of between 21 and 105 km (6-30 kbar) and at the temperatures between 700 and 1150°C (Fig.9.15). This overlaps the pressures and temperatures of crystallization of the ruby + garnet + fassaite from Beni Bousera, Morocco between 10 and 25 kbar (35 and 88 km) and between 800 and 1350°C, (Kornprobst *et al.*, (1990).

The overall depth interval deduced for the ruby samples is consistent with crystallisation in either the lower part of a thicker-than-average crust or else in the lithospheric mantle. The fact that both peridotitic and feldspathic xenoliths are abundant in the alkali basalts implies that the rising magmas scavenged wall-rock fragments from both crust and mantle. The depth range deduced for the ruby-bearing samples is broadly compatible with the occurrence of spinel as the dominant aluminous phase in the associated peridotite xenoliths suggesting that the former were probably

sampled from mantle depths. In their study of spinel-lherzolite xenoliths in Thai alkali basalts, Promprated *et al.* (1999) were unable to constrain equilibration pressures tightly, but deduced temperatures of ca 1000 to 1130°C. Within error, these values agree with the temperature range deduced in this study, indicating that the latter could have crystallized in the same thermal regime as the spinel-lherzolites. Promprated *et al* (1999) argued that the spinel-lherzolites record P-T conditions that reflect the asthenospheric upwelling event responsible for the late-Cenozoic alkali basaltic volcanism.

3) A model for the origin of Thai corundum

In Thailand sapphires and rubies are always found in the same locality. Sapphires are dominant in the localities in western part of the country (Shan-Thai block) but rubies are dominant in the eastern part of the country (Indochina block). The proportional change from sapphires to ruby is apparent in Chanthaburi and Trat areas (Figure. 4.11, Table 4.1). This suggests that the source of corundum beneath Thailand produced both rubies and sapphires under 13-30 kbar (46-105 km) and 1000 – 1150°C of the eclogite-facies or high pressure granulite-facies conditions at the base of a very thick continental crust or within the upper mantle (Figure 9.15). Note that this range of P-T conditions is based on the stable condition of both sapphires and rubies. The fact that rubies are rich in chromium and poor in gallium suggests that they formed in a pre-existing metamorphic rock with mafic composition. The fact that sapphires are rich in Ga and high field strength elements and poor in Cr consistent with their formation in syenitic metamorphic rocks by the intrusion of highly evolved fractionated magma (such as carbonatitic magma) moving from the mantle to deep in the crust where it reacted with the host metamorphic rock. Cr is most sensitive to fractionation (Matzat and Shiraki, 1978) that it is used up by fractionation and so it is not available for reaction between magma and host rock at high levels. Ga in the fractionated magma and host rock is the source of gallium in sapphires.

A model to explain the origin of Thai corundum based on the information of this study, is given in Figure 10.2. In this model, the first stage of corundum formation (Figure 10.2, A) is the development of ruby in metamorphic rocks of mafic composition (ruby–garnet-clinopyroxenite or ruby-garnet-pyriclasite); the formation is probably due to a gabbro or basalt intruding into the peridotitic host rocks in the upper mantle. The age of ruby formed in this way is unknown. Sapphires then formed as a consequence of

intrusion of highly evolved magma into lower crustal rocks, probably Precambrian gneiss, to give nepheline syenite carbonatite and gabbro. This process was probably the consequence of tectonic rifting in the Thai region, which is known to have taken place in the middle Tertiary.

In the Neogene (Figure 10.2, B), alkali basalt diatremes formed due to the upwelling asthenosphere under Thailand during the crustal extension. This caused alkali basaltic magma to ascend to the Earth's surface very rapidly along the fractures in the crust. In this stage the magma in the conduits picked up the materials (corundum, xenocrysts and xenoliths) which were encountered on the way up to the surface.

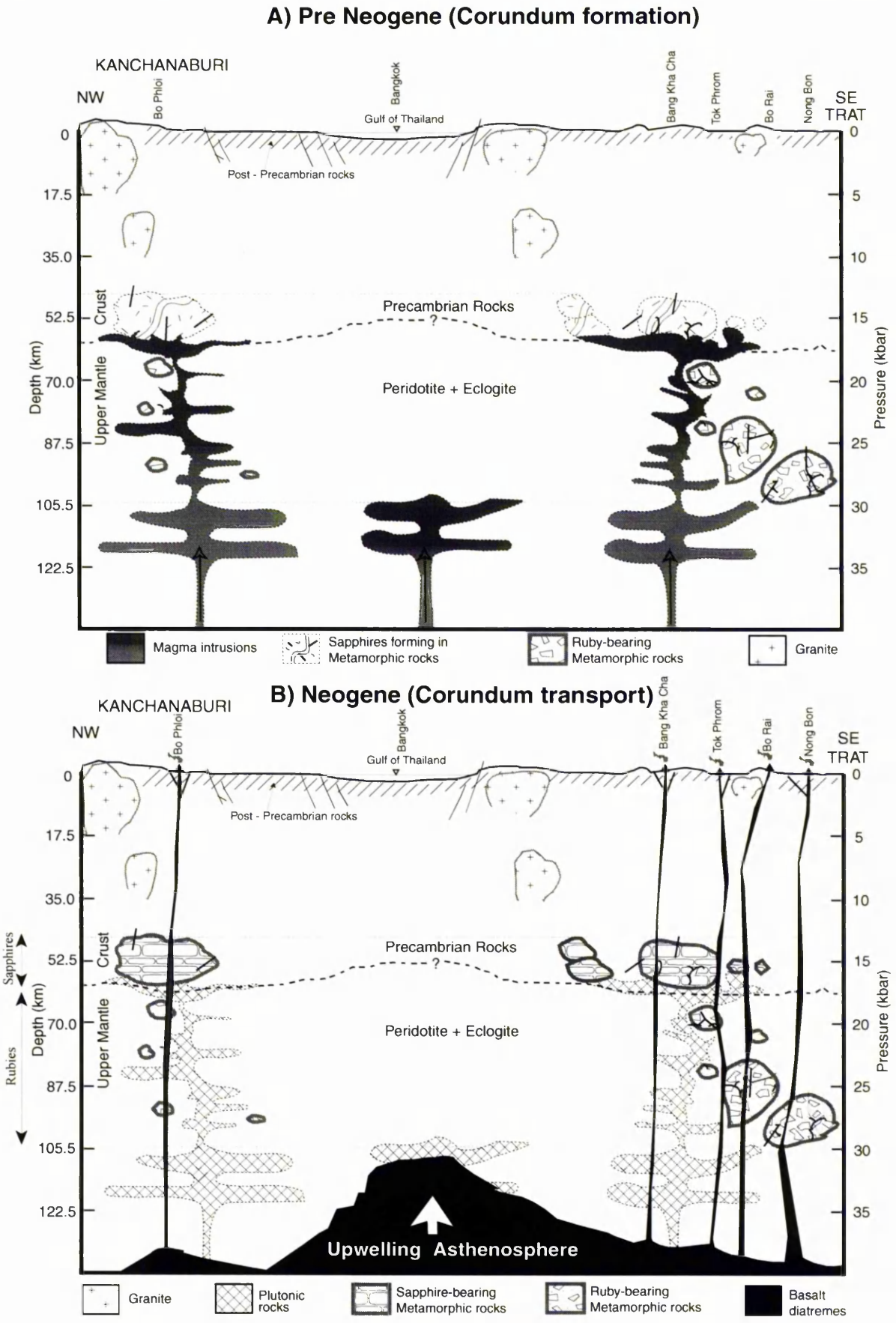

Figure 10.2 Model of corundum origin beneath Thailand (46-105 km depth or under 13-30 kbar). Rubies were crystallized in the relatively deeper and more mafic metamorphic rocks than sapphires. A) Highly evolved magmas reacting with metamorphic rocks in the lower crust to generate sapphires. B) Alkali basalt erupted in the Neogene and picked corundums up to the Earth's surface.

10.3 Recommendation for future work

The results of this study have substantially met the aims of the thesis. However there are still many points which are in doubt and need to be identified for future work. Some of these are as follows.

1) Ta-Nb-Sn contents in sapphires from Ban Huai Sai should be studied in more detail regarding the nature of their incorporation in the corundum structure.

2) The cathodoluminescent characteristics of corundum in terms of the nature of the quenchers or activators should be subject to quantitative examination. The position of the luminescence in the light spectra of samples of different colours should be studied.

3) Oxygen isotope geochemistry in corundum should be examined to establish the fingerprinting of different geological environments of corundums throughout the world. This could be compared to the oxygen isotopes in the rocks which are suspected to be the source of corundums. Oxygen isotopes could be used to distinguish between natural and synthetic corundums. The oxygen isotope geochemistry has been studied in certain corundums and in emerald.

4) More mineral inclusions in corundum should be searched for and analysed, especially coexisting mineral inclusions in single corundum grain to provide more accurate P-T conditions.

5) Internal standards of the spectrum of elements in synthetic corundum should be produced for using with LA-ICP-MS to analyse corundum samples.

References

Akimoto, S., Matsui, Y. and Syono, Y., 1976. High pressure crystal chemistry of orthosilicates and the formation of the mantle transition zone. *In*: Strens, R.G. (ed.). *The physics and chemistry of minerals and rocks*. pp. 327-363. New York: John Wiley & Sons.

Aranyakanon, P, Sampatavanija, S. and Ruengsuwan, J., 1970. Report on Gem Deposits of Si Sa Ket: Econ. Geol. Div., Dept. Min., Bangkok, Thailand (Published in Thai). 12 pp.

Aspen, P. Upton, B.G.J. and Dickin, A.P., 1990. Anorthoclase, sanidine and associated megacrysts in Scottish alkali basalts: high-pressure syenitic debris from upper mantle sources? *Eur. J. Mineral.*, 2: 503-517.

Barker, A.S.Jr., 1963. Infrared lattice vibration and dispersion in corundum. *Physical Review*, 132(4), 1475-1481.

Barkov, A.Y., Laajoki, K.V.O., Men' Shikov, Y.P., Alapieti, T.T. and Sivonen, S.J., 1997. First terrestrial occurrence of titanium-rich pyrrhotite, marcasite and pyrite in a fenitized xenolith from the Khibina alkaline complex, Russia. Canadian Mineralogist, 35(4): 875-885.

Barkov, A.Y., Martin, R.F., Men' Shikov, Y.P., Savchenko, Y.E., Thibault, Y. and Laajoki, K.V.O., 2000. Edgarite, $FeNb_3S_6$, first natural niobium-rich sulfide from the Khibina alkaline complex, Russian Far North: evidence for chalcophile behavior of Nb in a fenite. Contrib Mineral Petrol, 138: 229-236.

Barr, S.M. and Dostal, J., 1986. Petrochemistry and origin of megacrysts in Upper Cenozoic basalts, Thailand. *Journal of Southeast Asian Earth Sciences*, 1(2): 107-116.

Barr, S.M. and James, D.E., 1990. Trace element characteristics of Upper Cenozoic basaltic rocks of Thailand, Kampuchea and Vietnam. *Journal of Southeast Asian Earth Sciences*, 4 (3), 233-242.

Barr, S.M. and MacDonald, A.S., 1978. Geochemistry and petrogenesis of late Cenozoic alkaline basalts of Thailand. *Geol. Soc. Malaysia, Bulletin*, 10: 25-52.

Barr, S.M. and MacDonald, A.S., 1979. Palaeomagnetism, age, and geochemistry of the Den Chai basalt, northern Thailand. *Earth and Planetary Science Letters*, 46: 113-24.

Barr, S.M. and Macdonald, A.S., 1981. Geochemistry and geochronology of late Cenozoic basalts of Southeast Asia. *Geol. Soc. Amer. Bull.*, 92 (Part 2): 1069-1142.

Barr, S.M., MacDonald, A.S., Haile, N.S., and Reynolds, P.H., 1976. Paleomagnetism and age of the Lampang basalt (North Thailand) and age of the underlying pebble tools, *Jour. Geol Soc. Thailand*, 2(1-2): 1-10.

Barron, L.M., Lishmund, S.R., Oakes, G.M., Barron, B.J. and Sutherland, F.L., 1996. Subduction model for the origin of some diamonds in the Phanerozoic of eastern New South Wales. *Australian Journal of Earth Sciences*, 43: 257-267.

Belt, R.F., 1967. Hydrothermal ruby: Infrared spectra and X-ray topography. *J. Appl. Phys.*, 38: 2688-2689.

Ben-Avraham, Z. and Uyeda, S., 1973. Evolution of the China Basin and the Mesozoic palaeogeography of Borneo. *Earth Plan. Sci. Letters*, 18: 365-376.

Beran, A., 1991. Trace hydrogen in Verneuil-grown corundum and its colour varieties-an IR spectroscopic study. *Eur. J. Mineral.*, 3: 971-975.

Berman, R.G., 1990. Mixing properties of Ca-Mg-Fe-Mn garnets. *American Mineralogist*, 75: 328-344.

Bignell, J.D. and Snelling, N.J., 1977. K-Ar ages on some basic igneous rocks from peninsular Malaysia and Thailand, *Geol. Soc. Malaysia Bull.*, 8: 89-93.

Bloxam, T.W. and Allen, J.B., 1960. Glaucophane-schist, eclogite and associated rocks from Knockormal in the Girvan-Ballantrae complex, south Ayrshire. *Transactions of the Royal Society of Edinburgh*, 64: 1-27.

Bosshart, G., 1982. Distinction of natural and synthetic rubies by ultraviolet spectrophotometry. *J. Gemm.*, 18(2): 145-160.

Boyd, F.R., 1960. Garnet peridotites and the system $CaSiO_3$-$MgSiO_3$-Al_2O_3. *Mineralogical Society of America Special Paper*, 3: 63-75.

Brearley, A.J., 1986. An electron optical study of muscovite breakdown in pelitic xenoliths during pyrometamorphism. *Mineralogical Magazine*, 50: 385-397.

Brown, G.E.Jr., 1982. Olivines and silicate spinels. *In* Ribbe, P.H. (ed). *Reviews in mineralogy, Vol 5, 2nd ed. Orthosilicates,* pp. 275-381. Mineralogical Society of America.

Bunopas, S. and Bunjitradulya, S., 1975. Geology of Amphoe Bo Phloi, North Kanchanaburi with special notes on the "Kanchanaburi Series", *Jour, Geol. Soc. Thailand,* 1(1-2): 51-67.

Bunopas, S. and Vella, P., 1992. 'Geotectonics and geologic evolution of Thailand', In: *Proceedings of the National Conference on "Geologic Resources of Thailand: Potential for Future Development"* (C. Piencharoen, ed. In chief), Dept. Mineral Resources, Bangkok, Thailand, pp. 209-228.

Bunopas, S., 1992. Regional stratigraphic correlation in Thailand, In: *Proceedings of the National Conference on "Geologic Resources of Thailand: Potential for Future Development"* (C. Piencharoen, ed. In chief), Dept. Mineral Resources, Bangkok, Thailand, pp. 189-208.

Burns, R., 1970. Mineralogical applications of crystal field theory. Cambridge: Cambridge University Press. 224 pp.

Burns, R., 1983. Colours of gem. *Chemistry in Britain*, 19(12): 1004-1007.

Burns, R., 1985. Electronic spectra of minerals. *In*: Berry, F.J. and Vaughan, D.J. (ed). *Chemical bonding and spectroscopy in mineral chemistry*, pp. 63-101. London: Chapman and Hall.

Cao, R-L. and Zhu, S-H., 1987. Mantle xenoliths and alkali-rich host rocks in eastern Chiana. *In*: Nixon, P.H. (ed). *Mantle xonoliths*, pp. 177-180. John Wiley & Sons, Ltd.

Carlson, W. and Lindsley, D.H., 1988. Thermochemistry of pyroxenes on the join $Mg_2Si_2O_6$-$CaMgSi_2O_6$. *American Mineralogist*, 73: 242-252.

Cartwright, I. and Barnicoat, C., 1986. The generation of quartz-normative melts and corundum-bearing restites by crustal anatexis: petrogenetic modelling based on an example from the Lewisian of North-West Scotland. *J. metamorphic Geol.*, 3: 79-99.

Charoenprawat, A., 1986. Geology of Wang Chin and Ban Bo Khaeo areas, Phrae Province: A report of Geolo. Surv. Div., Dept. Miner. Res, Bangkok, Thailand (in Thai). pp 34.

Charusiri, P., Kosuwan, S. and Imsamut, S., 1997. Tectonic evolution in Thailand: from Bunopas (1981)s to a new scenario. In: *Proceedings of the International Conference on "Stratigraphy and Tectonics Evolution of Southeast Asia and the South Pacific"*, pp. 414-420. (P. Dheeradilok, ed. In chief), Bangkok, Thailand, 19-24 August,.

Chenery, S.R.N. and Cook, J.M., 1993. Determination of rare earth elements in single mineral grains by laser ablation microprobe-inductively coupled plasma mass spectrometry-preliminary study. *J. Anal. Atom. Spectrom.*, 8: 299-303.

Chinner, G.A., Smith, J.V. and Knowles, C.R., 1969. Transition metal contents of Al_2SiO_5 polymorphs. *American Journal of Science*, 267-A: 96-113.

Christensen, J.N., Halliday, A.N., Lee, D-C., and Hall, C.M., 1995. In situ Sr isotopic analysis by laser ablation. *Earth and Planetary Science Letters,* 136: 79-85.

Chuwong, M., Sinthusen, S. and Hansawek, R., 1995. Preliminary evaluation on future prospecting for potential of sapphire deposit in Amphoe Bo Phloi, Changwat Kanchanaburi. In: *Proceedings of the National Conference on "Progress and Vision of Geological Resource Development"*, pp. 177-193. Dept. Mineral. Resources, Bangkok, Thailand.

Clapsopoulos, I., 1991. Petrology, geochemistry and origin of Pliocene - Pleistocene potassium-rich volcanic rocks from Greece. Ph.D. Thesis, Department of Geology, The University of Manchester. 252 pp.

Coenraads R.R., Sutherland, F.L. and Kinny, P.D., 1990. The origin of sapphires: U-Pb dating of zircon inclusions sheds new light. *Mineralogical Magazine*, 54: 113-122.

Coenraads, R.R., 1992a. Sapphires and rubies associated with volcanic provinces: Inclusions and surface features shed new light on their origin. *Austral. Gem.*, 18(3): 70-78.

Coenraads, R.R., 1992b. Surface features on natural rubies and sapphires derived from volcanic provinces. *J. Gemm.*, 23(3): 151-160.

Coenraads, R.R., Vichit, P. and Sutherland, F.L., 1995. An unusual sapphire-zircon-magnetite xenolith from the Chanthaburi Gem Province, Thailand. *Mineralogical Magazine*, 59: 465-479.

Cole, J.M. and Crittenden, S., 1997. Early Tertiary basin formation and the development of Lacustrine and quasi-lacustrine/marine source rocks on the Sundra Shelf of SE Asia. *In*: Fraser, A. J., Matthews, S. J. & Murphy, R. W. (eds), *Petreoleum Geology of Southeast Asia*, Geological Society Special Publication No. 126, pp. 147-183.

Coleman, R.G., Lee, D.E., Beatty, L.B. and Brannock, W.W., 1965. Eclogites and eclogites: their differences and similarities. *Bull. Geol. Soc. Amrica,* 76: 483-508.

Cook, W.B. and Perkowitz, S., 1985. Temperature dependence of the far-infrared ordinary-ray optical constants of sapphire. *Applied Optics*, 24(12): 1773-1775.

Dao *et al.*, 1997. Diamond inclusions in corundum. *In*: John, M.L. and Koivula, J.L., Gem News. *Gem & Gemology*, 33(4): 299.

Dawson, J.B. and Stephens, W.E., 1975. Statistical analysis of garnets from kimberlites and associated xenoliths. *Journal of Geology*, 83: 589-607.

Deer, W.A., Howie, R.A. and Zussman, J., 1996. An introduction to the Rock-forming minerals, 2nd ed. Longman. 696 pp.

Deer, W.A., Howie, R.A. and Zussman, J., 1997a. Rock-forming minerals, Vol. 1A, Orthosiligcates silicates, 2nd ed. London: The Geological Society. 919 pp.

Deer, W.A., Howie, R.A. and Zussman, J., 1997b. Rock-forming minerals vol. 2A, Single-chain silicates, 2nd ed. London: The Geological Society. 668 pp.

Dele-Dubois, M.L. and Schbnell, H.J., 1987. Identification of inclusions in natural ruby or emerald and in synthetic minerals by Raman microspectrometry. *Terra Cognita*, 7: 14-15.

Dewey, J.F., Cande, S., Pitman, W.C. III., 1989. Tectonic evolution of India/Eurasia collision zone. *Eclogae Geologicae Helvetiae*, 82: 717-734.

Dheeradilok, P., Wongwanich, T., Tansathiean, W. and Chaodumrong, P., 1992. An introduction to geology of Thailand. In: *Proceedings of the National Conference on "Geologic Resources of Thailand: Potential for Future Development"* (C. Piencharoen, ed. In chief), Dept. Mineral Resources, Bangkok, Thailand, pp. 737-752.

Dirlam, D.M., Misiorowski, E.B., Tozer, R., Stark, K.B. and Bassett, A.M., 1992. Gem wealth of Tanzania. *Gems & Gemology*, 28(2): 80-102.

Droop, G.T.R. and Charnley, N.R., 1985. Comparative geobarometry of pelitic hornfelses associated with the Newer Gabbros: a preliminary study. *J. Geol. Soc. London*, 142: 53-62.

Droop, G.T.R. and Treloar, P.J., 1981. Presures of metamorphism in the thermal aureole of the Etive Granite Complex. *Scott. J. Geol.*, 17(2): 85-102.

Droop, G.T.R., 1987. A general equation for estimating Fe^{3+} concentrations in ferromagnesian silicates and oxides from microprobe analyses, using stoichiometric criteria. *Mineralogical Magazine*, 51: 431-435.

Droop, G.T.R., 1989. Reaction history of garnet-sapphirine granulites and conditions of Archaean high-pressure granulite-facies metamorphism in the Central Limpopo Mobile Belt, Zimbabwe. *J. metamorphic Geol.*, 7: 383-403.

Du Toit, A.L., 1918. Plumasite (corundum – Aplite) and titaniferous magnetite rocks from Natal. *Trans. Geol. Soc. South Africa*, 21(53): 53-75.

Dudley, R.J., 1976. The use of cathodoluminescence in the identification of soil materials. *Journal of Soil Science*, 27: 487-494.

Dunham, A.C. and Wilkinson, F.C.F., 1978. Accuracy, precision and detection limits of energy- dispersive electron microprobe analyses of silicates. *X-ray Spectrometry*, 7: 50-56.

Eigenmann, K. and Günthard, Hs.H., 1971. Hydrogen incorporation in doped α-Al_2O_3 by high temperature redox reactions. *Chemical Physics Letters*, 12(1): 12-15.

Ellis, DJ. and Green, D.H., 1979. An experimental study of the effect of Ca upon garnet-clinopyroxene Fe-Mg exchange equilibria. *Contrib Mineral Petrol*, 71: 13-22.

Estep-Barnes, P., 1977. Infrared spectroscopy. *In*: Zussman, J. (ed) *Physical methods in determinative mineralogy* (2nd ed.), pp. 529-603. London: Academic Press.

Fadini, A. and Schnepel, F.M., 1989. Vibrational spectroscopy: Methods and Application. New York: John Wiley & Sons.

Farmer, V.C., 1974. Vibrational spectroscopy in mineral chemistry. *In*: Farmer, V.C. (ed). *The infrared spectra of minerals*, Mineralogical society Monograph 4, pp. 1-10. Mineralogical Society, London.

Fedorovich, J.S., Richards, J.P., Jain, J.C., Kerrich, R., and Fan, J., 1993. A rapid method for REE and trace-element analysis using laser sampling ICP-MS on direct fusion whole-rock glasses. *Chemical Geology*, 106: 229-249.

Feenstra, A., 1985. Metamorphism of bauxites on Naxos, Greece. Geologica Ultraiectina, Mededelingen van het Instituut voor Aardwetenschappen der Rijksuniversiteit te Utrecht, No. 39. 206 pp.

Fitton, G., 1997. X-ray fluorescence spectrometry. *In* Gill, R. (ed). *Modern analytical geochemistry,* pp. 87-115. Singapore: Longman.

Fritsch, E. and Rossman, G., 1988. An update on color in gems. Part 3: colors caused by band gaps and physical phenomena. *Gems & Gemology*, Summer: 81-102.

Frye, K., 1974. Modern mineralogy. New Jersey: Prentice-Hall, Inc. 325 pp.

Fuhrman, M.L. and Lindsley, D.H., 1988. Ternary-feldspar modeling and thermometry. *American Mineralogist*, 73: 201-215.

Gaal, R.A.P., 1976-77. Cathodoluminescence of gem materials. *Gems & Gemology*, 15: 238-244.

Game, P.M., 1954. Zoisite-amphibolite with corundum from Tanganyika. *Min. Mag.* 230(226): 458-466.

Geschwind, S. and Remeika, J.P., 1961. Paramagnetic resonance of Gd^{3+} in Al_2O_3. *Physical Review*, 122(3): 757-761.

GIA, 1992. Colored stones, Assignment 32. Gemological Institute of America.

GIA, 1992. Gem reference guide. Gemological Institute of America. 270 pp.

GIA, 1993. Gem Identification Lab Manual. Gemological Institute of America. 66 pp.

Gogard, G. and Mabit, J-L., 1998. Peraluminous sapphirine formed during retrogression of a kyanite-bearing eclogite from Pays de Léon, Armorican Massif, France. *Lithos*, 43: 15-29.

Gordon, R.G. and Jurdy, D.M., 1986. Cenozoic global plate motions. *J. Geophys. Res.* 91(B.12): 12389-12406.

Govindaraju, K., 1989. Composition of working values and sample description for 272 geostandards. *Geostandards Newsletters*, 13(special issue): 1-113.

Griffith, W.P., 1974. Raman spectroscopy of minerals. *In*: Farmer, V.C. (ed). *The infrared spectra of minerals*, Mineralogical society Monograph 4, pp. 119-135. Mineralogical Society, London.

Griffith, W.P., 1978. Advances in the Raman and infrared spectroscopy of minerals. *In* : Clark, R.J.H. and Hester, R.E. (eds). *Spectroscopy of inorganic-based materials*, Advances in spectroscopy Vol. 14, pp. 119-186. John Wiley & Sons Ltd.

Gübelin, E.J. and Koivula, J.I., 1986. Photoatlas of inclusion in gemstones. Zürich: Switzerland, ABC Edition. 532 pp.

Gummer, W.K. and Burr, S.V., 1946. Nephelinized paragneisses in the Bancroft area, Ontario. *The Journal of Geology*, 54(3): 137-168.

Guo, J., O'Reilly, S.Y. and Griffin, W.L., 1996a. Corundum from basaltic terrains: a mineral inclusion approach to the enigma. *Contrib Mineral Petrol*, 122: 368-386.

Guo, J., O'Reilly, S.Y. and Griffin, W.L., 1996b. Zircon inclusions in corundum megacrysts: I. Trace element geochemistry and clues to the origin of corundum megacrysts in alkali basalts. *Geochimica et Cosmochimica Acta*, 60(13): 2347-2363.

Hada, S. and Bunopas, S., 1997. Terraine analysis and tectonics of the Nan_Chantha Buri sutrure zone (Abstract). *In*: *Proceedings of the International Conference on "Stratigraphy and Tectonics Evolution of Southeast Asia and the South Pacific"* (P. Dheeradilok, ed. In chief), Bangkok, Thailand, 19-24 August, 303.

Hada, S., Bunopas, S., Ishii, K. and Yoshikura, S., 1997. Rift-drift history and the amalgamation of Shan-Thai and Indochina/East Malaya Blocks. In: *Proceedings of the International Conference on "Stratigraphy and Tectonics Evolution of Southeast Asia and the South Pacific"*, pp. 273-286. (P. Dheeradilok, ed. In chief), Bangkok, Thailand, 19-24 August.

Haggerty, S.E., 1991. Oxide mineralogy of the Upper Mantle. *In*: Lindley, D.H. (ed.). *Oxide minerals: petrologic and magnetic significance. Reviews in mineralogy Vol. 25*, pp. 355-416. Mineralogical Society of America.

Hall, A.J., McConville, P., Boyce, A.J. and Fallick, A.E., 1994. A high chromium corundum (ruby) inclusion in diamond from the São Luiz alluvial mine, Brazil. *Mineralogical Magaszine*, 58: 490-493.

Hänni, H.A., Kiefert, L., and Chalain, J.P., 1997. A Raman microscope in the gemmological laboratory: first experiences of application. *J. Gemm.*, 25(6): 394-406.

Hansawek, R. and Pattamalai, K., 1997. Kanchanaburi sapphire deposits. In: *the proceedings of the international conference on stratigraphy and tectonic evolution of Southeast Asia and the south pacific*, p. 717. Bangkok, Thailand.

Henderson, B. and Imbusch, G.F., 1989. Optical spectroscopy of inorganic solids, Monographs on the physics and chemistry of materials. New York: Oxford University Press. 645 pp.

Herzberg, C.T. and Chapman, N.A., 1976. Clinopyroxene geothermometry of spinel lherzolite. *American Mineralogist*, 61: 626-637.

Holland, T.J.B. and Powell, R., 1985. An internally consistent thermodynamic dataset with uncertainties and correlations: 2. Data and results. *J. metamorphic Geol.*, 3: 343-370.

Holland, T.J.B. and Powell, R., 1990. An enlarged and updated internally consistent thermodynamic dataset with uncertainties and correlations: the system K_2O-Na_2O-CaO-MgO-MnO-FeO-Fe_2O_3-Al_2O_3-TiO_2-SiO_2-C-H_2-O_2. *J. metamorphic Geol.*, 8: 89-124.

Holland, T.J.B. and Powell, R., 1998. An internally consistent thermodynamic data set for phases of petrological interest. *J. Metamorphic Geol.*, 16: 309-343.

Horrocks, P.C., 1983. A corundum and sapphirine paragenesis from the Limpopo Mobile Belt, southern Africa. *J. metamorphic Geol.*, 1: 13-23.

Hughes, R.W., 1997. Ruby & Sapphire. Boulder: RWH Publishing. 511 pp.

Hutchison, C.S., 1989. Geological Evolution of Southeast Asia. Oxford University Press, Oxford Monograph on Geology and Geophysics, 13: 368.

Intasopha, S.B., 1993. Petrology and geochronology of the volcanic rocks of Central Thailand Volcanic Belt. PhD. Thesis (unpublished), the University of New Brunswick, Canada. 242 pp.

Irvine, T.N. and Baragar, W.R.A., 1971. A guide to chemical classification of the common volcanic rocks. *Canadian Journal of Earth Sciences*, 8: 523-548.

Isayev, Y.N. and Kkhoan, F., 1976. Some features of the deep-seated structure of the crust of Vietnam. *Internat. Geol. Rev.*,18: 945-948.

Jackson, S.E., Longerich, H.P., Dunning, C.R., and Fryer, B.J., 1992. The application of laser ablation microprobe-inductively coupled plasma-mass spectrometry (LA-ICP-MS) to in-situ trace elements determinations in minerals. *Can. Minerals*, 30: 1049-1064.

Jarvis, K.E. and Williams, J.G., 1993. Laser ablation inductively coupled plasma mass spectrometry (LA-ICP-MS): a rapid technique for the direct, quantitative determination of major, trace and rare-earth elements in geological samples. *Chemical Geology*, 106: 251-262.

Jarvis, K.E., 1997. Inductively coupled plasma-mass spectroscopy (ICP-MS). *In* Gill, R. (ed). *Modern analytical geochemistry,* pp. 171-187. Singapore: Longman.

Jarvis, K.E., Gray, A.L., and Houk, R.F., 1992. Handbook of inductively coupled plasma mass spectroscopy. Glasgow: Blackie, 375 pp.

Jeffries, T.E., Perkins, W.T. and Pearce, N.J.G., 1995. Measurements of trace elements in basalts and their phenocrysts by laser probe microanalysis inductively coupled plasma mass spectroscopy (LA-ICP-MS). *Chemical Geology*, 121: 131-144.

Johnson, M.L., Mercer, M.E., Fritsch, E., Maddison, P. and Shigley, J.E., 1995. "Ti-Sapphire": Czochralski-pulled synthetic pink sapphire from Union Carbide. *Gems & Gemology*, 31(3): 188-195.

Johnston, G.P., Muenchausen, R., Smith, D.M., Fahrenholtz, W., and Foltyn, S., 1992. Reactive laser ablation synthesis of nanosize alumina powder. *J. Am. Ceram. Soc.*, 75(12): 3293-3298.

Jones, M.P., 1987. Applied mineralogy: A quantitative approach. Oxford: Graham & Trotman.

Jungyusuk, N. and Khositanont, S., 1992. Volcanic rocks and associated mineralization in Thailand. In: *proceedings of the National Conference on "Geologic Resources of Thailand: Potential for Future Development"*, pp. 552-538. 17-24 November, Department of Mineral Resources, Bangkok Thailand. .

Jungyusuk, N. and Sirinawin, T., 1983. Cenozoic basalts of Thailand. In: *Proceedings of the Conference on "Geology & Mineral Resources of Thailand"*, 19-28 November, Dept. Mineral. Resources, Bangkok, Thailand. 9 pp.

Jurewicz, A.J.G. and Watson, E.B., 1988. Cations in olivine, Part 1: Calcium partitioning and Ca-Mg distribution between olivines and coexisting melts, with petrologic applications. *Contrib. Mineral. Petrol.*, 99: 176-185.

Kammerling, R.C., 1995. Sapphire mining in Laos. Gem News. *Gems & Gemology*, 31: 282-283.

Kent, R.W., Hardarson, B.S., Saunders, A.D. and Storey, M., 1996. Plateaux acient and modern: Geochemical and sedimentological perspectives on Archean oceanic magmatism. *Lithos*, 37: 129-142.

Kerr, A.C., 1998. Mineral chemistry of the Mull-Morvern Tertiary lava succession, western Scotland. *Mineralogical Magazine*, 62(3): 295-312.

Kettle, S.F.A., 1969. Coordination compounds. Bath: Thomas Nelson and Son Ltd. 220 pp.

Koivula, J.I., 1987. Sapphirine (not sapphire) in a ruby from Bo Rai, Thailand. *J. Gemm.*, 20(6): 369-370.

Koivula, J.I., 1991. Inclusion of the month: Native element inclusions. *Lapidary Journal*, 44(11): 48.

Kornprobst, J., Piboule, M., Roden, M. and Tabit, A., 1990. Corundum-bearing garnet clinopyroxenites at Beni Bousera (Morocco): Original plagioclase-rich Gabbros recrystallized at depth within the mantle? *Journal of Petrology*, 31, part 3: 717-745.

Krauskopf, K. and Bird, D., 1995. Introduction to geochemistry. 3th ed. New York: McGraw-Hill, Inc. 647 pp.

Krzemnicki, M.S., Hänni, H.A., Guggenheim, R. and Mathys, D., 1996. Investigations on sapphires from an alkali basalt, South West Rwanda. *J. Gemm.*, 25(2): 90-106.

Le Maitre R.W, Bateman, P., Dudek, A., Keller, J., Lameyre, J., Le Bas., M.J., Sabine, P.A., Schmid, R., Sorensen, H., Streckeisen, A., Woolley, A.R. and Zanettin, B., 1989. A classification of igneous rocks and glossary of terms. Oxford: Blackwell Scientific Publications. 193 pp.

Lechler, P.J. and Desilets, M.O., 1987. A review of the use of loss on ignition as a measurement of total volatiles in whole-rock analysis. *Chemical Geology*, 63: 341-344.

Lee, J.D., 1977. A new concise inorganic chemistry, 3rd ed. London: Van Nostrand Reinhold Company. 505 pp.

Lee, T.-Y. Lawver, L.A., 1995. Cenozoic plate reconstruction of Southeast Asia. *Tectonophysics*, 251: 85-138.

Lensch, G., 1971. Das Vorkommen von Sapphirin im Pridotitkörper von Finero (Zone von Ivrea, Italienische Westalpen). *Contrib Mineral Petrol*, 31: 145-153.

Leverenze, H.W., 1968. An introduction to luminescence of solids. New York: Dover.

Levinson, A.A. and Cook, F.A., 1994. Gem corundum in alkali basalt: Origin and occurrence. *Gem & Gemology*, 30(4): 253-262.

Liati, A. and Seidel, E., 1996. Metamorphic evolution and geochemistry of kyanite eclogites in central Rhodope, northern Greece. *Contrib Mineral Petrol*, 123: 293-307.

Liese, H.C., 1975. Selected terrestrial minerals and their infrared absorption spectral data (4000-300 cm^{-1}). *In*: Karr, C. Jr. (ed). *Infrared and Raman spectroscopy of Lunar and terrestrial minerals*, pp. 197-229. New York: Academic Press.

Limsuwan, R., 1999. "Bore-Pile Drilling" a new choice for deep sampling for placer deposits of gemstone. In: *Proceedings of symposium on mineral, energy, and water resources of Thailand: towards the year 2000,* Bangkok, Thailand. pp. 485-495.

Loeffler, B.M. and Burns, R.G., 1976. Shedding light on the color of gems and materials. *American Scientist*, 636-647.

Longsley, I.M., 1997. The tectonostratigraphic evolution of SE Asia. In: Fraser, A. J., Matthews, S. J. & Murphy, R. W. (eds), *Petreoleum Geology of Southeast Asia*, Geological Society Special Publication No. 126, pp. 31-339.

Lovering, J.F. and White, A.J.R., 1969. Granulitic and eclogitic inclusions from basic pipes at Delegate, Australia. *Contrib. Mineral. Petrol.*, 21: 9-52.

MacGetchin, T.R. and Silver, L.T., 1970. Compositional relatios from kimberlites and related rocks in the Moses Rock Dike, San Juan County, Utah. *American Mineralogist*, 55: 1738-1771.

MacKenzie, W.S., Donaldson, C.H. and Guilford, C., 1997. Atlas of igneous rocks and their textures. Longman. 148 pp.

Mantajit, N., 1997. Stratigraphy and tectonics of Thailand. In: *Proceedings of the International Conference on "Stratigraphy and Tectonics Evolution of Southeast Asia and the South Pacific"* (P. Dheeradilok, ed. In chief), Bangkok, Thailand, 19-24 August, 1-26.

Marshall, D.J., 1988. Cathodoluminescence of geological materials. Boston: Unwin Hyman. 146 pp.

Martin, F., Merigoux, H., and Zecchini, P., 1989. Reflectance infrared spectroscopy in gemology. *Gem & Gemology*, 25(4): 226-231.

Mattey, D.P., 1997. Gas source mass spectrometry: isotopic composition of lighter elements. *In* Gill, R. (ed). *Modern analytical geochemistry*, pp. 154-170. Singapore: Longman.

Matzat, E. and Shiraki, K., 1978. Chromium. *In* : Wedepohl, K.H. (ed). *Handbook of geochemistry vol II/3, Element Cr (24) to Br (35)*. Berlin: Spinger-Verlag.

McCabe, R., Celaya, M., Cole, J., Han, H-C., Ohnstad, T., Paijitprapapon, V. and Thitipawarn, V., 1988. Extension tectonics: The Neogene opening of the North-South trending basins of central Thailand. *Journal of Geophysics Research*, 93 (B10): 11899-11910.

McClue, D.S., 1962. Optical spectra of transition-metal ions in corundum. *J. Chem. Phys.*, 36: 2757-2779.

Meschede, M., 1986. A method of discriminating between different types of mid-ocean ridge basalts and continental tholeiites with the Nb-Zr-Y diagram. *Chem. Geol.*, 56: 207-218.

Metcalfe, I., 1988. Origin and assembly of Southeast Asian continental terranes. In: *Audley-Charles, M. G. & Hallam, A., (eds), Gondwana and Tethys.* Geological Society, London, Special Publication, No. 37: 101-118.

Metcalfe, I., 1997. The Palaeo-Tethys and Palaeozoic-Mesozoic tectonic evolution of Southeast Asia. In: *Proceedings of the International Conference on "Stratigraphy and Tectonics Evolution of Southeast Asia and the South Pacific"* (P. Dheeradilok, ed. In chief), Bangkok, Thailand, 19-24 August. pp. 260-272.

Meyer, H.O.A. and Gübelin, E., 1981. Ruby in diamond. *Gem & Gemology*, 17: 153-156.

Meyer, H.O.A., 1968. Chrome pyrope: an inclusion in diamond. *Science*, 160: 1446-1447.

Middlemost, E.A.K., 1975. The basalt clan. *Earth Sci. Rev.*, 11: 337-364.

Middlemost, E.A.K., 1989. Iron oxidation ratios, norms and the classification of volcanic rocks. *Chemical Geology*, 77: 19-26.

Miller, J., 1989. Cathodoluminescence microscopy. *In*: Tucker, M. (ed.). *Technique in sedimentology*, pp. 174-190. Oxford: Blackwell Scientific Publications.

Mitchell, A.H.G. and Garson, M.S., 1981. Mineral deposits and global tectonics settings. London: Academic Press. 42 pp.

Moazzen, M., 1999. Contact metamorphic process in Etive aureole, Scotland. PhD Thesis, Department of Earth Sciences, The University of Manchester. 392 pp.

Moon, A.R. and Phillips, M.R., 1984. An electron microscopy study of exolved phases in natural black Australian Sapphire. *Micron and Microscopica Acta*, 15(3): 143-146.

Morimoto, N., Fabries, J., Ferguson, A.K., Ginzburg, I.V., Ross, M., Seifert, F.A., Zussman, J., Aoki K. and Gottardi, G., 1988. Nomenclature of pyroxenes. *American Mineralogist,* 73: 1123-1133.

Moyd, L., 1949. Petrology of nepheline and corundum rocks of Southeastern Ontario. *American Mineralogist*, 34: 736-751.

Muhlmeister, S., Fritsch, E., Shigley, J.E., Devouard, B. and Laurs, B.M., 1998. Separating natural and synthetic rubies on the basis of trace-element chemistry. *Gems & Gemology,* 34(2): 80-101.

Mukasa, S.B., Fischer, G.M. and Barr, S.M., 1996. The character of the subcontinental mantle in Southeast Asia: evidence from isotopic and elemental compositions of extension-related Cenozoic basalts in Thailand. *In*: Basu, A. and Hart, S. (eds). *Earth process: reading the isotopic code, Geophysical Monograph 95,* pp. 233-252. American Geophysical Union.

Mukaza, S.B., Zhou, P. and Barr, S.M., 1994. Geochemical character of mantle sources beneath continental Souteast Asia: a Nd-Sr-Pb isotopic and major– and trace-element study of Cenozoic basalts in Thailand. *American Geophysical Union-Transactions*, 75, Suppl.: 736.

Nassau, K., 1980. The causes of colour. *Scientific American*, 243: 106-123.

Nassau, K., 1981. Raman spectroscopy as a gemstone test. *J. Gemm.*, 17: 306-320.

Nassau, K., 1983. The physics and chemistry of color: the fifteen causes of color. New York: John Wiley and Son. 454 pp.

Nassau, K., 1987. The fifteen causes of color: The physics and chemistry of color. *Color research and application*, 12(1): 4-26.

Newnham, R.E. and De Haan, Y.M., 1962. Refinement of the α Al_2O_3, Ti_2O_3, V_2O_3, and Cr_2O_3 structures. *Zeitschrift für Kristallographie, Bd.* 117: 235-237.

O'Keeffe, M. and Hyde, B.G., 1996. Crystal structures, I. Patterns and symmetry, Mineralogical Society of America Monograph. Washington, D.C: Mineralogical Society of America. 453 pp.

Orgel, L.E., 1966. An Introduction to transition-metal chemistry ligand-field theory. London: Methuen & Co Ltd. 186 pp.

Orlov, Yu.L., 1973. The mineralogy of diamond. New York: John Wiley & Son. 235 pp.

Osipowicz, T., Tay, T.S, Orlic, I., Tang, S.M., and Watt, F., 1995. Nuclear microscopy of rubies: Trace elements and inclusions. *Nuclear Instruments and Methods in Physics Research B,* No. 104: 590-594.

Panjasawatwong, Y and Youngsnong, M., 1995. Chiang Khong corundum-bearing basalt, Amphoe Chiang Khong, Changwat Chiang Rai. *A paper presented in the Seminar on "Gemological Sciences in Thailand"*, at the University of Suranari Technology, Nakhon Ratchasima, Thailand, Dec. 1994. 15 pp.

Panjasawatwong, Y., 1983. Chemical variation within a single basalt flow at Den Chai, Phrae: Paper presented at the Annual Technical Meeting, Dept. Geol. Sci., Chiang Mai University, Chiang Mai. Feb. 1-2 (Cited in Jungyusuk and Sirinawin, 1983).

Pearce N.J.G., Perkins, W.T., Abell, I., Duller, G.A.T. and Fuge, R., 1992. Mineral microanalysis by laser ablation inductively coupled plasma mass spectrometry. *J. Anal. Atom. Spectrom.*, 7: 53-57.

Pearce, T.H., Gorman, B.E. and Birkett, T.C., 1975. The TiO_2-K_2O-P_2O_5 diagram: a method of discriminating between oceanic and non-oceanic basalts. *Earth Planet. Sci. Lett.*, 24: 419-426.

Peltzer, G. and Tapponnier, P., 1988. Formation of strike-slip faults, rifts, and basins during the Indian-Asia collision: an experimental approach. *Journal of Geophysics Research*, 93: 15085-15117.

Peretti , A., Mullis, J. and Mouawad, F., 1996. The role of fluorine in the formation of colour zoning in rubies from Mong Hsu, Myanmar (Burma). *J. Gemm.*, 25(1): 3-19.

Peretti , A., Schmetzer, K, Bernhardt, H.J. and Mouawad, F., 1995. Rubies from Mong Hsu. *Gems & Gemology*, 31(1): 2-26.

Perkins, W.T. and Pearce, N.J.G., 1995. Mineral microanalysis by laserprobe inductively coupled plasma mass spectrometry. *In* Potts, P.J., Bowles, J.F.W., Reed, S.J.B., and Cave, M.R. (eds). *Microprobe Techniques in the Earth Sciences*, pp. 291-325. London: Chapman & Hall.

Phillippi, C.M., 1970. Analytical infrared spectra of particlulate alpha-aluminas. *In*: Grove, E.L. and Perkins, A.J. (eds). *Developments in applied spectroscopy Vol 7B*, pp. 23-33. New York: Plenium Press.

Phillips, W.R., 1971. Mineral optics principles and techniques. San Franciscos: W.H. Freeman and Company. 249 pp.

Pisutha-Arnond, V., Wathanakul, P. and Intasopa, S., 1999. New Evidences on the origin of Kanchanaburi Sapphire. Symposium on Mineral, Energy, and Water Resources of Thailand: Twards the year 2000. Bangkok, Thailand (Abstract).

Piyasin, S., 1975. Geology of Uttaradit, Sheet NE 47-11: Report of investigation, No 15, Dept. Miner. Res., Bangkok, Thailand. 68 pp.

Polachan, S., Pradidtan, S., Tongtaow, C., Janmaha, S., Intarawijitr, K. and Sangsuwan C., 1991. Development of Cenozoic basins in Thailand. *Marine and Petroleum Geology,* 8: 84-97.

Porto, S.P.S. and Krishnan, R.S., 1967. Raman effects of corundum. *The Journal of Chemical Physics*, 47(3): 1009-1012.

Potts, P.J., 1987. A handbook of silicate rock analysis. London: Blackie. 621 pp.

Powell, R. and Holland, T.J.B., 1985. An internally consistent thermodynamic dataset with uncertainties and correlations: 1. Methods and a worked example. *J. metamorphic Geol.*, 3: 327-342.

Powell, R. and Holland, T.J.B., 1988. An internally consistent dataset with uncertainties and correlations: 3. Applications to geobarometry, worked examples and computer program. *J. metamorphic Geol.*, 6: 173-204.

Powell, R., 1978. Equilibrium thermodynamics in petrology: an introduction. London: Harper & Row, Publishers. 244 pp.

Pradidtan, S. and Dook, R., 1992. Petroleum geology of the Northern Part of the gulf of Thailand. In: *Proceedings of the National Conference on "Geologic Resources of Thailand: Potential for Future Development"* (C. Piencharoen, ed. In chief), Dept. Mineral Resources, Bangkok, Thailand, pp. 235-246.

Presnall, D.C., Dixon, S.A., Dixon, J.R., O'Donnell, T.H., Brenner, N.L., Schrock, R.L. and Dycus, D.W., 1978. Liquidus phase relations on the join diopside-forsterite-anorthite from 1 atm to 20 kbar: Their bearing on the generation and crystallization of basaltic magma. *Contrib. Mineral. Petrol.*, 66: 203-220.

Promprated, P., Taylor, L.A. and Snyder, G.A., 1999. Petrochemistry of the mantle beneath Thailand: Evidence from peridotite xenoliths. *International Geology Review*, 41: 506-530.

Ramsey, M.H., 1997. Sampling and sample preparation. *In*: Gill, R. (ed). *Modern analytical geochemistry*, pp. 12-28. Singapore: Addison Wesley Longman Ltd.

Reed, P.G., 1994. Dictionary of gemmology. 2nd ed. Oxford: Butterworth-Heinemann Ltd. 266 pp.

Reed, S.J.B., 1996. Electron microprobe analysis and scanning electron microscopy in geology. Cambridge: Cambridge University Press. 201 pp.

Reed, S.J.B., 1997. Electron microprobe analysis, 2nd ed. Cambridge: Cambridge University Press. 326 pp.

Richter, B. and Fuller, M., 1996. Palaeomagnetism of the Sibumasu and Indochina blocks: implications for the extrusion tectonic model. In: *Hall, R. and Blundell, D (eds), Tectonic Evolution of Southeast Asia*, Geological Society, London, Special Publication No. 106: 203-204.

Riddle, C., 1993. Analysis of geologial materials. New York: Marcel Dekker, Inc. 463 pp.

Rodolfo, K.F., 1969. Bathymetry and marine geology of the Andaman Basin and tectonic implications for Southeast Asia. *Bull. Geol. Soc. Amer.*, 80: 1203-1230.

Roedder, E., 1984. Fluid inclusions. Reviews in Mineralogy Vol. 12. Mineralogical Society of America. 646 pp.

Rossman, G.R. and Smyth, J., 1990. Hydroxyl contents of accessory minerals in minerals in mantle eclogites and related rocks. *American Mineralogist*, 75: 775-780.

Rossman, G.R., 1988. Optical spectroscopy. *In*: Hawthorne, F.R. (ed). *Spectroscopic methods in mineralogy and geology*. Reviews in Mineralogy, Vol. 18, pp. 207-254. Mineralogical Society of America.

Rowland, A.P., 1997. Atomic absorption spectrometry and other solution methods. *In*: Gill, R. (ed). *Modern analytical geochemistry*, pp. 67-86. Singapore: Addison Wesley Longman Ltd.

Russell, J.D., 1974. Vibrational spectroscopy in mineral chemistry. *In*: Farmer, V.C. (ed). *The infrared spectra of minerals.* Mineralogical society Monograph 4. pp. 11-25. Mineralogical Society, London.

Rydzak, J.W. and Cannon, R., 1989. Fourier transform infrared microspectroscopy method to determine stress in sapphire. *J. Am. Ceram. Soc.*, 72 (8): 1559-1561.

Sanchez, J.L., Osipowicz, T., Tang, S.M., Tay, T.S and Winn, T.T., 1997. Micro-PIXE analysis of trace element concentration of natural rubies from different locations in Myamar. *Nuclear Instruments and Methods in Physics Research B*, No. 130: 682-686.

Sasada, M., Ratanasthien, B., and Soponpongpipat, R., 1987. New K/Ar ages from the Lampang Basalt, Northern Thailand, *Geol. Surv. Japan, Bull.*, 38(1): 13-20.

Schairer, J.F. and Yagi, K., 1952. The system FeO-Al_2O_3-SiO_2. *American Journal of Science*, Bowen Vol.: 471-512.

Schmetzer, K. and Bank, H., 1980. Explanations of the absorption spectra of natural and synthetic Fe- and Ti-containing corundums. *Neues Jahrbuch für Mineralogie, Abhandlungen*, 139: 216-225.

Schmetzer, K. and Bank, H., 1981. The colour of natural corundum. *N. Jb. Miner. Mh.*, 11(2): 59-68.

Schmetzer, K. and Kiefert, L., 1990. Spectroscopic evidence for heat treatmenmt of blue sapphires from Sri Lanka – additional data. *J. Gemm.*, 22(2): 80-82.

Schmetzer, K., Bank, H. and Gübelin, E., 1980. The alexandrite effect in minerals: chrysoberyl, garnet, corundum, fluorite. *N. Jb. Miner. Abh.*, 138(2): 147-164.

Schmetzer, K., Bosshart, G. and Hänni, H.A., 1983. Naturally-coloured and treated yellow and orange-brown sapphires. *J Gemm.*, 18(7): 607-622.

Schwarz, D., Petsch, E.J. and Kanis, J., 1996. Sapphires from the Andranondambo Region, Madagascar. *Gems & Gemology*, 32(2): 80-90.

Shriver, D.F. and Atkins, P.W., 1999. Inorganic chemistry. 3rd ed. Oxford University Press. 763 pp.

Sills, J.D., Ackermand, D., Herd, R.K. and Windley, B.F., 1983. Bulk composition and mineral parageneses of sappirine-bearing rocks along a gabbro-lherzolite contact at Finero, Iverea Zone, N Italy. *J. metamorphic Geol.*, 1: 337-351.

Simkin, T. and Smith, J.V., 1970. Minor element distribution in olivine. *J. Geol.*, 78: 304-325.

Sirinawin, T., 1981. *Geochemistry and genetic significance of gem-bearing basalt in Chanthaburi - Trat area*: Unpubl. M.Sc. Thesis, Dept. Geological Sciences, Chiang Mai University, Thailand (in Thai with English abstract). 87 pp.

Sivabovorn, V., Paichitprapaporn, V. and Tansatein, S., 1976. *Geology of Phratabong-Chanthaburi 1:250,000 (Sheet ND48-9, ND48-13)*: A report of Geol Surv. Div., Dept. Miner. Res., Bangkok, Thailand, (in Thai). 51 pp.

Skoog, D.A., Holler, F.J., and Nieman, T.A., 1998. Principles of instrumental analysis. (5th ed). Philadelphia: Saunders College Publishing.

Smirnov, V.I., 1968. The sources of ore-forming fluids. *Econ. Geol.* 63: 380-389.

Smith, A.L., 1974. Infrared spectroscopy. *In* Robinson, J.W. (ed.). *Handbook of spectroscopy Vol. II.* p. 61. Cleveland: CRC Press.

Smith, C.P., 1995. A contribution to understanding the infrared spectra of rubies from Mong Hsu, Myanmar. *J. Gemm.*, 24(5): 321-335.

Smith, D.G.W., 1969. Pyrometamorphism of phyllites by a dolerite plug. *Journal of Petrology*, 10(1): 20-55.

Sobolev, N.V., 1965. Xenolith of eclogite with ruby. *Dockl. Acad. Sci. USSR, Earth Sci. Sect.*, 157: 79-82.

Sobolev, N.V., Kuznetsova, I.K. and Zyuzin, N.I., 1968. The petrology of grospydite xenoliths from the Zagadochnaya kimberlite pipe in Yakutia. *Journal of Petrology*, 9: 253-280.

Solomonov, V.I., Mikhailov, S.G., Osipov, V.V., Lipchak, A.I., Avdonin, V.N. and Vasilevskaya, M.E., 1996. A spectral-luminescent technique for gemmology. *J. Gemm.*, 25(4): 299-305.

Sriprasert, B., 1997. Geochemistry and petrology of Thoeng Basalt, Changwat Chiang Rai. Master Thesis, Department of Geology, Chiang Mai University (Manuscript).

Stephens, W.E. and Dawson, J.B., 1977. Statistical comparison between pyroxenes from kimberlites and their associated xenoliths. *Journal of Geology*, 85: 433-449.

Stern, W.B. and Hänni, H.A., 1982. Energy dispersive X-ray spectrometry: A non-destructive tool in gemmology. *J.Gemm.*, 1982, 18(4): 285-296.

Sutherland, F.L. and Coenraads, R.R., 1996. An unusual ruby-sapphire-sapphirine-spinel assemblage from the Tertiary Barrington volcanic province, New South Wales, Australia. *Mineralogical Magazine*, 60: 623-638.

Sutherland, F.L. and Schwarz, D., 1997. Gem corundum from Australia and Southeast Asia. *In*: Johnson, M.L. and Koivula, J.I., Gem News. *Gem &Gemology*, 33(4): 302.

Sutherland, F.L., 1996. Alkaline rocks and gemstones, Australia: a review and synthesis. *Australian Journal of Earth Sciences*, 43: 323-343.

Sutherland, F.L., 1998. Gem corundum origins from eruptive sources. In: *Abstract & Programme of 17th General Meeting*, International Mineralogical Association, August 9-14, Toronto, Canada. p. A13.

Sutherland, F.L., Hoskin, P.W.O., Fanning C.M. and Coenraads, R.R., 1998a. Models of corundum origin from alkali basaltic terrains: a reappraisal. *Contrib. Mineral. Petrol.*, 133: 356-372.

Sutherland, F.L., Schwarz, D., Jobbins, E.A., Coenraads, R.R., and Webb, G., 1998b. Distinctive gem corundum suites from discrete basalt fields: a comparative study of Barrington, Australia, and West Pailin, Cambiodia, gemfields. *J.Gemm.*, 26(2): 65-85.

Sutthirat, C., Charusiri. P, Farrar, E., and Clark, A.H., 1994. New $^{40}Ar/^{39}Ar$ geochronology and characteristics of some Cenozoic basalts in Thailand, Proceedings of the International Symposium on: Stratigraphic Correlation of Southeast Asia 15-20 November, Bangkok, Thailand. pp. 306-321.

Sutthirat, C., Droop, G.T.R., Henderson, C.M.B. and Manning, D.A.C., 1999. Petrography and mineral chemistry of xenoliths and xenocrysts in Thai corundum-

realted basalts: implication for the upper mantle and lower crust beneath Thailand. Proceedings of the Symposium on Mineral, Energy, and Water Resources of Thailand: Towards the year 2000. Bangkok, Thailand. pp. 152-161.

Sutthirat, C., Thayapink, S. and Hansawek, R., 1995. New sapphire occurrences and Characteristics of associated basalts in Changwat Lanpang. In: *Proceedings of the National Conference on "Progress and Vision of Geological Resource Development"*, pp. 195-209. Dept. Mineral. Resources, Bangkok, Thailand.

Sylvester, P.J. and Ghaderi, M., 1997. Trace element analysis of scheelite by excimer laser ablation-inductively coupled plasma by excimer laser ablation-inductively coupled plasma-mass spectrometry (ELA-ICP-MS) using a synthetic silicate glass standard. *Chemical Geology*, 141: 49-65.

Tang, S.M., Tang, S.H., Mok, K.F., Retty, A.T. and Tay, T.S., 1989. A study of natural and synthetic rubies by PIXE. *Applied Spectroscopy*, 43(2): 219-223.

Tang, S.M., Tang, S.H., Tay, T.S and Retty, A.T., 1988. Analysis of Burmese and Thai rubies by PIXE. *Applied Spectroscopy*, 42(1): 44-48.

Tansathien, W., Polprasit, C., and Paijitprapaporn, V., 1976. Geological Map of Thailand, 1:250,000, ND48-13, 1st ed. Geological Survey, Department of Mineral resources, Thailand.

Tapponnier, O., Peltzer, G. and Armijo, R., 1986. On the mechanism of the collision between India and Asia: Collision Tectonics, Geological Society of London, Special; Publication 19. pp. 115-157.

Tapponnier, P., Peltzer, G., Le Dain, A.Y., Armijo, R. and Cobbold, P., 1982. Propagating extrusion tectonics in Asia; New insight from simple experiments with plasticine. *Geology*, 10: 611-616.

Thanasuthipitak, T. and Sirinawin, T., 1986. Petrochemistry of gem-bearing basalt in the Nong Bon area, Trat Province, Eastern Thailand. GEOSEA V Proceedings Vol. II, *Geol. Soc. Malaysia, Bulletin* 20: 503-521.

Thanasuthipitak, T., 1978. A review of igneous rocks of Thailand, *In*: Nutalaya, P., ed., *Proceedings of 3rd regional resources of Southeast Asia,* pp. 775-782. Bangkok, Asian Institute of Technology.

Thomas, H.H., 1922. On certain xenolithic Tertiary minor intrusions in the Island of Mull (Argyllshire). *The Quarterly Journal of the Geological Society of London*, 78 (311): 229-261.

Thomson, R.N., 1982. British Tertiary volcanic province. *Scott. J. Geol.*, 18: 49-107.

Trewin, N., 1989. Use of the scanning microscope in sedimentology. *In*: Tucker, M. (ed.). *Technique in sedimentology,* pp. 244-253. Oxford: Blackwell Scientific Publications.

Turnock, A.C. and Eugster, H.P., 1962. Fe-Al Oxides: Phase relationships below 1,000°C. *Journal of Petrology*, 3(part 3): 533-565.

Upton, B.G.J, Aspen, P. and Chapman, N.A., 1983. The upper mantle and deep crust beneath the British Isles: evidence from inclusions in volcanic rocks. *J. geol. Soc. London*, 140: 105-121.

Upton, B.G.J. Hinton, R.W., Aspen, P., Finch, A. and Valley, J.W., 1999. Megacrysts and associated xenoliths: evidence for migration of geochemically enriched melts in the upper mantle beneath Scotland. *Journal of Petrology*, 40(6): 935-956.

Vichit, P., 1976. A Report on Sapphire deposits at Ban Ta Koi, Nam Yun, Ubon Ratchathani Province, Eastern Thailand: Eco. Geol. Div., Dept. Min. Res., Bangkok, Thailand. (in Thai). 5 pp.

Vichit, P., 1987. Gemstones in Thailand. *J. Geol. Soc Thailand*, 9: 108-133.

Vichit, P., 1992. Gemstones in Thailand. National conference on "Geologic resources of Thailand: Potential for future development", 17-24 November. Department of Mineral Resources, Bangkok, Thailand. pp. 124-150.

Vichit, P., Udompornvirat, S., Tritra-ngan, A. and Jariyawat, P., 1988. A Report on gem deposits in Wichian Buri Area, Phetchabun Province: Economic Geology Report, Econ. Geol. Div., Dept. Miner. Res, Bangkok, No. 61/1988. 145 pp. (in Thai).

Vichit, P., Vudhichativanich, S., and Hansawek, R., 1978. The distribution and characteristics of corundum-bearing basalts in Thailand, *J. Geol. Soc. Thailand*, 3 (1): M4-1 - M4-38.

Volynets, F.K., Vorob'ev, V.G., and Sidorova, E.A., 1972. Infrared absorption bands in corundum crystals. *Journal of Applied Spectroscopy*, 10: 665-667. Translated from *Zhurnal Prikladnoi Spektroskopii* 1969, 10(6): 981-984.

Walsh, J.N., 1997. Inductively coupled plasma-atomic emission spectrometry (ICP-AES). *In* Gill, R. (ed). *Modern analytical geochemistry*, pp. 41-66. Singapore: Longman.

Waltham, T., 1999. The ruby mines of Mogok. *Geology Today*, 15(4): 143-149.

Watson, G.H., Daniels, W.B., and Wang, C.S., 1981. Measurements of Raman intensities and pressure dependence of phonon frequencies in sapphire. *J. Appl. Phys.*, 52(2): 956-958.

Webster, R., 1998. Gems: Their sources, descriptions and identification. Oxford: Butterworth-Heinemann. 1026 pp.

Wefers, K., and Bell, G.M., 1972. *Oxides and Hydroxides of Aluminium*. Technical Paper No. 19, Alcoa Research Laboratories, USA.

White, W.B., 1975. Structural interrelation of Lunar and terrestrial minerals by Raman spectroscopy. *In* : Karr, C.Jr. (ed). *Infrared and Raman Spectroscopy of Lunar and terrestrial Minerals*, pp. 325-358. New York: Academic Press.

Wilcock, I. and Bosshart, G., 1997. Diamond inclusions in corundum. *In*: John, M.L. and Koivula, J.L., Gem News. *Gem & Gemology*, 33(4): 299.

Willemse, J. and Viljoen, E.A., 1970. The fate of argillaceous material in the gabbroic magma of the Bushveld complex. *The Geological Society of South Africa*, Special Publication 1, Symposium on the Bushveld Igneous Complex and other Layered Intrusions: 336-366.

Wilson, M., 1989. Igneous petrogenesis. London: Unwin Hyman. 466 pp.

Wood, B.J. and Fraser, D.G., 1977. Elementary thermodynamics for geologists. Oxford: Oxford University Press. 303 pp.

Wood, B.J., 1979. Activity-composition relationships in $Ca(Mg,Fe)Si_2O_6$-$CaAl_2SiO_6$ clinopyroxene solid solutions. *American Journal of Science*, 279: 854-875.

Yaemniyom, N., 1982. The petrochemical study of corundum-bearing basalts at Bo Phloi district, Kanchanaburi. Master thesis, Dept. of Geology, Chulalongkorn University, Thailand. 100 pp.

Yamamoto, M., 1991. Occurrences and petrochemistry of the Lampang and Sop Prap basalt, northern Thailand. *Rep. Res. Inst. Natural Resources, Min. Coll. Akita Univ.*, No. 56: 85-94.

Zhou, P. and Mukasa, S.B., 1997. Nd-Sr-Pb isotopic, and major- and trace-element geochemistry of Cenozoic lavas from the Khorat Plateau, Thailand: sources and petrogenesis. *Chemical Geology*, 137: 175-193.

Appendix 1-1

1. Local names used in Thailand

Name	Meaning
Ao	bay, gulf
Amphoe	district; secondary administrative centre
Ban, Mu Ban	village, small community
Bo	well, shaft, hole, precious-mineral deposit in alluvium
Changwat	provincial capital, city; primary administrative centre
Doi	mount, mountain, or a prominent peak of a mountain (northern region)
Haad	beach
Huai	gully, creek
Kaeng	rapids
Khao	hill, isolated mountain
Khlong	stream, canal (central only)
Khwae	stream, a principal tributary of a river
King Amphoe	group of villages, larger than tambon but smaller than amphoe
Ko	island
Laem	a peninsula or a seaward point of land
Mae	river
Mae Nam, Nam Mae	large river
Muang	town, city
Nam	stream, river
Nam Tok	waterfall
Pha	cliff, a hill with a steep cliff
Phu	hill or mountain (especially in north-eastern area)
Tambon	group of villages; tertiary administrative centre
Tham	cave
Wat	temple

Modified from: Proceedings of the National Conference on "Geologic Resources of Thailand: Potential for Future Development", Dept. Mineral Resources, Bangkok, Thailand 17-24 Nov. 1992, p.vii.

2. Official division of the areas in Thailand

Thailand is divided into 6 regions namely northern region, central region, eastern region, western region, northeastern region, and southern region. It is divided into 76 Changwats (provinces) throughout the country.

1) "Changwat"

There are 76 Changwats (up to 1997) in Thailand e.g. Krung Thep Maha Nakhon (Bangkok Metropolis or Bangkok) (we do not use "Changwat" in front of "Krung Thep..." or "Bangkok"), Changwat Chiang Rai, Changwat Khanchanaburi, Changwat

Chanthaburi, Changwat Phetchabun, Changwat Ubon Ratchathani, Changwat Phuket, etc.. Changwat is divided into "Amphoe" King Amphoe" or "Khet. There are several Amphoes in a Changwat depending on how big of its area, amount of population, or other facilities. For example, there are 5 Amphoes in Changwat Trat namely Amphoe Muang Trat, Amphoe Khao Saming, Amphoe Bo Rai, Amphoe Khlong Yai, and Amphoe Laem Ngop.

2) "Amphoe", "King Amphoe", or "Khet".

Generally, we use "Amphoe", whereas "King Amphoe" is used for a small Amphoe which is almost established to be Amphoe. "Khet" is only used instead of Amphoe in Bangkok. Each Amphoe is divided into various Tambons (= districts).

3) "Tambon" or "Kwaeng"

Tambon is divided into many Mu Bans (= villages) called shortly as "Ban". Mu Ban is a smallest official community in Thailand. "Kwaeng" is only used instead of Tambon of Bangkok.

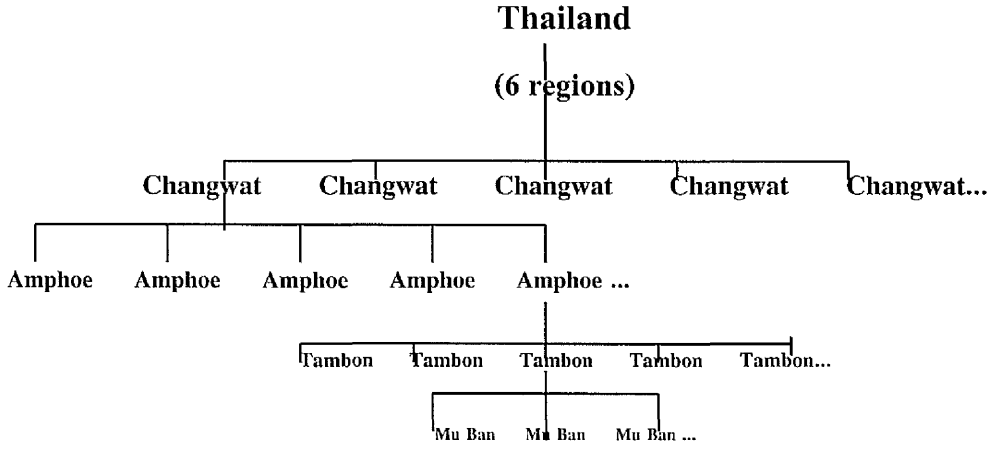

APPENDIX 2-1
ROCK DESCRIPTION

[Arranged in the order of CK, BN, SP, DC, KS, BP, NY, PW, TP, and NB.]

Sample CK1

1. Observations

i) Hand specimen

Colour : Greyish black.

Grain size : Aphanitic.

Obvious phenocrysts : -

Obvious xenocrysts :

1) Anhedral Ulvöspinel-magnetite with vitreous lustre and conchoidal fracture, up to 0.7x1.2 cm.
2) Ulvöspinel-magnetite (3x5 mm). Anhedral opaque with metallic lustre and magnetism.

Obvious xenoliths : Ultramafic nodules. Up to 0.5x1.1 cm.

Obvious amygdales : Round amygdales, up to 5x6 mm, filled with carbonate (? calcite).

Weathering : Surface of specimen is weathered to reddish brown colour and partly shiny lustre. The fracture surfaces are covered by green weathering product, probably clay mineral. The thickness of weathered zone from the surface into the core is up to 3 mm.

ii) Thin section

Phenocrysts : Total mode 1%.

Olivine : Euhedral skeletal phenocrysts up to 1.6 mm long. Some grains are altered to iddingsite. Mode < 1%.

Titanaugite : Subhedral prisms up to 1.8 mm long. Pale pinkish brown. Weak pleochroism. Mode <<< 1%.

Xenocrysts : Total mode 5%.

2Apatite : Sub-rounded irregular to ellipsoidal xenocrysts up to 1.9 mm long. Slightly turbid : show striations? // cleavage. Containing ? metamict zircon inclusion. No reaction rim.

Plagioclase : Well rounded xenocryst 1.5x0.9 mm. Reaction rim.. Showing albite twin.

Olivine : Anhedral xenocryst, 0.55 mm long. Reaction rim.

Ulvöspinel-magnetite : Large sub-rounded xenocrysts. Up to 1.7x3.0 mm. Ulvö spinel-magnetite -matrix contact marked by high concentration of Ulvö spinel-magnetite granules in matrix.

Spinel : Angular brown spinel: 0.2x0.6 mm, Some parts of the rim composed of Ulvöspinel-magnetite granules.

Clinopyroxene : large elongate rounded shape xenocrysts. Up to 3.7 mm long. Showing pale brownish reaction rim.

? Quartz : [Colourless, 1st-order grey-yellow interference colour, no cleavage, fractured,] Two rounded xenocrysts up to 0.7 mm diameter. Surrounded completely by ~0.05 mm thick reaction rim composed of very fine grains or laths of ? clinopyroxene.

Brown aggregate : Large (7x5 mm) rounded aggregate of dark brown (almost opaque) lamellar or feathery masses of ? glass in a paler partially interference colour matrix. Possibly melted plagioclase ? At the rim marked by high concentration of Ulvö spinel-magnetite granules in aggregate.

Xenoliths : -

Matrix : Total mode ~93%.

Plagioclase : Tiny laths up to 0.15 mm long. Euhedral. Lamellar twinning. Mode 10%.

Olivine : Tiny granules up to 0.05 mm long. Euhedral. Mode ~15%.

Ulvöspinel-magnetite : Tiny equant granules << 0.01 mm diameter. Mode 20%.

Glass : Brown. Mode ~47%.

Weathering products : Mode ~ 1%. Orange-brown to light green. Similar to iddingsite. Developed from olivine phenocrysts and in patches in some parts of slide.

Amygdales : Total mode ~1%. Oval shape up to 1.7x2.8 mm. Filled with carbonate (?calcite).

2. Name : Olivine-Phyric Basalt with Xenocrysts

3. Interpretation :

Crystallisation history :

1) Crystallisation of olivine in phenocrysts.
2) Crystallisation of olivine + clinopyroxene in phenocrysts.
3) Crystallisation of olivine + plagioclase + Ulvöspinel-magnetite in matrix.
4) Quenching of glass.

Magma type : Probably alkali olivine basalt ? (Ti-rich augite is only clinopyroxene).

Origin of xenocrysts :

Mantle : Spinel / Olivine / Clinopyroxene.

? : Apatite / Plagioclase / Ulvöspinel-magnetite / ?Quartz / Brown aggregate.

Sample CK2

1. Observations

i) Hand specimen

Colour : Greyish black.

Grain size : Aphanitic.

Obvious phenocrysts : Ulvöspinel-magnetite . Anhedral. Elongate vitreous Ulvöspinel-magnetite up to 1 cm long.

Obvious amygdales : Rounded amygdales, up to 1.5 mm diameter.

Weathering : The surface is weathered to yellowish brown colour. The thickness of weathering zone from the surface into the body of specimen is ~3 mm.

ii) Thin section

Phenocrysts : Total mode <1%.

Olivine : Euhedral skeletal phenocrysts up to 0.8 mm long. Mode <1%. No zoning apparent.

Ti-augite : Rare euhedral prisms up to 0.3x0.1 mm. Mode <<<1%. Pale pinkish brown. Very weak pleochroism. "Hour-glass" sector zoning apparent in PPL and XPL.

Xenocrysts : Total mode 5%.

Spinel : Two xenocrysts visible:

1) Ellipsoidal grey-brown spinel : 1.0x0.3 mm. Unzoned.
2) Rounded grey-green spinel : 0.2 mm diameter. Unzoned.

Both are completely surrounded by a thin (<0.02 mm) opaque reaction rim.

Apatite : Sub-rounded irregular to ellipsoidal xenocrysts up to mm diameter. Slightly turbid : show striations ?// cleavage. No reaction rim.

Plagioclase : Small rounded xenocryst (0.3 mm diameter). Clean rim. Sieve-like interior-cavities filled with brown ?glass in a paler partially interference colour. Possibly melted plagioclase?

?Quartz : [Colourless, 1st order grey interference colour, no cleavage, fractured, uniaxial +ve]. Single rounded xenocryst 0.4 mm diameter. Surrounded completely by ~0.1 mm thick reaction rim composed of colourless glass (near xenocryst) and tiny elongated prisms of ?clinopyroxene.

Xenoliths : Total mode <1%.

Ulvöspinel-magnetite + Apatite : Irregular 3x2 mm. xenolith consisting of 2 grains of Ulvöspinel-magnetite and one euhedral apatite. The xenolith encloses an amygdale filled with calcite. Ulvö spinel-magnetite -matrix contract marked by high concentration of Ulvö spinel-magnetite granules in matrix.

Quartzite : Small, irregular 0.2x0.1 mm polycrystalline quartzite xenolith composed of several quartz grains (max. diameter 0.1 mm). Completely surrounded by a 0.1 mm thick reaction rim composed of randomly oriented needles of ? clinopyroxene.

Matrix. Total mode ~92%.

Plagioclase : Tiny laths up to 0.1 mm long. Euhedral. Lamellar twinning. Mode 15%.

Olivine : Tiny granules up to 0.2 mm long. Euhedral. Some skeletal. Mode 15%.

Ulvöspinel-magnetite : Tiny equant granules. Ca. 10 microns diameter. Mode 15%.

Glass : Brown. Mode ~47%.

Weathering products : Orange-brown. Similar to iddingsite. Developed in patches in some parts of slide.

Amygdales. Total mode ~ 1%.

Round. Up to ~ 0.1 mm diameter. Filled with carbonate (?calcite)

2. Name : Olivine-Phyric Basalt with Xenocrysts and Xenoliths.

3. Interpretation :

Crystallisation history :

1) Crystallisation of Olivine in phenocrysts

2) Crystallisation of Olivine + Clinopyroxene in phenocrysts.

3) Crystallisation of Olivine + Plagioclase + Ulvö spinel-magnetite in matrix.

4) Quenching of Glass.

Magma type : Probably alkali olivine basalt ? (Ti-rich augite in only clinopyroxene).

Origin of Xenoliths / Xenocrysts :

Crust : Quartzite

Mantle : Spinel

? : Apatite + Ulvöspinel-magnetite / Plagioclase.

Sample CK3

1. Observations

i) Hand specimen

Colour : Greyish black.

Grain size : Aphanitic.

Obvious xenocrysts :

1) Large xenocrysts of black vitreous lustre mineral, 2 direction obvious cleavages, 2x1.4 cm, ?pyroxene.

2) Ulvöspinel-magnetite , elongate opaque metallic lustre and magnetism, 1 cm long.

Obvious xenoliths : Ultramafic nodule, Angular shape, 0.8 cm long.

Obvious amygdales : Round to Oval shape, up to 0.1 cm diameter filled with carbonate (?calcite).

Weathering : The specimen is weathered at its surface to yellowish brown. The weathering mantle near the surface is ~0.3 cm thick.

ii) Thin section

Phenocrysts : Total mode <1%.

Olivine : Euhedral skeletal phenocrysts up to 0.45 mm long < 1%. No zoning appearance.

Titanaugite : Rare euhedral prisms up to 0.23 mm long. <<<1%. Pale pinkish brown. Very weak pleochroism. "Hour-glass" sector zoning apparent in PPL and XPL.

Xenocrysts : Total mode ~2%.

Apatite : Sub-rounded to elongate xenocrysts, up to 0.9 mm long. Slightly turbid : showing striations ? // cleavage. No reaction rim.

Olivine : Elongate xenocryst up to 1.2 mm long. Showing reaction rim and resorption zoning in brown colour.

Ulvöspinel-magnetite : sub-rounded xenocryst up to 0.9 mm diameter. Ulvöspinel-magnetite -matrix contact marked by high concentration of Ulvöspinel-magnetite granules.

Brown aggregate : Angular shape (0.7x2.0 mm). Dark brown lamellar or scale masses of ?glass in a paler partially interference colour matrix. Possibly melted amphibole ?

Spinel : Angular brown green spinel (0.3x1.5 mm) Spinel-matrix contact marked by high concentration of magnetic granules.

Xenoliths : Total mode ~ 3%.

Spinel + Clinopyroxene: Large sub-rounded 4x5 mm. xenolith consisting of a large grain of clinopyroxene, showing undulated extinction (sub-grain), brown (Ti-rich) resorption rim which contact to the matrix; and green-brown spinel (with accumulation of Ulvöspinel-magnetite granules at the contact of spinel-matrix).

Quartzite : Ellipsoid xenoliths 0.2 mm long. Showing undulated extinction. Completely surrounded by 0.05 mm thick reaction rim containing radiated small laths of yellow interference colour minerals, probably clinopyroxene ?

Ulvöspinel-magnetite + Apatite : Sub-rounded, 1x1.7 mm xenolith, consisting of 2 gains of Ulvöspinel-magnetite , probably Ulvöspinel-magnetite and ellipsoid apatite crystal (0.3x0.6 mm). Apatite shows striation along the length of the crystal.

Matrix : Total mode ~93%.

Plagioclase : Tiny laths up to ~0.2 mm long. Euhedral. Lamellar twinning. Mode 15%.

Olivine : Tiny granules up to 0.15 mm long. Euhedral. Some skeletal. Mode 15%.

Ulvöspinel-magnetite : Tiny equant granules <<0.01 mm diameter. Mode 25%.

Glass : Brown. Mode 38%.

Weathering products : Orange-brown, similar to iddingsite. Developed in patches in some parts of slide. Greenish yellow colloform mineral in some part of matrix.

Amygdales : Total mode <<1%.

Round, up to ~0.7 mm diameter. Filled with carbonate (?calcite).

2. Name : Olivine-Phyric Basalt with Xenocrysts and Xenoliths.

3. Interpretation :

Crystallisation history :

1) Crystallisation of olivine in phenocrysts

2) Crystallisation of olivine + clinopyroxene in phenocrysts

3) Crystallisation of olivine + plagioclase + Ulvö spinel-magnetite in matrix.

4) Quenching of glass.

Magma type : Probably alkali olivine basalt ? (Ti-rich augite is only clinopyroxene).

Origin of xenoliths/xenocrysts :

Crust : Quartzite

Mantle : Spinel

? : Apatite + Ulvöspinel-magnetite / Unknown mineral.

Sample CK3/1

1. Observations

i) Hand specimen

Colour : Greyish black.

Grain size : Aphanitic.

Obvious xenocrysts :

1) Large xenocrysts of black vitreous lustre mineral, 2 direction obvious cleavages, 2x1.4 cm, ?pyroxene.

2) Ulvöspinel-magnetite , elongate opaque metallic lustre and magnetism, 1 cm long.

Obvious xenoliths : Ultramafic nodule, Angular shape, 0.8 cm long.

Obvious amygdales : Round to Oval shape, up to 0.1 cm diameter filled with carbonate (?calcite).

Weathering : The specimen is weathered at its surface to yellowish brown. The weathering mantle near the surface is ~0.3 cm thick.

ii) Thin section

Phenocrysts : Total mode 1%.

Olivine : Euhedral phenocrysts up to 03x0.35 mm. Skeletal. Most are altered to yellow-orange (? iddingsite). Mode <1%

Clinopyroxene: Rare euhedral xenocrysts. Up to 0.1x0.2 mm. Pale pinkish brown. Resorption zoning. Mode <<<1%.

Xenocrysts : Total mode 3%

Spinel: 1). A grey sub-rounded xenocrysts (0.5x0.6 mm). At the rim (<0.02 mm thick) has the accumulation of tiny (<0.01 mm diameter) granules of Ulvö spinel-magnetite .

2). Two irregular deep green (up to 0.2 mm diameter) xenocrysts. At the rim shows the same characteristic.

Olivine: Sub-rounded xenocryst (up to 0.3x0.3 mm). Alteration rim (<0.01 mm thick) of iddingsite. Unzoned.

Apatite: Sub-rounded elongate xenocrysts. Up to 0.6x1.4 mm. Striation. [length show, 1st order grey 11 extinction].

Melted amphibole: A large (6.0x10.0 mm) aggregated, composed of mainly the brown tiny prismatic crystals (up to 0.1 mm long), [2nd order interference colour] ? clinopyroxene granules (up to 0.1 mm diameter) and glass. There are parts of greenish brown amphibole (?hornblende) remaining at the core (up to 1.0 mm long). The oval cavities (up to 1.2 mm diameter) filled with ? clay mineral or amorphous [colourless, isotopic].

Melted xenocryst: A sub-rounded aggregate (1.2x1.8 mm) composed of glass and mantled by a layer (~0.2 mm thick) of tiny needles and laths of ? clinopyroxene (up to 0.1 mm long). In the glass (at core) contains very tiny granules of ? clinopyroxene (<<<<0.01 mm).

Ulvöspinel-magnetite : An irregular xenocryst (0.20x0.45 mm).

Xenoliths : -

Matrix : Total mode 94%.

Olivine : Tiny granules up to 0.15 mm diameter. Euhedral. Some skeletal. Mode 15%.

Plagioclase feldspar: Tiny laths. Up to 0.15 mm long. Euhedral. Lamellar twinning. Mode 15%

Ulvöspinel-magnetite : Tiny granules,<0.02 mm diameter. Euhedral. Mode 25%.

Glass : Brown. Mode 39%.

Amygdales : Total mode 2%.

Rounded amygdales. Up to 8 mm diameter. Filled with carbonate (?calcite) which shows layers of radiated structure with black and brown impurities. Some are empty.

2. Name : Olivine-Phyric Basalt with Xenocrysts.

3. Interpretation :

Crystallisation history :

1) Crystallisation of olivine in phenocrysts
2) Crystallisation of olivine + clinopyroxene in phenocrysts
3) Crystallisation of olivine + plagioclase + Ulvö spinel-magnetite in matrix.
4) Quenching of glass.

Magma type : Probably alkali olivine basalt ?

Origin of xenoliths/xenocrysts :

Crust : -

Mantle : Spinel / Olivine /

? : Apatite / Melted amphibole / Melted xenocryst / Ulvöspinel-magnetite .

<u>Sample CK4</u>

1. Observations

i) Hand specimen

Colour : Greyish black.

Grain size : Aphanitic.

Obvious phenocrysts : -

Obvious xenocrysts :

1) Clinopyroxene. Black vitreous lustre, conchoidal fracture , and anhedral mineral up to 2x4 mm.
2) Ulvöspinel-magnetite . Black metallic lustre anhedral mineral. Magnetism. Up to 2x3 mm.

Obvious amygdales : Rounded to oval amygdales, up to 6 mm long.

Weathering : The surface is weathered to reddish brown material. The thickness of weathering mantle is ~2 mm.

ii) Thin section

Phenocrysts : Total mode ~1%.

Olivine: Euhedral skeletal phenocrysts up to 0.62 mm long. No zoning. Mode <1%.

Ti-augite: Euhedral prisms, up to 0.25 mm. Mode <<<1%. Pale pinkish brown. Very weak pleochroism. "hour-glass" sector zoning in PPL and XPL.

Xenocrysts : Total mode ~5%.

Clinopyroxene : Angular to rounded ellipsoid xenocrysts, up to 5.5 mm long. Showing resorption rim in brown colour.

Spinel : Two xenocrysts visible.

1) Tiny sub-rounded green-brown spinel: 0.1 mm diameter.
2) Sub-rounded brown-green spinel : 0.2x0.25 mm. Completely surrounded by a thin (<0.02 mm) opaque reaction rim.

Apatite : Sub-rounded irregular to elongate xenocrysts, up to 0.4 x 2.1 mm. Slightly turbid. Showing striations ? // cleavage.

Brown aggregate : Large (0.5x1.0 mm) irregular shape. Containing plagioclase lamellar, granular of low interference colour mineral, probably ?glass in matrix. Possibly melted ?amphibole.

Xenoliths : Total mode <1%.

Ulvöspinel-magnetite + Apatite : Sub-angular to sub-rounded Ulvöspinel-magnetite crystals, up to 1.8x3.0 mm. Containing tiny subhedral crystal of apatite, up to 2.0 mm diameter. Xenoliths-matrix contact marked by high concentration of Ulvöspinel-magnetite granules in matrix.

Matrix : Total mode 92%.

Plagioclase : Tiny laths up to 0.35 mm long. Euhedral. Lamellar twinning . Mode 15%.

Olivine : Tiny granules up to 0.1 mm long. Euhedral. Some skeletal. Mode 15%.

Ulvöspinel-magnetite : Tiny equant granules, <<0.1 mm diameter. Mode 20%.

Glass : Brown. Mode ~42%.

Weathering products : 1). Orange-brown. Similar to iddingsite.

2) Yellow-green. Colloform apparent.

Both developed in some parts of matrix.

Amygdales : Total mode <1%.

Rounded amygdales. Up to 0.75 mm diameter. Filled with carbonate (?calcite). Some are empty.

2. Name : Olivine-Phyric Basalt with Xenocrysts and Xenoliths.

3. Interpretation :

Crystallisation history :

1) Crystallisation of olivine in phenocrysts.
2) Crystallisation of olivine + clinopyroxene in phenocrysts.
3) Crystallisation of olivine + plagioclase + Ulvöspinel-magnetite in matrix.
4) Quenching or glass.

Magma type : Probably alkali olivine basalt? (Ti-rich augite is only clinopyroxene).

Origin of xenoliths / xenocrysts :

Mantle : Spinel.

? : Ulvöspinel-magnetite + Apatite / Clinopyroxene / Brown aggregate.

<u>Sample CK5</u>

1. Observations

i) Hand specimen

Colour : Greyish black.

Grain size : Aphanitic

Obvious phenocrysts : -

Obvious xenocrysts : Ulvöspinel-magnetite . Euhedral, sub-rounded xenocrysts. Up to 0.4 mm diameter.

Obvious xenoliths : -

Obvious amygdales : Empty and carbonate filled amygdales. Round and oval shapes. Up to 8 mm long.

Weathering : The surface of specimen is weathered to reddish brown and yellow materials. At the margin of empty amygdales is crusted with white clay mineral?.

ii) Thin section

Phenocrysts : Total mode 1%.

Olivine : Euhedral skeletal phenocrysts : up to 1.5x0.7 mm. No zoning. Mode <1%.

Clinopyroxene : Subhedral crystals, up to 0.2x0.4 mm. No zoning. The rims are altered to orange-brown. Pinkish brown colour. Weak pleochroism. Showing unclean sector zoning in PPL and XPL. Mode <<1%.

Xenocrysts : Total mode ~5%.
- **Olivine :** Irregular xenocrysts: 0.45x0.8 mm. Iddingsite alteration rim (<<0.01 mm thick).
- **?Melted clinopyroxene :** Irregular xenocrysts, up to 0.4x1.0 mm. Composed of the masses of tiny crystals.
- **Spinel :** Sub-rounded spinels: up to 0.8x1.3 mm. Grey-brown colour.
- **Apatite :** Sub-rounded xenocrysts: up to 0.9x1.5 mm. Slightly turbid Showing striation along the length of crystals. Some grains show 3 directions of cleavage.
- **Unknown minerals :** Two unknown minerals:
  1) [1st order interference colour, no cleavage, probably ?quartz] Sub-rounded xenocrysts up to 0.2 mm diameter. Completely surrounded by tiny laths of yellow interference colour minerals, ? clinopyroxene.
  2) Light brown colour. Wedge shape (0.3x0.6 mm). 3 directions of cleavage, ?apatite.
- **Brown aggregate :** Large dark brown aggregate (2x5 mm). Almost opaque lamellar or feathery masses of ?glass in a paler partially interference colour matrix. Possibly melted plagioclase ?.
- **Plagioclase :** Angular xenocryst: 0.2x0.2 mm. Showing resorption zoning in XPL.
- **Ulvöspinel-magnetite s :** Sub-angular to sub-rounded xenocrysts (up to 1.5x1.7 mm). Showing curved fractures.

Xenoliths : Total mode ~ 1%.
- **Spinel + Olivine :** Sub-rounded elongate xenolith (0.8x2.0 mm). Consisting of large grey-brown spinel and rounded olivine (0.25 mm diameter).
- **Ulvöspinel-magnetite + Apatite :** Irregular xenoliths up to 0.50x1.00 mm, containing tiny rounded apatite (0.15 mm diameter). Ulvöspinel-magnetite - matrix contact marked by high concentration of Ulvöspinel-magnetite granules in matrix.
- **Quartzite :** Sub-rounded xenolith (0.2 mm diameter). Completely surrounded by reaction rim (0.02 mm thick), composed of randomly oriented ?clinopyroxene laths.

Matrix : Total mode 93%.
- **Plagioclase :** Tiny laths up to 0.2 mm long. Euhedral-lamellar twinning. Mode 15%.
- **Olivine :** Tiny granules up to 0.1 mm long. Euhedral. Some skeletal. Mode 15%
- **Ulvöspinel-magnetite :** Tiny equant granules <<0.01 mm diameter. Mode 25%.
- **Glass :** Brown. Mode ~43%.
- **Weathering products :**
  1) Orange-brown. Similar to iddingsite. Developed in patches in some parts of slide. Some granules of olivine altered to iddingsite.
  2) Green-yellow. Developed in patches in some parts of slide. Showing colloform characteristic.

(**Remark** : This sample has a high degree of alteration).

Amygdales : Total mode ~1%.
Round to oval shape up to 2.0x3.0 mm. Filled with carbonate (? calcite). Some are empty.

2. **Name : Olivine-Phyric Basalt with Xenocrysts and Xenoliths.**
3. **Interpretation :**
   - **Crystallisation history :**
     1) Crystallisation of olivine in phenocrysts.
     2) Crystallisation of olivine + clinopyroxene in phenocrysts.
     3) Crystallisation of olivine + plagioclase + Ulvöspinel-magnetite in matrix.
     4) Quenching or glass.
   - **Magma type :** Probably alkali olivine basalt ? (Ti-rich augite is only clinopyroxene).
   - **Origin of xenoliths /xenocrysts :**
     - **Crust :** Quartzite.
     - **Mantle :** Spinel / Spinel + Olivine / Olivine / Clinopyroxene.
     - **? :** Ulvöspinel-magnetite + Apatite / Apatite / Brown aggregate.

Sample CK6

1. **Observations**
   - **i) Hand specimen**
     - **Colour :** Greyish black.
     - **Grain size :** Very fine
     - **Obvious phenocrysts :** -
     - **Obvious xenocrysts :** Irregular shaped Ulvöspinel-magnetite (0.8x1.0 cm).
     - **Obvious xenoliths :** -
     - **Obvious amygdales :** Rounded to oval amygdales : up to 3.5x4.0 mm. Some are empty.
     - **Weathering :** The surface of specimen is weathered to yellowish brown. The thickness zone of weathering zone is < 1mm.
   - **ii) Thin section**
     - **Phenocrysts :** Total mode ~1%.
       - **Olivine :** Euhedral skeletal crystals : up to 0.45x0.7 mm. Some are elongate skeletal crystals, up to 1.0 mm long. Mode <1%. No zoning.
       - **Clinopyroxene :** Tabular phenocrysts : up to 0.15x0.30 mm. Pinkish brown. Weak pleochroism. Some crystals show "hour-glass" sector zoning. << 1%.
     - **Xenocrysts :** Total mode ~5%.
       - **Olivine :** Sub-angular to sub-rounded xenocrysts : up to 0.8x1.0 mm. Unzoned.
       - **Spinel :** Two xenocrysts visible :
         1) Sub-rounded grey-brown spinel : 2.0x2.5 mm. Unzoned.
         2) Angular dark brown spinel : 0.1x0.3 mm. Unzoned.

         Both are completely surrounded by a thin (<0.02 mm) opaque reaction rim.
       - **Clinopyroxene :** Ellipsoidal xenocrysts : 0.1x0.3 mm. Ti-rich at rim. Showing zoning in XPL.
       - **Ulvöspinel-magnetite :** Large irregular to sub-round xenocrysts : up to. 3.0 mm diameter.
       - **Apatite :** Irregular xenocrysts : up to 0.8 mm long. Slightly turbid. Showing striation.
       - **Brown aggregate :** Large oval aggregate : 2.0x4.5 mm. Composed of dark brown (almost opaque) lamellar or feathery masses of ? glass in a paler partially interference colour matrix (? Clinopyroxene). Possibly plagioclase ?.
       - **Unknown minerals :** [1st order grey to yellow, low relief, ? quartz]. Irregular xenocryst (0.15x0.40 mm). Completely surrounded by a rim (0.05 mm thick) composed of randomly oriented tiny laths of ?clinopyroxene.
     - **Xenoliths -**
     - **Matrix :** Total mode 93%.
       - **Plagioclase :** Tiny laths up to 0.2 mm long. Euhedral. Lamellar twinning . Mode 15%.
       - **Olivine :** Tiny granules up to 0.1 mm long. Euhedral. Some skeletal. Mode 15%.
       - **Ulvöspinel-magnetite :** Tiny equant granules <<0.01 mm diameter. Mode 20%
       - **Glass :** Brown . Mode ~43%.
       - **Weathering products :** Some olivine in matrix altered to iddingsite. Orange-brown.
     - **Amygdales :** Total mode ~1%.
       Round amygdales : up to ~30 mm diameter. Filled with carbonate (? calcite).
2. **Name : Olivine-Phyric Basalt with Xenocrysts**
3. **Interpretation :**
   - **Crystallisation history :**
     1) Crystallisation of olivine in phenocrysts.
     2) Crystallisation of olivine + clinopyroxene in phenocrysts.
     3) Crystallisation of olivine + plagioclase + Ulvöspinel-magnetite in matrix.
     4) Quenching or glass.
   - **Magma type :** Probably alkali olivine basalt ? (Ti-rich augite is only clinopyroxene).
   - **Origin of xenocrysts :**
     - **Mantle :** Spinel / Olivine.

? : Clinopyroxene / Ulvöspinel-magnetite / Apatite / Brown aggregate / Unknown mineral.

Sample BN1

1. Observations

i) Hand specimen

Colour : Dark grey.
Grain size : Very fine
Obvious phenocrysts : -
Obvious xenocrysts : -
Obvious xenoliths : Ultramafic nodules : up to 0.4x1.2 cm.
Obvious amygdales : -
Weathering : The specimen is rather fresh but there is a thin weathering to white and pale yellow layer in fractures.

ii) Thin section

Phenocrysts : Total mode ~1%.

Olivine : Euhedral crystals : up to 0.5 mm long. <1%. Unzoned. Some crystals show penetration twin. Some skeletal.

Titanaugite : Rare euhedral prism up to 0.1x0.3 mm. <<<1%. Pale pinkish brown. Very weak pleochroism. "Hour-glass" sector zoning appearance in PPL and XPL.

Xenocrysts : Total mode ~1%.

Spinel : Irregular green-brown xenocryst (0.9x1.2 mm). Completely surrounded by a thin (~0.01 mm) opaque reaction rim.

Yellow Aggregate : Irregular (up to 0.4 x 1.1 mm) aggregates of yellow granule masses of ?clinopyroxene [2nd order yellow interference colour]. Probably ?melted clinopyroxene.

Clinopyroxene : Oval slightly green xenocrysts (1.3x1.7 mm). Resorption zoning, Ti-rich (brown) at rim. Leucite surrounding outside the margin.

Olivine : Irregular xenocrysts up to 0.85 x 1.90 mm. Slightly reaction rim. Undulated extinction (dislocation lattices).

Xenoliths : Total mode ~5%.

Quartzite : Irregular xenolith (0.6 x0.8mm). Composed of several subhedral quartz crystals. Showing undulated extinction. Slightly reaction rim.

Melted xenoliths : Large aggregates. Up to 7.0x9.0 mm. Composed of glass and needle-like to swallow tail (up to 0.75 mm long) clinopyroxene in core. Surrounded by a thick (~3.00 mm) layer containing of various minerals:
1) Radiated euhedral twinning plagioclase laths (up to 0.6 mm long)
2) Euhedral tabular to equant clinopyroxene crystals (up to 0.05x0.3 mm). Some are hollow.
3) Colloform of fibrous unknown mineral [1st ordered grey interference colour, brown in PPL].
4) Colloform of fibrous orangy brown unknown mineral [2nd order yellow interference colour, ? clinopyroxene].

Matrix : Total mode 93%.

Olivine : Tiny granules up to 0.15 mm long. Anhedral. Unzoned. Mode 7%

Clinopyroxene : Tiny laths up to 0.1 mm long. Euhedral. Mode 15%.

Plagioclase : Tiny laths up to 0.7 mm long. Euhedral. Lamellar twinning. Mode 15%.

Ulvöspinel-magnetite : Tiny granules up to 0.1 mm long. Mode 25%. Glass : Colourless. Mode 31%.

Weathering products :
1) Orange-brown. Developed in fracture and some parts of matrix.
2) Yellow green . Developed at the fractures of olivine crystals.

Amygdales : -

2. Name : Olivine-Phyric Basalt With Xenocrysts And Xenoliths

3. Interpretation :

Crystallisation History :
1) Crystallisation of olivine in phenocrysts.
2) Crystallisation of olivine + clinopyroxene in phenocrysts
3) Crystallisation of olivine + clinopyroxene + plagioclase + Ulvöspinel-magnetite in matrix.
4) Quenching of glass and core of melted xenoliths.

Magma type : Probably alkali olivine basalt? (Ti-rich augite is only clinopyroxene).

Origin of xenocrysts :
Crust : Quartzite.
Mantle : Spinel / olivine / Clinopyroxene.
? : Melted xenoliths / Yellow aggregate.

Sample BN2

1. Observations

i) Hand specimen

Colour : Dark grey.
Grain size : Very fine.
Obvious phenocrysts : -
Obvious xenocrysts : Black mineral (3.0x5.0 mm). Conchoidal fracture. Vitreous lustre.
Obvious xenoliths : Undefined very pale green dull xenoliths. Irregular shape. Up to 3.0x4.0 mm.
Obvious amygdales : -
Weathering : The surface of specimen is weathered to pale brown colour. The weathered zone is very thin (<< 1 mm).

ii) Thin section

Phenocrysts : Total mode 1%.

Olivine : Euhedral skeletal equant to prism phenocrysts: up to 0.3x0.7 mm. Unzoned. Mode <1%.

Titanaugite : Rare euhedral prism up to 0.1x0.25 mm. <<<1%. Pale pinkish brown. Very weak pleochroism. "Hour-glass" sector zoning apparent in PPL and XPL.

Xenocrysts : Total mode 3%.

Clinopyroxene : Sub-rounded xenocrysts. Up to 1 mm diameter. Thick (up to 0.4 mm) reaction rim composed of tiny granules of ?clinopyroxene.

Orthopyroxene : Irregular (up to 1.5 x 2.2 mm) xenocrysts. Some are completely surrounded by 0.7 mm thick reaction rim composed of tiny granules of ? clinopyroxene.

Yellow Aggregate : Angular (up to 0.9 x 1.1 mm) masses of tiny yellow granules. [2nd order yellow interference colour]. Probably melted clinopyroxene ?.

Olivine : Irregular xenocrysts up to 1.3x1.7 mm. Slightly reaction rim. Alteration product (yellowish green) along fractures. Undulated extinction (dislocation lattice). Some grains show resorption zoning at rim with high Fe rim (higher interference colour) and high Mg core (lower interference colour).

?Feldspar : [1st order grey] . Resorption rim.

Xenoliths : Total mode ~ 2%.

Plagioclase : Irregular xenolith (0.6 x 1.0 mm) Resorption zoning at rim (<<<0.1 mm thick). Showing ? Carlsbad twin.

? Melted xenoliths : Sub-rounded aggregates of various minerals. Up to 3.5x4.5 mm. Containing glass and some equant clinopyroxene crystals (up to mm diameter). Completely surrounded by very thick (up to 1.4 mm) layer of various minerals:
1) Radiated euhedral Carlsbad twin plagioclase laths (up to 0.05x0.5 mm long).
2) Granules and laths of clinopyroxene crystals (up to 0.2 mm long).

?Quartzite : Irregular 0.7x0.9mm polycrystalline brown quartzite, composed of several quartz grains (max. diameter 0.1 mm). Unclean inter-grain boundaries. The xenolith enclose 2 irregular (~0.1 mm

diameter) carbonate (?calcite) aggregates.

Olivine + Spinel + Clinopyroxene : Olivine shows sub-grain aggregates (uneven extinction).

Matrix : Total mode 94%.

Olivine : Tiny granules up to 0.1 mm long. Euhedral. Mode 7%.

Clinopyroxene : Tiny clinopyroxene laths up to 0.05 mm long. Euhedral. Mode 25%.

Ulvöspinel-magnetite : Tiny equant granules up to 0.1 mm diameter. Mode 15%.

Plagioclase : Tiny laths up to 0.1 mm long. Euhedral. Lamellar twinning . Mode 10%.

Glass : Colourless. Mode 37%.

Weathering products : Yellowish green formed at the fractures of olivine crystals. Orange-brown formed in some parts of thin section.

2. Name Olivine-Phyric Basalt with Xenocrysts and Xenoliths.

3. Interpretation :

Crystallisation History :

1) Crystallisation of olivine in phenocrysts.
2) Crystallisation of clinopyroxene in phenocrysts.
3) Crystallisation of olivine + clinopyroxene + Ulvö spinel-magnetite + plagioclase.
4) Quenching of glass.

Magma type : Probably alkali olivine basalt ? (Ti-rich augite is only clinopyroxene)

Origin of xenoliths /xenocrysts :

Crust : ?Quartzite

Mantle : Olivine / Clinopyroxene / Orthopyroxene.

? : Melted xenoliths / Plagioclase / Yellow aggregate.

Sample BN3

1. Observations

i) Hand specimen

Colour : Dark grey.

Grain size : Very fine.

Obvious phenocrysts : -

Obvious xenocrysts :

1) Black opaque angular xenocrysts. Up to 5x8 mm.
2) Amphibole. Dark brown irregular xenocrysts, 1 cm long. Step-like cleavages. Vitreous lustre.

Obvious xenoliths :

1) Quartzite xenoliths : Sub-rounded. Up to 1 cm long.
2) Large pieces of rock: Up to 1.2x1.8 cm. Irregular shape. White-grey colour.

Obvious amygdales : -.

Weathering : Weathered surface is white to brown. Fe-oxide stain in the fractures.

ii) Thin section

Phenocrysts : Total mode 1%.

Olivine : Euhedral skeletal phenocrysts up to 0.65 mm long. No zoning. <1%.

Clinopyroxene : Rare euhedral prism to equant phenocrysts up to mm long. Pale pinkish brown. Very weak pleochroism. Oscillatory-sector zoning appears in XPL.<<<1%.

Xenocrysts : Total mode 2%.

Amphibole : Euhedral green to yellow brown xenocrysts : up to 4.0x9.0 mm. Perfect cleavages (~120, 60 degrees).

Spinel : Sub-rounded brown xenocrysts. Up to 0.3x0.5 mm. Unzoned. Completely surrounded by a thin (<0.02 mm) opaque reaction rim.

Olivine : Irregular xenocrysts: up to 0.6x1.9 mm. Unzoned. Completely surrounded by reaction rim.

Ulvöspinel-magnetite : Irregular curved fracture xenocrysts : up to 0.4x2.0 mm. Ulvöspinel-magnetite -matrix contact marked by high concentration of Ulvöspinel-magnetite granules in matrix.

Clinopyroxene : Sub-rounded xenocrysts. Up to 0.60x0.95 mm. Resorption zoning at rim by showing brown colour. (Ti -rich rim).

Biotite : An elongate black aggregate. Composed of very tiny black or brown granules . Showing foliation bands of accumulation. Between the bands is filled with matrix. Probably melted biotite. <<<< 1%.

Orthopyroxene : <<<< 1%.

Xenoliths : Total mode ~2%.

?Volcanic rock xenoliths : Large sub-rounded up to 4x6 mm. pale brown xenoliths. Turbid. Composed mainly of dust-like materials. (?glass and tiny granules of ?clinopyroxene). Some contain plagioclase feldspar crystals. Probably ? dacite xenoliths.

Quartzite : Small irregular 0.3x0.5mm. polycrystalline quartzite xenolith. Composed of several quartz grains (max. diameter 0.08 mm). Completely surrounded by a thin (<0.01 mm) cumulative layer of tiny laths of clinopyroxene in matrix.

Matrix : Total mode 94%.

Olivine : Tiny granules up to 0.2 mm long. Euhedral. Some skeletal. Mode 7%.

Clinopyroxene : Tiny laths up to 0.1 mm long. Euhedral. Mode 20%.

Ulvöspinel-magnetite : Tiny equant granules up to 0.05 mm diameter. Mode 20%.

Plagioclase : Tiny laths up to 0.1 mm long. Euhedral. Lamellar twinning. Mode <1%.

Glass : Colourless. Mode 46%.

Weathering products :

1) Some grains of olivine altered to orange-brown ? iddingsite.
2) Reddish brown stain embedded in fractures.

Amygdales : Total mode <1%.

Oval amygdales : up to ~0.6x0.9 mm. Filled with carbonates (?calcite) and brown / yellow / black layers of colloform minerals.

2. Name : Olivine-Phyric Basalt with Xenocrysts and Xenoliths.

3. Interpretation :

Crystallisation History :

1) Crystallisation of olivine in phenocrysts.
2) Crystallisation of olivine + clinopyroxene in phenocrysts.
3) Crystallisation of olivine + clinopyroxene + Ulvö spinel-magnetite + plagioclase in matrix.
4) Quenching of glass.

Magma type : Probably alkali olivine basalt ? (Ti-rich augite is only clinopyroxene).

Origin of xenoliths /xenocrysts :

Crust : Quartzite.

Mantle : Spinel, Olivine.

? : Volcanic rock xenoliths.

? : Amphibole / Ulvöspinel-magnetite / Clinopyroxene.

Sample BN4

1. Observations

i) Hand specimen

Colour : Dark grey.

Grain size : Very fine

Obvious phenocrysts : -

Obvious xenocrysts : -

Obvious xenoliths :

1) Ultramafic nodules 1x3 mm.
2) Undefined yellow dull xenoliths up to 1 x 3 mm.

Obvious amygdales : -

Weathering : Yellow-brown developed in surface of cavities in the specimen.

ii) Thin section

Phenocrysts : Total mode 2%.

Olivine : Euhedral phenocrysts up to 0.6 mm long. No zoning. <1%.

Ti Augite : Subhedral phenocrysts up to 0.4x0.5 mm. ~1%. Pale green core, pinkish brown rim (Ti-rich). Weak

pleochroism. Showing oscillatory-sector zoning in XPL.

Xenocrysts : Total mode 1%.

Olivine : Sub-rounded xenocrysts: up to 0.9x1.1 mm. Showing reaction zoning at rim Fe-rich: more extinction than core (Mg-rich)).

Clinopyroxene : Irregular (up to 0.6x1.6 mm) xenocrysts. Containing of tiny equant clinopyroxene crystals (up to 0.1 mm diameter). Pinkish brown at rim. Probably melted clinopyroxene.

Xenoliths : Total mode ~5%.

Spinel-harzburgite : Large angular (up to 8x8 mm) polycrystalline harzburgite xenoliths. Composed of

1) Several subhedral of olivine grains (up to 0.5x0.6 mm). Some show undulated extinction (deformed lattices). Mode ~80% of xenolith.
2) Anhedral orthopyroxene grains (up to 0.4x0.7 mm). Mode ~18% of xenolith.
3) Irregular brown spinel (up to 0.65 mm long).

Clinopyroxene : Small, irregular 0.4x0.4 mm. xenolith. Composed of 3 clinopyroxene grains (max. diameter 0.3 mm). Showing resorption brown zoning (Ti-rich) at rim, pale core.

Matrix : Total mode 91%.

Clinopyroxene : Tiny laths up to 0.2 mm long. Euhedral. No zoning. Mode 25%.

Olivine : Tiny granules up to 0.1 mm long. Euhedral. Mode 5%.

Ulvöspinel-magnetite : Tiny equant granules up to 0.1 mm diameter. Mode 15%.

Plagioclase : Tiny laths up to 0.2 mm long. Euhedral. Lamellar twinning . Mode 10%.

Glass : Colourless. Mode ~36% Some areas (up to 0.9x2.2 mm) of glass matrix contain brown to black slender dendritic form mineral.

Weathering products : Orange-brown. Similar to iddingsite. Developed in patches in some parts of slide.

Amygdales : Total mode <<1%.
Sub-rounded up to 0.15 mm. Filled with carbonates (?calcite).

2. Name : Olivine-Phyric Basalt With Xenocrysts And Xenoliths

3. Interpretation :

Crystallisation history :

1) Crystallisation of olivine in phenocrysts.
2) Crystallisation of olivine + clinopyroxene in phenocrysts.
3) Crystallisation of olivine + clinopyroxene + Ulvö spinel-magnetite + plagioclase in matrix.
4) Quenching of glass.

Magma type : Probably alkali olivine basalt ? (Ti-rich augite is only clinopyroxene).

Origin of xenoliths /xenocrysts :

Mantle : Spinel-harzburgite / Olivine / Clinopyroxene.

Sample BN5

1. Observations

i) Hand specimen

Colour : Dark grey.
Grain size : Very fine.
Obvious phenocrysts : -
Obvious xenocrysts :
Obvious xenoliths : Undefined irregular brown to white xenoliths, up to 4x5 mm.
Obvious amygdales : -.
Weathering : -

ii) Thin section

Phenocrysts : Total mode 1%.

Olivine : Euhedral phenocrysts up to 0.4x0.45 mm long. Unzoned. Showing alteration rim of iddingsite (yellowish green to brown). <1%.

Ti Augite : Rare euhedral prism up to 0.1x0.3 mm. Pale pinkish brown rim Very weak pleochroism. "Hour-glass" sector zoning apparent in PPL and XPL. <<1%.

Xenocrysts : Total mode 1%.

Olivine : Sub-rounded xenocrysts: up to 0.8 mm diameter. Undulated extinction (indicating deformed lattices). Resorption zoning (Fe-rich rim, Mg-rich core) marked by more extinction at rim than core.

Spinel : Dark brown irregular xenocryst (0.4x0.6 mm). Completely surrounded by a thick (0.15 mm) opaque reaction rim.

Plagioclase : Irregular colourless xenocrysts. Up to 0.2x1.1 mm. Showing resorption zoning in XPL.

Xenoliths : Total mode ~ 5%.

Quartzite : Sub-rounded colourless and brown stain polycrystalline quartzites. Up to 8x10 mm. Containing several quartz grains (max. diameter 1.0 mm). Completely surrounded by a thick (~0.3 mm) reaction rim composed of randomly oriented needle of ? clinopyroxene.

Spinel + Olivine : Irregular 2.0x3.6 mm. of xenolith consisting of 3 grains of anhedral olivine (up to 1.8x2.0 mm) and one anhedral brown spinel crystal (1.2x1.5 mm). Spinel shows opaque (~0.05 mm thick) reaction rim at the part which contact to the matrix. One of olivine crystals shows undulated extinction.

?Plagioclase or ?Zeolite : Irregular up to 1.2x1.5 mm. Colourless aggregates composed of random orientation tabular (up to 0.25x0.50 mm). Euhedral crystals. [1st order grey interference colour]. Completely surrounded by a reaction rim (~0.3 mm thick) composed of randomly oriented ?clinopyroxene needles.

Matrix : Total mode 93%.

Plagioclase : Tiny laths up to 0.4 mm long. Euhedral. Lamellar twinning. Mode 15%.

Clinopyroxene : Tiny laths up to 0.1 mm long. Euhedral. Mode 15%.

Olivine : Tiny granules up to 0.2 mm long. Euhedral. Some hollow. Mode 10%.

Ulvöspinel-magnetite : Tiny equant granules up to 0.2 mm diameter. Mode 15%.

Glass : Colourless. Mode 38%.

Weathering products :

1) Some olivine crystals altered to iddingsite (yellow-green brown).
2) Orange-brown. Developed in patched in some parts of matrix.

Amygdales : -

2. Name : Olivine-Phyric Basalt with Xenocrysts and Xenoliths.

3. Interpretation :

Crystallisation history :

1) Crystallisation of olivine in phenocrysts.
2) Crystallisation of olivine + clinopyroxene in phenocrysts.
3) Crystallisation of olivine + clinopyroxene + plagioclase + Ulvöspinel-magnetite in matrix.
4) Quenching of glass.

Magma type : Probably alkali olivine basalt ? (Ti-rich augite is only clinopyroxene).

Origin of xenocrysts / xenoliths :

Crust : Quartzite.
Mantle : Spinel + Olivine / Spinel / Olivine.
? : Plagioclase / ?Plagioclase or ?Zeolite.

Sample BN6

1. Observations

i) Hand specimen

Colour : Dark grey.
Grain size : Very fine
Obvious phenocrysts : -
Obvious xenocrysts : Sub-rounded metallic lustre xenocrysts. Black. Up to 1 mm diameter. Ulvö spinel-magnetite .

Obvious xenoliths : White dull irregular patches of xenoliths, up to 2x4 mm.
Obvious amygdales : -.
Weathering : Yellow brown. Developed in a thin (<1 mm) layer on the surface of the specimen.

ii) Thin section

Phenocrysts : Total mode 2%.

Olivine : Euhedral skeletal phenocrysts up to 1.6 mm long. <1% . No zoning apparent

Titanaugite : Rare euhedral equant to prismatic crystals. up to 0.15x0.05 mm. Pale pinkish brown. Very weak pleochroism. "Hour-glass" sector zoning apparent in XPL. <<1%.

Ulvöspinel-magnetite : Sub-rounded phenocrysts. Up to 0.3 mm diameter. <<<1%.

Xenocrysts : Total mode ~1%.

Orthopyroxene : Elongate xenocryst (0.9x2.5 mm). Completely surrounded by thick (0.5 mm) reaction rim composed of dense granules of ? clinopyroxene. The xenocryst-matrix contact marked by (0.5 mm thick) containing ?devitrified needle-like glass, blebs (lamellars) of Ulvöspinel-magnetite (up to 0.15 mm long), and clinopyroxene laths (up to 0.05 mm long).

Olivine : Irregular xenocrysts up to 1.0x1.8 mm. Showing sub-grain structure (undulated extinction). The grain boundaries and fracture zone are altered to iddingsite (yellow brown).

Clinopyroxene : Euhedral xenocrysts up to 0.4x0.8 mm. Connection to the matrix by reaction rim (0.15 mm thick) composed of tiny Ti-rich (brown) clinopyroxene granules.

Xenoliths : Total mode ~1%.

Harzburgite : Irregular (1.5x2.5 mm) harzburgite xenoliths. Composed of:

1) Olivine. Subhedral crystals up to 0.6 mm long. Mode 80%.
2) Orthopyroxene. Subhedral crystals up to 0.2x0.6 mm. Mode 15%.
3) Clinopyroxene. An irregular grain, 0.3x0.4 mm. Showing weak pleochroism (brown-green) and Ti-rich (brown) rim at clinopyroxene-matrix contact. Mode 5%.

Olivine + Clinopyroxene : Irregular xenolith (1.4x2.2 mm). Composed of:

1) Olivine. Several large irregular crystals : up to 0.5x1.3 mm. Containing sub-grain structure (deformed before involved to the melt). Showing reaction rim (~0.02 mm thick), composed of tiny granules of Ulvöspinel-magnetite .
2) Clinopyroxene . Two sub-rounded grains up to 0.2x0.3 mm. Resorption zoning at the contact to the melt marked by brown layer (<0.1 mm thick).
3) An irregular mass (0.3x0.8 mm) mass of tiny granules of ? clinopyroxene (<0.01 mm diameter).

Matrix : Total mode 95%.

Olivine : Tiny granules up to 0.2 mm long. Euhedral. Some are hollow. Unzoned. Mode 10%.

Clinopyroxene : Tiny laths up to 0.15 mm long. Euhedral. Mode 20%.

Plagioclase : Tiny laths up to 0.15 mm long. Euhedral. Lamellar twinning. Mode 15%.

Ulvöspinel-magnetite : Tiny equant granules up to 0.02 mm diameter. Mode 20 %.

Glass : Colourless. Mode 30%.

Weathering products : -

1) Iddingsite. Yellow brown. Developed at the boundaries and fractures of olivine crystals.
2) Clay minerals. Yellow green. Developed in patched of some parts of thin section.

Amygdales : Total mode <<1%.
Rounded. Up to 0.15 mm diameter. Filled with carbonate (?calcite).

2. Name : Olivine-Phyric Basalt with Xenocrysts and Xenoliths.

3. Interpretation :

Crystallisation history :

1) Crystallisation of olivine in phenocrysts.
2) Crystallisation of olivine + clinopyroxene + Ulvö spinel-magnetite in phenocrysts.
3) Crystallisation of olivine + clinopyroxene + plagioclase + Ulvöspinel-magnetite in matrix.
4) Quenching of glass.

Magma type : Probably alkali olivine basalt ? (Ti-rich augite is only clinopyroxene).

Origin of xenoliths / xenocrysts :

Mantle : Harzburgite / Olivine + Clinopyroxene / Olivine (has been deformed before involved to the melt).

<u>Sample SP1</u>

1. Observations

i) Hand specimen

Colour : Dark brown.
Grain size : Aphanitic.
Obvious phenocrysts : Olivine crystals, up to 1x2 mm. Sub-rounded. Yellowish green.
Obvious xenocrysts : -
Obvious xenoliths : -
Obvious amygdales : Oval. Up to 0.5x1.0 cm. Some are empty. Some are filled with carbonate (?calcite) or yellow to reddish brown minerals (?clay minerals). Mode ~15%.
Weathering : Reddish brown layer on the surface (very thin <0.1 mm). White and brown layer (~<0.01 mm thick), encrusts on the wall of empty vesicles.
Density : Usual.

ii) Thin section

Phenocrysts : Total mode 10%.

Olivine : Euhedral skeletal phenocrysts up to 1.9 mm long. Mode 10%. Alteration rim (up to 0.1 mm thick) iddingsite (orange-brown). Some grains are carbonate pseudomorph after olivine.

Xenocrysts : -
Xenoliths : -
Matrix : Total mode 75%.

Olivine : Tiny granules up to 0.2 mm long. Euhedral. Most of them are carbonate pseudomorph after olivine. Mode 2%.

Clinopyroxene : Tiny laths up to 0.12 mm long. Euhedral. "Hour-glass" sector zoning in XPL. Mode 7%.

Plagioclase : Euhedral laths up to 0.05x0.4 mm. Lamellar twinning. Showing sub-parallel arrangement of crystals called "trachytic texture". Mode 25%.

Ulvöspinel-magnetite : Tiny equant granules up to ~0.01 mm diameter. Mode 7%.

Glass : Brown. Mode 34%.

Weathering products : Orange-brown. Iddingsite. Developed in some parts of matrix especially at the tiny granules of olivine.

Amygdales : Total mode ~15%.
Oval shape. Up to 3.5x6.0 mm diameter. Some are partly filled with colloform of fibrous crystals of unknown mineral. Some are filled with:

1) Carbonate (?Calcite) in core. Several irregular grains (up to 0.8x1.7 mm).
2) Aragonite ?. [1st order yellow interference colour, 2v ~15-20 , Biax. -ve]. Subhedral and polysynthetic twin crystals.
3) Band of colloform orange-brown mineral (up to <<0.01 mm thick).
4) Druse of columnar crystals of an isometric mineral at the out most of amygdale (up to 0.15

mm thick). Some are filled with radiated fibrous orangy brown or yellow green mineral.

2. **Name : Amygdaloidal Olivine-Phyric Basalt.**
3. **Interpretation :**

Crystallisation history :

1) Crystallisation of olivine in phenocryst.
2) Crystallisation of olivine + plagioclase + clinopyroxene + Ulvöspinel-magnetite in matrix.
3) Quenching of glass.

Magma type : Probably alkali olivine basalt ? (Ti-rich augite is only clinopyroxene).

Sample SP2

1. **Observations**

i) **Hand specimen**

Colour : Dark brown.
Grain size : Aphanitic.
Obvious phenocrysts : Olivine. Euhedral. Yellowish green. Up to 3 mm long. Mode ~5%.
Obvious xenocrysts : -
Obvious xenoliths : -
Obvious amygdales : Round to oval. Up to 0.4x1.7 cm. Some are empty. Some are filled with carbonate (?calcite) Mode ~15%.
Weathering : Yellowish brown. Developed as a thin layer (~0.02 mm thick) on the surface of the specimen. On the walls of empty vesicles encrusted with white to yellow ? clay mineral.
Density : Usual.

ii) **Thin section**

Phenocrysts : Total mode 5%.
Olivine : Euhedral phenocrysts up to 1.0 mm long. Mode 5%. Alteration rim (up to 0.02 mm thick) is iddingsite (orange-brown). Some grains are carbonate pseudomorph after olivine. Some are arranged in cluster called "glomeroporphyritic texture".
Xenocrysts : -
Xenoliths : -
Matrix : Total mode 70%.
Olivine : Tiny granules up to 0.3 mm long. Euhedral. Most of them are replaced with carbonate (?calcite). Mode 1%.
Clinopyroxene : Tiny laths, up to 0.1 mm long. Euhedral. Mode 7%.
Plagioclase : Small laths up to 0.32 mm long. Euhedral. Lamellar twinning. Showing sub-parallel arrangement of crystals called "trachytic texture". Mode 25%.
Ulvöspinel-magnetite : Tiny equant granules up to ~0.01 mm diameter. Mode 5%.
Glass : Brown. Mode 32%.
Weathering products : Orange-brown. ? Iddingsite. Developed in some parts of matrix.
Amygdales : Total mode ~15%.
Oval to round. Up to 3x10 mm. Some are empty. Some are partly filled with orange-brown fibrous colloform minerals (up to 0.05 mm thick). Some are filled with carbonate (subhedral calcite crystals, up to 1.0x1.4 mm) in core, and layer 0.2 mm thick) of druse of columnar isometric colourless crystals (up to 0.05x0.15 mm).

2) **Name : Amygdaloidal Olivine-Phyric Basalt.**
3) **3. Interpretation :**

Crystallisation history :

1) Crystallisation of olivine in phenocryst.
2) Crystallisation of olivine + plagioclase + clinopyroxene + Ulvöspinel-magnetite in matrix.
3) Quenching of glass.

Magma type : Probably alkali olivine basalt ? (Ti-rich augite is only clinopyroxene).

Sample SP3

1. **Observations**

i) **Hand specimen**

Colour : Dark brown.
Grain size : Aphanitic (in matrix).
Obvious phenocrysts : Olivine. Yellowish green Euhedral. Up to 1.0x2.0 mm. Mode ~7%.
Obvious xenocrysts : -
Obvious xenoliths : -
Obvious amygdales : Round to oval. Up to 0.8x1.3cm. Some are empty. Some are filled with carbonate (?calcite). Mode ~15%.
Weathering :

1) Yellowish brown. Developed as a layer (~0.2 mm thick) covering on the surface of specimen.
2) White and dull layer of the wall of vesicles.

Density : Usual.

ii) **Thin section**

Phenocrysts : Total mode 7%.
Olivine : Euhedral phenocrysts. Some skeletal. Up to 1.4 mm long. Some grains are in cluster ("glomeroporphyritic texture"). Unzoned. Iddingsite alteration rim (up to ~0.02 mm thick).
Xenocrysts : -
Xenoliths : -
Matrix : Total mode 75%.
Olivine : Tiny euhedral granules up to 0.2 mm long. Some are altered to iddingsite (orange-brown). Mode <1%.
Titanaugite : Tiny laths : up to 0.1 mm long. Euhedral. Pale pinkish brown. Very weak pleochroism. "Hour-glass" sector zoning apparent in XPL. Mode 7%.
Plagioclase : Small laths up to 0.4 mm long. Euhedral. Lamellar twinning. Sub-parallel arrangement ("trachytic texture"). Mode 25%.
Ulvöspinel-magnetite : Tiny equant granules up to ~0.01 mm diameter. Mode 10%.
Glass : Brown. Containing tiny needle-like crystals (up to mm long) of unknown minerals (probably ? apatite or ? zircon). Mode 38%.
Weathering products : Orange-brown. Probably ?iddingsite. Developed in patches in some parts of thin section.
Amygdales : Total mode ~18%.
Round to oval. Up to 3x5 mm. Some are partly filled with yellow-brown fibrous colloform mineral (0.15 mm thick) at the margin of vesicles. Some are filled with

1) Carbonate (?calcite) at core (several subhedral calcite crystals (max. 0.4x0.5 mm)
2) Thin layer (<0.01 mm) of yellow-brown colloform mineral.
3) Druse (up to 0.15 mm thick) of columnar colourless crystals (up to 0.1x0.15 mm), surrounding the colloform mineral and calcite core respectively.

2. **Name : Amygdaloidal Olivine-Phyric Basalt.**
3. **Interpretation :**

Crystallisation history :

1) Crystallisation of olivine in phenocryst.
2) Crystallisation of olivine + plagioclase + titanaugite + Ulvöspinel-magnetite in matrix.
3) Quenching of glass.

Magma type : Probably alkali olivine basalt ? (Titanaugite is only clinopyroxene).

Sample SP4

1. **Observations**

i) **Hand specimen**

Colour : Greyish brown.
Grain size : Aphanitic.
Obvious phenocrysts : Olivine. Yellowish to brown (altered). Euhedral. Up to 1.0x1.5 mm long. Mode ~5%.
Obvious xenocrysts : -
Obvious xenoliths : -
Obvious amygdales : Vesicles. Sub-rounded to Elongate. Up to 0.7x1.2 cm. Mode ~40%.
Weathering : The surface of the specimen is encrusted with yellowish brown layer (0.01 mm) material, probably ? clay mineral. The wall of vesicles are covered with very thin (<0.01 mm). White ? clay mineral.
Density : Usual.

ii) **Thin section**

Phenocrysts : Total mode 5%.
Olivine : Euhedral. Up to 1.4 mm long. Rims are altered to iddingsite, orange-brown, up to 0.1 mm thick. Some crystals are arranged in cluster called "glomeroporphyritic texture".
Xenocrysts : -
Xenoliths : -
Matrix : Total mode 55%.
Olivine : Tiny granules up to 0.1 mm diameter. Euhedral. Most of them are altered to iddingsite. Mode ~1%.
Titanaugite : Tiny laths. Up to 0.13 mm long. Euhedral. "Hour-glass" sector zoning in XPL. Mode ~5%.
Plagioclase : Tiny laths up to 25 mm long. Euhedral. Lamellar twinning. Showing trachytic texture. Mode ~19%.
Ulvöspinel-magnetite : Tiny equant granules up to ~0.01 mm diameter. Euhedral. Mode 10 %
Glass : Brown. Containing tiny needle-like crystals (<<0.01 mm long), probably ?apatite or ?zircon. Mode 20%.
Weathering products : Orange-brown. ? Iddingsite. Developed in patches in some parts of thin section.
Amygdales : Total mode ~40%.
Round to irregular shape. Up to 5.0x8.0 mm. The wall is encrusted by a druse (up to 0.1 mm thick) of colourless-crystals (up to 0.05x0.10 mm). The druse is encrusted by orange-brown colloform mineral.

2. Name : Vesicular-Olivine Phyric Basalt.
3. Interpretation :
Crystallisation history :
1) Crystallisation of olivine in phenocryst.
2) Crystallisation of olivine + plagioclase + titanaugite + Ulvöspinel-magnetite in matrix.
3) Quenching of glass.
Magma type : Probably alkali olivine basalt ? (Titanaugite is only clinopyroxene).

Sample SP5
1. Observations
i) Hand specimen
Colour : Greyish brown.
Grain size : Aphanitic.
Obvious phenocrysts : Yellowish brown. Altered olivine. Irregular, up to 1.5x2.0 mm. Mode ~5%.
Obvious xenocrysts : -
Obvious xenoliths : -
Obvious amygdales Vesicles. Elongate irregular up to 0.6x1 cm. Mode ~ 30%.
Texture : Vesicular.
Weathering : Yellowish brown. Developed as a thin layer (<0.01 mm). Covering the surface of specimen. The wall of vesicles are encrusted by a thin layer (<0.01 mm) of white mineral.
Density : Light.
ii) Thin section
Phenocrysts : Total mode 5%.
Olivine : Euhedral. Some skeletal. Up to 0.9 mm long. Unzoned. Grain boundaries are altered to iddingsite (orange-brown), up to ~0.05 mm thick. Some crystals are arranged in cluster, "glomeroporphyritic texture".
Xenocrysts : -
Xenoliths : -
Matrix : Total mode 60%.
Olivine : Tiny granules . Euhedral. up to 0.1mm diameter. Most of them are completely altered to iddingsite (orange-brown). Mode ~1%.
Plagioclase : Small laths. Euhedral. Up to 0.1x0.3 mm. Lamellar twinning. Sub-parallel arrangement, "trachytic texture". Mode ~20%.
Ti-augite : Tiny laths. Euhedral. Up to 0.12 mm long. "Hour-glass" sector zoning in XPL. Mode 7%.
Ulvöspinel-magnetite : Tiny equant granules . Euhedral. Up to ~0.03 mm diameter. Mode 15%.
Glass : Brown. Containing tiny needle-like crystals (up to 0.1 mm long), probably ? apatite or ?zircon. Mode 17%.
Weathering products : Orange-brown. Developed in patches in some parts of matrix.
Amygdales : Total mode ~35%.
Irregular empty vesicles. Up to 6x8 mm. At the wall of vesicles are encrusted by the druse (0.15 mm thick) of columnar colourless isometric mineral (up to 0.05 x0.1 mm). The druse is encrusted by a thin layer (<0.01 mm) of colloform brown material.

2. Name : Vesicular Olivine-Phyric Basalt.
3. Interpretation :
Crystallisation history :
1) Crystallisation of olivine in phenocryst.
2) Crystallisation of olivine + plagioclase + clinopyroxene + Ulvöspinel-magnetite in matrix.
3) Quenching of glass.
Magma type : Probably alkali olivine basalt ? (Ti-rich augite is only clinopyroxene).

Sample DC1
1. Observations
i) Hand specimen
Colour : Greyish black..
Grain size : Aphanitic.
Obvious phenocrysts : -
Obvious xenocrysts : -
Obvious xenoliths : Ultramafic nodules. Up to 2 x 2.4 cm.
Obvious amygdales : -
Texture : -
Weathering : Thin layer (<< 0.05 mm) of white material partly covering on the surface of the specimen.
Density : Normal.
ii) Thin section
Phenocrysts : Total mode 3%.
Olivine : Euhedral. Up to 0.4 x 0.7 mm. Unzoned. Alteration rim as the brown-green mineral, probably clay mineral ? Mode 1%.
Ti-augite : Stubby prisms. Up to 0.15 x 0.20 mm. Euhedral. Oscillatory zoning. Ti-rich rim (as a stronger in brown colour than core). Pinkish brown to very pale green. Mode << 1 %.
Ulvöspinel-magnetite : Irregular phenocrysts. Up to 2.0 x 4.5 mm. Mode <<< 1%.
Xenocrysts : Total mode 1%.
Orthopyroxene : Angular xenocryst, 0.5 x 1.0 mm. Completely surrounded by non-uniform reaction rim (up to 0.2 mm thick), composed of masses of tiny (<<<0.05 mm) ? clinopyroxene and Ulvöspinel-magnetite granules.
Unknown mineral : Sub-angular 1.5 x 1.8 mm. xenocryst. [1st order grey-yellow interference colour, 2 direction-cleavage (~80°, 100°)]. Fractured and altered to yellow-brown cryptocrystalline mineral (low relief, high interference colour). Completely surrounded by 0.1 mm. reaction rim, composed of tiny laths (up to 0.1 mm long) of ? clinopyroxene.
Olivine : Irregular xenocrysts. Up to 0.7 x 1.1 mm. Resorption rim marked by higher interference colour than core.
Xenoliths : Total mode 3 %.
Dunite : Angular xenocryst (3.0 x 3.5 mm). Composed of anhedral olivine crystals, up to 1.2x1.9 mm, uneven extinction (indication deformed lattices). The xenolith mantled by 0.2 mm. reaction rim, consisting of masses of tiny (<<<0.05 mm) ? Clinopyroxene granules.
Quartzite : Irregular xenoliths. Up to 1.4 x 3.4 mm. Composed of small anhedral quartz grains (up to 0.3 mm long0, undulated extinction.

Completely surrounded by 0.1 mm. reaction rim, consisting of tiny ? clinopyroxene laths (up to 0.01 mm long).

?Alkali feldspar or ? Zeolite : [Colourless, low relief, 1st order grey interference colour]. Sub angular xenoliths. Up to 1.7 x 2.5 mm. Composed of the small grains (up to 0.3 mm diameter) of alkali feldspar or zeolite ?. Consertal texture. Some show fan-like texture. Completely surrounded by a 0.2 mm. layer of the tiny ? clinopyroxene laths (up to 0.1 mm long).

Matrix : Total mode 93%.

Olivine : Tiny granules. Up to 0.1 mm long. Euhedral. Unzoned. Mode 10%.

Ti-augite : Tiny laths. Up to 0.1 mm long. Euhedral. "Hour-glass" sector zoning. Pinkish brown to green pleochroism. Mode 15%.

Plagioclase : Tiny laths. Up to 0.3 mm long. Euhedral. Lamellar twinning. Sub-parallel arrangement or "trachytic texture". Mode 10 %.

Glass : Colourless. Mode 48%.

Weathering products : Green, brown. Developed in patches in some parts of slide. Probably clay mineral ?

Amygdales : -

2. Name : Olivine-Phyric Basalt with Xenocrysts and Xenoliths.

3. Interpretation :

Crystallisation history :

1) Crystallisation of olivine in phenocrysts.
2) Crystallisation of olivine + Ti-augite + ulvöspinel-magnetite in phenocrysts.
3) Crystallisation of olivine + plagioclase + Ti-augite in matrix.
4) Quenching of glass.

Magma type : Probably alkali olivine basalt ? (Ti-rich augite is the only clinopyroxene)

Origin of xenocrysts and xenoliths:

Crust : Quartzite / ?Alkali feldspar or ?Zeolite.

Mantle : Dunite / Olivine.

? : Orthopyroxene / Unknown mineral.

Sample DC2

1. Observations

i) Hand specimen

Colour : Greyish black.

Grain size : Aphanitic.

Obvious phenocrysts : -

Obvious xenocrysts : -

Obvious xenoliths : Ultramafic nodules. Up to 2.0x 3.0 cm.

Obvious amygdales : -

Weathering : The surface of specimen is weathered to yellow-brown and formed as a thin (~0.5 mm) layer.

Density : Normal.

ii) Thin section

Phenocrysts : Total mode 2%.

Olivine : Euhedral. Up 0.4x1.8 mm. Unzoned. Fractures and grain boundaries are altered to green-brown, probably ?clay mineral. Mode ~1%.

Ti-augite : Stubby prisms. Up to 0.2 mm long. Euhedral. "Hour-glass" sector zoning in XPL. Pinkish brown in PPL. Mode <<<1%.

Xenocrysts : Total mode <1%.

Orthopyroxene : Sub-rounded xenocryst (1.4x1.8 mm). Slightly reaction rim.

Xenoliths : Total mode 70%.

Quartzite : A large 5x9 mm quartz aggregate. Composed of several crumbs of quartz, up to 0.3 mm long. Undulatory extinction. Between the quartz grains are filled with irregular brown microlite (<0.01 mm) mineral (2nd order orange-red interference colour, probably ? clinopyroxene) and carbonate (?calcite). The microlite mineral is also cumulated as a 0.1 mm. layer surrounding the xenolith. Some areas are occupied by brown cryptocrystalline mineral, showing fibrous radiated texture, formed as rounded clumps, up to 0.9 mm diameter. Apatite, tiny euhedral crystal (diameter 20 μm.), at margin of quartzite.

Spinel-lherzolite : Large sub-rounded xenoliths (3 cm diameter). Allotriomorphic granular texture. Cross-cut by alteration veins (up to 0.4 mm thick) veins of green-brown mineral probably ?clay mineral. Composed of :

1) Olivine. Anhedral up to 4.8 x 6.0 mm. Fractured. Uneven extinction (deformed latticed). The olivine rim at the boarder to matrix is higher in interference colour than is the core. Mode ~ 80 % of this xenolith.
2) Orthopyroxene. Irregular crystals. Up to 3.5 x 6.0 mm. Fractures and cleavages are filled with microlite crystals of olivine?. Undulatory extinction. Mode ~ 8% of this xenolith.
3) Clinopyroxene. Irregular crystals. Up to 2.8 x 3.0 mm. Pale green. Surrounded by a spongy border zone (~0.3 mm thick). Mode ~8%.
4) Spinel. Euhedral to irregular elongated brown crystals. Up to 0.7x3.6 mm. Most are inter granular between olivine grains. Some enclose a tiny round olivine crystal (up to 0.3 mm diameter). Mode ~4% of this xenolith.

Matrix : Total mode 27%.

Plagioclase : Tiny laths. Up to 0.3 mm long Euhedral. Lamellar twinning. Sub-parallel arrangement ("trachytic texture"). Mode 5%.

Olivine : Tiny granules. Up to 0.15 mm long. Euhedral. Unzoned. Mode 4%.

Clinopyroxene : Tiny laths. Up to 0.1 mm long. Euhedral. Mode 4%.

Ulvöspinel-magnetite : Tiny granules. Up to 0.1 mm diameter. Mode 2%.

Glass : Colourless. Mode 12%.

Weathering products : Green, brown. Developed in patches in some parts of slide. Probably ?clay mineral.

Amygdales : Total mode ~1%.

Irregular amygdales. Up to 0.3 x 1.9 mm. Filled with ?zeolite. [1st order grey interference colour], formed in radiated texture. Some are empty and encrusted with very thin layer (<<<0.1 mm) layer of colloform cryptocrystalline mineral at the wall.

2. Name : Olivine-Phyric Basalt with Xenocryst and Xenoliths.

3. Interpretation :

Crystallisation history :

1) Crystallisation of olivine in phenocrysts.
2) Crystallisation of olivine + Ti-augite in phenocrysts.
3) Crystallisation of olivine + Ti-augite + plagioclase + Ulvöspinel-magnetite in matrix.
4) Quenching of glass.

Magma type : Probably alkali olivine basalt ? (Ti-rich augite is only clinopyroxene).

Origin of xenocrysts and xenoliths:

Crust : Quartz aggregates.

Mantle : Spinel-lherzolite.

? : Orthopyroxene.

Sample DC3

1. Observations

i) Hand specimen

Colour : Greyish black..

Grain size : Aphanitic.

Obvious phenocrysts : -

Obvious xenocrysts :

Obvious xenoliths : Ultramafic nodules. Up to 0.5 x 1.0 cm.

Obvious amygdales : Irregular. Up to 2x5 mm. Filled with white mineral probably ?zeolite.
Weathering : The surface of specimen is encrusted with an extremely thin yellow-green to white layer of mineral, probably ?clay mineral
Density : Normal.

ii) Thin section
Phenocrysts : Total mode ~3%.
Olivine : Euhedral. Up to 0.3x0.6 mm. Unzoned. Grain boundaries are altered to green-brown, probably ? clay mineral. Mode 1%.
Ti-augite : Euhedral. Up to 0.2 x 0.4 mm. Pinkish brown to pale green in PPL. "Hour-glass" sector zoning in XPL. Mode <<1%.
Plagioclase : Prismatic euhedral phenocrysts. Up to 0.5 mm long. Lamellar twinning. Mode <<<1%.
Xenocrysts : Total mode <1%.
Olivine : Sub-angular xenocrysts : Up to 1.9 x 2.2 mm. Uneven extinction. Fractures are altered to brown-green mineral, probably ?clay mineral.
Spinel : Sub-angular green-brown spinel (0.3 x 0.4 mm). Completely surrounded by opaque (0.1 mm thick) rim.
Plagioclase : Sub angular 0.4x0.7 xenocrysts of plagioclase. Lamellar twinning. Some parts of crystal are altered to brown and turbid.
Xenoliths : Total mode 1%.
Olivine + Clinopyroxene : Sub-angular xenolith (3.6x3.6 mm). Composed of 3 euhedral olivine crystals (up to 2.9x3.6 mm) and a sub-rounded clinopyroxene crystal (1 mm long). The rim of clinopyroxene is crumbled into small pieces and the matrix contact part is Ti-rich (marked by brown zone in PPL).
Matrix : Total mode 94%.
Olivine : Tiny granules. Up to 0.2 mm long. Euhedral. Unzoned. Some are altered to ?iddingsite. Mode 5%.
Clinopyroxene : Tiny laths. Up to 0.1 mm long. Euhedral. "Hour-glass" sector zoning in XPL. Mode 10%
Plagioclase feldspar : Tiny laths. Up to 0.3 mm long. Euhedral. Lamellar twinning. Sub-parallel arrangement ("trachytic texture"). Mode 15%.
Ulvöspinel-magnetite : Tiny granule up to 0.2 mm diameter. Probably Ulvö spinel-magnetite . Mode 7%.
Glass : Colourless. Mode 57%.
Weathering products : Green, brown. Developed in patches in some parts of slide. Probably ?clay mineral or ?iddingsite.
Amygdales : Total mode <1%.
Sub-rounded amygdales. Up to 0.4 x 0.9 mm. Filled with colourless, 1st order grey interference colour mineral, probably zeolite laths up to 0.3 mm long and forming in fan-like texture.

2. Name : Olivine-Phyric Basalt with Xenocrysts and Xenoliths.
3. Interpretation :
Crystallisation history :
1) Crystallisation of olivine in phenocrysts.
2) Crystallisation of olivine + Ti-augite + plagioclase in phenocrysts.
3) Crystallisation of olivine + Ti-augite + plagioclase + Ulvöspinel-magnetite in matrix.
4) Quenching of glass.
Magma type : Probably alkali olivine basalt ? (Ti-rich augite is only clinopyroxene).
Origin of xenocrysts and xenoliths:
Crust : -
Mantle : Olivine/ Spinel / Olivine + Clinopyroxene.
? : Plagioclase.

<u>Sample DC4</u>
1. Observations
i) Hand specimen
Colour : Green-grey.
Grain size : Aphanitic.
Obvious phenocrysts : -
Obvious xenocrysts : -
Obvious xenoliths : -
Obvious amygdales : -
Texture : -
Weathering : Some part of specimen are altered to be green mineral, probably chlorite?. The surface of specimen is encrusted by a thin layer (<<0.01 mm.) yellow brown material.
Density : Normal.

ii) Thin section
Phenocrysts : Total mode 36%.
Plagioclase : Euhedral prism. Up to 0.2x1.1 mm. Lamellae twinning. Parts of the crystal are altered to be other mineral [2nd order orange-red, blue interference colours]. Subradial arrangement. Mode ~20%.
Clinopyroxene : Euhedral prisms. Up to 0.35x1.1 mm.. Deep brown at core, pale brown at rim. Most are crumbled. Continuous zoning. Intergranular texture (occupying between plagioclase phenocrysts). Mode 15 %.
Ulvöspinel-magnetite : Irregular phenocrysts. Up to 0.3x0.8 mm. Fractured. Mode <1%.
Xenocrysts : -
Xenoliths : -
Matrix : Total mode 64%.
Clinopyroxene : Granules. Euhedral. Some skeletal. Up to 0.1 mm. diameter. Strong brown at core, pale brown at rim in PPL. Mode ~5%.
?Devitrified glass or ?Plagioclase : [1st order grey interference colour]. No crystal boundary apparent, containing the brown turbid minute granules (<<0.01 mm). Mode 20%.
Ulvöspinel-magnetite : Tiny granules. Up to 0.1 mm. Mode 1%.
Plagioclase : Tiny granules. Anhedral. Up to 0.15 mm. Mode 5%.
Weathering products : Green mineral, probably ? chlorite [2v ~20°, Biax. -ve, anomalous blue interference colour] and carbonate (? calcite). Developed in secondary veins (up to 0.7 mm thick) and in patches in matrix. Mode 33%.
Amygdales : -

2. Name : Plagioclase Phyric Basalt ?
3. Interpretation :
Crystallisation history :
1) Crystallisation of plagioclase and clinopyroxene in phenocrysts..
2) Crystallisation of Ulvöspinel-magnetite in phenocrysts.
3) Crystallisation of plagioclase + clinopyroxene + Ulvöspinel-magnetite in matrix.
4) Quenching of glass in matrix.
Magma type : Tholeiitic basalt?
Origin of xenocrysts and xenoliths: -
(Remark : This specimen is extremely altered).

<u>Sample DC5</u>
1. Observations
i) Hand specimen
Colour : Green-grey.
Grain size : Aphanitic.
Obvious phenocrysts : -
Obvious xenocrysts : -
Obvious xenoliths : -
Obvious amygdales : -
Weathering : Green mineral, probably ?chlorite fills in the fractures.
Density : Normal.

ii) Thin section
Phenocrysts : Total mode 45%.
Plagioclase : Euhedral. Prismatic phenocrysts. Up to 0.2x1.5 mm. Lamellar twinning. Parts of crystals are altered to colourless mineral [2nd order orange-red, blue interference colour]. Subradial arrangement. Mode 25%.
Clinopyroxene : Euhedral prisms. Up to 0.6x1.7 mm. Deep brown at core, pale brown at rim. Most are crumbled. Subophitic texture.

Intergranular texture (clinopyroxene occupying between plagioclase phenocrysts). Mode 20%.

Xenocrysts : -

Xenoliths : -

Matrix : Total mode 55%.

Clinopyroxene : Tiny granules. Up to 0.05 mm diameter. Brown. Mode ~20%.

Plagioclase : Tiny granules. Up to 0.1 mm. diameter. Mode 5%.

Ulvöspinel-magnetite : Euhedral granules. Up to 0.1x0.2 mm. Mode 7%.

Weathering products : 1) Green mineral, probably ?chlorite [anomalous blue interference colour]. Developed in veins (max. 0.9 mm. thick) and in patches of matrix. Mode 20%.
2) Carbonate (calcite?), filling in veins associated with chlorite. Mode 3%.

Amygdales : -

2. Name : Plagioclase Phyric Basalt.

3. Interpretation :

Crystallisation history :

1) Crystallisation of plagioclase and clinopyroxene in phenocrysts.
2) Crystallisation of plagioclase + clinopyroxene + Ulvöspinel-magnetite in matrix.
3) Quenching of glass in matrix.

Magma type : Tholeiitic basalt?.

Origin of xenocrysts and xenoliths: -

Crust : -

Mantle : -

(Remark: This specimen is extremely altered).

<u>Sample KS1</u>

1. Observations

i) Hand specimen

Colour : Dark grey.

Grain size : Aphanitic.

Obvious phenocrysts : 1) Plagioclase feldspar laths. Up to 4 mm long. <<1%.
2) Olivine. Up to 2 mm. Altered to brown. <<1%.

Obvious xenocrysts : -

Obvious xenoliths : -

Obvious amygdales : Elongate amygdales. Up to 3x7 mm. The orientation is along the fracture direction. Filled with white mineral, probably ?calcite.

Weathering : The specimen contains abundant fractures aligned in 1 direction. The surface is weathered as the small circular holes (up to ~1 cm diameter). The surface is also partly covered with brown material (<0.5 mm thick).

Density : Normal.

ii) Thin section

Phenocrysts : Total mode 3%.

Plagioclase : Euhedral. Up to 1.5x2.4 mm. Continuous zoning at rim and homogenous core. Spongy texture. Lamellar twinning. Embayment and filled with matrix (Ulvö spinel-magnetite granules + clinopyroxene laths). Mode ~2%. An85.

Olivine : Subhedral hollow phenocrysts. Up to 0.5.x1.0 mm. Unzoned. Fractures are altered to orange-brown, probably ? iddingsite. Mode ~1%.

Xenocrysts : -

Xenoliths : -

Matrix : Total mode 96%.

Plagioclase : Laths. Up to 0.5 mm long. Euhedral. An_{55} Lamellar twinning. "Trachytic texture". Mode 20%.

Olivine : Tiny granules. Up to 0.2 mm long. Euhedral Hollow crystals. Unzoned. Mode 10%.

Clinopyroxene : Tiny laths. Up to 0.1 mm. Euhedral. Mode 5%.

Ulvöspinel-magnetite : Tiny granules. Up to 0.1 mm long. Euhedral. Mode 7%.

Apatite : Euhedral, Ø upto 20 μm. Mode <<< 1%

Glass : Colourless. Mode 44%.

Amygdales : Total mode <<1%.

Rounded amygdales. Up to 1.0x1.3 mm. Filled with ?zeolite [1st order grey interference colour, subhedral, max. 0.4 mm diameter].

2. Name : Olivine- Plagioclase- Phyric Basalt.

3. Interpretation :

Crystallisation history :

1) Crystallisation of olivine in phenocrysts.
2) Crystallisation of olivine + plagioclase in phenocrysts.
3) Crystallisation of olivine + plagioclase + clinopyroxene + Ulvöspinel-magnetite in matrix.
4) Quenching of glass.

Magma type : Olivine basalt.

Origin of xenocrysts and xenoliths: -

<u>Sample KS2</u>

1. Observations

i) Hand specimen

Colour : Dark grey.

Grain size : Aphanitic.

Obvious phenocrysts : Small laths of plagioclase. Up to 3 mm long. <1%.

Obvious xenocrysts : -

Obvious xenoliths : -

Obvious amygdales : Sub-angular amygdales. Up to 7 mm diameter. Filled with white mineral, probably ? zeolite.

Weathering : The surface is covered with yellowish brown material, <0.05 mm thick.

ii) Thin section

Phenocrysts : Total mode 4%.

Plagioclase : Prismatic euhedral phenocrysts. Up to 0.6 x 1.3 mm. Sieve texture Some show oscillatory zoning. Lamellar twinning. Embayment filled with matrix. Mode ~3%.

Olivine : Euhedral phenocrysts. Up to 0.6x0.8 mm. Unzoned. Grain boundaries and fractures are altered to green, brown, probably ?clay mineral. Mode < 1%.

Xenocrysts : -

Xenoliths : -

Matrix : Total mode 95%.

Plagioclase : Laths. Up to 0.6 mm long. Euhedral. Lamellar twinning. Sub parallel arrangement ("Trachytic texture"). Mode 20%.

Olivine : Tiny granules . Up to 0.3 mm long. Euhedral and hollow crystals. Unzoned. Mode 5%.

Ulvöspinel-magnetite : Tiny granules. Up to 0.05 mm diameter. Euhedral. Mode 7%.

Clinopyroxene : Developed in patches as oikocrysts enclosing the laths of plagioclase and the granules of Ulvöspinel-magnetite . Brown in PPL. "Ophimottled texture". Mode 20%.

Glass : Colourless. Mode 43%.

Amygdales : Total mode <1%.
Sub-rounded amygdales. Up to 1.7x1.4 mm. Filled with pale brown cryptocrystalline mineral, probably zeolite.

2. Name : Olivine-Phyric Ophimottled Basalt.

3. Interpretation :

Crystallisation history :

1) Crystallisation of olivine in phenocrysts.
2) Crystallisation of olivine + plagioclase in phenocrysts.
3) Crystallisation of olivine + plagioclase + Ulvöspinel-magnetite + clinopyroxene in matrix.
4) Quenching of glass.

Magma type : Probably alkali basalt

Origin of xenoliths / xenocrysts :-

<u>Sample KS3</u>

1. Observations

i) Hand specimen

Colour : Dark grey.

Grain size : Aphanitic.

Obvious phenocrysts : 1) Olivine. Up to ~1 mm diameter. Altered to brown. <<<1%.
2) Plagioclase laths. Up to 3 mm long. <<1%.

Obvious xenocrysts : -

Obvious xenoliths -

Obvious amygdales : -
Texture : -
Weathering : The specimen contains a lot of fractures, 1 direction alignment. The surface is encrusted with brown-dark brown material (<0.05 mm thick).
Density : -

ii) Thin section
Phenocrysts : Total mode 3%.
Plagioclase : Euhedral phenocrysts. Up to 1.3x4.7 mm. Continuous zoning at rim and homogenous core. Lamellar twinning. Some show spongy core. Glomeroporphyritic texture. (accumulating with olivine). Mode ~2%.
Olivine : Euhedral phenocrysts. Up to 0.4x0.5 mm. Some are uneven extinction. Mode ~1%.
Xenocrysts : -
Xenoliths : -
Matrix : Total mode 96%.
Plagioclase : Prismatic euhedral crystals. Up to 0.1 x 0.7 mm. Oscillatory zoning. Lamellar twinning. Sub-parallel arrangement, "trachytic texture". Mode 20%.
Olivine : Euhedral hollow crystals. Up to 0.2 mm long. Unzoned. Some are altered to iddingsite. Mode 10%.
Clinopyroxene : Tiny laths. Up to 0.1 mm long. Euhedral. Mode 10%.
Ulvöspinel-magnetite : Tiny granules. Up to 0.05 mm diameter. Euhedral. Mode 15%.
Glass : Colourless. Mode ~41%.
Amygdales : Total mode <<1%.
Sub-rounded amygdale (0.8x1.1 mm). Filled with ?zeolite.

2. Name : Olivine- Plagioclase- Phyric Basalt.
3. Interpretation :
Crystallisation history :
1) Crystallisation of olivine in phenocrysts.
2) Crystallisation of olivine + plagioclase in phenocrysts.
3) Crystallisation of olivine + plagioclase + Ulvöspinel-magnetite + clinopyroxene in matrix.
4) Quenching of glass.

Magma type : Probably Alkali basalt ?
Origin of xenoliths / xenocrysts : -

Sample KS4
1. Observations
i) Hand specimen
Colour : Dark grey.
Grain size : Aphanitic.
Obvious phenocrysts : Plagioclase laths. Up to 4 mm long.
Obvious xenocrysts : -
Obvious xenoliths : -
Obvious amygdales : Elongate amygdales. Up to 2x5 mm. Filled with white mineral, probably zeolite.
Weathering : The specimen has abundant fractures arranged in one direction. The surface is covered with brown dull material (<0.1 mm thick).
Density : Normal

ii) Thin section
Phenocrysts : Total mode 8%.
Plagioclase : Prismatic euhedral phenocrysts. Up to 0.4x3.1 mm. Lamellar twinning. Some show continuous zoning at rim and homogeneous composition at core. Accumulated with olivine phenocrysts, "glomeroporphyritic texture". Mode 5%.
Olivine : Sub-angular anhedral phenocrysts. Up to 1.1 x 1.3 mm. Fractured. Some parts are altered to iddingsite. No reaction rim. Unzoned. Mode ~3%.
Ulvöspinel-magnetite : Sub-rounded phenocrysts, 0.3 mm diameter. The rim is accumulated with masses of tiny granules (<<0.01 mm diameter) of Ulvöspinel-magnetite . <<<< 1%.
Xenocrysts : -
Xenoliths : -
Matrix : Total mode ~92%.
Plagioclase : Prismatic laths. Up to 0.15x1.1 mm. Euhedral. Lamellar twinning. Sub-parallel arrangement, "trachytic texture". Mode 25%.
Olivine : Euhedral hollow crystals. Up to 0.2 mm long. Unzoned. Some are altered to green to yellow-orange, probably ?iddingsite and ?chlorite. Mode 7%.
Clinopyroxene : Tiny laths. Up to 0.15 mm long. Euhedral. "Hour-glass" sector zoning in XPL. Mode 10%.
Ulvöspinel-magnetite : Tiny granules. Up to 0.5 mm diameter. Euhedral. Mode 15%.
Glass : Colourless. Mode ~35%.
Amygdales : Total mode <1%.
Rounded amygdales. Up to 1.4 x 2.3 mm. Filled with aggregate of ?zeolite.

2. Name : Olivine- Plagioclase- Phyric Basalt.
3. Interpretation :
Crystallisation history :
1) Crystallisation of olivine in phenocrysts.
2) Crystallisation of plagioclase + Ulvöspinel-magnetite in phenocrysts.
3) Crystallisation of olivine + plagioclase + clinopyroxene + Ulvöspinel-magnetite in matrix.
4) Quenching of glass.

Magma type : Probably alkali olivine basalt ? (Ti-rich augite is only clinopyroxene).
Origin of xenoliths /xenocrysts : -

Sample KS5
1. Observations
i) Hand specimen
Colour : Dark grey.
Grain size : Aphanitic.
Obvious phenocrysts : Sub-angular phenocrysts. Up to 1.0 mm diameter. Grey-black colour. Conchoidal fracture. Vitreous lustre. ?Pyroxene.
Obvious xenocrysts : -
Obvious xenoliths : -
Obvious amygdales : -
Weathering : The surface of sample contains some holes (up to 1.5 cm diameter) and is covered with brown dull material.
Density : Normal.

ii) Thin section
Phenocrysts : Total mode 8%.
Olivine : Euhedral phenocrysts. Up to 0.4 x1.6 mm. Resorption rim (indicated by higher interference colour than core). Fractured. The fractures are altered to ?chlorite or ?iddingsite. Mode 5%.
Plagioclase : Prismatic euhedral phenocrysts. Up to 0.5 x1.7 mm. Continuous zoning. Lamellar twinning. Some show spongy core with homogeneous rim (~1 mm thick) but the cavities in core are filled with tiny granules (<<0.1 mm diameter) of ?clinopyroxene and Ulvöspinel-magnetite . Mode 3%.
Xenocrysts : -
Xenoliths : -
Matrix : Total mode 92%.
Plagioclase : Prismatic euhedral crystals. Up to 0.1x1.0 mm. Some show continuous zoning. Lamellar twinning. Sub-parallel arrangement called "trachytic texture". Mode 25%.
Olivine : Euhedral crystals. Up to 1.0x1.7 mm. Unzoned. Some grains are altered to iddingsite. Mode 7%.
Ulvöspinel-magnetite : Tiny granules Up to 0.1 mm long. Euhedral. Mode 12%.
Clinopyroxene : Developed in patched as the oikocrysts embedded or partly embedded by plagioclase laths and Ulvöspinel-magnetite crystals, called "ophimottled texture". The patches are irregular shape, up to 0.5x1.0 mm. Brown to very pale green in PPL. Mode 25%.

Glass : Colourless. Mode 32%.

Amygdales : Total mode <1%.
Irregular amygdales. Up to 1.1x2.5 mm. Filled with turbid colourless mineral, probably ?zeolite.

2. Name : Olivine-Phyric-Ophimottled Basalt.

3. Interpretation :

Crystallisation history :
1) Crystallisation of olivine in phenocrysts.
2) Crystallisation of olivine + plagioclase in phenocrysts.
3) Crystallisation of olivine + plagioclase + Ulvöspinel-magnetite + clinopyroxene in matrix.
4) Quenching of glass.

Magma type : Probably Alkali basalt

Origin of xenoliths / xenocrysts : -

Sample BP1

1. Observations

i) Hand specimen

Colour : Dark grey.

Grain size : Aphanitic.

Obvious phenocrysts : -

Obvious xenocrysts :
1) Black sub-angular xenocrysts. Up to 0.9x1.5 cm. Vitreous lustre. 2 directions of cleavage. ? Clinopyroxene.
2) Olivine. Sub-rounded. Up to 0.2 cm diameter.

Obvious xenoliths :
1) Ultramafic nodules. Up to 0.5 cm.
2) Aggregates of white + green minerals. Probably gabbro. Sub-rounded. Up to 2.0 cm diameter.

Obvious amygdales : -

Texture : -

Weathering : The surface of specimen is altered to orange-yellow. The weathering mantle is 0.5 cm thick.

Density : Normal.

ii) Thin section

Phenocrysts : Total mode 3%.

Olivine : Euhedral phenocrysts. Up to 0.4 mm long. Unzoned. Grain boundaries are altered to green (probably clay mineral or green mica ?). Mode ~1 %.

Clinopyroxene : Euhedral stubby prisms. Up to 0.2x0.5 mm. Pinkish brown to pale green pleochroism. Reaction rim. Mode < 1%.

Ulvöspinel-magnetite : Irregular phenocrysts. Up to 0.5 mm long. Mode <<<1%.

Xenocrysts : Total mode 5%.

Spinel : Up to 2.7 x 3.2 mm. Sub-angular brown-black xenocrysts. Curved fractures.

Olivine : Angular xenocrysts. Up to 1.2 x 2.3 mm. Undulated extinction. Resorption zoning indicated by higher interference colour at rim more than core. Grain boundaries or fractures are altered to green-brown, probably ?clay mineral.

Olivine overgrown by ?clinopyroxene : "Corona texture" up to 0.8 x 1.7 mm. Sub-angular olivine crystals (up to 0.6 x 0.7 mm) are overgrown or surrounded by clinopyroxene, non-uniform width (up to ~0.3 mm thick). Clinopyroxene has Ti-rich rim (marked by a ~ 0.05 mm. pinkish brown layer).

Clinopyroxene : Subhedral xenocrysts. Up to 0.6x1.3 mm. Turbid core. Mantled by a layer of pinkish brown Ti-rich reaction rim (~ 0.1 mm thick).

Xenoliths : Total mode 10 %.

?Alkali feldspar + Plagioclase + Clinopyroxene + Glass : Aggregates. Up to 0.5 x 1.2 cm.. Composed of :-
1) Alkali feldspar crystals. Up to 2.0 x 2.5 mm. Turbid. Tartan twinning. Simple twinning.
2) Plagioclase anhedral crystal. (0.8x0.9 mm). Lamellar twinning.
3) Clinopyroxene laths. Up to 0.2x0.25 mm. Cumulated as a non-uniform layer (~1.0 mm thick) at rim of xenolith.
4) Glass. Brown. Developed between mineral grains and near the margin of xenoliths.

Matrix : Total mode 82%.

Olivine : Tiny granules. Euhedral. Up to 0.1 mm long. Unzoned. Mode 5%.

Ti-augite : Tiny laths. Up to 0.3 mm long. "Hour-glass" sector zoning. Mode 15%.

Ulvöspinel-magnetite : Tiny granules. Up to 0.1 mm diameter. Mode 10%.

Plagioclase feldspar : Developed in patches as oikocrysts enclosing the tiny laths of Ti-augite and tiny granules of Ulvöspinel-magnetite . "Ophimottled texture" and interstice. Up to 2.0 mm diameter. Mode 7%.

Glass : Colourless and brown. Mode 45%.

Weathering products : Brown green. Developed as specks in some parts of matrix. Probably ?clay mineral.

Amygdales : -

2. Name : Olivine-Phyric Ophimottled Basalt.

3. Interpretation :

Crystallisation history :
1) Crystallisation of olivine in phenocrysts.
2) Crystallisation of olivine + clinopyroxene + Ulvö spinel-magnetite in phenocrysts.
3) Crystallisation of olivine + Ti-augite + Ulvöspinel-magnetite + plagioclase.
4) Quenching of glass and melted xenoliths.

Magma type : Probably alkali olivine basalt ? (Ti-rich augite is only clinopyroxene)

Origin of xenocrysts and xenoliths:

Crust : ?Alkali feldspar + Plagioclase + Clinopyroxene + Glass.

Mantle : Spinel/ Olivine/ Olivine overgrown by clinopyroxene / Clinopyroxene.

Sample BP2

1. Observations

i) Hand specimen

Colour : Dark grey.

Grain size : Aphanitic.

Obvious phenocrysts : -

Obvious xenocrysts : Black vitreous lustre rounded xenocrysts. Conchoidal fracture. Up to 0.2 mm diameter. Probably ?spinel.

Obvious xenoliths : Sub-rounded xenoliths. Up to 0.7 x 1.2 cm. Composed of white / green minerals. Some contain cavities.

Obvious amygdales : White mineral probably ?feldspar filling in the cavities in with irregular shape (up to 1 cm long).

Weathering : The specimen is weathered at the surface as a non-uniform width (up to 0.8 cm thick) of orange-yellow material, ?clay mineral.

Density : Normal.

ii) Thin section

Phenocrysts : Total mode 3%.

Olivine : Euhedral phenocrysts. Up to 0.25 x 0.4 mm. Unzoned. The boundaries and fractures of grain are altered to green-brown, probably ?clay mineral or ?iddingsite. Some are overgrown by Ti-augite, "corona texture" and the rim of Ti-augite has growth zoning (Ti-rich rim is pinkish brown 0.05 mm thick). Mode ~1%.

Clinopyroxene : Euhedral prismatic phenocrysts. Up to 0.2x0.5 mm. Ti-rich rim marked by pinkish brown layer (~0.1 m. thick). Pinkish brown to pale green pleochroism. Mode ~ 1 %.

Plagioclase : Euhedral prisms. Up to 0.3x0.9 mm. Lamellar twinning. Enclosing tiny clinopyroxene laths (up to 0.1 mm long) and tiny granules of Ulvö spinel-magnetite s (<0.05 mm diameter). "Ophitic texture". Mode 1%.

Xenocrysts : Total mode 5%.

Unknown mineral : [1st order grey-yellow interference colour, Biax. +ve, 2v ~30 - 60 , 2 directions of cleavage (65 , 115)]. Sub-rounded up to 3.6 mm diameter xenocrysts. Completely surrounded by a thick (0.7 mm) reaction rim (spongy rim). The reaction rim contains glass and clinopyroxene laths (up to 0.2 mm long).

Olivine : Irregular xenocrysts. Up to 0.7x1.6 mm. Higher interference colour at rim than core. Uneven extinction. The grain boundaries are altered to be green-brown, probably ?clay mineral.

Clinopyroxene : A sub-rounded 1.1 mm xenocryst. Pinkish brown to pale green pleochroism. Surrounded by reaction rim (up to 0.4 mm thick). Tiny granules (~0.05 mm) of ulvöspinel-magnetite are accumulated at rim.

?Clinopyroxene aggregate : Sub-angular aggregates. Up to 1.1x1.7 mm. Composed of tiny clinopyroxene granules (<<0.02 mm). Probably melted clinopyroxene ?.

Xenoliths : Total mode 10 %.

?Crustal xenoliths : Sub-angular xenoliths. Up to 1x1.7 cm.. Composed of :-

1) Alkali feldspar. Irregular crystals. Up to 0.6x1.1 mm. "Consertal texture". Some show "tartan" twinning.
2) Plagioclase. Developed the hollow laths. (up to 0.8 mm long). The gaps and between grains are filled with brown glass. Fan-like texture.
3) Fibrous mineral. Fan-like or spherulitic texture. Developed from alkali feldspar. Pale brown.
4) Clinopyroxene laths. Up to 0.1 mm long. Abundant in the rim of xenoliths. Swallow tail.
5) Green-brown stain of cryptocrystalline mineral. Developed in some areas of xenoliths.

Matrix : Total mode 82%.

Olivine : Tiny granules. Euhedral. Up to 0.2 mm long. Unzoned. Mode 5%.

Clinopyroxene : Tiny laths. Euhedral. Up to 0.3 mm long. "Hour-glass" sector zoning. Mode 10%.

Ulvöspinel-magnetite : Tiny granules. Up to 1 mm diameter. Mode 10%.

Alkai feldspar : Developed in patches as oikocrysts enclosing the tiny laths of clinopyroxene and tiny granules of Ulvö spinel-magnetite . Up to 1 mm diameter. "Ophimottled texture" and interstice. Mode 7 %.

Glass : Colourless. Mode 50%.

Weathering products : Brown-green. Developed as specks in some parts of slide. Probably ?clay mineral.

Amygdales : -

2. **Name : Olivine-Phyric Ophimottled Basalt with Xenocrysts and Xenoliths.**
3. **Interpretation :**

Crystallisation history :

1) Crystallisation of olivine in phenocrysts.
2) Crystallisation of olivine + clinopyroxene + plagioclase in phenocrysts.
3) Crystallisation of olivine + clinopyroxene + Ulvö spinel-magnetite + plagioclase in matrix.
4) Quenching of glass.

Magma type : Probably alkali olivine basalt ? (Ti-rich augite is only clinopyroxene).

Origin of xenocrysts and xenoliths:

Crust : ?Crustal xenoliths.

Mantle : Olivine / Clinopyroxene / Clinopyroxene aggregate.

? : Unknown mineral.

Sample BP3

1. **Observations**

i) Hand specimen

Colour : Dark grey.

Grain size : Aphanitic.

Obvious phenocrysts : -

Obvious xenocrysts :

1) Olivine sub-rounded xenocrysts. Up to 1 mm long.
2) Ellipsoidal Ulvöspinel-magnetite s, up to 2 mm long.

Obvious xenoliths :

1) Ultramafic nodule. Up to 0.5 mm diameter.
2) ?Gabbroic xenoliths. Angular shape, up to 1.5 cm long. Containing plagioclase feldspar and ferromagnesian minerals.

Obvious amygdales :

Texture : -

Weathering : The surface of specimen is developed to orange-yellow. There is weathered zone (up to 0.8 cm thick) near the surface, in greyish yellow. Some xenoliths are altered to green and orange-yellow.

Density : Normal.

ii) Thin section

Phenocrysts : Total mode 1%.

Clinopyroxene : Stubby euhedral prism. Up to 0.20x0.40 mm. Showing discontinuous zoning in XPL and spongy appearance. Mode <1%.

Olivine : Subhedral. Up to 0.25 mm long. Unzoned. At the fractures and rims are altered to green mineral. Mode <1%.

Xenocrysts : Total mode 5%.

Orthopyroxene : Colourless. Irregular crystals (up to 1.5x2.8 mm) Exhibiting streaky lamellar. Parallel extinction.

Olivine : Irregular xenocrysts. Up to 1.0x1.5 mm. Continuous zoning in XPL.

Clinopyroxene : Irregular xenocrysts. Up to 2.8x3.2 mm. Pale green with resorption zoning as a Ti-rich rim (brown in PPL). Reaction corona (0.4 mm thick).

Turbid aggregate : A large turbid stubby prismatic aggregate (0.3x6.0 mm). Containing turbid mineral (?glass). Fractures filled with green ? clinopyroxene.

?Clinopyroxene aggregate : Irregular aggregate, up to 1.0x1.4 mm. Containing tiny ?clinopyroxene granules (up to 0.05 mm diameter).

Alkai feldspar : Sub angular xenocrysts (up to 0.4x0.5 mm). Lamellar twinning.

Unknown mineral : [1st order grey interference colour, Biax. +ve]. Colourless. Sub angular (up to 0.7x0.8 mm). Probably ? alkali feldspar.

Xenoliths : Total mode 20%.

?Crustal xenoliths : Large irregular xenoliths. Up to 1.7x1.7 cm.. Containing 3 zones (from core to rim) :

1) Carbonate (?calcite), up to 1.5x3.2 mm.
2) Aggregate of ?plagioclase laths. (up to 0.35x1.4 mm). Lamellar twinning. Some crystals shows fan-shaped radiate arrangements. Some exhibit the rectangular to rhombic gap in the core and filled with brown glass. Some form in bow tie twin. Aggregate (2x2 mm) of plagioclase irregular crystals. Containing 5 plagioclase crystals up to 1.0x1.4 mm. This zone is 3.6 mm thick and the brown glass is occupied between the mineral grains. (Relicts of melted plagioclase ?).
3) The out most zone (~2 mm thick). Containing aggregate of plagioclase laths (same as 2)) and tiny laths of euhedral clinopyroxene crystals (up to 0.1x0.4 mm), hollow and swallow tail.

Ultramafic nodule : Angular (0.4x0.9 mm) xenolith. Consisting of crystals of olivine (up to 0.3x0.5 mm). Reaction rim.

Matrix : Total mode 74%.

Olivine : Tiny granules subhedral crystals. Up to 0.2 mm diameter. Unzoned.

Alteration rim as the green mineral. Mode 2%.

Clinopyroxene : Tiny laths of clinopyroxene. Up to 0.05x0.1 mm. Euhedral. Pinkish brown-green pleochroism. "Hour-glass" sector zoning in XPL. Mode 25 %

Ulvöspinel-magnetite : Tiny granules up to 0.2 mm. Mode 10%.

Glass : Brown. Mode 30%.

Alkai feldspar : Developed as small oikocrysts enclosing clinopyroxene laths and Ulvöspinel-magnetite granules (chadacrysts), "Ophimottled texture" and interstice. up to ~0.5 mm diameter. Mode 7%.

Weathering products : Green to brown. Developed in patches in some parts of thin section. Probably ? chlorite and ?iddingsite.

Amygdales : -

2. **Name : Olivine-Phyric Ophimottled Basalt with Xenocrysts and Xenoliths.**
3. **Interpretation :**

Crystallisation history :

1) Crystallisation of olivine in phenocrysts.
2) Crystallisation of olivine + clinopyroxene in phenocrysts.
3) Crystallisation of olivine + clinopyroxene + Ulvö spinel-magnetite + plagioclase in ground mass.
4) Quenching of glass and melted xenoliths.

Magma type : Probably alkali olivine basalt ? (Ti-rich augite is only clinopyroxene)

Origin of xenocrysts and xenoliths:

Crust : ?Crustal xenoliths.

Mantle : Ultramafic nodule / Olivine / Orthopyroxene / Clinopyroxene / Clinopyroxene aggregate.

? : Turbid aggregate / Plagioclase / Unknown mineral.

<u>Sample BP4</u>

1. **Observations**

i) Hand specimen

Colour : Dark grey.

Grain size : Aphanitic.

Obvious phenocrysts : -

Obvious xenocrysts :

1) Sub-rounded black ?pyroxene(1.7x3.0 cm). Striation, conchoidal fracture, vitreous lustre.
2) Ulvöspinel-magnetite . Sub-angular crystal (1.0x1.5 cm).

Obvious xenoliths : Sub-rounded xenoliths. Up to 0.7 cm diameter. Composed of white and green minerals. Probably altered plagioclase.

Obvious amygdales : -

Weathering : The surface of specimen is orange-yellow. The weathering zone near the surface is 1.0 cm thick.

ii) Thin section

Phenocrysts : Total mode 1%.

Olivine : Subhedral phenocrysts up to 0.9 mm long. Some skeletal. The grain boundaries are altered to green mineral. Mode < 1%.

Titanaugite : Euhedral prisms up to 0.1x0.5 mm. Oscillatory sector zoning apparent in XPL. Pinkish brown, green. Mode <<<1%.

Xenocrysts : Total mode 5%.

Olivine : Irregular xenocrysts. Up to 1.1x2.7 mm. Uneven extinction. Unzoned.

Clinopyroxene : Angular xenocrysts. Up to 0.5x0.8 mm. Completely surrounded by reaction rim (~0.1 mm thick.). Some show spongy core and Ti-rich at rim (brown).

Alkali feldspar : Sub-angular xenocrysts. Up to 0.5x0.9 mm. Tartan pattern (albite + pericline twin). Probably ? microcline [2v ~80 , Biax. -ve]. Some grains do not show twin [Biax. +ve, 2v ~80.].

Sieve texture feldspar : Sub angular xenocrysts. Up to 0.7x1.1 mm. Consisting mainly of turbid material (probably ?glass) in a fine-mesh-like arrangement of alkali feldspar and clinopyroxene.

?Clinopyroxene aggregate : Irregular aggregates. Up to 0.5x1.7 mm. Consisting mainly of tiny clinopyroxene granules (up to 0.1 mm diameter). Probably melted ? clinopyroxene.

Xenoliths : Total mode 20 %.

Clinopyroxene + Olivine : Sub-rounded large 1x1.7 cm xenolith consisting of 2 mineral grains (clinopyroxene and olivine) and plagioclase aggregates :-

1) Clinopyroxene. Rounded very large (1.5 cm diameter). Pinkish brown. Thin Ti rich rim (~0.5 mm). Good 2 direction cleavages.
2) Olivine . Angular (2.7x2.9 mm) grain. Unzoned.
3) Sub-rounded aggregates (up to 2 mm long) occupied in the cavities of the large clinopyroxene (in 1)). Consisting of plagioclase laths (up to 0.1x0.7 mm). Showing spherulitic texture or fan-shaped radiate arrangement. Some are bow-tie twin. In the fractures of the large clinopyroxene grain are also filled with plagioclase aggregate.

Ultramafic nodule : Large (0.5x0.6 mm) sub-round nodule. Consisting of :

1) Two olivine grains of olivine (up to 0.3x0.5 mm), resorption rim (Fe-rich) marked by higher interference colour than core. A larger grain shows uneven extinction indicating the deformed lattices. A small oval (0.2x0.5 mm) crystal included in a large olivine grain, probably ? plagioclase [1st order grey, 2v=70 degree, Biax. +ve]
2) A small (0.9x1.0 mm) angular clinopyroxene. Reaction rim (~0.1 mm thick).

?Crustal xenoliths : Irregular aggregates. Up to 1.0x1.7 mm. Containing of (from core to rim):

1) Alkali feldspar ? Stubby prismatic euhedral crystals to irregular crystals. up to 0.2x0.4 mm. Simple twin.
2) Dark green clinopyroxene laths. Up to 0.2 mm long. Cumulated in a layer (~0.5 mm thick) surrounding the core of ?alkali feldspar crystals.

Matrix : Total mode 74%.

Olivine : Tiny granules . Up to 0.15 mm diameter. Anhedral. Unzoned. Mode 5%.

Clinopyroxene : Tiny laths. Up to 0.1 mm long. Euhedral. "Hour-glass" sector zoning. Mode 7%.

Ulvöspinel-magnetite : Tiny granules. Up to 0.15 mm diameter. Mode 10%.

Alkai feldspar : Developed as small oikocrysts (up to ~0.5 mm diameter) enclosing clinopyroxene laths and Ulvöspinel-magnetite crystals (chadacrysts). "Ophimottled texture" and interstice. Mode 7%.

Glass : Brown. Mode 45%.

Weathering products : Green , brown. Probably ?clay minerals or ? iddingsite. Developed in some parts of matrix.

Amygdales : -

2. **Name : Olivine-Phyric Ophimottled Basalt with Xenocrysts and Xenoliths.**
3. **Interpretation :**

Crystallisation history :

1) Crystallisation of olivine.
2) Crystallisation of olivine + clinopyroxene in phenocrysts.
3) Crystallisation of olivine + clinopyroxene + Ulvö spinel-magnetite + plagioclase in ground mass.
4) Quenching of glass.

Magma type : Probably alkali olivine basalt ? (Ti-rich augite is only clinopyroxene).

Origin of xenoliths / xenocrysts :

Crust : ?Crustal xenoliths / Alkali feldspar.

Mantle : Ultramafic nodule / Clinopyroxene + Olivine / Olivine / Clinopyroxene / Clinopyroxene aggregate.

? : Sieve texture feldspar.

Sample BP5

1. Observations

i) Hand specimen

Colour : Dark grey.

Grain size : Aphanitic.

Obvious phenocrysts : -

Obvious xenocrysts : ?Clinopyroxene. Black vitreous lustre. Conchoidal fracture. Irregular xenocrysts (up to 4.0x7.0 mm).

Obvious xenoliths : Ultramafic nodule. Up to 0.8 mm diameter.

Obvious amygdales : -

Texture : -

Weathering : Orange-yellow. Developed on the surface (2 mm thick). Some xenoliths near the surface are altered to white and brown minerals, probably ? clay minerals.

Density : Normal.

ii) Thin section

ii) Thin section

Phenocrysts : Total mode 5%.

Olivine : Subhedral. Up to 1.5 mm long. Unzoned. Grain boundaries and fractures are slightly altered to green-brown mineral, probably clay mineral. Mode ~3%.

Ti-augite : Euhedral crystals. Up to 0.2x0.8 mm. Overgrowth zoning. Pinkish brown and high concentration of tiny Ulvöspinel-magnetite granules at rim, pale green to core. Mode <1%.

Alkai feldspar : Stubby prismatic euhedral crystals. Up to 0.7x1.3 mm. Lamellar twinning. Enclosing tiny laths (up to 0.25 mm long) of clinopyroxene, tiny granules (<0.02 mm diameter) of Ulvöspinel-magnetite , and tiny granules (up to 0.1 mm diameter) of olivine chadacrysts: "Subophitic texture". Mode ~1%.

Xenocrysts : Total mode 1%.

Olivine : Irregular xenocryst. Up to 1.0x2.8 mm. Resorption zoning marked by higher interference colour at rim more than core in XPL.

Clinopyroxene: Irregular xenocrysts. Up to 1.1 x 1.5 mm. Ti-rich rim (pinkish brown). Completely surround by reaction rim.

Clinopyroxene aggregate : Sub-angular aggregates. Up to 0.8 x 1.1 mm. Consisting of very fine granules of ? clinopyroxene. Probably melted clinopyroxene?

Xenoliths : Total mode ~5%.

?Crustal xenoliths : Large aggregates. Up to 0.7x1.2 cm. Composed of (from core to rim) :

1) Spherulitic clusters (up to 1.8x2.5 mm) Radiated arrangement of fibrous cryptocrystalline fibrous crystals, probably ?clinopyroxene. Sparsely occupied by long hollow clinopyroxene laths (up to 0.5 mm long).
2) Brown glass zone (~2.0 mm thick). Cut by thin (~0.05 mm) veins of carbonate (?calcite) and Fe-oxides.
3) Zone (~ 1.7 mm thick) of aggregate. Composed of fan-like shaped swallow-tail and hollow plagioclase laths (up to 0.4 mm long, filled with brown glass) and hollow euhedral clinopyroxene crystals(up to 0.23 x0.5 mm). Clinopyroxene crystals are high accumulated at rim.

Matrix : Total mode ~90%.

Ti-rich augite : Tiny laths up to 0.2 mm long. Euhedral. "Hour-glass" sector zoning. Mode 20%.

Olivine : Tiny granules. Euhedral. Up to 0.15 mm diameter. Unzoned. Mode ~2%.

Alkai feldspar : Developed in patches of oikocrysts (up to 0.5 mm diameter) enclosing tiny clinopyroxene laths Ulvöspinel-magnetite granules. "Ophimottled texture" and interstice. Mode 7%.

Ulvöspinel-magnetite : Tiny granules, up to 0.2 mm diameter. Mode 15%.

Glass : Brown. Mode ~46%.

Weathering products : Green-brown. Developed as specks in some parts of this slide.

Amygdales : -

2. Name : Olivine-Phyric Subophitic Basalt with Xenocrysts and Xenoliths.

3. Interpretation :

Crystallisation history :

1) Crystallisation of olivine in phenocrysts.
2) Crystallisation of olivine + clinopyroxene in phenocrysts.
3) Crystallisation of olivine + Ti-rich augite + plagioclase + Ulvöspinel-magnetite in matrix.
4) Quenching of glass.

Magma type : Probably alkali olivine basalt ? (Ti-rich augite is only clinopyroxene).

Origin of xenoliths / xenocrysts :

Crust : Crustal xenoliths.

? : Olivine / Clinopyroxene / Clinopyroxene aggregate.

Sample BP6

1. Observations

i) Hand specimen

Colour : Dark grey.

Grain size : Aphanitic.

Obvious phenocrysts : -

Obvious xenocrysts : Black irregular xenocrysts. Vitreous lustre. Conchoidal fracture. ?Spinel.

Obvious xenoliths :

1) Ultramafic nodules. Up to 3.0 mm diameter.
2) White-green patches of xenoliths. Up to ~1 cm diameter. Composed of ?plagioclase and other minerals (can not be identified by unaided eyes).

Obvious amygdales :-

Texture : -

Weathering : The surface is altered to yellowish brown. Very thin (<0.5 mm) weathering surface.

Density : Normal

ii) Thin section

Phenocrysts : Total mode 3%.

Olivine : Subhedral phenocrysts. Up to 0.3 x 0.6 mm. Unzoned. Mode < 3%

Ti-rich augite : Subhedral phenocrysts. Up to 0.2 x 0.5 mm. Turbid core, Ti-rich rim (pinkish brown in PPL). Mode <<<1%.

Xenocrysts : Total mode 5%.

?Unknown mineral : [Colourless, 1st order yellow interference colour, straight extinction, 2 direction cleavage (46 , 134), Uni.? ve, a part of crystal showing lamellar twinning]. Angular crystal, 1.6x2.7 mm. Reaction rim.

?Alkali feldspar : Large prism euhedral crystal, 1.2x2.5 mm. Resorption rim and the rim containing tiny laths of ?clinopyroxene.

Spinel : Greenish brown irregular rounded xenocryst, 0.88x2.88 mm. Dark brown at rim.

Olivine : Angular xenocrysts. Up to 0.9x1.7 mm. Resorption rim (marked by higher interference colour more than core). Some grains showing undulated extinction.

Clinopyroxene:. Elongate rounded xenocrysts. Up to 0.8 x 1.7 mm.

Reaction rim (up to 0.2 mm thick) contains high Ti (pinkish brown in PPL).

Xenoliths : Total mode 10%.

Quartzite : Large aggregate (0.7x1.2 cm). Composed of :

1) Quartzite in core. Consisting of angular quartz grains (up to 0.3 mm diameter). Showing undulated extinction. Boundaries between grains look like the fractures and filled with light brown glass.

2) Clusters of cryptocrystalline fibrous radiated crystals (spherulitic texture) are form in some parts of quartzite area. Up to 1.5 mm diameter.

3) Mantle zone (~1.0 mm thick). Consisting of fan-like shaped plagioclase laths (up to 0.5 mm long, showing swallow-tail) and stubby prismatic euhedral clinopyroxene (up to 0.1x0.2 mm, long (up to 1.5 mm) swallow-tail).

Plagioclase + Clinopyroxene + Ulvöspinel-magnetite : Rounded aggregates. Up to 2.3 mm. diameter. Consisting of: prismatic euhedral crystals of plagioclase, up to 0.5x1.5 mm, lamellar twinning; massive granular clinopyroxene crystals and a large clinopyroxene crystal (~0.5 mm); irregular long (~0.5 mm) crystals of Ulvöspinel-magnetite . Probably gabbro xenoliths ?.

Spinel + Clinopyroxene : Irregular (~0.5 mm diameter) xenolith consisting of one grain of green-brown spinel and one grain of ?clinopyroxene. Clinopyroxene crystal is partly embedded in spinel crystal and showing reaction rim at the contact.

Matrix : Total mode ~82%.

Olivine : Tiny granules. Up to 0.1 mm diameter. Euhedral. Unzoned. Mode <1%.

Ti-augite : Tiny laths. Up to 0.2 mm long. Euhedral. "Hour-glass" sector and oscillatory zoning in individuals. Mode 20%.

Ulvöspinel-magnetite : Tiny granules. Up to 0.1 mm diameter. Mode 15%

Plagioclase Developed in patches as oikocrysts (up to ~0.2 mm diameter) enclosing the tiny clinopyroxene laths and tiny Ulvöspinel-magnetite granules. "Ophimottled texture" and interstice. Mode 5%.

Glass : Colourless. Mode ~41%.

Weathering products : Orange-brown, green. Developed as small mottle areas in some parts of slide.

Amygdales : -

2. **Name : Olivine-Phyric Ophimottled Basalt with Xenoliths and Xenocrysts.**
3. **Interpretation :**

Crystallisation history :

1) Crystallisation of olivine in phenocrysts.
2) Crystallisation of olivine + clinopyroxene in phenocrysts.
3) Crystallisation of olivine + clinopyroxene + Ulvö spinel-magnetite + plagioclase in matrix.
4) Quenching of glass.

Magma type : Probably alkali olivine basalt ? (Ti-rich augite is only clinopyroxene).

Origin of xenoliths /xenocrysts :

Crust : Quartzite

Mantle : Spinel / Spinel + Clinopyroxene / Clinopyroxene.

? : Plagioclase + Clinopyroxene + Ulvöspinel-magnetite / Olivine / Unknown mineral / ? Alkali feldspar.

Sample BP7

1. **Observations**

i) Hand specimen

Colour : Dark grey.

Grain size : Aphanitic.

Obvious phenocrysts : -

Obvious xenocrysts :

1) A large euhedral clean crystal (1.7x1.8 cm.) of ?alkali feldspar.

2) Sub-angular black mineral. Up to 1x1 cm. Vitreous lustre. Conchoidal fracture. ? Clinopyroxene.

Obvious xenoliths :

1) Ultramafic nodules (3x5 mm).

2) The patches of white and green microcrystalline mineral. Up to 0.7 mm diameter.

Obvious amygdales : -

Weathering : The surface of this specimen is changed to be orange -yellow. The zone of weathering from the surface to the core is up to 1.5 cm thick.

Density : Normal.

ii) Thin section

Phenocrysts : Total mode 3%.

Olivine : Euhedral phenocrysts. Up to 0.3 x0.7 mm long. Unzoned. Mode ~1%.

Clinopyroxene : Subhedral phenocrysts. Up to 0.5 x 0.6 mm. Resorption zoning. Ti-rich rim (pinkish brown in PPL). Very weak pleochroism, pale green to pinkish brown in PPL). Mode <<1%.

Alkai feldspar : Sub-angular prismatic. Up to 0.6 x 1.5 mm. reaction rim (~0.1 mm thick), cumulative of (~0.1 mm long) ?clinopyroxene needles. Mode <1%.

Xenocrysts : Total mode 10%.

Olivine : Sub-angular xenocryst. Up to 1.00 x 1.65 mm. Resorption zoning (indicated by higher interference colour than core).

?Alkali feldspar : Sub-angular xenocrysts. Up to 1.0x1.3 cm. Embedded by 4 rounded aggregates (up to 0.8 x 1.6 mm) of glass-alkali feldspar forming in sieve texture. Numerous fractures filled with small crystals of ? plagioclase laths and carbonate (? calcite).

Xenoliths : Total mode 15%.

Alkali feldspar + Nepheline + ?Plagioclase + Clinopyroxene + Ulvöspinel-magnetite : Aggregates. Up to 2 x 2 mm. Composed of :

1) Fractured and turbid alkali feldspar. Irregular crystals, up to 1 mm diameter. Abundant in the core. Some grains show tartan twinning. There are some tiny granules(<0.05 mm diameter) of Ulvöspinel-magnetite s.

2) Mantle zone (~0.4 mm thick) consisting of small laths of ? plagioclase (up to 0.1x0.2 mm), bow tie twinning, and tiny laths of clinopyroxene (up to 0.5 mm long).

Matrix : Total mode ~72%.

Olivine : Tiny granules. Euhedral. Up to 0.2 mm long. Unzoned. Mode ~5%.

Ti-augite : Tiny laths. Euhedral. Up to 0.2 mm long. "Hour-glass" sector zoning. Mode 10%.

Alkai feldspar : Developed in patches as a oikocrysts. (up to 0.5 mm diameter). Enclosing clinopyroxene laths and Ulvöspinel-magnetite granules. "Ophimottled texture. Mode 3%.

Ulvöspinel-magnetite : Tiny granules. Up to 0.1 mm diameter. Mode 10%.

Glass : Brown. Mode ~44%.

Weathering products : Green, developed at the boundaries of some olivine grains probably ?clay mineral. Orange-brown, developed in patches in some parts of this slide, probably ? iddingsite.

Amygdales : -

2. **Name : Olivine-Phyric-Ophimottled Basalt with Xenocrysts and Xenoliths.**
3. **Interpretation :**

Crystallisation history :

1) Crystallisation of olivine in phenocrysts.
2) Crystallisation of olivine + clinopyroxene + plagioclase in phenocrysts.
3) Crystallisation of olivine + clinopyroxene + plagioclase in matrix.
4) Quenching of glass.

Magma type : Probably alkali olivine basalt ? (Ti-rich augite is only clinopyroxene).

Origin of xenoliths / xenocrysts :

Crust : Alkali feldspar + ?Plagioclase + Clinopyroxene + Ulvöspinel-magnetite xenoliths / Alkali feldspar.

Mantle : Olivine.

Sample BP8

1. Observations

i) Hand specimen

Colour : Dark grey.

Grain size : Aphanitic.

Obvious phenocrysts : -

Obvious xenocrysts :

1) Clean angular xenocrysts. Up to 3 x 5 mm. ? Alkali feldspar.
2) Black, conchoidal fracture, vitreous lustre, sub-angular. Up to 1.5 mm diameter. ?Spinel.
3) Black-brown. Step-like fracture (2 direction perfect cleavage), vitreous lustre. Up to 2 mm long. Sub-angular crystals. ?Clinopyroxene.

Obvious xenoliths :

1) Angular ultramafic xenoliths. Up to 6 x 8 mm.
2) Sub-angular xenoliths. Up to 1.4x1.7 cm. Composed of white mineral (probably clay mineral ?), black, grey, yellow-green minerals (can not identify by unaided eyes).
3) White rounded spots. Up to 4 mm diameter. Probably alkali feldspar.

Obvious amygdales : -

Weathering : The surface of this specimen is altered to orange yellow. The weathering zone near the surface is up to 1 cm thick.

Density : Normal.

ii) Thin section

Phenocrysts : Total mode 2%.

Olivine : Euhedral phenocrysts. Up to 0.3 x 0.35 mm. Unzoned. Mode <1%.

Clinopyroxene : Euhedral phenocrysts. Up to 0.3 x 0.4 mm. Reaction rim marked by Ti-rich rim (pinkish brown in PPL). Showing reaction zoning in XPL. The core is turbid in some crystals. Mode <<1%.

Plagioclase : <<< 1%.

Xenocrysts : Total mode 7%.

Clinopyroxene : Sub-angular crystals. Up to 1.8 x 3.5 mm. Resorption zoning (~0.1 mm thick at rim).

Spinel : Sub-rounded xenocrysts. Greenish brown. Up to 2.0x2.3 mm. Completely surrounded by dark green to opaque (0.1 mm thick) reaction rim.

Olivine : Irregular xenocryst. Up to 0.5x1.5 mm. Showing resorption rim (marked by higher extinction than core). Some grains show undulated or uneven extinction indicating they has been strained.

Nepheline : Sub angular xenocrysts. Up to 0.9x1.5 mm. Resorption rim (i.e. strongly zoned at the margin) and tiny laths of clinopyroxene are cumulated at rim. [1st order grey, Biax., 2v ~ 90 degree, colourless in PPL]. Mode <<<<1%.

Alkali feldspar : Stubby prismatic to sub rounded xenocrysts. Up to 2x2 mm. Cloudy inclusion (probably ?clay alteration products). Fractured. Resorption zoning. A part of the grain melted and recrystallised to tiny clinopyroxene laths (up to 0.1 mm long) and clean ?alkali feldspar crystals (up to 0.2 mm long).

Ulvöspinel-magnetite : Sub-rounded xenoliths, 0.4 mm diameter.

Xenoliths : Total mode 20%.

Unknown xenoliths : Angular aggregates. Up to 0.7x1.0 cm (relicts of quench melted alkali feldspar). Composed of :

1) Alkali feldspar subhedral crystals. Up to 1.1 x 1.1 mm. Cloudy inclusion (probably ?clay alteration products). Fractured. Resorption zoning at the rim-matrix contact to the matrix. Partly recrystallised to the quenching texture of sieve-like ?alkali feldspar and of fibrous fan-liked brown mineral.
2) Spherulitic or fan-like shaped aggregates of pale brown fibrous crystals.
3) Carbonate (?calcite) aggregates are filled in 2 cavities (~0.5 mm diameter).
4) Rounded brown spots (up to 1.2 mm diameter) of cryptocrystalline mineral, probably clay mineral ?
5) Clinopyroxene laths. Up to 0.25 mm long. Cumulated at the rim of xenoliths.
6) Tiny orange-brown irregular crystals of unknown mineral. Up to 2 mm diameter.

Spinel + Olivine : A small 0.5 x 0.6 mm. xenolith consisting of 0.4 mm diameter olivine and 0.3 long irregular green-brown spinel. The part of the spinel at the matrix contact side has the ~ 0.1 mm thick opaque reaction rim.

Olivine + Clinopyroxene : A small (0.4x0.5 mm) sub-angular xenolith. Consisting of subhedral (0.4 mm long) clinopyroxene with Ti-rich rim (pinkish brown) at rim-matrix contact and a long olivine crystal (0.4 mm) with slightly reaction rim.

Matrix : Total mode ~71%.

Olivine : Tiny granules. Up to 0.2 mm long. Euhedral. Unzoned. Mode 5%.

Ti-augite : Tiny laths. Up to 0.2 mm long. Euhedral. "Hour-glass" sector zoning. Mode 10%.

Ulvöspinel-magnetite : Tiny granules. Up to ~0.05 mm diameter. Mode 15%.

Alkai feldspar : Developed in patches as oikocrysts enclosing clinopyroxene laths and Ulvöspinel-magnetite granules. "Ophimottled texture" and interstice. Mode ~5%.

Apatite : up to 70 µm. diameter, <<<< 1%.

Glass : Colourless. Mode ~41%

Weathering products : Brown to black spots around unknown xenoliths.

Amygdales : -

2. Name : Olivine-Phyric Ophimottled Basalt with Xenocrysts and Xenoliths.

3. Interpretation :

Crystallisation history :

1) Crystallisation of olivine in phenocrysts.
2) Crystallisation of olivine + clinopyroxene in phenocrysts.
3) Crystallisation of olivine + clinopyroxene + Ulvö spinel-magnetite + plagioclase in matrix.
4) Quenching of glass.

Magma type : Probably alkali olivine basalt ? (Ti-augite is only clinopyroxene).

Origin of xenoliths / xenocrysts :

Crust : ? Unknown xenoliths / Alkali feldspar.

Mantle : Spinel + Olivine / Spinel / Olivine + Clinopyroxene / Olivine / Clinopyroxene.

? : Unknown mineral / Ulvöspinel-magnetite.

Sample BP9

1. Observations

i) Hand specimen

Colour : Dark grey.

Grain size : Aphanitic.

Obvious phenocrysts : -

Obvious xenocrysts : Black mineral. Irregular xenocrysts. 3 x 5 mm. Conchoidal fractured. Vitreous lustre. ?Clinopyroxene.

Obvious xenoliths :

1) Ultramafic nodules. Up to 2 cm diameter.

2) Aggregates of white and brown minerals. Up to 5x8 mm.

Obvious amygdales : Rounded amygdale. 2 mm diameter. Filled with white mineral (?calcite).

Weathering : The surface of this specimen section is weathered to orange brown. The weathering zone from the surface to the core is up to 8 mm.

Density : Normal.

ii) Thin section

Phenocrysts : Total mode 3%.

Clinopyroxene : Euhedral prisms. Up to 0.5 mm long. Pinkish brown to pale green pleochroism. Growth zoning, Ti-rich rim. Mode ~1%.

Olivine : Euhedral phenocrysts. Up to 0.4 mm long. No zoning. Grain boundaries are altered to green-brown [probably ?clay mineral]. Mode ~1%.

Alkai feldspar : Prismatic euhedral phenocrysts. Up to 0.4 x 1.0 mm. Lamellar twinning. Bow-tie twinning. Enclosing the tiny laths (~0.1 mm long) of clinopyroxene and tiny granules (up to ~ 0.05 mm) of Ulvö spinel-magnetite . Mode <<1%. "Ophitic texture".

Xenocrysts : Total mode 5%.

Clinopyroxene : Angular xenocrysts. Up to 1.3 x 3.0 mm. Pinkish brown to pale green. Completely surrounded by reaction rim (up to 0.5 mm thick). Ti-rich rim.

Olivine : Angular xenocryst. Up to 1.0 x 1.7 mm. Irregular extinction. Higher interference colour at rim more than core. Boundaries and fractures are altered to yellow-green to brown minerals (probably ?clay mineral).

Alkali feldspar : Rounded 0.1 mm. xenocryst. Tartan twin. Surrounded by the accumulation of tiny laths of clinopyroxene.

Nepheline : Sub angular xenocrysts.(1.1x2.2 mm). Reaction rim (0.1 mm thick). [1st order grey interference colour, Biax. +ve, 2v ~15°, no cleavage].

Xenoliths : Total mode 10%.

Olivine + Clinopyroxene : Large 0.4x0.5 cm. sub-rounded xenolith. Composed of a large olivine crystal and small 0.6x0.7 sub-rounded clinopyroxene crystal. Olivine shows resorption rim (higher interference colour than core). Clinopyroxene is completely surrounded by reaction rim (~0.2 mm. thick) and very weak pleochroism from pale green to pinkish brown in PPL.

Alkali feldspar + Plagioclase + Clinopyroxene + Apatite + Zircon + Calcite : Rounded to irregular aggregates. Up to 5x7 mm. Composed of :

1) Alkali feldspar. Mass of grain-supported irregular crystals (up to 0.9x1.2 mm). [1st order interference colour, 2v ~60-70°, Biax. +ve].

2) Mass of plagioclase. Formed as small hollow laths (up to 1.5 m. long, the gaps between grains filled with brown glass.

3) Clinopyroxene stubby prism and tiny laths. Up to 0.5 mm long. Some are hollow. Developed as a layer (up to 0.7 mm thick), completely surrounding the xenoliths.

4) Apatite large anhedral crystal with biaxial optic figure.

5) Zircon. A tiny crystal.

6) Rounded amygdales. Up to 0.5 mm diameter. Filled with small calcite crystals (~0.1 mm diameter).

Matrix : Total mode ~82%.

Olivine : Tiny granules. Euhedral. Up to 0.1 mm long. Unzoned. Mode ~5%.

Ti-augite : Tiny laths. Euhedral. Up to 0.2 mm long. "Hour-glass" sector zoning. Pinkish brown to pale green pleochroism. Mode 10%.

Ulvöspinel-magnetite : Tiny granules. Up to ~0.1 mm. Mode 10%.

Alkai feldspar : Developed in patches as oikocrysts (up to 1 mm diameter) enclosing the tiny laths of clinopyroxene and Ulvöspinel-magnetite granules. "Ophimottled texture" and interstice. Mode 5%.

Apatite : Up to 70 μm diameter. <<<< 1%.

Glass : Colourless. Mode 52%.

Weathering products : Brown-green. Developed as specks in some area of matrix. Probably ?clay mineral.

Amygdales : -

2. Name : Olivine-Phyric Ophimottled Basalt with Xenocrysts and Xenoliths.

3. Interpretation :

Crystallisation history :

1) Crystallisation of olivine in phenocrysts.

2) Crystallisation of olivine + clinopyroxene + plagioclase in phenocrysts.

3) Crystallisation of olivine + clinopyroxene + Ulvö spinel-magnetite + plagioclase in matrix.

4) Quenching of glass.

Magma type : Probably alkali olivine basalt ? (Ti-rich augite is only clinopyroxene).

Origin of xenocrysts / xenoliths :

Crust : Alkali feldspar.

Mantle : Olivine + Clinopyroxene / Olivine / Clinopyroxene.

? : Unknown mineral / Alkali feldspar + Plagioclase + Clinopyroxene + Carbonate..

<u>Sample NY1</u>

1. Observations

i) Hand specimen

Colour : Grey-black.

Grain size : Aphanitic (but coarser than the samples from other localities of this study).

Obvious phenocrysts : -

Obvious xenocrysts : -

Obvious xenoliths : -

Obvious amygdales : Rounded amygdales. Up to 2 mm. Filled with white mineral, probably ?zeolite. The sample contains a lot of minute (<1 mm) irregular patches of mineral, probably ?zeolite.

Weathering : The surface of specimen is partly encrusted with thin (<0.01 mm) dark brown material.

Density : Normal.

Other : The sample shows of minute mineral, Ulvöspinel-magnetite .

ii) Thin section

Phenocrysts : Total mode 8%.

Olivine : Euhedral skeletal phenocrysts. Up to 0.5 x 0.7 mm. Fractured. Resorption rim (indicated by higher interference colour than core). Fractures are altered to green and brown minerals (?chlorite and ? iddingsite). Mode 7%.

Clinopyroxene : Subhedral phenocrysts. Up to 0.2 x 0.4 mm. "Hour-glass" sector zoning in XPL. Brown at rim, pale brown at core in PPL. Mode <<<1%.

Xenocrysts : -

Xenoliths : -

Matrix : Total mode 91%.

Olivine : Sub-rounded crystals. Up to 0.15 mm diameter. Unzoned. Mode 7%.

Ti-augite : Euhedral prisms. Up to 0.1x0.3 mm. "Hour-glass" sector zoning in XPL. Brown rim and pale green-brown core. Mode 20%.

Ulvöspinel-magnetite : Equant or long prisms. Up to 0.05x0.5 mm magnetite. Mode 5%.

Plagioclase and Alkali feldspars : Euhedral prisms. Up to 0.1x0.8 mm. Lamellar twinning. Mode 25%.

Zeolite : Colourless. Aggregates of small (<0.05 mm) irregular crystals forming in "consertal texture". [1st order grey interference colour, lower relief than plagioclase feldspar]. Mode 34%.

Amygdales : Total mode <1%.

Round. Up to 1.5 mm diameter. Filled with two minerals : ?zeolite formed in turbid as a outer layer (~0.4 mm thick); carbonate (?calcite) at core.

2. Name : Olivine-Phyric Basalt.

3. Interpretation :

Crystallisation history :

1) Crystallisation of olivine in phenocrysts.
2) Crystallisation of olivine + clinopyroxene in phenocrysts.
3) Crystallisation of olivine + clinopyroxene + plagioclase + Ulvöspinel-magnetite in matrix.
4) Quenching of glass.

Magma type : Probably alkali olivine basalt ? (Ti-augite is only clinopyroxene).

Origin of xenoliths / xenocrysts : -

Sample NY2

1. Observations

i) Hand specimen

Colour : Grey-black.

Grain size : Aphanitic (but coarser than the samples from other localities of this study).

Obvious phenocrysts : -

Obvious xenocrysts : -

Obvious xenoliths : -

Obvious amygdales : Rounded amygdales. Up to 3.5 mm diameter. Filled with white mineral (<1 mm) irregular patches of white mineral, probably ? zeolite.

Weathering : The surface is encrusted by brown material (<0.01 mm thick).

Density : Normal

Other : The sample shows glitter of minute mineral, probably ?Ulvöspinel-magnetite .

ii) Thin section

Phenocrysts : Total mode 8%.

Olivine : Euhedral phenocrysts. Up to 0.2x0.7 mm. Unzoned. Fractured. The fracture zones are altered to green or red-brown minerals (probably chlorite? And ?iddingsite). Resorption zoning (indicated by higher interference colour in rim than core). Mode 7%.

Clinopyroxene : Euhedral stubby prisms. Up to 0.15x0.3 mm. Brown in rim, pale green-brown in core in PPL. "Hour-glass" sector zoning in XPL. Mode <1%.

Xenocrysts : -

Xenoliths : -

Matrix : Total mode 91%.

Olivine : Sub rounded crystals. Up to 0.15 mm diameter. Unzoned. Mode 7%.

Ti-augite Euhedral prisms. Up to 0.1x0.7 mm. Brown rim and weak brown to pale green core in PPL. "Hour-glass" sector zoning in XPL. Mode 15 %

Ulvöspinel-magnetite : Euhedral to irregular shapes. Up to 0.1x0.5 mm. Lamellar twinning. Mode 5%.

Plagioclase and Alkali feldspars: Euhedral prisms. Up to 0.1x0.5 mm. Lamellar twinning. Mode 25%.

Zeolite : Brown, turbid. Aggregates of small (<0.05 mm) irregular crystals forming in "consertal texture". [1st order grey interference colour, lower relief than plagioclase feldspar].. Mode 39%.

Weathering products : Green, yellow-brown. Developed in patches in some parts of matrix. Probably ?chlorite and ?iddingsite.

Amygdales : Total mode <1%.

Rounded amygdales, up to 3.6 mm diameter, filled with fibrous cryptocrystalline brown mineral showing fan-shaped texture.

2. Name : Olivine-Phyric Basalt ?

3. Interpretation : -

Crystallisation history :

1) Crystallisation of olivine in phenocrysts.
2) Crystallisation of olivine + clinopyroxene in phenocrysts.
3) Crystallisation of olivine + clinopyroxene + plagioclase + Ulvöspinel-magnetite in matrix.
4) Quenching of glass.

Magma type : Probably alkali olivine basalt ? (Ti-rich augite is only clinopyroxene).

Origin of xenocrysts / xenoliths : -

Sample NY3

1. Observations

i) Hand specimen

Colour : Grey-black.

Grain size : Aphanitic (but coarser than the samples from other localities in this study).

Obvious phenocrysts : -

Obvious xenocrysts : -

Obvious xenoliths : -

Obvious amygdales : -

Weathering : The surface is encrusted by to yellow-brown material (<0.5 mm thick). The fractures are filled with white and brown minerals.

Density : Normal.

ii) Thin section

Phenocrysts : Total mode 8%.

Olivine : Euhedral. Some skeletal phenocrysts. Up to 0.7x1.0 mm. Unzoned. Fractured. The fracture zones are altered to iddingsite. Mode 7 %.

Ti-augite : Stubby euhedral prisms. Up to 0.2x0.5 mm. Brown rim, green-brown core in PPL. "Hour-glass" sector zoning in XPL.

Xenocrysts : -

Xenoliths : -

Matrix : Total mode 91%.

Olivine : Sub-angular equant crystals. Up to 0.15 mm diameter. Unzoned. Mode 7%.

Ti-augite : Euhedral prisms. Up to 0.15x0.6 mm. Brown rim, pale green-brown core in PPL. "Hour-glass" sector zoning in XPL. Mode 20%.

Plagioclase : Euhedral laths. Up to 0.12x0.7 mm. Lamellar twinning. Mode 25%.

Ulvöspinel-magnetite : Euhedral to angular crystals. Up to 0.2 mm diameter. Mode 4%.

?Devitrified glass or ? zeolite : Light brown turbid aggregates of small (<0.05 mm) crystals forming as "consertal texture". [1st order grey interference colour, lower relief than plagioclase feldspar].. Mode 35%.

Amygdales : Total mode <1%. Rounded amygdales. Up to 0.5 mm. Filled with ? zeolite.

2. Name : Olivine-Phyric Basalt ?

3. Interpretation :

Crystallisation history :

1) Crystallisation of olivine in phenocrysts.
2) Crystallisation of olivine + Ti-augite in phenocrysts.
3) Crystallisation of olivine + Ti-augite + plagioclase + Ulvöspinel-magnetite in matrix.
4) Quenching of glass.

Magma type : Probably alkali olivine basalt ? (Ti-rich augite is only clinopyroxene)

Origin of xenocrysts and xenoliths: -

Sample NY4

1. Observations

i) Hand specimen

Colour : Grey-black.

Grain size : Aphanitic.

Obvious phenocrysts : -

Obvious xenocrysts : -

Obvious xenoliths : -

Obvious amygdales : Rounded amygdales. Up to 3 mm diameter. Some are partly filled. The sample contains a lot of minute (<1 mm) irregular patches of white mineral, probably ?zeolite.

Weathering : The specimen is mantled by orange-brown material (~5 mm thick).
Density : Normal.
Other : The sample shows some glitter of minute mineral, probably Ulvöspinel-magnetite ?.

ii) **Thin section**
Phenocrysts : Total mode 8%.
Olivine : Euhedral phenocrysts. Up to 0.6 x 1.1 mm. Some show resorption rim (higher in interference colour than core). Fractured. The fractures are altered to green to orange brown minerals, probably ?chlorite and ? iddingsite. Mode 7%.
Clinopyroxene : Long prismatic phenocrysts. Up to 0.2x0.8 mm. Brown rim, pale green-brown core in PPL. Mode << 1 %.
Xenocrysts : -
Xenoliths :. -
Matrix : Total mode 92%.
Olivine : Euhedral crystals. Up to 0.2 mm long. Some are hollow. Unzoned. Mode 5%.
Ti-augite : Prismatic euhedral crystals. Up to 0.1x0.4 mm. Brown rim, pale green-brown core in PPL. "Hour-glass" sector zoning in XPL. Mode 15%.
Plagioclase : Euhedral lath. Up to 0.1x1.0 mm. Lamellar twinning. Mode 30%.
Ulvöspinel-magnetite : Euhedral to irregular crystals. Up to 0.25 mm diameter. Mode 5%.
?Devitrified glass or ?Zeolite : Colourless. Aggregates of small (<0.1 mm) irregular crystals forming in "consertal textured". [1st order grey interference colour, lower relief than plagioclase feldspar]. Mode 37%.
Amygdales : -

2. **Name : Olivine-Phyric Basalt ?**
3. **Interpretation :**
Crystallisation history :
1) Crystallisation of olivine in phenocrysts.
2) Crystallisation of olivine + clinopyroxene in phenocrysts.
3) Crystallisation of olivine + clinopyroxene + plagioclase + Ulvöspinel-magnetite in matrix.
4) Quenching of glass.
Magma type : Probably alkali olivine basalt ? (Ti-rich augite is only clinopyroxene).
Origin of xenocrysts and xenoliths: -

<u>Sample NY5</u>
1. **Observations**
i) **Hand specimen**
Colour : Grey-black.
Grain size : Aphanitic.
Obvious phenocrysts : -
Obvious xenocrysts : -
Obvious xenoliths :
Obvious amygdales : Rounded amygdales. Up to 3.0 mm diameter. Completely or partly filled with white mineral, probably ?zeolite. The sample contains abundant minute (<1 mm) irregular patches of white mineral, probably ?zeolite.
Weathering : The surface is mantled by a thick (up to 6 mm) layer of orange-brown weathered material.
Density : Normal.
Other : The sample shows some glitter of minute mineral, probably ?Ulvöspinel-magnetite .

ii) **Thin section**
Phenocrysts : Total mode 8%.
Olivine : Euhedral phenocrysts. Up to 0.9x1.0 mm. Some show resorption rim (indicated by higher in interference colour than core. Fractured. The fractures are altered to ?chlorite (green) and ?iddingsite (orange-brown). Mode 7%.
Titanaugite : Euhedral stubby prismatic phenocrysts. Up to 0.25x0.38 mm. Brown rim, pale green-brown core in PPL. Very weak pleochroism, pale green to pale brown. "Hour-glass" sector zoning in XPL. Mode <1%.
Xenocrysts : -
Xenoliths : -
Matrix : Total mode 92%.
Olivine : Sub-angular equant crystals. Up to 0.1 mm diameter. Unzoned. Mode 3%.
Clinopyroxene : Tiny granule to prismatic euhedral crystals. Up to 0.1x0.4 mm. Brown rim and pale green-brown core in PPL. Some show continuous zoning rim, homogeneous core in XPL. Mode 15%.
Plagioclase : Euhedral laths. Up to 0.1x0.5 mm. Lamellar twinning. Mode 25%.
Ulvöspinel-magnetite : Irregular to euhedral crystals. Up to 0.1x0.5 mm. Mode 4%.
?Devitrified glass or ?Zeolite : Colourless to pale brown. Aggregates of small (<0.05 mm) crystals, forming in "consertal texture". [1st order grey interference colour, lower relief then plagioclase]. Mode 45%.
Amygdales : -

2. **Name : Olivine-Phyric Basalt ?**
3. **Interpretation :**
Crystallisation history :
1) Crystallisation of olivine in phenocrysts.
2) Crystallisation of olivine + Ti-augite in phenocrysts.
3) Crystallisation of olivine + clinopyroxene + plagioclase + Ulvöspinel-magnetite in matrix.
4) Quenching of glass.
Magma type : Probably alkali basalt ? (Ti-rich augite is only clinopyroxene)
Origin of xenocrysts and xenoliths: -

<u>Sample PW1</u>
1. **Observations**
i) **Hand specimen**
Colour : Grey-brown.
Grain size : Very fine.
Obvious phenocrysts : -
Obvious xenocrysts :
Sub-rounded xenocrysts. Up to 2x3 cm. Vitreous lustre black, probably pyroxene.
Obvious xenoliths : -
Obvious amygdales :
Irregular amygdales. Up to 0.2x0.8 cm, filled with white, yellow-grey mineral probably ?zeolite. Some are empty.
Weathering : The specimen is fairly altered as it looks brown but it is still hard as normal.
Density : Normal

ii) **Thin section**
Phenocrysts : Total mode 7%.
Olivine : Euhedral phenocrysts. Up to 0.5x0.8 mm. Some skeletal. Unzoned. The rim (~0.05 mm thick) is altered to ?iddingsite (orange-red). Some are completely altered to iddingsite. Mode ~7%.
Clinopyroxene : Euhedral crystals. Up to 0.4x0.5 mm. Pale- brown, deep brown rim(~0.05 thick). Some are spongy rim. Mode <<<1%.
Xenocrysts : Total mode 2%.
Clinopyroxene : Two elongate-rounded xenocrysts. Up to 5.0 x 9.0 mm. Rimmed by orange turbid alteration rim (0.2 mm thick).
Olivine : Irregular xenocryst. Up to 0.9 x 1.0 mm. Unzoned. Alteration rim (0.1 mm thick).
Aggregate: Sub-rounded aggregate (1.0x1.8 mm). Composed of the tiny granules (up to 0.05 mm diameter) of ? clinopyroxene. Mantled by alteration rim (0.7 mm thick) of iddingsite.
Xenoliths : Total mode 1%.
Unknown: Sub-angular xenolith (2.5x1.0 mm), composed of 9 angular crystals (up to 0.15x0.3 mm,). Some show 1 good direction cleavage. [1st order grey, 2v~0-5 degree, Biax. ve].
Spinel-websterite: A xenolith 1.1x1.1 mm, composed of: 2 subhedral clinopyroxene crystals(up to 0.2x0.4

mm); 2 sub-rounded orthopyroxene crystals (up to 0.3 mm diameter); and 4 subhedral brown spinel crystals (up to 0.15 mm long). The orthopyroxene crystals have been altered to ? clinopyroxene or ?iddingsite (up to 0.2 mm thick) at the rim.

Spinel-lherzolite: Angular xenoliths (up to 1.7x2.4 mm), composed of mainly sub-angular olivine crystals (up to 0.7x0.7 mm); irregular clinopyroxene crystals(up to 0.13x0.50 mm); an orthopyroxene crystal(0.1x0.4 mm); and 3 angular brown spinel crystals (up to 0.2x0.2 mm). The xenolith is slightly altered to iddingsite at rim (<<0.01 mm thick).

Plagioclase feldspar + Alkali feldspar: A xenolith (0.2x0.3 mm). Composed of 5 crystals (up to 0.2 mm diameter). Lamellar twinning resorption rim (<0.02 mm thick).

Matrix : Total mode ~80%.

Olivine : Tiny granules. Up to 0.3 mm diameter. Completely altered to ? iddingsite. Mode 3%.

Clinopyroxene: Tiny laths. Up to <0.01 mm long. Euhedral. Mode 15%.

Ulvöspinel-magnetite : Tiny granules. Up to <0.01 mm diameter. Euhedral. Mode 15%.

Glass : Brown. Some are altered to reddish brown material. Mode 47%.

Amygdales : Total mode 10%.

Irregular. Up to 1.2x2.5 mm. Most are empty. Some are filled with tiny laths of ? plagioclase feldspar (up to 0.2 mm long) and green clinopyroxene (up to 0.15 mm long). The vesicles are aligned in one direction.

2. Name : Vesicular Olivine-Phyric Basalt with Xenocrysts and Xenoliths.

3. Interpretation :

Crystallisation history :

1) Crystallisation of olivine in phenocrysts.
2) Crystallisation of clinopyroxene in phenocrysts.
3) Crystallisation of olivine + clinopyroxene + Ulvö spinel-magnetite in matrix.
4) Quenching of glass.

Magma type : Alkali olivine basalt

Origin of xenocrysts / xenoliths :

Crust : -

Mantle : Spinel-websterite / Spinel-lherzolite.

? : Plagioclase feldspar xenolith / ?Unknown xenolith.

Sample PW2

1. Observations

i) Hand specimen

Colour : Grey - brown.

Grain size : Very fine.

Obvious phenocrysts : -

Obvious xenocrysts :

Black ?pyroxene. Irregular. Up to 0.7x0.7 cm. Vitreous lustre.

Obvious xenoliths :

1) Vesicular angular basalt xenoliths. Up to 0.9x1.0 cm.
2) ?Ultramafic nodules. Up to 0.7x1.0 cm. Altered to brown or red material.

Obvious amygdales :

Ellipsoidal amygdales. Up to 1 mm. Filled with white mineral (probably ? zeolite).

Weathering : The specimen is fairly altered as it looks brown but it is still hard as normal.

Density : Normal

ii) Thin section

Phenocrysts : Total mode 7%.

Olivine : Euhedral phenocrysts. Up to 0.2x0.5 mm. Skeletal or hollow. Some are twin red. Unzoned. Alteration rim (<0.02 mm thick) (? iddingsite, orange-red).

Xenocrysts : Total mode 3%.

Spinel: A small angular xenocryst, 0.1x0.2 mm. Brown. Mantled by opaque reaction rim (~0.1 mm thick).

Clinopyroxene : Rounded xenocrysts. Up to 8.0 x 8.0 mm. Spongy rim (0.15 mm thick).

Olivine : Irregular xenocrysts. Up to 2.0x2.6 mm. Alteration rim (<0.05 mm) in orange-brown.

Xenoliths : Total mode 30%.

Basalt: Vesicular basalt xenoliths, up to 11x12 mm. Sub-rounded. containing more abundant vesicles than in host basalt. The vesicles (15% compared with itself) are rounded, up to 2 mm diameter. The matrix of xenolith is dark brown (darker than the matrix of host basalt). There is an unknown mineral embedded in a xenolith [sub-rounded, 0.8x1.0 mm , isotopic resorption rim (~0.2 mm thick) and an isotopic core, 1st order grey]. The phenocryst is olivine crystal euhedral up to 0.2x0.5 mm.

Matrix : Total mode 59%.

Olivine : Tiny granules. Up to 0.05 mm diameter. Unzoned 2%.

Clinopyroxene: Tiny laths. <0.05mm long. Mode 20%.

Glass : Brown. Mode 37%.

Weathering products: Orange-brown. Developed in patches in some area of thin section.

Amygdales : Total mode <1%.

Irregular amygdales. Up to 0.2 mm across. Filled with ?zeolite.

2. Name : Olivine Phyric Basalt with Xenocrysts and Xenoliths.

3. Interpretation :

Crystallisation history :

1) Crystallisation of olivine in phenocrysts.
2) Crystallisation of olivine + clinopyroxene in matrix.
3) Quenching of glass.

Magma type : Alkali olivine basalt.

Origin of xenocrysts / xenoliths :

Crust : -

Mantle : Spinel / Clinopyroxene / Olivine / Basalt xenoliths (the fragments of the previous basaltic flow erupted and crystallised before this magma body?).

Sample PW3

1. Observations

i) Hand specimen

Colour : Grey-brown.

Grain size : Very fine.

Obvious phenocrysts : -

Obvious xenocrysts :

Angular black pyroxene. Up to 0.2 x 0.8 mm. Vitreous lustre.

Obvious xenoliths :

Sub-angular xenoliths. Up to 0.6 x 0.8 mm. Composed of white-pale green mineral.

Obvious amygdales :

Sub-rounded vesicles. Max. 2.0 mm diameter.

Weathering : The specimen is altered as it looks brown but it is still hard as normal.

Density : Normal.

ii) Thin section

Phenocrysts : Total mode 7%.

Olivine : Euhedral skeletal phenocrysts. Up to 0.5x0.9 mm. The rim is altered to iddingsite (orange-brown). Mode 7%.

Clinopyroxene: Subhedral phenocrysts. Up to 0.2x0.3 mm. Resorption rim. Colourless. Unzoned. Mode <<<1%. Less altered than olivine.

Xenocrysts : Total mode 2%.

Spinel: Three angular xenocrysts. Slightly green brown. Up to 0.2x0.4 mm. Rimmed by opaque layer (~0.05 mm thick).

Clinopyroxene : Sub-rounded xenocrysts. Up to 2.0 x 5.0 mm. Rimmed by a layer (0.1 mm thick) of very tiny granules of ?clinopyroxene. Most abundant than other xenocrysts.

Orthopyroxene: Sub-angular xenocrysts (up to 0.6x1.1 mm). Colourless. Spongy rim (~0.2 mm thick) composed of tiny granules of ? clinopyroxene.

Olivine : Sub-angular xenocrysts. Up to 0.9x1.3 mm. Unzoned. The rim is altered to iddingsite (orange-brown) (0.05 mm thick). Fractured.

Plagioclase feldspar: A prismatic xenocryst (1.2x1.8 mm). Subhedral. Resorption zoning (the resorption rim is ~0.1 mm thick). Turbid. Fractured. Enclosing 2 small needle-crystals. Lamellar twinning.

Xenoliths : Total mode 3%.

Aggregate: A large angular turbid aggregate (7.0x9.0 mm). Brown. Composed of
1) Sub-rounded turbid plagioclase feldspar crystals. Up to 2 mm diameter. Resorption zoning. Some show twinning lamellar.
2) Tiny turbid laths of ? clinopyroxene. Up to 0.1 mm long.
3) Short needles of black mineral (<0.05 mm long).
4) Irregular cavities. Up to 0.5 x1.0 mm.

Lherzolite: A large angular xenolith (1.6x3.6 mm). Slightly resorption rim. Composed of :
1) Olivine crystals. Up to 0.6x2.6 mm. Showing sub grained (unknown extinction).
2) Orthopyroxene. 4 Irregular grains. Up to 0.3x0.4 mm.
3) Clinopyroxene. 2 irregular grains. Up to 0.4x0.8 mm. Showing resorption rim (spongy rim, ~0.1 mm thick) at the grain--matrix contact. Undulated extinction.
4) Five angular slightly green brown spinel. Up to 0.1x0.2 mm. Rimmed by opaque layer (<0.01 mm thick).

Orthopyroxene + Clinopyroxene + Olivine: A large irregular orthopyroxene (1.3x1.3 mm). Spongy rim (~0.1 mm thick) composed of tiny granules of ? clinopyroxene. Two sub-angular grains (up to 0.2x0.3 mm) of clinopyroxene and one sub-angular grain (0.2x0.2 mm) are embedded in the orthopyroxene grain.

Olivine + Spinel: A big (1.3x1.6 mm) subhedral olivine. Alteration margin (~0.05 mm thick) of iddingsite (orange-brown). Three brown sub-angular spinel grains (up to 0.18x0.35 mm) are embedded in the olivine. Spinel grains show dark rims (up to 0.03 mm thick).

Matrix : Total mode 78%.

Olivine : Tiny granules. Up to 0.03 mm diameter. Altered to iddingsite. Mode 2%.

Clinopyroxene: Tiny laths. Up to 0.05mm long. Euhedral. Mode ~ 20%.

Ulvöspinel-magnetite : Tiny granules. Up to 0.05 mm diameter. Euhedral. Mode ~20%.

Glass : Brown or colourless. Mode 36%.

Alkali feldspar : interstice <<<<< 1%.

Weathering products: Developed in black and brown in some parts of slide.

Amygdales : Total mode 10%.
Empty irregular vesicles. Up to 1.7x4.0 mm.

2. **Name : Vesicular Olivine Phyric Basalt with Xenocrysts and Xenoliths.**
3. **Interpretation :**
   Crystallisation history :
   1) Crystallisation of olivine in phenocrysts.
   2) Crystallisation of clinopyroxene in phenocrysts.
   3) Crystallisation of olivine + clinopyroxene + Ulvö spinel-magnetite in matrix.
   4) Quenching of glass.
   Magma type : Alkali olivine basalt
   Origin of xenocrysts / xenoliths :
   Crust : -
   Mantle : Lherzolite / Orthopyroxene + Olivine + Clinopyroxene / Olivine + Spinel / Olivine / Clinopyroxene / Orthopyroxene.
   ? : Aggregate / Plagioclase feldspar.

Sample PW4

1. **Observations**
   i) Hand specimen
   Colour : Grey-brown.
   Grain size : Very fine.
   Obvious phenocrysts : -
   Obvious xenocrysts :
   Angular black pyroxene. Up to 0.5x0.7 mm. Vitreous lustre.
   Obvious xenoliths : -
   Obvious amygdales :
   Empty elongate vesicles. Mode 30%.
   Weathering : The specimen is altered as it looks brown but it is still hard as normal.
   Density : Light.
   ii) Thin section
   Phenocrysts : Total mode 4%.

Olivine : Euhedral skeletal phenocrysts. Up to 0.4x0.6 mm. The rim (~0.05 mm thick) is altered to iddingsite(orange - brown). Mode 4%.

Clinopyroxene: Subhedral phenocrysts. Up to 0.2 mm diameter. Pale-green brown. Resorption rim. Zoning. Mode <<<1%.

Xenocrysts : Total mode 10%.

Clinopyroxene : Sub-rounded to angular xenocrysts. Up to 6.0 x 14.0 mm. Pale green brown. Completely surrounded by a uniform resorption layer (~0.2 mm thick) composed of tiny granules of ?clinopyroxene. Round red-brown aggregate (0.4 mm diameter is included in the grain. Some are pale green-brown core and deep brown rim (0.02 mm thick). Some are spongy margin and show undulated extinction. Move abundant than olivine.

Olivine : Angular xenocrysts. Up to 1.4 x2.5 mm. Colourless. Thin (~0.01 mm) alteration rim(?iddingsite).

Spinel: Irregular pale-green brown spinel (0.18x0.20 mm). Rimmed by opaque layer (up to 0.1 mm thick).

Xenoliths : Total mode <<1%.

Clinopyroxene + Spinel: Irregular xenolith (1.0x2.0 mm). Composed of
1) Four clinopyroxene grains. Angular. Pale-green brown. Up to 0.6x0.7 mm. Some grains are spongy and altered to orange-brown at rim.
2) A brown spinel grain (0.2x0.4 mm). Sub-angular. No opaque rim.

Matrix : Total mode 55%.

Olivine : Tiny granules. Up to 0.02 mm diameter. Altered to iddingsite. Mode 5%.

Clinopyroxene: Tiny laths. Up to 0.05mm long. Euhedral. Mode 15%.

Ulvöspinel-magnetite : Tiny granules. Up to 0.02 mm diameter. Euhedral 10%.

Glass : Brown, colourless. Mode 25%.

Amygdales : Total mode 30%.
Empty irregular-elongate vesicles. Up to 2.2x4.6 mm.

2. **Name : Vesicular Olivine Phyric Basalt with Xenocrysts and Xenoliths.**
3. **Interpretation :**
   Crystallisation history :
   1) Crystallisation of olivine in phenocrysts.
   2) Crystallisation of clinopyroxene in phenocrysts.
   3) Crystallisation of olivine + clinopyroxene + Ulvö spinel-magnetite in matrix.
   4) Quenching of glass.
   Magma type : Alkali olivine basalt
   Origin of xenocrysts / xenoliths :
   Crust : -
   Mantle : Clinopyroxene / Olivine / Spinel / Clinopyroxene + Spinel.

Sample PW5

1. Observations
   - i) Hand specimen
     - **Colour :** Grey-brown.
     - **Grain size :** Very fine.
     - **Obvious phenocrysts :** -
     - **Obvious xenocrysts :** Black xenocrysts. Rounded. Up to 0.4x1.0 cm. Vitreous lustre. Probably clinopyroxene.
     - **Obvious xenoliths :** A large fragment of ultramafic nodule (1.0x2.0 cm) composed of dark green-black mineral gains. (Altered).
     - **Obvious amygdales :** Rounded vesicles. Up to 2.0 cm diameter. Few are filled with white dull mineral.
     - **Weathering :** The specimen is altered as it looks brown but it is still hard as normal.
     - **Density :** Normal.
   - ii) Thin section
     - **Phenocrysts :** Total mode 5%.
       - **Olivine :** Euhedral skeletal phenocrysts. Up to 0.5x0.9 mm. Colourless. Unzoned. Some are twin crystals. The rim is altered to orange -brown ? iddingsite. Mode 5%.
       - **Clinopyroxene:** Subhedral phenocrysts. Up to 0.3x0.3 mm. Pale-green brown. Very weak pleochroism. Brown resorption rim (<0.02 mm thick). Mode <<<1%.
     - **Xenocrysts :** Total mode 10%.
       - **Clinopyroxene :** Well-round margin and elongate crystals. Pale-green brown. Up to 5.5x15.5 mm. Completely surrounded by a uniform resorption layer (~0.12 mm thick) composed of very tiny granules of ?clinopyroxene. One of them has very thick spongy rim (up to 1.6 mm thick). One of them shows undulated extinction.
       - **Olivine :** Subhedral xenocrysts. Up to 1.1x1.8 mm. Sub-grain. Corroded rim. The rim (~0.1 mm thick) is altered to red -brown.
       - **Spinel:** A rounded green-brown spinel (0.2 mm long). Rimmed by opaque layer (<0.02 mm thick).
       - **Turbid aggregate:** Turbid irregular brown aggregates. Up to 1.0x3.0 mm. Composed of mainly brown glass, tiny ?clinopyroxene laths (up to 0.05 mm long), and turbid dark dust-like material.
       - **Brown aggregate:** Rounded brown aggregates. Up to 0.6x1.0 mm. Composed of tiny granules (up to 0.02 mm diameter) of ?clinopyroxene. Probably melted clinopyroxene xenocrysts. The outer layer is altered to red brown.
     - **Xenoliths :** Total mode 5%.
       - **Olivine + Clinopyroxene:** Sub-angular xenolith (1.4x1.7 mm). A largest grain of olivine shows sub-grained (uneven extinction). Two small grains (olivine: 0.2 mm across; clinopyroxene: 0.1 mm across) are associated with a largest olivine grain.
       - **Olivine + Spinel:** Irregular xenolith (1.2x2.0 mm). Composed of
         1) An olivine subhedral grain (1.0x0.8 mm). The rim (~0.08 mm) is altered to red-brown. One part of grain is composed of a mass (~0.5 mm across) of tiny granules (<0.01 mm diameter) of ?clinopyroxene.
         2) Green-brown spinel. Sub-angular (0.6x0.9 mm). Enclosing 2 rounded grains (up to 0.2 mm diameter) of olivine. The spinel is rimmed by opaque layer(0.08 mm thick).
       - **Basalt:** Elongate (1.0x3.5 mm). Angular xenolith. Same composition of host basalt but the xenolith matrix is darker and finer than in the host rock.
     - **Matrix :** Total mode 73%.
       - **Olivine :** Tiny granules. Up to 0.02 mm diameter. Altered to iddingsite. Mode 3%.
       - **Clinopyroxene:** Tiny laths. Up to 0.08 mm long. Euhedral. Mode 25%.
       - **Ulvöspinel-magnetite :** Tiny granules Up to 0.05 mm diameter. Euhedral. Mode 20%.
       - **Glass :** Brown, colourless. Mode 25%.
     - **Amygdales :** Total mode 7%. Long irregular vesicles (up to 0.4x2.3 mm). The rim are accumulated with tiny laths of clinopyroxene.
2. **Name : Olivine Phyric Basalt with Xenocrysts and Xenoliths.**
3. **Interpretation :**
   - **Crystallisation history :**
     1) Crystallisation of olivine in phenocrysts.
     2) Crystallisation of clinopyroxene in phenocrysts.
     3) Crystallisation of olivine + clinopyroxene + Ulvö spinel-magnetite in matrix.
     4) Quenching of glass.
   - **Magma type :** Alkali olivine basalt
   - **Origin of xenocrysts / xenoliths :**
     - **Crust :** -
     - **Mantle :** Clinopyroxene / Olivine / Spinel / Olivine + Clinopyroxene / Olivine + Spinel / Basalt xenolith.
     - **? :** Turbid aggregates / Brown aggregate

Sample PW6

1. Observations
   - i) Hand specimen
     - **Colour :** Grey-brown.
     - **Grain size :** Very fine.
     - **Obvious phenocrysts :** Altered to brown material.
     - **Obvious xenocrysts :**
       1) Black vitreous lustre mineral. Probably ? clinopyroxene. Round, 0.5x0.7 cm.
       2) Olivine 0.2x0.5 mm. Yellow green.
     - **Obvious xenoliths :** Basaltic xenoliths. Up to 0.6x1.0 cm. More vesicle than host rock.
     - **Obvious amygdales :** Empty vesicles.
     - **Weathering :** The specimen is altered as it looks brown and the phenocrysts and some xenocrysts are altered to yellow brown but this specimen is still hard as normal.
     - **Density :** Normal
   - ii) Thin section
     - **Phenocrysts :** Total mode 5%.
       - **Olivine :** Euhedral skeletal phenocrysts Up to 0.4x0.8 mm. The rim is altered to orange-brown (?iddingsite). Some are twinned. Mode 5%.
       - **Clinopyroxene:** Euhedral phenocrysts. Up to 0.20 mm long. Pale green-brown but deeper brown rim (~0.20 mm thick). Mode <<<1%.
     - **Xenocrysts :** Total mode 2%.
       - **Clinopyroxene :** Sub-angular xenocrysts. Up to 4.0x5.0 mm. Pale green-brown. Completely surrounded by a resorption brown layer (0.6 mm thick) which is composed of very tiny granules of ?clinopyroxene and red-brown branching mineral (~0.3 mm long).
       - **Olivine :** Subhedral to irregular xenocrysts. Up to 2.0 x2.8 mm. Colourless. Fractured. The rim (<0.02 mm thick) is altered to red-brown (iddingsite).
       - **Spinel:** An angular (0.1 mm long) slightly-green brown spinel grain. Rimmed by opaque layer (~0.05 mm thick).
     - **Xenoliths :** Total mode 7%.
       - **Basalt:** The fragments of basalt. Irregular brown (up to 3 mm long). The mineral composition is the same as host basalt but it is darker and matrix is finer than host basalt. The xenoliths contain olivine and clinopyroxene phenocrysts, olivine, spinel, and clinopyroxene xenocrysts as well as more abundant and bigger vesicles (up to 1.3 mm diameter;

mode ~25% of xenolith) than in the host rock.

Matrix : Total mode 79%.

Olivine : Tiny granules. Up to 0.03 mm diameter. Altered to red-brown (iddingsite). Mode 2%.

Clinopyroxene: Tiny laths. Up to 0.08 mm long. Euhedral. Mode 20%.

Ulvöspinel-magnetite : Tiny granules. Up to 0.05 mm diameter. Euhedral. Mode 10%.

Glass : Brown, colourless. Mode 47%.

Amygdales : Total mode 7%.

Empty oval or irregular amygdales. Up to 1x2 mm. Clinopyroxene laths always accumulate near the edge of the vesicles.

2. Name : Olivine Phyric Basalt with Xenocrysts and Xenoliths.

3. Interpretation :

Crystallisation history :

1) Crystallisation of olivine in phenocrysts.
2) Crystallisation of clinopyroxene in phenocrysts.
3) Crystallisation of olivine + clinopyroxene + Ulvö spinel-magnetite in matrix.
4) Quenching of glass.

Magma type : Alkali olivine basalt

Origin of xenocrysts / xenoliths :

Crust : -

Mantle : Clinopyroxene / Olivine / Spinel / Basalt xenoliths.

Sample TP1

1. Observations

i) Hand specimen

Colour : Dark grey.

Grain size : Very fine

Obvious phenocrysts : -

Obvious xenocrysts : Angular to sub-rounded dark grey minerals, up to 0.8x1.5 cm. Mantled by white mineral (?zeolite).

Obvious xenoliths : An angular Ultramafic nodule, 0.4 mm diameter.

Obvious amygdales : Irregular, up to 0.2x1.0 cm. filled with white mineral (?zeolite).

Weathering : The specimen is weathered at the surface marked by yellow-brown layer (< 1 mm thick).

Density : Normal.

ii) Thin section

Phenocrysts : Total mode 3% (including microphenocrysts).

Olivine : Skeletal euhedral or hollow crystals, up to 0.4x0.8 mm, containing a deep embayment filled with matrix. No zoning. Mode ~2%.

Ti-augite: Euhedral crystal, up to 0.35x0.60 mm. Brown colour (pale core and intense rim).

Ulvöspinel-magnetite : Sub- angular. Up to 0.25 mm long. <<< 1%.

Xenocrysts : Total mode 2%.

Olivine : Anhedral angular olivine, up to 0.9 x 1.8 mm. Fractured. Resorption rim accumulated by the tiny ? olivine granules (~0.05 mm diameter). Undulated extinction. Lower interference colour (2^{nd} order yellow) than of the phenocrysts (2^{nd} order blue). Mode <<1%.

Clinopyroxene : Anhedral rounded crystal. Up to 2.9 mm diameter. Resorption (brown rim 10.2 mm thick). Some are spongy (sieve-texture) included by olivine granules (0.2 mm diameter). Augite (2v 25°, Biax. $^{+}$ve). Mode 1%.

Brown aggregates (?Melted clinopyroxene): Two sub-rounded and very large aggregates, up to 5 mm diameter. Turbid core and mantled by resorption brown rim (~0.05 mm thick). The core consists of a brown cryptocrystalline mineral showing sub-radiate texture (2^{nd} order yellow interference colour). The matrix is composed of the spongy mineral (2^{nd} order blue interference colour). The aggregates are cross cut and partly mantled by the veins (0.2 mm thick) of ?zeolite crystals, up to 0.1x0.3 mm. [Probably ? natrolite, 1^{st} order orange, euhedral prisms, // extinction, length slow]. Mode 1%.

Xenoliths : Total mode <<<1%.

Peridotite nodule: A large xenolith, 3.3x3.6 mm. Composed of 3 anhedral crystals of olivine, up to 3 mm lone. Showing lattice deformation (i.e. uneven extinction). Reaction rim and accumulated by the tiny euhedral pale-green and brown-rim minerals, up to 0.2 mm long (?clinopyroxene).

Matrix : Total mode 93%.

Olivine : Tiny granules, up to 0.5 mm long. Euhedral. Unzoned. Some altered to yellow-green (iddingsite). Mode ~10%

Ti-augite : Tiny laths, up to 0.1 mm long, prismatic euhedral. Sector zoning. Mode 10%.

Ulvöspinel-magnetite : Tiny equant granules. Ca. 0.02 mm diameter. Mode 15%.

Plagioclase feldspar : Developed in patches as oikocrysts enclosing the tiny clinopyroxene laths and Ulvö spinel-magnetite (Poikilitic texture or "ophimottled texture"). Mode 10%.

Glass : Brown. Mode 48%.

Weathering products : Orange brown. Similar to iddingsite. Developed in patches in some parts of slide.

Amygdales : Total mode <1%.

Rounded to irregular shaped, up to 0.4 mm long. Filled with ?zeolite (Natrolite).

2. Name : Olivine-Phyric Basalt with Xenocrysts and Xenoliths.

3. Interpretation :

Crystallisation history :

1) Crystallisation of olivine.
2) Crystallisation of olivine + clinopyroxene + Ulvö spinel-magnetite in phenocrysts.
3) Crystallisation of olivine + clinopyroxene + Ulvö spinel-magnetite + plagioclase feldspar in matrix.
4) Quenching of glass.

Magma type : Probably alkali olivine basalt ? (Ti-rich augite is only clinopyroxene)

Origin of xenocrysts and xenoliths:

Crust :-

Mantle : Ultramafic nodule / Olivines / Clinopyroxene.

Sample TP1/2 (Note : Portion from TP1)

1. Observations

i) Hand specimen

Colour : Dark grey.

Grain size : Very fine.

Obvious phenocrysts : -

Obvious xenocrysts: Angular brown-grey aggregate, 0.4x0.6 cm, (mantled by a layer(~0.2 cm thick) of white-mineral (?zeolite)).

Obvious xenoliths : -

Obvious amygdales : Irregular, up to 0.2x0.6 cm, filled with ?zeolite.

Weathering : The specimen is altered at the surface marked by encrusted with thin brown to black layer (<0.05 mm).

Density : Normal.

ii) Thin section

Phenocrysts : Total mode 3%.

Olivine : Euhedral crystals, up to 0.8x2.0 mm. Hollow or skeletal grains embedded with matrix. Unzoned. Mode 2 %.

Clinopyroxene : Euhedral prismatic or stubby crystals. Up to 0.30x0.30 mm. Pale green core and brown rim. Some show spongy core. Mode <1%.

Xenocrysts : Total mode 5%.

Olivine : Sub-angular xenocrysts, 1.2x0.8 mm. Uneven extinction. Resorption rim. Mode <<1%.

Clinopyroxene : Sub-angular xenocryst, 0.6x0.7 mm. Brown (pale core and intense rim). The brown layer is 0.05 mm thick. Resorption rim. Mode <<1%.

Aggregate (?Melted clinopyroxene): Brown aggregate, 0.3x1.7 mm. Spongy core and thin brown rim (~0.03 mm thick). Mantled by ? glass and tiny needle-liked crystals. The core mineral is 2nd order yellow, probably ?clinopyroxene. Mode ~1%.

Aggregates: Not well-defined boundary aggregates, up to 3.0x7.0 mm. rounded shape. Composed of plagioclase feldspar laths(up to 0.1x0.3 mm) with lamellar twinning; "hour-glass" sector zoned Ti-augite laths, up to 0.2 mm long; rounded to irregular amygdales filled with ?zeolite, up to 1 mm diameter; tiny granules of Ulvöspinel-magnetite , <0.01 mm.; glass. Mode ~3%.

?Spinel: A brown-green xenocrysts. Sub-angular 0.1x0.2 mm. grain. Rimmed by opaque layer (<0.05 mm thick). Mode <<<<1%.

Ulvöspinel-magnetite : An irregular xenocrysts, 0.5 mm long. Reaction rim. Mode <<<1%.

Xenoliths : -

Matrix : Total mode 91%.

Olivine : Tiny granules up to 0.05 mm diameter. Euhedral. Unzoned. Mode ~10%.

Clinopyroxene : Tiny laths up to 0.1 mm long. Euhedral prisms. "Hour-glass" sector zoning. Mode 15%.

Ulvöspinel-magnetite : Tiny granules. Up to 0.01 mm diameter. Euhedral crystals. Mode 15%.

Plagioclase feldspar and zeolite: Tiny laths, up to 0.1 mm long. Euhedral prisms. Lamellar twinning. Poikilitic texture. Mode 2%.

Glass : Brown. Mode 49%.

Weathering products : Developed in patches, in orange-brown or green, in some parts of thin section.

Amygdales : Total mode <1%.

Rounded amygdales. Up to 0.6 mm diameter. Filled with ?zeolite {?natrolite, 1st order orange, prisms, parallel extinction, length slow].

2. Name : Olivine-Phyric Basalt with Xenocrysts.

3. Interpretation :

Crystallisation history :

1) Crystallisation of olivine.
2) Crystallisation of olivine + clinopyroxene in phenocrysts.
3) Crystallisation of olivine + clinopyroxene + Ulvö spinel-magnetite + plagioclase feldspar in matrix.
4) Quenching of glass.

Magma type : Probably alkali olivine basalt ? (Ti-rich augite is only clinopyroxene).

Origin of xenocrysts and xenoliths:

Crust : -

Mantle : Spinel / Olivine / Clinopyroxene.

? : Aggregates / Ulvöspinel-magnetite .

Sample TP1/3

1. Observations

i) Hand specimen

Colour : Dark grey.

Grain size : Very fine.

Obvious phenocrysts : -

Obvious xenocrysts : -

Dark grey. Sub-rounded to rounded. Aggregates, up to 0.7x1.0 cm..

Obvious xenoliths : Ultramafic nodule, 0.8x1.5 cm.

Obvious amygdales : Irregular amygdales, up to 0.6x0.8 cm, filled with white mineral, probably ?zeolite.

Weathering: The surface of specimen is altered to brown material formed in a thin layer(<0.05 mm).

Density : Normal.

ii) Thin section

Phenocrysts : Total mode 2%.

Olivine: Euhedral phenocrysts, up to 0.5x1.8 mm. Unzoned. Some are skeletal or hollow. Some are altered to green mineral (?chlorite). Mode 1%.

Clinopyroxene : Brown euhedral phenocrysts, up to 0.7x1.6 mm. Spongy core and clean rim (0.1 mm thick). The spongy core of some grains is altered to yellow-green mineral. The prismatic euhedral microphenocrysts show sector zoning. Mode <1%.

Xenocrysts : Total mode 2%.

Sieve-texture ?Clinopyroxene : Sub-angular xenocrysts, up to 2.0x4.2 mm. The core is spongy, composed of massive tiny granules of ? clinopyroxene. The overgrown rim, 0.1 mm thick, is clean.

Unknown mineral : Sub-rounded xenocrysts, up to 0.5x0.7 mm. [1st order white, length slow, Biax. -ve, 2 directions-cleavages (90), parallel extinction, probably ?orthopyroxene]. Rimmed by a layer (0.15 mm thick) of massive tiny ?clinopyroxene granules (<0.01 mm across).

Xenoliths : Total mode 7%.

Websterite: A large xenolith, 8.0x17.0 mm, mantled by brown resorption rim (0.2 mm thick). Composed of: clinopyroxene grains, irregular, up to 7.2x10.8 mm; orthopyroxene grains, irregular, up to 4.5x9.9 mm, uneven extinction.

Matrix : Total mode 88%.

Olivine: Tiny granules. Up to 0.1 mm diameter. Euhedral. Unzoned. Mode 10%.

Ti-augite: Tiny laths. Up to 0.1 mm long. Euhedral prisms. Sector zoning. Mode 20%.

Ulvöspinel-magnetite : Tiny granules. Up to 0.08 mm. Euhedral. Mode 10%.

?Plagioclase feldspar or ?zeolite: Tiny laths, up to 0.18 mm. Euhedral. Twinning lamella. Some developed in patches as oikocrysts enclosing Ti-augite laths and Ulvöspinel-magnetite granules, ("ophimottled texture"). Mode 7%.

Glass: Colourless and embedded with needle crystals of unknown mineral. Mode 41%.

Weathering products : Green-brown. Developed in patches in some parts of thin section.

Amygdales : Total mode <<1%.

Irregular amygdales, up to 0.4x0.5 mm. Filled with ?zeolite.

2. Name : Olivine-Phyric Basalt with Xenocrysts and Xenoliths.

3. Interpretation :

Crystallisation history :

1) Crystallisation of olivine in phenocrysts.
2) Crystallisation of olivine + clinopyroxene in phenocrysts.
3) Crystallisation of olivine + clinopyroxene + Ulvö spinel-magnetite + plagioclase feldspar in ground mass.
4) Quenching of glass.

Magma type : Probably alkali olivine basalt ? (Ti-rich augite is only clinopyroxene)

Origin of xenocrysts and xenoliths:

Crust : -

Mantle : Clinopyroxene / Websterite / ?Unknown mineral

Sample TP2

1. Observations

i) Hand specimen

Colour : Dark grey.
Grain size : Very fine.
Obvious phenocrysts : -
Obvious xenocrysts :
1) Sub-rounded dark grey xenocrysts. Up to 0.7x1.2 cm. Sub-vitreous lustre on the flat surface.
2) Yellowish grey dull xenocrysts, 0.3x0.5 cm. Rounded shape.
Obvious xenoliths : -
Obvious amygdales :
Irregular elongate amygdales. Up to 0.2x1.7 cm. Filled with ?zeolite.
Weathering : The surface of thin section is altered to yellow-brown material, <0.01 mm thick.

ii) Thin section
Phenocrysts : Total mode 4%.
Olivine : Euhedral phenocrysts. Up to 0.4xx0.6 mm. Some skeletal. Unzoned. Some are altered to iddingsite. Mode 3%.
Clinopyroxene: Euhedral phenocrysts. Up to 0.8x1.0 mm. Brown. Pale-greenish brown core and more deep brown rim (<0.1 mm thick). Some are spongy at core. Mode 1%.
Xenocrysts : Total mode 25%.
Sieve texture ?Clinopyroxene: Large brown xenocrysts. Up to 7x12 mm. Angular shaped. Core is spongy or sieve texture and overgrown rim (~0.1 mm) is deeper brown than core. Some show shief-liked aggregate in core. Some are included with tiny granules of euhedral olivine (~0.15 mm). Partly mantled by the ?zeolite or glass layer(~1.8 mm thick).
Spinel: A triangular shaped spinel (0.2 mm). Dark rim (~0.05 mm thick). And green-brown core.
Unknown mineral: A colourless block xenocryst, 1.5x2.0 mm. Marginal zoning. Rimmed by some quenched swallow-tail clinopyroxene crystals and glass layer (~0.1 mm thick). Probably ?plagioclase [1st order white, Biax. +ve, 2v ~30 , length fast].
Aggregate of Ulvöspinel-magnetite : A longitudinal aggregate (size 0.5x3.6 mm) of tiny granules (~0.01 mm diameter) of brown and Ulvöspinel-magnetite s (Ulvöspinel-magnetite). Probably melted biotite.
Xenoliths : Total mode <<1%.
Clinopyroxenite: A curved-boundary xenolith, 0.9x3.0 mm. Composed of 4 crystals of clinopyroxene, up to 0.5x1.5 mm. The xenolith is rimmed by brown resorption layer (~0.05 mm thick). One grain in the middle has spongy rim (~0.03 mm thick).
Matrix : Total mode 70%.
Olivine : Tiny granules . Up to 0.05 mm diameter. Euhedral. Unzoned. Mode 7%.
Clinopyroxene : Tiny laths. Up to 0.15 mm long. Euhedral prisms. Mode ~15%.
Ulvöspinel-magnetite : Tiny granules. Up to 0.02 mm. Euhedral. Mode 15%.
Plagioclase feldspar : Developed in laths (~0.2 mm long) or in patches as oikocrysts enclosing clinopyroxene laths and Ulvöspinel-magnetite granules. Lamellar twinning. Poikilitic texture. Mode 7%.
Glass : Colourless, embedded by tiny crystals of unknown mineral. Mode 26%.
Amygdales : Total mode <1%.
Irregular amygdales. Up to 0.3x0.8 mm. Filled up with colourless mineral probably ? zeolite [1st order grey or orange, length slow] crystals. One of amygdale is rimmed by a layer (~0.2 mm thick) of tiny clinopyroxene laths (~0.1 long).

2. Name : Olivine-Phyric Basalt with Xenocrysts and Xenoliths.
3. Interpretation :
Crystallisation history :
1) Crystallisation of olivine in phenocrysts.
2) Crystallisation of olivine + clinopyroxene in phenocrysts.
3) Crystallisation of olivine + clinopyroxene + Ulvö spinel-magnetite + plagioclase feldspar or zeolite in ground mass.
4) Quenching of glass.
Magma type : Probably alkali olivine basalt ? (Ti-rich augite is only clinopyroxene).
Origin of xenoliths / xenocrysts :
Crust : -
Mantle : Clinopyroxenite / Sieve-texture clinopyroxene / Spinel.
? : Unknown mineral / Aggregate of Ulvö spinel-magnetite s.

<u>Sample TP3</u>

1. Observations
i) Hand specimen
Colour : Dark grey.
Grain size : Very fine.
Obvious phenocrysts : -
Obvious xenocrysts : Dark grey to brown xenocrysts, up to 0.6x1.0 mm. Sub-rounded.
Obvious xenoliths : -
Obvious amygdales : -
Texture : -
Weathering : The specimen is altered at the surface marked by the brown-yellow spot or thin layer (~1 mm).
Density : Normal.

ii) Thin section
Phenocrysts : Total mode 4%.
Olivine : Euhedral phenocrysts. Up to 0.5x0.8 mm. Unzoned. Some skeletal. Mode 3% (including microphenocrysts).
Clinopyroxene: Euhedral phenocryst. Up to 0.3x0.5 mm, zoning. Spongy core and clean rim (thickness of 0.1 mm). Brown. Some are pale-green at core and brown rim. Mode 1%.
Xenocrysts : Total mode 5%.
Clinopyroxene: Irregular to rounded xenocrysts. Up to 0.8 x 1.2 mm. Rimmed by brown layer (<0.05 mm thick).
Aggregates: Brown and turbid aggregates. Sub-angular, up to 6.0x9.0 mm. Spongy core and partly rimmed by a brown clean layer (up to 0.2 mm thick), included by tiny granules (~0.1 mm diameter) of ?olivine and rounded amygdale (fill with ? zeolite, up to 0.2 mm). Probably ? melted clinopyroxene [2nd order yellow].
Xenoliths : Total mode ~2%.
Olivine + Clinopyroxene: A xenolith 1.7x3.6 mm. Consists of a large angular olivine crystal and a small (0.2x0.6) clinopyroxene crystal. The xenolith shows brown resorption rim (~0.1 mm thick). Four euhedral brownish green spinel crystals (up to 0.25x0.35 mm) included in olivine. The olivine also contains some tiny 2 phase-inclusions.
Websterite: A large sub-rounded xenolith (6.0x7.0 mm). Consisting of mainly clinopyroxene crystals (up to 0.9x2 mm) and orthopyroxene crystals (up to 0.1 mm, diameter). Some crystals are altered to opaque turbid mass. The crystals has spongy rim (0.2 mm thick).
Matrix : Total mode ~88%.
Olivine : Tiny granules. Up to 0.05 mm diameter. Unzoned. Mode ~7%.
Clinopyroxene: Tiny laths. Up to 0.1 mm long. Brown-zoned. Mode 15%.
Ulvöspinel-magnetite : Tiny granules, euhedral, (< 0.01mm.). Mode 10%.
Plagioclase : Poikilitic texture. Mode 5 %.
Zeolite : Interstice. Mode <<<< 1%.
Glass : Brown. Mode ~50%.

Amygdales : Total mode<1%.
Irregular amygdales. Up to 1x4 mm. Filled with ?zeolite [1st order grey, prismatic crystals, up to 0.2x0.6 mm] and ?calcite.

2. Name : Olivine-Phyric Basalt with Xenocrysts and Xenoliths.

3. Interpretation :

Crystallisation history :
1) Crystallisation of olivine in phenocrysts.
2) Crystallisation of clinopyroxene in phenocrysts.
3) Crystallisation of olivine + clinopyroxene + Ulvö spinel-magnetite in matrix.
4) Quenching of glass.

Magma type : Probably alkali olivine basalt ? (Ti-rich augite is only clinopyroxene).

Origin of xenoliths / xenocrysts :

Crust : -

Mantle: Clinopyroxene / Olivine + Clinopyroxene / Websterite.
? : Aggregates.

Sample TP4

1. Observations

i) Hand specimen

Colour : Dark grey.
Grain size : Very fine.
Obvious phenocrysts: -
Obvious xenocrysts : Brown xenocrysts, up to 0.3x0.7 cm.
Obvious xenoliths : Black sub-rounded xenoliths. Up to 0.5x0.4 cm.
Obvious amygdales : Irregular amygdales. Up to 0.3x0.4 cm, filled with ?zeolite(white).
Texture : -
Weathering : The surface of the specimen is altered to yellow-brown material (<1 mm thick).
Density : Normal

ii) Thin section

Phenocrysts : Total mode 4%.
Olivine : Euhedral phenocrysts. Up to 0.5 x 0.5 mm. Unzoned. Some skeletal. Mode 3%.
Clinopyroxene: Euhedral phenocrysts. Up to 0.5x0.6 mm. Pale green-brown core (some spongy at core) and brown rim (<0.01 mm thick). "Hour-glass" sector zoning. Mode <1%.

Xenocrysts : Total mode 1%.
Olivine : Anhedral xenocrysts. Up to 1.0 x 1.5 mm. Resorption zoning, marked by interference colour difference between core and rim.
Aggregates: Rounded aggregates, up to 1.3x2.3 mm. Brown. Spongy core and clean rim (<0.05 mm thick). Probably melted ?clinopyroxene.
Ulvöspinel-magnetite aggregates: Elongate shaped aggregates. Up to 0.4x2.7 mm. Accumulation of tiny euhedral Ulvöspinel-magnetite granules (Ulvöspinel-magnetite , size <0.01 mm). Probably ?melted biotite.

Xenoliths : Total mode 1%.
Quartzite : A large irregular xenolith (5.0x10 mm). Composed of : the fragments of angular quartz grains (up to 0.2x0.3 mm) with undulated extinction. Mantled by the turbid-brown cryptocrystalline mineral. Some parts contain irregular amygdales (up to 0.5x1.0 mm) , filled with ?zeolite. The xenolith is rimmed by a thin (<0.03 mm) layer of the very tiny laths of ?clinopyroxene.

Matrix : Total mode 93%.
Olivine : Tiny granules. Up to 0.5 mm diameter. Euhedral. Unzoned. Mode 10%.
Clinopyroxene: Tiny laths. Up to 0.01 mm long. Euhedral. Zoning. Mode 20%.
Ulvöspinel-magnetite : Tiny granules. Up to 0.02 mm diameter. Euhedral. Mode 15%.
Glass : Brown. Mode 48%.

Amygdales : Total mode <1%.
Irregular amygdales. Up to 4x3 mm. Filled with ?zeolite.

2. Name : Olivine-Phyric Basalt with Xenocrysts and Xenoliths

3. Interpretation :

Crystallisation history :
1) Crystallisation of olivine in phenocrysts.
2) Crystallisation of olivine + clinopyroxene in phenocrysts.
3) Crystallisation of olivine + clinopyroxene + Ulvö spinel-magnetite in ground mass.
4) Quenching of glass.

Magma type : Probably alkali olivine basalt ? (Ti-rich augite is only clinopyroxene).

Origin of xenoliths /xenocrysts :

Crust : Quartzite.
Mantle : Olivine
? : Aggregates / Ulvöspinel-magnetite aggregates?

Sample TP5

1. Observations

i) Hand specimen

Colour : Dark grey.
Grain size: Very fine..
Obvious phenocrysts : -
Obvious xenocrysts :
1) Black angular phenocryst, 0.2x0.3 cm. Vitreous lustre.
2) Grey-brown angular phenocrysts, up to 0.4x0.8 cm. Dull.
Obvious xenoliths : -
Obvious amygdales : -
Weathering : The surface of the sample is weathered to an orange-brown layer (<0.1 mm thick).
Density : Normal.

ii) Thin section

Phenocrysts : Total mode 4%.
Olivine : Euhedral phenocrysts. Up to 0.4x0.8 mm. Skeletal. Unzoned. Mode 3%.
Clinopyroxene : Euhedral phenocrysts. Up to 0.5x0.8 mm. Brown. Some are spongy at core and clean at rim(~0.1 mm thick). Some are clean but the rim is deeper brown and the core is pale brown or pale-green brown. Mode <1%. Some show "Hour-glass" sector zoning.

Xenocrysts : Total mode 5%.
Clinopyroxene: Sub- angular xenocrysts. Up to 4.0x5.0 mm. Showing good 1-direction cleavage. Pale brown core but mantled by a darker brown rim (~1 mm thick).
Olivine : Irregular xenocryst. Up to 0.7 x 1.4 mm. Resorption interference colour (at rim).
Aggregates: Brown sub-rounded aggregates Up to 1.7x2.3 mm. Composed of spongy materials and included by ? clinopyroxene laths (up to 0.2 mm long). Probably ?melted clinopyroxene. At the aggregate-matrix contact, there is a layer (up to 0.2 mm thick) of ?zeolite.

Xenoliths : -

Matrix : Total mode 90%.
Olivine : Tiny granules. Up to 0.05 mm diameter. Unzoned. Mode 5%.
Clinopyroxene: Tiny laths. Up to 0.1 mm long. Euhedral. Mode 25%.
Ulvöspinel-magnetite : Tiny granules. Up to ~0.03 mm diameter. Euhedral. Mode 20%.
?Plagioclase feldspar : Developed in small patches (up to 0.2x1.5 mm) as oikocrysts including clinopyroxene laths and Ulvöspinel-magnetite granules. Some show lamellar twinning. Mode ~3%.
Glass : Brown. Mode 37%.

Amygdales : Total mode <<1%.
Irregular amygdales. Up to 0.3x1.8 mm. Filled with ?zeolite. [Prismatic or blocky euhedral crystals, up to 0.2x0.2 mm, 1st order orange].

2. Name : Olivine-Phyric Basalt with Xenocrysts.

3. Interpretation :

Crystallisation history :
1) Crystallisation of olivine in phenocrysts.
2) Crystallisation of clinopyroxene in phenocrysts.

3) Crystallisation of olivine + clinopyroxene + Ulvö spinel-magnetite in ground mass.
4) Quenching of glass.

Magma type : Probably alkali olivine basalt ? (Ti-rich augite is only clinopyroxene).

Origin of xenoliths / xenocrysts :

Crust : -

Mantle : Olivine / Clinopyroxene.

? : Aggregates

Sample TP6

1. Observations

i) Hand specimen

Colour : Dark grey.

Grain size : Very fine.

Obvious phenocrysts : -

Obvious xenocrysts :

1) Grey brown angular xenocrysts. Up to 0.5x0.7 cm. Dull.

2) Black vitreous sub-rounded xenocrysts. Up to 0.5x0.8 cm. Probably pyroxene.

Obvious xenoliths : -

Obvious amygdales :

Irregular empty amygdales. Up to 0.6x1.3 cm. Partly filled with white globular formed ?zeolite.

Weathering : The specimen is weathered near the surface marked by yellow-grey colour(~3 mm thick).

Density : Normal.

ii) Thin section

Phenocrysts : Total mode 8%.

Olivine : Euhedral skeletal phenocrysts. Up to 0.7 x 1.5 mm. Unzoned. One of these filled with spongy irregular ? clinopyroxene crystals (up to 0.2x0.4 mm) in the hollow area (0.2x0.4 mm). Some are twinned crystals. Mode 5%.

Clinopyroxene : Euhedral phenocrysts. Up to 0.5x 0.6 mm. Spongy core and clean rim (0.05 thick). Brown but pale green-brown core. "Hour-glass" sector zoning. Mode 2%.

Ulvöspinel-magnetite : Subhedral phenocrysts. Up to 0.2x0.3 mm. Mode <<<1%.

Xenocrysts : Total mode 3%.

Orthopyroxene: A large 2.0x4.0 mm. angular xenocrysts. Resorption zoning. The rim (up to 0.4 mm thick) is spongy and including the tiny laths or needles (up to 0.2 mm long) of clinopyroxene.

Olivine: Subhedral xenocrysts. Up to 0.8 x 1.3 mm. Undulated extinction and resorption interference colour (at rim).

Aggregates: Sub-angular brown and turbid aggregates. Up to 5.0x7.0 mm. Some are clean at rim (~0.05 mm thick). The cores of some aggregates shows branching texture. Around the aggregate is the layers (~1 mm thick) of ?zeolite.

Xenoliths : Total mode <1%.

Olivine + Orthopyroxene : An xenoliths, 1.9x2.8 mm. Consisting of a large crystal of olivine and a small (0.4x1.1 mm) orthopyroxene crystal. Olivine shows resorption interference colour at rim but orthopyroxene shows resorption spongy layer(~0.06 mm) at rim where the xenolith contacts to the matrix.

Clinopyroxene : Sub-angular xenolith (1.5x2.1 mm) , consists of 2 clinopyroxene crystals (1.5x2.1 mm and 0.5x1.0 mm. in sizes respectively). Brown. Clean core but spongy rim (~0.4 mm thick). The outmost rim (~0.05 mm thick) is intense brown (Ti-rich).

Matrix : Total mode 88%.

Olivine : Tiny granules. Up to 0.05 mm diameter. Unzoned. Mode 5%.

Clinopyroxene: Tiny laths. Up to 0.1 mm long. Euhedral. Brown. "Hour-glass" sector zoning. Mode 25%.

Ulvöspinel-magnetite : Tiny granules. Up to 0.03 mm diameter. Euhedral. Mode 20%.

Plagioclase : Developed in patches , some in lath(~0.1 mm long) with lamellar twinning. Mode 5%.

Glass : Brown. Mode 33%.

Amygdales : Total mode <<1%.

Irregular amygdales. Up to 0.3x0.4 mm. Filled with ?zeolite.

2. Name : Olivine-Phyric Basalt with Xenocrysts and Xenoliths.

3. Interpretation :

Crystallisation history :

1) Crystallisation of olivine in phenocrysts.
2) Crystallisation of olivine + clinopyroxene in phenocrysts.
3) Crystallisation of olivine + clinopyroxene + Ulvö spinel-magnetite + plagioclase in matrix.
4) Quenching of glass.

Magma type : Probably alkali olivine basalt ? (Ti-augite is only clinopyroxene).

Origin of xenoliths / xenocrysts :

Crust : .

Mantle : Orthopyroxene / Olivine / Olivine + Orthopyroxene / Clinopyroxene.

? : Aggregate.

Sample NB1

1. Observations

i) Hand specimen

Colour : Grey.

Grain size : Very fine.

Obvious phenocrysts : -

Obvious xenocrysts :

1) Ulvöspinel-magnetite . Opaque. Metallic lustre. Angular. Up to 0.4x0.6 cm.
2) White, dull. Elongate unknown xenocrysts (0.5x1.8 cm).

Obvious xenoliths : -

Obvious amygdales :

Irregular amygdales. Up to 0.5x0.7 cm. Filled with carbonate? Some are empty.

Weathering : The specimen is weathered at the surface in yellow-orange, up to ~1 cm.

Density : Heavy.

ii) Thin section

Phenocrysts : Total mode 6%.

Olivine : Euhedral phenocrysts. Up to 0.2 x 0.3 mm. Colourless. Some are hollow. Resorption zoning. Twinning. Mode 5%.

Clinopyroxene : Euhedral pale brown phenocrysts. Up to 0.2x0.5 mm. Spongy core but clean deep-brown rim (0.02 mm thick). Resorption zoning. Mode 1%.

Xenocrysts : Total mode 5%.

Ulvöspinel-magnetite : Two angular opaque xenocrysts (6.0x8.0 mm and 1.0x1.3 mm respectively). Fractured. The fracture zones are filled with cryptocrystalline mineral and ?calcite.

Clinopyroxene: Angular xenocrysts. Up to 4.0x5.0 mm. Pale green-brown. Spongy and mantled by clean rim (~ 0.10 mm thick). Some are clean at core by spongy deeper brown at rim. Enclosing 3 tiny granules of euhedral ?olivine (up to 0.1 mm diameter). The grain-matrix contact contains some cavities. One of them contains the branch-liked texture of turbid ? clinopyroxene (cryptocrystalline) and 0.1 mm diameter spots of Ulvöspinel-magnetite .

Xenoliths : -

Matrix : Total mode 87%.

Olivine : Tiny granules. Up to 0.05 mm diameter. Unzoned. Mode 5%.

Clinopyroxene: Tiny laths. Up to 0.15 mm long. Euhedral. Brown. Mode 25%.

Ulvöspinel-magnetite : Tiny granules. Up to 0.02 mm diameter. Euhedral. Mode 15%.

Nepheline : Poikilitic texture. 5%.

Glass : Colourless. Mode 37%.

Weathering products: Developed in orange-brown as the small patches in some area of slide.

Amygdales : Total mode 2%.
Oval amygdales. Up to 1.2x2.4 mm. Filled with carbonate (?calcite). Some are empty.

2. Name : Olivine-Phyric Basalt with Xenocrysts

3. Interpretation :

Crystallisation history :
1) Crystallisation of olivine in phenocrysts.
2) Crystallisation of clinopyroxene in phenocrysts.
3) Crystallisation of olivine + clinopyroxene + Ulvö spinel-magnetite + ?plagioclase feldspar in matrix.
4) Quenching of glass.

Magma type : Alkali basalt

Origin of xenoliths / xenocrysts :
Crust : -
Mantle : Clinopyroxene
? : Ulvöspinel-magnetite

Sample NB2

1. Observations

i) Hand specimen
Colour : Grey.
Grain size : Very fine.
Obvious phenocrysts : -
Obvious xenocrysts :
Black. Sub angular xenocrysts (up to 0.6x1.0 cm). Probably clinopyroxene.
Obvious xenoliths : -
Obvious amygdales :
Very tiny rounded vesicles, < 0.02 mm diameter.
Weathering : The specimen is mantled by the dull yellow brown material (~0.2 cm thick).
Density : Heavy.

ii) Thin section
Phenocrysts : Total mode 6%.
Olivine : Euhedral phenocrysts. Up to 0.28x0.40 mm. Colourless. Unzoned. Penetration twinning. Some are hollow or skeletal. Mode 5%.
Clinopyroxene : Euhedral phenocrysts. Up to 0.15x0.3 mm. Pale brown at core but deeper brown at rim (~0.05 mm thick). Some are turbid or spongy at core. Resorption zoning. Mode ~1%.

Xenocrysts : Total mode 5%.
Clinopyroxene: Angular xenocrysts (up to 6.0x9.0 mm). Slightly green pale brown. Fractured. Rimmed by the 2 uniform layers. The outer thin layer (up to 0.1 mm thick) is clean deeper brown. The inner layer (up to 0.5 mm thick) is brown, spongy, and turbid, composed of very tiny ?clinopyroxene granules (melted or resorption of the xenocryst).
Ulvöspinel-magnetite : Three small sub-rounded xenocrysts. Up to 0.4x0.75 mm.

Xenoliths : -

Matrix : Total mode 88%.
Olivine : Tiny granules. Up to 0.03 mm diameter. Euhedral. Unzoned. Some are penetration twinning. Mode 2%.
Clinopyroxene: Tiny laths. Up to 0.1 mm long. Euhedral. Mode 25%.
Ulvöspinel-magnetite : Tiny granules. Up to 0.02 mm diameter. Euhedral. Mode 20%.
Glass : Colourless. Mode 41%.
Weathering products: Orange-brown. Developed in patches in some parts of slide.

Amygdales : Total mode <<1%.
Sub-rounded amygdales. Up to 1.2x2.3 mm. Filled with brown cryptocrystalline mineral with globular texture at the margin (probably Fe- oxide?). Some are empty..

2. Name : Olivine-Phyric Basalt with Xenocrysts

3. Interpretation :

Crystallisation history :
1) Crystallisation of olivine in phenocrysts.
2) Crystallisation of clinopyroxene in phenocrysts.
3) Crystallisation of olivine + clinopyroxene + Ulvö spinel-magnetite in matrix.
4) Quenching of glass.

Magma type : Probably alkali olivine basalt ?

Origin of xenoliths / xenocrysts :
Crust : -
Mantle : Clinopyroxene.
? : Ulvöspinel-magnetite .

Sample NB3

1. Observations

i) Hand specimen
Colour : Grey.
Grain size : Very fine.
Obvious phenocrysts : -
Obvious xenocrysts :
Dark green-black vitreous lustre xenocrysts. Sub-angular 0.4x0.5 cm. Probably pyroxene.
Obvious xenoliths : -
Obvious amygdales :
Elongate-irregular vesicles. Up to 2 mm long.
Weathering : The specimen is weathered near the surface (up to ~0.5 cm thick) as the yellow brown material.
Density : Normal.

ii) Thin section
Phenocrysts : Total mode 6%.
Olivine : Euhedral phenocrysts. Up to 0.15 x 0.4 mm. Colourless. Unzoned. Some are hollow. Penetration twinning. Mode 5%.
Clinopyroxene : Euhedral phenocrysts. Up to 0.3x 0.9 mm. Pale green-brown. Spongy core but deeper brown clean rim (~0.08 mm thick). Resorption zoning. Mode 1%.

Xenocrysts : Total mode 3%.
Spinel: 1) A tiny brown square xenocryst (0.1x0.1 mm). Rimmed by opaque layer (< 0.01 mm thick).
2) A green rectangular-shaped (0.05x0.1 mm). Rimmed by opaque layer (<0.02 mm thick).
Ulvöspinel-magnetite : A large sub-rounded opaque xenocryst (3.5x6.0 mm). Showing one good direction of cleavage. Exfoliated fractures. Probably Ulvöspinel-magnetite .
Clinopyroxene: Sub-angular xenocryst. Up to 4.6x6.0 mm. Completely surrounded by 2 resorption layers. The outer is a thin (~0.05 mm) clean deeper brown layer. The inner layer (~0.35 mm thick) composed of the turbid mass of very tiny granules of melted ? clinopyroxene. The core is clean slightly-green brown.
?Melted clinopyroxene: A rounded aggregate (0.5 mm diameter). Brown and turbid. Composed of very tinny (<0.01 mm) granules of ? clinopyroxene. Rimmed by a thin (0.02 mm) of clean brown layer.

Xenoliths : Total mode <<<1%.
Aggregate: A brown turbid irregular aggregate (1.7x4.0 mm). Composed of orange-brown cryptocrystalline material (probably ?Fe-oxides) and the colourless euhedral ?alkali feldspar. The feldspar crystals (up to 0.2x0.2 mm) and laths (up to 0.3 mm long). [Carlsbad twin, Probably ? sanidine, Biax. $^{+}$ve, 2v ~30]. Some areas are the rounded vesicles (up to 0.6 mm diameter). Filled with orange-brown cryptocrystalline mineral (?Fe-oxide). [Probably ? melted crustal xenolith].

Matrix : Total mode 90%.
Olivine : Tiny granules. Up to 0.02 mm diameter. Euhedral. Unzoned. Mode 3%.
Clinopyroxene: Tiny laths. Up to 0.1 mm long. Pale green-brown. Euhedral. "Hour-glass" sector zoning. Mode 25%.

Ulvöspinel-magnetite : Tiny granules. Up to 0.05 mm diameter. Euhedral. Mode 20%.

Nepheline: Developed as the small patches (~0.2 mm diameter) as oikocrysts, enclosing the tiny clinopyroxene laths and Ulvöspinel-magnetite granules. "Poikilitic texture". Mode 5%.

Glass : Colourless. Mode 37%.

Weathering products: Reddish-brown. Developed in patches in some parts of this polished section.

Amygdales : Total mode <1%.

Elongate-irregular amygdales. Up to 0.5x2.1 mm. Filled with green-brown or orange-brown cryptocrystalline mineral, ? Fe-oxides. Some are empty.

2. Name : Olivine-Phyric Basalt with Xenocrysts and Xenoliths.

3. Interpretation :

Crystallisation history :

1) Crystallisation of olivine in phenocrysts.
2) Crystallisation of clinopyroxene in phenocrysts.
3) Crystallisation of olivine + clinopyroxene + Ulvö spinel-magnetite + ?plagioclase feldspar in matrix.
4) Quenching of glass.

Magma type : Probably alkali olivine basalt ?

Origin of xenoliths / xenocrysts :

Crust :

Mantle : Spinel / Clinopyroxene / ?Melted clinopyroxene.

? : Ulvöspinel-magnetite / Aggregate.

Sample NB4

1. Observations

i) Hand specimen

Colour : Dark grey.

Grain size : Very fine.

Obvious phenocrysts : -

Obvious xenocrysts :

Angular clinopyroxene xenocrysts. Up to 0.8x1.0 cm. Vitreous lustre. Black.

Obvious xenoliths : -

Obvious amygdales :

Elongate vesicles. Up to 3 mm long.

Weathering : The specimen is weathered at the surface (~2 mm thick) as yellow brown material.

Density : Normal.

ii) Thin section

Phenocrysts : Total mode 6%.

Olivine : Euhedral phenocrysts. Up to 0.3x0.5 mm. Some are skeletal or hollow. Penetration twinning. Unzoned. Mode 5%.

Clinopyroxene : Euhedral phenocrysts. Up to 0.3x0.5 mm. Pale green-brown. Spongy core and clean deeper brown rim (~0.05 mm thick). Resorption zoning. Mode <1%.

Xenocrysts : Total mode 3%.

Olivine : Irregular xenocrysts. Up to 0.5x0.9 mm. Colourless. Unzoned.

Clinopyroxene: Sub-angular xenocryst. Up to 4.6x13.2 mm. Pale-green brown. Rimmed by 2 different layers. The outer layer (~0.1 mm thick) is clean deeper brown (overgrown clinopyroxene). The inner layer (0.4 mm thick) is brown and turbid, composed of very tiny ?clinopyroxene granules, some are branch-liked. The xenocrysts enclose the tiny rounded mineral (reddish brown, ~0.08 mm diameter).

Aggregate of Ulvöspinel-magnetite : An elongate (0.6x2.3 mm) aggregate of the masses of tiny opaque euhedral granules (Ulvöspinel-magnetite , <<<0.01 mm) and ?clinopyroxene laths (up to 0.2 mm long). Probably melted xenocryst.

Xenoliths : Total mode <<<1%.

Olivine + Spinel: 1) Subhedral olivine (4.5x6.5 mm) crystal. Clear colourless. Very thin (<0.03 mm). Orange-brown alteration rim. Unzoned.

2) Tiny brown spinel (<0.05 mm diameter). The margin at the spinel-matrix contact has the opaque layer (<0.02 mm thick).

Matrix : Total mode 90%.

Olivine : Tiny granules. Up to 0.02 mm diameter. Unzoned. Mode 3%

Clinopyroxene: Tiny laths. Up to 0.1 mm long. Euhedral. Pale green brown. "Hour-glass" sector zoning. Mode 25%.

Ulvöspinel-magnetite : Tiny granules. Up to 0.03 mm diameter. Euhedral. Mode 20%.

Nepheline : Developed as the oikocrysts (~0.5 mm diameter) enclosing the tiny laths of clinopyroxene and tiny granules of Ulvöspinel-magnetite (Poikilitic texture). Mode ~7%.

Glass : Colourless. Mode 35%.

Weathering products: Orange-brown. Developed in patches in some parts of slide.

Amygdales : Total mode <1%.

Elongate amygdales. Up to 0.5x2.0 mm. Partly filled with yellow-green and orange-brown cryptocrystalline mineral. Probably ? Fe-oxide.

2. Name : Olivine-Phyric Basalt with Xenocrysts and Xenolith.

3. Interpretation :

Crystallisation history :

1) Crystallisation of olivine in phenocrysts.
2) Crystallisation of clinopyroxene in phenocrysts.
3) Crystallisation of olivine + clinopyroxene + Ulvö spinel-magnetite + ?plagioclase feldspar in matrix..
4) Quenching of glass.

Magma type : Probably alkali olivine basalt ?

Origin of xenoliths / xenocrysts :

Crust : -

Mantle : Olivine / Clinopyroxene / Olivine + Spinel

? : Aggregate of Ulvöspinel-magnetite .

Sample NB5/1

1. Observations

i) Hand specimen

Colour : Grey.

Grain size : Very fine.

Obvious phenocrysts : -

Obvious xenocrysts :

1) Red sub-rounded garnet, 0.3x1.0 cm. Rimmed by white material (~0.01 cm thick).
2) Black pyroxene, 0.6x1.2 cm. Vitreous lustre. Fractured. Showing 1 direction cleavage.

Obvious xenoliths : -

Obvious amygdales :

Elongate tiny vesicles (<0.01 mm diameter).

Weathering : The margin of specimen is altered to the pale grey (up to 0.5 cm thick) and the yellow-brown material covers on some parts of the surface.

Density : Normal.

ii) Thin section

Phenocrysts : Total mode 3%.

Olivine : Euhedral skeletal phenocrysts. Up to 0.4 x 0.5 mm. Some show corrosion rim. Mode ~2%.

Clinopyroxene : Euhedral colourless to brown phenocrysts. Up to 0.28x0.5 mm. Resorption zoning. Some are hollow. Mode 1%.

Xenocrysts : Total mode 2%.

Garnet: A large sub-rounded margin xenocryst (3.0x10.0 mm). Showing at least 2 alteration layers (up to 0.8 mm/layer thick) at the margin and in the fracture. The layer is orange-brown, showing fibrous cryptocrystalline structure. The gap between the layers is filled with matrix material [the alteration layers could be formed before this xenocrysts came into the host magma].

Clinopyroxene: Angular xenocrysts. Up to 0.9x2.2 mm. Pale green-brown but deeper brown reaction rim (up to 0.05 mm thick). Showing spongy margin

(up to 0.1 mm thick). Some are completely spongy xenocrysts or showing sieve-texture.

Unknown aggregate: A sub-rounded turbid aggregate (0.95x1.9 mm). Composed of colourless mineral [1st order grey, probably ?zeolite or ?tridymite, up to 1 mm long]. Some parts are altered to green mineral. Probably zeolite pseudomorph after feldspar ?

Ulvöspinel-magnetite aggregate: Two elongate (0.6x2.3 mm and 0.1x0.7 mm respectively) black aggregates. Composed of very tiny granules of (<<0.01 mm diameter) of Ulvöspinel-magnetite . Showing foliation bands of accumulation. Probably melted biotite?.

Xenoliths : -

Matrix : Total mode 94%.

Olivine : Tiny granules. Up to 0.05 mm diameter. Euhedral. Mode 10%.

Clinopyroxene: Tiny laths. Up to 0.12 mm long. Euhedral. Mode 30%.

Ulvöspinel-magnetite : Tiny granules. Up to 0.05 mm diameter. Euhedral. Mode 20%.

Glass : ?Devitrified. Colourless. Mode 34%.

Weathering products: Orange-brown (? iddingsite). Developed in specks or patches in some parts of slide.

Amygdales : Total mode <1%.

Irregular empty amygdales. Up to 0.4x0.6 mm. Partly filled with orange-brown globular mineral (? Fe-oxides) at the rim.

2. Name : Olivine-Phyric Basalt with Xenocrysts

3. Interpretation :

Crystallisation history :

1) Crystallisation of olivine in phenocrysts.
2) Crystallisation of clinopyroxene in phenocrysts.
3) Crystallisation of olivine + clinopyroxene + Ulvö spinel-magnetite in matrix.
4) Quenching of glass.

Magma type : Probably alkali olivine basalt.

Origin of xenoliths / xenocrysts :

Crust : -

Mantle : Garnet / Clinopyroxene.

? : Elongate opaque aggregates.

Sample NB5/2

1. Observations

i) Hand specimen

Colour : Grey.

Grain size : Very fine.

Obvious phenocrysts : -

Obvious xenocrysts :

1) Dark red garnet. Rounded (0.65x0.95 cm). Fractured. Surrounded by a white layer (~0.02 mm thick).
2) Black sub-rounded pyroxene crystals. Up to 0.3x0.7 cm. Vitreous lustre.

Obvious xenoliths : -

Obvious amygdales : Elongate empty amygdales. Up to 0.1x0.2 cm.

Weathering : The margin of specimen is altered to the pale grey (up to 0.5 cm thick) and the yellow-brown material covers on some parts of the surface.

Density : Normal.

ii) Thin section

Phenocrysts : Total mode 6%.

Olivine : Euhedral phenocrysts. Up to 0.21 x 0.35 mm. Some are hollow or skeletal. Some show penetration twin. Unzoned. Mode 5%.

Clinopyroxene : Euhedral. Up to 0.3x 0.4 mm. Pale green-brown core and brown rim (~0.05 mm thick). Mode ~1%.

Xenocrysts : Total mode 7%.

Garnet: A rounded-margin piece of xenocryst (6.0x8.0 mm). Pale brown. Fractured. Surrounded by at least 2 different layers. The inner layer (~0.3 mm thick) is brown composed of fibrous-texture cryptocrystalline mineral. This kind of mineral also develops as layers inside the fractures. The outer layer (~0.1 mm thick) composed of the masses of very fine granules (<<0.01 mm diameter, 2nd order yellow), probably reaction product between the inner layer and the melt.

Clinopyroxene: Pale green brown angular xenocryst. Up to 4.0x4.0 mm. Clean rim (~0.05 mm thick) surrounding the sponger layer (~0.4 mm thick) and the clean core. Spongy layers also extend into the fractures. One of theses contains inclusions of elongate-round opaque or orange material (~0.1 mm long). Some show only clean thin rim and spongy core (i.e. the clean core was completely altered).

Apatite : A triangular-shaped xenocryst (0.6x0.7 mm). High relief. Mineral inclusion within the crystal. Brown. Very dark brown rim. [3 direction cleavages, 3x60°, isotopic].

Biotite : An elongate (0.4x5.0 mm) black aggregate. Composed of very tiny granules (<<0.01 mm diameter) of Ulvöspinel-magnetite (Ulvö spinel-magnetite). Showing foliation bands of accumulation. Between the bands is filled with matrix. Probably melted biotite.

Xenoliths : Total mode <<<1%.

Pyroxenite: An irregular xenolith (0.3x1.0 mm) composed of 3 crystals of clinopyroxene (Max. dimension : 0.4x0.6 mm). Pale green-brown and deeper brown resorption rim (<0.02 mm thick).

Matrix : Total mode 86%.

Olivine : Tiny granules. Up to 0.05 mm diameter. Euhedral. Unzoned. Mode 10%.

Clinopyroxene: Tiny laths. Up to 0.1 mm long. Euhedral. Mode 25%.

Ulvöspinel-magnetite : Tiny granules. Up to 0.03 mm diameter. Euhedral. Mode 20%.

Glass : Colourless. Mode 31%.

Weathering products: Orange-red to orange-brown. Developed in specks or patches in some parts of the thin section.

Amygdales : Total mode <1%.

Sub-rounded amygdales. Up to 0.3x0.6 mm. Partly filled with globular-texture brown mineral (? Fe-oxides).

2. Name : Olivine-Phyric Basalt with Xenocrysts and Xenolith

3. Interpretation :

Crystallisation history :

1) Crystallisation of olivine in phenocrysts.
2) Crystallisation of clinopyroxene in phenocrysts.
3) Crystallisation of olivine + clinopyroxene + Ulvö spinel-magnetite in matrix.
4) Quenching of glass.

Magma type : Probably alkali olivine basalt ?

Origin of xenoliths / xenocrysts :

Crust :

Mantle : Garnet / Clinopyroxene / Pyroxenite.

Appendix 2-2

The results of standard rocks run by the XRF compared to results obtained from the literature.

Sample	W-1[a]				NIMN[b]			
Source	1. Literature[c]	2. XRF (this study)	Difference (1-2)	%	1. Literature[c]	2. XRF (this study)	Difference (1-2)	%
Major elements (wt%)								
SiO_2	52.46	52.03	0.43	0.8	52.64	52.31	0.33	0.6
Al_2O_3	15	16.14	-1.14	-7.6	16.5	16.55	-0.05	-0.3
Fe_2O_3T	11.11	10.57	0.54	4.9	8.91	9.19	-0.28	-3.1
MgO	6.62	6.02	0.6	9.1	7.5	6.36	1.14	15.2
CaO	11	11.22	-0.22	-2.0	11.5	12.11	-0.61	-5.3
Na_2O	2.16	2.79	-0.63	-29.2	2.46	2.91	-0.45	-18.3
K_2O	0.64	0.65	-0.01	-1.6	0.25	0.3	-0.05	-20.0
TiO_2	1.07	1	0.07	6.5	0.2	0.24	-0.04	-20.0
MnO	0.167	0.1	0.067	40.1	0.18	0.1	0.08	44.4
P_2O_5	0.13	0.14	-0.01	-7.7	0.03	0.09	-0.06	-200.0
Total	100.357	100.66	-0.303	-0.3	100.17	100.16	0.01	0.0
H_2O^+	0.53	not analysed	-	-	0.33	not analysed	-	-
CO_2	0.06	not analysed	-	-	0.1	not analysed	-	-
Fe_2O_3	1.43	not analysed	-	-	0.8	not analysed	-	-
FeO	8.76	not analysed	-	-	7.3	not analysed	-	-
Trace elements (ppm)								
Nb	9.9	13	-3.1	-31.3	2	2	0	0.0
Zr	99	108	-9	-9.1	23	31	-8	-34.8
Y	26	26	0	0.0	7	12	-5	-71.4
Sr	186	209	-23	-12.4	260	258	2	0.8
Rb	21.4	23	-1.6	-7.5	6	6	0	0.0
Zn	84	84	0	0.0	68	54	14	20.6
Cu	113	140	-27	-23.9	14	5	9	64.3
Ni	75	89	-14	-18.7	120	147	-27	-22.5
Cr	119	173	-54	-45.4	30	52	-22	-73.3
Ce	23.5	22	1.5	6.4	6	6	0	0.0
Nd	14.6	10	4.6	31.5	3	0	3	100.0
V	257	288	-31	-12.1	220	196	24	10.9
La	11	32	-21	-190.9	3	21	-18	-600.0
Ba	162	186	-24	-14.8	100	103	-3	-3.0
Sc	35	39	-4	-11.4	38	41	-3	-7.9

[a] W-1, Diabase from the United States Geological Survey (USGS), Reston. [b] NIMN, Norite from the National Institue for Mineralogy, South Africa. [c]Govindaraju, 1989.

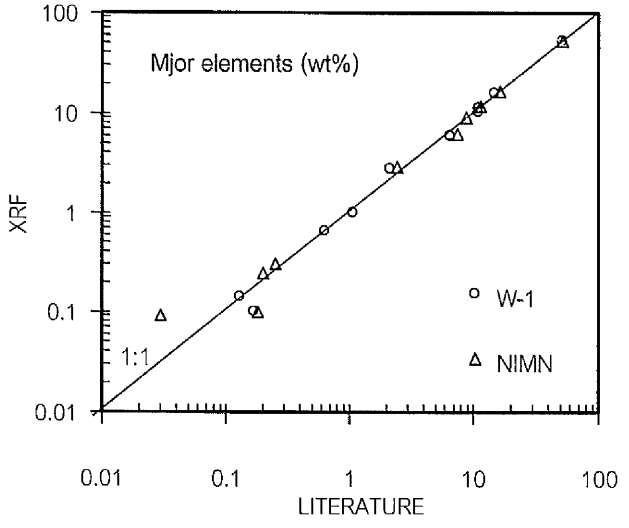

Appendix 2-3

Chemical composition and data treatment for normative mineral calculation of rock samples.

Original data from XRF (wt%)																	
	CK1	CK2	CK3	CK4	CK5	CK6	BN1	BN2	BN3	BN4	BN5	BN6	SP1	SP2	SP3	SP4	SP5
SiO_2	46.48	45.70	46.27	45.64	45.69	46.17	44.60	44.17	47.09	46.15	47.36	45.69	50.93	49.61	50.97	52.23	52.30
Al_2O_3	15.47	15.68	15.42	15.97	15.74	15.72	14.67	14.50	14.23	15.23	15.33	15.47	16.79	15.79	16.85	17.57	17.52
Fe_2O_3	12.28	12.24	12.21	12.21	12.16	12.03	11.91	11.85	12.16	11.04	10.18	11.21	9.27	9.73	9.64	9.62	9.51
MgO	6.06	6.34	6.47	6.55	6.51	6.70	9.58	10.36	6.98	9.51	10.32	8.85	5.08	5.02	5.26	4.53	4.65
CaO	10.35	10.12	10.05	9.35	10.39	9.84	9.55	9.50	9.88	8.48	8.62	8.89	9.49	11.53	8.87	8.78	8.69
Na_2O	2.22	2.56	2.41	2.95	2.24	2.37	3.97	3.95	5.21	3.75	3.83	4.09	2.32	2.18	2.28	2.27	2.32
K_2O	3.04	3.15	3.05	3.09	3.11	3.09	2.39	2.37	1.25	2.95	1.52	2.69	3.21	3.17	3.18	2.11	2.11
TiO_2	3.03	3.04	3.01	3.06	3.00	2.96	2.37	2.38	2.36	1.90	2.06	2.05	2.07	2.14	2.11	2.16	2.15
MnO	0.17	0.15	0.15	0.15	0.16	0.16	0.15	0.15	0.15	0.15	0.11	0.15	0.11	0.11	0.11	0.11	0.10
P_2O_5	0.86	0.90	0.87	0.86	0.90	0.87	0.63	0.61	0.63	0.66	0.61	0.71	0.72	0.70	0.73	0.73	0.75
Total	99.96	99.88	99.91	99.83	99.90	99.91	99.82	99.84	99.94	99.82	99.94	99.80	99.99	99.98	100.00	100.11	100.10
Data from Wet. Chem. (wt%)																	
H_2O^-	0.61	0.55	0.61	0.64	0.72	0.64	0.43	0.39	1.00	0.58	0.60	0.53	1.43	1.41	1.39	2.74	3.07
LOI	3.31	2.47	3.67	2.56	3.14	3.31	1.44	1.61	2.04	1.54	2.94	1.98	4.90	5.50	4.43	5.04	4.51
FeO	4.06	1.64	7.14	8.33	3.14	7.48	4.96	5.09	4.23	2.23	3.69	4.69	1.87	1.59	1.85	3.25	0.34
True Fe_2O_3 = (Total Fe_2O_3 fr. XRF) - 1.111344 x (true FeO fr. wet chem.), to give the data below.																	
SiO_2	46.63	45.90	46.43	45.85	46.00	46.33	44.91	44.54	47.28	46.31	47.74	45.91	51.24	49.59	50.86	52.58	52.77
Al_2O_3	15.22	15.43	15.18	15.74	15.44	15.48	14.44	14.26	13.99	14.96	15.02	15.21	16.43	15.52	16.57	17.18	17.08
Fe_2O_3	7.77	10.42	4.28	2.95	8.67	3.72	6.40	6.19	7.46	8.56	6.08	6.00	7.19	7.96	7.58	6.01	9.13
FeO	4.06	1.64	7.14	8.33	3.14	7.48	4.96	5.09	4.23	2.23	3.69	4.69	1.87	1.59	1.85	3.25	0.34
MgO	6.07	6.34	6.47	6.54	6.49	6.69	9.31	10.00	6.94	9.25	9.94	8.66	5.09	5.06	5.29	4.54	4.64
CaO	10.50	10.24	10.16	9.38	10.51	9.92	9.62	9.56	9.97	8.41	8.55	8.86	9.48	11.68	8.98	8.76	8.64
Na_2O	2.19	2.52	2.38	2.90	2.20	2.34	3.89	3.87	5.02	3.67	3.75	3.99	2.27	2.17	2.26	2.23	2.27
K_2O	3.01	3.13	3.03	3.08	3.08	3.07	2.36	2.35	1.23	2.93	1.49	2.67	3.16	3.13	3.13	2.04	2.05
TiO_2	2.92	2.92	2.90	2.93	2.90	2.87	2.41	2.42	2.41	2.00	2.14	2.14	2.15	2.23	2.21	2.24	2.21
MnO	0.18	0.18	0.18	0.18	0.18	0.18	0.17	0.17	0.18	0.17	0.19	0.17	0.21	0.22	0.22	0.21	0.21
P_2O_5	0.82	0.86	0.83	0.82	0.85	0.83	0.61	0.58	0.60	0.63	0.58	0.68	0.68	0.66	0.69	0.69	0.70
Total	99.37	99.58	98.98	98.70	99.46	98.91	99.08	99.03	99.31	99.12	99.17	98.98	99.77	99.81	99.64	99.73	100.04
Mg'[Mg/(Mg+Fe^{2+})]	0.73	0.87	0.62	0.58	0.79	0.61	0.77	0.78	0.75	0.88	0.83	0.77	0.83	0.85	0.84	0.71	0.96
Nat. Fe_2O_3/FeO	1.91	6.35	0.60	0.35	2.76	0.50	1.29	1.22	1.76	3.84	1.65	1.28	3.85	5.01	4.09	1.85	26.86
H_2O^-	0.61	0.55	0.61	0.64	0.72	0.64	0.43	0.39	1.00	0.58	0.60	0.53	1.43	1.41	1.39	2.74	3.07
LOI	3.31	2.47	3.67	2.56	3.14	3.31	1.44	1.61	2.04	1.54	2.94	1.98	4.90	5.50	4.43	5.04	4.51
Adjustment of 1). Fe_2O_3 / FeO 2). volatiles free and 3) recalculated total to 100%																	
Root name[a]	TB	T/B	TB	T/B	TB	TB	T/B	T/B	T/B	T/B	TB	T/B	TB	TB	TB	BA	BA
1) Before using the data for CIPW norm calculation, The Fe_2O_3/FeO has to be adjusted to the ideal ratio:																	
Fe_2O_3/FeO[b]	0.30	0.20	0.30	0.20	0.30	0.30	0.30	0.30	0.30	0.30	0.30	0.30	0.30	0.30	0.30	0.30	0.30
Fe_2O_3	2.61	1.87	2.60	1.86	2.58	2.56	2.53	2.52	2.58	2.35	2.16	2.38	1.97	2.07	2.05	2.04	2.02
FeO	8.70	9.33	8.65	9.31	8.62	8.52	8.44	8.40	8.62	7.82	7.21	7.94	6.57	6.89	6.83	6.82	6.74

[a] Classification based on Total alkalis versus silica after Le Maitre et al. (1989)

TB = Trachybasalt, T/B = Tephrite/Basanite, BA = Basaltic andesite, B = Basalt, PT = Phonotephrite

[b] Iron oxidation ratios after Middlemost (1989)

Example for Fe_2O_3,FeO calculation: (Sample CK1):

$Fe_2O_3/FeO = .30$.....1

Total Fe_2O_3 = true Fe_2O_3 + 1.111344 x trueFeO = 7.77 + 1.111344 x 4.06 = 12.28, or

$FeO = (12.28 - Fe_2O_3)/1.111344$.....2

Sustitute 2 in 1:

$Fe_2O_3 = 0.30(12.28-Fe_2O_3)/1.111344$

So, $Fe_2O_3 = 2.61$.....3

Substitute 3 in 1:

FeO =8.70, which gives the ratio of Fe_2O_3/FeO = 0.30

The data with adjusted Fe_2O_3 are as follows:

SiO_2	46.63	45.90	46.43	45.85	46.00	46.33	44.91	44.54	47.28	46.31	47.74	45.91	51.24	49.59	50.86	52.58	52.77
Al_2O_3	15.22	15.43	15.18	15.74	15.44	15.48	14.44	14.26	13.99	14.96	15.02	15.21	16.43	15.52	16.57	17.18	17.08
Fe_2O_3	2.61	1.87	2.60	1.86	2.58	2.56	2.53	2.52	2.58	2.35	2.16	2.38	1.97	2.07	2.05	2.04	2.02
FeO	8.70	9.33	8.65	9.31	8.62	8.52	8.44	8.40	8.62	7.82	7.21	7.94	6.57	6.89	6.83	6.82	6.74
MgO	6.07	6.34	6.47	6.54	6.49	6.69	9.31	10.00	6.94	9.25	9.94	8.66	5.09	5.06	5.29	4.54	4.64
CaO	10.50	10.24	10.16	9.38	10.51	9.92	9.62	9.56	9.97	8.41	8.55	8.86	9.48	11.68	8.98	8.76	8.64
Na_2O	2.19	2.52	2.38	2.90	2.20	2.34	3.89	3.87	5.02	3.67	3.75	3.99	2.27	2.17	2.26	2.23	2.27
K_2O	3.01	3.13	3.03	3.08	3.08	3.07	2.36	2.35	1.23	2.93	1.49	2.67	3.16	3.13	3.13	2.04	2.05
TiO_2	2.92	2.92	2.90	2.93	2.90	2.87	2.41	2.42	2.41	2.00	2.14	2.14	2.15	2.23	2.21	2.24	2.21
MnO	0.18	0.18	0.18	0.18	0.18	0.18	0.17	0.17	0.18	0.17	0.19	0.17	0.21	0.22	0.22	0.21	0.21
P_2O_5	0.82	0.86	0.83	0.82	0.85	0.83	0.61	0.58	0.60	0.63	0.58	0.68	0.68	0.66	0.69	0.69	0.70
Total	98.85	98.72	98.81	98.59	98.85	98.79	98.69	98.67	98.82	98.50	98.78	98.62	99.25	99.22	99.09	99.33	99.33
H_2O	0.61	0.55	0.61	0.64	0.72	0.64	0.43	0.39	1.00	0.58	0.60	0.53	1.43	1.41	1.39	2.74	3.07
LOI	3.31	2.47	3.67	2.56	3.14	3.31	1.44	1.61	2.04	1.54	2.94	1.98	4.90	5.50	4.43	5.04	4.51
Fe_2O_3/FeO	0.30	0.20	0.30	0.20	0.30	0.30	0.30	0.30	0.30	0.30	0.30	0.30	0.30	0.30	0.30	0.30	0.30
2) Volatiles free: By substracting H2O$^-$ and LOI from the Total and Recalculated to 100 %. (Middlemost, 1989). (However CO2 data is not available, the norm will not have calcite).																	
2.1) Volatiles free:																	
SiO_2	44.78	44.50	44.42	44.36	44.20	44.48	44.06	43.64	45.83	45.31	46.03	44.74	47.97	46.14	47.87	48.46	48.74
Al_2O_3	14.62	14.96	14.52	15.23	14.84	14.86	14.17	13.97	13.56	14.64	14.48	14.82	15.38	14.44	15.60	15.83	15.78
Fe_2O_3	2.51	1.81	2.48	1.80	2.48	2.45	2.48	2.47	2.51	2.30	2.09	2.32	1.84	1.92	1.93	1.88	1.87
FeO	8.36	9.05	8.28	9.01	8.28	8.18	8.28	8.23	8.35	7.65	6.95	7.74	6.15	6.41	6.43	6.28	6.22
MgO	5.83	6.15	6.19	6.33	6.24	6.42	9.13	9.80	6.73	9.05	9.58	8.44	4.77	4.71	4.98	4.18	4.29
CaO	10.08	9.93	9.72	9.08	10.10	9.52	9.44	9.37	9.66	8.23	8.24	8.63	8.88	10.87	8.45	8.07	7.98
Na_2O	2.10	2.44	2.28	2.81	2.11	2.25	3.82	3.79	4.87	3.59	3.62	3.89	2.13	2.02	2.13	2.06	2.10
K_2O	2.89	3.03	2.90	2.98	2.96	2.95	2.32	2.30	1.19	2.87	1.44	2.60	2.96	2.91	2.95	1.88	1.89
TiO_2	2.80	2.83	2.77	2.83	2.79	2.76	2.36	2.37	2.34	1.96	2.06	2.09	2.01	2.07	2.08	2.06	2.04
MnO	0.17	0.17	0.17	0.17	0.17	0.17	0.17	0.17	0.17	0.17	0.18	0.17	0.20	0.20	0.21	0.19	0.19
P_2O_5	0.79	0.83	0.79	0.79	0.82	0.80	0.60	0.57	0.58	0.62	0.56	0.66	0.64	0.61	0.65	0.64	0.65
Total	94.93	95.70	94.53	95.39	94.99	94.84	96.82	96.67	95.78	96.38	95.24	96.11	92.92	92.31	93.27	91.55	91.75
3) Recalculated to 100 % (Final adjusted data and ready for CIPW norm calculation).																	
SiO_2	47.17	46.49	46.99	46.50	46.53	46.90	45.51	45.14	47.84	47.02	48.33	46.55	51.63	49.98	51.33	52.93	53.13
TiO_2	2.95	2.96	2.94	2.97	2.93	2.91	2.44	2.45	2.44	2.03	2.17	2.17	2.17	2.25	2.23	2.26	2.22
Al_2O_3	15.40	15.63	15.36	15.96	15.62	15.67	14.63	14.45	14.16	15.19	15.21	15.42	16.55	15.64	16.72	17.30	17.20
Fe_2O_3	2.64	1.89	2.63	1.89	2.61	2.59	2.57	2.55	2.62	2.38	2.19	2.42	1.99	2.08	2.07	2.06	2.04
FeO	8.80	9.45	8.76	9.44	8.72	8.63	8.55	8.51	8.72	7.94	7.30	8.05	6.62	6.95	6.89	6.86	6.78
MnO	0.18	0.18	0.18	0.18	0.18	0.18	0.17	0.17	0.18	0.17	0.19	0.17	0.21	0.22	0.22	0.21	0.21
MgO	6.14	6.42	6.55	6.63	6.57	6.77	9.43	10.14	7.02	9.39	10.06	8.78	5.13	5.10	5.34	4.57	4.67
CaO	10.62	10.37	10.28	9.51	10.63	10.04	9.75	9.69	10.09	8.54	8.66	8.98	9.55	11.77	9.06	8.82	8.70
Na_2O	2.22	2.55	2.41	2.94	2.23	2.37	3.94	3.92	5.08	3.73	3.80	4.05	2.29	2.19	2.28	2.25	2.29
K_2O	3.04	3.17	3.07	3.12	3.12	3.11	2.39	2.38	1.24	2.97	1.51	2.71	3.18	3.15	3.16	2.05	2.06
P_2O_5	0.83	0.87	0.84	0.83	0.86	0.84	0.62	0.59	0.61	0.64	0.59	0.69	0.69	0.67	0.70	0.69	0.70
Total	100.00	100.00	100.00	100.00	100.00	100.00	100.00	100.00	100.00	100.00	100.00	100.00	100.00	100.00	100.00	100.00	100.00

Appendix 2-3 (continued)

Original data from XRF (wt%)																		
	DC1	DC2	DC3	DC4	DC5	KS1	KS2	KS3	KS4	KS5	BP1	BP2	BP3	BP4	BP5	BP6	BP7	BP8	BP9
SiO_2	47.31	46.90	47.33	47.16	47.53	47.94	48.16	48.48	48.27	47.97	48.44	48.14	48.82	48.59	48.32	48.69	48.80	48.84	48.12
Al_2O_3	15.36	14.64	15.65	14.29	14.26	16.78	17.22	16.81	16.67	16.88	14.92	14.65	14.98	15.14	15.11	14.68	14.75	14.72	14.38
Fe_2O_3	10.33	10.25	10.35	13.04	12.86	10.45	10.82	10.33	10.56	11.22	9.55	9.61	9.43	9.54	9.40	9.48	9.45	9.15	9.29
MgO	9.81	11.93	9.59	8.85	8.68	6.39	6.79	5.98	6.38	7.07	6.94	8.01	7.04	7.11	6.77	6.98	7.79	7.32	8.27
CaO	8.36	8.00	8.38	10.55	10.26	9.56	9.81	9.70	9.57	9.59	8.98	8.87	8.22	8.25	8.62	8.51	7.97	8.11	8.62
Na_2O	3.97	3.79	3.93	2.42	2.43	3.49	3.17	3.24	3.23	3.20	4.73	3.89	5.07	5.05	5.40	5.42	5.06	5.38	4.14
K_2O	1.55	1.41	1.44	0.55	0.51	1.92	1.18	1.94	1.79	1.20	2.95	3.43	2.98	2.89	2.92	2.79	2.73	3.04	3.77
TiO_2	2.31	2.10	2.33	2.79	3.04	2.11	1.98	2.10	2.19	2.06	1.88	1.86	1.96	1.93	1.87	1.90	1.89	1.84	1.79
MnO	0.20	0.20	0.21	0.23	0.22	0.21	0.20	0.21	0.21	0.22	0.22	0.20	0.20	0.21	0.21	0.21	0.21	0.19	0.21
P_2O_5	0.64	0.59	0.65	0.37	0.41	1.09	0.70	1.08	1.04	0.65	0.89	0.85	0.77	0.77	0.86	0.77	0.78	0.77	0.83
Total	99.84	99.81	99.86	100.25	100.20	99.94	100.03	99.87	99.91	100.06	99.50	99.51	99.41	99.48	99.48	99.43	99.43	99.36	99.42
Data from Wet. Chem. (wt%)																			
H_2O^-	0.76	0.62	0.70	0.19	0.23	0.37	0.46	0.44	0.52	0.53	0.29	0.48	0.51	0.65	0.60	0.41	0.67	0.50	0.61
LOI	3.26	2.58	2.90	4.02	3.52	2.24	2.11	2.45	2.06	2.24	3.18	3.06	2.66	2.76	3.09	2.61	2.79	2.84	2.44
FeO	6.39	2.67	2.05	4.88	3.18	3.71	5.17	6.31	3.67	4.90	3.48	2.32	1.32	1.74	5.41	3.50	2.14	5.69	2.58
True Fe_2O_3 = (Total Fe_2O_3 fr. XRF) - 1.111344 x (true FeO fr. wet chem.) , to give the data below.																			
SiO_2	47.17	46.63	47.17	47.72	47.86	47.90	47.98	48.63	48.36	47.84	48.88	48.32	49.36	49.04	48.83	49.31	49.38	49.46	48.29
Al_2O_3	14.88	14.03	15.19	13.74	13.75	16.95	17.70	16.87	16.74	17.31	14.40	14.11	14.45	14.64	14.68	14.17	14.22	14.19	13.85
Fe_2O_3	3.23	7.28	8.07	7.62	9.33	6.33	5.07	3.32	6.48	5.77	5.68	7.03	7.96	7.61	3.39	5.59	7.07	2.83	6.42
FeO	6.39	2.67	2.05	4.88	3.18	3.71	5.17	6.31	3.67	4.90	3.48	2.32	1.32	1.74	5.41	3.50	2.14	5.69	2.58
MgO	10.66	13.15	10.38	9.34	9.24	6.47	6.87	5.99	6.46	7.21	7.27	8.55	7.39	7.45	7.05	7.32	8.27	7.72	8.86
CaO	8.36	8.02	8.38	10.37	10.16	9.41	9.56	9.57	9.43	9.35	9.01	8.88	8.31	8.33	8.66	8.58	8.04	8.20	8.63
Na_2O	3.96	3.79	3.92	2.45	2.47	3.48	3.14	3.27	3.25	3.17	4.65	3.91	4.92	4.91	5.16	5.20	4.89	5.15	4.11
K_2O	1.51	1.37	1.41	0.57	0.53	1.88	1.13	1.91	1.75	1.16	3.01	3.54	3.04	2.95	2.99	2.84	2.76	3.12	3.93
TiO_2	2.26	2.07	2.28	2.67	2.88	2.06	1.93	2.07	2.14	1.99	1.90	1.86	1.92	1.94	1.88	1.92	1.89	1.85	1.79
MnO	0.19	0.20	0.20	0.22	0.22	0.20	0.19	0.20	0.21	0.22	0.23	0.20	0.20	0.22	0.21	0.21	0.21	0.19	0.21
P_2O_5	0.67	0.62	0.69	0.39	0.43	1.11	0.73	1.10	1.06	0.67	0.93	0.88	0.81	0.81	0.90	0.81	0.81	0.81	0.87
Total	99.28	99.83	99.74	99.97	100.05	99.50	99.47	99.24	99.55	99.59	99.44	99.60	99.68	99.64	99.16	99.45	99.68	99.21	99.54
$Mg'[Mg/(Mg+Fe^{2+})]$	0.75	0.90	0.90	0.77	0.84	0.76	0.70	0.63	0.76	0.72	0.79	0.87	0.91	0.88	0.70	0.79	0.87	0.71	0.86
Nat. Fe_2O_3/FeO	0.51	2.73	3.94	1.56	2.93	1.71	0.98	0.53	1.77	1.18	1.63	3.03	6.03	4.37	0.63	1.60	3.30	0.50	2.49
H_2O	0.76	0.62	0.70	0.19	0.23	0.37	0.46	0.44	0.52	0.53	0.29	0.48	0.51	0.65	0.60	0.41	0.67	0.50	0.61
LOI	3.26	2.58	2.90	4.02	3.52	2.24	2.11	2.45	2.06	2.24	3.18	3.06	2.66	2.76	3.09	2.61	2.79	2.84	2.44
Adjustment of 1). Fe_2O_3 / FeO 2). volatiles free and 3) recalculated total to 100%																			
Root name[a]	TB	TB	TB	B	B	TB	B	TB	TB	B	PT	PT	PT	PT	PT	PT	PT	PT	PT
1) Before using the data for CIPW norm calculation, The Fe_2O_3/FeO has to be adjusted to the ideal ratio:																			
Fe_2O_3/FeO[b]	0.30	0.30	0.30	0.20	0.20	0.30	0.20	0.30	0.30	0.20	0.35	0.35	0.35	0.35	0.35	0.35	0.35	0.35	0.35
Fe_2O_3	2.20	2.18	2.20	1.99	1.96	2.22	1.65	2.20	2.24	1.71	2.29	2.30	2.26	2.28	2.25	2.27	2.26	2.19	2.23
FeO	7.32	7.26	7.33	9.94	9.81	7.40	8.25	7.32	7.48	8.56	6.54	6.58	6.45	6.53	6.43	6.49	6.47	6.26	6.36
[a]Classification based on Total alkalis versus silica after Le Maitre et al. (1989)																			
TB = Trachybasalt, T/B = Tephrite/Basanite, BA = Basaltic andesite, B = Basalt, PT = Phonotephrite																			
[b]Iron oxidation ratios after Middlemost (1989)																			
The data with adjusted Fe_2O_3 are as follows:																			
SiO_2	47.17	46.63	47.17	47.72	47.86	47.90	47.98	48.63	48.36	47.84	48.88	48.32	49.36	49.04	48.83	49.31	49.38	49.46	48.29
Al_2O_3	14.88	14.03	15.19	13.74	13.75	16.95	17.70	16.87	16.74	17.31	14.40	14.11	14.45	14.64	14.68	14.17	14.22	14.19	13.85
Fe_2O_3	2.20	2.18	2.20	1.99	1.96	2.22	1.65	2.20	2.24	1.71	2.29	2.30	2.26	2.28	2.25	2.27	2.26	2.19	2.23
FeO	7.32	7.26	7.33	9.94	9.81	7.40	8.25	7.32	7.48	8.56	6.54	6.58	6.45	6.53	6.43	6.49	6.47	6.26	6.36
MgO	10.66	13.15	10.38	9.34	9.24	6.47	6.87	5.99	6.46	7.21	7.27	8.55	7.39	7.45	7.05	7.32	8.27	7.72	8.86
CaO	8.36	8.02	8.38	10.37	10.16	9.41	9.56	9.57	9.43	9.35	9.01	8.88	8.31	8.33	8.66	8.58	8.04	8.20	8.63
Na_2O	3.96	3.79	3.92	2.45	2.47	3.48	3.14	3.27	3.25	3.17	4.65	3.91	4.92	4.91	5.16	5.20	4.89	5.15	4.11
K_2O	1.51	1.37	1.41	0.57	0.53	1.88	1.13	1.91	1.75	1.16	3.01	3.54	3.04	2.95	2.99	2.84	2.76	3.12	3.93
TiO_2	2.26	2.07	2.28	2.67	2.88	2.06	1.93	2.07	2.14	1.99	1.90	1.86	1.92	1.94	1.88	1.92	1.89	1.85	1.79
MnO	0.19	0.20	0.20	0.22	0.22	0.20	0.19	0.20	0.21	0.22	0.23	0.20	0.20	0.22	0.21	0.21	0.21	0.19	0.21
P_2O_5	0.67	0.62	0.69	0.39	0.43	1.11	0.73	1.10	1.06	0.67	0.93	0.88	0.81	0.81	0.90	0.81	0.81	0.81	0.87
Total	99.18	99.32	99.15	99.40	99.31	99.09	99.13	99.13	99.13	99.19	99.10	99.13	99.11	99.10	99.04	99.12	99.20	99.14	99.12
H_2O	0.76	0.62	0.70	0.19	0.23	0.37	0.46	0.44	0.52	0.53	0.29	0.48	0.51	0.65	0.60	0.41	0.67	0.50	0.61
LOI	3.26	2.58	2.90	4.02	3.52	2.24	2.11	2.45	2.06	2.24	3.18	3.06	2.66	2.76	3.09	2.61	2.79	2.84	2.44
Fe_2O_3/FeO	0.30	0.30	0.30	0.20	0.20	0.30	0.20	0.30	0.30	0.20	0.35	0.35	0.35	0.35	0.35	0.35	0.35	0.35	0.35
2) Volatiles free: By substracting H2O and LOI from the Total and Recalculated to 100 %. (Middlemost, 1989). (However CO2 data is not available, the norm will not have calcite).																			
2.1) Volatiles free:																			
SiO_2	45.26	45.13	45.46	45.70	46.05	46.64	46.74	47.21	47.10	46.50	47.17	46.59	47.78	47.35	47.01	47.81	47.66	47.79	46.80
Al_2O_3	14.28	13.58	14.64	13.16	13.23	16.50	17.24	16.38	16.30	16.83	13.90	13.61	13.99	14.14	14.13	13.74	13.72	13.71	13.42
Fe_2O_3	2.11	2.11	2.12	1.90	1.89	2.16	1.61	2.13	2.19	1.66	2.21	2.22	2.19	2.21	2.17	2.20	2.18	2.12	2.16
FeO	7.02	7.03	7.07	9.52	9.44	7.21	8.04	7.11	7.29	8.32	6.31	6.34	6.25	6.30	6.19	6.29	6.24	6.05	6.16
MgO	10.23	12.73	10.00	8.94	8.89	6.30	6.69	5.82	6.29	7.01	7.02	8.24	7.15	7.19	6.79	7.10	7.98	7.46	8.59
CaO	8.02	7.76	8.08	9.93	9.78	9.16	9.31	9.29	9.18	9.09	8.69	8.56	8.04	8.04	8.34	8.32	7.76	7.92	8.36
Na_2O	3.80	3.67	3.78	2.35	2.38	3.39	3.06	3.17	3.17	3.08	4.49	3.77	4.76	4.74	4.97	5.04	4.72	4.98	3.98
K_2O	1.45	1.33	1.36	0.55	0.51	1.83	1.10	1.85	1.70	1.13	2.90	3.41	2.94	2.85	2.88	2.75	2.66	3.01	3.81
TiO_2	2.17	2.00	2.20	2.56	2.77	2.01	1.88	2.01	2.08	1.93	1.83	1.79	1.86	1.87	1.81	1.86	1.82	1.79	1.73
MnO	0.18	0.19	0.19	0.21	0.21	0.19	0.19	0.19	0.20	0.21	0.22	0.19	0.19	0.21	0.20	0.20	0.20	0.18	0.20
P_2O_5	0.64	0.60	0.66	0.37	0.41	1.08	0.71	1.07	1.03	0.65	0.90	0.85	0.78	0.78	0.87	0.79	0.78	0.78	0.84
Total	95.16	96.12	95.55	95.19	95.56	96.48	96.56	96.24	96.55	96.42	95.63	95.59	95.94	95.69	95.35	96.10	95.74	95 80	96.07
3) Recalculated to 100 % (Final adjusted data and ready for CIPW norm calculation).																			
SiO_2	47.56	46.95	47.57	48.01	48.19	48.34	48.40	49.06	48.79	48.23	49.32	48.75	49.80	49.48	49.30	49.75	49.78	49.89	48.72
TiO_2	2.28	2.08	2.30	2.69	2.90	2.08	1.95	2.09	2.16	2.01	1.92	1.88	1.94	1.96	1.90	1.94	1.91	1.87	1.81
Al_2O_3	15.00	14.13	15.32	13.82	13.85	17.11	17.86	17.02	16.89	17.45	14.53	14.23	14.58	14.77	14.82	14.30	14.33	14.31	13.97
Fe_2O_3	2.21	2.19	2.22	2.00	1.98	2.24	1.66	2.22	2.26	1.73	2.31	2.32	2.28	2.31	2.27	2.29	2.28	2.21	2.24
FeO	7.38	7.31	7.40	10.00	9.88	7.47	8.32	7.38	7.55	8.63	6.59	6.63	6.51	6.59	6.49	6.54	6.52	6.32	6.41
MnO	0.19	0.20	0.20	0.22	0.22	0.20	0.19	0.20	0.21	0.22	0.23	0.20	0.20	0.22	0.21	0.21	0.21	0.19	0.21
MgO	10.75	13.24	10.47	9.40	9.30	6.53	6.93	6.04	6.52	7.27	7.34	8.63	7.46	7.52	7.12	7.39	8.34	7.79	8.94
CaO	8.43	8.07	8.45	10.43	10.23	9.50	9.64	9.65	9.51	9.43	9.09	8.96	8.38	8.41	8.74	8.66	8.10	8.27	8.71
Na_2O	3.99	3.82	3.95	2.46	2.49	3.51	3.17	3.30	3.28	3.20	4.69	3.94	4.96	4.95	5.21	5.25	4.93	5.19	4.15
K_2O	1.52	1.38	1.42	0.57	0.53	1.90	1.14	1.93	1.77	1.17	3.04	3.57	3.07	2.98	3.02	2.87	2.78	3.15	3.96
P_2O_5	0.68	0.62	0.70	0.39	0.43	1.12	0.74	1.11	1.07	0.68	0.94	0.89	0.82	0.82	0.91	0.82	0.82	0.82	0.88
Total	100.00	100.00	100.00	100.00	100.00	100.00	100.00	100.00	100.00	100.00	100.00	100.00	100.00	100.00	100.00	100.00	100.00	100.00	100.00

Appendix 2-3 (continued)

Original data from XRF (wt%)	NY1	NY2	NY3	NY4	NY5	PW1	PW2	PW3	PW4	PW5	PW6	TP1	TP2	TP3	TP4	TP5	TP6	NB1	NB2	NB3	NB4	NB5
SiO_2	49.46	49.46	49.58	50.09	49.51	44.58	44.60	44.73	45.87	43.83	43.81	44.53	44.45	44.47	44.06	44.46	43.92	41.74	43.41	43.24	42.83	42.81
Al_2O_3	16.36	16.29	16.24	16.03	16.28	12.46	11.95	12.02	13.26	12.06	10.94	13.11	13.32	13.20	13.35	13.18	13.30	13.01	13.63	13.33	13.61	13.45
Fe_2O_3	11.39	11.37	11.27	11.15	11.43	14.90	14.57	15.11	14.70	14.38	14.80	12.78	12.73	12.73	12.80	12.71	12.66	14.43	15.18	14.24	14.90	14.51
MgO	6.11	6.05	5.78	6.25	6.13	8.72	9.16	8.77	8.73	10.15	11.81	9.52	9.55	9.67	10.23	9.80	9.75	8.47	7.79	7.57	8.32	7.52
CaO	8.52	8.35	8.39	8.44	8.45	10.68	10.69	10.79	11.42	10.30	10.27	9.62	9.21	9.32	9.09	9.28	9.68	11.14	11.16	10.90	10.94	10.85
Na_2O	2.96	3.20	3.42	2.76	2.99	3.30	4.09	3.16	1.65	4.31	3.59	3.71	3.88	3.88	3.70	3.79	3.81	4.57	2.80	3.93	3.13	4.01
K_2O	2.18	2.20	2.23	2.18	2.17	1.13	0.76	1.16	0.26	0.91	0.73	2.47	2.56	2.53	2.57	2.56	2.53	2.27	1.39	2.04	1.86	2.17
TiO_2	1.97	2.00	1.98	1.95	1.97	3.33	3.28	3.38	3.35	3.14	3.24	3.19	3.36	3.22	3.25	3.22	3.46	3.44	3.83	3.80	3.63	3.79
MnO	0.20	0.20	0.20	0.20	0.21	0.24	0.22	0.23	0.21	0.22	0.22	0.23	0.20	0.21	0.21	0.20	0.21	0.24	0.22	0.22	0.22	0.22
P_2O_5	0.64	0.65	0.64	0.64	0.64	1.14	1.08	1.11	1.10	1.12	1.01	0.90	0.89	0.92	0.94	0.94	0.90	1.30	1.31	1.26	1.24	1.24
Total	99.79	99.77	99.73	99.69	99.78	100.48	100.40	100.46	100.55	100.42	100.42	100.16	100.15	100.15	100.20	100.14	100.22	100.61	100.72	100.53	100.68	100.57
Data from Wet. Chem. (wt%)																						
H_2O^-	0.59	0.76	0.82	0.79	0.70	2.11	1.67	2.09	3.07	1.55	1.67	0.43	0.38	0.51	0.50	0.38	0.51	0.93	1.89	1.37	1.50	1.20
LOI	3.41	3.50	3.68	3.29	3.30	3.23	3.67	3.41	4.50	3.07	3.36	2.21	2.11	2.10	2.22	2.21	2.68	2.74	3.65	2.65	3.02	2.61
FeO	5.79	5.75	9.36	5.86	6.16	2.94	2.50	0.92	1.02	2.04	3.01	5.51	4.26	6.24	6.30	6.08	5.76	6.24	3.61	3.17	3.02	3.71
True Fe_2O_3 = (Total Fe_2O_3 fr. XRF) - 1.111344 x (true FeO fr. wet chem.) , to give the data below.																						
SiO_2	50.00	50.03	50.35	50.92	50.14	44.38	44.13	44.45	45.73	43.46	42.72	44.21	44.27	44.12	43.84	44.20	43.76	42.79	44.53	44.12	43.54	43.86
Al_2O_3	16.16	16.07	16.08	15.66	16.09	12.74	12.70	12.85	13.06	12.63	12.96	12.87	12.99	12.91	12.97	12.91	12.94	12.55	13.05	12.92	13.00	12.91
Fe_2O_3	4.96	4.98	0.87	4.64	4.58	11.63	11.79	14.09	13.57	12.11	11.45	6.66	8.00	5.80	5.80	5.95	6.26	7.50	11.17	10.72	11.54	10.39
FeO	5.79	5.75	9.36	5.86	6.16	2.94	2.50	0.92	1.02	2.04	3.01	5.51	4.26	6.24	6.30	6.08	5.76	6.24	3.61	3.17	3.02	3.71
MgO	6.16	6.09	5.75	6.33	6.17	9.26	9.69	9.20	9.35	10.80	12.37	10.33	10.34	10.52	11.10	10.63	10.56	8.77	8.04	7.82	8.74	7.75
CaO	8.48	8.32	8.32	8.40	8.39	10.51	10.48	10.54	11.29	10.07	9.87	9.56	9.17	9.28	9.02	9.22	9.60	10.80	10.91	10.69	10.73	10.63
Na_2O	3.00	3.24	3.43	2.80	3.02	3.30	3.98	3.13	1.64	4.15	3.43	3.71	3.86	3.86	3.68	3.77	3.78	4.33	2.79	3.85	3.12	3.92
K_2O	2.15	2.18	2.20	2.15	2.14	1.10	0.75	1.12	0.30	0.89	0.71	2.49	2.57	2.55	2.59	2.58	2.54	2.24	1.36	2.02	1.83	2.15
TiO_2	1.95	1.98	1.95	1.93	1.94	3.03	2.98	3.05	3.09	2.86	2.88	3.01	3.07	2.97	2.98	2.96	3.12	3.05	3.35	3.33	3.22	3.32
MnO	0.19	0.20	0.19	0.20	0.20	0.26	0.21	0.23	0.21	0.22	0.21	0.25	0.20	0.22	0.21	0.20	0.21	0.26	0.22	0.22	0.21	0.22
P_2O_5	0.67	0.69	0.67	0.67	0.67	1.16	1.10	1.12	1.13	1.13	1.01	0.94	0.93	0.96	0.97	0.97	0.94	1.29	1.31	1.27	1.25	1.25
Total	99.51	99.53	99.17	99.56	99.50	100.31	100.31	100.70	100.39	100.36	100.62	99.54	99.66	99.43	99.45	99.47	99.47	99.82	100.34	100.13	100.20	100.11
$Mg'[Mg/(Mg+Fe^{tot})]$	0.65	0.65	0.65	0.66	0.64	0.85	0.87	0.95	0.94	0.90	0.88	0.77	0.81	0.75	0.76	0.76	0.77	0.71	0.80	0.81	0.84	0.79
Nat Fe_2O_3/FeO	0.86	0.87	0.09	0.79	0.74	3.96	4.72	15.31	13.30	5.94	3.81	1.21	1.88	0.93	0.92	0.98	1.09	1.20	3.09	3.38	3.82	2.80
H_2O^-	0.59	0.76	0.82	0.79	0.70	2.11	1.67	2.09	3.07	1.55	1.67	0.43	0.38	0.51	0.50	0.38	0.51	0.93	1.89	1.37	1.50	1.20
LOI	3.41	3.50	3.68	3.29	3.30	3.23	3.67	3.41	4.50	3.07	3.36	2.21	2.11	2.10	2.22	2.21	2.68	2.74	3.65	2.65	3.02	2.61
Adjustment of 1), Fe_2O_3 / FeO 2). volatiles free and 3) recalculated total to 100%																						
Root name[a]	T/B	T/B	T/B	B	T/B	T/B	T/B	T/B	B	T/B	T/B	T/B	T/B	T/B	T/B	T/B	T/B	T/B	T/B	T/B	T/B	T/B
1) Before using the data for CIPW norm calculation, The Fe_2O_3/FeO has to be adjusted to the ideal ratio:																						
Fe_2O_3/FeO[b]	0.30	0.30	0.30	0.20	0.30	0.20	0.20	0.20	0.20	0.20	0.20	0.30	0.30	0.30	0.30	0.30	0.30	0.30	0.20	0.20	0.20	0.30
Fe_2O_3	2.42	2.42	2.40	1.70	2.43	2.27	2.22	2.30	2.24	2.19	2.26	2.72	2.71	2.71	2.72	2.70	2.69	3.07	2.32	2.17	2.27	3.08
FeO	8.07	8.06	7.99	8.50	8.10	11.36	11.11	11.52	11.21	10.97	11.29	9.06	9.02	9.02	9.07	9.01	8.97	10.22	11.58	10.86	11.36	10.28
[a]Classification based on Total alkalis versus silica after Le Maitre et al. (1989)																						
T/B = Trachybasalt, T/B = Tephrite/Basanite, B/A = Basaltic andesite, B = Basalt, PT = Phonotephrite																						
[b]Iron oxidation ratios after Middlemost (1989)																						
The data with adjusted Fe_2O_3 are as follows:																						
SiO_2	50.00	50.03	50.35	50.92	50.14	44.38	44.13	44.45	45.73	43.46	42.72	44.21	44.27	44.12	43.84	44.20	43.76	42.79	44.53	44.12	43.54	43.86
Al_2O_3	16.16	16.07	16.08	15.66	16.09	12.74	12.70	12.85	13.06	12.63	12.96	12.87	12.99	12.91	12.97	12.91	12.94	12.55	13.05	12.92	13.00	12.91
Fe_2O_3	2.42	2.42	2.40	1.70	2.43	2.27	2.22	2.30	2.24	2.19	2.26	2.72	2.71	2.71	2.72	2.70	2.69	3.07	2.32	2.17	2.27	3.08
FeO	8.07	8.06	7.99	8.50	8.10	11.36	11.11	11.52	11.21	10.97	11.29	9.06	9.02	9.02	9.07	9.01	8.97	10.22	11.58	10.86	11.36	10.28
MgO	6.16	6.09	5.75	6.33	6.17	9.26	9.69	9.20	9.35	10.80	12.37	10.33	10.34	10.52	11.10	10.63	10.56	8.77	8.04	7.82	8.74	7.75
CaO	8.48	8.32	8.32	8.40	8.39	10.51	10.48	10.54	11.29	10.07	9.87	9.56	9.17	9.28	9.02	9.22	9.60	10.80	10.91	10.69	10.73	10.63
Na_2O	3.00	3.24	3.43	2.80	3.02	3.30	3.98	3.13	1.64	4.15	3.43	3.71	3.86	3.86	3.68	3.77	3.78	4.33	2.79	3.85	3.12	3.92
K_2O	2.15	2.18	2.20	2.15	2.14	1.10	0.75	1.12	0.30	0.89	0.71	2.49	2.57	2.55	2.59	2.58	2.54	2.24	1.36	2.02	1.83	2.15
TiO_2	1.95	1.98	1.95	1.93	1.94	3.03	2.98	3.05	3.09	2.86	2.88	3.01	3.07	2.97	2.98	2.96	3.12	3.05	3.35	3.33	3.22	3.32
MnO	0.19	0.20	0.19	0.20	0.20	0.26	0.21	0.23	0.21	0.22	0.21	0.25	0.20	0.22	0.21	0.20	0.21	0.26	0.22	0.22	0.21	0.22
P_2O_5	0.67	0.69	0.67	0.67	0.67	1.16	1.10	1.12	1.13	1.13	1.01	0.94	0.93	0.96	0.97	0.97	0.94	1.29	1.31	1.27	1.25	1.25
Total	99.25	99.27	99.32	99.26	99.29	99.37	99.35	99.52	99.25	99.37	99.70	99.14	99.13	99.12	99.15	99.15	99.11	99.37	99.45	99.27	99.27	99.38
H_2O^-	0.59	0.76	0.82	0.79	0.70	2.11	1.67	2.09	3.07	1.55	1.67	0.43	0.38	0.51	0.50	0.38	0.51	0.93	1.89	1.37	1.50	1.20
LOI	3.41	3.50	3.68	3.29	3.30	3.23	3.67	3.41	4.50	3.07	3.36	2.21	2.11	2.10	2.22	2.21	2.68	2.74	3.65	2.65	3.02	2.61
Fe_2O_3/FeO	0.30	0.30	0.30	0.20	0.30	0.20	0.20	0.20	0.20	0.20	0.20	0.30	0.30	0.30	0.30	0.30	0.30	0.30	0.20	0.20	0.20	0.30
2) Volatiles free: By substracting H2O and LOI from the Total and Recalculated to 100 %. (Middlemost, 1989). (However CO2 data is not available, the norm will not have calcite).																						
2.1) Volatiles free:																						
SiO_2	47.98	47.88	48.07	48.83	48.12	42.00	41.76	41.99	42.24	41.44	40.56	43.03	43.16	42.96	42.64	43.05	42.35	41.31	42.95	42.33	41.56	42.18
Al_2O_3	15.51	15.38	15.35	15.02	15.44	12.06	12.02	12.14	12.06	12.04	12.31	12.53	12.66	12.57	12.61	12.57	12.52	12.09	12.32	12.40	12.41	12.42
Fe_2O_3	2.32	2.31	2.29	1.63	2.33	2.15	2.10	2.18	2.07	2.09	2.14	2.64	2.64	2.63	2.65	2.63	2.60	2.95	2.19	2.08	2.17	2.97
FeO	7.75	7.71	7.62	8.15	7.77	10.75	10.51	10.89	10.35	10.46	10.72	8.81	8.79	8.78	8.82	8.77	8.68	9.85	10.93	10.42	10.85	9.89
MgO	5.91	5.83	5.49	6.07	5.92	8.76	9.17	8.69	8.64	10.30	11.75	10.05	10.08	10.24	10.80	10.35	10.22	8.45	7.59	7.50	8.34	7.45
CaO	8.14	7.96	7.91	8.05	8.05	9.95	9.92	9.96	10.43	9.60	9.37	9.31	8.94	9.04	8.77	8.98	9.29	10.40	10.30	10.26	10.24	10.22
Na_2O	2.88	3.10	3.27	2.68	2.90	3.12	3.77	2.96	1.51	3.96	3.26	3.61	3.76	3.76	3.58	3.67	3.66	4.17	2.63	3.69	2.98	3.77
K_2O	2.06	2.09	2.10	2.06	2.05	1.04	0.71	1.06	0.28	0.85	0.67	2.42	2.51	2.48	2.52	2.51	2.46	2.16	1.28	1.94	1.75	2.07
TiO_2	1.87	1.90	1.86	1.85	1.86	2.87	2.82	2.88	2.85	2.73	2.73	2.93	2.99	2.89	2.90	2.88	3.02	2.94	3.16	3.20	3.07	3.19
MnO	0.18	0.19	0.18	0.19	0.19	0.25	0.20	0.22	0.19	0.21	0.20	0.24	0.19	0.21	0.20	0.19	0.20	0.25	0.21	0.21	0.20	0.21
P_2O_5	0.64	0.66	0.64	0.64	0.64	1.10	1.04	1.06	1.04	1.08	0.96	0.91	0.91	0.93	0.94	0.94	0.91	1.24	1.24	1.22	1.19	1.20
Total	95.25	95.01	94.82	95.18	95.29	94.03	94.01	94.02	91.68	94.75	94.67	96.50	96.64	96.51	96.43	96.56	95.92	95.70	93.91	95.25	94.75	95.57
3) Recalculated to 100 % (Final adjusted data and ready for CIPW norm calculation).																						
SiO_2	50.38	50.40	50.69	51.30	50.50	44.66	44.42	44.67	46.07	43.74	42.85	44.59	44.66	44.51	44.22	44.58	44.15	43.06	44.78	44.44	43.86	44.14
TiO_2	1.96	1.99	1.96	1.94	1.95	3.05	3.00	3.06	3.11	2.88	2.89	3.04	3.10	3.00	3.01	2.99	3.15	3.07	3.37	3.35	3.24	3.34
Al_2O_3	16.28	16.19	16.19	15.78	16.21	12.82	12.78	12.91	13.16	12.71	13.00	12.98	13.10	13.03	13.08	13.02	13.06	12.63	13.12	13.01	13.09	12.99
Fe_2O_3	2.44	2.43	2.41	1.71	2.45	2.29	2.24	2.32	2.26	2.21	2.26	2.74	2.73	2.73	2.74	2.72	2.72	3.09	2.33	2.19	2.29	3.10
FeO	8.13	8.12	8.04	8.57	8.16	11.43	11.18	11.58	11.29	11.04	11.32	9.13	9.10	9.10	9.15	9.08	9.05	10.29	11.64	10.94	11.45	10.35
MnO	0.19	0.20	0.19	0.20	0.20	0.26	0.21	0.23	0.21	0.22	0.21	0.25	0.20	0.22	0.21	0.20	0.21	0.26	0.22	0.22	0.21	0.22
MgO	6.21	6.13	5.79	6.38	6.21	9.32	9.75	9.24	9.42	10.87	12.41	10.42	10.43	10.61	11.20	10.72	10.65	8.83	8.08	7.88	8.80	7.80
CaO	8.54	8.38	8.38	8.46	8.45	10.58	10.55	10.59	11.38	10.13	9.90	9.64	9.25	9.36	9.10	9.30	9.69	10.87	10.97	10.77	10.81	10.70
Na_2O	3.02	3.26	3.45	2.82	3.04	3.32	4.01	3.15	1.65	4.18	3.44	3.74	3.89	3.89	3.71	3.80	3.81	4.36	2.81	3.88	3.14	3.94
K_2O	2.17	2.20	2.22	2.17	2.16	1.11	0.75	1.13	0.30	0.90	0.71	2.51	2.59	2.57	2.61	2.60	2.56	2.25	1.37	2.03	1.84	2.16
P_2O_5	0.68	0.70	0.67	0.67	0.67	1.17	1.11	1.13	1.14	1.14	1.01	0.95	0.94	0.97	0.98	0.98	0.95	1.30	1.32	1.28	1.26	1.26
Total	100.00	100.00	100.00	100.00	100.00	100.00	100.00	100.00	100.00	100.00	100.00	100.00	100.00	100.00	100.00	100.00	100.00	100.00	100.00	100.00	100.00	100.00

Appendix 2-4

Appendix 2-4 Chemical composition and CIPW normative mineral composition of Thai basalts. (Standards 6a + 6F linear calibration). *s* = standard deviation; %RSD = *s* x 100/mean ; **M' = [Mg/(Mg+Fe^{2+})]**

Locality	CHIANG KHONG, CK									BAN NONG, BN								
Weight % Oxides	CK1	CK2	CK3	CK4	CK5	CK6	mean	*s*	%RSD	BN1	BN2	BN3	BN4	BN5	BN6	mean	*s*	%RSD
SiO_2	46.63	45.90	46.43	45.85	46.00	46.33	46.19	0.32	0.7	44.91	44.54	47.28	46.31	47.74	45.91	46.12	1.27	2.7
Al_2O_3	15.22	15.43	15.18	15.74	15.44	15.48	15.42	0.20	1.3	14.44	14.26	13.99	14.96	15.02	15.21	14.65	0.49	3.3
Fe_2O_3	7.77	10.42	4.28	2.95	8.67	3.72	6.30	3.06	48.5	6.40	6.19	7.46	8.56	6.08	6.00	6.78	1.02	15.1
FeO	4.06	1.64	7.14	8.33	3.14	7.48	5.30	2.72	51.3	4.96	5.09	4.23	2.23	3.69	4.69	4.15	1.07	25.8
MgO	6.07	6.34	6.47	6.54	6.49	6.69	6.43	0.21	3.3	9.31	10.00	6.94	9.25	9.94	8.66	9.02	1.13	12.5
CaO	10.50	10.24	10.16	9.38	10.51	9.92	10.12	0.42	4.2	9.62	9.56	9.97	8.41	8.55	8.86	9.16	0.64	7.0
Na_2O	2.19	2.52	2.38	2.90	2.20	2.34	2.42	0.26	10.9	3.89	3.87	5.02	3.67	3.75	3.99	4.03	0.50	12.3
K_2O	3.01	3.13	3.03	3.08	3.08	3.07	3.07	0.04	1.4	2.36	2.35	1.23	2.93	1.49	2.67	2.17	0.67	30.8
TiO_2	2.92	2.92	2.90	2.93	2.90	2.87	2.91	0.02	0.7	2.41	2.42	2.41	2.00	2.14	2.14	2.25	0.18	8.1
MnO	0.18	0.18	0.18	0.18	0.18	0.18	0.18	0.00	0.0	0.17	0.17	0.18	0.17	0.19	0.17	0.18	0.01	4.8
P_2O_5	0.82	0.86	0.83	0.82	0.85	0.83	0.84	0.02	2.0	0.61	0.58	0.60	0.63	0.58	0.68	0.61	0.04	6.2
Total	99.37	99.58	98.98	98.70	99.46	98.91	99.17	0.35	0.4	99.08	99.03	99.31	99.12	99.17	98.98	99.11	0.12	0.1
Mg'	0.73	0.87	0.62	0.58	0.79	0.61	0.70	0.11	16.4	0.77	0.78	0.75	0.88	0.83	0.77	0.79	0.05	6.3
Nat. Fe_2O_3/FeO	1.91	6.35	0.60	0.35	2.76	0.50	2.08	2.30	110.5	1.29	1.22	1.76	3.84	1.65	1.28	1.84	1.00	54.6
H_2O^-	0.61	0.55	0.61	0.64	0.72	0.64	0.63	0.06	8.9	0.43	0.39	1.00	0.58	0.60	0.53	0.59	0.22	37.0
LOI	3.31	2.47	3.67	2.56	3.14	3.31	3.08	0.47	15.2	1.44	1.61	2.04	1.54	2.94	1.98	1.93	0.55	28.7
Trace elements (ppm)																		
Nb	122	119	123	121	119	121	121	2	1.3	103	101	111	119	87	116	106	12	11.1
Zr	403	395	400	386	386	389	393	7	1.9	334	332	379	401	306	393	358	39	10.8
Y	57	57	57	55	57	58	57	1	1.7	50	50	55	54	47	55	52	3	6.4
Sr	897	872	879	829	870	834	864	27	3.1	826	809	979	947	782	944	881	85	9.6
Rb	47	44	47	44	49	46	46	2	4.2	88	87	66	107	64	127	90	24	26.9
Zn	80	75	78	79	82	77	79	2	3.1	72	79	85	79	56	74	74	10	13.5
Cu	50	43	49	55	53	44	49	5	9.7	52	64	50	45	51	42	51	8	15.0
Ni	78	65	73	71	71	69	71	4	6.1	155	143	105	175	256	164	166	50	30.1
Cr	78	82	80	82	73	81	79	3	4.3	235	210	184	211	251	234	221	24	10.8
Ce	97	92	116	109	111	98	104	9	9.1	117	74	105	138	51	120	101	32	32.1
Nd	39	41	51	47	47	35	43	6	13.8	46	45	38	50	17	52	41	13	31.1
V	290	289	275	285	286	285	285	5	1.9	308	304	281	217	232	236	263	40	15.1
La	42	38	25	22	34	43	34	9	25.8	45	35	35	49	34	45	41	7	16.2
Ba	388	252	238	224	321	233	276	65	23.6	1027	1021	1009	1002	322	1013	899	283	31.5
Sc	27	20	22	25	25	17	23	4	16.4	29	29	31	15	22	25	25	6	23.6
CIPW normative minerals (%)																		
Q																		
Or	17.97	18.73	18.14	18.44	18.44	18.38	18.35	0.26	1.4	14.12	14.07	7.33	17.55	8.92	16.02	13.00	4.03	31.0
Ab	14.62	10.66	14.01	12.12	11.88	14.00	12.88	1.55	12.1	7.53	5.93	20.64	11.23	23.89	10.75	13.33	7.27	54.6
An	23.06	21.82	22.01	21.12	23.38	22.92	22.39	0.87	3.9	15.16	14.79	12.16	15.92	19.97	15.88	15.65	2.53	16.2
Ne	2.26	5.92	3.46	6.91	3.78	3.28	4.27	1.77	41.4	13.98	14.76	12.11	11.01	4.48	12.74	11.51	3.69	32.1
Di	19.72	19.58	19.11	16.86	19.30	17.38	18.66	1.22	6.5	23.50	23.67	27.58	17.94	15.34	19.50	21.26	4.47	21.0
Hy																		
Ol	11.01	12.89	11.93	14.21	11.87	12.83	12.46	1.11	8.9	15.91	17.06	10.34	17.56	18.74	15.88	15.92	2.94	18.4
Mt	3.83	2.74	3.81	2.74	3.78	3.75	3.44	0.54	15.8	3.73	3.70	3.80	3.45	3.17	3.51	3.56	0.23	6.6
Il	5.60	5.62	5.58	5.64	5.56	5.52	5.59	0.04	0.8	4.63	4.65	4.63	3.85	4.12	4.12	4.33	0.35	8.0
Ap	1.92	2.02	1.95	1.92	1.99	1.95	1.96	0.04	2.0	1.44	1.37	1.41	1.48	1.37	1.60	1.45	0.09	6.0
Total	99.99	99.98	100.00	99.96	99.98	100.01	99.99	0.02	0.0	100.00	100.00	100.00	99.99	100.00	100.00	100.00	0.00	0.0

Appendix 2-4 (Continued).

Locality	SOP PRAP, SP								DEN CHAI, DC							
Weight % oxides	SP1	SP2	SP3	SP4	SP5	mean	s	%RSD	DC1	DC2	DC3	DC4	DC5	mean	s	%RSD
SiO_2	51.24	49.59	50.86	52.58	52.77	51.41	1.31	2.5	47.17	46.63	47.17	47.72	47.86	47.31	0.49	1.0
Al_2O_3	16.43	15.52	16.57	17.18	17.08	16.56	0.66	4.0	14.88	14.03	15.19	13.74	13.75	14.32	0.67	4.7
Fe_2O_3	7.19	7.96	7.58	6.01	9.13	7.58	1.14	15.0	3.23	7.28	8.07	7.62	9.33	7.11	2.30	32.4
FeO	1.87	1.59	1.85	3.25	0.34	1.78	1.03	58.1	6.39	2.67	2.05	4.88	3.18	3.83	1.77	46.3
MgO	5.09	5.06	5.29	4.54	4.64	4.92	0.32	6.5	10.66	13.15	10.38	9.34	9.24	10.55	1.58	15.0
CaO	9.48	11.68	8.98	8.76	8.64	9.51	1.26	13.2	8.36	8.02	8.38	10.37	10.16	9.06	1.11	12.3
Na_2O	2.27	2.17	2.26	2.23	2.27	2.24	0.04	1.9	3.96	3.79	3.92	2.45	2.47	3.32	0.79	23.7
K_2O	3.16	3.13	3.13	2.04	2.05	2.70	0.60	22.2	1.51	1.37	1.41	0.57	0.53	1.08	0.48	45.0
TiO_2	2.15	2.23	2.21	2.24	2.21	2.21	0.03	1.6	2.26	2.07	2.28	2.67	2.88	2.43	0.33	13.7
MnO	0.21	0.22	0.22	0.21	0.21	0.21	0.01	2.6	0.19	0.20	0.20	0.22	0.22	0.21	0.01	6.5
P_2O_5	0.68	0.66	0.69	0.69	0.70	0.68	0.02	2.2	0.67	0.62	0.69	0.39	0.43	0.56	0.14	25.0
Total	99.77	99.81	99.64	99.73	100.04	99.80	0.15	0.1	99.28	99.83	99.74	99.97	100.05	99.77	0.30	0.3
Mg'	0.83	0.85	0.84	0.71	0.96	0.84	0.09	10.5	0.75	0.90	0.90	0.77	0.84	0.83	0.07	8.4
Nat. Fe_2O_3/FeO	3.85	5.01	4.09	1.85	26.86	8.33	10.42	125.1	0.51	2.73	3.94	1.56	2.93	2.33	1.33	56.8
H_2O^-	1.43	1.41	1.39	2.74	3.07	2.01	0.83	41.2	0.76	0.62	0.70	0.19	0.23	0.50	0.27	53.9
LOI	4.90	5.50	4.43	5.04	4.51	4.88	0.43	8.9	3.26	2.58	2.90	4.02	3.52	3.26	0.56	17.1
Trace elements (ppm)																
Nb	125	133	128	134	133	131	4	3.0	89	80	89	26	29	63	32	51.5
Zr	632	611	609	443	434	546	98	18.0	305	273	307	286	307	296	15	5.2
Y	49	52	51	50	53	51	2	3.1	47	45	48	69	71	56	13	22.9
Sr	3325	3033	3054	1138	1070	2324	1120	48.2	726	647	749	253	255	526	251	47.8
Rb	110	111	98	117	131	113	12	10.6	46	50	48	14	14	34	19	54.3
Zn	64	64	69	67	64	66	2	3.5	64	59	62	90	82	71	14	19.2
Cu	43	45	47	48	47	46	2	4.3	56	53	57	82	69	63	12	19.0
Ni	115	119	121	107	112	115	6	4.9	314	566	290	137	142	290	175	60.3
Cr	145	152	147	151	144	148	4	2.4	309	574	287	246	266	336	135	40.1
Ce	109	109	116	106	96	107	7	6.8	89	88	87	15	37	63	35	55.1
Nd	31	34	49	43	51	42	9	21.3	37	30	24	13	19	25	9	38.0
V	200	203	202	225	220	210	12	5.5	237	220	234	311	329	266	50	18.8
La	43	33	46	28	39	38	7	19.4	26	27	20	23	11	21	6	30.0
Ba	541	554	538	532	539	541	8	1.5	324	292	339			318	24	7.5
Sc	16	18	19	23	23	20	3	15.7	25	23	20	36	33	27	7	24.8
CIPW normative minerals (%)																
Q	0.39		0.17	6.56	6.62	3.44	3.64	106.1								
Or	18.79	18.62	18.67	12.12	12.17	16.07	3.59	22.3	8.98	8.16	8.39	3.37	3.13	6.41	2.90	45.2
Ab	19.38	17.62	19.29	19.04	19.38	18.94	0.75	4.0	21.79	19.45	22.97	20.82	21.07	21.22	1.29	6.1
An	25.47	23.52	26.04	31.03	30.55	27.32	3.31	12.1	18.51	17.32	19.86	24.97	25.03	21.14	3.64	17.2
Ne		0.50				0.50	0.00	0.0	6.48	6.97	5.66			6.37	0.66	10.4
Di	14.15	24.83	11.66	6.71	6.56	12.78	7.48	58.5	15.10	14.88	14.00	19.66	18.57	16.44	2.50	15.2
Hy	13.22		15.30	15.66	15.92	15.03	1.23	8.2				10.90	13.64	12.27	1.94	15.8
Ol		6.07				6.07	0.00	0.0	20.01	24.65	19.90	11.36	9.18	17.02	6.50	38.2
Mt	2.88	3.02	3.00	2.99	2.96	2.97	0.05	1.8	3.20	3.17	3.22	2.90	2.87	3.07	0.17	5.6
Il	4.12	4.27	4.23	4.29	4.21	4.22	0.07	1.6	4.33	3.95	4.37	5.11	5.51	4.65	0.64	13.7
Ap	1.60	1.55	1.62	1.60	1.62	1.60	0.03	1.8	1.58	1.44	1.62	0.90	1.00	1.31	0.34	25.6
Total	100.00	100.00	99.98	100.00	99.99	99.99	0.01	0.0	99.98	99.99	99.99	99.99	100.00	99.99	0.01	0.0

Appendix 2-4 (Continued).

Locality	KHOK SAMRAN, KS								BO PHLOI, BP											
Weight % oxides	KS1	KS2	KS3	KS4	KS5	mean	*s*	%RSD	BP1	BP2	BP3	BP4	BP5	BP6	BP7	BP8	BP9	mean	*s*	%RSD
SiO_2	47.90	47.98	48.63	48.36	47.84	48.14	0.34	0.7	48.88	48.32	49.36	49.04	48.83	49.31	49.38	49.46	48.29	48.99	0.45	0.9
Al_2O_3	16.95	17.70	16.87	16.74	17.31	17.11	0.39	2.3	14.40	14.11	14.45	14.64	14.68	14.17	14.22	14.19	13.85	14.30	0.27	1.9
Fe_2O_3	6.33	5.07	3.32	6.48	5.77	5.39	1.29	23.8	5.68	7.03	7.96	7.61	3.39	5.59	7.07	2.83	6.42	5.95	1.80	30.3
FeO	3.71	5.17	6.31	3.67	4.90	4.75	1.10	23.2	3.48	2.32	1.32	1.74	5.41	3.50	2.14	5.69	2.58	3.13	1.55	49.4
MgO	6.47	6.87	5.99	6.46	7.21	6.60	0.46	7.0	7.27	8.55	7.39	7.45	7.05	7.32	8.27	7.72	8.86	7.76	0.64	8.2
CaO	9.41	9.56	9.57	9.43	9.35	9.46	0.10	1.0	9.01	8.88	8.31	8.33	8.66	8.58	8.04	8.20	8.63	8.52	0.32	3.8
Na_2O	3.48	3.14	3.27	3.25	3.17	3.26	0.13	4.1	4.65	3.91	4.92	4.91	5.16	5.20	4.89	5.15	4.11	4.77	0.46	9.7
K_2O	1.88	1.13	1.91	1.75	1.16	1.57	0.39	24.8	3.01	3.54	3.04	2.95	2.99	2.84	2.76	3.12	3.93	3.13	0.37	11.9
TiO_2	2.06	1.93	2.07	2.14	1.99	2.04	0.08	3.9	1.90	1.86	1.92	1.94	1.88	1.92	1.89	1.85	1.79	1.88	0.05	2.4
MnO	0.20	0.19	0.20	0.21	0.22	0.20	0.01	5.6	0.23	0.20	0.20	0.22	0.21	0.21	0.21	0.19	0.21	0.21	0.01	5.6
P_2O_5	1.11	0.73	1.10	1.06	0.67	0.93	0.22	23.1	0.93	0.88	0.81	0.81	0.90	0.81	0.81	0.81	0.87	0.85	0.05	5.6
Total	99.50	99.47	99.24	99.55	99.59	99.47	0.14	0.1	99.44	99.60	99.68	99.64	99.16	99.45	99.68	99.21	99.54	99.49	0.20	0.2
Mg'	0.76	0.70	0.63	0.76	0.72	0.71	0.05	7.4	0.79	0.87	0.91	0.88	0.70	0.79	0.87	0.71	0.86	0.82	0.08	9.4
Nat. Fe_2O_3/FeO	1.71	0.98	0.53	1.77	1.18	1.23	0.52	42.1	1.63	3.03	6.03	4.37	0.63	1.60	3.30	0.50	2.49	2.62	1.80	68.6
H_2O^-	0.37	0.46	0.44	0.52	0.53	0.46	0.07	14.0	0.29	0.48	0.51	0.65	0.60	0.41	0.67	0.50	0.61	0.52	0.12	23.4
LOI	2.24	2.11	2.45	2.06	2.24	2.22	0.15	6.8	3.18	3.06	2.66	2.76	3.09	2.61	2.79	2.84	2.44	2.83	0.24	8.7
Trace elements (ppm)																				
Nb	46	31	47	44	27	39	9	23.8	157	157	151	153	163	156	155	151	150	155	4	2.6
Zr	358	253	371	373	252	321	63	19.7	414	413	398	403	418	393	388	404	405	404	10	2.5
Y	51	47	50	51	46	49	2	4.8	53	54	50	51	51	48	50	49	56	51	3	5.0
Sr	1748	1142	1921	1945	1157	1583	403	25.4	1076	1151	1013	1012	1126	1000	1011	1089	1112	1066	58	5.4
Rb	19	13	19	18	15	17	3	16.0	75	212	68	65	90	81	61	71	286	112	80	71.6
Zn	81	85	79	79	92	83	5	6.6	75	77	74	76	73	73	72	72	78	74	2	2.9
Cu	51	64	49	46	66	55	9	16.6	53	57	45	51	50	56	44	47	51	50	5	9.0
Ni	33	105	38	44	119	68	41	60.2	190	218	163	189	179	171	234	168	215	192	25	13.0
Cr	50	124	52	55	130	82	41	49.9	227	250	217	250	248	208	429	239	241	257	66	25.9
Ce	156	74	192	163	93	136	50	36.8	148	141	149	132	157	151	130	145	153	145	9	6.3
Nd	65	35	52	55	35	48	13	27.2	41	52	44	41	46	54	42	59	45	47	6	13.6
V	231	235	246	240	253	241	9	3.6	221	210	224	219	215	235	222	211	200	217	10	4.6
La	48	30	51	46	26	40	11	28.3	60	61	56	57	57	55	51	51	57	56	3	6.1
Ba	458	178	514	440	156	349	169	48.3	462	476	452	470	516	456	469	483	489	475	20	4.1
Sc	29	20	23	18	20	22	4	19.6	22	21	15	13	15	22	18	17	14	17	4	20.1
CIPW normative minerals (%)																				
Q																				
Or	11.23	6.74	11.41	10.46	6.91	9.35	2.33	25.0	17.97	21.10	18.14	17.61	17.85	16.96	16.43	18.62	23.40	18.68	2.20	11.8
Ab	25.66	26.83	27.93	27.76	27.08	27.05	0.90	3.3	16.94	12.30	18.72	18.35	16.74	18.50	20.66	17.69	9.18	16.56	3.58	21.6
An	25.30	31.12	25.91	26.12	29.78	27.65	2.62	9.5	9.60	10.58	8.44	9.27	8.12	6.96	8.75	6.43	7.78	8.44	1.30	15.4
Ne	2.19					2.19	0.00	0.0	12.32	11.40	12.60	12.75	14.81	14.05	11.41	14.21	14.05	13.07	1.26	9.6
Di	11.78	9.68	11.96	11.42	10.25	11.02	1.00	9.1	23.64	22.51	22.35	21.81	23.60	24.66	20.93	23.48	23.78	22.97	1.16	5.0
Hy		2.31	0.17	0.82	0.60	0.98	0.93	95.4												
Ol	14.05	15.50	12.86	13.57	17.50	14.70	1.84	12.5	10.36	13.11	10.87	11.26	9.86	9.99	13.00	10.93	13.08	11.38	1.34	11.7
Mt	3.25	2.41	3.22	3.28	2.51	2.93	0.43	14.8	3.35	3.36	3.31	3.35	3.29	3.32	3.31	3.20	3.25	3.30	0.05	1.6
Il	3.95	3.70	3.97	4.10	3.82	3.91	0.15	3.9	3.65	3.57	3.68	3.72	3.61	3.68	3.63	3.55	3.44	3.61	0.09	2.4
Ap	2.59	1.71	2.57	2.48	1.58	2.19	0.50	22.8	2.18	2.06	1.90	1.90	2.11	1.90	1.90	1.90	2.04	1.99	0.11	5.6
Total	100.00	100.00	100.00	100.01	100.03	100.01	0.01	0.0	100.01	99.99	100.01	100.02	99.99	100.02	100.02	100.01	100.00	100.01	0.01	0.0

Appendix 2-4 (Continued).

Locality	NAM YUN, NY								PHLOI WAEN, PW								
Weight % oxides	NY1	NY2	NY3	NY4	NY5	mean	s	%RSD	PW1	PW2	PW3	PW4	PW5	PW6	mean	s	%RSD
SiO_2	50.00	50.03	50.35	50.92	50.14	50.29	0.38	0.8	44.38	44.13	44.45	45.73	43.46	42.72	44.15	1.02	2.3
Al_2O_3	16.16	16.07	16.08	15.66	16.09	16.01	0.20	1.2	12.74	12.70	12.85	13.06	12.63	12.96	12.82	0.16	1.3
Fe_2O_3	4.96	4.98	0.87	4.64	4.58	4.00	1.76	44.0	11.63	11.79	14.09	13.57	12.11	11.45	12.44	1.11	8.9
FeO	5.79	5.75	9.36	5.86	6.16	6.58	1.56	23.7	2.94	2.50	0.92	1.02	2.04	3.01	2.07	0.92	44.5
MgO	6.16	6.09	5.75	6.33	6.17	6.10	0.21	3.5	9.26	9.69	9.20	9.35	10.80	12.37	10.11	1.26	12.4
CaO	8.48	8.32	8.32	8.40	8.39	8.38	0.07	0.8	10.51	10.48	10.54	11.29	10.07	9.87	10.46	0.49	4.7
Na_2O	3.00	3.24	3.43	2.80	3.02	3.10	0.24	7.8	3.30	3.98	3.13	1.64	4.15	3.43	3.27	0.89	27.3
K_2O	2.15	2.18	2.20	2.15	2.14	2.16	0.03	1.2	1.10	0.75	1.12	0.30	0.89	0.71	0.81	0.30	37.4
TiO_2	1.95	1.98	1.95	1.93	1.94	1.95	0.02	1.0	3.03	2.98	3.05	3.09	2.86	2.88	2.98	0.09	3.1
MnO	0.19	0.20	0.19	0.20	0.20	0.20	0.01	2.8	0.26	0.21	0.23	0.21	0.22	0.21	0.22	0.02	8.8
P_2O_5	0.67	0.69	0.67	0.67	0.67	0.67	0.01	1.3	1.16	1.10	1.12	1.13	1.13	1.01	1.11	0.05	4.7
Total	99.51	99.53	99.17	99.56	99.50	99.45	0.16	0.2	100.31	100.31	100.70	100.39	100.36	100.62	100.45	0.17	0.2
Mg'	0.65	0.65	0.52	0.66	0.64	0.63	0.06	9.3	0.85	0.87	0.95	0.94	0.90	0.88	0.90	0.04	4.4
Nat. Fe_2O_3/FeO	0.86	0.87	0.09	0.79	0.74	0.67	0.33	48.7	3.96	4.72	15.31	13.30	5.94	3.81	7.84	5.11	65.1
H_2O^-	0.59	0.76	0.82	0.79	0.70	0.73	0.09	12.4	2.11	1.67	2.09	3.07	1.55	1.67	2.03	0.56	27.7
LOI	3.41	3.50	3.68	3.29	3.30	3.44	0.16	4.7	3.23	3.67	3.41	4.50	3.07	3.36	3.54	0.51	14.4
Trace elements (ppm)																	
Nb	65	64	66	61	67	65	2	3.6	169	170	168	157	159	153	163	7	4.4
Zr	228	239	224	232	230	231	6	2.4	543	546	540	547	524	483	531	25	4.7
Y	42	41	41	44	42	42	1	2.9	59	57	60	61	55	57	58	2	3.8
Sr	631	694	579	654	615	635	43	6.8	1558	1548	1558	1732	1450	1321	1528	136	8.9
Rb	26	28	28	26	34	28	3	11.6	235	107	227	226	103	182	180	61	33.9
Zn	98	98	99	96	97	98	1	1.2	142	140	139	136	135	128	137	5	3.6
Cu	80	75	80	78	75	78	3	3.2	59	51	61	50	55	64	57	6	9.9
Ni	188	181	178	169	193	182	9	5.1	250	240	249	414	291	511	326	112	34.3
Cr	192	186	195	196	188	191	4	2.3	188	198	185	247	276	417	252	89	35.2
Ce	67	71	53	72	49	62	11	17.1	174	179	181	185	173	194	181	8	4.3
Nd	24	10	23	30	18	21	7	35.6	57	80	75	83	75	74	74	9	12.2
V	193	187	197	194	198	194	4	2.2	327	294	315	270	266	311	297	25	8.4
La	23	37	36	25	25	29	7	23.0	58	61	61	66	54	64	61	4	7.0
Ba	65	84	57	65	68	68	10	14.7	533	420	594	164	416	359	414	150	36.1
Sc	17	14	18	13	16	16	2	13.3	19	26	27	26	22	25	24	3	12.7
CIPW normative minerals (%)																	
Q																	
Or	12.82	13.00	13.12	12.82	12.77	12.91	0.15	1.1	6.56	4.43	6.68	1.77	5.32	4.20	4.83	1.82	37.7
Ab	25.56	27.59	29.20	23.86	25.73	26.39	2.05	7.8	16.09	15.50	16.26	13.96	12.17	11.32	14.22	2.10	14.7
An	24.44	23.03	22.12	23.97	24.19	23.55	0.96	4.1	16.79	14.64	17.74	27.60	13.25	17.92	17.99	5.05	28.1
Ne									6.51	9.99	5.63		12.57	9.63	8.87	2.81	31.7
Di	11.00	11.40	12.33	11.15	10.90	11.36	0.58	5.1	22.87	24.76	22.37	17.43	23.97	19.88	21.88	2.75	12.5
Hy	9.83	6.26	4.13	16.52	10.48	9.44	4.73	50.1				22.85			22.85	0.00	0.0
Ol	7.50	9.79	10.33	3.95	7.13	7.74	2.53	32.8	19.38	19.16	19.55	4.54	21.44	25.94	18.34	7.23	39.4
Mt	3.54	3.52	3.49	2.48	3.55	3.32	0.47	14.1	3.32	3.25	3.36	3.28	3.20	3.28	3.28	0.06	1.7
Il	3.72	3.78	3.72	3.68	3.70	3.72	0.04	1.0	5.79	5.70	5.81	5.90	5.47	5.49	5.69	0.18	3.1
Ap	1.58	1.62	1.55	1.55	1.55	1.57	0.03	2.0	2.71	2.57	2.62	2.64	2.64	2.34	2.59	0.13	5.0
Total	99.99	99.99	99.99	99.98	100.00	99.99	0.01	0.0	100.02	100.00	100.02	99.97	100.03	100.00	100.01	0.02	0.0

Appendix 2-4 (Continued).

Locality	TOK PHROM, TP									NONG BON ,NB							
Weight % oxides	TP1	TP2	TP3	TP4	TP5	TP6	mean	s	%RSD	NB1	NB2	NB3	NB4	NB5	mean	s	%RSD
SiO_2	44.21	44.27	44.12	43.84	44.20	43.76	44.07	0.21	0.5	42.79	44.53	44.12	43.54	43.86	43.77	0.66	1.5
Al_2O_3	12.87	12.99	12.91	12.97	12.91	12.94	12.93	0.04	0.3	12.55	13.05	12.92	13.00	12.91	12.89	0.20	1.5
Fe_2O_3	6.66	8.00	5.80	5.80	5.95	6.26	6.41	0.84	13.2	7.50	11.17	10.72	11.54	10.39	10.26	1.61	15.7
FeO	5.51	4.26	6.24	6.30	6.08	5.76	5.69	0.76	13.4	6.24	3.61	3.17	3.02	3.71	3.95	1.31	33.2
MgO	10.33	10.34	10.52	11.10	10.63	10.56	10.58	0.28	2.7	8.77	8.04	7.82	8.74	7.75	8.22	0.50	6.0
CaO	9.56	9.17	9.28	9.02	9.22	9.60	9.31	0.23	2.4	10.80	10.91	10.69	10.73	10.63	10.75	0.11	1.0
Na_2O	3.71	3.86	3.86	3.68	3.77	3.78	3.78	0.07	2.0	4.33	2.79	3.85	3.12	3.92	3.60	0.63	17.5
K_2O	2.49	2.57	2.55	2.59	2.58	2.54	2.55	0.04	1.4	2.24	1.36	2.02	1.83	2.15	1.92	0.35	18.2
TiO_2	3.01	3.07	2.97	2.98	2.96	3.12	3.02	0.06	2.1	3.05	3.35	3.33	3.22	3.32	3.25	0.12	3.8
MnO	0.25	0.20	0.22	0.21	0.20	0.21	0.22	0.02	8.7	0.26	0.22	0.22	0.21	0.22	0.23	0.02	8.6
P_2O_5	0.94	0.93	0.96	0.97	0.97	0.94	0.95	0.02	1.8	1.29	1.31	1.27	1.25	1.25	1.27	0.03	2.0
Total	99.54	99.66	99.43	99.46	99.47	99.47	99.50	0.08	0.1	99.82	100.34	100.13	100.20	100.11	100.12	0.19	0.2
Mg'	0.77	0.81	0.75	0.76	0.76	0.77	0.77	0.02	2.9	0.71	0.80	0.81	0.84	0.79	0.79	0.05	5.9
Nat. Fe_2O_3/FeO	1.21	1.88	0.93	0.92	0.98	1.09	1.17	0.36	31.3	1.20	3.09	3.38	3.82	2.80	2.86	1.00	35.0
H_2O^-	0.43	0.38	0.51	0.50	0.38	0.51	0.45	0.06	14.0	0.93	1.89	1.37	1.50	1.20	1.38	0.36	25.9
LOI	2.21	2.11	2.10	2.22	2.21	2.68	2.26	0.21	9.5	2.74	3.65	2.65	3.02	2.61	2.93	0.43	14.7
Trace elements (ppm)																	
Nb	128	125	129	130	125	125	127	2	1.8	168	175	177	168	178	173	5	2.8
Zr	430	421	431	432	427	430	429	4	0.9	539	557	550	532	543	544	10	1.8
Y	49	47	49	48	49	51	49	1	2.7	59	62	64	59	62	61	2	3.5
Sr	1076	1069	1081	1086	1078	1097	1081	10	0.9	1534	1491	1446	1428	1407	1461	51	3.5
Rb	63	62	85	59	60	90	70	14	19.8	210	231	344	237	257	256	52	20.4
Zn	112	111	112	105	110	109	110	3	2.4	131	146	147	142	146	142	7	4.7
Cu	68	73	65	71	75	78	72	5	6.6	54	69	68	71	66	66	7	10.3
Ni	211	231	241	226	207	229	224	13	5.7	127	187	153	140	140	149	23	15.4
Cr	178	194	189	188	176	181	184	7	3.8	88	88	96	92	90	91	3	3.7
Ce	130	140	131	141	125	165	139	14	10.3	188	228	205	189	179	198	19	9.8
Nd	45	52	66	63	47	37	52	11	21.5	79	88	102	89	91	90	8	9.2
V	308	308	294	307	315	328	310	11	3.6	312	346	336	338	341	335	13	3.9
La	49	60	45	54	43	55	51	6	12.7	69	63	60	67	62	64	4	5.8
Ba	499	535	493	522	507	594	525	37	7.1	580	765	814	847	635	728	116	15.9
Sc	22	19	19	22	26	27	23	3	15.1	18	22	22	22	23	21	2	9.1
CIPW normative minerals (%)																	
Q																	
Or	14.83	15.31	15.19	15.42	15.37	15.13	15.21	0.21	1.4	13.30	8.10	12.00	10.87	12.77	11.41	2.06	18.1
Ab	6.55	6.97	6.20	5.77	6.51	4.58	6.10	0.84	13.8	2.45	17.25	9.54	9.79	8.90	9.59	5.25	54.7
An	11.20	10.62	10.49	11.31	10.78	10.96	10.89	0.32	3.0	8.23	19.13	12.07	16.17	11.37	13.39	4.28	31.9
Ne	13.59	14.06	14.47	13.88	13.89	14.98	14.15	0.50	3.5	18.66	3.54	12.62	9.09	13.24	11.43	5.58	48.8
Di	24.46	23.41	23.80	22.02	23.27	24.82	23.63	0.99	4.2	30.18	21.83	26.95	23.84	27.24	26.01	3.24	12.5
Hy																	
Ol	17.40	17.61	17.94	19.64	18.29	17.40	18.05	0.85	4.7	13.87	17.34	14.31	17.83	12.74	15.22	2.24	14.7
Mt	3.97	3.96	3.96	3.97	3.94	3.94	3.96	0.01	0.3	4.48	3.38	3.17	3.32	4.49	3.77	0.66	17.5
Il	5.77	5.89	5.70	5.71	5.68	5.98	5.79	0.12	2.1	5.83	6.40	6.36	6.15	6.34	6.22	0.24	3.8
Ap	2.20	2.18	2.25	2.27	2.27	2.20	2.23	0.04	1.8	3.01	3.06	2.96	2.92	2.92	2.97	0.06	2.0
Total	99.97	100.01	100.00	99.99	100.00	99.99	99.99	0.01	0.0	100.01	100.03	99.98	99.98	100.01	100.00	0.02	0.0

Appendix 3-1 Chemical composition of olivine in basalt samples.

Locality	CHIANG KHONG, CK																												
Occurrence	Phenocryst						Groundmass																						
Analysis No	CK13-OL1	CK14-OL2	CK15-OL1	CK18-OL1	CK17-OL1	CK29-OL3	CK13-OL5	CK13-OL6	CK13-OL8	CK13-OL10	CK14-OL3	CK15-OL2	CK15-OL4	CK15-OL5	CK16-OL5	CK16-OL6	CK16-OL7	CK16-OL8	CK17-OL2	CK18-OL2	CK18-OL3	CK29-OL1	CK29-OL2	CK29-OL4	CK29-OL6	CK29B-OL1	CK29B-OL4	CK315-OL1	CK315B-L1	CK315B-L2
SiO_2	39.49	40.00	39.01	38.83	38.60	37.82	38.57	38.76	39.23	39.13	40.23	39.88	38.55	39.20	38.73	39.49	38.69	39.66	39.02	38.65	39.24	37.55	37.71	37.89	37.79	37.39	37.54	38.28	37.76	38.04
TiO_2																							0.19						0.24	
Al_2O_3																						0.40		0.44	0.55				0.31	
FeO	16.10	15.97	17.78	22.00	20.84	22.43	22.42	22.51	19.92	18.16	16.22	15.93	21.71	16.63	21.28	18.44	22.99	18.71	19.73	22.97	20.09	24.47	24.31	23.88	24.58	24.43	24.67	21.34	24.51	24.12
MnO		0.21	0.38	0.48	0.48	0.32	0.39	0.50	0.24	0.26			0.29	0.23	0.29	0.20	0.29	0.33	0.27	0.50	0.37	0.44	0.62	0.54	0.38	0.54	0.46	0.38	0.54	0.49
MgO	43.59	43.60	41.75	38.76	39.16	37.36	38.23	37.91	40.08	41.60	43.41	44.09	38.71	42.65	39.21	41.89	38.19	41.77	40.76	37.62	40.66	35.42	35.59	35.52	36.08	35.99	36.29	39.51	35.73	36.03
CaO	0.38	0.31	0.27	0.41	0.32	0.39	0.26	0.38	0.25	0.34	0.30	0.31	0.31	0.37	0.33	0.34	0.40	0.32	0.29	0.40	0.33	0.62	0.54	0.53	0.56	0.42	0.41	0.20	0.53	0.44
Na_2O						0.56																		0.44	0.53	0.44	0.60	0.45	0.63	
NiO												0.29																		
Cr_2O_3																														
Total	99.56	100.10	99.19	100.47	99.40	99.13	99.87	100.06	99.73	99.49	100.16	100.50	99.57	99.08	99.83	100.36	100.56	100.79	100.07	100.15	100.68	99.32	99.29	99.82	100.76	99.21	100 22	100.36	100.94	99.39
Numbers of ions on the basis of 4 O																														
Si	1.001	1.007	1.002	1.004	1.004	0.996	1.005	1.009	1.010	1.003	1.012	1.001	1.004	1.002	1.004	1.004	1.004	1.005	1.001	1.008	1.003	0.995	1.001	0.997	0.988	0.996	0.989	0.990	0.985	1.005
Ti	0	0	0	0	0	0	0	0	0	0	0	0	0	0	0	0	0	0	0	0	0	0	0.004	0	0	0	0	0	0.005	0
Al	0	0	0	0	0	0	0	0	0	0	0	0	0	0	0	0	0	0	0	0	0	0.012	0	0.014	0.017	0	0	0	0.009	0
Fe^{2+}	0.341	0.336	0.382	0.476	0.453	0.494	0.489	0.490	0.429	0.389	0.341	0.334	0.473	0.355	0.461	0.392	0.499	0.396	0.424	0.501	0.429	0.542	0.539	0.526	0.538	0.544	0.544	0.461	0.535	0.533
Mn	0.000	0.004	0.008	0.010	0.011	0.007	0.009	0.011	0.005	0.006	0.000	0.000	0.006	0.005	0.006	0.004	0.006	0.007	0.006	0.011	0.008	0.010	0.014	0.012	0.008	0.012	0.010	0.008	0.012	0.011
Mg	1.647	1.637	1.599	1.494	1.519	1.467	1.485	1.471	1.539	1.590	1.627	1.650	1.503	1.625	1.515	1.587	1.477	1.578	1.560	1.462	1.549	1.399	1.408	1.394	1.407	1.429	1.426	1.523	1.390	1.419
Ca	0.010	0.008	0.008	0.011	0.009	0.011	0.007	0.011	0.007	0.009	0.008	0.008	0.009	0.010	0.009	0.009	0.011	0.009	0.008	0.011	0.009	0.018	0.015	0.015	0.016	0.012	0.011	0.005	0.015	0.012
Na	0	0	0	0	0	0.029	0	0	0	0	0	0	0	0	0	0	0	0	0	0	0	0	0	0.022	0.027	0.023	0.031	0.022	0.032	0
Ni	0	0	0	0	0	0	0	0	0	0	0	0.006	0	0	0	0	0	0	0	0	0	0	0	0	0	0	0	0	0	0
Cr	0	0	0	0	0	0	0	0	0	0	0	0	0	0	0	0	0	0	0	0	0	0	0	0	0	0	0	0	0	0
Total	2.999	2.993	2.998	2.996	2.996	3.010	2.995	2.991	2.990	2.997	2.988	2.999	2.996	2.998	2.996	2.996	2.996	2.995	2.999	2.992	2.997	2.985	2.990	2.994	3.007	3.016	3.017	3.015	2.998	2.986
Fo% (Mgx100/ ($Mg+Fe^{2+}$))	82.8	83.0	80.7	75.9	77.0	74.8	75.2	75.0	78.2	80.3	82.7	83.1	76.1	82.1	76.7	80.2	74.8	79.9	78.6	74.5	78.3	72.1	72.3	72.6	72.4	72.4	72.4	76.7	72.2	72.7

Appendix 3-1 (Continued).

Locality	CHIANG KHONG, CK																	BAN NONG, NAM CHO, BN												
Occurrence	Groundmass																	Phenocryst												
Analysis No	CK315B-L4	CK315C-L1	CK315C-L2	CK315C-L3	CK519A-L5	CK519A-L8	CK519A-L9	CK519A-L10	CK519A-OL13	CK519A-OL14	CK519A-OL16	CK519A-OL17	CK519A-OL20	CK519A-OL23	CK519B-OL1	CK519B-OL3	CK519B-OL4	BN132-OL20	BN132-OL21	BN132-OL22	BN134-O15	BN134-O17	BN134-O5	BN134-O6	BN134-O7	BN135-O16	BN135-O17	BN135-O18	BN135-O19	BN135-O20
SiO_2	38.30	38.36	37.50	37.66	39.00	39.37	38.94	37.50	38.68	39.12	38.45	37.68	38.41	38.38	37.95	37.75	38.32	40.52	40.31	38.81	38.61	38.39	39.19	38.90	38.14	39.44	38.99	41.13	40.43	41.07
TiO_2	0.17														0.21															
Al_2O_3		0.35	0.25				0.44	0.41		0.39		0.29	0.34	0.33	0.32															
FeO	24.42	22.28	24.02	24.26	18.08	16.76	17.87	26.95	19.04	19.14	21.14	23.59	22.18	23.59	24.01	24.10	22.09	12.38	15.31	20.21	22.41	24.45	18.90	18.33	22.98	20.08	20.71	10.38	13.51	10.89
MnO	0.55	0.58	0.44	0.68	0.29		0.27	0.49			0.40	0.33	0.22	0.37	0.53	0.40	0.24	0.24	0.35	0.41	0.43	0.65	0.20	0.29	0.44	0.28	0.40		0.22	
MgO	36.12	38.09	36.35	36.28	42.11	43.08	42.37	34.35	40.58	41.22	39.31	36.66	38.52	37.01	36.23	36.38	38.92	46.56	44.51	39.67	38.22	36.25	41.59	41.34	37.66	40.39	40.04	48.36	46.22	48.44
CaO	0.49	0.33	0.49	0.51	0.20	0.23	0.30	0.51	0.23	0.26	0.27	0.42	0.40	0.36	0.57	0.56	0.33		0.13	0.14	0.30	0.32	0.25	0.26	0.26	0.12	0.18			
Na_2O	0.47	0.49	0.39	0.31				0.38	0.42	0.41	0.33	0.40			0.46	0.51	0.51		0.25											
NiO																										0.07		0.40		0.40
Cr_2O_3																														
Total	100.52	100.74	99.67	99.71	99.89	99.69	100.46	100.81	99.23	100.83	100.20	99.74	100.32	100.38	100.63	99.70	100.61	99.70	100.87	99.23	99.97	100.07	100.12	99.12	99.47	100.37	100.32	100.27	100.37	100.81
Numbers of ions on the basis of 4 O																														
Si	1.004	0.992	0.990	0.997	0.995	0.998	0.986	0.992	0.998	0.992	0.994	0.991	0.994	0.999	0.992	0.998	0.991	1.007	1.005	1.007	1.005	1.009	1.001	1.002	1.002	1.009	1.003	1.007	1.003	1.003
Ti	0.0033	0	0	0	0	0	0	0	0	0	0	0	0	0	0.0042	0	0	0	0	0	0	0	0	0	0	0	0	0	0	0	0
Al	0	0.0107	0.0077	0	0	0	0.0130	0.0127	0	0.0117	0	0.0091	0.0105	0.0102	0.0100	0	0	0	0	0	0	0	0	0	0	0	0	0	0	0	0
Fe^{2+}	0.535	0.482	0.530	0.537	0.386	0.355	0.378	0.596	0.411	0.406	0.457	0.519	0.480	0.513	0.525	0.533	0.478	0.257	0.319	0.439	0.488	0.537	0.404	0.395	0.505	0.430	0.445	0.213	0.280	0.222
Mn	0.012	0.013	0.010	0.015	0.006	0.000	0.006	0.011	0.000	0.000	0.009	0.007	0.005	0.008	0.012	0.009	0.005	0.005	0.007	0.009	0.010	0.015	0.004	0.005	0.010	0.006	0.009	0.000	0.005	0.000
Mg	1.412	1.469	1.431	1.432	1.602	1.629	1.600	1.354	1.561	1.559	1.515	1.437	1.486	1.436	1.411	1.434	1.501	1.724	1.654	1.535	1.484	1.420	1.584	1.588	1.475	1.541	1.535	1.765	1.709	1.764
Ca	0.014	0.009	0.014	0.015	0.005	0.006	0.008	0.015	0.006	0.007	0.008	0.012	0.011	0.010	0.016	0.016	0.009	0	0.003	0.004	0.008	0.009	0.007	0.007	0.007	0.003	0.005	0.000	0.000	0.000
Na	0.0241	0.0244	0.0201	0.0160	0	0	0	0.0193	0.0209	0.0202	0.0165	0.0203	0	0	0.0235	0.0259	0.0256	0	0.012	0	0	0	0	0	0	0	0	0	0	0
Ni	0	0	0	0	0	0	0	0	0	0	0	0	0	0	0	0	0	0	0	0	0	0	0	0	0	0.001	0	0.008	0	0.008
Cr	0	0	0	0	0	0	0	0	0	0	0	0	0	0	0	0	0	0	0	0	0	0	0	0	0	0	0	0	0	0
Total	3.005	3.006	3.008	3.011	2.998	2.994	2.998	3.004	3.003	3.002	3.005	3.003	2.992	2.985	3.000	3.015	3.014	2.993	3.001	2.993	2.995	2.991	2.999	2.998	2.998	2.991	2.997	2.993	2.997	2.997
Fo% (Mgx100/ (Mg+Fe^{2+}))	72.5	75.3	73.0	72.7	80.6	82.1	80.9	69.4	79.2	79.3	76.8	73.5	75.6	73.7	72.9	72.9	75.9	87.0	83.8	77.8	75.3	72.5	79.7	80.1	74.5	78.2	77.5	89.3	85.9	88.8

Appendix 3-1 Chemical composition of olivine in basalt samples.

Appendix 3-1 (Continued).

Locality	BAN NONG, NAM CHO, BN																												
Occurrence	Phenocryst												Microphenocryst												Groundmass				
Analysis No	BN135-O21	BN323-OL4	BN323-OL5	BN325-OL1	BN326-OL1	BN326-OL5	BN326-OL6	BN329-OL1	BN329-OL2	BN330-OL1	BN330-OL2	BN446-OL3	BN139-OL1	BN323-OL6	BN326-OL3	BN326-OL4	BN328-OL1	BN328-OL2	BN328-OL3	BN328-OL4	BN329-OL3	BN329-OL4	BN330-OL3	BN330-OL4	BN330-OL5	BN133-OL1	BN133-OL5	BN133-OL7	BN133-OL8	BN133-OL9
SiO_2	39.19	40.17	41.08	41.19	39.87	39.62	40.33	40.90	39.76	39.70	39.62	38.25	37.83	40.23	39.52	39.90	39.87	39.57	39.00	39.45	39.82	39.24	38.88	39.29	39.39	37.88	37.48	37.50	37.32	37.69
TiO_2																												0.18		
Al_2O_3												0.33														0.47	0.41	0.36	0.40	0.26
FeO	20.13	12.23	9.11	8.91	16.45	16.34	12.90	10.26	15.81	17.62	16.08	24.27	24.67	15.92	15.46	16.63	15.23	16.89	19.32	17.66	15.56	18.78	18.36	19.10	18.53	25.24	25.98	25.47	25.19	25.30
MnO	0.36				0.23	0.27	0.27	0.24	0.26		0.24	0.64	0.53	0.26	0.38	0.28		0.30	0.24			0.38	0.30	0.24	0.21	0.68	0.70	0.75	0.70	0.62
MgO	40.55	46.35	48.58	49.78	43.02	43.03	45.88	48.42	43.67	42.05	43.87	36.64	36.19	43.79	43.61	43.02	43.96	42.87	40.06	41.81	44.12	40.89	41.22	40.83	41.16	35.24	34.66	35.34	35.03	35.30
CaO		0.24	0.14	0.11	0.24	0.24	0.21	0.10	0.23	0.35	0.34	0.31	0.28	0.33	0.28	0.20	0.20	0.24	0.39	0.26	0.34	0.38	0.31	0.34	0.32	0.51	0.47	0.54	0.57	0.30
Na_2O												0.55														0.43	0.68	0.60		0.36
NiO		0.30	0.47	0.34				0.64																						
Cr_2O_3																														
Total	100.23	99.29	99.37	100.31	99.80	99.50	99.58	100.57	99.72	99.72	100.15	100.98	99.50	100.53	99.25	100.02	99.25	99.86	99.01	99.18	99.84	99.67	99.07	99.81	99.62	100.68	100.38	100.72	99.21	100.02
Numbers of ions on the basis of 4 O																														
Si	1.005	1.003	1.010	1.002	1.009	1.006	1.006	1.001	1.005	1.010	0.999	0.997	1.002	1.008	1.003	1.008	1.008	1.004	1.010	1.010	1.003	1.007	1.002	1.007	1.009	0.995	0.994	0.989	0.996	0.997
Ti	0	0	0	0	0	0	0	0	0	0	0	0	0	0	0	0	0	0	0	0	0	0	0	0	0	0	0	0.003	0	0
Al	0	0	0	0	0	0	0	0	0	0	0	0.010	0	0	0	0	0	0	0	0	0	0	0	0	0	0.014	0.013	0.011	0.013	0.008
Fe^{2+}	0.432	0.255	0.187	0.181	0.348	0.347	0.269	0.210	0.334	0.375	0.339	0.529	0.547	0.334	0.328	0.351	0.322	0.358	0.418	0.378	0.328	0.403	0.396	0.410	0.397	0.554	0.576	0.562	0.562	0.560
Mn	0.008	0.000	0.000	0.000	0.005	0.006	0.006	0.005	0.005	0.000	0.005	0.014	0.012	0.005	0.008	0.006	0.000	0.006	0.005	0.000	0.000	0.008	0.007	0.005	0.005	0.015	0.016	0.017	0.016	0.014
Mg	1.550	1.726	1.780	1.805	1.623	1.629	1.707	1.767	1.645	1.595	1.649	1.424	1.429	1.636	1.650	1.621	1.657	1.621	1.546	1.595	1.657	1.564	1.584	1.561	1.572	1.380	1.370	1.390	1.394	1.392
Ca	0.000	0.006	0.004	0.003	0.007	0.007	0.006	0.003	0.008	0.009	0.009	0.009	0.008	0.009	0.007	0.005	0.005	0.006	0.011	0.007	0.009	0.011	0.008	0.009	0.009	0.014	0.013	0.015	0.016	0.009
Na	0	0	0	0	0	0	0	0	0	0	0	0.028	0	0	0	0	0	0	0	0	0	0	0	0	0	0.022	0.035	0.030	0	0.019
Ni	0	0.006	0.009	0.007	0	0	0	0.013	0	0	0	0	0	0	0	0	0	0	0	0	0	0	0	0	0	0	0	0	0	0
Cr	0	0	0	0	0	0	0	0	0	0	0	0	0	0	0	0	0	0	0	0	0	0	0	0	0	0	0	0	0	0
Total	2.995	2.997	2.990	2.998	2.991	2.994	2.994	2.999	2.995	2.990	3.001	3.011	2.998	2.992	2.997	2.992	2.992	2.996	2.990	2.990	2.997	2.993	2.998	2.993	2.991	3.000	3.017	3.017	2.997	3.002
Fo% (Mgx100/ (Mg+Fe^{2+}))	78.2	87.1	90.5	90.9	82.3	82.4	86.4	89.4	83.1	81.0	83.0	72.9	72.3	83.1	83.4	82.2	83.7	81.9	78.7	80.8	83.5	79.5	80.0	79.2	79.8	71.3	70.4	71.2	71.3	71.3

Appendix 3-1 (Continued).

Locality	BAN NONG, NAM CHO																			SOP PRAP, SP										
Occurrence	Groundmass																			Phenocryst										
Analysis No	BN133-L10	BN133-L13	BN133-L15	BN134-OL9	BN134-O19	BN134-O20	BN134-O21	BN134-O22	BN134-O24	BN135-O22	BN135-O23	BN135-O24	BN135-O25	BN135-O26	BN135-O27	BN139-OL2	BN139-OL4	BN139-OL6	BN139-OL8	SP154-OL2	SP154-OL3	SP154-OL4	SP154-OL5	SP154-OL6	SP155-OL1	SP155-OL3	SP155-OL4	SP155-OL6	SP155-OL7	SP155-OL8
SiO_2	37.94	37.32	37.78	38.42	37.66	38.18	38.02	37.42	37.67	37.72	38.12	37.82	38.67	38.06	38.08	37.50	37.43	37.64	37.73	39.74	39.34	39.88	40.00	39.74	39.86	39.68	39.45	39.89	39.89	39.59
TiO_2		0.19																												
Al_2O_3	0.52	0.31	0.28																											
FeO	25.47	25.62	25.63	24.40	25.93	26.09	25.41	25.49	25.79	26.17	25.81	25.66	24.98	25.66	25.89	25.72	26.42	26.69	25.84	16.10	16.90	16.03	15.98	17.17	17.12	17.35	17.16	17.14	17.41	17.33
MnO	0.64	0.63	0.56	0.52	0.54	0.58	0.72	0.60	0.58	0.49	0.47	0.69	0.39	0.62	0.54	0.86	0.73	0.71	0.65	0.27	0.24		0.35	0.26	0.32	0.35	0.38	0.26	0.24	0.35
MgO	35.30	34.98	35.45	36.97	34.87	35.05	34.87	35.08	35.06	35.36	35.03	35.12	36.57	34.56	35.12	34.91	34.66	34.68	34.65	43.02	42.64	43.18	43.07	42.73	42.58	42.98	42.50	42.43	42.32	42.54
CaO	0.50	0.44	0.34	0.32	0.39	0.52	0.42	0.45	0.50	0.52	0.55	0.47	0.25	0.54	0.51	0.53	0.46	0.57	0.53	0.25	0.25	0.25	0.18	0.29	0.28	0.24	0.30	0.27	0.32	0.26
Na_2O			0.59	0.33																										
NiO																								0.38						
Cr_2O_3																														
Total	100.63	99.49	100.89	100.96	99.39	100.41	99.43	99.04	99.60	100.26	99.98	99.76	100.85	99.44	100.14	99.52	99.71	100.28	99.42	99.38	99.37	99.34	99.59	100.56	100.17	100.60	99.80	99.98	100.16	100.06
Numbers of ions on the basis of 4 O																														
Si	0.996	0.995	0.992	1.001	1.005	1.008	1.012	1.002	1.003	0.999	1.010	1.005	1.009	1.014	1.008	1.001	1.000	1.000	1.007	1.009	1.003	1.011	1.012	1.004	1.008	1.001	1.003	1.011	1.010	1.004
Ti	0	0.004	0	0	0	0	0	0	0	0	0	0	0	0	0	0	0	0	0	0	0	0	0	0	0	0	0	0	0	0
Al	0.016	0.010	0.009	0	0	0	0	0	0	0	0	0	0	0	0	0	0	0	0	0	0	0	0	0	0	0	0	0	0	0
Fe^{2+}	0.559	0.571	0.563	0.532	0.579	0.576	0.565	0.570	0.574	0.580	0.572	0.570	0.545	0.571	0.573	0.574	0.590	0.593	0.577	0.342	0.360	0.340	0.338	0.363	0.362	0.366	0.365	0.363	0.369	0.368
Mn	0.014	0.014	0.012	0.012	0.012	0.013	0.016	0.014	0.013	0.011	0.010	0.015	0.009	0.014	0.012	0.019	0.017	0.016	0.015	0.006	0.005	0	0.008	0.005	0.007	0.007	0.008	0.006	0.005	0.007
Mg	1.381	1.390	1.388	1.437	1.388	1.380	1.383	1.400	1.392	1.396	1.383	1.391	1.422	1.372	1.385	1.389	1.380	1.374	1.379	1.628	1.621	1.632	1.625	1.609	1.606	1.617	1.612	1.603	1.598	1.609
Ca	0.014	0.013	0.010	0.009	0.011	0.015	0.012	0.013	0.014	0.015	0.016	0.013	0.007	0.016	0.014	0.015	0.013	0.016	0.015	0.007	0.007	0.007	0.005	0.008	0.008	0.007	0.008	0.007	0.009	0.007
Na	0	0	0.030	0.017	0	0	0	0	0	0	0	0	0	0	0	0	0	0	0	0	0	0	0	0	0	0	0	0	0	0
Ni	0	0	0	0	0	0	0	0	0	0	0	0	0	0	0	0	0	0	0	0	0	0	0	0.008	0	0	0	0	0	0
Cr	0	0	0	0	0	0	0	0	0	0	0	0	0	0	0	0	0	0	0	0	0	0	0	0	0	0	0	0	0	0
Total	2.987	2.996	3.009	3.007	2.995	2.992	2.988	2.998	2.997	3.001	2.990	2.995	2.991	2.986	2.992	2.999	3.000	3.000	2.993	2.991	2.997	2.989	2.988	2.996	2.992	2.999	2.997	2.989	2.990	2.996
Fo% (Mgx100/ ($Mg+Fe^{2+}$))	71.2	70.9	71.1	73.0	70.6	70.5	71.0	71.0	70.8	70.7	70.8	70.9	72.3	70.6	70.8	70.8	70.0	69.9	70.5	82.7	81.8	82.8	82.8	81.6	81.6	81.5	81.5	81.5	81.3	81.4

Appendix 3-1 (Continued).

Locality	SOP PRAP, SP																														
Occurrence	Phenocryst																														
Analysis No	SP155-OL9	SP155-OL10	SP155-OL11	SP155-OL12	SP155-OL13	SP155-OL14	SP155-OL15	SP155-OL16	SP155-OL17	SP155-OL18	SP155-OL19	SP155-OL20	SP155-OL21	SP155-OL22	SP155-OL23	SP155-OL31	SP155-OL32	SP155-OL33	SP155-OL34	SP155-OL35	SP155-OL36	SP155-OL37	SP155-OL38	SP155-OL40	SP155-OL42	SP155-OL43	SP155-OL44	SP155-OL45	SP161-OL3	SP161-OL4
SiO_2	39.82	39.36	39.57	39.42	39.55	39.75	39.54	39.47	39.36	39.86	39.37	39.67	39.76	39.75	39.51	40.12	39.52	39.61	39.87	39.96	39.68	39.89	39.31	39.64	39.63	39.68	39.51	39.77	39.80	39.93
TiO_2																														
Al_2O_3																														
FeO	17.43	17.36	17.88	17.18	16.94	17.09	17.05	17.06	16.97	17.39	16.59	16.63	17.32	17.29	17.44	15.71	15.44	15.96	16.01	15.18	17.45	16.02	16.04	16.84	16.13	15.89	16.03	17.22	16.00	15.68
MnO	0.28	0.34	0.32	0.39	0.20	0.20	0.21	0.35	0.25	0.21	0.31	0.39	0.32	0.30	0.33	0.26	0.22	0.24	0.27	0.27	0.25	0.24	0.27	0.30	0.27	0.35	0.24	0.29		
MgO	42.68	42.53	41.75	42.34	42.55	43.04	42.42	42.44	42.37	42.51	42.67	42.71	42.02	42.13	41.99	43.51	43.66	43.34	43.70	44.14	42.21	43.60	42.90	43.10	42.76	43.07	43.10	41.52	43.50	43.49
CaO	0.34	0.31	0.24	0.36	0.20	0.23	0.24	0.26	0.26	0.23	0.24	0.25	0.32	0.26	0.34	0.20	0.26	0.27	0.25	0.30	0.45	0.26	0.29	0.21	0.32	0.22	0.35	0.29	0.27	0.24
Na_2O																														
NiO						0.38							0.32					0.36												
Cr_2O_3																														
Total	100.55	99.90	99.76	99.68	99.43	100.69	99.47	99.59	99.20	100.19	99.17	99.64	100.05	99.73	99.61	99.79	99.09	99.78	100.11	99.85	100.03	100.01	98.81	100.08	99.10	99.20	99.23	99.08	99.57	99.33
Numbers of ions on the basis of 4 O																														
Si	1.005	1.001	1.009	1.004	1.007	1.002	1.007	1.005	1.006	1.009	1.005	1.007	1.010	1.011	1.008	1.011	1.004	1.003	1.004	1.006	1.007	1.006	1.005	1.003	1.009	1.009	1.005	1.017	1.007	1.011
Ti	0	0	0	0	0	0	0	0	0	0	0	0	0	0	0	0	0	0	0	0	0	0	0	0	0	0	0	0	0	0
Al	0	0	0	0	0	0	0	0	0	0	0	0	0	0	0	0	0	0	0	0	0	0	0	0	0	0	0	0	0	0
Fe^{2+}	0.368	0.369	0.381	0.366	0.361	0.360	0.363	0.363	0.362	0.368	0.354	0.353	0.368	0.368	0.372	0.331	0.328	0.338	0.337	0.319	0.370	0.338	0.343	0.356	0.344	0.338	0.341	0.368	0.338	0.332
Mn	0.006	0.007	0.007	0.008	0.004	0.004	0.005	0.008	0.005	0.005	0.007	0.008	0.007	0.006	0.007	0.005	0.005	0.005	0.006	0.006	0.005	0.005	0.006	0.006	0.006	0.008	0.005	0.006	0	0
Mg	1.606	1.613	1.587	1.608	1.616	1.617	1.611	1.612	1.614	1.604	1.623	1.617	1.591	1.597	1.596	1.635	1.653	1.636	1.641	1.656	1.597	1.639	1.634	1.626	1.623	1.632	1.635	1.583	1.640	1.641
Ca	0.009	0.008	0.007	0.010	0.005	0.006	0.007	0.007	0.007	0.006	0.006	0.007	0.009	0.007	0.009	0.005	0.007	0.007	0.007	0.008	0.012	0.007	0.008	0.006	0.009	0.006	0.010	0.008	0.007	0.006
Na	0	0	0	0	0	0	0	0	0	0	0	0	0	0	0	0	0	0	0	0	0	0	0	0	0	0	0	0	0	0
Ni	0	0	0	0	0	0.008	0	0	0	0	0	0	0.006	0	0	0	0	0.007	0	0	0	0	0	0	0	0	0	0	0	0
Cr	0	0	0	0	0	0	0	0	0	0	0	0	0	0	0	0	0	0	0	0	0	0	0	0	0	0	0	0	0	0
Total	2.995	2.999	2.991	2.996	2.993	2.998	2.993	2.995	2.994	2.991	2.995	2.993	2.990	2.989	2.992	2.989	2.996	2.997	2.996	2.994	2.993	2.994	2.995	2.997	2.991	2.991	2.995	2.983	2.993	2.989
Fo% (Mgx100/ ($Mg+Fe^{2+}$))	81.4	81.4	80.6	81.5	81.8	81.8	81.6	81.6	81.7	81.3	82.1	82.1	81.2	81.3	81.1	83.2	83.4	82.9	83.0	83.8	81.2	82.9	82.7	82.0	82.5	82.9	82.7	81.1	82.9	83.2

Appendix 3-1 (Continued).

Locality	SOP PRAP, SP																DEN CHAI, DC													
Occrurrence	Phenocryst								Groundmass								Phenocryst													
Analysi No	SP161-OL5	SP161-OL7	SP161-OL8	SP161-OL9	SP161-OL11	SP161-OL12	SP161-OL13	SP161-OL14	SP155-OL61	SP155-OL67	SP155-OL68	SP155-OL69	SP156-OL39	SP161-OL1	SP161-OL2	SP161-OL10	DC162-OL1	DC162-OL2	DC162-OL3	DC162-OL4	DC162-OL5	DC162-OL6	DC162-OL7	DC162-OL9	DC162-L13	DC162-L14	DC162-L18	DC263-OL1	DC263-OL2	DC263-OL3
SiO_2	39.57	40.12	39.28	39.54	39.88	39.52	40.10	39.74	39.64	39.15	39.40	38.85	39.67	39.72	39.58	39.62	40.00	40.35	40.62	40.67	40.24	40.20	39.76	39.99	41.18	41.16	39.23	40.11	40.82	38.95
TiO_2																														
Al_2O_3																														
FeO	16.30	16.23	17.59	17.15	17.01	16.15	15.13	15.58	16.81	18.44	17.58	19.06	16.72	16.70	16.86	16.95	15.47	14.88	14.43	15.20	14.33	14.30	17.70	14.73	10.28	10.29	20.63	14.53	10.50	19.45
MnO	0.25	0.24	0.20	0.33	0.32	0.28		0.21	0.24	0.36	0.35	0.38	0.25	0.36	0.48	0.43	0.30				0.19	0.19	0.27	0.25	0.23		0.20	0.24		0.25
MgO	43.00	43.21	41.86	42.33	42.19	43.45	43.92	43.56	42.74	41.44	41.80	40.94	42.49	42.30	42.98	42.08	44.12	44.80	45.63	44.86	45.08	44.88	42.59	44.63	48.79	48.61	40.35	45.08	47.90	40.29
CaO	0.33	0.24	0.31	0.31	0.35	0.23	0.15	0.22	0.28	0.29	0.35	0.38	0.25	0.29	0.28	0.34	0.19	0.29	0.22	0.24	0.25	0.26	0.23	0.22		0.15	0.29	0.25		0.29
Na_2O									0.32	0.46	0.32	0.44																		
NiO								0.39									0.31	0.46					0.40			0.45		0.32		
Cr_2O_3																														
Total	99.44	100.04	99.24	99.67	99.75	99.63	99.30	99.70	100.02	100.14	99.80	100.06	99.38	99.38	100.17	99.41	100.39	100.78	100.90	100.96	100.09	99.83	100.95	99.82	100.47	100.66	100.70	100.51	99.22	99.24
Numbers of ions on the basis of 4 O																														
Si	1.005	1.011	1.006	1.007	1.013	1.002	1.012	1.005	1.004	1.000	1.005	0.997	1.010	1.011	1.002	1.010	1.004	1.005	1.006	1.009	1.005	1.007	1.003	1.004	1.005	1.004	1.004	1.001	1.009	1.007
Ti	0	0	0	0	0	0	0	0	0	0	0	0	0	0	0	0	0	0	0	0	0	0	0	0	0	0	0	0	0	0
Al	0	0	0	0	0	0	0	0	0	0	0	0	0	0	0	0	0	0	0	0	0	0	0	0	0	0	0	0	0	0
Fe^{2+}	0.346	0.342	0.377	0.365	0.361	0.342	0.319	0.329	0.356	0.394	0.375	0.409	0.356	0.356	0.357	0.361	0.325	0.310	0.299	0.315	0.299	0.300	0.373	0.309	0.210	0.210	0.441	0.303	0.217	0.420
Mn	0.005	0.005	0.004	0.007	0.007	0.006	0	0.005	0.005	0.008	0.008	0.008	0.005	0.008	0.010	0.009	0.006	0.000	0.000	0.000	0.004	0.004	0.006	0.005	0.005	0.000	0.004	0.005	0.000	0.006
Mg	1.629	1.624	1.598	1.606	1.597	1.642	1.653	1.642	1.614	1.578	1.590	1.567	1.612	1.606	1.622	1.600	1.650	1.663	1.684	1.660	1.679	1.676	1.601	1.671	1.775	1.768	1.539	1.677	1.765	1.552
Ca	0.009	0.007	0.008	0.009	0.010	0.006	0.004	0.006	0.008	0.008	0.009	0.011	0.007	0.008	0.008	0.009	0.005	0.008	0.006	0.006	0.007	0.007	0.006	0.006	0.000	0.004	0.008	0.007	0.000	0.008
Na	0	0	0	0	0	0	0	0	0.016	0.023	0.016	0.022	0	0	0	0	0	0	0	0	0	0	0	0	0	0	0	0	0	0
Ni	0	0	0	0	0	0	0	0.008	0	0	0	0	0	0	0	0	0.006	0.009	0	0	0	0	0.008	0	0	0.009	0	0.006	0	0
Cr	0	0	0	0	0	0	0	0	0	0	0	0	0	0	0	0	0	0	0	0	0	0	0	0	0	0	0	0	0	0
Total	2.995	2.989	2.994	2.993	2.987	2.998	2.988	2.995	3.003	3.011	3.003	3.014	2.990	2.989	2.998	2.990	2.996	2.995	2.994	2.991	2.995	2.993	2.997	2.996	2.995	2.996	2.996	2.999	2.991	2.993
Fo% (Mgx100/ ($Mg+Fe^{2+}$))	82.5	82.6	80.9	81.5	81.6	82.7	83.8	83.3	81.9	80.0	80.9	79.3	81.9	81.9	82.0	81.6	83.6	84.3	84.9	84.0	84.9	84.8	81.1	84.4	89.4	89.4	77.7	84.7	89.0	78.7

Appendix 3-1 (Continued).

Locality	DEN CHAI, DC																		KHOK SAMRAN, KS										
Occurrence	Phenocryst					Microphenocryst								Groundmass						Phenocryst									
Analysis No	DC263-OL4	DC263-OL5	DC271-OL10	DC271-OL11	DC271-OL12	DC161-OL15	DC161-OL16	DC264-OL1	DC264-OL2	DC264-OL3	DC264-OL4	DC264-OL5	DC264-OL6	DC1K-OL1	DC157-OL4	DC157-OL5	DC3-OL8	DC3-OL10	DC376A-OL2	KS110-O1	KS110-O2	KS110-O3	KS110-O4	KS110-O5	KS110-O6	KS110-O7	KS110-O8	KS110-O9	KS110-O10	KS110-O11
SiO_2	38.40	41.04	40.16	39.01	39.16	38.83	41.12	40.33	39.18	39.66	40.42	41.26	38.61	37.90	38.94	38.83	39.38	38.27	37.73	39.20	39.09	38.85	39.06	38.88	39.16	39.06	39.13	39.48	39.16	39.24
TiO_2																			0.18											
Al_2O_3														0.35			0.29	0.33	0.24											
FeO	23.19	10.39	15.03	21.81	20.80	21.82	9.73	14.38	19.97	18.18	14.58	10.99	21.23	22.72	20.60	22.37	17.53	21.54	24.57	19.09	19.18	20.37	20.56	20.02	21.15	20.14	19.90	19.59	19.18	19.63
MnO	0.57		0.27	0.45	0.32	0.48	0.26	0.22	0.37	0.23	0.15		0.32	0.37	0.28	0.30	0.26	0.30	0.60	0.31	0.28		0.32	0.28	0.25	0.34	0.43	0.26		
MgO	37.37	48.32	44.34	39.02	39.86	38.54	48.79	44.60	40.12	42.46	45.17	48.02	39.32	37.46	40.13	38.12	42.48	37.96	35.26	40.96	40.83	40.18	40.36	40.30	39.93	40.26	40.84	40.56	40.75	40.59
CaO	0.36	0.11	0.17	0.41	0.32	0.40	0.10	0.15	0.28	0.22	0.30	0.16	0.31	0.30	0.31	0.41	0.25	0.35	0.40	0.18	0.26	0.27	0.15	0.21	0.24	0.12	0.18	0.22	0.29	0.17
Na_2O														0.64				0.52												
NiO			0.49				0.35					0.33										0.46								
Cr_2O_3																														
Total	99.89	99.87	100.45	100.70	100.45	100.07	100.33	99.68	99.92	100.74	100.62	100.77	99.80	99.74	100.27	100.03	100.19	99.26	99.23	99.74	99.64	100.13	100.45	99.69	100.72	99.92	100.48	100.11	99.38	99.63
Numbers of ions on the basis of 4 O																														
Si	1.005	1.008	1.005	1.005	1.006	1.007	1.005	1.011	1.008	1.002	1.005	1.008	1.002	0.994	1.002	1.009	0.999	1.001	1.001	1.006	1.005	1.001	1.002	1.003	1.004	1.005	1.001	1.011	1.008	1.009
Ti	0	0	0	0	0	0	0	0	0	0	0	0	0	0	0	0	0	0	0.004	0	0	0	0	0	0	0	0	0	0	0
Al	0	0	0	0	0	0	0	0	0	0	0	0	0	0.011	0	0	0.009	0.010	0.008	0	0	0	0	0	0	0	0	0	0	0
Fe^{2+}	0.508	0.213	0.315	0.470	0.447	0.473	0.199	0.301	0.430	0.384	0.303	0.225	0.461	0.498	0.443	0.486	0.372	0.471	0.545	0.410	0.412	0.439	0.441	0.432	0.453	0.434	0.426	0.419	0.413	0.422
Mn	0.013	0.000	0.006	0.010	0.007	0.011	0.005	0.005	0.008	0.005	0.003	0.000	0.007	0.008	0.006	0.007	0.006	0.007	0.013	0.007	0.006	0	0.007	0.006	0.005	0.007	0.009	0.006	0	0
Mg	1.459	1.768	1.655	1.499	1.526	1.490	1.777	1.667	1.539	1.600	1.675	1.749	1.521	1.465	1.539	1.477	1.606	1.481	1.395	1.567	1.565	1.543	1.544	1.550	1.526	1.545	1.558	1.548	1.563	1.556
Ca	0.010	0.003	0.004	0.011	0.009	0.011	0.003	0.004	0.008	0.006	0.008	0.004	0.009	0.008	0.009	0.011	0.007	0.010	0.011	0.005	0.007	0.007	0.004	0.006	0.007	0.003	0.005	0.006	0.008	0.005
Na	0	0	0	0	0	0	0	0	0	0	0	0	0	0.032	0	0	0	0.026	0	0	0	0	0	0	0	0	0	0	0	0
Ni	0	0	0.010	0	0	0	0.007	0	0	0	0	0.007	0	0	0	0	0	0	0	0	0	0.009	0	0	0	0	0	0	0	0
Cr	0	0	0	0	0	0	0	0	0	0	0	0	0	0	0	0	0	0	0	0	0	0	0	0	0	0	0	0	0	0
Total	2.995	2.992	2.995	2.995	2.994	2.993	2.995	2.989	2.992	2.998	2.995	2.992	2.998	3.017	2.998	2.991	2.997	3.007	2.983	2.994	2.995	2.999	2.998	2.997	2.996	2.995	2.999	2.989	2.992	2.991
Fo% (Mgx100/ ($Mg+Fe^{2+}$))	74.2	89.2	84.0	76.1	77.4	75.9	89.9	84.7	78.2	80.6	84.7	88.6	76.8	74.6	77.6	75.2	81.2	75.9	71.9	79.3	79.1	77.9	77.8	78.2	77.1	78.1	78.5	78.7	79.1	78.7

Appendix 3-1 (Continued).

Locality	KHOK SAMRAM, KS																													
Occurrence	Phenocryst														Groundmass															
Analysis No	KS211-OL2	KS211-OL3	KS211-OL4	KS211-OL5	KS211-OL6	KS211-OL7	KS211-OL9	KS211-OL11	KS211-OL12	KS213-OL1	KS214-OL1	KS214-OL2	KS214-OL8	KS214-OL9	KS110-O12	KS110-O14	KS110-O15	KS17-O1	KS17-O2	KS17-O4	KS18-O1	KS18-O2	KS211-OL8	KS211-OL10	KS213-OL2	KS213-OL3	KS213-OL4	KS213-OL5	KS213-OL6	KS213-OL7
SiO_2	39.65	39.27	39.94	39.32	39.71	39.27	39.20	37.88	38.84	39.07	39.32	39.01	38.30	38.90	38.59	38.50	37.77	37.29	38.51	39.11	38.09	37.92	37.03	36.64	38.22	38.40	37.27	37.62	37.48	39.11
TiO_2																														
Al_2O_3																														
FeO	19.23	18.56	17.97	19.06	17.37	18.58	19.61	26.83	20.85	20.38	17.55	19.36	25.04	20.31	21.80	23.53	27.20	27.80	22.08	18.89	21.38	24.44	31.05	30.00	24.35	23.20	28.13	28.50	27.45	23.63
MnO	0.11	0.22	0.19	0.27			0.41	0.27	0.37	0.24	0.29	0.29	0.34	0.26	0.50	0.32	0.50	0.51	0.63	0.26	0.24	0.51	0.51	0.41	0.34	0.41	0.41	0.48	0.47	0.37
MgO	41.60	41.41	42.22	41.31	42.55	41.85	40.64	34.75	39.97	40.50	41.86	40.68	36.45	39.90	38.91	37.61	34.45	33.61	37.97	41.18	39.17	36.44	31.28	31.66	37.00	37.60	33.33	33.67	33.90	37.53
CaO	0.27	0.22	0.20	0.21	0.26	0.13	0.18	0.31	0.22	0.20	0.24	0.26	0.25	0.26	0.26	0.33	0.30	0.33	0.34	0.23	0.30	0.39	0.42	0.37	0.28	0.24	0.44	0.30	0.34	0.33
Na_2O																														
NiO																														
Cr_2O_3																														
Total	100.85	99.66	100.52	100.17	99.88	99.83	100.04	100.04	100.26	100.38	99.26	99.60	100.37	99.62	100.06	100.28	100.22	99.54	99.52	99.66	99.19	99.70	100.30	99.07	100.17	99.84	99.58	100.56	99.63	100.98
Numbers of ions on the basis of 4 O																														
Si	1.005	1.006	1.010	1.004	1.008	1.00	1.01	1.01	1.00	1.00	1.01	1.00	1.01	1.01	1.00	1.00	1.00	1.00	1.01	1.00	1.00	1.00	1.004	1.002	1.002	1.005	1.003	1.003	1.005	1.012
Ti	0	0	0	0	0	0	0	0	0	0	0	0	0	0	0	0	0	0	0	0	0	0	0	0	0	0	0	0	0	0
Al	0	0	0	0	0	0	0	0	0	0	0	0	0	0	0	0	0	0	0	0	0	0	0	0	0	0	0	0	0	0
Fe^{2+}	0.408	0.397	0.380	0.407	0.368	0.40	0.42	0.60	0.45	0.44	0.38	0.42	0.55	0.44	0.47	0.51	0.61	0.63	0.48	0.41	0.47	0.54	0.704	0.686	0.534	0.508	0.633	0.635	0.615	0.511
Mn	0.002	0.005	0.004	0.006	0	0	0.01	0.01	0.01	0.01	0.01	0.01	0.01	0.01	0.01	0.01	0.01	0.01	0.01	0.01	0.01	0.01	0.012	0.009	0.007	0.009	0.009	0.011	0.011	0.008
Mg	1.572	1.581	1.591	1.573	1.609	1.59	1.55	1.38	1.54	1.55	1.60	1.56	1.43	1.54	1.51	1.46	1.37	1.35	1.48	1.58	1.53	1.43	1.264	1.291	1.446	1.467	1.338	1.339	1.355	1.448
Ca	0.007	0.006	0.005	0.006	0.007	0.00	0.01	0.01	0.01	0.01	0.01	0.01	0.01	0.01	0.01	0.01	0.01	0.01	0.01	0.01	0.01	0.01	0.012	0.011	0.008	0.007	0.013	0.009	0.010	0.009
Na	0	0	0	0	0	0	0	0	0	0	0	0	0	0	0	0	0	0	0	0	0	0	0	0	0	0	0	0	0	0
Ni	0	0	0	0	0	0	0	0	0	0	0	0	0	0	0	0	0	0	0	0	0	0	0	0	0	0	0	0	0	0
Cr	0	0	0	0	0	0	0	0	0	0	0	0	0	0	0	0	0	0	0	0	0	0	0	0	0	0	0	0	0	0
Total	2.995	2.994	2.990	2.996	2.992	3.00	2.99	2.99	3.00	3.00	2.99	3.00	2.99	2.99	3.00	3.00	3.00	3.00	2.99	3.00	3.00	3.00	2.996	2.998	2.998	2.995	2.997	2.997	2.995	2.988
Fo% (Mgx100/ ($Mg+Fe^{2+}$))	79.4	79.9	80.7	79.4	81.4	80.1	78.7	69.8	77.4	78.0	81.0	78.9	72.2	77.8	76.1	74.0	69.3	68.3	75.4	79.5	76.6	72.7	64.2	65.3	73.0	74.3	67.9	67.8	68.8	73.9

Appendix 3-1 (Continued).

Locality	KHOK SAMRAN, KS					BO PHLOI, BP																						
Occurrence	Groundmass					Phenocryst												Microphenocryst			Groundmass							
Analysis No.	KS214-OL4	KS214-OL5	KS214-L6/2	KS214-OL7	KS214-OL10	BP733-OL2	BP736-OL4	BP81-OL4	BP87-OL1	BP87-OL2	BP87-OL4	BP912-OL1	BP912-OL2	BP912-OL3	BP924-OL1	BP924-OL2	BP924-OL3	BP83-OL2	BP82-OL3	BP82-OL9	BP733-OL1	BP733-OL3	BP733-OL4	BP734-OL3	BP734-OL4	BP734-OL5	BP736-OL1	BP736-OL2	BP736-OL3	BP736-OL5
SiO_2	39.72	37.96	36.79	36.20	37.13	39.27	40.29	38.38	37.56	38.72	37.74	37.80	38.23	37.87	38.13	37.85	38.40	37.85	37.42	37.59	38.21	38.24	38.12	37.93	38.40	38.21	38.07	38.23	38.17	38.21
TiO_2																														
Al_2O_3																														
FeO	17.91	25.53	26.84	33.12	32.15	19.36	14.93	24.09	26.01	20.32	26.21	25.07	25.30	25.29	25.46	24.87	25.32	25.90	26.47	26.04	23.85	24.06	23.83	24.79	23.81	23.82	23.55	23.67	23.10	23.75
MnO	0.37	0.21	0.38	0.69	0.60	0.42	0.43	0.69	0.84	0.51	0.63	0.72	0.76	0.62	0.78	0.85	0.56	0.78	0.66	0.75	0.65	0.87	0.86	0.76	0.66	0.73	0.91	0.76	0.82	0.76
MgO	41.78	36.22	34.57	29.29	30.22	40.87	44.09	37.27	35.08	39.46	35.00	35.60	35.81	35.55	35.38	35.55	35.71	35.40	34.84	34.56	36.66	36.60	36.40	35.63	36.94	36.40	36.18	36.42	36.89	36.61
CaO	0.19	0.31	0.33	0.44	0.51			0.25	0.25	0.13	0.26	0.33	0.40	0.34	0.35	0.35	0.35	0.33	0.28	0.30	0.30	0.33	0.33	0.35	0.24	0.28	0.29	0.33	0.27	0.24
Na_2O																														
NiO						0.38	0.42			0.40																				
Cr_2O_3			0.23																											
Total	99.97	100.23	99.14	99.74	100.61	100.31	100.16	100.68	99.73	99.54	99.84	99.52	100.50	99.67	100.09	99.47	100.35	100.26	99.68	99.25	99.66	100.10	99.54	99.36	100.05	99.44	99.00	99.41	99.25	99.56
Numbers of ions on the basis of 4 O																														
Si	1.011	1.000	0.991	1.000	1.009	1.005	1.011	1.001	1.001	1.005	1.004	1.004	1.006	1.005	1.008	1.005	1.010	1.002	0.999	1.006	1.006	1.005	1.006	1.008	1.007	1.009	1.009	1.009	1.007	1.007
Ti	0	0	0	0	0	0	0	0	0	0	0	0	0	0	0	0	0	0	0	0	0	0	0	0	0	0	0	0	0	0
Al	0	0	0	0	0	0	0	0	0	0	0	0	0	0	0	0	0	0	0	0	0	0	0	0	0	0	0	0	0	0
Fe^{2+}	0.381	0.563	0.605	0.765	0.730	0.414	0.313	0.526	0.579	0.441	0.583	0.557	0.556	0.561	0.563	0.552	0.557	0.573	0.591	0.583	0.525	0.529	0.526	0.551	0.522	0.526	0.522	0.522	0.510	0.523
Mn	0.008	0.005	0.009	0.016	0.014	0.009	0.009	0.015	0.019	0.011	0.014	0.016	0.017	0.014	0.017	0.019	0.013	0.017	0.015	0.017	0.014	0.019	0.019	0.017	0.015	0.016	0.020	0.017	0.018	0.017
Mg	1.585	1.423	1.388	1.206	1.224	1.559	1.649	1.450	1.393	1.526	1.388	1.409	1.404	1.406	1.394	1.408	1.400	1.397	1.387	1.379	1.440	1.433	1.432	1.407	1.444	1.433	1.430	1.433	1.451	1.439
Ca	0.005	0.009	0.009	0.013	0.015	0.000	0.000	0.007	0.007	0.004	0.007	0.009	0.011	0.010	0.010	0.010	0.010	0.009	0.008	0.009	0.008	0.009	0.009	0.010	0.007	0.008	0.008	0.009	0.008	0.007
Na	0	0	0	0	0	0	0	0	0	0	0	0	0	0	0	0	0	0	0	0	0	0	0	0	0	0	0	0	0	0
Ni	0	0	0	0	0	0.008	0.008	0	0	0.008	0	0	0	0	0	0	0	0	0	0	0	0	0	0	0	0	0	0	0	0
Cr	0	0	0.005	0	0	0	0	0	0	0	0	0	0	0	0	0	0	0	0	0	0	0	0	0	0	0	0	0	0	0
Total	2.989	3.000	3.007	3.000	2.991	2.995	2.989	2.999	2.999	2.995	2.996	2.996	2.994	2.995	2.992	2.995	2.990	2.998	3.001	2.994	2.994	2.995	2.994	2.992	2.993	2.991	2.991	2.991	2.993	2.993
Fo% (Mgx100/ ($Mg+Fe^{2+}$))	80.6	71.7	69.7	61.2	62.6	79.0	84.0	73.4	70.6	77.6	70.4	71.7	71.6	71.5	71.2	71.8	71.5	70.9	70.1	70.3	73.3	73.1	73.1	71.9	73.4	73.2	73.3	73.3	74.0	73.3

Appendix 3-1 (Continued).

Locality	BO PHLOI, BP																			NAM YUN, NY										
Occurrence	Groundmass																			Phenocryst										
Analysis No	BP736-OL6	BP81-OL6	BP81-OL7	BP81-OL8	BP81-OL9	BP82-OL5	BP82-OL7	BP82-OL8	BP82-OL10	BP82A-OL2	BP83-OL3	BP86-OL4	BP86-OL5	BP86-OL6	BP86-OL7	BP87-OL3	BP922-OL5	BP924-OL4	BP929-OL7	NY131-OL1	NY131-OL2	NY131-OL3	NY131-OL4	NY131-OL5	NY131-OL6	NY131-OL7	NY132-OL1	NY132-OL2	NY132-OL5	NY133-OL2
SiO_2	38.17	38.34	38.10	37.76	38.07	38.15	37.83	37.78	37.86	38.12	38.28	38.08	37.96	37.80	37.98	37.77	37.98	38.11	38.14	37.55	37.52	37.69	37.29	37.67	37.38	37.39	37.81	38.00	37.48	37.07
TiO_2																														
Al_2O_3																														
FeO	23.34	26.18	26.19	25.76	26.56	25.74	26.15	26.12	26.14	25.49	26.43	26.82	26.43	26.46	26.52	26.09	25.34	25.01	24.15	28.11	28.60	25.71	27.82	28.33	28.40	28.91	27.05	26.05	29.40	26.64
MnO	0.87	0.83	0.79	0.87	0.69	0.89	0.99	0.82	0.64	0.77	0.70	0.77	0.65	0.73	0.55	0.73	0.84	0.75	0.88	0.46	0.32	0.27	0.39	0.38	0.24	0.36	0.32	0.38	0.39	0.30
MgO	36.96	35.04	35.13	35.47	34.90	34.74	34.74	34.79	34.71	35.16	35.16	34.68	34.70	34.99	34.89	34.89	36.06	35.53	36.12	33.99	33.35	35.57	33.25	33.57	33.75	33.26	34.80	35.52	32.71	34.17
CaO	0.32	0.28	0.31	0.26	0.37	0.31	0.34	0.32	0.40	0.32	0.33	0.34	0.42	0.30	0.35	0.34	0.31	0.35	0.31	0.30	0.29	0.26	0.26	0.37	0.27	0.43	0.27	0.39	0.36	0.26
Na_2O																														0.54
NiO																														
Cr_2O_3																														
Total	99.66	100.67	100.51	100.11	100.58	99.83	100.04	99.82	99.75	99.84	100.90	100.68	100.16	100.28	100.29	99.81	100.53	99.76	99.59	100.40	100.09	99.50	99.02	100.32	100.04	100.34	100.24	100.34	100.35	99.23
Numbers of ions on the basis of 4 O																														
Si	1.004	1.010	1.006	1.001	1.006	1.013	1.005	1.005	1.008	1.010	1.007	1.007	1.007	1.002	1.006	1.005	1.000	1.009	1.008	1.001	1.005	1.002	1.008	1.006	1.001	1.002	1.004	1.003	1.006	0.996
Ti	0	0	0	0	0	0	0	0	0	0	0	0	0	0	0	0	0	0	0	0	0	0	0	0	0	0	0	0	0	0
Al	0	0	0	0	0	0	0	0	0	0	0	0	0	0	0	0	0	0	0	0	0	0	0	0	0	0	0	0	0	0
Fe^{2+}	0.513	0.577	0.578	0.571	0.587	0.571	0.581	0.581	0.582	0.565	0.581	0.593	0.586	0.587	0.588	0.580	0.558	0.554	0.534	0.627	0.641	0.572	0.629	0.632	0.636	0.648	0.600	0.575	0.660	0.598
Mn	0.019	0.019	0.018	0.019	0.015	0.020	0.022	0.018	0.014	0.017	0.016	0.017	0.015	0.016	0.012	0.016	0.019	0.017	0.020	0.010	0.007	0.006	0.009	0.009	0.005	0.008	0.007	0.008	0.009	0.007
Mg	1.449	1.376	1.383	1.401	1.375	1.375	1.376	1.380	1.377	1.389	1.379	1.367	1.373	1.383	1.378	1.384	1.415	1.402	1.423	1.351	1.332	1.410	1.340	1.336	1.348	1.328	1.377	1.398	1.309	1.368
Ca	0.009	0.008	0.009	0.007	0.010	0.009	0.010	0.009	0.011	0.009	0.009	0.010	0.012	0.009	0.010	0.010	0.009	0.010	0.009	0.008	0.008	0.007	0.008	0.011	0.008	0.012	0.008	0.011	0.010	0.008
Na	0	0	0	0	0	0	0	0	0	0	0	0	0	0	0	0	0	0	0	0	0	0	0	0	0	0	0	0	0	0.028
Ni	0	0	0	0	0	0	0	0	0	0	0	0	0	0	0	0	0	0	0	0	0	0	0	0	0	0	0	0	0	0
Cr	0	0	0	0	0	0	0	0	0	0	0	0	0	0	0	0	0	0	0	0	0	0	0	0	0	0	0	0	0	0
Total	2.996	2.990	2.994	2.999	2.994	2.987	2.995	2.995	2.992	2.990	2.993	2.993	2.993	2.998	2.994	2.995	3.000	2.991	2.992	2.999	2.995	2.998	2.992	2.994	2.999	2.998	2.996	2.997	2.994	3.010
Fo% (Mgx100/ ($Mg+Fe^{2+}$))	73.8	70.5	70.5	71.1	70.1	70.6	70.3	70.4	70.3	71.1	70.3	69.7	70.1	70.2	70.1	70.5	71.7	71.7	72.7	68.3	67.5	71.1	68.1	67.9	67.9	67.2	69.6	70.9	66.5	69.6

Appendix 3-1 (Continued).

Locality	NAM YUN, NY							PHLOI WAEN, PW																						
Occurrence	Pheno.	Microphe no.	Groundmass					Phenocryst																				Microphenocryst		
Analysis No	NY133-OL4	NY131-OL9	NY131-OL8	NY131-L10	NY132-OL3	NY132-OL4	NY133-OL3	PW12-OL10	PW12-OL11	PW13-OL8	PW14-OL9	PW14-OL10	PW15-OL1	PW15-OL5	PW18-OL1	PW18-OL2	PW213-OL7	PW213-OL9	PW319-OL1	PW321-OL1	PW322-OL5	PW323-OL5	PW323-OL7	PW323-OL8	PW324-OL5	PW324-OL6	PW324-OL7	PW123-OL1	PW123-OL2	PW13-OL9
SiO_2	36.56	35.38	34.54	36.12	36.64	36.03	37.27	39.20	39.73	41.39	39.65	39.54	40.99	39.70	41.08	39.48	39.37	39.99	40.85	39.79	39.81	39.82	39.47	40.15	39.60	39.75	39.54	41.31	39.66	39.92
TiO_2																														
Al_2O_3	0.27																													
FeO	30.32	39.74	40.97	34.21	34.00	36.93	26.67	19.16	16.62	9.62	15.98	18.31	10.26	16.64	9.75	15.98	20.22	15.84	10.41	15.98	15.90	16.34	16.88	15.76	16.89	18.23	17.03	9.19	16.48	16.52
MnO	0.44	0.56	0.78	0.41	0.51	0.77	0.37		0.20		0.22	0.22				0.25	0.25	0.27		0.23		0.35	0.23	0.27		0.27				0.26
MgO	30.83	24.04	22.25	28.74	29.19	26.75	34.05	40.70	43.09	49.31	43.12	41.64	48.07	43.09	48.38	43.41	40.64	43.25	48.25	43.77	43.36	42.38	42.60	43.40	42.86	42.08	42.98	49.04	42.45	43.44
CaO	0.36	0.46	0.54	0.42	0.42	0.48	0.33	0.29	0.24		0.16	0.31		0.16			0.17	0.17		0.24	0.19	0.23		0.26	0.11	0.22	0.23	0.12	0.27	0.27
Na_2O	0.48						0.52																							
NiO													0.33		0.39									0.32					0.39	
Cr_2O_3																														
Total	99.25	100.17	99.08	99.91	100.76	100.97	99.20	99.35	99.88	100.31	99.13	100.03	99.64	99.59	99.60	99.13	100.64	99.53	99.50	100.01	99.25	99.12	99.18	100.15	99.46	100.56	99.78	99.66	99.23	100.41
Numbers of ions on the basis of 4 O																														
Si	1.001	1.005	1.003	1.000	1.003	1.001	1.002	1.009	1.006	1.007	1.008	1.007	1.009	1.007	1.010	1.004	1.005	1.012	1.007	1.003	1.009	1.014	1.007	1.010	1.007	1.007	1.003	1.010	1.011	1.005
Ti	0	0	0	0	0	0	0	0	0	0	0	0	0	0	0	0	0	0	0	0	0	0	0	0	0	0	0	0	0	0
Al	0.009	0	0	0	0	0	0	0	0	0	0	0	0	0	0	0	0	0	0	0	0	0	0	0	0	0	0	0	0	0
Fe^{2+}	0.694	0.944	0.995	0.792	0.778	0.858	0.600	0.412	0.352	0.196	0.340	0.390	0.211	0.353	0.200	0.340	0.432	0.335	0.214	0.337	0.337	0.348	0.360	0.332	0.359	0.386	0.361	0.188	0.351	0.348
Mn	0.010	0.013	0.019	0.010	0.012	0.018	0.008	0	0.004	0	0.005	0.005	0	0	0	0.005	0.005	0.006	0	0.005	0	0.008	0.005	0.006	0	0.006	0	0	0	0.005
Mg	1.258	1.018	0.963	1.186	1.191	1.108	1.365	1.562	1.626	1.789	1.635	1.582	1.764	1.629	1.773	1.646	1.547	1.631	1.772	1.645	1.639	1.609	1.621	1.628	1.624	1.589	1.626	1.788	1.612	1.630
Ca	0.011	0.014	0.017	0.013	0.012	0.014	0.009	0.008	0.007	0	0.004	0.009	0	0.004	0	0	0.005	0.005	0	0.006	0.005	0.006	0	0.007	0.003	0.006	0.006	0.003	0.007	0.007
Na	0.025	0	0	0	0	0	0.027	0	0	0	0	0	0	0	0	0	0	0	0	0	0	0	0	0	0	0	0	0	0	0
Ni	0	0	0	0	0	0	0	0	0	0	0	0	0.006	0	0.008	0	0	0	0	0	0	0	0	0.006	0	0	0	0	0.008	0
Cr	0	0	0	0	0	0	0	0	0	0	0	0	0	0	0	0	0	0	0	0	0	0	0	0	0	0	0	0	0	0
Total	3.008	2.995	2.997	3.000	2.997	2.999	3.011	2.991	2.994	2.993	2.992	2.993	2.991	2.993	2.990	2.996	2.995	2.988	2.993	2.997	2.991	2.986	2.993	2.990	2.993	2.993	2.997	2.990	2.989	2.995
Fo% (Mgx100/ ($Mg+Fe^{2+}$))	64.4	51.9	49.2	60.0	60.5	56.4	69.5	79.1	82.2	90.1	82.8	80.2	89.3	82.2	89.8	82.9	78.2	83.0	89.2	83.0	82.9	82.2	81.8	83.1	81.9	80.5	81.8	90.5	82.1	82.4

Appendix 3-1 (Continued).

Locality	PHLOI WAEN, PW																												
Occurrence	Microphenocryst																												Ground mass
Analysis No	PW14-OL3	PW14-OL4	PW14-OL5	PW14-OL6	PW14-OL7	PW14-OL8	PW210-OL8	PW210-OL9	PW210-OL11	PW210-OL14	PW210-OL15	PW210-OL16	PW212-OL13	PW212-OL14	PW212-OL15	PW212-OL16	PW213-OL11	PW213-OL12	PW227-OL1	PW227-OL2	PW227-OL4	PW227-OL5	PW318-OL1	PW318-OL3	PW318-OL4	PW319-OL2	PW319-OL3	PW319-OL4	PW320-OL6	PW213-OL8
SiO_2	39.52	39.50	39.55	39.02	39.73	39.76	39.55	39.93	39.79	39.42	39.74	39.75	39.57	39.88	40.04	40.85	40.14	39.74	39.77	39.87	38.97	39.37	40.10	40.78	39.91	39.51	39.61	40.52	39.56	39.89
TiO_2																														
Al_2O_3																														
FeO	17.27	16.41	16.88	17.36	16.26	15.94	17.02	15.93	17.15	17.15	17.27	17.60	17.04	16.24	17.11	9.79	15.94	16.64	16.27	16.78	18.86	16.66	16.87	9.83	16.08	17.04	17.16	10.07	16.73	16.10
MnO		0.24		0.32			0.23	0.22				0.24		0.23	0.20	0.08				0.25	0.25		0.23		0.23	0.34		0.09		
MgO	42.61	43.10	43.33	42.10	43.53	43.29	42.95	43.18	43.23	43.05	42.64	42.71	42.55	43.48	42.92	48.59	43.75	43.27	43.17	43.01	41.38	42.58	42.81	48.66	43.37	42.58	42.72	47.74	43.11	42.96
CaO	0.27	0.19	0.22	0.20	0.18	0.18	0.28	0.21	0.20	0.23	0.29	0.18	0.21	0.25	0.21	0.08	0.25	0.17	0.23	0.21	0.27	0.23	0.18		0.16	0.21	0.29	0.04	0.21	0.23
Na_2O																														
NiO				0.33	0.32											0.43								0.43				0.39		
Cr_2O_3																0.05												0.03		
Total	99.67	99.43	99.96	99.33	100.02	99.17	100.03	99.47	100.37	99.85	99.94	100.48	99.37	100.08	100.47	99.86	100.08	99.82	99.45	100.12	99.72	98.85	100.19	99.69	99.76	99.69	99.78	98.89	99.61	99.17
Numbers of ions on the basis of 4 O																														
Si	1.005	1.004	1.001	1.000	1.003	1.009	1.002	1.011	1.004	1.000	1.007	1.004	1.008	1.006	1.009	1.003	1.009	1.006	1.008	1.007	1.000	1.007	1.012	1.003	1.009	1.005	1.006	1.006	1.004	1.013
Ti	0	0	0	0	0	0	0	0	0	0	0	0	0	0	0	0	0	0	0	0	0	0	0	0	0	0	0	0	0	0
Al	0	0	0	0	0	0	0	0	0	0	0	0	0	0	0	0	0	0	0	0	0	0	0	0	0	0	0	0	0	0
Fe^{2+}	0.367	0.349	0.357	0.372	0.343	0.338	0.361	0.337	0.362	0.364	0.366	0.372	0.363	0.342	0.360	0.201	0.335	0.352	0.345	0.355	0.405	0.356	0.356	0.202	0.340	0.362	0.364	0.209	0.355	0.342
Mn	0	0.005	0	0.007	0	0	0.005	0.005	0	0	0	0.005	0	0.005	0.004	0.002	0	0	0	0.005	0.005	0.000	0.005	0	0.005	0.007	0	0.002	0	0
Mg	1.615	1.633	1.635	1.609	1.639	1.638	1.622	1.630	1.626	1.629	1.611	1.609	1.616	1.635	1.612	1.779	1.640	1.632	1.632	1.620	1.583	1.624	1.611	1.784	1.634	1.614	1.617	1.767	1.631	1.626
Ca	0.007	0.005	0.006	0.006	0.005	0.005	0.008	0.006	0.005	0.006	0.008	0.005	0.006	0.007	0.006	0.002	0.007	0.005	0.006	0.006	0.007	0.006	0.005	0	0.004	0.006	0.008	0.001	0.006	0.006
Na	0	0	0	0	0	0	0	0	0	0	0	0	0	0	0	0	0	0	0	0	0	0	0	0	0	0	0	0	0	0
Ni	0	0	0	0.007	0.007	0	0	0	0	0	0	0	0	0	0	0.008	0	0	0	0	0	0	0	0.009	0	0	0	0.008	0	0
Cr	0	0	0	0	0	0	0	0	0	0	0	0	0	0	0	0.001	0	0	0	0	0	0	0	0	0	0	0	0.001	0	0
Total	2.995	2.996	2.999	3.000	2.997	2.991	2.998	2.989	2.996	3.000	2.993	2.996	2.992	2.994	2.991	2.996	2.991	2.994	2.992	2.993	3.000	2.993	2.988	2.997	2.991	2.995	2.994	2.994	2.996	2.987
Fo% (Mgx100/ ($Mg+Fe^{2+}$))	81.5	82.4	82.1	81.2	82.7	82.9	81.8	82.9	81.8	81.7	81.5	81.2	81.7	82.7	81.7	89.9	83.0	82.3	82.5	82.0	79.6	82.0	81.9	89.8	82.8	81.7	81.6	89.4	82.1	82.6

Appendix 3-1 (Continued).

Locality	PHLOI WAEN, PW				TOK PHROM, TP																								
Occurrence	Groundmass				Phenocryst																								
Analysis No	PW213-OL10	PW320-OL8	PW322-OL6	PW323-OL6	TP1315-OL1	TP1315-OL2	TP1315-OL6	TP1319-OL1	TP1319-OL2	TP1320-OL1	TP1320-OL2	TP1320-OL3	TP1320-OL4	TP1320-OL5	TP1320-OL6	TP1320-OL7	TP1320-OL8	TP1320-OL9	TP1330-OL1	TP1330-OL2	TP1330-OL3	TP1330-OL4	TP1330-OL5	TP1330-OL12	TP131-OL1	TP131-OL2	TP131-OL3	TP131-OL8	TP131-OL9	TP13K-OL1
SiO_2	39.49	39.77	39.75	39.50	39.18	38.51	39.09	38.13	38.93	38.51	39.21	38.51	38.67	38.36	38.52	38.99	38.80	38.85	38.28	38.24	37.97	37.97	39.02	38.36	39.17	39.12	38.93	39.12	38.34	38.53
TiO_2																														
Al_2O_3									0.44																					0.46
FeO	19.72	16.48	16.58	16.07	20.99	23.19	21.04	21.50	18.63	22.63	20.24	24.02	23.30	24.37	24.39	22.06	23.77	23.21	21.91	24.24	23.07	23.08	19.44	23.87	22.16	21.73	21.36	21.28	23.96	20.78
MnO	0.22	0.38			0.39	0.33	0.43	0.41	0.25	0.50	0.30	0.53	0.44	0.47	0.52	0.44	0.39	0.37	0.31	0.37	0.37	0.42	0.21	0.51	0.53	0.31	0.28	0.25	0.41	0.41
MgO	40.42	43.24	42.72	43.46	39.72	38.07	39.66	38.63	40.95	38.15	40.13	36.65	37.87	37.10	37.01	38.99	37.75	37.51	38.51	37.18	37.86	37.36	40.47	37.02	38.86	39.05	39.78	39.81	37.11	39.76
CaO	0.44	0.17	0.18	0.24	0.32	0.25	0.27	0.31	0.19	0.27	0.24	0.46	0.34	0.46	0.42	0.29	0.27	0.29	0.20	0.44	0.31	0.34	0.21	0.41	0.24	0.24	0.12	0.17	0.26	0.16
Na_2O								0.71	0.32																					0.41
NiO																			0.37											
Cr_2O_3																														
Total	100.29	100.05	99.23	99.26	100.60	100.34	100.48	99.69	99.99	100.06	100.11	100.17	100.62	100.76	100.85	100.77	100.98	100.23	99.58	100.47	99.58	99.17	99.35	100.16	100.96	100.46	100.48	100.63	100.08	100.82
Numbers of ions on the basis of 4 O																														
Si	1.010	1.005	1.011	1.003	1.006	1.002	1.005	0.996	0.994	1.003	1.007	1.009	1.004	1.001	1.004	1.005	1.005	1.011	1.000	1.000	0.997	1.001	1.007	1.005	1.008	1.009	1.002	1.004	1.004	0.987
Ti	0	0	0	0	0	0	0	0	0	0	0	0	0	0	0	0	0	0	0	0	0	0	0	0	0	0	0	0	0	0
Al	0	0	0	0	0	0	0	0	0.013	0	0	0	0	0	0	0	0	0	0	0	0	0	0	0	0	0	0	0	0	0.014
Fe^{2+}	0.422	0.348	0.353	0.341	0.451	0.505	0.452	0.469	0.398	0.493	0.435	0.526	0.506	0.532	0.532	0.475	0.515	0.505	0.479	0.530	0.507	0.509	0.419	0.523	0.477	0.469	0.460	0.457	0.525	0.445
Mn	0.005	0.008	0	0	0.008	0.007	0.009	0.009	0.005	0.011	0.006	0.012	0.010	0.010	0.011	0.010	0.009	0.008	0.007	0.008	0.008	0.009	0.005	0.011	0.011	0.007	0.006	0.005	0.009	0.009
Mg	1.541	1.629	1.620	1.646	1.520	1.477	1.521	1.504	1.559	1.482	1.537	1.431	1.466	1.443	1.438	1.498	1.458	1.456	1.500	1.450	1.482	1.469	1.557	1.445	1.490	1.501	1.526	1.524	1.450	1.519
Ca	0.012	0.005	0.005	0.006	0.009	0.007	0.007	0.009	0.005	0.007	0.006	0.013	0.009	0.013	0.012	0.008	0.007	0.008	0.006	0.012	0.009	0.010	0.006	0.012	0.007	0.007	0.003	0.005	0.007	0.004
Na	0	0	0	0	0	0	0	0.036	0.016	0	0	0	0	0	0	0	0	0	0	0	0	0	0	0	0	0	0	0	0	0.020
Ni	0	0	0	0	0	0	0	0	0	0	0	0	0	0	0	0	0	0	0.008	0	0	0	0	0	0	0	0	0	0	0
Cr	0	0	0	0	0	0	0	0	0	0	0	0	0	0	0	0	0	0	0	0	0	0	0	0	0	0	0	0	0	0
Total	2.990	2.995	2.989	2.997	2.994	2.998	2.995	3.022	2.997	2.997	2.993	2.991	2.996	2.999	2.998	2.995	2.995	2.989	3.000	3.000	3.003	2.999	2.993	2.995	2.992	2.991	2.998	2.996	2.996	3.006
Fo% (Mgx100/ ($Mg+Fe^{2+}$))	78.5	82.4	82.1	82.8	77.1	74.5	77.1	76.2	79.7	75.0	78.0	73.1	74.3	73.1	73.0	75.9	73.9	74.2	75.8	73.2	74.5	74.3	78.8	73.4	75.8	76.2	76.9	76.9	73.4	77.3

Appendix 3-1 (Continued).

Locality	TOK PHROM																								BONG BON, NB				
Occurrence	Phenocryst				Micropheno.		Groundmass																		Phenocryst				
	TP13K-OL2	TP13K-OL5	TP324-OL1	TP324-OL4	TP1317-OL1	TP1317-OL4	TP1315-OL3	TP1315-OL4	TP1315-OL5	TP1317-OL2	TP1317-OL3	TP1317-OL5	TP1317-OL7	TP1317-OL8	TP1330-OL6	TP1330-OL7	TP1330-OL8	TP1330-OL9	TP1330-OL40	TP1330-OL41	TP1330-OL42	TP131-OL4	TP131-OL6	TP131-OL11	TP324b-OL2	NB51OP-OL1	NB51OP-OL44	NB51OP-OL2	NB51OP-OL3	NB51OP-OL4
SiO_2	39.05	38.00	39.35	39.20	38.20	38.36	38.56	38.64	38.60	38.22	38.01	38.02	38.56	38.18	38.34	38.45	38.24	38.63	38.25	38.46	38.12	38.57	39.05	38.53	38.05	39.20	39.45	39.56	39.35	39.38
TiO_2																									0.18					
Al_2O_3	0.44	0.35	0.30																											
FeO	19.45	21.80	18.17	21.10	23.15	22.51	23.03	23.86	23.05	23.39	24.32	24.44	23.18	23.95	22.06	23.82	24.09	23.71	23.19	22.21	24.10	23.80	22.13	24.08	25.76	17.48	17.84	17.16	16.94	16.97
MnO	0.20	0.37	0.39	0.39	0.38	0.39	0.45	0.40	0.40	0.33	0.50	0.62	0.49	0.46	0.32	0.43	0.52	0.43	0.56	0.43	0.51	0.46	0.31	0.39	0.48	0.24		0.19	0.36	
MgO	40.47	37.90	41.08	39.13	37.32	37.70	37.68	36.82	38.38	37.44	36.85	36.49	37.44	37.06	38.06	37.42	36.68	37.05	37.40	38.09	36.75	37.44	38.91	37.36	35.43	42.04	42.20	42.42	42.38	42.46
CaO	0.11	0.27	0.17	0.14	0.26	0.20	0.33	0.33	0.27	0.21	0.47	0.43	0.30	0.39	0.23	0.41	0.42	0.36	0.32	0.33	0.38	0.30	0.20	0.31	0.43	0.19	0.18	0.15	0.18	0.26
Na_2O	0.48	0.43	0.32	0.31																										
NiO																														
Cr_2O_3																														
Total	100.46	99.46	99.77	100.26	99.31	99.16	100.04	100.05	100.70	99.58	100.16	100.00	99.97	100.05	99.01	100.53	99.95	100.18	99.72	99.52	99.86	100.56	100.60	100.67	100.33	99.15	99.66	99.47	99.20	99.07
Numbers of ions on the basis of 4 O																														
Si	0.996	0.993	1.006	1.011	1.005	1.008	1.006	1.011	1.000	1.004	0.999	1.001	1.008	1.002	1.006	1.003	1.005	1.010	1.003	1.005	1.003	1.005	1.007	1.004	1.004	1.005	1.006	1.008	1.005	1.006
Ti	0	0	0	0	0	0	0	0	0	0	0	0	0	0	0	0	0	0	0	0	0	0	0	0	0.004	0	0	0	0	0
Al	0.013	0.011	0.009	0	0	0	0	0	0	0	0	0	0	0	0	0	0	0	0	0	0	0	0	0	0	0	0	0	0	0
Fe^{2+}	0.415	0.476	0.388	0.455	0.509	0.494	0.502	0.522	0.500	0.514	0.534	0.538	0.506	0.525	0.484	0.519	0.529	0.518	0.509	0.486	0.530	0.518	0.477	0.524	0.568	0.374	0.380	0.366	0.362	0.363
Mn	0.004	0.008	0.008	0.009	0.008	0.009	0.010	0.009	0.009	0.007	0.011	0.014	0.011	0.010	0.007	0.010	0.011	0.009	0.012	0.009	0.011	0.010	0.007	0.009	0.011	0.005	0	0.004	0.008	0
Mg	1.539	1.476	1.565	1.504	1.464	1.476	1.466	1.437	1.483	1.466	1.444	1.433	1.459	1.450	1.490	1.454	1.437	1.443	1.463	1.485	1.442	1.454	1.496	1.451	1.394	1.606	1.604	1.611	1.615	1.618
Ca	0.003	0.008	0.005	0.004	0.007	0.005	0.009	0.009	0.008	0.006	0.013	0.012	0.008	0.011	0.006	0.012	0.012	0.010	0.009	0.009	0.011	0.008	0.005	0.009	0.012	0.005	0.005	0.004	0.005	0.007
Na	0.024	0.022	0.016	0.015	0	0	0	0	0	0	0	0	0	0	0	0	0	0	0	0	0	0	0	0	0	0	0	0	0	0
Ni	0	0	0	0	0	0	0	0	0	0	0	0	0	0	0	0	0	0	0	0	0	0	0	0	0	0	0	0	0	0
Cr	0	0	0	0	0	0	0	0	0	0	0	0	0	0	0	0	0	0	0	0	0	0	0	0	0	0	0	0	0	0
Total	3.001	3.001	2.998	2.997	2.995	2.992	2.994	2.989	3.000	2.996	3.001	2.999	2.992	2.998	2.994	2.997	2.995	2.990	2.997	2.995	2.997	2.995	2.993	2.996	2.992	2.995	2.994	2.992	2.995	2.994
Fo% (Mgx100/ ($Mg+Fe^{2+}$))	78.8	75.6	80.1	76.8	74.2	74.9	74.5	73.3	74.8	74.1	73.0	72.7	74.2	73.4	75.5	73.7	73.1	73.6	74.2	75.4	73.1	73.7	75.8	73.4	71.0	81.1	80.8	81.5	81.7	81.7

Appendix 3-1 (Continued).

Locality	NONG BON, NB																								
Occurrence	Microphenocryst																								
Analysis No	NB131-OL3	NB131-OL4	NB131-OL5	NB131-OL9	NB133-OL1	NB133-OL2	NB133-OL4	NB133-OL5	NB133-OL6	NB133-OL7	NB133-OL9	NB133-OL10	NB133-OL11	NB133-OL12	NB5139-OL1	NB5139-OL3	NB5139-OL4	NB5139-OL5	NB5139-OL6	NB51OM-L1	NB51OM-L2	NB51OM-L3	NB51OM-L4	NB51OM-L5	NB51OM-L6	NB51OM-L7
SiO_2	39.17	38.70	38.97	38.37	39.41	39.37	39.16	38.93	39.36	39.32	39.00	38.94	38.40	39.62	39.82	39.23	39.49	39.11	39.08	39.97	39.52	39.43	38.81	38.42	39.20	39.69
TiO_2																										
Al_2O_3																										
FeO	19.56	18.74	19.42	22.23	18.08	18.10	19.04	19.25	17.69	20.42	19.84	18.86	22.26	17.24	17.25	19.52	19.19	19.03	19.80	16.89	17.13	17.19	20.61	20.15	18.17	17.51
MnO	0.20	0.35	0.41	0.26		0.26		0.29	0.27	0.29	0.23	0.21	0.33	0.28	0.29	0.30		0.26	0.21	0.19	0.19		0.26	0.28	0.23	0.22
MgO	40.40	40.97	40.55	37.93	41.87	41.56	41.52	40.68	42.02	40.33	40.16	41.10	37.99	42.36	42.91	40.74	41.36	41.35	40.40	42.73	42.70	42.32	39.69	40.13	41.62	42.32
CaO	0.31	0.25	0.18	0.30	0.18	0.28	0.23	0.21	0.24	0.32	0.25	0.21	0.44	0.19	0.17	0.17	0.29	0.19	0.34	0.24	0.15	0.26	0.28	0.29	0.18	0.21
Na_2O																										
NiO		0.32																								
Cr_2O_3																										
Total	99.65	99.33	99.53	99.10	99.53	99.57	99.95	99.36	99.58	100.67	99.48	99.31	99.42	99.70	100.43	99.96	100.33	99.94	99.84	100.01	99.68	99.20	99.65	99.26	99.39	99.95
Numbers of ions on the basis of 4 O																										
Si	1.008	0.999	1.005	1.007	1.007	1.007	1.002	1.004	1.005	1.005	1.007	1.003	1.005	1.008	1.005	1.006	1.006	1.002	1.005	1.011	1.005	1.007	1.005	0.998	1.005	1.008
Ti	0	0	0	0	0	0	0	0	0	0	0	0	0	0	0	0	0	0	0	0	0	0	0	0	0	0
Al	0	0	0	0	0	0	0	0	0	0	0	0	0	0	0	0	0	0	0	0	0	0	0	0	0	0
Fe^{2+}	0.421	0.404	0.419	0.488	0.386	0.387	0.407	0.415	0.378	0.437	0.428	0.406	0.487	0.367	0.364	0.419	0.409	0.407	0.426	0.357	0.364	0.367	0.446	0.438	0.389	0.372
Mn	0.004	0.008	0.009	0.006	0	0.006	0	0.006	0.006	0.006	0.005	0.004	0.007	0.006	0.006	0.007	0	0.006	0.005	0.004	0.004	0	0.006	0.006	0.005	0.005
Mg	1.550	1.576	1.558	1.484	1.595	1.585	1.583	1.564	1.600	1.538	1.546	1.578	1.483	1.607	1.615	1.558	1.571	1.579	1.550	1.611	1.619	1.611	1.532	1.553	1.591	1.602
Ca	0.009	0.007	0.005	0.008	0.005	0.008	0.006	0.006	0.007	0.009	0.007	0.006	0.012	0.005	0.005	0.005	0.008	0.005	0.009	0.006	0.004	0.007	0.008	0.008	0.005	0.006
Na	0	0	0	0	0	0	0	0	0	0	0	0	0	0	0	0	0	0	0	0	0	0	0	0	0	0
Ni	0	0.007	0	0	0	0	0	0	0	0	0	0	0	0	0	0	0	0	0	0	0	0	0	0	0	0
Cr	0	0	0	0	0	0	0	0	0	0	0	0	0	0	0	0	0	0	0	0	0	0	0	0	0	0
Total	2.992	3.001	2.995	2.993	2.993	2.993	2.998	2.996	2.995	2.995	2.993	2.997	2.995	2.992	2.995	2.994	2.994	2.998	2.995	2.989	2.995	2.993	2.995	3.002	2.995	2.992
Fo%(Mgx100/ (Mg+Fe^{2+}))	78.6	79.6	78.8	75.3	80.5	80.4	79.5	79.0	80.9	77.9	78.3	79.5	75.3	81.4	81.6	78.8	79.3	79.5	78.4	81.9	81.6	81.4	77.4	78.0	80.3	81.2

Appendix 3-1 (Continued).

Locality	NONG BON, NB																								
Occurrence	Microphenocryst																								
Analysis No	NB51OM-OL8	NB51OM-OL9	NB51OM-OL10	NB51OM-OL11	NB51OM-OL12	NB51OM-OL13	NB51OM-OL14	NB51OM-OL15	NB51OM-OL16	NB51OM-OL17	NB51OM-OL18	NB51OM-OL19	NB51OM-OL20	NB51OM-OL21	NB51OM-OL22	NB51OM-OL23	NB51OM-OL24	NB51OM-OL25	NB51OM-OL26	NB51OM-OL27	NB51OM-OL28	NB51OM-OL30	NB51OM-OL31	NB51OM-OL32	NB51OP-OL5
SiO_2	39.58	39.55	38.94	39.89	39.71	38.75	39.80	39.61	39.72	39.51	39.27	39.51	39.30	39.63	39.83	39.59	39.70	39.44	39.36	39.71	39.69	39.26	39.74	39.47	39.20
TiO_2																									
Al_2O_3																									
FeO	17.95	17.41	20.58	17.67	16.85	21.15	17.60	16.87	16.74	17.20	17.62	17.39	17.77	16.80	17.69	17.18	16.83	16.91	16.73	16.89	17.34	17.42	17.55	17.29	18.32
MnO	0.21			0.19		0.36		0.22		0.20	0.21			0.22					0.30	0.23		0.29	0.23		0.33
MgO	42.27	42.69	39.77	42.42	42.34	38.50	42.64	42.65	42.59	42.15	42.28	43.01	42.04	42.57	42.69	42.90	42.71	42.68	42.75	43.20	42.81	42.48	42.51	42.84	41.25
CaO	0.15	0.26	0.34	0.19	0.22	0.30	0.17	0.25	0.29	0.13	0.20	0.21	0.24	0.11	0.25	0.24	0.23	0.20	0.21	0.24	0.23	0.18	0.25	0.13	0.30
Na_2O																									
NiO	0.33																		0.39			0.32			
Cr_2O_3																									
Total	100.49	99.91	99.63	100.36	99.13	99.06	100.22	99.61	99.35	99.20	99.57	100.13	99.34	99.32	100.46	99.91	99.48	99.23	99.73	100.28	100.07	99.95	100.28	99.73	99.39
Numbers of ions on the basis of 4 O																									
Si	1.003	1.004	1.007	1.009	1.013	1.012	1.007	1.007	1.010	1.010	1.003	1.001	1.005	1.009	1.006	1.004	1.009	1.006	1.001	1.003	1.005	1.000	1.006	1.003	1.006
Ti	0	0	0	0	0	0	0	0	0	0	0	0	0	0	0	0	0	0	0	0	0	0	0	0	0
Al	0	0	0	0	0	0	0	0	0	0	0	0	0	0	0	0	0	0	0	0	0	0	0	0	0
Fe^{2+}	0.381	0.370	0.445	0.374	0.359	0.462	0.372	0.359	0.356	0.367	0.376	0.368	0.380	0.358	0.374	0.364	0.358	0.361	0.356	0.357	0.367	0.371	0.371	0.367	0.393
Mn	0.004	0	0	0.004	0	0.008	0	0.005	0	0.004	0.005	0	0	0.005	0	0	0	0	0.007	0.005	0	0.006	0.005	0	0.007
Mg	1.597	1.615	1.533	1.599	1.610	1.498	1.609	1.616	1.615	1.606	1.609	1.624	1.603	1.616	1.608	1.622	1.618	1.623	1.621	1.626	1.616	1.612	1.605	1.623	1.579
Ca	0.004	0.007	0.009	0.005	0.006	0.009	0.005	0.007	0.008	0.004	0.005	0.006	0.006	0.003	0.007	0.006	0.006	0.006	0.006	0.007	0.006	0.005	0.007	0.004	0.008
Na	0	0	0	0	0	0	0	0	0	0	0	0	0	0	0	0	0	0	0	0	0	0	0	0	0
Ni	0.007	0	0	0	0	0	0	0	0	0	0	0	0	0	0	0	0	0	0.008	0	0	0.007	0	0	0
Cr	0	0	0	0	0	0	0	0	0	0	0	0	0	0	0	0	0	0	0	0	0	0	0	0	0
Total	2.997	2.996	2.993	2.991	2.987	2.988	2.993	2.993	2.990	2.990	2.997	2.999	2.995	2.991	2.994	2.996	2.991	2.994	2.999	2.997	2.995	3.000	2.994	2.997	2.994
Fo% (Mgx100/ ($Mg+Fe^{2+}$))	80.8	81.4	77.5	81.1	81.8	76.4	81.2	81.8	81.9	81.4	81.1	81.5	80.8	81.9	81.1	81.7	81.9	81.8	82.0	82.0	81.5	81.3	81.2	81.5	80.1

Appendix 3-1 (Continued).

Locality	NONG BON, NB																						
Occurrence	Microphenocryst																						
Analysis No	NB5238-OL1	NB5238-OL2	NB5238-OL4	NB5238-OL5	NB5238-OL6	NB5239-OL1	NB5239-OL2	NB5239-OL3	NB5239-OL4	NB5239-OL5	NB5239-OL6	NB5239-OL8	NB5239-OL9	NB5239-OL10	NB5239-OL11	NB5239-OL12	NB5239-OL13	NB5239-OL15	NB5239-OL16	NB5239-OL17	NB5239-OL18	NB5239-OL19	NB5239-OL20	NB5239-OL21	NB5239-OL22
SiO_2	39.33	39.05	38.94	38.62	39.37	39.39	39.27	39.42	40.09	39.84	39.94	39.25	39.29	39.11	39.20	39.72	39.11	39.58	39.75	39.13	39.75	39.91	39.81	39.82	39.45
TiO_2																									
Al_2O_3																									
FeO	17.80	20.49	20.19	20.83	17.55	17.88	19.52	17.92	17.45	17.65	17.46	20.87	19.09	19.86	20.37	16.90	20.17	17.26	18.57	21.52	18.40	17.28	17.35	17.26	19.44
MnO	0.29		0.34	0.22	0.26	0.27	0.29	0.28	0.28		0.24	0.28	0.22	0.37	0.24		0.29	0.34		0.32					0.22
MgO	42.19	39.92	40.15	39.74	42.08	42.13	40.69	42.50	42.94	42.40	42.49	39.91	41.53	40.86	39.83	43.15	40.37	42.89	42.24	39.39	42.24	43.21	43.28	42.95	41.11
CaO	0.24	0.31	0.27	0.30	0.22	0.21	0.19	0.20	0.21	0.17	0.18	0.28	0.21	0.25	0.30	0.23	0.45	0.21	0.22	0.32	0.18	0.18	0.23	0.26	0.33
Na_2O																									
NiO							0.31	0.34						0.35		0.36								0.30	
Cr_2O_3																	0.17		0.21						
Total	99.84	99.78	99.89	99.72	99.48	99.88	100.26	100.66	100.97	100.07	100.31	100.59	100.34	100.80	99.94	100.35	100.55	100.28	100.97	100.68	100.56	100.58	100.66	100.58	100.54
Si	1.002	1.007	1.004	1.000	1.006	1.004	1.006	0.999	1.007	1.010	1.010	1.006	1.002	0.999	1.009	1.003	1.002	1.002	1.003	1.006	1.006	1.005	1.002	1.004	1.005
Ti	0	0	0	0	0	0	0	0	0	0	0	0	0	0	0	0	0	0	0	0	0	0	0	0	0
Al	0	0	0	0	0	0	0	0	0	0	0	0	0	0	0	0	0	0	0	0	0	0	0	0	0
Fe^{2+}	0.378	0.442	0.435	0.451	0.375	0.381	0.418	0.380	0.366	0.374	0.369	0.448	0.407	0.424	0.439	0.357	0.432	0.365	0.392	0.463	0.389	0.364	0.365	0.364	0.414
Mn	0.006	0	0.007	0.005	0.006	0.006	0.006	0.006	0.006	0	0.005	0.006	0.005	0.008	0.005	0	0.006	0.007	0	0.007	0	0	0	0	0.005
Mg	1.603	1.535	1.543	1.535	1.602	1.600	1.553	1.605	1.608	1.602	1.601	1.526	1.579	1.556	1.529	1.624	1.541	1.618	1.589	1.510	1.594	1.622	1.624	1.615	1.562
Ca	0.007	0.009	0.008	0.008	0.006	0.006	0.005	0.005	0.006	0.005	0.005	0.008	0.006	0.007	0.008	0.006	0.012	0.006	0.006	0.009	0.005	0.005	0.006	0.007	0.009
Na	0	0	0	0	0	0	0	0	0	0	0	0	0	0	0	0	0	0	0	0	0	0	0	0	0
Ni	0	0	0	0	0	0	0.006	0.007	0	0	0	0	0	0.007	0	0.007	0	0	0	0	0	0	0	0.006	0
Cr	0	0	0	0	0	0	0	0	0	0	0	0	0	0	0	0	0.003	0	0.004	0	0	0	0	0	0
Total	2.998	2.993	2.996	3.000	2.994	2.996	2.994	3.001	2.993	2.990	2.990	2.994	2.998	3.001	2.991	2.997	2.997	2.998	2.995	2.994	2.994	2.995	2.998	2.996	2.995
Fo% (Mgx100/ (Mg+Fe^{2+}))	80.9	77.6	78.0	77.3	81.0	80.8	78.8	80.9	81.4	81.1	81.3	77.3	79.5	78.6	77.7	82.0	78.1	81.6	80.2	76.5	80.4	81.7	81.6	81.6	79.0

Appendix 3-1 (Continued).

Locality	NONG BON, NB																							
Occurrence	Microphenocryst			Groundmass																				
Analysis No	NB5239-OL23	NB5239-OL24	NB5239-OL25	NB131-OL1	NB131-OL2	NB131-OL6	NB131-OL7	NB131-OL10	NB131-OL11	NB132-OL1	NB132-OL4	NB132-OL5	NB132-OL6	NB132-OL7	NB132-OL8	NB132-OL9	NB132-OL10	NB132-OL11	NB5238A-OL1	NB5238A-OL3	NB5238A-OL5	NB5238A-OL6	NB5238A-L12	NB5238A-L14	NB5238A-L15
SiO_2	39.22	39.74	40.44	38.05	38.96	37.51	38.85	39.32	38.88	39.04	38.94	39.29	38.67	38.50	37.89	38.70	38.91	39.55	38.47	39.29	39.40	38.83	39.39	38.89	38.51
TiO_2																									0.16
Al_2O_3																					0.31				
FeO	21.54	18.52	17.99	22.12	20.15	26.84	19.69	19.39	18.57	19.69	20.92	18.03	22.48	21.02	26.20	20.98	18.99	18.20	20.51	16.71	17.52	20.54	16.68	20.41	20.78
MnO	0.36	0.24		0.47	0.19	0.57	0.20	0.19	0.21	0.29	0.35	0.24	0.41	0.33	0.64	0.39			0.21			0.29	0.35	0.37	0.21
MgO	39.53	41.99	40.00	37.99	39.63	33.60	40.35	41.14	41.25	40.10	39.02	41.48	37.88	38.94	34.45	39.08	41.02	41.57	39.76	43.28	42.66	39.62	43.18	40.01	39.78
CaO	0.31	0.25	1.46	0.50	0.27	0.53	0.21	0.29	0.19	0.28	0.32	0.22	0.40	0.25	0.56	0.22	0.21	0.15	0.33	0.18	0.16	0.23	0.20	0.32	0.35
Na_2O																			0.52					0.36	0.41
NiO									0.41	0.37				0.31					0.30						
Cr_2O_3																									
Total	100.96	100.73	99.89	99.13	99.20	99.05	99.30	100.32	99.51	99.77	99.54	99.25	99.83	99.35	99.74	99.37	99.13	99.46	99.28	100.57	100.27	99.86	100.07	100.65	100.50
Numbers of ions on the basis of 4 O																									
Si	1.005	1.006	1.030	1.000	1.010	1.010	1.004	1.004	1.000	1.006	1.010	1.008	1.008	1.004	1.009	1.007	1.004	1.011	1.000	0.991	0.996	1.001	0.996	0.997	0.991
Ti	0	0	0	0	0	0	0	0	0	0	0	0	0	0	0	0	0	0	0	0	0	0	0	0	0.003
Al	0	0	0	0	0	0	0	0	0	0	0	0	0	0	0	0	0	0	0	0	0.009	0	0	0	0
Fe^{2+}	0.462	0.392	0.383	0.486	0.437	0.604	0.426	0.414	0.399	0.424	0.454	0.387	0.490	0.458	0.584	0.456	0.410	0.389	0.446	0.352	0.370	0.443	0.353	0.437	0.447
Mn	0.008	0.005	0	0.010	0.004	0.013	0.004	0.004	0.005	0.006	0.008	0.005	0.009	0.007	0.014	0.008	0	0	0.005	0	0	0.006	0.008	0.008	0.005
Mg	1.511	1.584	1.518	1.489	1.532	1.348	1.555	1.566	1.582	1.541	1.509	1.586	1.473	1.513	1.368	1.515	1.577	1.584	1.541	1.627	1.608	1.523	1.628	1.528	1.525
Ca	0.009	0.007	0.040	0.014	0.008	0.015	0.006	0.008	0.005	0.008	0.009	0.006	0.011	0.007	0.016	0.006	0.006	0.004	0.009	0.005	0.004	0.006	0.005	0.009	0.010
Na	0	0	0	0	0	0	0	0	0	0	0	0	0	0	0	0	0	0	0	0.026	0	0	0	0.018	0.021
Ni	0	0	0	0	0	0	0	0	0.008	0.008	0	0	0	0.007	0	0	0	0	0	0.006	0	0	0	0	0
Cr	0	0	0	0	0	0	0	0	0	0	0	0	0	0	0	0	0	0	0	0	0	0	0	0	0
Total	2.995	2.994	2.970	3.000	2.990	2.990	2.996	2.996	3.000	2.994	2.990	2.992	2.992	2.996	2.991	2.993	2.996	2.989	3.000	3.013	2.992	2.987	2.995	3.003	3.007
Fo% (Mgx100/ ($Mg+Fe^{2+}$))	76.6	80.2	79.9	75.4	77.8	69.1	78.5	79.1	79.8	78.4	76.9	80.4	75.0	76.8	70.1	76.9	79.4	80.3	77.6	82.2	81.3	77.5	82.2	77.8	77.3

Appendix 3-2 Chemical composition of CPX in basalt samples. (Note: $\Sigma Fe = Fe^{2+}+Fe^{3+}+Mn$; $mg^*=100xMg/(Mg+Fe^{2+}+Fe^{3+}+Mn)$.

Locality	CHIANG KHONG, CK																														
Occurrence	Phenocryst		Microphenocryst		Groundmass																										
Analysis No	CK18-CPX1	CK18-CPX2	CK13-CPX2	CK13-CPX3	CK210-CPX1	CK210-CPX2	CK210-CPX3	CK29-CPX1	CK29-CPX3	CK29-CPX4	CK29-CPX5	CK29B-CPX1	CK29B-CPX4	CK315A-CPX1	CK315B-CPX1	CK315B-CPX2	CK315B-CPX3	CK315B-CPX4	CK315B-CPX5	CK315B-CPX6	CK315B-CPX7	CK315B-CPX8	CK315B-CPX9	CK315C-CPX1	CK315C-CPX2	CK315C-CPX3	CK519B-CPX1	CK519B-CPX2	CK519B-CPX3	CK519B-CPX4
SiO_2	41.00	43.79	46.90	43.10	43.04	42.12	42.19	46.29	42.00	42.78	45.68	44.25	41.11	46.08	46.45	46.92	45.67	48.02	46.46	44.23	42.57	44.43	45.00	42.96	46.89	46.79	46.03	42.54	44.42	44.10
TiO_2	5.99	4.30	2.74	4.62	4.77	5.02	5.53	3.29	5.54	4.98	3.83	3.86	5.91	3.34	3.57	3.04	3.53	3.02	3.53	4.71	5.34	4.56	4.30	4.97	3.15	3.32	3.79	5.57	4.80	4.60
Al_2O_3	10.30	9.03	8.36	9.68	8.58	8.80	9.46	5.85	9.54	9.13	6.24	7.73	9.86	6.00	6.08	5.17	6.53	5.00	5.78	8.09	8.78	8.51	8.28	9.28	5.87	5.67	5.73	9.29	6.65	8.31
Fe_2O_3	4.44	3.19	2.56	4.02	3.05	2.68	3.38	1.81	3.58	2.40	1.86	3.09	4.16	2.13	2.46	3.19	4.04	2.26	1.60	3.53	3.43	3.36	1.98	1.98	1.36	1.94	1.66	3.06	2.01	3.03
FeO	4.56	5.09	4.45	4.35	5.33	6.56	5.03	5.90	4.88	5.90	6.70	4.86	4.95	6.05	5.63	4.51	4.36	5.71	6.04	4.97	5.38	4.30	5.95	5.99	5.74	6.03	6.97	5.33	7.44	5.04
MnO	0	0.25	0.19	0	0	0	0	0	0	0	0	0	0	0.22	0.20	0	0	0	0	0	0	0.24	0	0	0.29	0	0	0	0.23	0
MgO	9.91	10.87	12.71	11.07	10.77	10.68	10.61	12.27	10.61	10.47	11.91	11.41	10.34	12.33	12.60	12.74	12.26	13.21	12.63	11.58	10.83	11.56	11.41	10.76	12.52	12.82	12.02	10.80	10.93	11.43
CaO	22.54	22.64	20.78	22.39	22.08	21.32	21.77	21.78	21.80	22.08	21.47	21.85	21.68	21.47	21.78	21.90	22.04	21.91	21.57	21.80	21.65	22.41	22.14	21.80	21.75	21.57	21.54	21.92	21.14	21.67
Na_2O	0.71	0.54	0.92	0.63	0.68	0.77	0.86	0.71	0.78	0.73	0.70	0.81	0.81	0.56	0.64	0.79	0.76	0.62	0.54	0.86	0.77	0.71	0.70	0.79	0.62	0.57	0.65	0.76	0.85	0.77
K_2O	0	0	0	0	0.10	0	0.10	0	0.13	0	0.14	0	0.16	0.15	0.17	0.14	0.15	0.17	0.25	0.14	0.17	0.18	0.09	0	0.12	0.13	0.14	0.11	0.14	0.17
Cr_2O_3	0	0	0	0	0	0	0	0	0	0	0	0.19	0.23	0	0	0	0	0	0	0	0	0	0	0	0	0	0	0	0	0.18
Total	99.45	99.70	99.99	99.85	98.63	98.73	99.28	98.20	99.11	98.78	99.02	98.33	99.67	98.66	100.03	98.68	99.64	100.20	98.77	100.32	99.31	100.49	100.09	98.98	98.59	99.15	99.03	99.70	99.17	99.51
Numbers of ions on the basis of 6 O																														
Si	1.560	1.652	1.738	1.621	1.642	1.609	1.600	1.760	1.596	1.630	1.730	1.685	1.560	1.748	1.737	1.773	1.715	1.787	1.757	1.655	1.616	1.657	1.684	1.630	1.773	1.762	1.744	1.607	1.692	1.662
Ti	0.171	0.122	0.076	0.131	0.137	0.144	0.158	0.094	0.158	0.143	0.109	0.110	0.169	0.095	0.100	0.086	0.100	0.084	0.100	0.132	0.152	0.128	0.121	0.142	0.089	0.094	0.108	0.158	0.137	0.130
Al	0.462	0.402	0.365	0.429	0.386	0.396	0.423	0.262	0.427	0.410	0.278	0.347	0.441	0.268	0.268	0.230	0.289	0.219	0.258	0.357	0.393	0.374	0.365	0.415	0.262	0.252	0.256	0.414	0.298	0.369
Fe^{3+}	0.127	0.090	0.071	0.114	0.087	0.077	0.096	0.052	0.102	0.069	0.053	0.089	0.119	0.061	0.069	0.091	0.114	0.063	0.046	0.099	0.098	0.094	0.056	0.056	0.039	0.055	0.047	0.087	0.058	0.086
Fe^{2+}	0.145	0.161	0.138	0.137	0.170	0.210	0.160	0.187	0.155	0.188	0.212	0.155	0.157	0.192	0.176	0.142	0.137	0.178	0.191	0.156	0.171	0.134	0.186	0.190	0.182	0.190	0.221	0.168	0.237	0.159
Mn	0	0.008	0.006	0	0	0	0	0	0	0	0	0	0	0.007	0.006	0	0	0	0	0	0	0.007	0	0	0.009	0	0	0	0.007	0
Mg	0.562	0.611	0.702	0.621	0.612	0.608	0.600	0.696	0.601	0.595	0.672	0.648	0.585	0.697	0.702	0.718	0.687	0.733	0.712	0.646	0.613	0.642	0.637	0.608	0.706	0.720	0.679	0.608	0.620	0.642
Ca	0.919	0.915	0.825	0.902	0.903	0.873	0.884	0.887	0.888	0.901	0.871	0.891	0.881	0.873	0.872	0.886	0.887	0.874	0.874	0.874	0.880	0.895	0.888	0.886	0.881	0.870	0.874	0.887	0.862	0.875
Na	0.053	0.039	0.066	0.046	0.050	0.057	0.063	0.052	0.058	0.054	0.051	0.060	0.060	0.041	0.046	0.058	0.055	0.045	0.040	0.062	0.057	0.051	0.050	0.058	0.046	0.041	0.048	0.055	0.063	0.056
K	0	0	0	0	0.005	0	0.005	0	0.006	0	0.007	0	0.008	0.007	0.008	0.007	0.007	0.008	0.012	0.007	0.008	0.009	0.004	0.000	0.006	0.006	0.007	0.005	0.007	0.008
Cr	0	0	0	0	0	0	0	0	0	0	0	0.006	0.007	0	0	0	0	0	0	0	0	0	0	0	0	0	0	0	0	0.005
Total	4.000	4.000	4.000	4.000	4.000	4.000	4.000	4.000	4.000	4.000	4.000	4.000	4.000	4.000	4.000	4.000	4.000	4.000	4.000	4.000	4.000	4.000	4.000	4.000	4.000	4.000	4.000	4.000	4.000	4.000
Ca%(Wo%)	52.4	51.2	47.4	50.9	50.9	49.4	50.8	48.7	50.8	51.4	48.2	50.0	50.6	47.7	47.8	48.3	48.6	47.3	47.9	49.2	50.0	50.5	50.2	50.9	48.5	47.4	48.0	50.7	48.3	49.7
Mg%(En%)	32.0	34.2	40.3	35.0	34.5	34.4	34.5	38.2	34.4	33.9	37.2	36.4	33.6	38.1	38.5	39.1	37.6	39.7	39.1	36.4	34.8	36.2	36.0	34.9	38.8	39.2	37.3	34.7	34.8	36.4
ΣFe%(Fs%)	15.5	14.5	12.3	14.1	14.5	16.2	14.7	13.1	14.7	14.7	14.7	13.6	15.8	14.2	13.8	12.7	13.8	13.0	13.0	14.4	15.3	13.3	13.7	14.2	12.6	13.3	14.7	14.6	16.9	13.9
mg*	67.4	70.2	76.6	71.3	70.4	68.0	70.1	74.4	70.0	69.8	71.7	72.7	68.0	72.9	73.6	75.5	73.2	75.2	75.1	71.7	69.5	73.2	72.5	71.2	75.4	74.6	71.7	70.4	67.3	72.4

Appendix 3-2 (Continued).

Locality	Chiang Khong, CK							BAN NONG, NAM CHO, BN																							
Occurrence	Groundmass							Phenocryst?				Phenocryst						Phenocryst (Core)							Phenocryst (Rim)							MicroPH	MicroPH (Spongy core)
Analysis No	CK519B-CPX5	CK519B-CPX6	CK519B-CPX7	CK519B-CPX8	CK519B-CPX9	CK519B-CPX10	CK519B-CPX12	BN132-CPX21	BN132-CPX22	BN132-CPX23	BN134-CPX1	BN134-CP1	BN134-CP2	BN324-CPX1	BN324-CPX2	BN324-CPX3	BN133-CPX2	BN446-CPX1	BN446-CPX3	BN446-CPX5	BN447-CPX3	BN447-CPX7	BN133-CPX4	BN446-CPX1	BN446-CPX3	BN446-CPX5	BN447-CPX3	BN447-CPX7	BN323-CPX2	BN133-CPX3
SiO_2	46.06	45.15	47.21	40.32	44.34	42.02	44.66	48.96	49.17	49.00	48.65	48.52	48.02	49.86	50.41	50.01	46.33	50.78	50.18	49.76	46.29	51.80	42.45	45.77	45.66	45.81	40.28	46.47	42.79	46.64
TiO_2	3.99	4.17	3.50	6.41	4.53	5.61	3.94	1.03	0.83	1.03	1.43	1.28	1.34	0.74	0.76	0.52	1.02	0.45	0.69	0.92	2.74	0.97	4.28	2.61	2.99	2.99	5.09	2.92	3.91	1.08
Al_2O_3	6.19	6.04	5.35	11.10	7.74	10.04	7.09	5.42	5.41	5.24	7.09	7.08	7.05	5.11	5.31	4.77	11.05	3.05	5.76	4.91	6.90	3.93	10.56	7.84	7.20	7.53	11.07	7.30	9.29	11.38
Fe_2O_3	2.78	2.71	2.41	4.98	1.73	2.58	3.47	2.14	2.35	1.34	3.95	1.90	2.59	2.99	3.29	3.53	3.74	2.94	3.26	2.29	4.42	0.00	5.36	5.09	2.85	2.22	5.78	4.74	5.64	5.37
FeO	6.01	6.80	5.76	4.03	6.85	5.74	5.63	9.19	8.84	9.76	5.38	7.08	6.18	8.13	7.54	7.00	4.00	11.82	1.18	8.77	3.40	4.13	3.30	2.80	6.02	5.95	2.98	3.13	3.02	2.79
MnO	0	0	0.27	0	0	0	0	0	0	0.25	0.22	0.20	0.22	0.34	0.40	0.49	0	0.34	0	0.38	0	0	0	0.23	0	0	0	0.20	0	0.21
MgO	12.22	11.74	12.57	10.20	11.63	10.37	11.86	11.54	11.68	11.44	12.10	11.83	12.03	12.04	12.17	12.28	10.30	11.49	15.35	12.13	12.48	15.69	10.82	12.38	11.87	11.39	9.88	12.05	11.02	10.64
CaO	21.34	21.43	21.98	21.85	21.47	21.87	21.47	19.98	20.02	19.97	21.10	20.54	20.36	19.35	19.42	19.63	21.57	18.91	22.09	19.98	22.29	21.87	22.51	22.01	21.55	22.13	22.82	22.82	22.60	21.86
Na_2O	0.85	0.70	0.73	0.86	0.54	0.70	0.85	0.89	0.91	0.76	1.14	0.97	1.02	1.20	1.39	1.24	1.36	0.92	0.81	0.86	0.78	0.52	0.83	0.82	0.63	0.80	0.68	0.89	0.86	1.46
K_2O	0.13	0.13	0.18	0.12	0.10	0.10	0.09	0	0	0	0	0	0	0	0	0	0	0	0	0	0	0	0	0	0	0	0.10	0	0	0
Cr_2O_3	0	0	0	0	0	0	0	0	0.30	0.27	0	0	0	0	0	0	0	0	0	0	0	0.55	0	0.19	0	0	0	0	0	0
Total	99.94	99.41	100.42	100.31	99.32	99.28	99.84	99.13	99.51	99.06	101.05	99.39	98.80	99.77	100.69	99.46	99.36	100.68	99.32	99.99	99.29	99.65	100.44	99.73	98.96	99.26	98.93	100.53	98.92	101.44
Numbers of ions on the basis of 6 O																														
Si	1.727	1.711	1.760	1.519	1.677	1.594	1.679	1.852	1.852	1.858	1.792	1.816	1.806	1.868	1.867	1.875	1.726	1.912	1.840	1.865	1.736	1.900	1.586	1.710	1.727	1.725	1.537	1.725	1.624	1.703
Ti	0.113	0.119	0.098	0.182	0.129	0.160	0.111	0.029	0.024	0.029	0.040	0.036	0.038	0.021	0.021	0.015	0.028	0.013	0.019	0.026	0.077	0.027	0.120	0.073	0.085	0.085	0.146	0.082	0.112	0.030
Al	0.273	0.270	0.235	0.493	0.345	0.449	0.314	0.241	0.240	0.234	0.308	0.312	0.313	0.226	0.232	0.211	0.485	0.135	0.249	0.217	0.305	0.170	0.465	0.345	0.321	0.334	0.498	0.319	0.416	0.490
Fe^{3+}	0.079	0.077	0.068	0.141	0.049	0.074	0.098	0.061	0.067	0.038	0.110	0.054	0.073	0.084	0.092	0.100	0.105	0.083	0.090	0.065	0.125	0	0.151	0.143	0.081	0.063	0.166	0.132	0.161	0.148
Fe^{2+}	0.188	0.215	0.179	0.127	0.217	0.182	0.177	0.291	0.278	0.309	0.166	0.222	0.194	0.255	0.234	0.219	0.124	0.372	0.036	0.275	0.107	0.127	0.103	0.087	0.191	0.187	0.095	0.097	0.096	0.085
Mn	0	0	0.008	0	0	0	0	0	0	0.008	0.007	0.006	0.007	0.011	0.012	0.016	0	0.011	0	0.012	0	0	0	0.007	0	0	0	0.006	0	0.006
Mg	0.683	0.663	0.698	0.573	0.656	0.587	0.665	0.651	0.656	0.647	0.664	0.660	0.674	0.672	0.672	0.687	0.572	0.645	0.839	0.677	0.698	0.858	0.603	0.689	0.669	0.640	0.562	0.667	0.624	0.579
Ca	0.857	0.870	0.878	0.881	0.870	0.889	0.864	0.810	0.808	0.812	0.833	0.824	0.820	0.777	0.771	0.788	0.861	0.763	0.868	0.802	0.896	0.859	0.901	0.881	0.873	0.893	0.933	0.907	0.919	0.855
Na	0.062	0.052	0.053	0.063	0.040	0.051	0.062	0.065	0.067	0.056	0.081	0.070	0.074	0.087	0.100	0.090	0.098	0.067	0.058	0.062	0.057	0.037	0.060	0.059	0.046	0.059	0.050	0.064	0.049	0.103
K	0.006	0.006	0.009	0.006	0.005	0.005	0.004	0	0	0	0	0	0	0	0	0	0	0	0	0	0	0	0	0	0	0	0.005	0	0	0
Cr	0	0	0	0	0	0	0	0	0.009	0.008	0	0	0	0	0	0	0	0	0	0	0	0.016	0	0.005	0	0	0	0	0	0
Total	4.000	4.000	4.000	4.000	4.000	4.000	4.000	4.000	4.000	4.000	4.000	4.000	4.000	4.000	4.000	4.000	4.000	4.000	4.000	4.000	4.000	4.000	4.000	4.000	4.000	4.000	4.000	4.000	4.000	4.000
Ca%(Wo%)	47.4	47.6	47.9	51.2	48.5	51.3	47.9	44.7	44.7	44.7	46.8	46.7	46.4	43.2	43.3	43.6	51.8	40.7	47.3	43.8	49.1	46.6	51.3	48.7	48.1	50.1	53.1	50.1	51.1	51.1
Mg%(En%)	37.8	36.3	38.1	33.3	36.6	33.9	36.8	35.9	36.3	35.7	37.3	37.4	38.1	37.4	37.7	37.9	34.4	34.4	45.8	37.0	38.2	46.5	34.3	38.1	36.9	35.9	32.0	36.8	34.7	34.6
ΣFe%(Fs%)	14.8	16.0	13.9	15.6	14.8	14.8	15.2	19.4	19.1	19.6	15.9	15.9	15.5	19.4	19.0	18.5	13.8	24.9	6.9	19.2	12.7	6.9	14.4	13.2	15.0	14.0	14.9	13.0	14.3	14.3
mg*	71.9	69.4	73.2	68.1	71.2	69.6	70.7	64.9	65.5	64.5	70.2	70.1	71.1	65.8	66.5	67.2	71.4	59.0	86.9	65.8	75.1	87.1	70.4	74.4	71.1	71.9	68.3	73.9	70.8	70.8

Appendix 3-2 (Continued).

Locality	BAN NONG, NAM CHO, BN							SOP PRAP, SP												DEN CHAI, DC											
Occurrence	Groundmass							Groundmass												Microphenocryst					Groundmass						
Analysis No	BN134-CP4	BN135-CPX2	BN446-CPX8	BN447-CPX1	BN447-CPX2	BN6-CPX2	BN6-CPX3	SP1A-CPX2	SP1A-CPX3	SP1b-CPX1	SP1b-CPX2	SP1b-CPX3	SP1b-CPX4	SP1b-CPX5	SP1b-CPX6	SP1b-CPX7	SP1b-CPX8	SP1b-CPX9	SP1b-CPX10	DC264-CPX3	DC264-CPX4	DC264-CPX5	DC264-CPX6	DC264-CPX7	DC160-CPX1	DC160-CPX2	DC160-CPX3	DC160-CPX4	DC160-CPX5	DC1K-CPX2
SiO_2	43.83	44.46	43.55	44.23	47.43	43.70	43.78	43.87	45.57	43.23	44.31	41.84	44.23	47.78	45.89	46.32	44.10	45.44	47.17	45.05	48.92	45.96	46.42	46.00	44.05	46.16	44.30	44.77	43.78	43.55
TiO_2	3.83	3.79	3.92	3.49	2.12	4.38	4.02	4.59	3.44	4.63	4.17	5.63	3.89	2.85	3.36	3.56	4.57	4.03	2.89	3.35	2.27	2.85	3.24	2.98	4.10	3.39	4.11	4.02	4.32	4.14
Al_2O_3	9.04	8.89	9.27	8.64	5.76	9.87	9.54	8.36	6.91	8.05	8.20	9.54	8.10	5.11	6.80	6.53	7.97	7.20	5.21	8.38	5.06	8.11	6.27	7.91	8.45	7.04	8.39	7.10	8.73	8.35
Fe_2O_3	3.99	4.76	3.09	4.85	3.70	2.46	5.06	3.98	2.55	2.98	2.71	3.64	2.77	1.02	2.73	3.48	1.90	1.62	3.11	2.43	3.28	2.70	2.46	3.09	4.88	4.30	4.99	6.35	3.83	4.60
FeO	4.50	3.75	5.24	3.42	4.46	6.19	4.11	3.71	5.00	5.15	5.00	5.25	6.19	6.51	4.47	4.28	6.29	5.90	4.07	4.71	3.94	4.31	5.58	3.56	4.18	4.02	3.60	3.65	4.53	3.74
MnO	0	0	0.25	0	0	0.23	0.22	0	0	0	0	0	0	0	0	0.25	0	0	0	0	0	0	0	0	0	0	0.30	0.20	0	0
MgO	10.50	10.83	10.60	11.68	12.47	10.06	10.76	11.49	12.20	11.35	11.70	10.66	11.25	13.22	12.24	12.47	11.25	11.90	13.45	11.82	13.63	12.19	12.11	12.39	11.39	12.32	11.29	12.04	11.01	11.14
CaO	22.70	22.44	21.86	22.37	22.25	22.90	22.96	21.74	21.86	21.45	21.48	21.03	21.41	21.77	21.86	21.67	21.69	22.14	21.61	22.71	22.70	22.79	22.15	22.83	22.59	22.41	22.67	22.04	22.37	22.02
Na_2O	0.77	1.03	0.89	0.80	0.84	0.73	0.65	0.90	0.70	0.78	0.83	1.04	0.83	0.52	0.81	0.93	0.84	0.73	0.80	0.43	0.70	0.49	0.62	0.60	0.64	0.77	0.77	0.78	0.74	0.86
K_2O	0	0	0.12	0	0	0.13	0	0.13	0.13	0.10	0	0.10	0.11	0	0.09	0.10	0	0.11	0.12	0	0	0	0	0	0	0	0	0	0	0	0
Cr_2O_3	0	0	0	0.27	0	0	0.24	0.22	0	0	0	0	0	0	0.21	0	0	0	0	0.67	0.20	0.70	0	0.79	0	0	0	0	0	0.17
Total	99.15	99.94	99.44	100.00	99.26	101.29	101.33	98.98	98.74	98.16	98.62	99.32	99.50	99.13	98.59	99.84	99.22	99.69	98.81	99.54	100.71	100.10	98.84	100.14	100.26	100.41	100.44	100.94	99.30	98.57
Numbers of ions on the basis of 6 O																														
Si	1.661	1.667	1.643	1.655	1.780	1.626	1.628	1.659	1.722	1.652	1.679	1.586	1.669	1.794	1.727	1.731	1.668	1.704	1.773	1.692	1.803	1.712	1.756	1.710	1.652	1.718	1.657	1.670	1.655	1.658
Ti	0.109	0.107	0.111	0.098	0.060	0.122	0.112	0.130	0.098	0.133	0.119	0.160	0.110	0.080	0.096	0.100	0.130	0.114	0.082	0.095	0.063	0.080	0.092	0.083	0.116	0.095	0.116	0.113	0.123	0.118
Al	0.404	0.393	0.412	0.381	0.255	0.433	0.418	0.373	0.308	0.362	0.366	0.426	0.360	0.226	0.303	0.288	0.355	0.318	0.231	0.371	0.220	0.356	0.279	0.347	0.374	0.309	0.370	0.312	0.389	0.375
Fe^{3+}	0.114	0.134	0.088	0.136	0.105	0.069	0.142	0.113	0.072	0.086	0.077	0.104	0.079	0.029	0.078	0.098	0.054	0.046	0.088	0.069	0.091	0.076	0.070	0.086	0.138	0.120	0.140	0.178	0.109	0.132
Fe^{2+}	0.142	0.118	0.166	0.107	0.140	0.193	0.128	0.117	0.158	0.164	0.159	0.166	0.195	0.204	0.141	0.134	0.199	0.185	0.128	0.148	0.122	0.134	0.176	0.111	0.131	0.125	0.113	0.114	0.143	0.119
Mn	0	0	0.008	0	0	0.007	0.007	0	0	0	0	0	0	0	0	0.008	0	0	0	0	0	0	0	0	0	0	0.010	0.006	0	0
Mg	0.593	0.605	0.596	0.651	0.698	0.558	0.597	0.648	0.687	0.647	0.661	0.602	0.633	0.740	0.690	0.695	0.634	0.665	0.753	0.662	0.749	0.677	0.683	0.687	0.637	0.684	0.630	0.669	0.620	0.632
Ca	0.921	0.902	0.884	0.897	0.895	0.913	0.915	0.881	0.885	0.878	0.872	0.854	0.865	0.876	0.885	0.867	0.879	0.890	0.870	0.914	0.897	0.910	0.898	0.909	0.907	0.894	0.909	0.881	0.906	0.898
Na	0.056	0.075	0.065	0.058	0.061	0.053	0.047	0.066	0.051	0.057	0.061	0.076	0.061	0.038	0.060	0.067	0.062	0.053	0.058	0.031	0.050	0.036	0.046	0.043	0.046	0.055	0.056	0.058	0.054	0.064
K	0	0	0.006	0	0	0.006	0	0.006	0.006	0.005	0	0.005	0.005	0	0.004	0.005	0	0.005	0.006	0	0	0	0	0	0	0	0	0	0	0	0
Cr	0	0	0	0.008	0	0	0.007	0.007	0	0	0	0	0	0	0.006	0	0	0	0	0.020	0.006	0.021	0	0.023	0	0	0	0	0	0.005
Total	4.000	4.000	4.000	4.000	4.000	4.000	4.000	4.000	4.000	4.000	4.000	4.000	4.000	4.000	4.000	4.000	4.000	4.000	4.000	4.000	4.000	4.000	4.000	4.000	4.000	4.000	4.000	4.000	4.000	4.000
Ca%(Wo%)	52.0	51.3	50.7	50.1	48.7	52.5	51.2	50.1	49.1	49.5	49.3	49.5	48.8	47.4	49.4	48.1	49.8	49.8	47.3	51.0	48.3	50.6	49.1	50.7	50.1	49.0	50.4	47.7	50.9	50.4
Mg%(En%)	33.5	34.4	34.2	36.4	38.0	32.1	33.4	36.8	38.1	36.4	37.4	34.9	35.7	40.0	38.5	38.6	35.9	37.2	41.0	36.9	40.3	37.7	37.4	38.3	35.1	37.5	35.0	36.2	34.9	35.5
∑Fe%(Fs%)	14.5	14.3	15.0	13.6	13.3	15.5	15.5	13.1	12.8	14.1	13.3	15.7	15.5	12.6	12.2	13.3	14.3	12.9	11.7	12.1	11.4	11.7	13.5	11.0	14.8	13.5	14.6	16.1	14.2	14.1
mg*	69.8	70.6	69.5	72.8	74.0	67.5	68.3	73.8	74.9	72.1	73.7	69.0	69.8	76.0	75.9	74.4	71.5	74.2	77.7	75.4	77.9	76.3	73.5	77.7	70.3	73.6	70.6	69.2	71.1	71.6

Appendix 3-2 (Continued).

Locality	DEN CHAI, DC																KHOK SAMRAN, KS												
Occurrence	Groundmass																Groundmass			Ophimottled texture in groundmass									
Analysis No	DC1K-CPX3	DC1K-CPX6	DC1K-CPX7	DC263-CPX2	DC3-CPX1	DC3-CPX2	DC3-CPX4	DC3-CPX5	DC3-CPX6	DC3-CPX7	DC3-CPX8	DC3-CPX9	DC3-CPX10	DC3-CPX11	DC376A-CPX2	DC376A-CPX3	KS1-CPX1	KS1X-CPX2	KS1X-CPX4	KS211-CPX1	KS211-CPX2	KS211-CPX3	KS211-CPX4	KS211-CPX5	KS211-CPX6	KS211-CPX7	KS211-CPX8	KS213-CPX1	KS213-CPX2	KS213-CPX3
SiO_2	48.36	46.87	47.85	45.90	45.81	44.27	47.44	45.80	44.13	47.82	44.46	48.04	46.04	47.64	47.43	44.29	49.62	49.64	49.83	47.04	47.75	47.69	47.48	48.21	46.21	45.61	47.52	47.59	47.77	48.64
TiO_2	2.26	2.64	2.43	3.53	2.96	3.99	2.96	3.21	4.29	2.53	3.61	2.55	3.46	2.50	2.65	4.25	1.70	1.67	1.62	3.07	2.79	2.66	2.86	2.81	3.36	3.32	2.90	2.28	2.61	3.48
Al_2O_3	4.45	5.60	5.19	6.63	6.41	8.61	5.73	6.74	8.20	6.12	8.01	4.83	7.10	5.19	5.81	8.16	3.14	3.12	2.73	5.86	5.07	4.95	5.02	4.14	5.87	6.22	4.56	4.77	4.77	4.23
Fe_2O_3	4.03	2.88	2.64	3.45	3.86	2.52	1.10	3.46	4.80	3.10	3.79	2.32	3.51	3.08	1.97	1.66	3.35	1.62	2.38	3.77	2.80	4.56	3.61	3.34	3.90	3.96	4.23	3.60	4.39	1.47
FeO	3.12	4.95	5.15	5.22	4.07	5.87	6.67	4.14	3.41	4.31	4.32	5.74	4.00	4.54	5.30	6.38	4.58	6.29	5.97	5.84	6.23	4.77	5.86	6.13	6.12	5.85	5.36	5.68	4.95	8.34
MnO	0	0	0	0.21	0.21	0	0	0	0	0.25	0	0	0	0	0	0	0	0	0.225	0.109	0	0.208	0.198	0	0	0	0.299	0	0.294	0.203
MgO	13.48	12.81	13.19	11.73	12.54	11.46	12.91	12.51	11.51	13.34	11.72	13.13	12.35	13.24	12.97	11.24	13.91	13.46	13.52	12.27	12.47	12.90	12.56	12.71	12.04	11.85	12.68	12.73	12.77	12.10
CaO	22.28	21.96	22.06	21.92	21.90	21.91	21.58	22.06	22.16	21.67	22.17	21.77	22.29	21.90	22.17	22.10	21.65	21.71	21.67	21.90	21.64	21.84	21.61	21.53	21.54	21.41	21.63	21.76	21.87	21.56
Na_2O	0.90	0.65	0.54	0.72	0.71	0.57	0.60	0.77	0.93	0.76	0.76	0.72	0.86	0.75	0.59	0.58	0.81	0.72	0.79	0.68	0.74	0.75	0.69	0.82	0.67	0.68	0.75	0.59	0.74	0.77
K_2O	0	0	0	0	0	0	0	0	0	0	0	0	0	0	0	0	0.00	0.00	0.00	0.00	0.00	0.00	0.00	0.00	0.00	0.00	0.00	0.00	0.00	0.00
Cr_2O_3	0	0	0.20	0	0	0	0	0	0.19	0	0	0	0	0	0	0	0	0	0	0	0	0	0	0	0	0	0	0	0	0
Total	98.87	98.62	99.25	99.60	98.71	99.66	99.36	98.99	99.62	100.20	99.19	99.41	99.82	99.07	99.61	98.97	98.76	98.52	99.06	100.54	99.48	100.32	99.90	99.68	99.70	98.90	99.92	99.00	100.16	100.80
Numbers of ions on the basis of 6 O																														
Si	1.814	1.771	1.796	1.730	1.732	1.666	1.779	1.724	1.660	1.772	1.677	1.800	1.719	1.787	1.773	1.679	1.864	1.873	1.873	1.756	1.796	1.780	1.782	1.812	1.743	1.734	1.785	1.799	1.787	1.816
Ti	0.064	0.075	0.068	0.100	0.084	0.113	0.083	0.091	0.121	0.070	0.102	0.072	0.097	0.070	0.075	0.121	0.048	0.047	0.046	0.086	0.079	0.075	0.081	0.079	0.095	0.095	0.082	0.065	0.073	0.098
Al	0.197	0.249	0.230	0.294	0.285	0.382	0.253	0.299	0.364	0.267	0.356	0.213	0.312	0.229	0.256	0.365	0.139	0.139	0.121	0.258	0.225	0.218	0.222	0.183	0.261	0.279	0.202	0.212	0.210	0.186
Fe^{3+}	0.114	0.082	0.075	0.098	0.110	0.071	0.031	0.098	0.136	0.087	0.107	0.066	0.099	0.087	0.055	0.047	0.095	0.046	0.067	0.106	0.079	0.128	0.102	0.095	0.111	0.113	0.119	0.102	0.123	0.041
Fe^{2+}	0.098	0.157	0.162	0.165	0.129	0.185	0.209	0.130	0.107	0.133	0.136	0.180	0.125	0.143	0.166	0.202	0.144	0.199	0.188	0.182	0.196	0.149	0.184	0.193	0.193	0.186	0.168	0.180	0.155	0.260
Mn	0	0	0	0.007	0.007	0	0	0	0	0.008	0	0	0	0	0	0	0	0	0.007	0.003	0	0.007	0.006	0	0	0	0.010	0	0.009	0.006
Mg	0.754	0.722	0.738	0.659	0.707	0.643	0.722	0.702	0.645	0.737	0.659	0.733	0.687	0.741	0.723	0.635	0.779	0.757	0.758	0.683	0.699	0.718	0.703	0.712	0.677	0.671	0.710	0.717	0.712	0.673
Ca	0.895	0.889	0.887	0.885	0.887	0.883	0.867	0.890	0.893	0.860	0.896	0.874	0.892	0.880	0.888	0.898	0.872	0.878	0.873	0.876	0.872	0.873	0.869	0.867	0.871	0.872	0.870	0.881	0.876	0.862
Na	0.066	0.048	0.039	0.053	0.052	0.042	0.044	0.056	0.068	0.055	0.055	0.052	0.063	0.055	0.043	0.042	0.059	0.053	0.058	0.049	0.054	0.054	0.050	0.060	0.049	0.050	0.054	0.043	0.054	0.056
K	0	0	0	0	0	0.004	0	0	0	0.004	0	0	0	0	0	0	0	0	0	0	0	0	0	0	0	0	0	0	0	0	0
Cr	0	0	0.006	0	0	0	0	0	0.006	0	0	0	0	0	0	0	0	0	0	0	0	0	0	0	0	0	0	0	0	0	0
Total	4.000	4.000	4.000	4.000	4.000	4.000	4.000	4.000	4.000	4.000	4.000	4.000	4.000	4.000	4.000	4.000	4.000	4.000	4.000	4.000	4.000	4.000	4.000	4.000	4.000	4.000	4.000	4.000	4.000	4.000
Ca%(Wo%)	48.1	48.1	47.7	48.8	48.2	49.6	47.4	48.9	50.1	47.1	49.8	47.2	49.5	47.6	48.5	50.3	46.1	46.7	46.1	47.3	47.2	46.6	46.6	46.5	47.0	47.3	46.4	46.9	46.7	46.8
Mg%(En%)	40.5	39.0	39.6	36.3	38.4	36.1	39.5	38.6	36.2	40.4	36.6	39.6	38.1	40.0	39.5	35.6	41.2	40.3	40.0	36.9	37.9	38.3	37.7	38.2	36.6	36.4	37.8	38.1	37.9	36.5
ΣFe%(Fs%)	11.4	12.9	12.7	14.8	13.3	14.4	13.1	12.5	13.6	12.5	13.6	13.2	12.4	12.4	12.1	14.0	12.6	13.0	13.8	15.8	14.9	15.1	15.7	15.4	16.4	16.2	15.8	15.0	15.3	16.7
mg*	78.1	75.2	75.7	71.0	74.3	71.5	75.0	75.5	72.6	76.4	73.0	74.9	75.5	76.4	76.6	71.8	76.6	75.6	74.3	70.1	71.8	71.7	70.6	71.2	69.0	69.2	70.5	71.8	71.2	68.6

Appendix 3-2 (Continued).

Locality	KHOK SAMRAN, KS																	BO PHLOI, BP												
Occurrence	Ophimottled texture in groundmass																	Phenocryst										Microphenocryst		
Analysis No	KS213-CPX4	KS213-CPX5	KS213-CPX6	KS213-CPX7	KS213-CPX8	KS213-CPX9	KS214-CPX1	KS214-CPX2	KS214-CPX3	KS214-CPX4	KS214-CPX5	KS214-CPX6	KS214-CPX7	KS214-CPX8	KS214-CPX9	KS3-CPX1	KS3-CPX3	BP733-CPX1	BP734-CPX2	BP922-CPX9	BP922-CPX11	BP922-CPX12	BP924-CPX12	BP930-CPX1	BP930-CPX2	BP930-CPX4	BP930-CPX5	BP922-CPX10	BP925-CPX1	BP925-CPX2
SiO_2	47.27	49.75	48.04	46.25	46.83	49.07	48.99	47.83	47.88	47.86	49.89	46.94	47.85	46.46	46.83	50.09	50.08	47.90	53.18	50.04	52.81	50.55	49.92	45.27	49.81	50.53	48.03	50.96	45.43	49.99
TiO_2	3.04	1.81	2.77	3.33	2.75	1.88	2.69	3.20	2.62	2.69	1.92	2.74	2.87	3.33	3.01	1.60	1.55	2.45	0.53	2.32	0.00	1.82	2.01	2.94	1.67	1.97	2.66	1.70	3.16	1.41
Al_2O_3	4.45	2.33	4.31	5.21	5.28	3.44	3.80	5.08	4.84	4.86	2.82	4.95	4.42	5.72	5.62	2.49	2.54	4.80	0.77	3.94	0.62	3.79	3.73	4.32	5.42	3.54	4.95	3.26	6.96	2.98
Fe_2O_3	2.24	2.04	4.33	4.09	5.02	3.67	2.61	4.36	3.75	2.51	2.70	3.81	2.51	4.27	3.47	1.08	1.54	2.26	2.17	2.82	1.56	3.31	3.75	11.15	2.85	4.53	4.66	3.06	5.95	3.28
FeO	6.95	6.85	5.50	5.63	4.75	5.35	7.03	5.52	5.68	6.54	6.34	5.61	6.55	5.28	6.08	6.94	7.13	8.41	5.81	4.63	8.87	4.09	3.58	1.94	4.09	2.61	3.12	3.98	2.49	4.09
MnO	0.197	0	0	0	0	0	0	0.269	0	0	0	0	0	0	0	0.215	0	0	0.47	0.21	0.82	0	0	0.25	0.06	0.24	0	0	0.23	0.16
MgO	12.10	13.79	12.66	12.27	12.42	13.76	12.62	12.35	12.63	12.67	13.65	12.63	12.49	12.05	12.35	13.48	13.28	12.39	14.35	13.05	11.51	13.58	13.37	11.81	13.82	13.85	12.79	13.77	11.86	13.23
CaO	21.59	21.50	21.67	21.35	21.69	21.61	21.86	21.79	22.06	21.75	21.49	21.86	21.90	21.77	21.82	21.13	21.39	20.25	21.61	22.79	24.57	22.90	22.84	21.55	21.98	23.00	23.69	22.85	23.33	23.06
Na_2O	0.62	0.46	0.89	0.75	0.82	0.60	0.75	0.94	0.68	0.58	0.68	0.53	0.63	0.84	0.57	0.76	0.69	0.66	0.97	1.00	0.32	0.96	1.04	1.28	0.89	1.12	0.77	1.01	0.74	0.79
K_2O	0.00	0.00	0.00	0.00	0.00	0.00	0.00	0.00	0.00	0.00	0.00	0.00	0.00	0.00	0.00	0.00	0.09	0	0	0	0	0	0	0	0	0	0	0	0	0
Cr_2O_3	0	0.179	0	0	0	0	0	0	0	0	0.217	0	0.181	0	0	0	0	0.27	0	0	0.20	0	0.21	0	0.41	0	0	0	0.23	0
Total	98.45	98.71	100.17	98.87	99.55	99.37	100.34	101.34	100.14	99.44	99.71	99.07	99.40	99.73	99.75	98.01	98.50	99.38	99.87	100.79	101.27	101.00	100.44	100.50	100.99	101.40	100.66	100.58	100.37	98.99
Numbers of ions on the basis of 6 O																														
Si	1.804	1.882	1.798	1.757	1.764	1.841	1.831	1.773	1.792	1.801	1.868	1.777	1.805	1.749	1.762	1.900	1.895	1.811	1.973	1.847	1.973	1.856	1.845	1.709	1.824	1.847	1.780	1.876	1.698	1.877
Ti	0.087	0.051	0.078	0.095	0.078	0.053	0.076	0.089	0.074	0.076	0.054	0.078	0.081	0.094	0.085	0.046	0.044	0.070	0.015	0.064	0	0.050	0.056	0.084	0.046	0.054	0.074	0.047	0.089	0.040
Al	0.200	0.104	0.190	0.233	0.234	0.152	0.167	0.222	0.213	0.216	0.124	0.221	0.197	0.254	0.249	0.111	0.113	0.214	0.033	0.171	0.027	0.164	0.163	0.192	0.234	0.153	0.216	0.141	0.307	0.132
Fe^{3+}	0.064	0.058	0.122	0.117	0.142	0.104	0.073	0.121	0.106	0.071	0.076	0.108	0.071	0.121	0.098	0.031	0.044	0.064	0.061	0.078	0.044	0.092	0.104	0.317	0.079	0.125	0.130	0.085	0.167	0.093
Fe^{2+}	0.222	0.217	0.172	0.179	0.149	0.168	0.220	0.171	0.178	0.206	0.199	0.178	0.207	0.166	0.191	0.220	0.226	0.266	0.180	0.143	0.277	0.125	0.111	0.061	0.125	0.080	0.097	0.123	0.078	0.128
Mn	0.006	0	0	0	0	0	0	0.008	0	0	0	0	0	0	0	0.007	0	0	0.015	0.007	0.026	0	0	0.008	0.002	0.007	0	0	0.007	0.005
Mg	0.688	0.777	0.707	0.695	0.697	0.770	0.703	0.683	0.704	0.711	0.762	0.713	0.702	0.676	0.693	0.763	0.749	0.698	0.794	0.718	0.641	0.743	0.736	0.665	0.754	0.754	0.707	0.756	0.660	0.740
Ca	0.882	0.871	0.869	0.869	0.875	0.869	0.875	0.865	0.884	0.877	0.862	0.886	0.885	0.878	0.880	0.859	0.867	0.820	0.859	0.901	0.983	0.901	0.904	0.871	0.862	0.901	0.941	0.901	0.934	0.928
Na	0.046	0.034	0.064	0.055	0.060	0.044	0.054	0.067	0.050	0.042	0.050	0.039	0.046	0.062	0.042	0.056	0.051	0.048	0.070	0.071	0.023	0.068	0.075	0.094	0.063	0.080	0.055	0.072	0.053	0.058
K	0	0	0	0	0	0	0	0	0	0	0	0	0	0	0	0	0.004	0	0	0	0	0	0	0	0	0	0	0	0	0
Cr	0	0.005	0	0	0	0	0	0	0	0	0.006	0	0.005	0	0	0	0	0.008	0	0	0.006	0	0.006	0	0.012	0	0	0	0.007	0
Total	4.000	4.000	4.000	4.000	4.000	4.000	4.000	4.000	4.000	4.000	4.000	4.000	4.000	4.000	4.000	4.000	4.000	4.000	4.000	4.000	4.000	4.000	4.000	4.000	4.000	4.000	4.000	4.000	4.000	4.000
Ca%(Wo%)	47.4	45.3	46.5	46.7	46.9	45.5	46.8	46.8	47.2	47.0	45.4	47.0	47.5	47.7	47.2	45.7	46.0	44.4	45.0	48.8	49.9	48.4	48.7	45.3	47.3	48.2	50.2	48.3	50.6	49.0
Mg%(En%)	36.9	40.4	37.8	37.4	37.4	40.3	37.6	36.9	37.6	38.1	40.1	37.8	37.6	36.7	37.2	40.6	39.7	37.8	41.6	38.9	32.5	39.9	39.7	34.6	41.4	40.4	37.7	40.5	35.8	39.1
ΣFe%(Fs%)	15.7	14.3	15.7	15.9	15.7	14.2	15.7	16.3	15.1	14.8	14.5	15.2	14.9	15.6	15.5	13.7	14.3	17.9	13.4	12.3	17.6	11.7	11.6	20.1	11.3	11.3	12.1	11.1	13.7	11.9
mg*	70.2	73.9	70.6	70.2	70.5	73.9	70.6	69.4	71.3	72.0	73.5	71.4	71.6	70.2	70.5	74.7	73.5	67.9	75.6	75.9	64.9	77.4	77.4	63.3	78.6	78.1	75.7	78.5	72.3	76.6

Appendix 3-CPX (Continued).

Locality	BO PHLOI, BP																												
Occurrence	MicroPH.	Groundmass																											
Analysis No	BP925-CPX3	PB736-CPX1	PB736-CPX2	PB736-CPX5	BP82-CPX1	BP82-CPX2	BP82-CPX3	BP82-CPX4	BP82A-CPX1	BP82A-CPX2	BP82A-CPX3	BP82A-CPX4	BP82A-CPX5	BP82A-CPX6	BP82A-CPX8	BP82A-CPX9	BP83-CPX1	BP921-CPX6	BP921A-CPX1	BP921A-CPX2	BP921A-CPX3	BP921A-CPX4	BP921A-CPX5	BP921A-CPX6	BP921A-CPX7	BP921A-CPX8	BP921B-CPX1	BP921B-CPX2	BP921B-CPX3
SiO_2	50.20	51.28	44.71	46.50	48.18	45.61	48.15	48.60	50.20	49.73	51.20	44.19	45.64	48.46	46.24	50.35	50.86	46.13	44.87	47.40	47.48	44.52	43.56	47.75	48.45	49.60	50.05	52.29	47.58
TiO_2	1.72	0.51	2.37	2.37	2.15	3.19	2.19	2.18	1.34	1.97	1.13	3.81	3.21	1.97	2.81	1.82	1.34	2.80	3.13	2.59	1.46	3.87	4.08	1.97	2.33	1.43	1.45	1.17	2.10
Al_2O_3	2.90	7.49	6.94	7.59	4.67	8.55	5.63	4.35	2.99	4.25	2.79	9.11	7.46	4.69	5.79	3.67	2.81	8.45	7.09	5.67	3.49	7.52	8.48	4.10	5.32	3.96	4.61	1.78	4.62
Fe_2O_3	2.56	1.25	10.17	5.34	3.85	3.47	2.31	3.05	1.62	2.93	2.31	2.84	4.57	2.63	3.39	2.32	3.87	3.67	4.49	4.80	1.68	3.52	6.75	1.56	4.04	3.14	2.98	1.80	2.96
FeO	4.84	2.42	0.61	1.81	3.79	3.75	4.60	4.01	5.48	4.62	5.45	5.21	4.11	4.24	6.66	4.91	3.88	3.42	4.54	3.20	5.76	4.65	2.58	5.35	3.76	3.87	3.75	5.95	4.72
MnO	0	0	0.20	0	0	0	0	0.25	0	0	0.21	0	0.27	0	0	0	0.27	0	0	0	0	0.23	0	0	0	0.20	0	0.19	0
MgO	13.25	15.72	15.05	11.96	13.00	11.66	12.63	13.17	13.70	13.37	13.83	11.06	11.73	13.36	11.18	13.75	13.18	11.81	11.62	12.63	12.50	11.08	11.15	12.85	12.78	13.57	13.76	14.01	12.70
CaO	22.60	18.21	18.35	22.14	23.17	21.96	22.49	23.11	23.61	22.36	22.40	21.39	22.50	22.51	21.86	21.91	23.55	22.52	22.46	22.55	23.70	22.31	22.10	23.12	22.32	22.49	22.15	22.45	22.91
Na_2O	0.90	1.73	0.96	1.34	0.62	1.02	0.78	0.59	0.93	0.99	0.82	1.03	0.87	0.76	0.85	1.04	0.91	0.94	0.78	1.01	0.79	0.92	1.26	0.61	1.27	1.01	0.97	0.89	0.84
K_2O	0	0	0	0	0	0	0	0	0	0	0	0	0	0	0	0	0	0	0.09	0.11	0	0.11	0.12	0	0	0	0	0.06	0.11
Cr_2O_3	0.20	0.94	0.38	0.60	0	0.52	0	0	0	0	0	0	0	0	0	0	0	0.74	0	0	0	0	0.18	0	0	0	0.34	0	0
Total	99.17	99.55	99.74	99.65	99.42	99.72	98.77	99.29	101.65	100.45	100.39	99.02	100.72	98.96	99.14	100.01	100.67	100.47	99.77	100.27	98.82	99.27	100.85	98.20	100.75	100.03	100.06	100.88	99.62
Numbers of ions on the basis of 6 O																													
Si	1.881	1.856	1.667	1.732	1.805	1.703	1.809	1.821	1.831	1.837	1.892	1.667	1.698	1.815	1.756	1.863	1.880	1.709	1.687	1.761	1.792	1.683	1.622	1.809	1.786	1.835	1.848	1.923	1.780
Ti	0.049	0.014	0.066	0.066	0.060	0.089	0.062	0.061	0.037	0.055	0.031	0.108	0.090	0.055	0.080	0.051	0.037	0.078	0.089	0.072	0.041	0.110	0.114	0.056	0.065	0.040	0.040	0.032	0.059
Al	0.128	0.320	0.305	0.333	0.206	0.376	0.249	0.192	0.129	0.185	0.121	0.405	0.327	0.207	0.259	0.160	0.123	0.369	0.314	0.248	0.155	0.335	0.372	0.183	0.231	0.172	0.200	0.077	0.204
Fe^{3+}	0.072	0.034	0.285	0.150	0.108	0.097	0.065	0.086	0.044	0.081	0.064	0.081	0.128	0.074	0.097	0.064	0.108	0.102	0.127	0.134	0.048	0.100	0.189	0.044	0.112	0.087	0.083	0.050	0.083
Fe^{2+}	0.152	0.073	0.019	0.056	0.119	0.117	0.145	0.126	0.167	0.143	0.168	0.164	0.128	0.133	0.212	0.152	0.120	0.106	0.143	0.099	0.182	0.147	0.081	0.170	0.116	0.120	0.116	0.183	0.148
Mn	0	0	0.006	0	0	0	0	0.008	0	0	0.006	0	0.008	0	0	0	0.008	0	0	0	0	0.007	0	0	0	0.006	0	0.006	0
Mg	0.740	0.848	0.837	0.664	0.726	0.649	0.708	0.736	0.745	0.736	0.762	0.622	0.651	0.746	0.633	0.759	0.726	0.653	0.651	0.700	0.703	0.625	0.619	0.726	0.702	0.748	0.757	0.768	0.708
Ca	0.907	0.706	0.733	0.884	0.930	0.878	0.905	0.928	0.923	0.885	0.887	0.865	0.897	0.903	0.889	0.869	0.933	0.894	0.905	0.897	0.958	0.903	0.882	0.938	0.882	0.891	0.876	0.885	0.918
Na	0.065	0.121	0.069	0.097	0.045	0.074	0.057	0.043	0.066	0.071	0.058	0.075	0.063	0.055	0.063	0.075	0.065	0.067	0.057	0.073	0.058	0.067	0.091	0.044	0.091	0.072	0.070	0.064	0.061
K	0	0	0	0	0	0	0	0	0	0	0	0	0	0	0	0	0	0	0.004	0.005	0	0.005	0.006	0	0	0	0	0.003	0.005
Cr	0.006	0.027	0.011	0.018	0	0.015	0	0	0	0	0	0	0	0	0	0	0	0.022	0	0	0	0	0.005	0	0	0	0.010	0	0
Total	4.000	4.000	4.000	4.000	4.000	4.000	4.000	4.000	4.000	4.000	4.000	4.000	4.000	4.000	4.000	4.000	4.000	4.000	4.000	4.000	4.000	4.000	4.000	4.000	4.000	4.000	4.000	4.000	4.000
Ca%(Wo%)	48.5	42.5	39.0	50.4	49.4	50.4	49.7	49.3	49.1	48.0	47.0	49.9	49.5	48.7	48.6	47.1	49.2	50.9	49.6	49.0	50.7	50.7	49.8	50.0	48.7	48.1	47.8	46.8	49.4
Mg%(En%)	39.6	51.0	44.5	37.9	38.6	37.3	38.8	39.1	39.6	39.9	40.4	35.9	35.9	40.2	34.6	41.1	38.3	37.2	35.7	38.2	37.2	35.0	35.0	38.6	38.8	40.4	41.3	40.6	38.1
∑Fe%(Fs%)	12.0	6.5	16.5	11.8	12.1	12.3	11.5	11.6	11.3	12.1	12.7	14.2	14.6	11.1	16.8	11.7	12.5	11.9	14.8	12.8	12.1	14.3	15.2	11.4	12.6	11.5	10.8	12.6	12.4
mg*	76.8	88.8	72.9	76.3	76.2	75.2	77.1	77.0	77.9	76.7	76.1	71.7	71.1	78.3	67.2	77.8	75.5	75.8	70.7	75.0	75.4	71.0	69.7	77.2	75.5	77.8	79.2	76.3	75.4

Appendix 3-2 (Continued).

Locality	BO PHLOI, BP														NAM YUN, NY														
Occurrence	Groundmass														Phenocryst		Phenocryst (core)							Microphenocryst						
Analysis No	BP921B-CPX4	BP921B-CPX5	BP921B-CPX6	BP921B-CPX7	BP921B-CPX8	BP924-CPX11	BP924-CPX13	BP924-CPX14	BP924A-CPX1	BP924A-CPX2	BP924A-CPX3	BP924A-CPX4	BP924A-CPX5	BP924A-CPX6	NY133-CPX2	NY133-CPX3	NY132-CPX4	NY132-CPX5	NY132-CPX11	NY132-CPX12	NY132-CPX13	NY133-CPX1	NY132-CPX8	NY131-CPX1	NY131-CPX2	NY131-CPX3	NY131-CPX4	NY131-CPX5	NY131-CPX6	NY131-CPX7
SiO_2	49.92	50.02	52.87	45.66	48.55	47.21	48.86	49.52	49.98	46.48	49.08	45.06	47.85	50.98	50.87	48.45	51.21	50.70	51.11	51.29	49.58	50.25	51.38	49.92	51.40	49.76	49.25	49.57	51.00	50.37
TiO_2	1.87	2.02	0.45	3.11	1.78	2.62	2.11	1.83	1.71	2.85	2.21	3.10	2.44	1.24	1.11	2.41	1.75	1.67	1.83	1.43	2.01	1.85	1.63	2.22	1.47	1.84	2.77	1.92	1.42	2.00
Al_2O_3	4.20	3.98	0.73	7.03	4.51	5.99	4.37	6.27	3.80	5.73	4.25	7.00	5.40	3.41	2.44	3.92	2.06	2.17	2.26	1.96	3.78	2.01	2.07	3.82	2.25	3.58	3.69	3.11	2.50	2.37
Fe_2O_3	2.97	3.53	0.61	4.30	3.12	5.54	4.38	0.00	3.02	3.29	1.00	3.96	3.02	2.48	1.63	3.16	2.69	1.78	1.85	2.40	1.90	0.60	1.90	3.12	2.25	3.29	2.86	1.77	2.27	3.14
FeO	4.33	3.86	10.31	3.89	4.23	2.27	3.25	6.60	4.29	4.66	6.35	4.43	4.57	4.94	5.76	5.62	6.85	7.04	7.56	5.82	6.38	8.30	7.51	5.50	6.12	4.95	7.11	6.33	6.55	6.53
MnO	0	0	0.41	0.20	0.24	0	0.21	0.27	0	0	0	0.27	0	0.28	0	0	0.21	0	0	0.22	0	0	0.26	0	0	0	0	0	0	0.27
MgO	13.38	13.51	12.09	11.61	13.18	11.71	12.71	11.54	13.41	12.54	12.96	11.41	12.63	13.65	14.56	12.81	13.53	13.67	13.51	14.52	13.42	13.18	13.36	13.52	14.30	13.77	12.55	13.46	14.06	13.15
CaO	22.22	22.06	21.54	22.44	22.72	22.70	22.70	20.67	22.01	22.48	21.97	22.41	22.64	22.15	21.55	21.11	21.84	21.84	22.31	21.91	22.17	21.26	22.17	22.31	21.95	22.16	22.13	21.90	21.50	22.01
Na_2O	1.02	1.25	0.91	0.92	1.17	1.42	1.11	1.48	0.99	0.63	0.78	0.98	0.77	1.01	0.65	1.08	0.79	0.59	0.55	0.57	0.52	0.67	0.63	0.76	0.66	0.71	0.76	0.57	0.67	0.78
K_2O	0	0.09	0	0	0	0	0	0	0.11	0.09	0	0.10	0.15	0	0	0	0	0	0	0	0	0	0	0	0	0	0	0	0	0
Cr_2O_3	0	0.45	0	0	0	0	0	0	0	0	0	0	0	0	0.35	0	0	0	0	0.27	0.30	0	0	0.19	0.19	0.30	0	0.20	0	0
Total	99.91	101.05	100.16	99.35	100.90	99.45	99.68	98.18	99.31	99.17	98.86	99.68	99.78	100.40	99.18	98.76	100.92	99.45	100.97	100.38	100.06	98.31	100.92	101.36	100.59	100.35	101.12	98.83	99.97	100.61
Numbers of ions on the basis of 6 O																														
Si	1.851	1.835	1.984	1.719	1.786	1.768	1.823	1.864	1.864	1.751	1.845	1.694	1.786	1.881	1.899	1.830	1.897	1.901	1.894	1.900	1.848	1.909	1.905	1.837	1.900	1.846	1.829	1.869	1.898	1.876
Ti	0.052	0.056	0.013	0.088	0.049	0.074	0.059	0.052	0.048	0.081	0.063	0.088	0.069	0.034	0.031	0.068	0.049	0.047	0.051	0.040	0.056	0.053	0.045	0.061	0.041	0.051	0.077	0.054	0.040	0.056
Al	0.184	0.172	0.032	0.312	0.196	0.264	0.192	0.278	0.167	0.254	0.188	0.310	0.237	0.148	0.107	0.174	0.090	0.096	0.099	0.085	0.166	0.090	0.090	0.166	0.098	0.156	0.161	0.138	0.109	0.104
Fe^{3+}	0.083	0.097	0.017	0.122	0.086	0.156	0.123	0	0.085	0.093	0.028	0.112	0.085	0.069	0.046	0.090	0.075	0.050	0.052	0.067	0.053	0.017	0.053	0.086	0.063	0.092	0.080	0.050	0.064	0.088
Fe^{2+}	0.134	0.118	0.324	0.122	0.130	0.071	0.101	0.208	0.134	0.147	0.199	0.139	0.143	0.152	0.180	0.177	0.212	0.221	0.234	0.180	0.199	0.264	0.233	0.169	0.189	0.153	0.221	0.200	0.204	0.203
Mn	0	0	0.013	0.006	0.007	0	0.007	0.009	0	0	0	0.009	0	0.009	0	0	0.007	0	0	0.007	0	0	0.008	0	0	0	0	0	0	0.008
Mg	0.740	0.739	0.677	0.652	0.723	0.654	0.707	0.648	0.746	0.704	0.726	0.639	0.703	0.751	0.810	0.721	0.747	0.764	0.746	0.802	0.746	0.747	0.739	0.741	0.788	0.761	0.695	0.757	0.780	0.730
Ca	0.883	0.867	0.866	0.905	0.896	0.911	0.908	0.834	0.880	0.907	0.885	0.902	0.905	0.876	0.862	0.854	0.867	0.877	0.886	0.870	0.885	0.865	0.881	0.879	0.869	0.880	0.881	0.885	0.857	0.878
Na	0.073	0.089	0.066	0.067	0.083	0.103	0.080	0.108	0.071	0.046	0.057	0.072	0.055	0.072	0.047	0.079	0.056	0.043	0.039	0.041	0.037	0.049	0.045	0.054	0.047	0.051	0.055	0.041	0.048	0.056
K	0	0.004	0	0	0	0	0	0	0.005	0.004	0	0.005	0.007	0	0	0	0	0	0	0	0	0	0	0	0	0	0	0	0	0
Cr	0	0.013	0	0	0	0	0	0	0	0	0	0	0	0	0.010	0	0	0	0	0.008	0.009	0	0	0.006	0.006	0.009	0	0.006	0	0
Total	4.000	4.000	4.000	4.000	4.000	4.000	4.000	4.000	4.000	4.000	4.000	4.000	4.000	4.000	4.000	4.000	4.000	4.000	4.000	4.000	4.000	4.000	4.000	4.000	4.000	4.000	4.000	4.000	4.000	4.000
Ca%(Wo%)	48.0	47.6	45.7	50.1	48.6	50.8	49.2	49.1	47.7	49.0	48.1	50.1	49.3	47.2	45.4	46.4	45.4	45.9	46.2	45.2	47.0	45.7	46.0	46.9	45.5	46.7	46.9	46.8	45.0	46.0
Mg%(En%)	40.2	40.6	35.7	36.1	39.2	36.5	38.3	38.2	40.5	38.0	39.5	35.5	38.3	40.4	42.7	39.1	39.2	40.0	38.9	41.6	39.6	39.5	38.6	39.5	41.3	40.4	37.0	40.0	41.0	38.3
∑Fe%(Fs%)	11.8	11.8	18.6	13.9	12.2	12.7	12.5	12.7	11.8	13.0	12.4	14.4	12.4	12.4	11.9	14.5	15.4	14.2	14.9	13.2	13.4	14.8	15.4	13.6	13.2	13.0	16.0	13.2	14.0	15.7
mg*	77.3	77.4	65.7	72.2	76.3	74.2	75.4	75.0	77.4	74.6	76.1	71.1	75.5	76.6	78.2	72.9	71.8	73.8	72.3	75.9	74.7	72.7	71.5	74.4	75.8	75.6	69.8	75.2	74.5	70.9

Appendix 3-2 (Continued).

Locality	NAM YUN, NY										PHLOI WAEN, PW											TOK PHROM, TP								
Occurrence	Microphenocryst		Microphenocryst (Rim)								Phenocryst							Phenocryst (Core)		Phenocryst (Rim)		Phenocryst			Phenocryst (Spongy core)				Pheno(Clean rim)	
Analysis No	NY131-CPX8	NY131-CPX9	NY133-CPX1	NY132-CPX1	NY132-CPX2	NY132-CPX3	NY132-CPX6	NY132-CPX7	NY132-CPX9	NY132-CPX10	PW121-CPX1	PW15-CPX1	PW18-CPX6	PW18-CPX4	PW215-CPX17	PW319-CPX7	PW319-CPX5	PW15-CPX3	PW15-CPX5	PW15-CPX2	PW15-CPX4	TP1320-CPX4	TP1320-CPX5	TP1330-CPX23	TP1331-CPX4	TP1330-CPX14	TP1330-CPX21	TP13K-CPX2	TP1331-CPX1	TP1331-CPX2
SiO_2	49.33	51.17	48.98	48.57	49.10	48.83	49.10	50.11	49.64	48.59	52.34	52.05	51.68	52.07	52.20	52.08	51.94	51.29	50.56	48.53	45.33	43.55	45.64	47.48	49.27	51.05	48.29	50.20	46.30	47.66
TiO_2	2.22	1.57	2.41	2.98	2.68	3.00	2.56	2.11	2.80	2.72	0.55	0.54	0.47	0.46	0.21	0.53	0.56	0.76	0.79	2.39	3.55	4.93	3.84	3.38	1.94	1.31	2.49	1.48	3.35	3.05
Al_2O_3	3.77	2.76	2.86	4.19	3.62	3.63	3.39	2.22	3.18	3.82	5.75	6.16	5.61	5.52	4.99	6.06	6.11	5.45	5.90	5.11	7.18	8.74	7.14	5.54	5.70	7.60	6.34	3.75	5.53	5.06
Fe_2O_3	3.61	2.22	1.49	0.98	2.92	2.22	2.74	2.74	1.73	2.18	1.78	0.24	0.50	0.00	1.33	0.49	0.70	0.39	1.46	2.78	4.84	5.10	3.46	4.23	0.84	0.00	3.19	0.42	4.90	4.38
FeO	5.26	5.99	9.03	8.34	6.62	8.20	8.06	8.28	8.34	7.62	1.10	2.58	2.25	2.60	1.77	2.33	2.03	6.46	5.22	4.18	2.62	2.91	3.87	3.07	5.93	4.52	4.19	5.13	3.02	3.31
MnO	0	0	0	0	0.21	0.25	0.22	0.27	0.27	0	0	0	0	0	0	0	0	0	0	0	0.213	0	0	0	0.21	0	0	0.23	0.22	0
MgO	13.32	14.36	11.66	12.32	12.67	11.65	11.99	11.60	12.23	12.28	15.16	14.56	15.17	15.00	16.36	14.85	14.91	12.85	12.77	13.09	11.88	11.52	11.83	13.48	13.22	13.74	13.40	14.29	12.72	13.32
CaO	22.07	22.06	21.46	21.67	21.77	21.86	20.83	22.06	21.78	21.82	21.20	20.42	20.59	20.78	21.05	21.15	21.03	21.53	21.33	23.18	23.21	23.01	23.13	23.11	20.41	19.75	21.10	22.14	23.27	23.01
Na_2O	0.80	0.59	0.84	0.58	0.82	0.83	1.01	0.93	0.76	0.66	1.68	1.73	1.42	1.35	1.02	1.47	1.52	1.09	1.26	0.64	0.79	0.77	0.68	0.67	1.03	1.35	1.05	0.58	0.57	0.69
K_2O	0	0	0	0	0	0	0	0	0	0	0	0	0	0	0	0	0	0	0	0	0	0	0	0	0	0	0	0	0	0
Cr_2O_3	0	0.29	0	0	0	0	0	0	0	0	0.82	1.12	0.86	0.77	0.96	0.60	0.57	0	0	0	0	0	0	0	0	0.95	0.31	0.26	0	0.18
Total	100.36	101.01	98.94	99.63	100.41	100.47	99.89	100.33	100.74	99.69	100.37	99.39	98.55	98.55	99.88	99.53	99.36	99.83	99.29	99.90	99.61	100.53	99.89	100.96	98.56	100.28	100.36	98.73	99.88	100.66
Numbers of ions on the basis of 6 O																														
Si	1.834	1.883	1.866	1.830	1.834	1.834	1.850	1.886	1.855	1.831	1.886	1.895	1.897	1.912	1.892	1.892	1.890	1.894	1.874	1.805	1.701	1.626	1.710	1.751	1.845	1.860	1.782	1.875	1.735	1.766
Ti	0.062	0.043	0.069	0.084	0.075	0.085	0.072	0.060	0.079	0.077	0.015	0.015	0.013	0.013	0.006	0.014	0.015	0.021	0.022	0.067	0.100	0.138	0.108	0.094	0.055	0.036	0.069	0.042	0.094	0.085
Al	0.165	0.120	0.128	0.186	0.159	0.161	0.150	0.099	0.140	0.170	0.244	0.264	0.243	0.239	0.213	0.259	0.262	0.237	0.258	0.224	0.318	0.384	0.315	0.241	0.251	0.326	0.275	0.165	0.244	0.221
Fe^{3+}	0.101	0.061	0.043	0.028	0.082	0.063	0.078	0.078	0.049	0.062	0.048	0.007	0.014	0	0.036	0.013	0.019	0.011	0.041	0.078	0.137	0.143	0.098	0.117	0.024	0	0.089	0.012	0.138	0.122
Fe^{2+}	0.163	0.184	0.288	0.263	0.207	0.258	0.254	0.261	0.261	0.240	0.033	0.079	0.069	0.080	0.054	0.071	0.062	0.199	0.162	0.130	0.082	0.091	0.121	0.095	0.186	0.138	0.129	0.160	0.095	0.102
Mn	0	0	0	0	0.007	0.008	0.007	0.009	0.009	0	0	0	0	0	0	0	0	0	0	0	0.007	0	0	0	0.007	0	0	0.007	0.007	0
Mg	0.738	0.788	0.662	0.692	0.706	0.653	0.674	0.651	0.681	0.690	0.814	0.790	0.830	0.821	0.884	0.805	0.809	0.707	0.705	0.726	0.665	0.641	0.661	0.741	0.738	0.746	0.737	0.796	0.711	0.735
Ca	0.879	0.869	0.876	0.875	0.871	0.880	0.841	0.890	0.872	0.881	0.819	0.796	0.810	0.818	0.817	0.824	0.820	0.852	0.847	0.924	0.933	0.920	0.928	0.913	0.819	0.771	0.834	0.886	0.934	0.913
Na	0.058	0.042	0.062	0.042	0.060	0.060	0.073	0.068	0.055	0.048	0.117	0.122	0.101	0.096	0.071	0.104	0.107	0.078	0.091	0.046	0.057	0.056	0.049	0.048	0.075	0.095	0.075	0.042	0.041	0.050
K	0	0	0	0	0	0	0	0	0	0	0	0	0	0	0	0	0	0	0	0	0	0	0	0	0	0	0	0	0	0
Cr	0	0.009	0	0	0	0	0	0	0	0	0.023	0.032	0.025	0.022	0.028	0.017	0.016	0	0	0	0	0	0	0	0	0.027	0.009	0.008	0	0.005
Total	4.000	4.000	4.000	4.000	4.000	4.000	4.000	4.000	4.000	4.000	4.000	4.000	4.000	4.000	4.000	4.000	4.000	4.000	4.000	4.000	4.000	4.000	4.000	4.000	4.000	4.000	4.000	4.000	4.000	4.000
Ca%(Wo%)	46.7	45.7	46.9	47.1	46.5	47.3	45.4	47.1	46.6	47.0	47.8	47.6	47.0	47.6	45.6	48.1	47.9	48.1	48.3	49.7	51.2	51.3	51.3	48.9	46.2	46.6	46.6	47.6	49.6	48.8
Mg%(En%)	39.2	41.4	35.4	37.3	37.7	35.1	36.3	34.5	36.4	36.8	47.5	47.3	48.2	47.8	49.3	47.0	47.3	40.0	40.2	39.1	36.5	35.7	36.6	39.7	41.6	45.1	41.2	42.8	37.7	39.3
ΣFe%(Fs%)	14.0	12.9	17.7	15.6	15.8	17.7	18.3	18.4	17.0	16.1	4.7	5.1	4.8	4.6	5.0	4.9	4.7	11.9	11.5	11.2	12.4	13.0	12.1	11.4	12.2	8.3	12.2	9.6	12.7	12.0
mg*	73.6	76.2	66.7	70.4	70.5	66.5	66.5	65.2	68.2	69.6	90.9	90.3	90.9	91.1	90.8	90.5	90.9	77.1	77.7	77.7	74.7	73.2	75.1	77.8	77.4	84.4	77.2	81.6	74.8	76.6

Appendix 3-2 (Continued).

Locality	TOK PHROM, TP																																
Occurrence	Phenocryst (Clean rim)							Microphenocryst								Groundmass																	
Analysis No	TP1331-CPX7	TP1331-CPX8	TP1330-CPX15	TP1330-CPX16	TP1330-CPX17	TP1330-CPX20	TP324-CPX4	TP1315-CPX1	TP1317-CPX16	TP1317-CPX17	TP1317-CPX18	TP1330-CPX24	TP1331-CPX9	TP1331-CPX10	TP1331-CPX17	TP1319-CPX3	TP1319-CPX4	TP1319-CPX5	TP1331-CPX19	TP1331-CPX20	TP1331-CPX21	TP13B-CPX1	TP13B-CPX2	TP13B-CPX4	TP13K-CPX3	TP324a-CPX1	TP324a-CPX2	TP324a-CPX3	TP324b-CPX1	TP324b-CPX2
SiO_2	47.79	48.81	49.70	47.81	46.31	47.00	42.01	47.84	47.08	42.48	48.52	48.20	46.72	43.84	43.33	46.57	43.08	41.94	48.74	48.57	46.72	48.78	45.70	45.89	45.02	47.14	46.23	43.66	44.03	43.75
TiO_2	3.24	2.62	1.70	3.30	3.36	3.15	5.91	2.62	3.02	5.19	2.34	2.71	3.54	4.63	5.61	3.33	5.14	6.02	2.95	2.77	3.57	2.42	3.86	3.25	3.99	3.19	3.68	4.90	4.79	5.30
Al_2O_3	5.05	4.40	6.74	5.50	6.55	6.00	9.60	5.45	5.60	8.89	4.13	4.40	6.02	8.32	8.54	5.48	8.24	9.06	4.35	4.82	5.47	4.90	6.93	5.74	6.85	5.32	6.84	7.84	8.02	8.43
Fe_2O_3	2.92	3.31	1.51	3.77	3.78	3.80	5.09	3.30	3.32	5.08	3.16	3.49	3.49	5.27	3.36	1.66	4.18	2.93	2.65	2.94	3.69	1.15	1.68	2.98	3.36	3.55	1.80	3.80	3.98	4.36
FeO	4.31	3.65	4.28	3.90	3.56	4.09	3.55	3.97	3.68	4.17	4.55	4.34	6.16	3.10	5.10	6.00	4.79	5.71	6.29	4.86	4.13	6.29	5.68	4.95	4.51	4.83	6.26	4.74	4.35	4.57
MnO	0	0	0	0	0	0	0	0	0	0	0.21	0	0.21	0	0	0	0	0	0	0	0	0	0	0	0	0.22	0	0	0	0
MgO	13.25	13.75	13.14	13.22	12.43	12.54	10.67	13.63	13.07	10.62	13.14	13.45	11.47	11.42	10.84	12.42	11.25	10.26	12.89	13.41	12.98	12.61	12.14	12.14	11.66	12.03	11.54	11.27	11.07	10.62
CaO	23.15	23.15	21.28	23.31	22.68	22.84	22.80	21.29	22.58	22.32	22.71	22.54	22.26	22.96	22.87	22.05	21.68	21.79	22.29	22.57	23.04	22.45	22.44	22.45	22.15	23.39	22.36	22.81	23.15	22.63
Na_2O	0.53	0.62	1.29	0.61	0.78	0.72	0.92	0.87	0.67	0.82	0.61	0.62	0.80	0.80	0.68	0.65	0.89	0.94	0.67	0.62	0.50	0.76	0.59	0.75	0.96	0.97	0.87	0.80	0.91	1.11
K_2O	0	0	0	0	0	0	0	0	0	0	0	0	0	0	0	0	0	0.10	0	0	0	0	0	0	0.10	0	0	0	0.15	0.11
Cr_2O_3	0	0	0.63	0.27	0.49	0.33	0	0	0.19	0.07	0	0.35	0	0.43	0.18	0.17	0	0.17	0	0	0	0.19	0	0	0	0	0	0	0	0
Total	100.24	100.31	100.26	101.68	99.93	100.45	100.80	98.96	99.21	99.64	99.36	100.11	100.66	100.76	100.50	98.66	99.67	99.40	100.82	100.57	100.09	99.82	99.33	98.65	99.11	101.49	100.04	100.36	101.16	101.33
Numbers of ions on the basis of 6 O																																	
Si	1.777	1.807	1.824	1.755	1.729	1.748	1.572	1.791	1.766	1.610	1.820	1.796	1.748	1.636	1.627	1.764	1.627	1.594	1.810	1.799	1.745	1.820	1.719	1.740	1.700	1.741	1.730	1.638	1.637	1.628
Ti	0.091	0.073	0.047	0.091	0.094	0.088	0.166	0.074	0.085	0.148	0.066	0.076	0.099	0.130	0.158	0.095	0.146	0.172	0.082	0.077	0.100	0.068	0.109	0.093	0.113	0.089	0.104	0.138	0.134	0.148
Al	0.221	0.192	0.291	0.238	0.288	0.263	0.423	0.240	0.248	0.397	0.182	0.193	0.265	0.366	0.378	0.244	0.367	0.406	0.190	0.211	0.241	0.216	0.307	0.256	0.305	0.231	0.302	0.346	0.351	0.370
Fe^{3+}	0.082	0.092	0.042	0.104	0.106	0.106	0.143	0.093	0.094	0.145	0.089	0.098	0.098	0.148	0.095	0.047	0.119	0.084	0.074	0.082	0.104	0.032	0.048	0.085	0.096	0.099	0.051	0.107	0.111	0.122
Fe^{2+}	0.134	0.113	0.131	0.120	0.111	0.127	0.111	0.124	0.115	0.132	0.143	0.135	0.193	0.097	0.160	0.190	0.151	0.181	0.195	0.151	0.129	0.196	0.179	0.157	0.142	0.149	0.196	0.149	0.135	0.142
Mn	0	0	0	0	0	0	0	0	0	0	0.007	0	0.007	0	0	0	0	0	0	0	0	0	0	0	0	0.007	0	0	0	0
Mg	0.734	0.759	0.719	0.724	0.692	0.695	0.595	0.761	0.731	0.600	0.735	0.747	0.639	0.635	0.607	0.701	0.633	0.582	0.714	0.740	0.723	0.701	0.681	0.686	0.656	0.662	0.644	0.630	0.614	0.589
Ca	0.923	0.918	0.836	0.917	0.908	0.910	0.914	0.854	0.907	0.906	0.913	0.900	0.892	0.918	0.920	0.895	0.877	0.887	0.887	0.896	0.922	0.898	0.904	0.912	0.896	0.926	0.896	0.917	0.922	0.902
Na	0.038	0.045	0.092	0.043	0.056	0.052	0.067	0.063	0.049	0.060	0.045	0.045	0.058	0.058	0.049	0.047	0.065	0.069	0.048	0.045	0.036	0.055	0.043	0.055	0.070	0.070	0.063	0.058	0.065	0.080
K	0	0	0	0	0	0	0	0	0	0	0	0	0	0	0	0	0	0.005	0	0	0	0	0	0	0.005	0	0	0	0.007	0.005
Cr	0	0	0.018	0.008	0.014	0.010	0	0	0.006	0.002	0	0.010	0	0.013	0.005	0.005	0	0.005	0	0	0	0.006	0	0	0	0	0	0	0	0
Total	4.000	4.000	4.000	4.000	4.000	4.000	4.000	4.000	4.000	4.000	4.000	4.000	4.000	4.000	4.000	4.000	4.000	4.000	4.000	4.000	4.000	4.000	4.000	4.000	4.000	4.000	4.000	4.000	4.000	4.000
Ca%(Wo%)	49.3	48.8	48.4	49.2	49.9	49.5	51.8	46.6	49.1	50.8	48.4	47.9	48.8	51.0	51.6	48.8	49.3	51.2	47.4	47.9	49.1	49.1	49.9	49.6	50.0	50.2	50.2	50.9	51.7	51.4
Mg%(En%)	39.2	40.3	41.6	38.8	38.1	37.8	33.7	41.5	39.6	33.6	39.0	39.7	35.0	35.3	34.1	38.2	35.6	33.5	38.2	39.6	38.5	38.4	37.6	37.3	36.7	36.0	36.0	35.0	34.4	33.6
ΣFe%(Fs%)	11.5	10.9	10.0	12.0	12.0	12.7	14.4	11.9	11.3	15.5	12.7	12.4	16.3	13.6	14.3	12.9	15.2	15.3	14.4	12.5	12.4	12.5	12.5	13.1	13.3	13.8	13.8	14.2	13.8	15.1
mg*	77.3	78.7	80.6	76.4	76.1	74.9	70.1	77.8	77.8	68.4	75.5	76.2	68.3	72.2	70.4	74.7	70.1	68.7	72.6	76.1	75.7	75.4	75.0	73.9	73.4	72.2	72.3	71.1	71.3	69.0

Appendix 3-2 (Continued).

Locality	TOK PHROM, TP				NONG BON, NB																									
Occurrence	Groundmass				Phenocryst							Phenocryst (Core)						Phenocryst (Clean core)			Phenocryst (Rim)								Micropheno.	
Analysis No	TP324b-CPX3	TP324c-CPX1	TP324c-CPX2	TP324c-CPX3	NB131-CPX3	NB133-CPX1	NB133-CPX6	NB51CP-CPX4	NB51CP-CPX7	NB51CP-CPX8	NB51CM-CPX7	NB132-CPX13	NB132-CPX8	NB132-CPX9	NB132-CPX10	NB133-CPX19	NB133-CPX20	NB51CP-CPX1	NB131-CPX1	NB51CP-CPX3	NB131-CPX1	NB132-CPX11	NB133-CPX18	NB132-CPX13	NB133-CPX8	NB133-CPX22	NB51CM-CPX6	NB51CP-CPX1	NB131-CPX5	NB131-CPX6
SiO_2	47.23	45.79	45.87	46.73	47.76	44.60	47.60	51.57	48.61	52.26	44.66	50.25	51.42	51.83	51.73	49.11	47.60	51.27	50.36	48.45	48.70	49.34	46.80	47.61	46.69	46.99	46.56	47.10	52.24	47.66
TiO_2	3.46	4.25	3.95	3.39	2.91	4.07	2.81	0.48	2.49	0.00	3.72	1.50	0.73	0.68	0.58	0.99	0.96	0.69	1.80	1.94	2.76	2.24	3.03	2.75	3.35	3.07	3.12	2.64	0.88	2.74
Al_2O_3	5.21	6.17	5.37	5.58	4.58	7.03	4.60	4.83	3.72	5.59	6.65	3.60	4.31	4.30	4.34	6.44	7.90	5.36	3.90	6.11	4.49	4.14	5.14	4.53	6.02	6.97	9.74	5.14	1.47	4.91
Fe_2O_3	3.72	4.18	3.54	4.67	4.76	4.98	4.10	1.06	3.59	1.29	5.89	2.18	1.18	1.45	1.28	0.00	0.00	0.94	2.77	4.60	2.88	2.43	4.07	3.24	3.40	5.35	4.94	4.43	1.84	4.32
FeO	4.31	5.14	4.92	3.93	2.94	3.37	3.25	3.85	3.66	2.22	2.26	3.51	4.22	3.96	4.02	7.26	9.18	5.96	3.32	3.41	3.95	4.18	3.18	3.66	3.65	2.04	2.60	2.87	6.30	3.30
MnO	0	0	0	0	0	0.26	0	0	0	0	0	0	0	0	0	0	0.20	0	0.22	0	0	0	0.22	0	0	0	0.21	0	0.19	0
MgO	13.24	12.13	12.30	12.20	13.27	11.43	12.77	14.34	13.27	15.87	11.70	13.84	14.69	14.87	14.65	15.78	16.34	13.41	14.01	12.18	13.16	13.25	12.53	12.69	12.08	11.46	9.75	12.00	13.45	12.45
CaO	22.76	22.72	22.54	22.90	23.49	23.43	23.68	22.41	23.58	19.89	23.24	23.38	22.23	22.08	22.11	17.69	14.34	21.19	23.83	21.34	23.66	23.61	23.70	23.47	23.46	21.95	19.90	23.93	22.48	23.50
Na_2O	0.68	0.78	0.58	1.03	0.65	0.64	0.67	0.85	0.61	1.40	0.83	0.71	0.70	0.83	0.84	2.77	3.56	1.06	0.61	1.56	0.65	0.64	0.56	0.66	0.78	1.80	2.76	0.81	0.79	0.83
K_2O	0	0	0.15	0.12	0	0	0	0	0	0	0	0	0	0	0	0	0	0	0	0	0	0	0	0	0	0	0	0	0	0
Cr_2O_3	0	0	0	0	0	0	0	0	0	1.00	0	0	0	0	0	0	0	0	0	0	0	0	0	0	0	0	0	0	0	0
Total	100.92	101.62	99.43	101.15	100.36	99.81	99.48	99.40	99.54	99.52	98.94	98.97	99.48	100.00	99.57	100.05	100.07	99.87	100.81	99.57	100.25	99.81	99.25	98.60	99.44	99.63	99.58	98.93	100.01	99.71
Numbers of ions on the basis of 6 O																														
Si	1.748	1.695	1.732	1.730	1.775	1.681	1.785	1.898	1.819	1.898	1.692	1.874	1.895	1.898	1.902	1.764	1.698	1.889	1.849	1.804	1.808	1.836	1.763	1.799	1.753	1.751	1.730	1.778	1.946	1.784
Ti	0.096	0.118	0.112	0.094	0.081	0.115	0.079	0.013	0.070	0	0.106	0.042	0.020	0.019	0.016	0.027	0.026	0.019	0.050	0.054	0.077	0.063	0.086	0.078	0.095	0.086	0.087	0.075	0.025	0.077
Al	0.227	0.269	0.239	0.243	0.201	0.312	0.203	0.210	0.164	0.239	0.297	0.158	0.187	0.185	0.188	0.273	0.332	0.233	0.169	0.268	0.196	0.182	0.228	0.202	0.266	0.306	0.426	0.229	0.065	0.217
Fe^{3+}	0.103	0.117	0.100	0.130	0.133	0.141	0.116	0.029	0.101	0.035	0.168	0.061	0.033	0.040	0.035	0	0	0.026	0.077	0.129	0.081	0.068	0.115	0.092	0.096	0.150	0.138	0.126	0.051	0.122
Fe^{2+}	0.134	0.159	0.155	0.122	0.092	0.106	0.102	0.119	0.115	0.068	0.072	0.109	0.130	0.121	0.124	0.218	0.274	0.184	0.102	0.106	0.123	0.130	0.100	0.116	0.114	0.064	0.081	0.091	0.196	0.103
Mn	0	0	0	0	0	0.008	0	0	0	0	0	0	0	0	0	0	0.006	0	0.007	0	0	0	0.007	0	0	0	0.007	0	0.006	0
Mg	0.730	0.670	0.693	0.673	0.735	0.642	0.714	0.787	0.740	0.859	0.661	0.769	0.807	0.812	0.803	0.845	0.869	0.737	0.767	0.676	0.728	0.735	0.704	0.715	0.676	0.637	0.540	0.675	0.747	0.695
Ca	0.903	0.901	0.912	0.908	0.936	0.946	0.952	0.884	0.946	0.774	0.943	0.934	0.878	0.866	0.871	0.681	0.548	0.837	0.937	0.851	0.941	0.941	0.956	0.950	0.943	0.876	0.792	0.968	0.897	0.942
Na	0.049	0.056	0.042	0.074	0.047	0.047	0.048	0.061	0.044	0.099	0.061	0.052	0.050	0.059	0.060	0.193	0.246	0.076	0.043	0.112	0.046	0.046	0.041	0.048	0.057	0.130	0.199	0.060	0.057	0.060
K	0	0	0.007	0.005	0	0	0	0	0	0	0	0	0	0	0	0	0	0	0	0	0	0	0	0	0	0	0	0	0	0
Cr	0	0	0	0	0	0	0	0	0	0.029	0	0	0	0	0	0	0	0	0	0	0	0	0	0	0	0	0	0	0	0	0
Total	4.000	4.000	4.000	4.000	4.000	4.000	4.000	4.000	4.000	4.000	4.000	4.000	4.000	4.000	4.000	4.000	4.000	4.000	4.000	4.000	4.000	4.000	4.000	4.000	4.000	4.000	4.000	4.000	4.000	4.000
Ca%(Wo%)	48.3	48.8	49.0	49.5	49.4	51.3	50.5	48.6	49.7	44.6	51.2	49.8	47.5	47.1	47.5	39.0	32.3	46.9	49.6	48.3	50.3	50.2	50.8	50.7	51.6	50.7	50.8	52.0	47.3	50.6
Mg%(En%)	39.1	36.3	37.2	36.7	38.8	34.8	37.9	43.3	38.9	49.5	35.8	41.1	43.7	44.1	43.8	48.5	51.2	41.3	40.6	38.4	38.9	39.2	37.4	38.2	36.9	36.9	34.7	36.3	39.4	37.3
∑Fe%(Fs%)	12.7	14.9	13.7	13.7	11.9	13.9	11.6	8.1	11.3	5.9	13.0	9.1	8.8	8.8	8.7	12.5	16.5	11.8	9.8	13.3	10.8	10.6	11.8	11.1	11.5	12.4	14.5	11.6	13.4	12.1
mg*	75.5	70.8	73.0	72.8	76.6	71.5	76.6	84.2	77.5	89.3	73.4	81.9	83.2	83.4	83.5	79.5	75.6	77.9	80.5	74.2	78.2	78.8	76.0	77.5	76.3	74.9	70.6	75.7	74.6	75.5

Appendix 3-2 (Continued).

Locality	NONG BON, NB																												
Occurrence	Microphenocrysr										Microphenocryst (Spongy)					Groundmass													
Analysis No	NB131-CPX7	NB133-CPX2	NB51OM-CPX1	NB51OM-CPX2	NB51OM-CPX3	NB51OM-CPX4	NB51OM-CPX5	NB5239-CPX3	NB5239-CPX4	NB133-CPX3	NB51OM-CPX1	NB51OM-CPX2	NB51OM-CPX3	NB51OM-CPX4	NB133-CPX3	NB132-CPX15	NB133-CPX5	NB5238A-CPX1	NB5238A-CPX2	NB5238A-CPX3	NB5238A-CPX4	NB5238A-CPX5	NB5238A-CPX6	NB5238A-CPX7	NB5238A-CPX9	NB5238A-CPX10	NB5238A-CPX11	NB5238A-CPX12	NB5238A-CPX13	NB5238A-CPX14
SiO_2	50.80	47.66	47.87	47.83	49.24	45.71	49.80	47.09	49.02	46.99	49.40	46.53	48.53	50.03	49.96	49.76	46.00	49.43	51.46	45.28	50.04	47.65	38.89	47.64	51.56	46.03	47.45	51.76	44.37	40.90
TiO_2	1.63	2.05	2.97	2.57	1.21	3.78	1.55	2.33	2.86	2.85	1.74	3.32	2.12	1.21	1.89	1.38	3.43	2.31	1.36	3.85	2.13	2.84	4.29	2.92	1.54	3.78	2.89	1.26	4.46	3.73
Al_2O_3	3.14	7.83	4.23	5.55	8.60	8.96	5.17	5.09	4.34	4.78	7.61	5.17	5.69	5.49	5.33	1.87	6.79	3.69	1.78	5.62	3.74	5.15	7.55	4.78	1.93	5.22	4.99	1.35	7.62	6.35
Fe_2O_3	1.73	3.97	4.13	1.36	2.04	9.82	0.00	7.95	4.19	4.37	4.56	4.78	3.95	3.49	1.37	5.94	4.84	1.65	0.60	3.63	1.95	2.39	4.09	3.79	2.15	2.56	3.11	1.68	5.12	0.07
FeO	5.68	4.89	3.74	6.53	3.45	1.59	6.46	1.74	3.48	3.28	2.43	3.60	4.20	2.21	5.90	1.34	3.04	5.08	7.19	4.49	4.90	5.04	3.86	3.95	5.61	5.47	4.79	6.27	3.47	6.79
MnO	0	0	0	0	0.20	0	0	0	0	0	0	0.24	0	0	0	0	0	0	0	0	0	0	0	0	0	0	0	0.21	0	0
MgO	13.04	10.75	13.34	11.91	12.60	8.16	13.24	11.04	13.16	12.50	11.43	11.92	12.38	13.68	13.39	13.52	11.24	13.63	13.42	12.25	13.61	12.66	10.29	13.35	13.79	12.25	12.71	13.50	11.66	10.24
CaO	22.77	20.41	23.25	21.62	21.67	16.87	21.00	22.54	24.09	23.72	20.21	23.16	22.38	21.89	20.99	24.68	22.67	22.82	22.39	22.48	23.17	22.95	26.01	22.70	22.81	22.59	23.00	23.00	22.81	25.39
Na_2O	0.89	1.86	0.56	0.88	1.32	4.38	0.80	1.75	0.73	0.61	2.58	0.83	1.08	1.36	1.03	0.79	1.29	0.70	0.75	0.70	0.74	0.68	0.93	0.81	0.88	0.54	0.70	0.81	1.00	0.72
K_2O	0	0	0	0	0	0	0	0	0	0	0	0	0	0	0	0	0	0.09	0.13	0	0.11	0	0	0	0	0.14	0	0	0	0
Cr_2O_3	0	0	0.19	0	0	0	0	0	0	0	0	0	0.2	0	0	0	0	0	0	0	0	0	0	0	0	0	0	0	0	0	0
Total	99.69	99.42	100.29	98.23	100.32	99.27	98.01	99.53	101.86	99.11	99.95	99.55	100.53	99.34	99.86	99.28	99.29	99.89	99.52	98.67	100.81	99.69	100.57	100.44	100.50	98.92	100.05	100.19	101.03	98.48
Numbers of ions on the basis of 6 O																														
Si	1.893	1.781	1.783	1.815	1.800	1.716	1.875	1.772	1.796	1.773	1.816	1.754	1.797	1.847	1.849	1.865	1.731	1.836	1.923	1.720	1.842	1.783	1.464	1.767	1.906	1.745	1.771	1.924	1.649	1.567
Ti	0.046	0.058	0.083	0.073	0.033	0.107	0.044	0.066	0.079	0.081	0.048	0.094	0.059	0.034	0.052	0.039	0.097	0.065	0.038	0.110	0.059	0.080	0.121	0.081	0.043	0.108	0.081	0.035	0.125	0.108
Al	0.138	0.345	0.186	0.248	0.370	0.396	0.229	0.226	0.187	0.213	0.330	0.230	0.248	0.239	0.233	0.083	0.301	0.161	0.078	0.251	0.162	0.227	0.335	0.209	0.084	0.233	0.219	0.059	0.334	0.287
Fe^{3+}	0.048	0.112	0.116	0.039	0.056	0.277	0	0.225	0.115	0.124	0.126	0.135	0.110	0.097	0.038	0.167	0.137	0.046	0.017	0.104	0.054	0.067	0.116	0.106	0.060	0.073	0.087	0.047	0.143	0.002
Fe^{2+}	0.177	0.153	0.116	0.207	0.105	0.050	0.203	0.055	0.107	0.104	0.075	0.114	0.130	0.068	0.183	0.042	0.096	0.158	0.225	0.143	0.151	0.158	0.121	0.123	0.173	0.173	0.150	0.195	0.108	0.218
Mn	0	0	0	0	0.006	0	0	0	0	0	0	0.008	0	0	0	0	0	0	0	0	0	0	0	0	0	0	0	0.007	0	0
Mg	0.725	0.599	0.741	0.674	0.686	0.457	0.743	0.620	0.719	0.703	0.626	0.670	0.683	0.753	0.739	0.755	0.630	0.755	0.747	0.694	0.747	0.706	0.577	0.738	0.760	0.692	0.707	0.748	0.646	0.585
Ca	0.909	0.817	0.928	0.879	0.849	0.679	0.847	0.909	0.946	0.959	0.796	0.935	0.888	0.866	0.832	0.991	0.914	0.908	0.896	0.915	0.914	0.920	1.049	0.902	0.903	0.917	0.920	0.916	0.908	1.042
Na	0.064	0.135	0.041	0.064	0.093	0.319	0.058	0.128	0.052	0.044	0.184	0.061	0.077	0.097	0.074	0.058	0.094	0.051	0.054	0.052	0.053	0.049	0.068	0.058	0.063	0.040	0.051	0.058	0.072	0.054
K	0	0	0	0	0	0	0	0	0	0	0	0	0	0	0	0	0	0.004	0.006	0	0.005	0	0	0	0	0.007	0	0	0	0
Cr	0	0	0.006	0	0	0	0	0	0	0	0	0	0.006	0	0	0	0	0	0	0	0	0	0	0	0	0	0	0	0	0	0
Total	4.000	4.000	4.000	4.000	4.000	4.000	4.000	4.000	4.000	4.000	4.000	4.000	4.000	4.000	4.000	4.000	4.000	4.000	4.000	4.000	4.000	4.000	4.000	4.000	4.000	4.000	4.000	4.000	4.000	4.000
Ca%(Wo%)	48.9	48.6	48.8	48.9	49.8	46.4	47.2	50.3	50.1	50.7	49.0	50.2	49.0	48.5	46.4	50.7	51.4	48.6	47.5	49.3	49.0	49.7	56.3	48.3	47.6	49.4	49.3	47.9	50.3	56.4
Mg%(En%)	39.0	35.6	39.0	37.5	40.3	31.2	41.4	34.3	38.1	37.2	38.6	36.0	37.7	42.2	41.2	38.6	35.5	40.4	39.6	37.4	40.0	38.1	31.0	39.5	40.1	37.3	37.9	39.1	35.8	31.7
ΣFe%(Fs%)	12.1	15.7	12.2	13.7	9.8	22.4	11.3	15.5	11.8	12.0	12.4	13.8	13.3	9.3	12.3	10.7	13.1	10.9	12.8	13.3	11.0	12.2	12.7	12.2	12.3	13.3	12.7	13.0	13.9	11.9
mg*	76.3	69.4	76.2	73.3	80.4	58.3	78.5	68.9	76.4	75.5	75.7	72.3	74.0	82.0	77.0	78.3	73.0	78.7	75.6	73.8	78.5	75.8	70.9	76.4	76.5	73.8	74.9	75.1	72.0	72.7

Appendix 3-2 (Continued).

Locality	NONG BON, NB																		
Occurrence	Groundmass																		
Analysis No	NB5238A-CPX15	NB5238A-CPX16	NB5238A-CPX17	NB5238A-CPX18	NB5238A-CPX19	NB5238A-CPX20	NB5238A-CPX21	NB5238A-CPX22	NB5238A-CPX24	NB5238A-CPX25	NB5238A-CPX27	NB5238A-CPX28	NB5238A-CPX29	NB5238A-CPX30	NB5239-CPX2				
SiO_2	45.32	43.30	45.55	51.62	43.52	46.38	47.97	48.08	49.15	48.44	47.65	49.26	47.06	46.71	47.73				
TiO_2	4.37	4.00	3.61	1.49	4.91	3.46	2.81	2.72	2.51	2.69	2.90	2.73	3.24	3.54	3.17				
Al_2O_3	6.27	7.01	6.37	1.62	7.67	6.11	4.82	4.27	4.09	4.14	4.60	4.39	5.29	5.54	4.75				
Fe_2O_3	3.48	1.73	3.54	0.73	3.62	2.34	3.93	2.39	2.11	3.23	2.87	3.11	3.47	3.84	4.79				
FeO	4.92	6.20	4.34	7.21	4.52	5.24	3.49	4.94	4.91	3.77	4.80	4.29	4.37	4.38	3.30				
MnO	0	0	0.21	0.2	0	0	0	0	0	0.20	0	0	0	0	0.25				
MgO	12.21	11.04	11.79	13.57	11.49	12.13	13.19	13.08	13.64	13.45	12.72	13.78	12.92	12.76	12.89				
CaO	22.43	24.03	22.65	22.84	22.63	22.76	23.11	22.70	22.83	23.03	23.02	23.17	22.81	22.83	23.81				
Na_2O	0.76	0.71	0.72	0.62	0.66	0.70	0.92	0.60	0.64	0.77	0.74	0.76	0.71	0.72	0.62				
K_2O	0	0	0.09	0	0	0	0	0.13	0.1	0	0.10	0	0.14	0	0				
Cr_2O_3	0	0	0	0	0.18	0	0.24	0	0	0	0	0	0	0	0				
Total	100.19	100.30	99.11	100.23	99.48	99.46	100.98	99.17	100.32	100.03	99.96	101.84	100.58	100.67	101.32				
Numbers of ions on the basis of 6 O																			
Si	1.697	1.625	1.722	1.919	1.646	1.743	1.769	1.806	1.820	1.801	1.780	1.799	1.747	1.736	1.764				
Ti	0.123	0.113	0.103	0.042	0.140	0.098	0.078	0.077	0.070	0.075	0.081	0.075	0.091	0.099	0.088				
Al	0.277	0.310	0.284	0.071	0.342	0.271	0.210	0.189	0.179	0.181	0.202	0.189	0.232	0.243	0.207				
Fe^{3+}	0.098	0.049	0.101	0.020	0.103	0.066	0.109	0.068	0.059	0.090	0.081	0.085	0.097	0.107	0.133				
Fe^{2+}	0.154	0.195	0.137	0.224	0.143	0.165	0.108	0.155	0.152	0.117	0.150	0.131	0.136	0.136	0.102				
Mn	0	0	0.007	0.006	0	0	0	0	0	0.006	0	0	0	0	0.008				
Mg	0.682	0.618	0.665	0.752	0.648	0.680	0.725	0.733	0.753	0.748	0.709	0.750	0.715	0.707	0.710				
Ca	0.900	0.966	0.917	0.910	0.917	0.916	0.913	0.914	0.906	0.917	0.921	0.906	0.907	0.909	0.943				
Na	0.055	0.052	0.053	0.045	0.048	0.051	0.066	0.044	0.046	0.055	0.053	0.054	0.051	0.052	0.044				
K	0	0	0.005	0	0	0	0	0.006	0.005	0	0.005	0	0.007	0	0				
Cr	0	0	0	0	0.005	0	0.007	0	0	0	0	0	0	0	0				
Total	4.000	4.000	4.000	4.000	4.000	4.000	4.000	4.000	4.000	4.000	4.000	4.000	4.000	4.000	4.000				
Ca%(Wo%)	49.1	52.9	50.2	47.6	50.6	50.2	49.2	48.9	48.4	48.9	49.5	48.4	48.9	48.9	49.7				
Mg%(En%)	37.2	33.8	36.4	39.3	35.8	37.2	39.1	39.2	40.3	39.7	38.1	40.1	38.5	38.0	37.5				
∑Fe%(Fs%)	13.8	13.3	13.4	13.1	13.6	12.6	11.7	11.9	11.3	11.4	12.4	11.6	12.5	13.1	12.8				
mg*	73.0	71.7	73.1	75.0	72.5	74.7	77.0	76.7	78.1	77.7	75.4	77.6	75.4	74.4	74.5				

Appendix 3-3 Chemical composition of feldspars in basalt samples.

Locality	CHIANG KHONG, CK																													
Occurrence	Groundmass																													
Analysis No	CK17-PL2	CK18-PL1	CK210-PL2	CK29B-PL2	CK29B-PL4	CK29B-PL5	CK29B-PL7	CK315A-PL1	CK315A-PL2	CK315A-PL3	CK315A-PL4	CK315A-PL5	CK315A-PL6	CK315A-PL7	CK315A-PL8	CK315A-PL9	CK315A-PL10	CK315A-PL11	CK315B-PL1	CK315B-PL2	CK315B-PL3	CK315B-PL4	CK315B-PL5	CK315B-PL6	CK315B-PL7	CK315B-PL8	CK315C-PL1	CK315C-PL2	CK315C-PL4	CK519A-PL3
SiO_2	50.86	50.56	50.69	51.52	52.63	50.56	51.80	51.68	51.97	52.78	51.84	52.59	52.96	53.25	53.25	52.58	52.91	51.98	52.88	53.05	52.61	52.70	52.65	53.40	52.09	56.84	52.06	51.48	51.85	53.00
TiO_2	0	0	0.36	0.20	0.44	0.20	0	0.47	0.30	0.33	0.21	0.73	0.32	0.23	0.32	0.46	0.23	0.30	0.18	0.23	0	0.29	0.31	0.46	0.28	0.71	0.27	0.56	0.33	0.27
Al_2O_3	28.96	29.56	29.16	29.24	27.72	29.58	28.33	29.01	28.74	28.67	29.09	27.26	29.10	28.31	27.87	27.69	28.94	29.49	28.56	28.94	29.26	29.57	29.08	29.34	28.63	23.69	29.85	27.59	28.62	28.52
$Fe_2O_3^*$	1.00	0.83	0.87	0.81	0.87	1.01	0.78	0.96	0.86	0.79	0.58	1.72	0.90	0.98	0.87	1.23	0.66	0.76	0.92	0.76	0.85	0.87	0.74	0.87	0.70	0.70	0.92	1.40	1.02	0.74
MgO	0	0	0.26	0	0	0	0	0.29	0	0	0	0.29	0.29	0.25	0	0.22	0.25	0	0.26	0	0.23	0.25	0	0	0	0.30	0.23	0.40	0	0.23
CaO	13.02	13.67	12.87	12.40	11.04	12.85	12.21	12.42	12.06	11.76	12.27	10.43	12.10	11.64	10.88	11.31	11.75	12.75	11.45	11.62	12.25	12.23	12.10	11.91	11.92	7.30	12.89	11.87	11.88	11.54
Na_2O	3.68	3.53	3.57	3.63	4.39	3.43	3.99	3.59	3.90	4.08	3.99	4.61	4.10	4.51	4.75	4.29	4.29	3.76	4.61	4.56	4.10	3.98	3.90	4.24	3.94	5.14	3.87	4.16	3.83	4.30
K_2O	0.66	0.53	0.59	0.64	0.97	0.52	0.69	0.70	0.76	0.76	0.67	1.25	0.71	0.70	0.85	0.82	0.74	0.57	0.74	0.84	0.64	0.66	0.69	0.84	0.74	3.40	0.60	1.01	0.71	0.79
BaO	0	0	0	0	0	0	0	0	0	0	0	0	0	0	0	0	0	0	0	0	0	0	0	0	0	0	0	0	0	0
Total	98.18	98.69	98.66	98.44	98.31	98.15	98.06	99.29	98.58	99.34	98.87	99.05	100.66	99.87	99.05	98.78	100.11	99.61	99.59	100.22	99.94	100.82	99.65	101.37	98.31	99.08	100.68	98.87	98.23	99.39
Numbers of ions on the basis of 32 O																														
Si	9.464	9.368	9.372	9.520	9.728	9.392	9.611	9.479	9.593	9.650	9.534	9.691	9.570	9.700	9.759	9.686	9.599	9.501	9.661	9.627	9.579	9.505	9.595	9.579	9.631	10.396	9.433	9.522	9.601	9.690
Ti	0	0	0.050	0.028	0.061	0.027	0.000	0.065	0.042	0.045	0.030	0.101	0.044	0.032	0.045	0.064	0.032	0.041	0.024	0.032	0	0.039	0.042	0.062	0.039	0.097	0.036	0.078	0.045	0.037
Al	6.350	6.454	6.354	6.368	6.037	6.476	6.194	6.270	6.253	6.177	6.305	5.920	6.197	6.079	6.020	6.012	6.187	6.353	6.150	6.190	6.279	6.286	6.246	6.202	6.239	5.106	6.374	6.015	6.244	6.144
Fe^{3+}	0.140	0.116	0.122	0.113	0.121	0.142	0.109	0.132	0.119	0.109	0.080	0.239	0.122	0.135	0.120	0.171	0.090	0.105	0.126	0.104	0.116	0.118	0.102	0.117	0.098	0.096	0.125	0.195	0.142	0.101
Mg	0	0	0.072	0	0	0	0	0.078	0	0	0	0.080	0.077	0.068	0	0.059	0.067	0	0.071	0	0.062	0.068	0	0	0	0.082	0.061	0.109	0	0.064
Ca	2.595	2.713	2.550	2.456	2.186	2.557	2.426	2.441	2.386	2.303	2.417	2.060	2.342	2.272	2.136	2.232	2.284	2.496	2.241	2.259	2.390	2.363	2.363	2.288	2.362	1.430	2.502	2.353	2.357	2.261
Na	1.326	1.269	1.281	1.301	1.573	1.234	1.434	1.276	1.395	1.445	1.423	1.646	1.436	1.592	1.688	1.531	1.509	1.331	1.632	1.604	1.448	1.393	1.377	1.474	1.412	1.822	1.361	1.490	1.374	1.523
K	0.157	0.126	0.139	0.152	0.229	0.122	0.164	0.164	0.179	0.177	0.158	0.293	0.163	0.163	0.198	0.192	0.171	0.134	0.172	0.194	0.149	0.153	0.160	0.193	0.175	0.792	0.139	0.238	0.167	0.185
Ba	0	0	0	0	0	0	0	0	0	0	0	0	0	0	0	0	0	0	0	0	0	0	0	0	0	0	0	0	0	0
Total	20.033	20.045	19.984	19.938	19.975	19.950	19.990	19.933	19.966	19.933	19.982	20.056	19.981	20.039	20.007	19.976	19.992	19.961	20.079	20.043	20.022	19.966	19.914	19.962	19.956	19.978	20.031	20.064	19.931	20.004
An	63.6	66.0	64.2	62.8	54.8	65.4	60.3	62.9	60.3	58.7	60.5	51.5	59.4	56.4	53.1	56.4	57.6	63.0	55.4	55.7	59.9	60.4	60.6	57.9	59.8	35.4	62.5	57.7	60.5	57.0
Ab	32.5	30.9	32.3	33.3	39.5	31.5	35.6	32.9	35.2	36.8	35.6	41.2	36.4	39.5	42.0	38.7	38.1	33.6	40.3	39.5	36.3	35.6	35.3	37.3	35.8	45.1	34.0	36.5	35.2	38.4
Or	3.8	3.1	3.5	3.9	5.7	3.1	4.1	4.2	4.5	4.5	3.9	7.3	4.1	4.1	4.9	4.9	4.3	3.4	4.3	4.8	3.7	3.9	4.1	4.9	4.4	19.6	3.5	5.8	4.3	4.7

* Total Fe as Fe_2O_3

Appendix 3-3 (Continued).

Locality	CHIANG KHONG, CK										BAN NONG, NAM CHO, BN																			
Occurrence	Groundmass										Groundmass																			
Analysis No	CK519A-PL4	CK519B-PL1	CK519B-PL2	CK519B-PL3	CK519B-PL4	CK519B-PL5	CK519B-PL7	CK519B-PL8	CK519B-PL9	CK519B-PL10	BN477-PL1	BN477-PL3	BN6-PL1	BN6-PL2	BN6-PL3	BN6-PL5	BN6-PL6	BN6-PL7	BN6-PL8	BN6-PL9	BN6-PL10	BN6-PL11	BN6-PL13	BN6-PL14	BN6-PL15	BN6-PL16	BN6-PL17	BN6-PL18	BN6-PL19	BN6-PL20
SiO_2	52.25	52.06	52.22	54.07	51.69	52.81	52.05	53.18	51.97	52.14	53.34	51.82	52.78	53.74	51.82	53.79	53.78	53.12	52.28	54.83	53.91	57.31	55.35	57.02	53.95	53.80	52.84	53.22	54.38	51.02
TiO_2	0.22	0.25	0.21	0.42	0.21	0.38	0.22	0.4	0.3	0.32	0.24	0.18	0	0	0	0	0	0	0	0	0	0	0	0.24	0	0	0	0	0	0
Al_2O_3	29.72	29.00	30.80	27.98	29.51	28.23	28.96	28.89	28.44	28.47	28.18	28.99	30.49	28.90	31.03	29.06	29.40	29.80	30.26	28.97	28.03	27.40	28.14	27.29	28.18	28.97	30.07	28.19	28.52	31.06
$Fe_2O_3^*$	0.70	0.82	0.67	0.90	0.90	1.23	0.69	0.69	0.80	1.20	0.74	0.66	0.67	0.72	0.76	0.56	0.67	0.98	0.64	0.79	0.49	0.47	0.80	0.53	0.88	0.77	0.80	0.97	0.69	0.90
MgO	0.28	0	0.3	0.34	0	0	0.24	0.28	0	0.23	0.28	0	0	0	0	0	0	0.27	0	0	0	0.37	0	0	0	0	0.22	0.43	0	0
CaO	12.45	12.26	13.34	11.24	12.84	11.65	12.22	11.80	11.87	11.85	10.88	11.89	13.28	11.93	13.89	12.14	12.41	12.51	13.23	11.41	10.68	9.34	10.62	9.33	11.79	11.74	12.82	11.33	11.48	14.14
Na_2O	3.95	4.19	3.59	4.74	3.53	4.09	4.15	4.38	4.04	3.71	4.68	4.40	3.87	4.60	3.45	4.45	4.41	4.09	3.75	4.62	4.91	5.89	5.10	5.68	4.33	4.37	4.36	4.22	4.44	3.45
K_2O	0.70	0.66	0.55	0.95	0.59	0.75	0.70	0.73	0.73	0.69	0.40	0.30	0.41	0.32	0.20	0.29	0.31	0.24	0.22	0.35	0.38	0.50	0.45	0.57	0.41	0.34	0.24	0.37	0.76	0.19
BaO	0	0	0	0	0	0	0	0	0	0	0	0	0	0	0	0	0.36	0	0	0	0.37	0.51	0	0	0	0.33	0	0	0	0
Total	100.27	99.24	101.85	100.85	99.27	99.14	99.48	100.35	98.15	98.61	98.73	98.24	101.49	100.19	101.15	100.29	101.34	101.01	100.38	100.97	98.77	101.78	100.46	100.65	99.76	100.31	101.36	98.73	100.26	100.76
Numbers of ions on the basis of 32 O																														
Si	9.490	9.557	9.353	9.751	9.483	9.689	9.526	9.637	9.631	9.616	9.778	9.580	9.465	9.726	9.331	9.720	9.658	9.553	9.467	9.820	9.886	10.168	9.954	10.189	9.795	9.736	9.489	9.761	9.830	9.246
Ti	0.030	0.035	0.028	0.057	0.029	0.052	0.030	0.055	0.042	0.044	0.033	0.024	0	0	0	0	0	0	0	0	0	0	0	0.032	0	0	0	0	0	0
Al	6.361	6.274	6.501	5.947	6.380	6.104	6.246	6.170	6.212	6.188	6.089	6.316	6.443	6.164	6.584	6.189	6.223	6.315	6.456	6.114	6.057	5.729	5.963	5.745	6.029	6.178	6.364	6.093	6.075	6.634
Fe^{3+}	0.096	0.114	0.090	0.122	0.124	0.170	0.095	0.094	0.112	0.167	0.102	0.092	0.090	0.097	0.103	0.076	0.090	0.132	0.088	0.107	0.068	0.063	0.108	0.071	0.120	0.104	0.108	0.134	0.093	0.122
Mg	0.075	0	0.080	0.091	0	0	0.065	0.076	0	0.063	0.076	0	0	0	0	0	0	0.073	0	0	0	0.098	0	0	0	0	0.060	0.118	0	0
Ca	2.422	2.411	2.560	2.172	2.524	2.290	2.396	2.291	2.357	2.341	2.136	2.355	2.550	2.312	2.680	2.351	2.387	2.410	2.567	2.188	2.098	1.775	2.047	1.785	2.293	2.276	2.467	2.226	2.223	2.746
Na	1.391	1.491	1.247	1.657	1.255	1.455	1.472	1.539	1.452	1.326	1.663	1.578	1.347	1.612	1.205	1.557	1.535	1.426	1.315	1.604	1.745	2.024	1.776	1.968	1.523	1.534	1.517	1.499	1.555	1.213
K	0.162	0.155	0.126	0.219	0.138	0.176	0.163	0.169	0.173	0.162	0.093	0.071	0.093	0.073	0.045	0.067	0.071	0.054	0.051	0.079	0.088	0.113	0.103	0.129	0.094	0.079	0.055	0.087	0.175	0.045
Ba	0	0	0	0	0	0	0	0	0	0	0	0	0	0	0	0	0.025	0	0	0	0.027	0.035	0	0	0	0.023	0	0	0	0
Total	20.028	20.037	20.010	20.047	19.933	19.936	20.033	20.030	19.977	19.907	19.971	20.016	19.988	19.985	19.950	19.960	19.989	19.964	19.944	19.912	19.968	20.005	19.950	19.920	19.888	19.930	20.061	19.918	19.951	20.005
An	60.9	59.4	65.1	53.7	64.4	58.4	59.4	57.3	59.2	61.1	54.9	58.8	63.9	57.8	68.2	59.1	59.8	62.0	65.3	56.5	53.4	45.4	52.1	46.0	58.6	58.5	61.1	58.4	56.2	68.6
Ab	35.0	36.8	31.7	40.9	32.1	37.1	36.5	38.5	36.5	34.6	42.7	39.4	33.8	40.3	30.7	39.2	38.4	36.7	33.4	41.4	44.4	51.7	45.3	50.7	38.9	39.4	37.6	39.3	39.3	30.3
Or	4.1	3.8	3.2	5.4	3.5	4.5	4.1	4.2	4.3	4.2	2.4	1.8	2.3	1.8	1.2	1.7	1.8	1.4	1.3	2.0	2.2	2.9	2.6	3.3	2.4	2.0	1.4	2.3	4.4	1.1

* Total Fe as Fe_2O_3

Appendix 3-3 (Continued).

Locality	SOP PRAP, SP																												
Occurrence	Groundmass																												
Analysis No.	SP1-PL1	SP154-PL1	SP154-PL2	SP154-PL3	SP154-PL4	SP155-PL1	SP155-PL3	SP155-PL4	SP155-PL5	SP155-PL6	SP155-PL7	SP155-PL8	SP155-PL9	SP155-PL11	SP155-PL12	SP155-PL15	SP155-PL1	SP155-PL2	SP155-PL4	SP155-PL6	SP155-PL9	SP161-PL5	SP161-PL6	SP161-PL7	SP161-PL8	SP161-PL9	SP161-PL10	SP161-PL11	SP161-PL12
SiO_2	52.96	53.46	53.46	52.79	53.43	53.77	53.44	52.95	52.84	53.61	53.60	53.40	53.60	53.38	54.30	54.01	53.63	53.69	53.64	54.00	52.82	53.39	54.00	53.84	53.31	53.35	53.45	53.58	52.94
TiO_2	0.32	0	0	0	0	0.27	0.24	0.17	0.20	0.28	0.21	0.18	0.48	0.25	0.24	0	0	0	0	0	0	0	0	0	0	0	0	0	0
Al_2O_3	27.98	28.20	27.78	28.58	27.01	28.05	28.07	28.06	27.41	28.08	27.90	28.41	25.76	27.40	27.53	27.88	27.62	27.67	27.70	27.38	27.80	27.77	27.02	27.61	28.20	27.83	27.65	27.73	28.52
$Fe_2O_3^*$	0.55	0.64	0.67	0.67	1.82	0.46	0.54	0.53	1.19	0.83	0.63	0.76	2.61	0.98	0.87	0.91	0.83	0.91	0.58	0.77	0.53	0.55	1.17	0.65	0.63	0.52	0.93	0.87	0.60
MgO	0.34	0	0	0	0	0	0	0	0	0	0	0	0.45	0	0	0	0	0	0	0	0	0	0	0	0	0	0	0	0
CaO	10.92	11.26	11.21	11.94	10.91	11.03	11.29	11.52	11.20	11.33	11.06	11.52	9.38	10.93	10.69	10.99	11.01	11.12	11.16	10.66	11.88	11.36	10.77	10.88	11.45	11.29	11.06	11.11	11.87
Na_2O	4.57	4.47	4.57	4.32	4.35	4.62	4.35	4.45	4.54	4.56	4.61	4.39	4.03	4.55	4.92	4.47	4.47	4.39	4.60	4.70	4.64	4.43	4.35	4.80	4.67	4.52	4.34	4.46	4.29
K_2O	0.65	0.63	0.83	0.63	0.87	0.72	0.70	0.70	0.77	0.69	0.72	0.69	1.83	0.75	0.78	0.66	0.80	1.04	0.75	0.96	0.65	0.70	1.05	0.80	0.76	0.76	0.73	0.68	0.60
BaO	0	0	0	0	0	0	0	0	0	0	0	0	0	0	0	0	0	0	0	0	0	0	0	0	0	0	0	0	0
Total	98.29	98.66	98.52	98.93	98.40	98.91	98.62	98.56	98.14	99.38	98.73	99.34	98.14	98.24	99.33	98.91	98.36	98.81	98.42	98.46	98.31	98.19	98.36	98.59	99.02	98.27	98.15	98.43	98.82
Numbers of ions on the basis of 32 O																													
Si	9.766	9.816	9.846	9.695	9.876	9.843	9.815	9.746	9.793	9.791	9.840	9.754	9.962	9.858	9.911	9.884	9.882	9.865	9.876	9.940	9.770	9.854	9.959	9.899	9.778	9.843	9.868	9.864	9.722
Ti	0.044	0	0	0	0	0.037	0.032	0.023	0.027	0.038	0.028	0.025	0.067	0.035	0.033	0	0	0	0	0	0	0	0	0	0	0	0	0	0
Al	6.081	6.101	6.029	6.187	5.884	6.052	6.077	6.086	5.987	6.044	6.036	6.116	5.641	5.963	5.920	6.012	5.998	5.992	6.011	5.939	6.059	6.039	5.873	5.983	6.096	6.050	6.014	6.017	6.173
Fe^{3+}	0.076	0.088	0.093	0.092	0.253	0.064	0.074	0.074	0.166	0.114	0.088	0.104	0.365	0.136	0.120	0.125	0.115	0.126	0.081	0.106	0.073	0.076	0.162	0.090	0.087	0.072	0.129	0.121	0.083
Mg	0.094	0	0	0	0	0	0	0	0	0	0	0	0.124	0	0	0	0	0	0	0	0	0	0	0	0	0	0	0	0
Ca	2.158	2.214	2.212	2.348	2.160	2.163	2.222	2.271	2.224	2.217	2.174	2.255	1.867	2.162	2.090	2.155	2.174	2.188	2.201	2.102	2.354	2.245	2.127	2.144	2.249	2.232	2.188	2.190	2.336
Na	1.633	1.592	1.631	1.539	1.560	1.640	1.548	1.588	1.630	1.616	1.639	1.554	1.452	1.629	1.742	1.586	1.597	1.562	1.642	1.676	1.663	1.584	1.556	1.710	1.662	1.617	1.552	1.592	1.529
K	0.152	0.148	0.194	0.147	0.206	0.168	0.164	0.165	0.181	0.160	0.169	0.161	0.435	0.177	0.181	0.154	0.188	0.243	0.175	0.224	0.153	0.165	0.246	0.188	0.178	0.179	0.172	0.159	0.140
Ba	0	0	0	0	0	0	0	0	0	0	0	0	0	0	0	0	0	0	0	0	0	0	0	0	0	0	0	0	0
Total	20.004	19.959	20.005	20.009	19.939	19.966	19.932	19.983	20.009	19.980	19.974	19.969	19.912	19.960	19.997	19.917	19.954	19.978	19.986	19.988	20.072	19.963	19.924	20.013	20.050	19.994	19.923	19.942	19.984
An	54.7	56.0	54.8	58.2	55.0	54.5	56.5	56.4	55.1	55.5	54.6	56.8	49.7	54.5	52.1	55.3	54.9	54.8	54.8	52.5	56.4	56.2	54.1	53.0	55.0	55.4	55.9	55.6	58.3
Ab	41.4	40.2	40.4	38.2	39.7	41.3	39.3	39.5	40.4	40.5	41.2	39.1	38.7	41.1	43.4	40.7	40.3	39.1	40.9	41.9	39.9	39.7	39.6	42.3	40.6	40.2	39.7	40.4	38.2
Or	3.8	3.8	4.8	3.6	5.2	4.2	4.2	4.1	4.5	4.0	4.3	4.1	11.6	4.5	4.5	3.9	4.7	6.1	4.4	5.6	3.7	4.1	6.3	4.7	4.4	4.4	4.4	4.0	3.5

* Total Fe as Fe_2O_3

Appendix 3-3 (Continued).

Locality	DEN CHAI, DC																								
Occurrence	Groundmass																								
Analysis No	DC157-PL1	DC157-PL2	DC157-PL4	DC157-PL5	DC157-PL6	DC160-PL3	DC160-PL8	DC160-PL9	DC161-PL3	DC161-PL4	DC162-PL1	DC162-PL3	DC162-PL4	DC162-PL5	DC162-PL6	DC164-PL3	DC1K-PL1	DC1K-PL4	DC263-PL2	DC263-PL4	DC264-PL4	DC264-PL6	DC264-PL7	DC264-PL8	DC264-PL9	DC264-PL10	DC264-PL11	DC264-PL12	DC271-PL1	DC271-PL3
SiO_2	51.74	56.70	54.48	52.47	51.78	55.92	56.99	55.33	51.61	52.30	52.19	52.80	54.73	54.43	52.67	53.19	52.09	51.86	56.46	52.90	52.83	52.49	52.52	52.96	52.47	51.92	49.31	52.63	52.65	53.03
TiO_2	0	0	0	0	0	0	0	0	0	0	0	0	0	0	0	0	0.218	0.28	0	0	0	0	0	0	0	0	0	0	0	0
Al_2O_3	28.94	26.42	28.07	29.11	29.23	26.29	26.28	27.00	29.58	28.42	29.34	28.68	27.65	28.79	29.31	28.41	28.75	28.62	24.70	28.46	29.28	28.73	28.66	29.09	29.37	29.03	31.19	28.96	28.93	28.86
$Fe_2O_3^*$	0.70	0.54	0.48	0.74	0.69	0.96	0.52	0.76	0.82	0.88	0.69	0.87	0.68	0.76	0.77	0.91	0.56	0.70	0.95	0.95	0.86	0.82	0.91	0.82	0.77	0.76	0.47	0.56	0.68	0.72
MgO	0	0	0	0	0	0	0	0	0	0	0	0	0	0	0	0	0.198	0.28	0	0	0	0	0	0	0	0	0	0	0	0
CaO	12.42	8.73	10.80	12.50	12.73	9.85	8.66	9.49	13.04	11.79	12.70	12.19	10.60	11.07	12.33	11.84	12.18	11.90	9.33	11.23	12.47	11.84	11.89	12.21	12.59	12.30	14.77	12.21	12.05	11.82
Na_2O	4.27	6.04	5.11	4.23	4.13	5.35	6.07	5.71	3.91	4.46	4.38	4.56	5.18	4.98	4.36	4.60	4.03	4.28	5.12	4.86	4.37	4.47	4.51	4.25	4.25	3.88	2.84	4.46	4.63	4.50
K_2O	0.34	0.62	0.37	0.25	0.30	1.06	0.74	0.55	0.31	0.40	0.31	0.24	0.79	0.29	0.34	0.26	0.24	0.26	1.31	0.34	0.27	0.33	0.61	0.43	0.23	0.75	0.29	0.32	0.24	0.28
BaO	0	0	0	0	0	0	0	0	0	0	0	0	0	0	0	0	0	0	0.78	0.28	0	0	0.35	0.28	0.18	0.43	0.23	0.17	0	0.39
Total	98.40	99.06	99.30	99.31	98.87	99.43	99.26	98.83	99.26	98.26	99.59	99.33	99.64	100.32	99.78	99.22	98.27	98.16	98.65	99.02	100.07	98.67	99.46	100.04	99.84	99.06	99.09	99.30	99.17	99.68
Numbers of ions on the basis of 32 O																														
Si	9.566	10.290	9.912	9.601	9.530	10.178	10.323	10.101	9.470	9.672	9.540	9.660	9.952	9.814	9.594	9.730	9.614	9.594	10.398	9.714	9.597	9.658	9.638	9.637	9.565	9.570	9.114	9.637	9.641	9.674
Ti	0	0	0	0	0	0	0	0	0	0	0	0	0	0	0	0	0.030	0.039	0	0	0	0	0	0	0	0	0	0	0	0
Al	6.306	5.652	6.019	6.277	6.341	5.640	5.610	5.808	6.397	6.193	6.320	6.183	5.925	6.117	6.292	6.124	6.254	6.239	5.362	6.160	6.269	6.230	6.198	6.239	6.309	6.306	6.795	6.250	6.243	6.225
Fe^{3+}	0.097	0.074	0.065	0.102	0.096	0.132	0.072	0.104	0.113	0.123	0.094	0.120	0.094	0.103	0.106	0.126	0.077	0.097	0.132	0.132	0.117	0.113	0.126	0.112	0.105	0.106	0.065	0.077	0.093	0.099
Mg	0	0	0	0	0	0	0	0	0	0	0	0	0	0	0	0	0.054	0.076	0	0	0	0	0	0	0	0	0	0	0	0
Ca	2.460	1.697	2.106	2.450	2.511	1.920	1.680	1.856	2.564	2.336	2.487	2.389	2.065	2.137	2.405	2.319	2.408	2.359	1.842	2.209	2.426	2.334	2.338	2.380	2.458	2.428	2.924	2.395	2.363	2.310
Na	1.529	2.127	1.802	1.501	1.474	1.889	2.130	2.020	1.389	1.600	1.561	1.619	1.826	1.740	1.540	1.633	1.443	1.533	1.826	1.730	1.540	1.594	1.606	1.500	1.501	1.388	1.017	1.583	1.643	1.591
K	0.080	0.144	0.087	0.059	0.071	0.245	0.172	0.128	0.073	0.093	0.071	0.056	0.184	0.067	0.079	0.061	0.057	0.060	0.308	0.080	0.063	0.078	0.143	0.100	0.052	0.175	0.067	0.075	0.057	0.064
Ba	0	0	0	0	0	0	0	0	0	0	0	0	0	0	0	0	0	0	0.056	0.020	0	0	0.025	0.020	0.013	0.031	0.017	0.012	0	0.028
Total	20.038	19.982	19.990	19.989	20.024	20.004	19.987	20.017	20.006	20.017	20.064	20.026	20.044	19.979	20.016	19.992	19.939	19.996	19.923	20.045	20.012	20.007	20.075	19.988	20.004	20.005	19.998	20.028	20.041	19.991
An	60.4	42.8	52.7	61.1	61.9	47.4	42.2	46.3	63.7	58.0	60.5	58.8	50.7	54.2	59.8	57.8	61.6	59.7	46.3	55.0	60.2	58.3	57.2	59.8	61.3	60.8	73.0	59.1	58.2	58.3
Ab	37.6	53.6	45.1	37.4	36.4	46.6	53.5	50.4	34.5	39.7	37.7	39.8	44.8	44.1	38.3	40.7	36.9	38.8	45.9	43.0	38.2	39.8	39.3	37.7	37.4	34.8	25.4	39.1	40.4	40.1
Or	2.0	3.6	2.2	1.5	1.7	6.1	4.3	3.2	1.8	2.3	1.7	1.4	4.5	1.7	2.0	1.5	1.5	1.5	7.7	2.0	1.6	2.0	3.5	2.5	1.3	4.4	1.7	1.9	1.4	1.6

* Total Fe as Fe_2O_3

Appendix 3-3 (Continued).

Locality	DEN CHAI, DC							KHOK SAMRAN, KS																						
Occurrence	Groundmass							Phenocryst																						
Analysis No	DC3-PL1	DC3-PL5	DC3-PL6	DC3-PL8	DC3-PL9	DC3-PL10	DC376A-PL2	KS110-P2	KS110-P3	KS110-P4	KS110-P6	KS110-P7	KS110-P9	KS110-P10	KS110-P11	KSI10-P13	KS110-P14	KS110-P15	KS110-P16	KS110-P17	KS110-P18	KS110-P19	KS110-P20	KS110-P21	KS110-P22	KS110-P23	KS110-P25	KS110-P26	KS110-P27	KS110-P28
SiO_2	51.09	56.27	52.09	53.73	53.17	51.71	52.35	54.05	54.51	53.85	52.02	54.59	54.14	54.67	54.65	54.18	51.61	54.11	54.31	52.71	53.97	54.45	54.20	54.46	54.02	54.30	53.07	53.79	53.86	54.71
TiO_2	0.22	0.34	0.22	0.26	0.20	0.18	0.19	0	0	0	0	0	0	0	0	0	0	0	0	0	0	0	0	0	0	0	0	0	0	0
Al_2O_3	29.46	27.00	29.07	27.60	27.85	29.88	28.62	28.05	27.98	27.99	29.28	27.83	28.38	28.46	27.90	27.65	29.69	28.06	28.22	28.89	28.44	28.01	27.88	27.89	28.28	28.43	28.69	28.42	28.62	27.77
$Fe_2O_3^*$	0.88	0.58	0.85	0.87	0.80	0.91	0.84	0.57	0.57	0.41	0.85	0.46	0.50	0.25	0.46	0.56	0.91	0.33	0.56	0.90	0.49	0.59	0.47	0.46	0.67	0.44	0.84	0.52	0.41	0.69
MgO	0	0.35	0	0	0.28	0.32	0	0	0	0	0	0	0	0	0	0	0	0	0	0	0	0	0	0	0	0	0	0	0	0
CaO	12.53	9.15	12.18	10.45	10.82	13.06	11.64	11.06	10.74	11.03	12.86	10.60	11.15	11.01	10.59	10.71	13.06	10.76	11.05	12.17	11.20	10.84	10.71	10.91	11.05	11.28	11.86	11.00	11.39	11.03
Na_2O	4.29	6.14	4.31	5.15	5.00	4.05	4.37	4.95	4.92	4.67	3.87	4.88	4.70	4.78	4.90	5.02	3.83	4.82	5.03	4.14	4.89	5.02	4.84	4.97	4.74	4.89	4.40	4.84	4.70	4.97
K_2O	0.24	0.44	0.29	0.31	0.30	0.19	0.31	0.49	0.56	0.48	0.29	0.52	0.55	0.49	0.55	0.51	0.26	0.51	0.53	0.30	0.42	0.48	0.42	0.49	0.50	0.42	0.35	0.41	0.39	0.56
BaO	0	0	0	0	0	0	0	0	0	0	0	0	0	0	0	0	0	0	0	0	0	0	0	0	0	0	0	0	0	0
Total	98.70	100.47	99.00	98.35	98.63	100.68	98.32	99.17	99.28	98.42	99.18	98.88	99.42	99.66	99.04	98.64	99.36	98.60	99.70	99.11	99.40	99.39	98.52	99.18	99.27	99.77	99.20	98.97	99.36	99.73
Numbers of ions on the basis of 32 O																														
Si	9.434	10.103	9.566	9.882	9.763	9.356	9.659	9.867	9.924	9.888	9.541	9.965	9.851	9.902	9.960	9.934	9.459	9.910	9.864	9.652	9.825	9.908	9.931	9.927	9.847	9.847	9.705	9.829	9.805	9.932
Ti	0.031	0.046	0.030	0.035	0.027	0.025	0.026	0	0	0	0	0	0	0	0	0	0	0	0	0	0	0	0	0	0	0	0	0	0	0	0
Al	6.410	5.713	6.290	5.982	6.027	6.372	6.223	6.034	6.005	6.056	6.328	5.986	6.085	6.076	5.992	5.973	6.413	6.057	6.040	6.235	6.101	6.006	6.020	5.990	6.076	6.077	6.182	6.119	6.141	5.940
Fe^{3+}	0.122	0.078	0.117	0.120	0.111	0.124	0.117	0.079	0.078	0.056	0.118	0.063	0.068	0.034	0.063	0.077	0.126	0.045	0.076	0.124	0.068	0.080	0.064	0.063	0.092	0.060	0.115	0.071	0.056	0.094
Mg	0	0.092	0	0	0.076	0.086	0	0	0	0	0	0	0	0	0	0	0	0	0	0	0	0	0	0	0	0	0	0	0	0
Ca	2.478	1.760	2.395	2.058	2.129	2.531	2.301	2.164	2.095	2.170	2.528	2.073	2.174	2.136	2.069	2.104	2.564	2.111	2.151	2.387	2.184	2.113	2.102	2.130	2.158	2.192	2.324	2.152	2.221	2.146
Na	1.535	2.137	1.534	1.836	1.780	1.419	1.564	1.753	1.735	1.661	1.376	1.727	1.658	1.678	1.731	1.785	1.360	1.713	1.772	1.470	1.726	1.770	1.720	1.757	1.676	1.720	1.560	1.715	1.657	1.750
K	0.055	0.100	0.068	0.072	0.071	0.044	0.073	0.113	0.130	0.113	0.068	0.120	0.128	0.114	0.127	0.119	0.061	0.119	0.124	0.069	0.097	0.111	0.098	0.114	0.116	0.096	0.081	0.095	0.091	0.129
Ba	0	0	0	0	0	0	0	0	0	0	0	0	0	0	0	0	0	0	0	0	0	0	0	0	0	0	0	0	0	0
Total	20.065	20.059	20.001	19.986	20.016	20.014	19.963	20.009	19.967	19.944	19.958	19.935	19.965	19.939	19.941	19.993	19.983	19.955	20.026	19.938	20.001	19.989	19.936	19.982	19.965	19.992	19.967	19.981	19.971	19.991
An	60.9	44.0	59.9	51.9	53.5	63.4	58.4	53.7	52.9	55.0	63.6	52.9	54.9	54.4	52.7	52.5	64.3	53.5	53.1	60.8	54.5	52.9	53.6	53.2	54.6	54.7	58.6	54.3	56.0	53.3
Ab	37.7	53.5	38.4	46.3	44.7	35.5	39.7	43.5	43.8	42.1	34.6	44.1	41.9	42.7	44.1	44.5	34.1	43.4	43.8	37.4	43.1	44.3	43.9	43.9	42.4	42.9	39.4	43.3	41.7	43.5
Or	1.4	2.5	1.7	1.8	1.8	1.1	1.8	2.8	3.3	2.9	1.7	3.1	3.2	2.9	3.2	3.0	1.5	3.0	3.1	1.8	2.4	2.8	2.5	2.8	2.9	2.4	2.0	2.4	2.3	3.2

* Total Fe as Fe_2O_3

Appendix 3-3 (Continued).

Locality	KHOK SAMRAN, KS																												
Occurrence	Phenocryst																											Groundmass	
Analysis No	KS110-P29	KS17-P1	KS17-P2	KS17-P3	KS17-P4	KS17-P5	KS17-P6	KS17-P7	KS17-P8	KS17-P9	KS17-P10	KS17-P11	KS17-P12	KS211-PL1	KS211-PL2	KS211-PL3	KS211-PL4	KS211-PL5	KS211-PL6	KS211-PL7	KS213-PL1	KS213-PL2	KS213-PL3	KS213-PL4	KS214-PL1	KS214-PL2	KS214-PL3	KS110-P30	KS110-P31
SiO_2	51.78	53.46	53.93	53.45	53.66	53.80	53.60	53.37	53.75	52.97	54.40	53.53	54.89	53.43	53.53	54.13	53.39	53.30	53.96	53.37	53.45	52.30	53.17	53.51	52.60	53.16	54.05	52.71	53.81
TiO_2	0	0	0	0	0	0	0	0	0	0	0	0	0	0	0	0	0	0	0	0	0	0	0	0	0	0	0	0	0
Al_2O_3	29.63	28.62	28.07	28.70	28.54	28.76	28.21	28.14	28.63	28.57	28.05	28.07	27.41	29.38	28.90	29.28	29.12	28.89	28.95	28.99	28.44	29.65	28.58	28.66	28.91	28.89	27.88	29.58	28.23
$Fe_2O_3^*$	0.81	0.53	0.38	0.35	0.56	0.58	0.52	0.66	0.71	0.51	0.49	0.48	0.54	0.51	0.45	0.43	0.52	0.50	0.33	0.70	0.30	0.61	0.43	0.58	0.87	0.56	0.59	0.68	0.82
MgO	0	0	0	0	0	0	0	0	0	0	0	0	0	0	0	0	0	0	0	0	0	0	0	0	0	0	0	0	0
CaO	12.94	11.70	11.25	11.64	11.58	11.76	11.15	11.62	11.72	11.90	10.64	11.25	9.96	12.09	11.87	12.19	12.56	12.21	12.13	12.29	11.84	13.13	11.88	11.80	12.59	12.35	11.02	12.61	11.48
Na_2O	3.87	4.57	4.99	4.56	4.78	4.61	4.91	4.75	4.56	4.50	5.07	4.78	5.59	4.51	4.54	4.55	4.34	4.62	4.54	4.49	4.81	4.11	4.71	4.78	4.12	4.30	4.97	4.13	4.77
K_2O	0.28	0.34	0.44	0.37	0.39	0.36	0.43	0.39	0.35	0.33	0.41	0.33	0.50	0.37	0.32	0.26	0.23	0.19	0.21	0.31	0.38	0.29	0.34	0.31	0.24	0.31	0.37	0.16	0.44
BaO	0	0	0	0	0	0	0	0	0	0	0	0	0	0	0	0	0	0	0	0	0	0	0	0	0	0	0	0	0
Total	99.31	99.22	99.04	99.08	99.51	99.88	98.82	98.93	99.73	98.77	99.05	98.43	98.88	100.29	99.62	100.84	100.15	99.72	100.12	100.15	99.21	100.07	99.11	99.62	99.34	99.56	98.88	99.86	99.56
Numbers of ions on the basis of 32 O																													
Si	9.487	9.759	9.858	9.765	9.773	9.760	9.822	9.786	9.766	9.722	9.919	9.839	10.023	9.663	9.734	9.724	9.671	9.696	9.755	9.676	9.768	9.513	9.731	9.740	9.623	9.687	9.889	9.579	9.803
Ti	0	0	0	0	0	0	0	0	0	0	0	0	0	0	0	0	0	0	0	0	0	0	0	0	0	0	0	0	0
Al	6.399	6.157	6.046	6.178	6.127	6.148	6.091	6.079	6.131	6.181	6.026	6.079	5.898	6.262	6.192	6.198	6.217	6.193	6.168	6.195	6.126	6.355	6.163	6.148	6.232	6.203	6.011	6.336	6.061
Fe^{3+}	0.111	0.073	0.052	0.048	0.077	0.079	0.071	0.091	0.097	0.071	0.068	0.066	0.074	0.069	0.062	0.058	0.071	0.069	0.046	0.096	0.042	0.083	0.060	0.079	0.120	0.077	0.081	0.093	0.112
Mg	0	0	0	0	0	0	0	0	0	0	0	0	0	0	0	0	0	0	0	0	0	0	0	0	0	0	0	0	0
Ca	2.539	2.288	2.202	2.279	2.259	2.286	2.189	2.283	2.282	2.340	2.078	2.215	1.949	2.343	2.313	2.346	2.437	2.380	2.350	2.387	2.318	2.558	2.329	2.301	2.468	2.412	2.160	2.454	2.241
Na	1.376	1.616	1.767	1.616	1.686	1.622	1.744	1.689	1.607	1.600	1.790	1.702	1.979	1.583	1.599	1.585	1.524	1.629	1.591	1.577	1.703	1.449	1.670	1.685	1.462	1.517	1.762	1.453	1.685
K	0.066	0.079	0.102	0.087	0.091	0.084	0.100	0.090	0.082	0.076	0.096	0.078	0.116	0.085	0.075	0.060	0.053	0.044	0.048	0.071	0.089	0.066	0.080	0.071	0.056	0.072	0.086	0.036	0.103
Ba	0	0	0	0	0	0	0	0	0	0	0	0	0	0	0	0	0	0	0	0	0	0	0	0	0	0	0	0	0
Total	19.978	19.973	20.028	19.973	20.014	19.979	20.018	20.019	19.965	19.990	19.977	19.979	20.039	20.005	19.976	19.971	19.973	20.010	19.958	20.003	20.044	20.025	20.033	20.024	19.960	19.968	19.989	19.951	20.004
An	63.8	57.4	54.1	57.2	56.0	57.3	54.3	56.2	57.5	58.3	52.4	55.4	48.2	58.4	58.0	58.8	60.7	58.7	58.9	59.1	56.4	62.8	57.1	56.7	61.9	60.3	53.9	62.2	55.6
Ab	34.6	40.6	43.4	40.6	41.8	40.6	43.2	41.6	40.5	39.8	45.2	42.6	48.9	39.5	40.1	39.7	38.0	40.2	39.9	39.1	41.4	35.6	40.9	41.5	36.7	37.9	44.0	36.9	41.8
Or	1.7	2.0	2.5	2.2	2.3	2.1	2.5	2.2	2.1	1.9	2.4	2.0	2.9	2.1	1.9	1.5	1.3	1.1	1.2	1.8	2.2	1.6	2.0	1.7	1.4	1.8	2.1	0.9	2.6

* Total Fe as Fe_2O_3

Appendix 3-3 (Continued).

Locality	KHOK SAMRAN, KS																													
Occurrence	Groundmass																													
Analysis No	KS110-P32	KS10-P33	KS110-P34	KS110-P35	KS110-P36	KS110-P38	KS110-P39	KS110-P40	KS110-P41	KS17-P13	KS17-P14	KS17-P15	KS17-P17	KS17-20	KS17-P21	KS17-P22	KS17-P23	KS17-P24	KS18-P1	KS18-P2	KS18-P3	KS18-P4	KS18-P5	KS18-P6	KS18-P7	KS18-P8	KS18-P9	KS211-PL8	KS211-PL9	KS211-PL10
SiO_2	52.59	53.02	52.54	53.22	52.49	53.59	53.62	54.25	52.09	52.59	52.80	52.78	53.83	52.88	52.70	52.74	53.07	52.02	52.19	52.74	53.28	52.16	52.28	52.20	53.19	52.63	52.31	51.40	52.29	52.66
TiO_2	0	0	0	0	0	0	0	0	0	0	0	0	0	0	0	0	0	0	0	0	0	0	0	0	0	0	0	0	0	0
Al_2O_3	29.36	28.18	29.06	28.05	28.58	28.42	28.13	27.64	29.38	29.02	28.40	28.57	28.58	29.00	28.90	28.85	28.81	29.43	29.37	28.94	28.79	29.14	28.67	28.81	28.48	29.05	29.09	29.89	29.54	28.87
$Fe_2O_3^*$	0.81	1.17	0.98	0.94	0.94	0.76	1.26	1.01	0.77	0.84	0.76	0.90	0.57	0.74	1.01	1.00	1.08	0.95	0.93	0.72	0.87	0.82	0.93	1.12	0.79	0.93	1.17	0.85	1.00	0.95
MgO	0	0	0	0	0	0	0	0	0	0	0	0	0	0	0	0	0	0	0	0	0	0	0	0	0	0	0	0	0	0
CaO	12.87	11.51	12.44	11.30	12.12	11.78	11.55	10.87	12.81	12.32	11.79	11.88	11.47	12.14	12.02	11.95	12.08	12.76	12.92	12.22	12.25	12.65	12.45	12.51	11.51	12.44	12.43	13.80	13.28	12.45
Na_2O	4.03	4.60	4.31	4.30	4.30	4.57	4.65	5.09	4.16	4.31	4.32	4.54	4.62	4.41	4.43	4.43	4.35	4.02	4.03	4.24	4.46	4.02	4.15	3.83	4.64	4.14	4.38	3.74	3.92	4.32
K_2O	0.31	0.35	0.23	0.56	0.37	0.36	0.36	0.33	0.33	0.30	0.30	0.27	0.38	0.22	0.28	0.27	0.30	0.29	0.24	0.33	0.24	0.29	0.30	0.31	0.34	0.29	0.28	0.23	0.21	0.32
BaO	0	0	0	0	0	0	0	0	0	0	0	0	0	0	0	0	0	0	0	0	0	0	0	0	0	0	0	0	0	0
Total	99.97	98.83	99.56	98.37	98.81	99.48	99.57	99.20	99.54	99.38	98.36	98.94	99.45	99.39	99.33	99.22	99.69	99.48	99.68	99.19	99.89	99.08	98.77	98.77	98.95	99.47	99.65	99.91	100.24	99.58
Numbers of ions on the basis of 32 O																														
Si	9.568	9.740	9.596	9.803	9.655	9.768	9.776	9.903	9.528	9.616	9.729	9.686	9.797	9.654	9.638	9.651	9.669	9.518	9.530	9.652	9.685	9.572	9.623	9.606	9.745	9.614	9.560	9.390	9.503	9.620
Ti	0	0	0	0	0	0	0	0	0	0	0	0	0	0	0	0	0	0	0	0	0	0	0	0	0	0	0	0	0	0
Al	6.294	6.102	6.255	6.088	6.197	6.105	6.046	5.947	6.333	6.255	6.167	6.178	6.130	6.239	6.229	6.221	6.186	6.346	6.320	6.241	6.168	6.301	6.221	6.248	6.149	6.253	6.265	6.436	6.327	6.216
Fe^{3+}	0.111	0.161	0.135	0.130	0.130	0.104	0.172	0.139	0.106	0.116	0.105	0.125	0.078	0.102	0.139	0.137	0.148	0.131	0.128	0.099	0.119	0.113	0.128	0.155	0.109	0.127	0.160	0.117	0.137	0.131
Mg	0	0	0	0	0	0	0	0	0	0	0	0	0	0	0	0	0	0	0	0	0	0	0	0	0	0	0	0	0	0
Ca	2.509	2.266	2.434	2.231	2.389	2.301	2.257	2.126	2.510	2.413	2.328	2.335	2.236	2.374	2.355	2.343	2.358	2.502	2.527	2.395	2.386	2.487	2.455	2.466	2.259	2.434	2.434	2.701	2.585	2.436
Na	1.423	1.638	1.526	1.537	1.534	1.614	1.645	1.802	1.476	1.529	1.544	1.617	1.628	1.562	1.572	1.570	1.538	1.425	1.425	1.506	1.572	1.429	1.479	1.365	1.648	1.467	1.551	1.325	1.380	1.531
K	0.073	0.082	0.054	0.131	0.087	0.085	0.083	0.076	0.076	0.070	0.070	0.062	0.088	0.050	0.064	0.063	0.069	0.068	0.057	0.076	0.054	0.068	0.071	0.073	0.080	0.067	0.064	0.053	0.049	0.075
Ba	0	0	0	0	0	0	0	0	0	0	0	0	0	0	0	0	0	0	0	0	0	0	0	0	0	0	0	0	0	0
Total	19.977	19.989	19.999	19.921	19.992	19.977	19.978	19.993	20.029	19.998	19.942	20.002	19.957	19.981	19.997	19.986	19.968	19.990	19.987	19.969	19.985	19.969	19.977	19.912	19.990	19.963	20.035	20.023	19.980	20.009
An	62.7	56.8	60.7	57.2	59.6	57.5	56.6	53.1	61.8	60.1	59.1	58.2	56.6	59.6	59.0	58.9	59.5	62.6	63.0	60.2	59.5	62.4	61.3	63.2	56.7	61.3	60.1	66.2	64.4	60.3
Ab	35.5	41.1	38.0	39.4	38.3	40.4	41.3	45.0	36.3	38.1	39.2	40.3	41.2	39.2	39.4	39.5	38.8	35.7	35.5	37.9	39.2	35.9	36.9	35.0	41.3	37.0	38.3	32.5	34.4	37.9
Or	1.8	2.1	1.3	3.4	2.2	2.1	2.1	1.9	1.9	1.7	1.8	1.6	2.2	1.3	1.6	1.6	1.7	1.7	1.4	1.9	1.4	1.7	1.8	1.9	2.0	1.7	1.6	1.3	1.2	1.9

* Total Fe as Fe_2O_3

Appendix 3-3 (Continued).

Locality	KHOK SAMRAN, KS																	BO PHLOI, BP								NAM YUN, NY				
Occurrence	Groundmass																	Phenocryst			Interstice in groundmass					Groundmass				
Analysis No	KS211-PL11	KS211-PL12	KS211-PL13	KS211-PL14	KS213-PL5	KS213-PL6	KS213-PL7	KS213-PL8	KS213-PL9	KS213-PL10	KS213-PL11	KS213-PL12	KS214-PL4	KS214-PL5	KS214-PL6	KS214-PL7	KS214-PL8	BP83-PL1	BP92-PL7	BP81-PL1	BP733-AF13	BP734-AF5	BP736-AF9	BP736-AF10	BP924-AF14	NY131-PL1	NY131-PL2	NY131-PL3	NY131-PL4	NY131-PL5
SiO_2	51.46	52.53	52.59	52.02	51.68	51.74	51.74	52.58	51.89	51.69	51.40	52.12	51.28	51.88	52.24	51.31	52.17	60.74	61.12	52.73	63.10	65.00	61.91	62.10	62.65	56.27	63.26	54.46	53.70	59.32
TiO_2	0	0	0	0	0	0	0	0	0	0	0	0	0	0	0	0	0	0.28	0	0	0	0	0	0	0	0	0	0	0	0
Al_2O_3	29.53	28.98	29.63	30.41	29.42	29.99	29.54	28.76	29.57	29.97	29.47	29.26	30.24	29.66	29.85	29.56	29.17	24.19	24.29	29.49	21.66	19.36	22.13	22.16	22.05	26.98	21.00	28.58	28.43	24.02
$Fe_2O_3^*$	1.03	0.90	0.85	0.77	0.90	0.75	0.76	0.80	1.05	0.52	0.64	0.87	0.64	1.03	1.00	0.66	0.97	0.37	0.34	0.59	0.48	0.45	0.24	0.41	0.42	0.69	0.60	0.66	0.64	0.47
MgO	0	0	0	0	0	0	0	0	0	0	0	0	0	0	0	0	0	0	0	0	0	0	0	0	0	0	0	0	0	0
CaO	13.68	12.43	13.20	13.61	13.19	13.48	13.16	12.34	13.19	13.40	13.43	12.70	13.92	13.29	13.26	13.47	12.86	5.69	5.46	12.64	3.02	1.05	3.67	3.30	2.71	9.57	2.66	11.52	11.57	6.35
Na_2O	3.83	4.18	3.93	3.64	4.05	3.90	3.78	4.38	3.74	3.83	3.75	4.18	3.33	3.90	3.95	3.78	4.05	7.37	7.14	4.33	7.42	5.94	7.61	7.54	7.58	5.76	7.33	4.76	4.69	7.24
K_2O	0.23	0.22	0.31	0.28	0.26	0.19	0.28	0.29	0.25	0.24	0.28	0.31	0.20	0.21	0.26	0.24	0.24	0.00	1.38	0.30	2.81	7.28	2.13	2.76	2.95	0.55	3.63	0.44	0.37	1.02
BaO	0	0	0	0	0	0	0	0	0	0	0	0	0	0	0	0	0	0	0	0	0.62	0.31	0.79	0.91	0	0	0	0	0	0
Total	99.76	99.24	100.50	100.71	99.51	100.06	99.25	99.16	99.68	99.65	98.97	99.42	99.61	99.95	100.56	99.02	99.47	98.65	99.71	100.08	99.11	99.39	98.47	99.18	98.36	99.81	98.47	100.42	99.40	98.42
Numbers of ions on the basis of 32 O																														
Si	9.421	9.615	9.526	9.408	9.471	9.423	9.488	9.639	9.480	9.443	9.463	9.542	9.376	9.460	9.468	9.443	9.547	10.900	10.914	9.577	11.376	11.794	11.245	11.240	11.334	10.162	11.465	9.823	9.789	10.780
Ti	0	0	0	0	0	0	0	0	0	0	0	0	0	0	0	0	0	0.038	0	0	0	0	0	0	0	0	0	0	0	0
Al	6.371	6.252	6.325	6.481	6.354	6.438	6.385	6.214	6.366	6.452	6.394	6.312	6.517	6.373	6.375	6.411	6.291	5.116	5.112	6.313	4.602	4.139	4.737	4.726	4.701	5.742	4.484	6.074	6.107	5.144
Fe^{3+}	0.142	0.124	0.116	0.104	0.125	0.103	0.105	0.110	0.144	0.071	0.089	0.12	0.088	0.141	0.136	0.092	0.134	0.050	0.045	0.080	0.065	0.061	0.032	0.056	0.058	0.093	0.082	0.090	0.088	0.064
Mg	0	0	0	0	0	0	0	0	0	0	0	0	0	0	0	0	0	0	0	0	0	0	0	0	0	0	0	0	0	0
Ca	2.683	2.438	2.561	2.636	2.590	2.631	2.586	2.424	2.582	2.622	2.648	2.49	2.726	2.596	2.574	2.656	2.522	1.094	1.044	2.460	0.584	0.204	0.714	0.640	0.525	1.852	0.516	2.225	2.258	1.236
Na	1.358	1.484	1.380	1.276	1.439	1.377	1.344	1.557	1.325	1.358	1.337	1.484	1.180	1.378	1.386	1.348	1.438	2.564	2.473	1.523	2.593	2.088	2.678	2.647	2.658	2.017	2.574	1.663	1.656	2.549
K	0.054	0.051	0.071	0.063	0.060	0.045	0.065	0.068	0.058	0.057	0.065	0.071	0.048	0.048	0.061	0.057	0.055	0	0.313	0.070	0.647	1.684	0.493	0.637	0.681	0.126	0.838	0.102	0.087	0.237
Ba	0	0	0	0	0	0	0	0	0	0	0	0	0	0	0	0	0	0	0	0	0.043	0.022	0.056	0.065	0	0	0	0	0	0
Total	20.028	19.964	19.979	19.969	20.039	20.017	19.972	20.012	19.956	20.003	19.997	20.02	19.935	19.996	20.000	20.008	19.987	19.761	19.901	20.024	19.911	19.992	19.956	20.011	19.957	19.992	19.958	19.978	19.985	20.009
An	65.5	61.4	63.8	66.3	63.3	64.9	64.7	59.9	65.1	65.0	65.4	61.6	68.9	64.5	64.0	65.4	62.8	29.9	27.3	60.7	15.3	5.1	18.4	16.3	13.6	46.4	13.1	55.8	56.4	30.7
Ab	33.2	37.4	34.4	32.1	35.2	34.0	33.6	38.5	33.4	33.6	33.0	36.7	29.8	34.3	34.5	33.2	35.8	70.1	64.6	37.6	67.8	52.5	68.9	67.4	68.8	50.5	65.5	41.7	41.4	63.4
Or	1.3	1.3	1.8	1.6	1.5	1.1	1.6	1.7	1.5	1.4	1.6	1.8	1.2	1.2	1.5	1.4	1.4	0.0	8.2	1.7	16.9	42.4	12.7	16.2	17.6	3.2	21.3	2.6	2.2	5.9

* Total Fe as Fe_2O_3

Appendix 3-3 (Continued).

Locality	NAM YUN, NY															PHLOI WAEN, PW			TOK PHROM, TP						
Occurrence	Groundmass															Interstice in groundmass			Interstice in GM		Poikilitic texture in groundmass				
Analysis No	NY131-PL6	NY131-PL7	NY131-PL8	NY131-PL9	NY132-AF1	NY132-AF2	NY132-AF3	NY132-AF4	NY132-AF5	NY132-AF6	NY132-AF7	NY132-AF9	NY132-AF10	NY133-AF2	NY133-AF4	PW318-AF1	PW318-F1/1	PW318-AF2	TP324b-AF1	TP324b-AF2	TP1319-PL2	TP324-PL1	TP324b-PL1	TP324b-PL3	TP324c-PL2	TP324c-PL3
SiO_2	65.91	65.85	64.61	59.38	66.06	66.09	64.52	64.94	65.38	62.17	62.42	65.15	65.66	64.97	64.16	65.62	65.10	65.92	65.38	65.30	57.26	56.99	56.99	55.66	57.91	60.35
TiO_2	0	0	0	0	0.24	0	0	0	0	0	0	0	0.22	0	0.30	0.23	0	0	0.36	0.55	0.67	0.29	0.32	0.31	0.71	0.63
Al_2O_3	19.21	19.10	20.64	24.59	19.22	19.20	18.79	20.12	18.89	22.31	21.47	19.05	19.05	19.23	19.27	17.20	16.73	18.22	19.47	18.55	25.39	26.08	26.97	27.12	25.70	23.61
$Fe_2O_3^*$	0.34	0	0	0.49	0	0	0.48	0.41	0.25	0.46	0.53	0.26	0.24	0.26	0.33	1.39	1.47	0.33	0.76	0.99	0.56	0.54	0.35	0.77	0.80	0.42
MgO	0	0	0	0	0	0	0	0	0	0	0	0	0	0	0.21	0	0	0	0.22	0.00	0.26	0.00	0.41	0.38	0.23	0.00
CaO	0.58	0.62	2.03	6.83	0.65	0.60	1.65	1.70	0.68	4.29	3.34	0.90	0.88	0.99	1.17	0	0	0	0.93	0.32	6.75	7.94	8.58	9.09	7.05	4.96
Na_2O	5.51	5.85	7.05	7.04	5.78	5.47	5.98	6.51	5.59	7.87	6.83	5.42	5.40	6.26	5.67	3.05	2.98	3.33	5.89	3.93	6.39	5.96	5.87	5.87	6.28	6.72
K_2O	8.43	7.97	4.99	0.99	8.15	8.37	7.53	6.22	8.20	2.03	3.75	8.40	8.45	6.64	7.08	11.94	11.91	12.22	7.24	10.58	0.80	0.71	0.59	0.46	0.79	2.03
BaO	0	0	0	0	0	0	0	0	0	0	0	0	0	0	0	0	0	0	0	0	0	0	0	0	0	0
Total	99.99	99.38	99.32	99.32	100.10	99.73	98.95	99.91	99.00	99.12	98.33	99.16	99.89	98.81	98.41	99.44	98.18	100.02	100.25	100.47	98.34	98.51	100.22	99.66	99.46	98.72
Numbers of ions on the basis of 32 O																										
Si	11.881	11.913	11.622	10.701	11.879	11.921	11.787	11.674	11.900	11.188	11.351	11.857	11.860	11.775	11.715	12.058	12.118	12.023	11.708	11.819	10.436	10.369	10.203	10.069	10.429	10.912
Ti	0	0	0	0	0.033	0	0	0	0	0	0	0	0.029	0	0.041	0.032	0	0	0.048	0.075	0.092	0.039	0.043	0.043	0.096	0.086
Al	4.082	4.072	4.376	5.223	4.072	4.082	4.045	4.263	4.052	4.732	4.601	4.085	4.056	4.107	4.146	3.725	3.669	3.917	4.108	3.956	5.454	5.593	5.690	5.782	5.453	5.030
Fe^{3+}	0.047	0	0	0.066	0	0	0.066	0.055	0.034	0.062	0.073	0.035	0.032	0.035	0.046	0.193	0.206	0.046	0.102	0.135	0.077	0.075	0.047	0.105	0.109	0.057
Mg	0	0	0	0	0	0	0	0	0	0	0	0	0	0	0.057	0	0	0	0.059	0	0.071	0	0.110	0.102	0.060	0
Ca	0.112	0.120	0.390	1.319	0.126	0.116	0.324	0.328	0.132	0.827	0.651	0.175	0.170	0.191	0.229	0	0	0	0.179	0.061	1.318	1.548	1.645	1.762	1.359	0.961
Na	1.926	2.051	2.458	2.460	2.015	1.911	2.119	2.270	1.974	2.745	2.406	1.911	1.892	2.198	2.007	1.088	1.076	1.176	2.044	1.377	2.257	2.104	2.036	2.059	2.191	2.354
K	1.939	1.838	1.144	0.227	1.869	1.926	1.754	1.427	1.904	0.466	0.869	1.949	1.946	1.536	1.649	2.799	2.827	2.843	1.654	2.442	0.185	0.165	0.134	0.105	0.181	0.469
Ba	0	0	0	0	0	0	0	0	0	0	0	0	0	0	0	0	0	0	0	0	0	0	0	0	0	0
Total	19.987	19.995	19.991	19.997	19.994	19.956	20.094	20.016	19.996	20.020	19.950	20.013	19.986	19.914	19.924	19.894	19.896	20.005	19.936	19.908	19.928	19.892	19.929	20.027	19.880	19.870
An	2.8	3.0	9.8	32.9	3.1	2.9	7.7	8.1	3.3	20.5	16.6	4.3	4.2	4.9	5.9	0.0	0.0	0.0	4.6	1.6	35.0	40.6	43.1	44.9	36.4	25.4
Ab	48.4	51.1	61.6	61.4	50.3	48.3	50.5	56.4	49.2	68.0	61.3	47.4	47.2	56.0	51.7	28.0	27.6	29.3	52.7	35.5	60.0	55.1	53.4	52.4	58.7	62.2
Or	48.7	45.9	28.7	5.7	46.6	48.7	41.8	35.5	47.5	11.5	22.1	48.3	48.6	39.1	42.4	72.0	72.4	70.7	42.7	62.9	4.9	4.3	3.5	2.7	4.9	12.4

*Total Fe as Fe_2O_3

Appendix 3-4 Chemical composition of ulvöspinel-magnetite in basalt samples.

Locality	CHIANG KHONG, CK											BAN NONG, NAM CHO, BN								
Occurrence	Groundmass											Groundmass								
Sample No	CK210-MT5	CK210-MT6	CK210-MT7	CK29-MT4	CK29-MT5	CK29-MT6	CK519B-MT1	CK519B-MT3	CK519B-MT4	CK519B-MT6	CK519B-MT7	BN134-MT1	BN134-MT4	BN135-M1	BN135-M4	BN135-M6	BN135-M7	BN6-MT1	BN6-MT2	BN6-MT3
SiO_2	0.26	0.28	0.27	0.29	0.22	0.20	0.32	0.33	0.33	0.30	0.31	0.26	1.42	0.59	3.22	0.31	0.48	0.48	0.53	0.29
TiO_2	22.55	22.86	23.64	23.47	24.07	23.82	23.30	23.33	23.29	23.12	23.77	22.72	21.07	21.13	21.17	23.65	22.99	21.57	22.97	22.17
Al_2O_3	5.10	4.96	4.22	4.91	4.23	4.53	4.88	4.54	5.08	4.83	3.85	2.55	4.08	5.05	4.49	4.23	4.80	3.02	1.14	1.85
Fe_2O_3	19.75	19.18	16.72	16.16	17.69	17.56	18.23	18.90	16.69	19.81	19.14	21.45	21.78	22.05	16.55	18.89	19.10	25.00	22.35	23.50
FeO	43.55	44.44	47.19	46.13	45.18	44.61	43.97	44.78	45.58	43.45	45.59	46.25	44.86	43.71	45.03	44.38	45.25	46.41	50.14	48.07
MnO	0.65	0.51	0.63	0.70	0.58	0.65	0.67	0.65	0.52	0.43	0.63	0.81	0.60	0.72	0.60	0.80	0.68	0.61	0.75	0.89
MgO	3.97	3.79	2.97	3.96	3.44	3.68	4.00	3.71	4.19	4.02	3.25	3.24	4.80	4.61	4.76	5.06	5.06	2.45	1.40	1.86
CaO	0.28	0.21	0.23	0.22	0.16	0.28	0.35	0.22	0.27	0.30	0.48	0.28	0.18	0.52	1.88	0.55	0	0	0.12	0.25
Na_2O	0.38	0.38	0	0	0.48	0.34	0.39	0.32	0	0.58	0.39	0	0	0	0	0	0	0.37	0	0
K_2O	0	0	0.10	0.11	0	0.11	0	0.10	0	0	0	0	0	0	0	0	0	0	0	0
NiO	0	0	0	0	0	0	0	0	0	0	0	0	0	0	0	0	0	0	0	0
Cr_2O_3	0.37	0.47	0.26	0.32	0.25	0.31	0.30	0.20	0.30	0.39	0.20	0.53	0.60	0.89	0.30	0.32	1.02	0.39	0.22	0.32
ZnO	0	0	0	0	0	0	0	0	0	0	0	0	0	0	0	0	0	0	0	0
Total	96.86	97.08	96.21	96.45	96.32	96.07	96.40	97.08	96.24	97.22	97.61	98.09	99.38	99.27	98.00	98.18	99.37	100.31	99.61	99.20
Numbers of ions on the basis of 32 O																				
Si	0.076	0.083	0.080	0.085	0.066	0.058	0.094	0.097	0.098	0.087	0.091	0.077	0.403	0.168	0.915	0.089	0.136	0.140	0.156	0.086
Ti	4.946	5.013	5.295	5.185	5.343	5.286	5.132	5.129	5.145	5.045	5.228	5.039	4.512	4.524	4.528	5.115	4.908	4.687	5.124	4.937
Al	1.753	1.704	1.480	1.698	1.472	1.575	1.683	1.563	1.758	1.650	1.326	0.886	1.370	1.694	1.506	1.433	1.605	1.029	0.398	0.645
Fe^{3+}	4.333	4.208	3.746	3.570	3.928	3.899	4.016	4.156	3.688	4.324	4.211	4.759	4.665	4.721	3.542	4.087	4.078	5.433	4.989	5.234
Fe^{2+}	10.619	10.833	11.751	11.327	11.147	11.009	10.766	10.945	11.195	10.540	11.150	11.402	10.680	10.403	10.708	10.670	10.739	11.211	12.436	11.899
Mn	0.161	0.126	0.159	0.174	0.144	0.163	0.167	0.161	0.129	0.105	0.156	0.201	0.145	0.173	0.145	0.195	0.163	0.150	0.188	0.224
Mg	1.725	1.647	1.317	1.734	1.514	1.617	1.745	1.617	1.835	1.739	1.417	1.426	2.036	1.957	2.016	2.170	2.142	1.056	0.619	0.820
Ca	0.088	0.065	0.072	0.070	0.052	0.087	0.109	0.069	0.084	0.093	0.151	0.087	0.054	0.160	0.572	0.168	0	0	0	0
Na	0.214	0.213	0	0	0.276	0.195	0.220	0.181	0	0.327	0.222	0	0	0	0	0	0	0.205	0	0
K	0	0	0.038	0.042	0	0.040	0	0.035	0	0	0	0	0	0	0	0	0	0	0	0
Ni	0	0	0	0	0	0	0	0	0	0	0	0	0	0	0	0	0	0	0	0
Cr	0.085	0.109	0.061	0.075	0.059	0.072	0.069	0.046	0.069	0.089	0.047	0.123	0.135	0.201	0.067	0.073	0.229	0.088	0.053	0.075
Zn	0	0	0	0	0	0	0	0	0	0	0	0	0	0	0	0	0	0	0	0
Total	24.000	24.000	24.000	24.000	24.000	24.000	24.000	24.000	24.000	24.000	24.000	24.000	24.000	24.000	24.000	24.000	24.000	24.000	24.000	24.000
%END-MEMBERS																				
Spinel	22.6	21.6	16.9	22.3	19.9	21.2	23.0	21.2	23.5	23.2	18.8	18.2	27.0	25.5	31.0	28.0	27.2	13.8	7.9	10.5
Hercynite	0	0	0	0	0	0	0	0	0	0	0	0	0	0	0	0	0	0	0	0
Gahnite	0	0	0	0	0	0	0	0	0	0	0	0	0	0	0	0	0	0	0	0
Galaxite	2.1	1.6	2.0	2.2	1.9	2.1	2.2	2.1	1.6	1.4	2.1	2.6	1.9	2.2	2.2	2.5	2.1	2.0	2.4	2.9
Magnetite	22.8	22.5	21.1	19.2	20.9	20.5	20.9	22.0	19.7	22.5	22.6	25.2	24.0	24.4	18.7	19.7	20.4	30.7	29.3	29.9
Chromite	0.4	0.6	0.3	0.4	0.3	0.4	0.4	0.2	0.4	0.5	0.3	0.7	0.7	1.0	0.4	0.4	1.1	0.5	0.3	0.4
Ulvöspinel	52.0	53.7	59.7	55.8	57.0	55.7	53.5	54.4	54.9	52.4	56.2	53.4	46.4	46.8	47.8	49.4	49.1	53.0	60.1	56.4
Total	100.0	100.0	100.0	100.0	100.0	100.0	100.0	100.0	100.0	100.0	100.0	100.0	100.0	100.0	100.0	100.0	100.0	100.0	100.0	100.0

Appendix 3-4 (Continued).

Locality	SOP PRAP, SP					DEN CHAI, DC														
Occurrence	Groundmass					Groundmass														
Sample No	SP1B-MT1	SP1B-MT4	SP1B-MT5	SP1B-MT7	SP1B-MT10	DC157-MT1	DC157-MT2	DC160-MT1	DC160-MT5	DC160-MT7	DC161-MT1	DC161-MT3	DC161-MT5	DC162-MT1	DC162-MT2	DC162-MT5	DC162-MT7	DC162-MT9	DC162-MT10	DC263-MT1
SiO_2	0.28	0.32	0.29	0.37	0.20	0.27	1.10	0.81	0.33	0.31	0.58	0.69	0.37	0.74	0.35	0.37	0.44	0.37	0.43	0.30
TiO_2	21.03	20.85	21.33	21.89	21.82	12.41	25.41	24.01	23.43	22.41	21.56	22.94	22.38	23.49	24.13	22.76	24.47	23.39	24.14	21.92
Al_2O_3	3.56	3.54	3.85	3.98	4.27	9.22	2.05	2.32	2.18	4.20	4.49	4.19	3.47	2.56	2.42	3.30	2.19	3.07	2.44	4.01
Fe_2O_3	22.98	23.44	21.56	21.13	21.71	17.28	15.07	18.15	20.43	21.76	21.48	19.36	21.71	19.19	19.17	20.93	18.48	20.65	19.05	20.60
FeO	43.02	42.53	44.58	43.03	42.71	36.33	49.35	47.89	46.59	45.15	44.70	46.38	45.28	47.20	47.91	46.06	48.40	46.43	47.80	44.80
MnO	0.59	0.61	0.63	0.65	0.59	0.75	0.64	0.89	0.76	0.70	0.65	0.67	0.85	0.69	0.62	0.73	0.75	0.76	0.61	0.60
MgO	2.77	2.98	3.40	3.68	3.78	4.96	3.73	3.52	3.59	4.59	4.57	4.34	4.08	3.69	3.43	4.16	3.42	4.21	3.66	4.36
CaO	0.24	0.29	0.27	0.16	0.22	0	0.25	0.19	0.22	0.13	0.17	0.18	0.23	0.30	0.26	0	0	0	0.15	0
Na_2O	0.45	0.38	0	0.39	0.42	0	0	0	0	0	0	0	0	0	0	0	0	0	0	0
K_2O	0	0.10	0	0	0	0	0	0	0	0	0	0	0	0	0	0	0	0	0	0
NiO	0	0	0	0	0	0	0	0	0	0	0	0	0	0	0	0	0	0	0	0
Cr_2O_3	0.24	0.27	0.29	0.41	0.52	18.36	0.81	0.80	0.79	0.85	1.54	0.96	0.70	0.83	0.89	1.37	0.65	0.55	0.83	2.03
ZnO	0	0	0	0	0	0	0	0	0	0	0	0	0	0	0	0	0	0	0	0
Total	95.14	95.31	96.19	95.68	96.23	99.59	98.40	98.56	98.31	100.09	99.74	99.70	99.07	98.69	99.19	99.68	98.81	99.43	99.12	98.62
Numbers of ions on the basis of 32 O																				
Si	0.084	0.095	0.087	0.109	0.059	0.076	0.321	0.235	0.097	0.089	0.165	0.196	0.108	0.216	0.103	0.106	0.130	0.108	0.125	0.086
Ti	4.775	4.722	4.783	4.896	4.847	2.593	5.579	5.278	5.176	4.787	4.612	4.917	4.863	5.147	5.281	4.918	5.384	5.070	5.278	4.761
Al	1.267	1.256	1.354	1.395	1.486	3.019	0.705	0.799	0.755	1.406	1.504	1.408	1.181	0.880	0.828	1.118	0.756	1.043	0.836	1.365
Fe^{3+}	5.222	5.309	4.837	4.728	4.822	3.611	3.309	3.990	4.516	4.650	4.596	4.151	4.718	4.205	4.199	4.523	4.068	4.477	4.167	4.477
Fe^{2+}	10.861	10.706	11.114	10.701	10.544	8.438	12.043	11.702	11.444	10.726	10.630	11.052	10.936	11.495	11.660	11.064	11.838	11.186	11.619	10.822
Mn	0.150	0.155	0.158	0.163	0.148	0.177	0.158	0.219	0.190	0.167	0.157	0.162	0.207	0.171	0.153	0.178	0.186	0.184	0.150	0.146
Mg	1.245	1.337	1.513	1.633	1.664	2.054	1.621	1.532	1.571	1.945	1.939	1.843	1.755	1.602	1.489	1.782	1.490	1.807	1.587	1.879
Ca	0.077	0.093	0.086	0.052	0.069	0	0.078	0.059	0.069	0.039	0.051	0.055	0.072	0.094	0.082	0	0	0	0.047	0
Na	0.263	0.224	0	0.227	0.240	0	0	0	0	0	0	0	0	0	0	0	0	0	0	0
K	0	0.040	0	0	0	0	0	0	0	0	0	0	0	0	0	0	0	0	0	0
Ni	0	0	0	0	0	0	0	0	0	0	0	0	0	0	0	0	0	0	0	0
Cr	0.057	0.065	0.067	0.095	0.121	4.032	0.186	0.185	0.183	0.191	0.346	0.215	0.159	0.190	0.205	0.312	0.150	0.126	0.191	0.464
Zn	0	0	0	0	0	0	0	0	0	0	0	0	0	0	0	0	0	0	0	0
Total	24.000	24.000	24.000	24.000	24.000	24.000	24.000	24.000	24.000	24.000	24.000	24.000	24.000	24.000	24.000	24.000	24.000	24.000	24.000	24.000
%END-MEMBERS																				
Spinel	16.4	17.7	19.3	21.5	21.8	25.9	21.3	19.9	20.1	24.7	24.9	23.8	22.4	20.8	19.1	22.6	18.9	22.9	20.3	23.7
Hercynite	0	0	0	0	0	0	0	0	0	0	0	0	0	0	0	0	0	0	0	0
Gahnite	0	0	0	0	0	0	0	0	0	0	0	0	0	0	0	0	0	0	0	0
Galaxite	2.0	2.0	2.0	2.1	1.9	2.2	2.1	2.8	2.4	2.1	2.0	2.1	2.7	2.2	2.0	2.3	2.4	2.3	1.9	1.8
Magnetite	28.7	28.7	26.3	24.7	25.1	20.2	17.3	20.9	23.3	23.6	23.7	21.7	24.2	22.0	22.2	23.2	21.4	22.7	21.7	23.0
Chromite	0.3	0.4	0.4	0.5	0.6	22.6	1.0	1.0	0.9	1.0	1.8	1.1	0.8	1.0	1.1	1.6	0.8	0.6	1.0	2.4
Ulvöspinel	52.6	51.1	52.0	51.2	50.5	29.0	58.3	55.4	53.3	48.6	47.6	51.3	49.9	53.9	55.7	50.4	56.6	51.4	55.1	49.0
Total	100.0	100.0	100.0	100.0	100.0	100.0	100.0	100.0	100.0	100.0	100.0	100.0	100.0	100.0	100.0	100.0	100.0	100.0	100.0	100.0

Appendix 3-4 (Continued).

Locality	DEN CHAI, DC							KHOK SAM RAN, KS												
Occurrence	Groundmass							Groundmass												
Sample No	DC263-MT2	DC264-MT1	DC264-MT3	DC264-MT4	DC264-MT5	DC264-MT6	DC264-MT7	KS110-M1	KS110-M2	KS110-M7	KS110-M8	KS17-M6	KS211-MT1	KS211-MT2	KS211-MT5	KS211-MT6	KS211-MT8	KS211-T10	KS211-T11	KS211-T12
SiO_2	0.65	0.61	0.50	0.89	1.09	0.41	3.04	0.43	0.58	0.40	0.88	0.52	0.30	0.41	0.39	0.34	0.33	0.52	0.33	0.33
TiO_2	21.61	17.62	21.71	19.71	17.87	19.04	20.90	22.01	22.97	22.72	23.15	24.09	25.88	25.72	26.53	25.98	27.13	26.43	25.43	26.56
Al_2O_3	4.45	5.96	4.49	4.80	5.46	5.10	4.80	2.19	1.37	1.08	1.41	1.14	1.15	1.30	1.52	1.49	1.68	1.64	1.54	1.42
Fe_2O_3	21.15	21.60	20.63	20.13	20.99	22.78	15.59	23.66	21.91	23.29	20.82	20.04	17.82	17.65	15.57	16.60	15.48	14.64	17.95	15.76
FeO	44.33	42.08	44.66	44.24	41.71	42.01	47.51	47.86	48.08	48.18	48.65	49.03	50.38	50.29	51.23	50.28	52.34	51.57	49.83	51.27
MnO	0.75	0.60	0.66	0.56	0.61	0.71	0.59	0.63	0.76	0.89	0.84	0.76	0.60	0.76	0.60	0.68	0.61	0.64	0.68	0.77
MgO	4.62	4.55	4.56	4.00	4.56	4.88	3.99	2.53	2.55	2.09	2.40	2.53	2.83	2.82	2.61	2.87	2.68	2.44	2.77	2.50
CaO	0.16	0	0	0.08	0.16	0.06	0.61	0	0.19	0.20	0.34	0.18	0.13	0	0.18	0	0	0.12	0.19	0.20
Na_2O	0	0	0	0	0	0	0	0	0	0	0	0	0	0	0	0	0	0	0	0
K_2O	0	0	0	0	0	0	0	0	0	0	0	0	0	0	0	0	0	0	0	0
NiO	0	0	0	0	0	0	0	0	0	0	0	0	0	0	0	0	0	0	0	0
Cr_2O_3	0.97	7.89	1.61	4.62	6.13	5.15	1.78	0.40	0.21	0	0.20	0.34	0.23	0	0	0	0	0.39	0	0.21
ZnO	0	0	0	0.18	0.31	0.02	0.13	0	0	0	0	0	0	0	0	0	0	0	0	0
Total	98.70	100.92	98.81	99.20	98.89	100.17	98.93	99.70	98.62	98.85	98.68	98.63	99.31	98.97	98.63	98.23	100.25	98.38	98.71	99.01
Numbers of ions on the basis of 32 O																				
Si	0.186	0.171	0.142	0.254	0.311	0.116	0.863	0.126	0.172	0.120	0.260	0.154	0.087	0.120	0.114	0.102	0.096	0.154	0.097	0.097
Ti	4.667	3.704	4.688	4.244	3.830	4.042	4.466	4.845	5.121	5.085	5.153	5.372	5.718	5.697	5.892	5.789	5.926	5.884	5.642	5.886
Al	1.505	1.962	1.520	1.620	1.834	1.697	1.606	0.754	0.480	0.378	0.491	0.397	0.397	0.452	0.528	0.519	0.574	0.573	0.536	0.492
Fe^{3+}	4.568	4.544	4.455	4.337	4.502	4.837	3.333	5.210	4.885	5.214	4.636	4.472	3.939	3.913	3.459	3.700	3.383	3.261	3.985	3.494
Fe^{2+}	10.644	9.836	10.721	10.593	9.942	9.913	11.287	11.712	11.917	11.987	12.037	12.159	12.377	12.387	12.650	12.454	12.709	12.764	12.293	12.633
Mn	0.183	0.143	0.159	0.136	0.146	0.170	0.141	0.156	0.190	0.225	0.210	0.191	0.149	0.190	0.149	0.170	0.151	0.160	0.169	0.191
Mg	1.976	1.897	1.950	1.706	1.939	2.054	1.689	1.103	1.126	0.929	1.058	1.118	1.238	1.240	1.151	1.266	1.162	1.075	1.218	1.096
Ca	0.050	0	0	0.026	0.048	0.017	0.185	0	0.061	0.064	0.108	0.058	0.041	0	0.056	0	0	0.039	0.060	0.063
Na	0	0	0	0	0	0	0	0	0	0	0	0	0	0	0	0	0	0	0	0
K	0	0	0	0	0	0	0	0	0	0	0	0	0	0	0	0	0	0	0	0
Ni	0	0	0	0	0	0	0	0	0	0	0	0	0	0	0	0	0	0	0	0
Cr	0.220	1.744	0.365	1.047	1.381	1.150	0.401	0.093	0.049	0	0.046	0.079	0.053	0	0	0	0	0.090	0	0.048
Zn	0	0	0	0.037	0.066	0.004	0.027	0	0	0	0	0	0	0	0	0	0	0	0	0
Total	24.000	24.000	24.000	24.000	24.000	24.000	24.000	24.000	24.000	24.000	24.000	24.000	24.000	24.000	24.000	24.000	24.000	24.000	24.000	24.000
%END-MEMBERS																				
Spinel	25.5	24.2	24.8	22.1	25.4	26.1	24.3	14.0	14.5	11.9	13.9	14.4	15.7	15.7	14.7	16.0	14.7	13.8	15.5	14.0
Hercynite	0	0	0	0	0	0	0	0	0	0	0	0	0	0	0	0	0	0	0	0
Gahnite	0	0	0	0.5	0.9	0	0.4	0	0	0	0	0	0	0	0	0	0	0	0	0
Galaxite	2.4	1.8	2.0	1.8	1.9	2.2	2.0	2.0	2.4	2.9	2.8	2.5	1.9	2.4	1.9	2.2	1.9	2.0	2.2	2.4
Magnetite	23.3	24.5	23.0	23.7	23.9	24.6	19.3	29.2	26.7	28.9	25.8	24.3	21.0	20.9	18.9	19.8	18.5	18.2	21.5	19.1
Chromite	1.1	9.4	1.9	5.7	7.3	5.9	2.3	0.5	0.3	0	0.3	0.4	0.3	0	0	0	0	0.5	0	0.3
Ulvöspinel	47.7	40.0	48.3	46.3	40.6	41.2	51.7	54.3	56.1	56.4	57.3	58.4	61.1	60.9	64.5	62.0	64.9	65.5	60.8	64.2
Total	100.0	100.0	100.0	100.0	100.0	100.0	100.0	100.0	100.0	100.0	100.0	100.0	100.0	100.0	100.0	100.0	100.0	100.0	100.0	100.0

Appendix 3-4 (Continued).

Locality	KHOK SAMRAN, KS													BO PHLOI, BP						
Occurrence	Groundmass													Groundmass						
Sample No	KS213-MT2	KS213-MT4	KS213-MT5	KS213-MT7	KS213-MT8	KS214-MT2	KS214-MT3	KS214-MT4	KS214-MT5	KS214-MT7	KS214-MT8	KS214-MT10	KS214-MT12	BP733-MT2	BP81-MT3	BP82A-MT3	BP85-MT1	BP9-MT1	BP9-MT2	BP922-MT1
SiO_2	0.30	0.27	0.32	0.24	0.32	0.30	0.55	0.42	0.42	0.40	0.32	0.31	0.30	0.44	0.18	0.22	0.34	0.46	0.34	0.18
TiO_2	25.86	25.91	26.00	25.78	24.47	15.82	26.68	26.30	26.65	26.97	26.24	26.40	26.13	18.24	20.62	21.26	11.27	20.50	21.85	20.01
Al_2O_3	1.73	1.23	1.48	1.66	1.60	6.68	1.29	1.32	1.45	1.61	1.71	1.28	1.52	1.53	1.84	0.48	10.99	0.82	0.55	2.80
Fe_2O_3	16.78	17.09	17.34	17.01	19.23	32.07	15.59	16.40	16.02	15.67	16.08	16.38	16.22	31.70	28.54	28.96	31.06	27.40	26.16	27.52
FeO	51.17	50.23	50.99	50.99	49.29	41.98	51.78	51.24	52.42	52.34	51.59	51.53	51.16	41.60	43.98	42.50	36.44	44.67	46.96	44.07
MnO	0.56	0.71	0.59	0.68	0.62	0.34	0.67	0.78	0.69	0.74	0.57	0.64	0.69	0.92	0.79	0.71	0.78	0.68	0.79	0.56
MgO	2.39	2.81	2.68	2.30	2.71	3.36	2.81	2.64	2.24	2.57	2.39	2.43	2.45	3.84	3.78	3.25	4.32	3.15	2.49	3.33
CaO	0	0	0	0	0	0	0	0	0.12	0	0	0	0	0	0.12	0.16	0	0.19	0.20	0.38
Na_2O	0	0	0	0	0	0	0	0	0	0	0	0	0	0	0	0.53	0	0	0	0
K_2O	0	0	0	0	0	0	0	0	0	0	0	0	0	0	0	0	0	0	0	0
NiO	0	0	0	0	0	0	0	0	0	0	0	0	0	0	0	0	0	0	0	0
Cr_2O_3	0	0.35	0	0	0.34	0	0.47	0.26	0.20	0	0	0	0.29	0.34	0	0.29	4.48	0.71	0.40	0.57
ZnO	0	0	0	0	0	0	0	0	0	0	0	0	0	0	0	0	0	0	0	0
Total	98.80	98.60	99.40	98.65	98.59	100.54	99.83	99.35	100.22	100.30	98.91	98.97	98.75	98.60	99.86	98.34	99.67	98.58	99.73	99.42
Numbers of ions on the basis of 32 O																				
Si	0.088	0.079	0.094	0.071	0.096	0.085	0.162	0.122	0.123	0.117	0.095	0.093	0.088	0.131	0.053	0.064	0.095	0.138	0.099	0.052
Ti	5.746	5.764	5.737	5.743	5.445	3.376	5.852	5.808	5.848	5.894	5.822	5.864	5.810	4.047	4.509	4.740	2.359	4.577	4.853	4.386
Al	0.602	0.428	0.510	0.581	0.559	2.232	0.444	0.457	0.498	0.552	0.595	0.446	0.528	0.531	0.631	0.166	3.603	0.286	0.193	0.960
Fe^{3+}	3.730	3.804	3.828	3.790	4.281	6.847	3.421	3.624	3.517	3.426	3.570	3.640	3.609	7.035	6.244	6.459	6.503	6.118	5.811	6.033
Fe^{2+}	12.641	12.425	12.511	12.631	12.191	9.961	12.627	12.582	12.788	12.716	12.726	12.728	12.646	10.262	10.693	10.535	8.478	11.088	11.596	10.737
Mn	0.141	0.178	0.146	0.170	0.156	0.080	0.165	0.194	0.171	0.183	0.141	0.161	0.174	0.229	0.195	0.178	0.183	0.170	0.197	0.138
Mg	1.052	1.240	1.174	1.014	1.194	1.419	1.222	1.154	0.972	1.113	1.050	1.068	1.078	1.687	1.638	1.436	1.793	1.396	1.096	1.444
Ca	0	0	0	0	0	0	0	0	0.039	0	0	0	0	0	0.036	0.051	0	0.061	0.062	0.119
Na	0	0	0	0	0	0	0	0	0	0	0	0	0	0	0	0.302	0	0	0	0
K	0	0	0	0	0	0	0	0	0	0	0	0	0	0	0	0	0	0	0	0
Ni	0	0	0	0	0	0	0	0	0	0	0	0	0	0	0	0	0	0	0	0
Cr	0	0.081	0	0	0.080	0	0.107	0.060	0.045	0	0	0	0.068	0.079	0	0.069	0.986	0.166	0.093	0.131
Zn	0	0	0	0	0	0	0	0	0	0	0	0	0	0	0	0	0	0	0	0
Total	24.000	24.000	24.000	24.000	24.000	24.000	24.000	24.000	24.000	24.000	24.000	24.000	24.000	24.000	24.000	24.000	24.000	24.000	24.000	24.000
%END-MEMBERS																				
Spinel	13.3	15.7	14.9	12.8	15.1	17.9	15.6	14.6	12.4	14.1	13.3	13.5	13.6	21.4	20.7	18.9	22.7	17.9	14.0	18.4
Hercynite	0	0	0	0	0	0	0	0	0	0	0	0	0	0	0	0	0	0	0	0
Gahnite	0	0	0	0	0	0	0	0	0	0	0	0	0	0	0	0	0	0	0	0
Galaxite	1.8	2.3	1.9	2.1	2.0	1.0	2.1	2.5	2.2	2.3	1.8	2.0	2.2	2.9	2.5	2.4	2.3	2.2	2.5	1.8
Magnetite	20.8	20.3	20.8	21.1	23.3	40.8	18.5	19.6	19.7	18.8	19.9	20.0	19.9	35.0	31.4	31.8	40.0	31.7	31.1	32.2
Chromite	0	0.4	0	0	0.4	0	0.6	0.3	0.3	0	0	0	0.4	0.4	0.0	0.3	6.1	0.9	0.5	0.7
Ulvöspinel	64.1	61.4	62.5	64.0	59.2	40.2	63.2	62.9	65.5	64.7	65.0	64.5	63.9	40.3	45.4	46.6	29.0	47.4	51.9	46.9
Total	100.0	100.0	100.0	100.0	100.0	100.0	100.0	100.0	100.0	100.0	100.0	100.0	100.0	100.0	100.0	100.0	100.0	100.0	100.0	100.0

Appendix 3-4 (Continued).

Locality	BO PHLOI, BP							NAM YUN, NY											
Occurrence	Groundmass							Groundmass											
Sample No	BP922-MT2	BP922-MT3	BP922-MT4	BP924-MT1	BP924-MT3	BP924-MT4	BP930-MT1	NY131-MT1	NY131-MT2	NY131-MT3	NY131-MT5	NY131-MT7	NY131-MT8	NY132-MT1	NY132-MT2	NY132-MT3	NY132-MT4	NY132-MT5	NY133-MT1
SiO_2	0.58	0.46	0.84	4.87	0.36	0.38	0.40	0.19	0.23	0.30	0.34	0.35	0.41	0.38	2.12	0.30	0.31	0.23	0.27
TiO_2	17.57	18.32	19.29	17.59	18.95	20.00	20.73	28.56	28.21	27.96	27.92	27.96	28.76	28.20	25.39	27.84	28.18	28.52	27.66
Al_2O_3	2.28	1.97	2.23	2.68	1.71	1.46	2.20	1.60	1.47	1.53	1.32	1.40	1.55	1.47	2.01	1.30	1.39	1.34	1.38
Fe_2O_3	31.60	31.55	27.85	21.09	29.98	28.05	26.77	12.48	12.95	13.41	13.50	13.16	11.23	12.59	12.85	14.33	12.88	12.92	14.82
FeO	43.28	41.18	42.83	46.06	44.21	45.16	45.15	54.00	53.78	53.94	54.05	53.90	54.84	54.30	53.63	53.90	54.55	54.50	51.09
MnO	0.88	0.78	0.81	0.59	0.83	0.70	0.88	0.48	0.54	0.57	0.65	0.41	0.65	0.45	0.61	0.65	0.47	0.65	0.52
MgO	2.63	3.40	2.90	3.42	2.56	2.71	3.38	2.30	2.14	2.03	1.87	2.09	1.88	2.02	1.96	2.02	1.78	1.94	2.05
CaO	0.21	1.35	1.63	1.66	0.12	0	0	0	0	0	0	0	0	0	0.15	0	0	0	0
Na_2O	0	0	0	0	0	0	0	0	0	0	0	0	0	0	0	0	0	0	0.48
K_2O	0	0	0	0	0	0	0	0	0	0	0	0	0	0	0	0	0	0	0
NiO	0	0	0	0	0	0	0	0	0	0	0	0	0	0	0	0	0	0	0
Cr_2O_3	0.69	0.24	0.19	0.46	0.29	0.34	0.45	0	0	0	0	0	0	0	0	0	0	0	0
ZnO	0	0	0	0	0	0	0	0	0	0	0	0	0	0	0	0	0	0	0
Total	99.71	99.24	98.57	98.42	99.01	98.80	99.96	99.62	99.32	99.74	99.66	99.28	99.31	99.40	98.71	100.34	99.56	100.09	98.26
Numbers of ions on the basis of 32 O																			
Si	0.170	0.135	0.247	1.401	0.106	0.113	0.117	0.057	0.066	0.089	0.101	0.103	0.120	0.111	0.621	0.088	0.090	0.066	0.080
Ti	3.873	4.028	4.265	3.808	4.222	4.463	4.529	6.292	6.245	6.166	6.177	6.195	6.368	6.240	5.610	6.114	6.241	6.280	6.165
Al	0.786	0.677	0.772	0.908	0.596	0.509	0.752	0.552	0.508	0.530	0.457	0.487	0.537	0.511	0.697	0.447	0.484	0.461	0.481
Fe^{3+}	6.969	6.942	6.159	4.568	6.682	6.260	5.851	2.751	2.869	2.959	2.988	2.917	2.487	2.787	2.841	3.149	2.854	2.847	3.304
Fe^{2+}	10.609	10.069	10.526	11.087	10.949	11.202	10.966	13.226	13.237	13.227	13.295	13.277	13.502	13.356	13.175	13.161	13.434	13.341	12.660
Mn	0.218	0.193	0.203	0.144	0.208	0.177	0.216	0.120	0.134	0.140	0.162	0.102	0.162	0.111	0.153	0.160	0.118	0.161	0.130
Mg	1.148	1.480	1.270	1.467	1.131	1.197	1.465	1.003	0.941	0.888	0.821	0.919	0.824	0.884	0.858	0.881	0.779	0.844	0.904
Ca	0.067	0.421	0.514	0.512	0.039	0	0	0	0	0	0	0	0	0	0.046	0	0	0	0
Na	0	0	0	0	0	0	0	0	0	0	0	0	0	0	0	0	0	0	0.275
K	0	0	0	0	0	0	0	0	0	0	0	0	0	0	0	0	0	0	0
Ni	0	0	0	0	0	0	0	0	0	0	0	0	0	0	0	0	0	0	0
Cr	0.159	0.055	0.043	0.106	0.067	0.080	0.104	0	0	0	0	0	0	0	0	0	0	0	0
Zn	0	0	0	0	0	0	0	0	0	0	0	0	0	0	0	0	0	0	0
Total	24.000	24.000	24.000	24.000	24.000	24.000	24.000	24.000	24.000	24.000	24.000	24.000	24.000	24.000	24.000	24.000	24.000	24.000	24.000
%END-MEMBERS																			
Spinel	14.8	19.9	17.5	24.1	14.4	15.2	18.6	12.6	11.9	11.2	10.4	11.6	10.5	11.2	11.7	11.1	9.9	10.6	11.8
Hercynite	0	0	0	0	0	0	0	0	0	0	0	0	0	0	0	0	0	0	0
Gahnite	0	0	0	0	0	0	0	0	0	0	0	0	0	0	0	0	0	0	0
Galaxite	2.8	2.6	2.8	2.4	2.7	2.2	2.7	1.5	1.7	1.8	2.0	1.3	2.1	1.4	2.1	2.0	1.5	2.0	1.7
Magnetite	38.6	35.8	33.3	27.3	36.5	33.9	30.7	15.4	16.1	16.8	17.1	16.6	14.3	16.0	17.4	17.8	16.5	16.1	18.3
Chromite	0.9	0.3	0.2	0.6	0.4	0.4	0.5	0	0	0	0	0	0	0	0	0	0	0	0
Ulvöspinel	42.9	41.5	46.1	45.6	46.1	48.3	47.5	70.5	70.3	70.2	70.5	70.5	73.2	71.4	68.8	69.1	72.2	71.2	68.2
Total	100.0	100.0	100.0	100.0	100.0	100.0	100.0	100.0	100.0	100.0	100.0	100.0	100.0	100.0	100.0	100.0	100.0	100.0	100.0

Appendix 3-4 (Continued).

Locality	PHLOI WAEN, PW				TOK PHROM, TP											NONG BON, NB				
Occurrence	Groundmass				Groundmass											Groundmass				
Sample No	PW2-MT1	PW2-MT2	PW2-MT3	PW214-MT1	TP1320-MT1	TP1320-MT2	TP1331-MT1	TP324a-MT1	TP324a-MT2	TP324a-MT3	TP324b-MT1	TP324b-MT2	TP324b-MT3	TP324c-MT1	TP324c-MT2	TP324c-MT3	NB132-MT1	NB132-MT3	NB132-MT4	NB133-MT5	NB5238A-MT6
SiO_2	0.14	0.26	0.28	1.72	0.36	1.13	0.38	0.23	0.22	0.23	0.25	0	0.29	0.22	0	0.26	5.30	0.31	0.24	3.68	0.21
TiO_2	8.94	31.07	0.75	11.78	22.42	21.53	23.35	23.08	24.27	23.19	22.88	22.19	24.40	22.55	23.34	23.26	19.79	20.86	20.50	22.68	21.78
Al_2O_3	0.38	0.36	0.52	0.28	4.28	4.69	3.99	2.72	1.31	2.51	2.05	2.42	0.44	2.67	1.99	2.28	2.57	2.14	2.38	1.23	2.22
Fe_2O_3	47.13	1.48	64.05	38.16	21.82	20.75	20.40	24.26	21.22	22.99	24.13	26.04	22.81	23.34	22.51	24.40	16.73	26.01	26.50	14.14	23.56
FeO	31.38	52.07	25.55	35.40	44.82	45.37	47.41	45.07	48.37	45.67	44.36	43.19	48.43	44.23	46.34	45.16	45.46	43.65	43.25	49.25	43.98
MnO	0.40	0.84	0.53	0.72	0.74	0.58	0.56	0.53	0.72	0.67	0.53	0.88	0.76	0.57	0.81	0.68	0.70	0.62	0.77	0.73	0.83
MgO	3.31	2.48	2.83	2.27	4.70	4.48	3.87	3.82	3.04	3.38	3.33	3.53	1.94	3.89	3.47	3.82	4.36	3.93	3.84	2.44	2.75
CaO	0.15	0.18	0.17	1.95	0.18	0.22	0.14	0.18	0.19	0.19	0.29	0.17	0.23	0.29	0.14	0.16	2.87	0.14	0.15	1.94	0.24
Na_2O	0	0	0	0	0	0	0	0.39	0	0.33	0.51	0.50	0.38	0.37	0	0.39	0	0	0	0	0.32
K_2O	0	0	0	0	0	0	0	0	0	0	0	0	0	0	0	0	0	0	0	0	0
NiO	0	0	0	0	0	0	0	0	0	0	0	0	0	0	0	0	0	0	0	0	0
Cr_2O_3	0	0.26	0.34	0	0.32	0.33	0.31	0	0.20	0.33	0.25	0.26	0	0	0	0.19	0	0	0	0	0
ZnO	0	0	0	0	0	0	0	0	0	0	0	0	0	0	0	0	0	0	0	0	0
Total	91.84	88.99	95.01	92.28	99.63	99.08	100.39	100.27	99.53	99.50	98.58	99.17	99.67	98.32	98.60	100.59	97.79	97.65	97.63	96.07	95.88
Numbers of ions on the basis of 32 O																					
Si	0.045	0.086	0.088	0.548	0.104	0.323	0.109	0.065	0.065	0.067	0.074	0	0.086	0.065	0	0.073	1.514	0.090	0.072	1.099	0.065
Ti	2.167	7.630	0.177	2.823	4.804	4.622	5.002	4.970	5.348	5.054	5.033	4.849	5.414	4.945	5.164	5.003	4.254	4.642	4.563	5.096	4.952
Al	0.143	0.137	0.192	0.106	1.437	1.578	1.338	0.919	0.452	0.857	0.706	0.829	0.152	0.917	0.689	0.768	0.867	0.746	0.831	0.432	0.792
Fe^{3+}	11.432	0.365	15.194	9.151	4.677	4.458	4.372	5.227	4.677	5.012	5.311	5.692	5.065	5.120	4.982	5.251	3.597	5.791	5.900	3.178	5.359
Fe^{2+}	8.459	14.217	6.735	9.433	10.677	10.830	11.291	10.791	11.848	11.064	10.852	10.493	11.949	10.781	11.398	10.802	10.862	10.800	10.702	12.303	11.119
Mn	0.109	0.233	0.141	0.193	0.178	0.140	0.134	0.128	0.179	0.165	0.132	0.218	0.189	0.140	0.201	0.164	0.170	0.155	0.193	0.184	0.212
Mg	1.593	1.205	1.331	1.079	1.998	1.908	1.645	1.630	1.328	1.459	1.452	1.527	0.853	1.692	1.522	1.631	1.858	1.732	1.692	1.087	1.239
Ca	0.051	0.061	0.058	0.666	0.055	0.067	0.041	0.055	0.058	0.059	0.092	0.052	0.072	0.092	0.043	0.050	0.878	0.045	0.047	0.622	0.078
Na	0	0	0	0	0	0	0	0.215	0	0.188	0.290	0.280	0.219	0.209	0	0.215	0	0	0	0	0.185
K	0	0	0	0	0	0	0	0	0	0	0	0	0	0	0	0	0	0	0	0	0
Ni	0	0	0	0	0	0	0	0	0	0	0	0	0	0	0	0	0	0	0	0	0
Cr	0	0.067	0.085	0	0.071	0.074	0.069	0	0.045	0.076	0.057	0.060	0	0	0	0.043	0	0	0	0	0
Zn	0	0	0	0	0	0	0	0	0	0	0	0	0	0	0	0	0	0	0	0	0
Total	24.000	24.000	24.000	24.000	24.000	24.000	24.000	24.000	24.000	24.000	24.000	24.000	24.000	24.000	24.000	24.000	24.000	24.000	24.000	24.000	24.000
%END-MEMBERS																					
Spinel	20.2	15.3	16.9	15.9	25.5	25.1	21.0	21.3	16.9	19.0	19.3	19.9	11.2	22.3	19.1	21.3	33.1	22.0	21.5	17.3	16.1
Hercynite	0	0	0	0	0	0	0	0	0	0	0	0	0	0	0	0	0	0	0	0	0
Gahnite	0	0	0	0	0	0	0	0	0	0	0	0	0	0	0	0	0	0	0	0	0
Galaxite	1.4	3.0	1.8	2.8	2.3	1.8	1.7	1.7	2.3	2.1	1.7	2.8	2.5	1.8	2.5	2.1	3.0	2.0	2.5	2.9	2.8
Magnetite	56.9	1.9	79.0	50.3	23.5	23.6	23.4	26.6	24.5	26.0	27.2	28.5	27.5	25.9	25.5	26.3	19.0	29.2	29.9	19.0	28.5
Chromite	0	0.4	0.4	0	0.4	0.4	0.4	0	0.2	0.4	0.3	0.3	0	0	0	0.2	0	0	0	0	0
Ulvöspinel	21.6	79.4	1.8	31.0	48.4	49.0	53.6	50.5	56.1	52.5	51.5	48.5	58.8	50.0	52.9	50.1	44.9	46.8	46.2	60.8	52.6
Total	100.0	100.0	100.0	100.0	100.0	100.0	100.0	100.0	100.0	100.0	100.0	100.0	100.0	100.0	100.0	100.0	100.0	100.0	100.0	100.0	100.0

Appendix 3-5 Chemical composition of apatite in basalt samples.

Locality	BO PHLOI, BP																KS
Occurrence	Groundmass																Groundmass
Analysis No	BP81-AP1	BP82A-AP1	BP82A-AP2	BP82A-AP3	BP921-AP1	BP921-AP2	BP921A-AP1	BP921A-AP2	BP921A-AP3	BP921B-AP1	BP921B-AP2	BP921B-AP3	BP921B-AP4	BP924-AP1	BP924A-AP1	BP924A-AP2	KS1-AP1
SiO_2	0	0	0	0	0	0	0	0	0.28	0.39	0.39	0.20	0.20	0	0.27	0.18	0.60
FeO*	0.33	0.29	0.27	0.32	0.47	0.27	0.26	0.35	0.44	0.43	0.42	0.27	0.28	0.23		0.36	0.32
MnO	0	0	0	0	0	0	0	0	0	0	0	0	0	0	0	0	0
MgO	0.08	0.27	0.19	0.24	0	0	0.23	0	0.32	0.26	0.26	0.30	0.28	0	0.21	0.23	0.35
CaO	54.18	52.30	52.69	53.04	53.09	53.01	52.30	52.11	52.90	51.31	51.56	52.02	51.68	53.95	51.79	51.74	53.02
Na_2O	0	0.75	0.33	0.24	0	0	0.28	0.34	0.31	0.38	0	0.36	0.48	0	0.45	0.40	0
K_2O	0	0.10	0.14	0.10	0	0	0.15	0.12	0	0	0.10	0	0.22	0	0.25	0.30	0.16
P_2O_5	43.03	41.31	41.58	41.22	42.24	41.65	40.77	41.10	41.37	39.83	40.82	40.99	40.80	42.37	40.63	40.65	40.27
Cl	0	0.87	0.65	0.28	0	0	0.63	0.40	0.76	0.94	0.85	0.91	0.83	0	0.77	0.64	
Ori. Total	97.62	95.89	95.85	95.44	95.80	94.93	94.62	94.42	96.38	93.54	94.40	95.05	94.77	96.55	94.37	94.50	94.72
-O≡Cl	0	0.20	0.15	0.06	0	0	0.14	0.09	0.17	0.21	0.19	0.21	0.19	0	0.17	0.14	0
Total	97.62	95.69	95.70	95.38	95.80	94.93	94.48	94.33	96.21	93.33	94.21	94.84	94.58	96.55	94.20	94.36	94.72
Numbers of ions on the basis of **12.5 O**																	
Si	0	0	0	0	0	0	0	0	0.024	0.034	0.034	0.018	0.017	0	0.024	0.015	0.052
Fe^{2+}	0.023	0.021	0.019	0.023	0.033	0.020	0.019	0.025	0.031	0.032	0.030	0.019	0.020	0.016	0.000	0.026	0.023
Mn	0	0	0	0	0	0	0	0	0	0	0	0	0	0	0	0	0
Mg	0.010	0.034	0.025	0.031	0	0	0.030	0	0.041	0.034	0.034	0.039	0.037	0	0.027	0.029	0.045
Ca	4.853	4.809	4.836	4.891	4.847	4.890	4.872	4.851	4.833	4.840	4.797	4.815	4.804	4.893	4.831	4.826	4.926
Na	0	0.124	0.054	0.040	0	0	0.047	0.058	0.051	0.064	0	0.060	0.081	0	0.076	0.067	0
K	0	0.011	0.015	0.011	0	0	0.016	0.014	0	0	0.011	0	0.024	0	0.028	0.033	0.018
P	3.045	3.002	3.015	3.003	3.048	3.036	3.001	3.023	2.987	2.969	3.001	2.998	2.997	3.036	2.995	2.996	2.957
Cl	0	0.063	0.047	0.020	0	0	0.046	0.030	0.055	0.070	0.062	0.067	0.061	0	0.056	0.047	0
Total	7.931	8.064	8.011	8.019	7.928	7.946	8.031	8.001	8.022	8.043	7.969	8.016	8.041	7.945	8.037	8.039	8.021

* Total Fe as FeO; H_2O is not analysed.

Appendix 3-6 Chemical composition of nepheline, leucite and zeolite in basalt samples.

Mineral/Locality	Nepheline/NONG BON, NB						Leucite/BAN NONG, NAM CHO, BN												Leucite,/BOPHLOI, BP			Leucite,/TOK PHROM. TP			Zeolite/ BN	Zeolite/ BP
Occurrence	?	Oikocryst of Poikilitic texture in groundmass					Interstice In groundmass												Interstice in groundmass			Interstice in GM	At Pheno.(CPX) Rim		Ground-mass	Interstice in GM
Analysis No	NB5238A-NE1	NB131-NE1	NB131-NE2	NB131-NE3	NB131-NE4	NB131-NE5	BN6-LEU1	BN6-LEU2	BN6-LEU3	BN6-LEU4	BN6-LEU5	BN6-LEU6	BN6-LEU7	BN6-LEU8	BN447-LEU2	BN447-LEU3	BN139-LEU7	BN139-LEU8	BN139-LEU9	BP924A-LEU2	BP924A-LEU3	BP921B-LEU1	TP324c-LEU1	TP1330-LEU1	TP1330-LEU2	BN446-ZE1	BP924A-ZE4
SiO_2	46.28	44.23	44.37	44.26	43.58	43.47	56.58	56.73	56.33	56.34	55.48	55.47	56.58	56.39	55.03	55.25	55.17	54.96	55.09	55.43	55.61	54.99	55.23	54.87	55.21	54.70	53.02
TiO_2	0	0	0	0	0	0	0	0	0	0.24	0	0	0	0	0	0.17	0	0	0	0	0	0	0.18	0.26	0	0	0
Al_2O_3	31.65	32.23	32.61	32.58	32.78	32.48	23.15	23.22	23.56	23.47	22.77	22.87	23.08	23.06	22.85	23.23	22.64	22.62	22.71	22.72	22.75	22.66	23.19	22.35	22.72	25.06	27.57
$Fe_2O_3^*$	1.04	1.11	0.95	1.03	0.93	1.23	0.42	0.52	0.70	0.53	0.62	0.52	0.51	0.50	0.48	0.47	0.27	0	0.25	0.27	0.67	0.53	0.74	0	0	0.77	1.01
FeO	-	-	-	-	-	-	-	-	-	-	-	-	-	-	-	-	-	-	-	-	-	-	-	-	-	-	-
MgO	0.77	0	0	0	0	0	0	0	0	0	0	0	0	0	0	0	0	0	0	0	0	0	0.32	0	0	0.36	0.60
CaO	0.00	0.53	0.50	0.35	0.56	0.39	0	0.25	0.18	0	0	0	0	0	0	0	0	0	0	0	0	0	0	0	0	0.61	0
Na_2O	16.67	16.44	17.09	17.03	16.95	17.07	0.27	0	0.48	0	0	0.26	0	0	0	0.28	0.16	0.71	0.76	0	0.32	0	0.22	0.35	0.49	11.95	15.53
K_2O	4.48	4.34	4.13	4.48	4.62	4.32	21.38	21.21	20.20	19.91	20.46	20.87	20.89	21.36	20.12	18.94	20.88	19.79	19.81	20.37	20.30	20.24	20.32	20.66	20.41	4.75	1.55
Total	100.89	98.88	99.65	99.73	99.42	98.96	101.80	101.93	101.45	100.49	99.33	99.99	101.06	101.31	98.48	98.34	99.12	98.08	98.62	98.79	99.65	98.42	100.20	98.49	98.83	98.20	99.28
Numbers of O	32						6																			80	
Si	8.720	8.528	8.492	8.480	8.394	8.407	2.015	2.015	2.004	2.014	2.018	2.011	2.022	2.017	2.015	2.013	10.756	10.775	10.751	2.024	2.017	2.017	1.994	2.018	2.019	25.683	24.541
Ti	0	0	0	0	0	0	0	0	0	0.007	0	0	0	0	0	0.005	0	0	0	0	0	0	0.005	0.007	0	0	0
Al	7.027	7.324	7.356	7.356	7.441	7.403	0.972	0.972	0.988	0.989	0.976	0.977	0.972	0.972	0.986	0.997	5.201	5.226	5.222	0.978	0.972	0.980	0.987	0.968	0.979	13.869	15.037
Fe^{3+}	0.147	0.161	0.137	0.149	0.135	0.179	0.011	0.014	0.019	0.014	0.017	0.014	0.014	0.014	0.013	0.013	0.040	0	0.037	0.007	0.018	0.015	0.020	0	0	0.271	0.352
Fe^{2+}	-	-	-	-	-	-	-	-	-	-	-	-	-	-	-	-	-	-	-	-	-	-	-	-	-	-	-
Mg	0.215	0	0	0	0	0	0	0	0	0	0	0	0	0	0	0	0	0	0	0	0	0	0.017	0	0	0.254	0.411
Ca	0	0.110	0.103	0.072	0.115	0.080	0	0.009	0.007	0	0	0	0	0	0	0	0	0	0	0	0	0	0	0	0	0.308	0
Na	6.090	6.144	6.341	6.325	6.331	6.399	0.019	0	0.033	0	0	0.018	0	0	0	0.020	0.061	0.271	0.287	0	0.022	0	0.015	0.025	0.035	10.877	13.932
K	1.076	1.068	1.007	1.095	1.135	1.066	0.972	0.961	0.917	0.908	0.949	0.965	0.953	0.975	0.940	0.880	5.193	4.948	4.932	0.949	0.939	0.947	0.936	0.969	0.952	2.844	0.916
Total	23.276	23.335	23.435	23.477	23.550	23.535	3.988	3.972	3.968	3.932	3.960	3.985	3.961	3.977	3.955	3.927	21.250	21.221	21.229	3.958	3.969	3.959	3.974	3.988	3.985	54.107	55.189
Ne	76.7	78.8	80.7	79.7	80.2	80.8																					
Ks	15.1	15.3	14.3	15.4	16.0	15.0																					
Q	8.3	5.9	5.1	4.9	3.7	4.2																					

*Total Fe as Fe_2O_3

Appendix 3-7 Chemical composition of CPX in alluvium, xenocryst and xenolith (Note: $\Sigma Fe = Fe^{2+}+Fe^{3+}+Mn$; $mg^*=100xMg/(Mg+Fe^{2+}+Fe^{3+}+Mn)$.

Locality	DEN CHAI, DC																					
Occurrence	Alluvium						Dunite xenolith			Spinel-Lherzolite xenolith												
Analysis No	DCCPX1-1	DCCPX2-2	DCCPX4-1	DCCPX4-3	DCCPX5-1	DCCPX5-3	DC164-PX11	DC164-PX12	DC164-PX16	DC266-CPX1	DC266-CPX2	DC269-CPX1	DC269-CPX2	DC269-CPX4	DC269-CPX5	DC269-CPX6	DC269-CPX7	DC270-CPX1	DC270-CPX2	DC270-CPX3	DC270-CPX4	DC271-CPX2	DC271-CPX4
SiO_2	48.41	47.14	48.55	48.12	47.58	48.14	52.19	52.09	51.77	52.12	52.16	51.89	51.50	51.86	51.42	51.76	51.39	52.00	51.93	52.08	51.85	51.30	51.88
TiO_2	1.08	1.94	1.28	1.34	1.58	1.63	0.71	0.60	0.72	0.58	0.48	0.57	0.56	0.56	0.67	0.58	0.63	0.55	0.49	0.61	0.64	0.62	0.70
Al_2O_3	9.23	8.95	9.17	8.85	8.97	9.21	7.10	7.00	4.51	7.23	4.90	7.49	5.38	7.04	5.52	7.07	3.98	7.13	7.14	7.17	4.63	4.75	4.38
Fe_2O_3	2.08	3.39	3.75	2.10	3.17	1.23	0.53	1.34	1.32	0.97	0.76	1.15	0.77	1.75	1.00	0.61	0.80	1.46	1.60	0.32	0.69	0.37	0.01
FeO	4.35	4.58	3.08	4.41	3.95	5.75	2.48	1.92	2.15	2.32	2.74	2.20	2.40	1.93	2.32	2.81	2.66	2.07	1.87	2.93	2.71	2.95	3.31
MnO	0.24	0	0.23	0.19	0.14	0	0	0	0	0	0	0	0	0	0	0	0.23	0	0	0	0	0	0
MgO	14.23	12.25	13.98	13.59	13.03	12.93	15.12	14.93	16.06	15.12	16.48	14.93	15.90	15.20	15.89	15.03	15.92	15.20	15.06	15.00	16.66	16.02	16.55
CaO	17.88	18.80	18.23	18.07	18.72	18.67	19.69	19.44	22.21	19.75	21.90	19.50	22.14	19.58	22.24	19.63	22.22	19.70	19.72	19.72	21.82	22.87	22.18
Na_2O	1.29	1.64	1.64	1.46	1.52	1.36	1.81	2.03	0.72	1.79	0.57	1.89	0.64	1.81	0.64	1.65	0.49	1.78	1.85	1.70	0.48	0	0
K_2O	0	0	0	0	0	0	0	0	0	0	0	0	0	0	0	0	0	0	0	0	0	0	0
Cr_2O_3	0	0	0	0	0	0	1.19	1.26	1.42	0.93	0.82	0.80	1.04	0.75	0.87	0.70	0.92	0.78	0.81	0.79	0.87	0.87	0.94
Total	98.80	98.69	99.91	98.12	98.65	98.91	100.83	100.60	100.87	100.82	100.80	100.42	100.32	100.47	100.58	99.84	99.24	100.66	100.47	100.33	100.33	100.11	100.42
Numbers of ions on the basis of 6 O																							
Si	1.787	1.760	1.774	1.792	1.770	1.785	1.870	1.870	1.871	1.867	1.881	1.865	1.867	1.865	1.860	1.873	1.889	1.866	1.867	1.875	1.879	1.872	1.884
Ti	0.030	0.054	0.035	0.037	0.044	0.045	0.019	0.016	0.020	0.016	0.013	0.015	0.015	0.015	0.018	0.016	0.017	0.015	0.013	0.016	0.017	0.017	0.019
Al	0.402	0.394	0.395	0.388	0.393	0.402	0.300	0.296	0.192	0.305	0.208	0.317	0.230	0.298	0.235	0.302	0.173	0.301	0.303	0.304	0.198	0.204	0.188
Fe^{3+}	0.058	0.095	0.103	0.059	0.089	0.034	0.014	0.036	0.036	0.026	0.021	0.031	0.021	0.047	0.027	0.017	0.022	0.039	0.043	0.009	0.019	0.010	0.000
Fe^{2+}	0.134	0.143	0.094	0.137	0.123	0.178	0.074	0.058	0.065	0.070	0.082	0.066	0.073	0.058	0.070	0.085	0.082	0.062	0.056	0.088	0.082	0.090	0.101
Mn	0.008	0	0.007	0.006	0.004	0	0	0	0	0	0	0	0	0	0	0	0.007	0	0	0	0	0	0
Mg	0.783	0.682	0.762	0.754	0.722	0.715	0.808	0.799	0.866	0.807	0.886	0.800	0.859	0.815	0.857	0.811	0.873	0.813	0.807	0.805	0.900	0.871	0.896
Ca	0.707	0.752	0.714	0.721	0.746	0.742	0.756	0.748	0.860	0.758	0.846	0.751	0.860	0.754	0.862	0.761	0.875	0.757	0.759	0.761	0.847	0.894	0.863
Na	0.093	0.119	0.116	0.105	0.109	0.098	0.126	0.141	0.050	0.124	0.040	0.132	0.045	0.126	0.045	0.116	0.035	0.124	0.129	0.119	0.034	0	0
K	0	0	0	0	0	0	0	0	0	0	0	0	0	0	0	0	0	0	0	0	0	0.017	0.022
Cr	0	0	0	0	0	0	0.034	0.036	0.041	0.026	0.023	0.023	0.030	0.021	0.025	0.020	0.027	0.022	0.023	0.023	0.025	0.025	0.027
Total	4.000	4.000	4.000	4.000	4.000	4.000	4.000	4.000	4.000	4.000	4.000	4.000	4.000	4.000	4.000	4.000	4.000	4.000	4.000	4.000	4.000	4.000	4.000
Ca%(Wo%)	41.8	45.0	42.5	43.0	44.3	44.4	45.7	45.6	47.1	45.6	46.1	45.6	47.4	45.0	47.4	45.5	47.1	45.3	45.6	45.7	45.8	47.9	46.4
Mg%(En%)	46.3	40.8	45.3	45.0	42.9	42.8	48.9	48.7	47.4	48.6	48.3	48.5	47.4	48.7	47.2	48.4	46.9	48.6	48.5	48.4	48.7	46.7	48.2
ΣFe%(Fs%)	11.8	14.2	12.2	12.1	12.8	12.7	5.4	5.7	5.5	5.8	5.6	5.9	5.2	6.3	5.4	6.1	6.0	6.1	6.0	5.8	5.5	5.4	5.4
mg*	79.7	74.1	78.9	78.9	77.0	77.1	90.1	89.5	89.6	89.4	89.6	89.2	90.2	88.6	89.8	88.8	88.7	88.9	89.0	89.3	89.9	89.7	89.9

Appendix 3-7 (Continued).

Locality	BO PHLOI, BP															
Occurrence	Alluvium						Xenocryst					Xenolith (Olivine+CPX)				
Analysis No	BPCPX1-1	BPCPX1-3	BPCPX1-4	BPCPX2-4	BPCPX2-4/1	BPCPX3-4	BP734-CPX1	BP924-CPX15	BP924-CPX16	BP924-CPX17	BP924-CPX18	BP9-CPX1	BP9-CPX5	BP9-CPX6	BP9-CPX7	BP9-CPX8
SiO_2	47.52	47.95	47.19	49.58	50.99	48.44	52.20	48.06	47.74	47.87	47.89	52.17	51.76	51.61	49.39	51.16
TiO_2	1.95	2.05	2.04	0.91	0.80	1.39	0.54	1.83	1.88	1.94	2.01	0.49	0.54	0.58	1.39	0.73
Al_2O_3	9.72	9.72	9.42	7.02	7.41	8.89	5.84	8.85	9.20	9.01	9.07	7.00	7.10	6.99	4.93	5.10
Fe_2O_3	4.20	4.59	3.39	1.79	2.86	1.22	1.50	1.39	3.84	2.02	2.61	0.40	0.65	1.96	2.97	2.06
FeO	3.05	2.89	4.11	3.63	2.54	4.73	1.22	5.14	2.91	4.59	4.29	2.80	2.64	1.48	3.08	2.89
MnO	0	0	0.195	0	0	0	0	0	0	0	0	0	0	0	0	0.24
MgO	11.81	12.27	11.55	15.06	15.52	13.04	15.17	12.41	12.72	12.55	12.38	15.78	15.61	15.76	13.25	15.08
CaO	20.55	20.66	20.37	18.16	18.81	19.87	21.64	20.38	20.40	20.28	20.43	19.48	19.16	19.42	22.45	21.68
Na_2O	1.76	1.71	1.57	1.38	1.60	1.24	1.49	1.24	1.52	1.31	1.41	1.49	1.59	1.68	1.05	0.87
K_2O	0	0	0	0	0	0	0	0	0	0	0	0	0	0	0	0
Cr_2O_3	0	0	0	0.527	0.461	0	1.08	0.19	0	0	0	0.95	0.97	1.04	0.97	0.85
Total	100.57	101.83	99.82	98.06	100.99	98.81	100.69	99.49	100.21	99.56	100.08	100.55	100.03	100.51	99.47	100.65
Numbers of ions on the basis of 6 O																
Si	1.741	1.735	1.747	1.838	1.832	1.795	1.878	1.778	1.750	1.769	1.762	1.872	1.867	1.854	1.835	1.861
Ti	0.054	0.056	0.057	0.025	0.022	0.039	0.015	0.051	0.052	0.054	0.056	0.013	0.015	0.016	0.039	0.020
Al	0.420	0.414	0.411	0.307	0.314	0.388	0.248	0.386	0.398	0.392	0.393	0.296	0.302	0.296	0.216	0.219
Fe^{3+}	0.116	0.125	0.094	0.050	0.077	0.034	0.041	0.039	0.106	0.056	0.072	0.011	0.018	0.053	0.083	0.056
Fe^{2+}	0.094	0.087	0.127	0.112	0.076	0.147	0.037	0.159	0.089	0.142	0.132	0.084	0.080	0.044	0.096	0.088
Mn	0	0	0.006	0	0	0	0	0	0	0	0	0	0	0	0	0.007
Mg	0.645	0.662	0.637	0.832	0.831	0.720	0.814	0.685	0.695	0.691	0.679	0.844	0.840	0.844	0.734	0.818
Ca	0.806	0.801	0.808	0.721	0.724	0.789	0.834	0.808	0.802	0.802	0.805	0.749	0.741	0.747	0.894	0.845
Na	0.125	0.120	0.112	0.099	0.111	0.089	0.104	0.089	0.108	0.093	0.101	0.104	0.111	0.117	0.075	0.062
K	0	0	0	0	0	0	0	0	0	0	0	0	0	0	0	0
Cr	0	0	0	0.015	0.013	0	0.031	0.006	0	0	0	0.027	0.028	0.029	0.029	0.025
Total	4.000	4.000	4.000	4.000	4.000	4.000	4.000	4.000	4.000	4.000	4.000	4.000	4.000	4.000	4.000	4.000
Ca%(Wo%)	48.6	47.8	48.3	42.0	42.4	46.7	48.4	47.8	47.4	47.4	47.7	44.4	44.1	44.3	49.5	46.6
Mg%(En%)	38.8	39.5	38.1	48.5	48.6	42.6	47.2	40.5	41.1	40.9	40.2	50.0	50.1	50.0	40.6	45.1
∑Fe%(Fs%)	12.6	12.7	13.6	9.5	9.0	10.7	4.5	11.7	11.5	11.7	12.1	5.6	5.8	5.8	9.9	8.3
mg*	75.5	75.7	73.7	83.7	84.4	80.0	91.3	77.6	78.1	77.8	76.9	89.9	89.6	89.7	80.4	84.4

Appendix 3-8 Chemical composition of spinel in alluvium, xenocryst, xenolith and inclusion in corundum.

Locality	DEN CHAI, DC																			
Occurrence	Gravel in alluvium					Xenocryst				Spinel lherzolite xenolith										
Sample No	DCSP7-1	DCSP8-2	DCSP8-3	DCSP9-2	DCSP9-3	DC161-SP4	DC376A-SP1 (Core)	DC376A-SP3 (Core)	DC376A-SP5 (Core)	DC266-SP1	DC266-SP5	DC269-SP1	DC269-SP2	DC269-SP3	DC270-SP3	DC270-SP4	DC270-SP5	DC270-SP6	DC271-SP2	DC271-SP3
SiO_2	0.19	0	0.35	0.20	0.26	2.95	0	0.30	0.20	0.26	0.35	0.21	0.32	0.25	0.31	0.27	0.19	0.26	0.21	0.28
TiO_2	0.59	0.53	0.65	0.50	0.54	2.13	0.54	0	0.27	0	0	0	0.21	0	0	0.16	0.20	0.18	0	0
Al_2O_3	58.30	58.32	59.23	59.00	59.11	36.40	51.46	32.82	57.13	58.38	58.07	58.26	58.08	57.98	57.93	57.91	58.04	57.85	57.81	58.01
Fe_2O_3	8.48	8.46	8.80	7.71	9.02	10.16	7.93	5.23	5.55	2.11	1.86	2.45	2.10	2.52	1.95	1.71	2.38	2.11	2.17	1.92
FeO	11.29	10.65	10.51	10.97	9.69	23.09	14.35	15.98	7.05	9.62	9.58	9.24	9.47	9.18	9.63	9.65	9.81	9.57	9.60	9.53
MnO	0	0	0	0	0	0.36	0	0	0	0	0.15	0	0.24	0	0	0	0	0	0	0
MgO	18.27	18.29	19.01	18.60	18.68	12.51	15.40	12.32	20.75	20.64	20.50	20.77	20.82	20.87	20.52	20.55	20.63	20.75	20.32	20.52
CaO	0	0	0	0	0	0.36	0	0	0	0	0	0	0	0	0	0	0	0	0.10	0
Na_2O	0.44	0.37	0.50	0.39	0.74	0	0.62	0.53	0.60	0	0	0	0	0	0	0	0	0	0	0
K_2O	0	0	0	0	0	0	0	0	0	0	0	0	0	0	0	0	0	0	0	0
NiO	0	0	0	0	0	0	0	0	0.43	0.37	0.48	0.51	0.43	0.34	0.42	0.47	0.35	0.30	0.49	0.47
Cr_2O_3	0	0	0	0	0	10.79	9.75	31.39	9.28	8.59	8.78	8.66	8.92	8.76	8.86	8.95	8.76	8.86	8.90	8.79
ZnO	0	0.49	0.49	0	0	0	0	0	0	0	0	0	0	0	0	0	0	0	0	0
Total	97.6	97.1	99.5	97.4	98.0	98.74	100.05	98.57	101.35	99.98	99.76	100.09	100.58	99.90	99.62	99.67	100.36	99.88	99.59	99.50
Numbers of ions on the basis of 32 O																				
Si	0.039	0	0.073	0.042	0.054	0.693	0	0.072	0.042	0.053	0.072	0.042	0.066	0.050	0.064	0.056	0.039	0.053	0.043	0.057
Ti	0.094	0.084	0.101	0.079	0.085	0.376	0.088	0	0.041	0	0	0	0.033	0	0	0.025	0.031	0.028	0	0
Al	14.562	14.631	14.478	14.695	14.600	10.068	13.127	9.238	13.725	14.168	14.133	14.126	14.033	14.081	14.120	14.110	14.067	14.064	14.117	14.149
Fe^{3+}	1.353	1.355	1.374	1.226	1.423	1.793	1.292	0.940	0.851	0.327	0.290	0.380	0.323	0.391	0.303	0.266	0.368	0.328	0.339	0.298
Fe^{2+}	2.000	1.896	1.822	1.938	1.699	4.531	2.597	3.191	1.202	1.657	1.654	1.589	1.623	1.583	1.666	1.668	1.687	1.651	1.664	1.649
Mn	0	0	0	0	0	0.072	0	0	0	0	0.025	0	0.042	0	0	0	0	0	0	0
Mg	5.771	5.804	5.877	5.860	5.838	4.376	4.968	4.386	6.305	6.334	6.313	6.370	6.363	6.411	6.328	6.335	6.325	6.380	6.277	6.330
Ca	0	0	0	0	0	0.090	0	0	0	0	0	0	0	0	0	0	0	0	0.022	0
Na	0.181	0.154	0.199	0.161	0.302	0	0.261	0.247	0.238	0	0	0	0	0	0	0	0	0	0	0
K	0	0	0	0	0	0	0	0	0	0	0	0	0	0	0	0	0	0	0	0
Ni	0	0	0	0	0	0	0	0	0.071	0.062	0.079	0.084	0.071	0.057	0.070	0.078	0.058	0.050	0.081	0.078
Cr	0	0	0	0	0	2.002	1.667	5.926	1.496	1.399	1.433	1.409	1.446	1.427	1.448	1.462	1.424	1.445	1.458	1.439
Zn	0	0.076	0.075	0	0	0	0	0	0	0	0	0	0	0	0	0	0	0	0	0
Total	24.000	24.000	24.000	24.000	24.000	24.000	24.000	24.000	24.000	24.000	24.000	24.000	24.000	24.000	24.000	24.000	24.000	24.000	24.000	24.000
%END-MEMBERS																				
Spinel	74.2	74.0	76.0	75.2	76.4	60.6	64.2	57.1	82.7	80.3	80.4	80.9	80.9	81.2	80.4	80.5	80.0	80.8	79.9	80.5
Hercynite	16.2	15.5	13.1	16.2	13.7	10.0	16.2	0.0	2.1	8.9	8.5	7.9	7.1	7.4	8.6	8.4	8.4	7.8	8.9	8.7
Gahnite	0	1.0	1.0	0	0	0	0	0	0	0	0	0	0	0	0	0	0	0	0	0
Galaxite	0	0	0	0	0	1.0	0	0	0	0	0.3	0	0.5	0	0	0	0	0	0	0
Magnetite	8.5	8.5	8.6	7.7	8.9	11.2	8.1	5.9	5.3	2.0	1.8	2.4	2.0	2.4	1.9	1.7	2.3	2.0	2.1	1.9
Chromite	0	0	0	0	0	12.5	10.4	37.0	9.3	8.7	9.0	8.8	9.0	8.9	9.1	9.1	8.9	9.0	9.1	9.0
Ulvöspinel	1.2	1.1	1.3	1.0	1.1	4.7	1.1	0	0.5	0	0	0	0.4	0	0	0.3	0.4	0.4	0	0
Total	100.0	100.0	100.0	100.0	100.0	100.0	100.0	100.0	100.0	100.0	100.0	100.0	100.0	100.0	100.0	100.0	100.0	100.0	100.0	100.0

Appendix 3-8 (Continued).

Locality	BO PHLOI, BP																		
Occurrence	Gravel in alluvium					Xenocryst													
Sample No	BPSP1-1	BPSP1-2	BPSP1-3	BPSP1-4	BPSP3-1	BP81-SP1	BP81-SP2	BP81-SP3	BP81-SP4	BP81-SP5	BP81-SP6	BP81-SP7	BP81-SP7.1	BP81-SP8	BP81-SP9	BP81-SP11	BP81-SP12	BP81-SP13	BP81-SP14	BP81-SP15
SiO_2	0.39	0.23	0.30	0.36	0.33	0.28	0.32	0.48	0.32	0.37	0.38	0.45	0.40	0.26	0.49	0.43	0.41	0.34	0.40	0.32
TiO_2	0.53	0.71	0.56	0.59	0.72	0.82	0.59	0.63	0.65	0.67	0.58	0.69	0.61	0.65	0.53	0.62	0.75	0.74	0.56	0.54
Al_2O_3	58.98	58.52	59.10	59.03	58.38	54.63	56.04	58.80	59.73	60.17	59.91	60.14	59.97	59.54	60.00	60.10	60.15	59.53	58.59	57.13
Fe_2O_3	6.32	8.15	8.22	6.85	8.53	9.09	8.97	5.76	6.27	6.51	6.32	5.82	5.98	6.49	6.79	5.66	5.95	5.91	6.60	8.08
FeO	12.80	11.46	11.65	12.82	11.51	19.87	17.88	16.43	13.46	13.43	13.54	13.55	13.40	13.23	13.25	13.94	14.08	14.64	16.40	17.39
MnO	0	0	0	0	0	0.24	0.33	0	0	0	0.29	0	0	0	0.21	0	0	0	0.24	0.38
MgO	18.87	18.92	18.95	18.90	18.60	13.88	15.03	16.82	18.79	18.96	18.61	19.03	18.97	18.61	19.03	18.65	18.75	17.82	16.67	15.70
CaO	0	0	0	0	0	0	0	0	0	0	0	0	0	0	0.16	0	0	0.10	0	0
Na_2O	0	0.30	0.31	0.00	0.41	0	0	0	0	0	0	0	0	0	0	0	0	0	0	0
K_2O	0	0	0	0	0	0	0	0	0	0	0	0	0	0	0	0	0	0	0	0
NiO	0	0	0	0.31	0	0	0	0	0	0.3	0	0	0	0.38	0	0	0	0.35	0	0
Cr_2O_3	0.34	0.32	0.28	0.41	0	0.25	0.19	0.23	0.22	0.26	0	0.33	0.42	0.26	0.25	0.27	0.27	0.25	0.29	0.24
ZnO	0	0	0	0	0	0	0.49	0	0	0	0	0	0	0	0	0	0	0	0	0
Total	98.23	98.61	99.38	99.28	98.47	99.04	99.84	99.14	99.43	100.67	99.63	100.01	99.74	99.43	100.71	99.68	100.36	99.68	99.74	99.78
Numbers of ions on the basis of 32 O																				
Si	0.082	0.048	0.063	0.076	0.068	0.061	0.069	0.101	0.066	0.075	0.079	0.093	0.084	0.054	0.101	0.089	0.085	0.071	0.085	0.068
Ti	0.084	0.112	0.088	0.093	0.114	0.135	0.096	0.100	0.102	0.103	0.090	0.107	0.095	0.102	0.082	0.097	0.116	0.116	0.088	0.087
Al	14.612	14.460	14.489	14.519	14.454	14.071	14.190	14.644	14.646	14.593	14.674	14.642	14.641	14.628	14.542	14.698	14.630	14.656	14.558	14.352
Fe^{3+}	1.000	1.286	1.286	1.076	1.348	1.494	1.450	0.916	0.981	1.007	0.989	0.904	0.932	1.018	1.051	0.884	0.924	0.929	1.046	1.297
Fe^{2+}	2.250	2.008	2.027	2.237	2.022	3.631	3.213	2.903	2.341	2.311	2.354	2.341	2.321	2.307	2.278	2.419	2.431	2.558	2.891	3.099
Mn	0	0	0	0	0	0.044	0.060	0	0	0	0.050	0	0	0	0.036	0	0	0	0.042	0.068
Mg	5.915	5.912	5.877	5.880	5.825	4.522	4.813	5.298	5.827	5.818	5.765	5.859	5.858	5.785	5.833	5.768	5.770	5.548	5.240	4.989
Ca	0	0	0	0	0	0	0	0	0	0	0	0	0	0	0.036	0	0	0.023	0	0
Na	0	0.120	0.124	0	0.168	0	0	0	0	0	0	0	0	0	0	0	0	0	0	0
K	0	0	0	0	0	0	0	0	0	0	0	0	0	0	0	0	0	0	0	0
Ni	0	0	0	0.052	0	0	0	0	0	0.050	0	0	0	0.064	0	0	0	0.058	0	0
Cr	0.057	0.054	0.046	0.068	0	0.043	0.032	0.038	0.036	0.042	0	0.053	0.069	0.043	0.040	0.045	0.044	0.041	0.049	0.041
Zn	0	0	0	0	0	0	0.078	0	0	0	0	0	0	0	0	0	0	0	0	0
Total	24.000	24.000	24.000	24.000	24.000	24.000	24.000	24.000	24.000	24.000	24.000	24.000	24.000	24.000	24.000	24.000	24.000	24.000	24.000	24.000
%END-MEMBERS																				
Spinel	74.7	75.5	75.2	74.7	75.0	57.0	60.7	67.1	73.4	73.9	72.8	74.1	74.0	73.4	74.2	72.9	72.9	70.7	66.2	62.9
Hercynite	17.6	14.7	15.4	17.0	15.1	31.2	27.1	25.7	18.9	18.3	19.3	18.6	18.6	18.7	17.5	20.1	19.6	21.8	25.3	26.8
Gahnite	0	0	0	0	0	0	1.0	0	0	0	0	0	0	0	0	0	0	0	0	0
Galaxite	0	0	0	0	0	0.5	0.8	0	0	0	0.6	0	0	0	0.5	0	0	0	0.5	0.9
Magnetite	6.3	8.0	8.0	6.7	8.4	9.3	9.1	5.7	6.1	6.3	6.2	5.7	5.8	6.4	6.6	5.5	5.8	5.8	6.5	8.1
Chromite	0.4	0.3	0.3	0.4	0	0.3	0.2	0.2	0.2	0.3	0	0.3	0.4	0.3	0.3	0.3	0.3	0.3	0.3	0.3
Ulvöspinel	1.0	1.4	1.1	1.2	1.4	1.7	1.2	1.2	1.3	1.3	1.1	1.3	1.2	1.3	1.0	1.2	1.5	1.4	1.1	1.1
Total	100.0	100.0	100.0	100.0	100.0	100.0	100.0	100.0	100.0	100.0	100.0	100.0	100.0	100.0	100.0	100.0	100.0	100.0	100.0	100.0

Appendix 3-8 (Continued).

Locality	BO PHLOI, BP											
Occurrence	Xenocryst						Xenolith (Spinel+Olivine)			Inclusion in corundum		
Sample No	BP81-SP16	BP82-SP4	BP83-SP2	BP83-SP3	BP83-SP4	BP85-SP1	BP82-SP1	BP82-SP2	BP82-SP3	BPEP13-SP1	BPEP13-SP2	BPEP13-SP3
SiO_2	0.28	0.33	0.29	0.70	0.32	0.27	0.36	0.33	0.26	0.39	0.39	0.43
TiO_2	0.75	1.27	0.30	0.88	1.26	0.24	0.16	0	1.18	0	0.29	0.35
Al_2O_3	54.97	50.90	51.94	43.39	43.47	51.55	51.52	50.54	41.15	56.67	56.41	56.39
Fe_2O_3	9.10	11.86	3.33	10.45	11.98	7.22	4.90	5.83	14.08	4.69	6.04	6.33
FeO	19.43	21.40	16.54	22.17	22.19	18.65	17.01	17.60	23.19	30.63	29.79	29.44
MnO	0.30	0.32	0.58	0.29	0.27	0.46	0.35	0.34	0.48	0.86	0.55	0.65
MgO	14.17	12.30	15.17	11.43	11.53	13.88	15.04	14.11	10.31	6.65	6.70	6.75
CaO	0	0	0	0	0	0	0	0	0	0	0	0
Na_2O	0	0	0	0	0	0	0	0	0	0	0.35	0.43
K_2O	0	0	0	0	0	0	0	0	0	0	0	0
NiO	0	0	0.36	0	0	0.44	0	0.38	0	0	0	0
Cr_2O_3	0.28	0	10.97	10.09	8.40	7.68	9.57	9.42	8.44	0.77	0.81	0.77
ZnO		0.704	0	0.527								
Total	99.29	99.08	99.46	99.92	99.40	100.39	98.92	98.55	99.08	100.66	101.33	101.54
Numbers of ions on the basis of 32 O												
Si	0.061	0.073	0.064	0.161	0.074	0.059	0.079	0.073	0.061	0.087	0.087	0.095
Ti	0.123	0.214	0.049	0.152	0.218	0.039	0.027	0	0.209	0	0.048	0.058
Al	14.093	13.429	13.340	11.739	11.808	13.287	13.319	13.226	11.402	14.902	14.730	14.690
Fe^{3+}	1.489	1.998	0.546	1.805	2.077	1.188	0.809	0.974	2.491	0.787	1.007	1.053
Fe^{2+}	3.534	4.005	3.014	4.255	4.277	3.411	3.121	3.269	4.560	5.715	5.519	5.442
Mn	0.055	0.060	0.106	0.057	0.052	0.084	0.065	0.065	0.096	0.162	0.104	0.122
Mg	4.596	4.105	4.930	3.912	3.963	4.526	4.920	4.671	3.614	2.211	2.214	2.223
Ca	0	0	0	0	0	0	0	0	0	0	0	0
Na	0	0	0	0	0	0	0	0	0	0	0.149	0.183
K	0	0	0	0	0	0	0	0	0	0	0	0
Ni	0	0	0.063	0	0	0.077	0	0.068	0	0	0	0
Cr	0.049	0	1.890	1.831	1.530	1.328	1.660	1.654	1.568	0.137	0.142	0.135
Zn	0	0.116	0	0.089	0	0	0	0	0	0	0	0
Total	24.000	24.000	24.000	24.000	24.000	24.000	24.000	24.000	24.000	24.000	24.000	24.000
%END-MEMBERS												
Spinel	57.9	51.8	62.6	49.9	50.0	57.6	62.1	59.4	45.5	27.9	28.5	28.8
Hercynite	30.3	30.8	20.2	23.6	24.1	25.2	21.3	23.3	25.3	64.2	62.4	61.5
Gahnite	0	1.5	0	1.1	0	0	0	0	0	0	0	0
Galaxite	0.7	0.8	1.3	0.7	0.7	1.1	0.8	0.8	1.2	2.0	1.3	1.6
Magnetite	9.3	12.5	3.4	11.3	13.0	7.4	5.1	6.1	15.6	4.9	6.3	6.6
Chromite	0.3	0	11.8	11.4	9.6	8.3	10.4	10.3	9.8	0.9	0.9	0.8
Ulvöspinel	1.5	2.7	0.6	1.9	2.7	0.5	0.3	0	2.6	0	0.6	0.7
Total	100.0	100.0	100.0	100.0	100.0	100.0	100.0	100.0	100.0	100.0	100.0	100.0

Appendix 7-1

COLOUR DESCRIPTION

In describing the colour of the coloured stones based on GIA (Gemological Institute of America) **hue, tone**, and **saturation** are used (GIA, 1992, 1993).

Hue is the pure spectral sensation or a term applied to the colour or wavelength of light (GIA, 1993, and Read, 1994). They are red, orange, yellow, green, blue, violet or purple. Hue is divided into two main groups, namely cool hues (e.g. green, blue, purple) and warm hues (e.g. yellow, orange, red).

Tone is the lightness or darkness of the hue. There are 11 levels, starting at 0, colourless (or white, when we talk about translucent or opaque stones), and ending at 10, black. (As with hue, more divisions are possible, but these, too, would only make verbal descriptions less consistent and more complicated.) For transparent gems, one normally deals with only steps 2-8.

Saturation (intensity) is the strength and purity of the hue. Described as: greyish (brownish) to vivid. Expressions like "bright red" "vibrant green" imply colours with highly saturated hues. However, "rust red" and olive green" refer to low-saturation hues that look brownish or greyish. (Warm hues like red, orange, and yellow look brownish in low saturations; cool hues like blue, blue-green, and violet look greyish.) The GIA Colour Grading System divides saturation variations into six levels that run from 1, greyish or brownish, through 6, vivid.

In some cases, the additional colours could be added e.g. colour banding, mottling, colour change, colour zoning, and pleochroism.

The hue chart, tone scale, and saturation scale are shown on the next two pages. We can describe the colour by giving hue terms and saturation numbers. For example Blue 5/6 means blue hue, tone 5, saturation 6.

Corundum colour
GIA gives the ranges of colour for corundum as follows:

Ruby: orangy red through strongly purplish red; tones 5-8; saturations 4-6.
Fine colour: Red 6/6.
Blue sapphire: violetish blue through greenish blue; tones 2-8; saturations 1-6.
Fine colour: violetish blue 6/6.

Fancy:
Green sapphire: blue-green through yellow-green; tones 2-8; saturations 1-3
Fine colour: very strongly bluish green 6/3; bluish green 6/3; very slightly bluish green 6/3
Orange sapphire: Yellowish orange through orangy red; tones 2-8; saturations 1-6
Fine colour: Orange-red 5/6; orange-red 6/6
Yellowish sapphire: greenish yellow through ornagy yellow; tones 2-4; saturations 1-5
Fine colour: yellow 3/5; orangy yellow 3/5

Pink sapphire: red through purple; tones 2-5; saturations 1-6
Fine colour: red-purple 4/6; reddish purple 4/6
Purple sapphire: red through bluish purple; tones 5-8; saturations 1-6
Fine colour: red-purple 6/6

HUE CHART

You can use the 31 hues shown here to describe gem colors. The consistency of printed color values is subject to the normal limitations of the four-color process. Use the opaque color samples here only as guidelines in estimating the hues of gemstones.

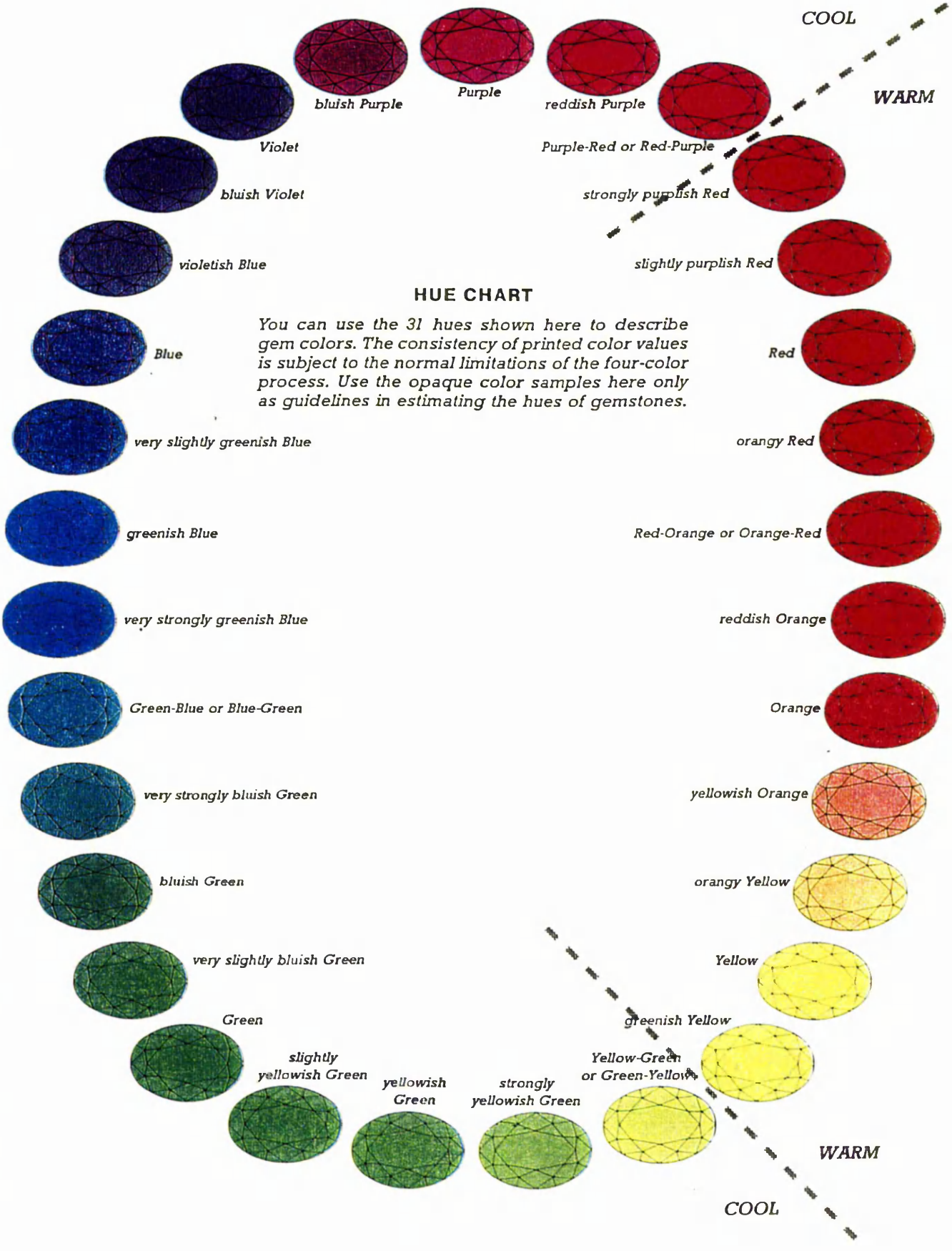

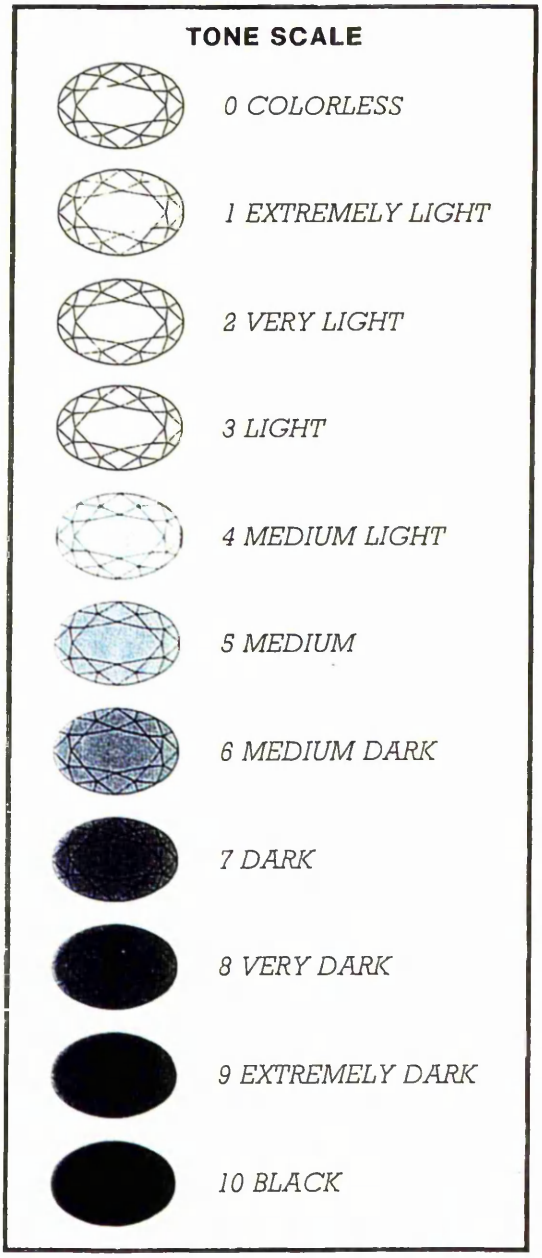

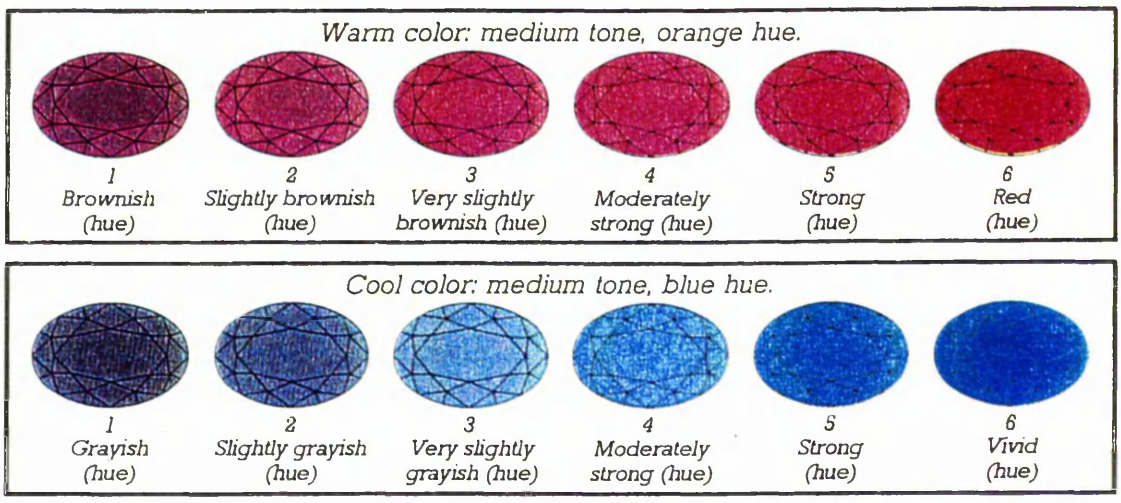

SATURATION SCALE

Appendix 8-1

Appendix 8-1 Description of the corundum samples from Thailand and other localities for the analysis by EPMA.

Locality, sample number	Colour (Hue)[1]	Tone/Saturation (based on GIA)[1]	Dimension (wxlxd; cm)	Comment
Ban Huai Sai, near Chiang Khong, set1				
CKEP1	very slightly greenish Blue	8/5	0.3x0.4x0.25	subhedral, hexagonal pyramid
CKEP2	very slightly greenish Blue	8/5	0.4x0.4x0.2	angular, anhedral
CKEP3	very slightly greenish Blue	8/5	0.3x0.25x0.2	subhedral, hexagonal pyramid
CKEP4	very slightly greenish Blue	7/4	0.4x0.5x0.4	subhedral, hexagonal pyramid, pinacoid
CKEP5	very slightly greenish Blue	7/4	0.3x0.3x0.2	subhedral, hexagonal pyramid, pinacoid
CKEP6	very slightly greenish Blue	7/4	0.3x0.4x0.2	euhedral, hexagonal prism, pinacoid
CKEP7	very slightly greenish Blue	7/3	0.4x0.5x0.2	angular, subhedral
CKEP8	very slightly greenish Blue	7/3	0.4x0.4x0.3	angular, subhedral
CKEP9	very slightly greenish Blue	6/3	0.3x0.6x0.2	angular, subhedral, pinacoid
CKEP10	very slightly greenish Blue	6/3	0.4x0.5x0.2	subhedral, hexagonal pyramid, pinacoid
CKEP11	very slightly greenish Blue	6/3	0.4x0.5x0.3	angular, subhedral, hexagonal pyramid
CKEP12	very slightly greenish Blue	6/3	0.3x0.4x0.2	very angular, anhedral
CKEP13	Green-Blue	5/2	0.3x0.5x0.2	angular, subhedral
CKEP14	Green-Blue	5/2	0.3x0.3x0.2	very angular, subhedral
CKEP15	Green-Blue	5/2	0.3x0.35x0.2	angular, anhedral
CKEP16	Green-Blue	5/2	0.3x0.5x0.1	very angular, subhedral
CKEP17	Green-Blue	5/2	0.2x0.4x0.2	angular, subhedral, hexagonal pyramid
CKEP18	Green-Blue	5/2	0.4x0.5x0.4	angular, subhedral, hexagonal pyramid, yellow core
CKEP19	orangy Yellow	5/2	0.4x0.5x0.3	angular, subhedral, hexagonal pyramid, slightly blue rim
CKEP20	orangy Yellow	5/2	0.35x0.45x0.2	angular, subhedral, hexagonal pyramid, slightly blue rim
CKEP21	orangy Yellow	5/2	0.4x0.4x0.3	angular, subhedral, colourless rim
CKEP22	orangy Yellow	5/2	0.4x0.6x0.15	angular, subhedral, hexagonal prism, pinacoid, slightly blue rim
CKEP23	orangy Yellow	5/2	0.35x0.4x0.3	angular, anhedral, slightly blue rim
CKEP24	orangy Yellow	5/2	0.3x0.45x0.2	angular, subhedral, slightly blue rim
CKEP25	bluish Purple	6/2	0.3x0.35x0.3	euhedral, hexagonal pyramid, pinacoid
CKEP26	Brown	10/-	0.4x0.7x0.2	angular, subhedral, pinacoid, chatoyancy
CKEP27	Brown	10/-	0.4x0.5x0.3	angular, subhedral, pinacoid, chatoyancy
CKEP28	Brown	10/-	0.4x0.4x0.15	angular, subhedral, pinacoid, chatoyancy
CKEP29	Brown	10/-	0.3x0.4x0.1	angular, subhedral, pinacoid, hexagonal prism, chatoyancy
CKEP30	Brown	10/-	0.3x0.3x0.1	angular, subhedral, pinacoid, hexagonal prism, chatoyancy
Ban Nong Nam Cho, Lam Pang				
BNEP1	Blue			(Polished section)
BNEP2	Blue			(Polished section)
BNEP3	Blue			(Polished section)
BNEP4	Blue			(Polished section)
Den Chai, Phrae				
DCEP1	very slightly greenish Blue	8/5	0.25x0.35x0.15	angular, subhedral
DCEP2	very slightly greenish Blue	8/5	0.3x0.4x0.3	very angular
DCEP3	very slightly greenish Blue	7/5	0.4x0.5x0.1	very angular, subhedral
DCEP4	Blue	10/-	0.3x0.35x0.3	hexagonal pyramid, pinacoid
DCEP5	very slightly greenish Blue	8/5	0.3x0.3x0.2	angular subhedral, pinacoid

Appendix 8-1 (Continued).

Locality, sample number	Colour (Hue)[1]	Tone/Saturation (based on GIA)[1]	Dimension (wxlxd; cm)	Comment
DCEP6	very slightly greenish Blue	5/4	0.35x0.5x0.25	sub-angular, anhedral
DCEP7	very slightly greenish Blue	5/4	0.4x0.4x0.2	angular, anhedral
DCEP8	very slightly greenish Blue	5/3	0.25x0.4x0.1	angular, subhedral
DCEP9	very slightly greenish Blue	6/3	0.25x0.3x0.1	rounded, anhedral
DCEP10	very slightly greenish Blue	7/3	0.25x0.3x0.15	sub-rounded, subhedral
DCEP11	very slightly greenish Blue	3/2	0.25x0.4x0.15	very angular, anhedral
DCEP12	very slightly greenish Blue	3/2	0.2x0.5x0.2	hexagonal pyramid
DCEP13	very slightly greenish Blue	3/2	0.2x0.25x0.15	angular, anhedral
DCEP14	very slightly greenish Blue	3/2	0.15x0.3x0.15	angular, anhedral
DCEP15	very slightly greenish Blue	3/2	0.2x0.3x0.15	sub-rounded, anhedral
DCEP16	Green-Blue	5/3	0.25x0.3x0.2	angular, anhedral
DCEP17	Green-Blue	5/3	0.15x0.2x0.2	hexagonal prism, pinacoid
DCEP18	Green-Blue	5/3	0.2x0.35x0.2	angular, anhedral
DCEP19	Green-Blue	5/3	0.15x0.3x0.1	hexagonal pyramid
DCEP20	Green-Blue	6/3	0.3x0.4x0.15	angular, anhedral
DCEP21	Green-Blue	6/3	0.2x0.35x0.1	angular, anhedarl
DCEP22	orangy Yellow	5/2	0.4x0.5x0.3	angular, anhedral, (tinct of blue)
DCEP23	orangy Yellow	5/2	0.3x0.4x0.2	angular, anhedral (tinct of blue)
DCEP24	orangy Yellow	5/2	0.3x0.4x0.2	sub-rounded, anhedral (tinct of blue)
DCEP25	orangy Yellow	5/2	0.25x0.35x0.25	angular, anhedral (tinct of blue)
DCEP26	yellowish Orange	5/3	0.15x0.3x0.2	angular, anhedral
DCEP27	Brown with golden chatoyancy	10/-	0.35x0.6x0.15	angular, subhedral, pinacoid
DCEP28	Brown with golden chatoyancy	10/-	0.25x0.2x0.22	hexagonal prism,pinacoid
DCEP29	Brown with golden chatoyancy	10/-	0.4x0.4x0.15	angular, subhedral, pinacoid
DCEP30	Brown with golden chatoyancy	10/-	0.35x0.45x0.2	angular, subhedral, pinacoid
DCEP31	Brown with golden chatoyancy	10/-	0.3x0.4x0.12	angular, subhedral, pinacoid
Bo Phloi, Kanchanaburi				
BPEP1	very slightly greenish Blue	7/5	0.6x0.7x0.25	tabular, subhedral
BPEP2	very slightly greenish Blue	7/5	0.4x0.7x0.2	tabular, subhedral
BPEP3	very slightly greenish Blue	7/5	0.3x0.7x0.2	very angular, tabular, subhedral
BPEP4	very slightly greenish Blue	7/5	0.3x0.4x0.2	very angular, subhedral
BPEP5	very slightly greenish Blue	5/3	0.3x0.5x0.1	sub-angular, tabular subhedral
BPEP6	very slightly greenish Blue	5/3	0.3x0.5x0.3	sub-angular, subhedral
BPEP7	very slightly greenish Blue	4/2	0.4x0.5x0.3	sub-angular, anhedral
BPEP8	very slightly greenish Blue	4/2	0.3x0.7x0.2	angular, anhedral
BPEP9	very slightly greenish Blue	3/2	0.4x0.6x0.2	sub-angular, subhedral, pinacoid, hexagonal prism
BPEP10	bluish Green	4/2	0.6x0.8x0.5	sub-angular, subhedral, pinacoid, hexagonal pyramid
BPEP11	bluish Green	4/2	0.4x0.5x0.3	sub-angular, subhedral, pinacoid, hexagonal prism
BPEP12	Yellow-Green	4/2	0.4x0.4x0.3	angular, subhedral
BPEP13	Violet	5/2	0.3x0.3x0.1	euhedral, hexagonal prism and pinacoid
BPEP14	bluish Purple	4/2	0.3x0.4x0.2	sub-angular, anhedral

Appendix 8-1 (Continued).

Locality, sample number	Colour (Hue)[1]	Tone/Saturation (based on GIA)[1]	Dimension (wxlxd; cm)	Comment
BPEP15	Brown	10/-	0.6x0.7x0.15	tabular, subhedral, hexagonal prism, pinacoid
BPEP16	Brown	10/-	0.3x0.4x0.15	tabular, very angular, subhedral, pinacoid
BPEP17	Brown	10/-	0.45x0.7x0.15	tabular, angular, subhedral, hexagonal prism, pinacoid
Khok Samran, Phetchabun				
KSEP1	very slightly greenish Blue	10/-	0.6x0.7x0.2	rounded, anhedral
KSEP2	very slightly greenish Blue	10/-	0.7x0.9x0.4	tabular, subhedral, hexagonal prism
KSEP3	very slightly greenish Blue	10/-	0.4x0.7x0.3	angular, subhedral, pinacoid, brown and chatoyancy on the pinacoid
KSEP4	very slightly greenish Blue	9/5	0.5x0.7x0.25	euhedral, hexagonal, pinacoid
KSEP5	very slightly greenish Blue	9/5	0.5x0.6x0.4	sub-angular, anhedral
KSEP6	very slightly greenish Blue	9/5	0.4x0.5x0.2	sub-angular, subhedral, pinacoid
KSEP7	very slightly greenish Blue	8/4	0.4x0.6x0.2	angular, subhedral, pinacoid
KSEP8	very slightly greenish Blue	8/4	0.5x0.6x0.4	sub-angular, subhedral, hexagonal pyramid
KSEP9	very slightly greenish Blue	8/4	0.5x0.6x0.3	very angular, anhedral
KSEP10	very slightly greenish Blue	6/3	0.5x0.7x0.1	angular, tabular, subhedral, pinacoid
KSEP11	very slightly greenish Blue	6/3	0.5x0.6x0.2	angular, tabular, subhedral, pinacoid
KSEP12	very slightly greenish Blue	6/3	0.5x0.6x0.15	angular, tabular, subhedral, pinacoid
Nam Yun, Ubonratchathani				
NYEP1	very slightly greenish Blue	8/5	0.5x0.7x0.3	sub-angular, anhedral
NYEP2	very slightly greenish Blue	8/5	0.3x0.6x0.2	angular, anhedral
NYEP3	very slightly greenish Blue	7/5	0.4x0.7x0.2	angular, anhedral
NYEP4	very slightly greenish Blue	7/5	0.4x0.6x0.2	angular, anhedral
NYEP5	very slightly greenish Blue	7/5	0.35x0.45x0.1	angular, subhedral, pinacoid
NYEP6	very slightly greenish Blue	7/4	0.5x0.5x0.25	sub-rounded, subhedral, pinacoid
NYEP7	very slightly greenish Blue	7/4	0.45x0.5x0.1	sub-rounded, subhedral, pinacoid, colour zoning (from core to rim)
NYEP8	very slightly greenish Blue	7/4	0.5x0.65x0.1	very angular, subhedral, pinacoid
NYEP9	very slightly greenish Blue	7/4	0.4x0.6x0.1	angular, subhedral, pinacoid, hexagonal prism, brown hexagonal zone
NYEP10	very slightly greenish Blue	7/4	0.4x0.4x0.3	angular, subhedral, hexagonal prism
NYEP11	very slightly greenish Blue	7/4	0.3x0.4x0.2	sub-rounded, anhedral
NYEP12	greenish-Blue	7/4	0.4x0.6x0.25	angular, subhedral
NYEP13	Green-Blue	8/5	0.4x0.7x0.3	angular, subhedral
NYEP14	Green-Blue	7/4	0.45x0.6x0.2	angular, anhedral
NYEP15	bluish Green	6/3	0.4x0.6x0.3	sub-rounded, anhedral
NYEP16	bluish Green	6/3	0.3x0.4x0.25	sub-rounded, euhedral, hexagonal pyramid, pinacoid
NYEP17	bluish Green	5/3	0.5x0.7x0.1	angular, subhedral, pinacoid
Bang Kacha, Chanthaburi				
BKCEP1	bluish Green	9/4	2.2x2.3x1.8	subhedral, hexagonal dipyramid, pinacoid
BKCEP2	bluish Green	9/4	2.2x2.3x1.8	subhedral, hexagonal dipyramid, pinacoid
BKCEP3	bluish Green	6/3	0.5x0.7x0.25	cut stone, unpolished
BKCEP4	Brown	10/0	0.8x1.1x0.25	tabular, subhedral, hexagonal prism, pinacoid
BKCEP5	Brown	10/0	0.3x0.5x0.35	sub-angular, subhedral, hexagonal prism, pinacoid

Appendix 8-1 (Continued).

Locality, sample number	Colour (Hue)[1]	Tone/Saturation (based on GIA)[1]	Dimension (wxlxd; cm)	Comment
BKCEP6	Brown	10/0	0.4x0.6x0.2	euhedral, hexagonal prism, pinacoid
BKCEP7	Brown	10/0	0.8x1.3x0.2	very angular, subhedral, hexagonal prism, pinacoid
BKCEP8	Brown	10/0	0.5x0.5x0.3	euhedral, hexagonal prism, pinacoid
BKCEP9	Brown	10/0	0.5x0.5x0.3	euhedral, hexagonal prism, pinacoid
BKCEP10	Brown	10/0	0.7x0.7x0.3	euhedral, hexagonal prism, pinacoid
BKCEP11	Brown	10/0	0.4x0.5x0.3	euhedral, hexagonal prism, pinacoid
BKCEP12	Brown	10/0	0.5x1.0x0.2	angular, subhedral, pinacoid
BKCEP13	Brown	10/0	0.6x0.8x0.2	angular, subhedral, hexagonal prism, pinacoid
Bo Rai, Trat (set 2, medium)				
BREP19	redish Purple	5/3	0.5x0.7x0.1	very angular, subhedral, pinacoid
BREP20	redish Purple	4/2	0.3x0.65x0.2	cut stone (marquise), unpolished
BREP21	Purple	3/2	0.4x0.4x0.3	very angular, anhedral, pinacoid
BREP22	bluish Purple	6/4	0.4x0.6x0.2	angular, anhedral
BREP23	bluish Purple	6/4	0.4x0.6x0.2	sub-rounded, anhedral
BREP24	very slightly greenish Blue	9/4	0.4x0.4x0.25	euhedral, hexagonal pyramid, pinacoid, translucent
BREP25	very slightly greenish Blue	9/4	0.5x0.6x0.4	euhedral, hexagonal pyramid, pinacoid, translucent
BREP26	very slightly greenish Blue	5/3	0.35x0.4x0.25	subhedral, hexagonal pyramid, pinacoid
BREP27	very strongly greenish Blue	4/2	0.3x0.3x0.2	angular, subhedral, hexagonal pyramid, pinacoid
BREP28	very strongly greenish Blue	3/1	0.3x0.3x0.1	very angular, subhedral, pinacoid
Bo Rai, Trat (set 2, small)				
BREP29	slightly purplish Red	6/4	0.25x0.35x0.2	sub-rounded, anhedral
BREP30	slightly purplish Red	6/4	0.2x0.4x0.2	sub-angular, anhedral
BREP31	slightly purplish Red	6/4	0.3x0.5x0.3	angular, anhedral
BREP32	slightly purplish Red	6/4	0.5x0.6x0.2	very angular, anhedral
BREP33	strongly purplish Red	4/3	0.3x0.3.5x0.2	sub-rounded, anhedral, hexagonal pyramid
BREP34	strongly purplish Red	4/3	0.5x0.6x0.3	angular, anhedral
BREP35	strongly purplish Red	4/3	0.4x0.5x0.2	angular, anhedral
BREP36	strongly purplish Red	4/3	0.3x0.5x0.3	angular, subhedral
BREP37	strongly purplish Red	4/3	0.3x0.35x0.2	angular, anhedral
BREP38	Purple-Red	5/3	0.3x0.4x0.2	angular, anhedral
BREP39	Purple-Red	5/3	0.2x0.3x0.2	angular, anhedral
BREP40	reddish Purple	5/4	0.3x0.3x0.05	sub-rounded, tabular, anhedral
BREP41	Purple	5/3	0.35x0.4x0.2	sub-rounded, anhedral
BREP42	Purple	5/3	0.4x0.5x0.1	sub-rounded, tabular, anhedral
BREP43	bluish Purple	5/3	0.3x0.4x0.3	very angular, anhedral
BREP44	bluish Purple	5/3	0.4x0.5x0.2	very angular, anhedral
BREP45	bluish Purple	5/3	0.4x0.35x0.2	very angular, anhedral
BRj			0.9x1.2x0.5	sub-angular, subhedral (pinacoid), associated with green vitreous-lustre minearal
Bo Na Wong, Chanthaburi				
NWEP9	reddish Purple	5/4	0.4x0.6x0.1	sub-rounded, anhedral
NWEP11	reddish Purple	4/3	0.4x0.7x0.4	rounded, anhedral
Nong Bon, Trat				
NBEP1	reddish Purple	5/4	0.4x0.6x0.2	very angular, anhedral
NBEP2	reddish Purple	5/3	0.5x0.8x0.15	very angular, anhedral
NBEP3	Purple	5/4	0.5x0.6x0.2	very angular, tabular, subhedral, pinacoid
NBEP4	Purple	5/3	0.6x0.8x0.9	very angular, anhedral
NBEP5	Purple	5/2	0.7x0.7x0.3	very angular, tabular, subhedral, pinacoid
NBEP6	Purple	5/2	0.4x0.5x0.3	very angular, anhedral
NBEP7	Purple	4/2	0.7x0.9x0.1	very angular, tabular, subhedral, pinacoid
NBEP8	Purple	4/2	0.5x0.6x0.2	sub-angular, anhedral
NBEP9	Purple	3/1	0.6x0.9x0.2	sub-angular, tabular, anhedral
NBEP10	bluish Purple	6/4	0.7x0.8x0.2	sub-rounded, anhedral
NBEP11	bluish Purple	5/1	0.6x0.9x0.4	sub-angular, anhedral
NBEP12	bluish Purple	6/5	0.5x0.7x0.2	sub-angular, tabular, anhedral
Mong Hsu, Myanmar, purchased from Taunggi (heated?)				
TYEP1	reddish Purple	5/5	0.4x0.4x0.3	angular, subhedral
TYEP2	reddish Purple	5/5	0.4x0.4x0.3	cut stone, unpolished
TYEP3	reddish Purple	5/5	0.4x0.4x0.2	angular, anhedral

Appendix 8-1 (Continued).

Locality, sample number	Colour (Hue)[1]	Tone/Saturation (based on GIA)[1]	Dimension (wxlxd; cm)	Comment
Viatnam (unknown specific source)				
VNEP1	slightly greenish Blue	6/4	0.5x0.8x0.2	very angular, tabular, subhedral, pinacoib
VNEP2	slightly greenish Blue	6/3	0.4x0.4x0.15	euhedral, hexagonal prism, pinacoid
VNEP3	slightly greenish Blue	7/4	0.4x0.5x0.4	sub-rounded, subhedral, pyramid
Africa (unknown specific source)				
AFEP1	Purple-Red	7/5	0.4x0.7x0.3	very angular, anhedral
AFEP2	Purple-Red	7/5	0.3x0.5x0.3	very angular, anhedral
AFEP3	Purple-Red	7/5	0.3x0.4x0.3	very angular, anhedral
Nigeria, Africa				
NAEP1	slightly greenish Blue	6/3	0.7x0.7x0.35	very angular, tabular, anhedral
NAEP2	slightly greenish Blue	7/3	0.5x0.5x0.3	angular, subhedral, hexagonal pyramid, pinacoid
NAEP3	slightly greenish Blue	3/1	0.5x0.7x0.4	euhedral, hexagonal pyramid, pinacoid
North Vietnam (unknown specific source)				
NVEP1	reddish Purple	5/3	0.4x0.7x0.2	very angular, tabular, anhedral
NVEP2	reddish Purple	5/3	0.3x0.5x0.2	angular, tabular, subhedral
NVEP3	reddish Purple	5/3	0.3x0.4x0.1	very angular, tabular, anhedral
Mong Hsu, Myanmar				
MSEP1	Purple	5/5	0.3x0.4x0.3	angular, subhedral, hexagonal pyramid,
MSEP2	Purple	5/5	0.4x0.5x0.3	angular, subhedral, hexagonal pyramid, black core
MSEP3	Purple	5/5	0.4x0.5x0.3	angular, subhedral, hexagonal pyramid, black core, //c-axis
MSEP4	Purple	5/5	0.5x0.6x0.4	angular, subhedral, hexagonal pyramid, black core
MSEP5	Purple	5/5	0.4x0.7x0.2	very angular, tabular anhedral
MSEP6	Purple	5/5	0.6x0.8x0.3	angular, subhedral, hexagonal prism, black core, perpen. to c-axis
MSEP7	Purple	5/5	0.5x0.5x0.3	angular, subhedral, hexagonal prism, black core
MSEP8	Purple	5/5	0.5x0.4x0.4	angular, subhedral, hexagonal pyramid, black core
BKCEP14	bluish Green	6/4	0.6x0.7x0.4	angular, subhedral, pinacoid, hexagonal pyramid, very slightly greenish Blue spot, perpen. to c-axis. (heated)
BKCEP15	bluish Green	6/4	0.5x0.7x0.3	angular, subhedral, pinacoid, hexagonal prism, very slightly greenish Blue spot, perpen. to c-axis. (heated)
BKCEP16	bluish Green	6/4	0.3x0.6x0.4	angular, subhedral, hexagonal pyramid, perpen. to c-axis. (heated)
BKCEP17	bluish Green	6/4	0.3x0.6x0.5	angular, subhedral, perpen. to c-axis. (heated)
BKCEP18	bluish Green	6/4	0.5x0.7x0.3	angular, subhedral, hexagonal pyramid, perpen. to c-axis. (heated)
BKCEP19	bluish Green	6/4	0.6x0.6x0.5	angular, subhedral, very slightly greenish Blue spot. (heated)
BKCEP20	bluish Green	6/4	0.6x0.8x0.3	angular, subhedral, hexagonal pyramid, very slightly greenish Blue spot, // c-axis. (heated)
BKCEP21	bluish Green	6/4	0.5x0.5x0.4	angular, subhedral, hexagonal pyramid, very slightly greenish Blue spot, // c-axis. (heated)

Appendix 8-1 (Continued).

Locality, sample number	Colour (Hue)[1]	Tone/Saturation (based on GIA)[1]	Dimension (wxlxd; cm)	Comment
SAMPLES LENT BY DR GTR DROOP				
Natal, S. Africa				
Δ 1556-1	grey	10/-	0.5x0.6x0.5	very angular, anhedral,
Δ 1556-2	grey	10/-	0.5x0.6x0.7	very angular, anhedral,
Δ 1556-3	grey	10/-	0.5x0.8x0.6	very angular, anhedral, parting
Bushveld intrusion, S. Africa				
18058-1	bluish purple	8/5	0.7x1.3x0.3	very angular, rhombohedral parting, associated with white unknown mineral
18058-2	bluish purple	8/5	0.4x0.7x0.2	"
18058-3	bluish purple	8/5	0.5x0.7x0.3	"
Limpopo belt, Zimbabwe				
BB14A-1	bluish Purple	5/1	0.3x0.5x0.7	very angular, anhedral associated with cordierite(green) and biotite
BB14A-2	bluish Purple	5/1	0.3x0.6x0.7	"
BB14A-3	bluish Purple	5/1	0.6x0.8x0.3	"
Tanzania				
CRM/ZOI-1	Purple	8/5	0.7x0.7x0.4	very angular, anhedral, associated with green zoisite
CRM/ZOI-2	Purple	8/5	0.5x0.7x0.3	"
CRM/ZOI-3	Purple	8/5	0.3x0.5x0.3	"
South India				
Δ 793	Red-Purple (Purple-Red)	7/6	0.6x0.8x0.4	parting, associated with ultramafic rock

[1] Colours are described based on Gem reference guide. Gemological Institute of America, 1992:

Blue sapphires include violetish Blue, Blue, very slightly greenish Blue, and greenish Blue; (tones 2-8; saturations 1-6).

Green sapphires include Green-Blue, very strongly bluish Green, bluish Green, very slightly bluish Green, Green, slightly yellowish Green, yellowish Green, yellowish Green, strongly yellowish Green, and Yellow-Green; (tones 2-8; saturations 1-3).

Yellow sapphires include greenish Yellow, Yellow, orangy Yellow; (tones 2-4; saturations 1-5).

Orange sapphires include yellowish Orange, Orange, reddish Orange, Red- Orange, orangy Red; (tones 2-8; saturations 1-6).

Rubies include orangy Red, Red, slightly purplish Red, strongly purplish Red; (tones 5-8; saturations 4-6).

Pink sapphires include Red, slightly purplish Red, strongly purplish Red, Purple-Red, reddish Purple, Purple; (tones 2-5; saturations 1-6).

Purple sapphires include Red, slightly purplish Red, strongly purplish Red, Purple-Red, reddish Purple, Purple, bluish Purple; (tones 5-8; saturations 1-6).

(More Detail, see Appendix 7-1)

Appendix 8-2

Appendix 8-2 Weight % oxides of trace elements in the corundum samples from **Thailand** and the **Democratic People's Republic of Laos** obtained by EPMA.

Locality/ Date & No. of analyses	Huai Sai, in the Democratic People's Republic of Laos, Tue. 23, Mar. 99 (25 analyses).																								
Colour	Blue								Green					Yellow?						Brown					Purple
Sample No	CKEP11	CKEP12	CKEP9	CKEP7	CKEP1	CKEP2	CKEP4	CKEP5	CKEP18	CKEP17	CKEP15	CKEP14	CKEP13	CKEP24	CKEP23	CKEP22	CKEP19	CKEP20	CKEP21	CKEP26	CKEP27	CKEP28	CKEP29	CKEP30	CKEP25
Point	#17	#18	#20	#21	#22	#23	#24	#25	#10	#14	#15	#16	#19	#7	#8	#9	#11	#12	#13	#1	#2	#3	#4	#5	#6
V_2O_5	0.005	0.000	0.000	0.000	0.004	0.001	0.000	0.000	0.000	0.001	0.000	0.001	0.001	0.001	0.004	0.001	0.000	0.000	0.007	0.001	0.000	0.005	0.001	0.000	0.013
NiO	0.000	0.000	0.000	0.000	0.000	0.000	0.000	0.000	0.000	0.000	0.000	0.000	0.000	0.000	0.000	0.000	0.000	0.000	0.000	0.000	0.000	0.000	0.000	0.000	0.000
Ga_2O_3	0.036	0.038	0.053	0.017	0.024	0.022	0.015	0.019	0.038	0.043	0.038	0.044	0.029	0.047	0.042	0.027	0.041	0.065	0.039	0.018	0.017	0.022	0.017	0.013	0.014
Fe_2O_3	0.567	1.145	0.454	0.354	0.617	0.763	0.525	0.765	0.712	1.207	0.930	1.081	0.668	1.200	0.465	0.506	0.631	0.641	0.313	0.549	0.490	0.307	0.704	0.526	0.350
MnO	0.000	0.000	0.000	0.000	0.000	0.000	0.000	0.000	0.000	0.000	0.000	0.001	0.000	0.000	0.000	0.000	0.000	0.000	0.000	0.000	0.000	0.000	0.000	0.000	0.000
Cr_2O_3	0.003	0.000	0.002	0.000	0.000	0.000	0.003	0.002	0.003	0.002	0.000	0.000	0.005	0.000	0.000	0.002	0.000	0.000	0.005	0.001	0.005	0.002	0.000	0.002	0.034
La_2O_3	0.000	0.000	0.001	0.000	0.000	0.002	0.001	0.003	0.001	0.000	0.000	0.000	0.000	0.000	0.001	0.001	0.002	0.000	0.001	0.002	0.000	0.000	0.001	0.003	0.002
TiO_2	0.133	0.078	0.115	0.012	0.132	0.049	0.019	0.183	0.046	0.129	0.045	0.005	0.035	0.003	0.081	0.038	0.014	0.013	0.534	0.050	0.007	0.018	0.104	0.004	0.020
SnO_2	0.000	0.030	0.007	0.002	0.003	0.003	0.002	0.003	0.016	0.075	0.013	0.003	0.014	0.002	0.005	0.000	0.007	0.011	0.002	0.000	0.002	0.000	0.000	0.002	0.001
SiO_2	0.009	0.000	0.000	0.000	0.000	0.000	0.000	0.000	0.000	0.000	0.000	0.000	0.000	0.000	0.000	0.000	0.000	0.000	0.000	0.000	0.000	0.000	0.003	0.001	0.000
Y_2O_3	0.000	0.000	0.000	0.004	0.005	0.000	0.000	0.000	0.000	0.001	0.000	0.000	0.000	0.000	0.000	0.003	0.000	0.000	0.000	0.004	0.000	0.000	0.000	0.000	0.000
Al_2O_3*	99.008	99.008	99.008	99.008	99.008	99.008	99.008	99.008	99.008	99.008	99.008	99.008	99.008	99.008	99.008	99.008	99.008	99.008	99.008	99.008	99.008	99.008	99.008	99.008	99.008
Total*	99.761	100.299	99.639	99.397	99.792	99.848	99.572	99.982	99.825	100.466	100.033	100.144	99.761	100.262	99.607	99.585	99.704	99.738	99.909	99.633	99.530	99.361	99.838	99.559	99.441

* The values are not genuine, as Al was not analysed.

Appendix 8-2 Weight % oxides of trace elements in the corundum samples from Thailand and the Democratic People's Republic of Laos obtained by EPMA.

Appendix 8-2 (Continued).

Locality/ Date & No. of analyses	Huai Sai, in the Democratic People's Republic of Laos, Mon. 10 July 2000 (22 analyses) & Sun. 16 July 2000 (55 analyses).																													
Colour	Blue																										Green			
Sample No	CKEP1	CKEP2	CKEP3	CKEP3	CKEP3	CKEP6	CKEP6	CKEP7	CKEP7	CKEP7	CKEP8	CKEP8	CKEP8	CKEP8	CKEP8	CKEP9	CKEP9	CKEP9	CKEP9	CKEP12	CKEP12	CKEP12	CKEP11	CKEP11	CKEP11	CKEP11	CKEP10	CKEP10	CKEP13	CKEP13
Point	#91	#92	#93	#94	#1	#2	#3	#4	#5	#6	#7	#8	#9	#10	#11	#15	#16	#17	#18	#19	#20	#21	#22	#12	#13					
V_2O_5	0.005	0.000	0.000	0.000	0.000	0.000	0.000	0.002	0.002	0.002	0.002	0.000	0.002	0.002	0.000	0.002	0.000	0.004	0.005	0.004	0.005	0.007	0.009	0.000	0.000					
Ga_2O_3	0.027	0.023	0.024	0.024	0.030	0.032	0.023	0.022	0.027	0.020	0.019	0.019	0.056	0.101	0.048	0.042	0.036	0.035	0.036	0.043	0.042	0.022	0.022	0.034	0.035					
Fe_2O_3	0.784	0.755	0.320	0.390	0.829	0.702	0.363	0.393	0.559	0.433	0.512	0.450	0.482	0.498	0.393	1.165	1.098	0.468	0.502	0.593	0.588	0.296	0.320	0.686	0.682					
MnO	0.000	0.000	0.000	0.000	0.000	0.000	0.000	0.000	0.000	0.000	0.000	0.000	0.000	0.000	0.000	0.000	0.000	0.000	0.000	0.000	0.000	0.000	0.000	0.000	0.000					
Cr_2O_3	0.003	0.000	0.000	0.000	0.001	0.000	0.000	0.000	0.000	0.004	0.000	0.001	0.000	0.001	0.003	0.000	0.000	0.000	0.000	0.000	0.000	0.009	0.004	0.000	0.000					
TiO_2	0.481	0.028	0.007	0.155	0.214	0.187	0.022	0.028	0.250	0.037	0.170	0.471	0.120	0.075	0.003	0.008	0.065	0.294	0.382	0.018	0.040	0.224	0.380	0.245	0.249					
SnO_2	0.010	0.001	0.001	0.001	0.013	0.011	0.001	0.001	0.005	0.000	0.005	0.005	0.014	0.011	0.001	0.003	0.019	0.003	0.003	0.001	0.001	0.000	0.001	0.023	0.023					
Ta_2O_5	0.009	0.001	0.045	0.002	0.010	0.016	0.001	0.011	0.026	0.005	0.101	0.000	0.020	0.043	0.006	0.000	0.009	0.007	0.016	0.033	0.065	0.000	0.005	0.039	0.037					
Nb_2O_5	0.006	0.000	0.027	0.003	0.001	0.007	0.001	0.004	0.149	0.007	0.195	0.003	0.003	0.044	0.000	0.000	0.001	0.003	0.007	0.006	0.033	0.000	0.000	0.017	0.014					
WO_3	0.009	0.004	0.000	0.000	0.004	0.005	0.000	0.000	0.004	0.000	0.004	0.000	0.008	0.023	0.003	0.000	0.000	0.000	0.000	0.001	0.001	0.000	0.000	0.004	0.005					
CuO	0.000	0.000	0.000	0.000	0.000	0.000	0.004	0.003	0.000	0.000	0.000	0.000	0.000	0.000	0.001	0.000	0.003	0.000	0.000	0.000	0.000	0.003	0.000	0.000	0.000					
Al_2O_3*	99.008	99.008	99.008	99.008	99.008	99.008	99.008	99.008	99.008	99.008	99.008	99.008	99.008	99.008	99.008	99.008	99.008	99.008	99.008	99.008	99.008	99.008	99.008	99.008	99.008					
Total*	100.340	99.820	99.433	99.584	100.109	99.969	99.423	99.472	100.029	99.516	100.015	99.957	99.712	99.806	99.467	100.227	100.239	99.820	99.959	99.707	99.783	99.567	99.750	100.056	100.052					

* The values are not genuine, as Al was not analysed.

Appendix 8-2 (Continued).

Locality/ Date & No. of analyses	Huai Sai, in the Democratic People's Republic of Laos, Mon. 10 July 2000 (22 analyses) & Sun. 16 July 2000 (55 analyses).																													
Colour	Green																Yellow?													
Sample No	CKEP13	CKEP17	CKEP17	CKEP16	CKEP16	CKEP16	CKEP15	CKEP15	CKEP15	CKEP14	CKEP14	CKEP14	CKEP18	CKEP18	CKEP18	CKEP19	CKEP19	CKEP20	CKEP20	CKEP21	CKEP21	CKEP21	CKEP24	CKEP24	CKEP24	CKEP24	CKEP23	CKEP23	CKEP22	
Point	#14	#40	#41	#42	#43	#44	#45	#46	#47	#48	#49	#50	#51	#52	#53	#54	#55	#56	#57	#58	#63	#64	#65	#66	#67	#68				
V_2O_5	0.000	0.000	0.000	0.000	0.000	0.000	0.002	0.000	0.000	0.000	0.000	0.000	0.002	0.000	0.000	0.002	0.000	0.005	0.005	0.007	0.000	0.000	0.002	0.005	0.002	0.002				
Ga_2O_3	0.035	0.051	0.047	0.023	0.026	0.024	0.038	0.036	0.042	0.046	0.044	0.038	0.039	0.040	0.047	0.070	0.070	0.042	0.046	0.047	0.047	0.046	0.048	0.047	0.044	0.028				
Fe_2O_3	0.699	1.358	1.260	0.536	0.538	0.555	0.961	0.932	0.959	1.158	1.167	0.886	0.659	0.671	0.633	0.641	0.656	0.316	0.389	0.389	1.458	1.400	1.222	0.468	0.393	0.560				
MnO	0.000	0.000	0.000	0.000	0.000	0.000	0.000	0.000	0.000	0.000	0.000	0.000	0.000	0.000	0.000	0.000	0.000	0.000	0.000	0.000	0.000	0.000	0.000	0.000	0.000	0.000				
Cr_2O_3	0.000	0.000	0.001	0.001	0.000	0.000	0.000	0.000	0.000	0.001	0.000	0.000	0.000	0.001	0.001	0.003	0.003	0.003	0.003	0.000	0.003	0.001	0.001	0.001	0.000	0.000				
TiO_2	0.060	0.007	0.123	0.043	0.035	0.048	0.042	0.025	0.043	0.003	0.003	0.072	0.013	0.013	0.025	0.007	0.012	0.554	0.289	0.357	0.012	0.012	0.002	0.017	0.072	0.057				
SnO_2	0.003	0.024	0.075	0.003	0.001	0.000	0.019	0.011	0.020	0.001	0.000	0.028	0.003	0.011	0.008	0.004	0.014	0.005	0.011	0.011	0.046	0.041	0.000	0.000	0.000	0.000				
Ta_2O_5	0.023	0.072	0.015	0.004	0.000	0.000	0.004	0.000	0.005	0.000	0.000	0.212	0.009	0.159	0.055	0.093	0.258	0.010	0.271	0.243	0.138	0.121	0.000	0.055	0.011	0.004				
Nb_2O_5	0.004	0.019	0.003	0.000	0.000	0.000	0.000	0.000	0.000	0.000	0.000	0.126	0.006	0.033	0.016	0.011	0.056	0.010	0.382	0.356	0.037	0.039	0.001	0.003	0.003	0.001				
WO_3	0.000	0.001	0.010	0.000	0.000	0.000	0.004	0.013	0.000	0.000	0.000	0.010	0.006	0.011	0.004	0.000	0.000	0.000	0.009	0.005	0.000	0.003	0.004	0.000	0.005	0.000				
CuO	0.000	0.000	0.000	0.000	0.000	0.000	0.000	0.003	0.000	0.000	0.000	0.000	0.000	0.000	0.000	0.000	0.000	0.000	0.000	0.000	0.000	0.000	0.000	0.000	0.001	0.000				
Al_2O_3*	99.008	99.008	99.008	99.008	99.008	99.008	99.008	99.008	99.008	99.008	99.008	99.008	99.008	99.008	99.008	99.008	99.008	99.008	99.008	99.008	99.008	99.008	99.008	99.008	99.008	99.008				
Total*	99.832	100.540	100.542	99.618	99.607	99.635	100.076	100.028	100.078	100.218	100.222	100.380	99.744	99.948	99.797	99.838	100.076	99.953	100.413	100.424	100.749	100.669	100.289	99.604	99.539	99.660				

* The values are not genuine, as Al was not analysed.

Appendix 8-2 (Continued).

Locality/ Date & No. of analyses	Huai Sai, in the Democratic People's Republic of Laos, Mon. 10 July 2000 (22 analyses) & Sun. 16 July 2000 (55 analyses).																									
Colour	Yellow?	Brown																					Purple			
Sample No	CKEP22	CKEP26	CKEP26	CKEP26	CKEP26	CKEP26	CKEP26	CKEP26	CKEP26	CKEP26	CKEP26	CKEP26	CKEP26	CKEP26	CKEP26	CKEP27	CKEP27	CKEP28	CKEP28	CKEP29	CKEP29	CKEP30	CKEP25	CKEP25	CKEP25	CKEP25
Point	#69	#70	#71	#72	#73	#74	#75	#76	#77	#78	#79	#80	#81	#82	#83	#84	#85	#86	#87	#88	#89	#90	#59	#60	#61	#62
V_2O_5	0.000	0.004	0.004	0.002	0.005	0.007	0.004	0.007	0.004	0.004	0.005	0.005	0.004	0.005	0.004	0.000	0.000	0.007	0.007	0.000	0.000	0.000	0.011	0.014	0.012	0.014
Ga_2O_3	0.031	0.020	0.020	0.022	0.022	0.017	0.016	0.019	0.019	0.019	0.017	0.016	0.016	0.016	0.019	0.023	0.019	0.020	0.022	0.020	0.017	0.016	0.017	0.016	0.019	0.019
Fe_2O_3	0.563	0.496	0.508	0.622	0.568	0.550	0.646	0.532	0.555	0.553	0.542	0.539	0.523	0.519	0.522	0.503	0.473	0.366	0.346	0.679	0.608	0.628	0.313	0.355	0.309	0.352
MnO	0.000	0.000	0.000	0.000	0.000	0.000	0.000	0.000	0.000	0.000	0.000	0.000	0.000	0.000	0.000	0.000	0.000	0.000	0.000	0.000	0.000	0.000	0.000	0.000	0.000	0.000
Cr_2O_3	0.000	0.001	0.006	0.000	0.000	0.001	0.001	0.003	0.001	0.003	0.001	0.004	0.000	0.000	0.000	0.000	0.000	0.006	0.001	0.000	0.001	0.001	0.042	0.025	0.029	0.031
TiO_2	0.100	0.010	0.017	0.098	0.047	0.025	0.128	0.010	0.088	0.100	0.010	0.010	0.012	0.013	0.012	0.007	0.003	0.057	0.048	0.027	0.007	0.093	0.010	0.043	0.027	0.115
SnO_2	0.004	0.000	0.000	0.001	0.000	0.000	0.001	0.000	0.001	0.001	0.001	0.000	0.000	0.001	0.000	0.000	0.000	0.000	0.000	0.000	0.000	0.001	0.000	0.000	0.000	0.000
Ta_2O_5	0.005	0.000	0.000	0.000	0.000	0.000	0.004	0.001	0.002	0.000	0.001	0.000	0.001	0.000	0.000	0.000	0.000	0.000	0.001	0.001	0.002	0.000	0.004	0.002	0.000	0.000
Nb_2O_5	0.000	0.000	0.000	0.000	0.001	0.000	0.000	0.000	0.000	0.000	0.000	0.000	0.000	0.000	0.001	0.003	0.000	0.003	0.000	0.001	0.000	0.001	0.000	0.000	0.000	0.001
WO_3	0.000	0.000	0.000	0.001	0.000	0.000	0.000	0.000	0.005	0.006	0.000	0.000	0.000	0.000	0.001	0.008	0.008	0.004	0.001	0.004	0.000	0.001	0.000	0.005	0.000	0.000
CuO	0.000	0.000	0.000	0.000	0.000	0.001	0.000	0.000	0.000	0.000	0.003	0.001	0.001	0.000	0.004	0.004	0.000	0.000	0.001	0.001	0.001	0.000	0.000	0.000	0.000	0.000
Al_2O_3*	99.008	99.008	99.008	99.008	99.008	99.008	99.008	99.008	99.008	99.008	99.008	99.008	99.008	99.008	99.008	99.008	99.008	99.008	99.008	99.008	99.008	99.008	99.008	99.008	99.008	99.008
Total*	99.711	99.539	99.562	99.754	99.651	99.611	99.809	99.580	99.684	99.694	99.589	99.584	99.565	99.563	99.570	99.555	99.511	99.470	99.436	99.742	99.645	99.751	99.405	99.469	99.404	99.540

* The values are not genuine, as Al was not analysed.

Appendix 8-2 (Continued).

Locality/ Date & No. of analyses	Ban Nong Nam Cho, Tue. 1, Jun. 99 (8 analyses).								Den Chai, Wed. 21, April 99 (24 analyses).																					
Colour	Blue								Blue											Green		Yellow			Brown					
Sample No	BNEP1	BNEP3	BNEP4	BNEP2	BNEP2	BNEP1	BNEP4	BNEP3	DCEP1	DCEP2	DCEP3	DCEP3	DCEP3	DCEP3	DCEP3	DCEP5	DCEP9	DCEP8	DCEP7	DCEP12	DCEP14	DCEP15	DCEP21	DCEP19.	DCEP17	DCEP23	DCEP25	DCEP22	DCEP30	DCEP29	DCEP28	DCEP27
Point	#18	#19	#20	#21	#22	#23	#24	#25	#13	#14	#15	#16	#17	#18	#19	#20	#21	#22	#23	#24	#25	#26	#27	#28	#29	#30	#31	#36	#32	#33	#34	#35
V_2O_5	0.003	0.001	0.005	0.007	0.007	0.002	0.008	0.001	0.001	0.004	0.001	0.004	0.003	0.001	0.001	0.001	0.001	0.003	0.006	0.001	0.004	0.000	0.001	0.000	0.000	0.013	0.000	0.000	0.005	0.002	0.002	0.011
NiO	0.000	0.000	0.000	0.000	0.000	0.000	0.000	0.000	0.000	0.000	0.000	0.000	0.000	0.000	0.000	0.000	0.000	0.000	0.000	0.000	0.000	0.000	0.000	0.000	0.000	0.000	0.000	0.000	0.000	0.000	0.000	0.000
Ga_2O_3	0.017	0.012	0.008	0.007	0.010	0.012	0.010	0.012	0.019	0.020	0.018	0.018	0.021	0.019	0.021	0.018	0.040	0.026	0.017	0.027	0.025	0.030	0.017	0.023	0.017	0.015	0.028	0.023	0.017	0.020	0.024	0.015
Fe_2O_3	1.114	0.489	0.570	0.525	0.478	0.951	0.497	0.482	1.955	1.548	1.628	1.536	1.543	1.474	1.467	1.966	0.378	0.614	0.450	0.382	0.300	0.502	0.865	1.564	0.459	0.382	0.444	0.347	0.406	1.489	0.378	0.396
MnO	0.000	0.000	0.000	0.000	0.000	0.000	0.000	0.000	0.000	0.000	0.000	0.000	0.000	0.000	0.000	0.000	0.000	0.000	0.000	0.000	0.000	0.000	0.000	0.000	0.000	0.000	0.000	0.000	0.000	0.000	0.000	0.000
Cr_2O_3	0.003	0.000	0.000	0.011	0.011	0.000	0.006	0.001	0.005	0.000	0.005	0.003	0.003	0.000	0.000	0.002	0.001	0.004	0.000	0.000	0.002	0.000	0.005	0.000	0.000	0.018	0.001	0.003	0.006	0.000	0.001	0.002
La_2O_3	0.003	0.000	0.000	0.001	0.001	0.000	0.002	0.000	0.000	0.002	0.001	0.000	0.001	0.000	0.002	0.000	0.000	0.000	0.000	0.001	0.000	0.002	0.002	0.002	0.000	0.000	0.002	0.000	0.000	0.000	0.002	0.000
TiO_2	0.024	0.067	0.023	0.026	0.023	0.030	0.022	0.046	0.073	0.044	0.049	0.035	0.054	0.052	0.061	0.052	0.151	0.147	0.103	0.064	0.233	0.017	0.021	0.044	0.007	0.022	0.008	0.026	0.021	0.033	0.242	0.022
SnO_2	0.000	0.000	0.000	0.000	0.000	0.001	0.001	0.000	0.000	0.003	0.001	0.001	0.001	0.000	0.000	0.000	0.004	0.000	0.000	0.002	0.001	0.002	0.001	0.003	0.000	0.000	0.003	0.000	0.000	0.000	0.000	0.001
SiO_2	0.000	0.000	0.000	0.000	0.003	0.000	0.000	0.000	0.000	0.000	0.013	0.000	0.000	0.000	0.000	0.000	0.001	0.000	0.000	0.000	0.012	0.000	0.000	0.000	0.000	0.000	0.000	0.000	0.000	0.000	0.000	0.000
Y_2O_3	0.000	0.004	0.000	0.000	0.000	0.000	0.000	0.000	0.000	0.002	0.000	0.003	0.004	0.000	0.000	0.000	0.000	0.004	0.000	0.000	0.003	0.000	0.000	0.000	0.001	0.004	0.000	0.000	0.000	0.000	0.000	0.001
Al_2O_3*	99.008	99.008	99.008	99.008	99.008	99.008	99.008	99.008	99.008	99.008	99.008	99.008	99.008	99.008	99.008	99.008	99.008	99.008	99.008	99.008	99.008	99.008	99.008	99.008	99.008	99.008	99.008	99.008	99.008	99.008	99.008	99.008
Total*	100.172	99.580	99.614	99.584	99.541	100.003	99.554	99.550	101.061	100.631	100.723	100.607	100.638	100.555	100.559	101.047	99.5837	99.8053	99.5844	99.4858	99.5876	99.5604	99.9204	100.644	99.492	99.4618	99.4952	99.4061	99.4631	100.552	99.6563	99.4566

* The values are not genuine, as Al was not analysed.

Appendix 8-2 (Continued).

Locality/ Date & No. of analyses	Bo Phloi, Sun. 16 July 2000 (39 analyses).																
Colour	Blue																
Sample No	BPEP1	BPEP1	BPEP2	BPEP2	BPEP3	BPEP3	BPEP4	BPEP9	BPEP9	BPEP8	BPEP8	BPEP7	BPEP7	BPEP6	BPEP6	BPEP5	BPEP5
Point	#1	#2	#3	#4	#5	#6	#7	#8	#9	#10	#11	#12	#13	#14	#15	#16	#17
V_2O_5	0.002	0.002	0.000	0.007	0.002	0.000	0.002	0.002	0.000	0.002	0.000	0.000	0.002	0.004	0.004	0.002	0.000
Ga_2O_3	0.023	0.024	0.024	0.030	0.023	0.023	0.020	0.012	0.013	0.013	0.013	0.019	0.017	0.012	0.013	0.023	0.023
Fe_2O_3	0.678	0.725	0.931	0.576	0.739	0.582	0.681	0.370	0.369	0.427	0.445	0.456	0.480	0.412	0.356	0.423	0.459
MnO	0.000	0.000	0.000	0.000	0.000	0.000	0.000	0.000	0.000	0.000	0.000	0.000	0.000	0.000	0.000	0.000	0.000
Cr_2O_3	0.000	0.000	0.001	0.000	0.000	0.000	0.000	0.000	0.001	0.001	0.004	0.000	0.003	0.000	0.000	0.003	0.000
TiO_2	0.025	0.028	0.038	0.264	0.078	0.035	0.023	0.005	0.005	0.008	0.008	0.007	0.005	0.017	0.013	0.013	0.012
SnO_2	0.000	0.001	0.001	0.000	0.000	0.000	0.000	0.000	0.000	0.000	0.000	0.000	0.000	0.000	0.000	0.000	0.001
Ta_2O_5	0.002	0.004	0.000	0.006	0.002	0.000	0.000	0.001	0.001	0.000	0.000	0.000	0.002	0.000	0.002	0.000	0.000
Nb_2O_5	0.000	0.000	0.000	0.003	0.001	0.000	0.000	0.000	0.000	0.001	0.001	0.000	0.000	0.000	0.000	0.000	0.000
WO_3	0.000	0.000	0.000	0.093	0.011	0.000	0.003	0.000	0.000	0.008	0.000	0.005	0.003	0.014	0.003	0.000	0.008
CuO	0.003	0.001	0.000	0.000	0.000	0.000	0.000	0.001	0.000	0.000	0.003	0.001	0.000	0.000	0.000	0.000	0.000
Al_2O_3*	99.008	99.008	99.008	99.008	99.008	99.008	99.008	99.008	99.008	99.008	99.008	99.008	99.008	99.008	99.008	99.008	99.008
Total*	99.740	99.793	100.004	99.987	99.865	99.648	99.736	99.400	99.398	99.469	99.483	99.496	99.520	99.466	99.399	99.472	99.510

* The values are not genuine, as Al was not analysed.

Appendix 8-2 Weight % oxides of trace elements in the corundum samples from Thailand and the Democratic People's Republic of Laos obtained by EPMA.

Appendix 8-2 (Continued).

Locality/ Date & No. of analyses	Bo Phioi, Sun. 16 July 2000 (39 analyses).																											
Colour	Green							Brown													Violet			Purple				
Sample No	BPEP10	BPEP10	BPEP11	BPEP11	BPEP11	BPEP12	BPEP12	BPEP17	BPEP17	BPEP17	BPEP17	BPEP17	BPEP17	BPEP17	BPEP16	BPEP16	BPEP16	BPEP15	BPEP15	BPEP15	BPEP13	BPEP13	BPEP13	BPEP14	BPEP14	BPEP14	BPEP14	BPEP14
Point	#18	#19	#20	#21	#22	#23	#24	#28	#29	#30	#31	#32	#33	#34	#35	#36	#37	#25	#26	#27	#38	#39						
V_2O_5	0.002	0.000	0.000	0.002	0.002	0.002	0.002	0.005	0.004	0.005	0.005	0.004	0.004	0.004	0.005	0.004	0.000	0.027	0.032	0.030	0.002	0.002						
Ga_2O_3	0.012	0.011	0.016	0.015	0.013	0.017	0.016	0.022	0.020	0.016	0.016	0.015	0.017	0.016	0.016	0.016	0.013	0.024	0.026	0.026	0.015	0.015						
Fe_2O_3	0.472	0.482	0.420	0.455	0.363	0.446	0.449	0.559	0.509	0.523	0.459	0.771	0.683	0.330	0.476	0.412	0.417	0.327	0.337	0.333	0.356	0.420						
MnO	0.000	0.000	0.000	0.000	0.000	0.000	0.000	0.000	0.000	0.000	0.000	0.000	0.000	0.000	0.000	0.000	0.000	0.000	0.000	0.000	0.000	0.000						
Cr_2O_3	0.000	0.000	0.000	0.003	0.000	0.000	0.001	0.001	0.001	0.000	0.004	0.004	0.003	0.004	0.000	0.001	0.000	0.035	0.038	0.038	0.032	0.053						
TiO_2	0.007	0.008	0.005	0.007	0.005	0.007	0.008	0.047	0.012	0.020	0.010	0.130	0.013	0.008	0.087	0.065	0.013	0.015	0.020	0.018	0.003	0.005						
SnO_2	0.000	0.000	0.001	0.000	0.001	0.001	0.000	0.000	0.000	0.001	0.000	0.000	0.001	0.000	0.000	0.001	0.000	0.000	0.000	0.000	0.000	0.000						
Ta_2O_5	0.000	0.000	0.000	0.000	0.001	0.000	0.000	0.001	0.000	0.000	0.001	0.000	0.000	0.001	0.000	0.000	0.000	0.001	0.000	0.002	0.000	0.000						
Nb_2O_5	0.000	0.001	0.000	0.000	0.000	0.000	0.000	0.001	0.001	0.000	0.000	0.001	0.000	0.000	0.000	0.000	0.000	0.000	0.000	0.000	0.000	0.000						
WO_3	0.005	0.008	0.013	0.003	0.000	0.000	0.001	0.000	0.006	0.000	0.008	0.010	0.000	0.005	0.003	0.003	0.000	0.003	0.004	0.004	0.016	0.000						
CuO	0.000	0.004	0.000	0.000	0.000	0.000	0.000	0.000	0.000	0.001	0.006	0.001	0.003	0.000	0.001	0.001	0.000	0.000	0.000	0.000	0.001	0.000						
Al_2O_3*	99.008	99.008	99.008	99.008	99.008	99.008	99.008	99.008	99.008	99.008	99.008	99.008	99.008	99.008	99.008	99.008	99.008	99.008	99.008	99.008	99.008	99.008						
Total*	99.505	99.522	99.463	99.491	99.394	99.481	99.486	99.645	99.562	99.575	99.518	99.944	99.732	99.377	99.596	99.511	99.452	99.440	99.465	99.459	99.434	99.502						

* The values are not genuine, as Al was not analysed.

Appendix 8-2 (Continued).

Locality/ Date & No. of analyses	Bo Phloi, Tue. 23, Mar. 99 (17 analyses).																	Khok Sam Ran										
																		Mon. 29/3/. 99 (1 anal.)	Tue. 13, Apr. 99 (11 analyses).									
Colour	Blue								Green		Brown			Violet	Purple	Blue												
Sample No	BPEP1	BPEP2	BPEP3	BPEP4	BPEP9	BPEP8	BPEP7	BPEP6	BPEP5	BPEP10	BPEP11	BPEP12	BPEP17	BPEP16	BPEP15	BPEP13	BPEP14	KSEP1	KSEP3	KSEP6	KSEP5	KSEP4	KSEP7	KSEP8	KSEP9	KSEP12	KSEP11	KSEP10
Point	#26	#27	#28	#29	#30	#31	#32	#33	#34	#35	#36	#37	#39	#40	#41	#38	#42	#24	#1	#2	#3	#4	#5	#6	#8	#7	#9	#10	#11
V_2O_5	0.001	0.002	0.004	0.000	0.000	0.001	0.003	0.003	0.002	0.000	0.004	0.000	0.005	0.000	0.002	0.028	0.001	0.002	0.002	0.003	0.001	0.001	0.000	0.003	0.000	0.001	0.003	0.004	0.000
NiO	0.000	0.000	0.000	0.000	0.000	0.000	0.000	0.000	0.000	0.000	0.000	0.000	0.000	0.000	0.000	0.000	0.000	0.000	0.000	0.000	0.000	0.000	0.000	0.000	0.000	0.000	0.000	0.000	0.000
Ga_2O_3	0.020	0.017	0.016	0.022	0.010	0.016	0.019	0.012	0.022	0.012	0.014	0.014	0.019	0.016	0.011	0.025	0.015	0.015	0.014	0.012	0.019	0.011	0.014	0.015	0.015	0.017	0.011	0.013	0.019
Fe_2O_3	0.612	0.536	0.556	0.668	0.364	0.431	0.451	0.389	0.451	0.465	0.402	0.436	0.439	0.317	0.356	0.302	0.327	1.482	1.833	1.548	1.607	1.367	1.600	1.441	1.413	1.624	1.451	1.610	1.575
MnO	0.000	0.000	0.000	0.000	0.000	0.000	0.000	0.000	0.000	0.000	0.001	0.000	0.000	0.000	0.000	0.000	0.000	0.000	0.000	0.000	0.000	0.000	0.000	0.000	0.000	0.003	0.000	0.000	0.000
Cr_2O_3	0.000	0.000	0.000	0.000	0.000	0.000	0.000	0.000	0.004	0.001	0.000	0.000	0.003	0.000	0.007	0.036	0.021	0.005	0.000	0.005	0.006	0.000	0.004	0.000	0.007	0.000	0.004	0.000	0.003
La_2O_3	0.000	0.003	0.001	0.000	0.000	0.000	0.000	0.000	0.000	0.000	0.000	0.001	0.000	0.003	0.000	0.000	0.000	0.000	0.000	0.000	0.000	0.002	0.000	0.000	0.001	0.000	0.001	0.000	0.001
TiO_2	0.011	0.055	0.019	0.016	0.009	0.007	0.007	0.015	0.015	0.007	0.006	0.008	0.009	0.012	0.014	0.017	0.004	0.082	0.048	0.182	0.084	0.121	0.107	0.008	0.018	0.079	0.040	0.056	0.033
SnO_2	0.000	0.004	0.000	0.000	0.000	0.002	0.000	0.003	0.000	0.000	0.000	0.002	0.000	0.000	0.000	0.000	0.000	0.000	0.000	0.001	0.001	0.004	0.001	0.000	0.000	0.002	0.003	0.001	0.000
SiO_2	0.000	0.000	0.000	0.000	0.000	0.000	0.000	0.000	0.000	0.000	0.000	0.000	0.000	0.000	0.000	0.007	0.000	0.000	0.000	0.000	0.000	0.000	0.000	0.000	0.002	0.000	0.000	0.000	0.002
Y_2O_3	0.000	0.000	0.000	0.000	0.000	0.001	0.000	0.000	0.000	0.000	0.000	0.002	0.004	0.003	0.000	0.000	0.000	0.000	0.000	0.000	0.001	0.000	0.000	0.000	0.000	0.000	0.000	0.000	0.000
Al_2O_3*	99.008	99.008	99.008	99.008	99.008	99.008	99.008	99.008	99.008	99.008	99.008	99.008	99.008	99.008	99.008	99.008	99.008	99.008	99.008	99.008	99.008	99.008	99.008	99.008	99.008	99.008	99.008	99.008	99.008
Total*	99.652	99.625	99.605	99.715	99.391	99.465	99.487	99.431	99.502	99.493	99.434	99.471	99.488	99.358	99.398	99.421	99.377	100.594	100.905	100.760	100.727	100.514	100.734	100.475	100.465	100.732	100.520	100.692	100.640

* The values are not genuine, as Al was not analysed.

Appendix 8-2 (Continued).

Locality/ Date & No. of analyses	Bang Ka Cha, Tue. 11, May 99 (16 analyses).																Bang Ka Cha , Tue. 14, Sept. 99 (11 analyses).										
Colour	Green	Brown															Bluish Green										
Sample No	BKCEP3	BKCEP4	BKCEP4	BKCEP4	BKCEP5	BKCEP8	BKCEP7	BKCEP7	BKCEP6	BKCEP6	BKCEP9	BKCEP9	BKCEP9	BKCEP9	BKCEP10	BKCEP11	BKCEP13	BKCEP14	BKCEP14	BKCEP14	BKCEP15	BKCEP15	BKCEP16	BKCEP17	BKCEP18	BKCEP19	BKCEP20	BKCEP21
Point	#1	#2	#3	#4	#5	#6	#7	#8	#9	#10	#11	#12	#13	#14	#15	#16	#7	#8	#9	#10	#11	#12	#13	#14	#15	#16	#17
V_2O_5	0.003	0.001	0.000	0.000	0.001	0.001	0.002	0.005	0.000	0.001	0.000	0.000	0.001	0.001	0.000	0.000	0.002	0.000	0.000	0.002	0.002	0.005	0.007	0.002	0.000	0.000	0.004
NiO	0.000	0.000	0.000	0.000	0.000	0.000	0.000	0.000	0.000	0.000	0.000	0.000	0.000	0.000	0.000	0.000	0.000	0.000	0.000	0.000	0.000	0.000	0.000	0.000	0.000	0.000	0.000
Ga_2O_3	0.025	0.022	0.022	0.018	0.017	0.022	0.021	0.018	0.017	0.018	0.018	0.019	0.018	0.023	0.014	0.021	0.027	0.019	0.034	0.024	0.023	0.030	0.028	0.031	0.031	0.017	0.030
Fe_2O_3	2.048	1.782	2.158	1.602	1.927	1.365	1.461	2.082	1.964	1.844	1.830	1.808	3.334	1.116	1.729	1.261	1.391	1.240	1.184	1.227	0.705	1.180	1.461	1.017	1.119	1.453	1.454
MnO	0.000	0.000	0.000	0.000	0.000	0.000	0.000	0.002	0.001	0.000	0.000	0.000	0.007	0.000	0.000	0.000	0.000	0.000	0.000	0.000	0.000	0.000	0.000	0.000	0.000	0.000	0.000
Cr_2O_3	0.004	0.000	0.000	0.000	0.000	0.000	0.004	0.002	0.005	0.002	0.002	0.000	0.001	0.001	0.000	0.002	0.000	0.004	0.004	0.004	0.004	0.007	0.001	0.000	0.000	0.003	0.003
La_2O_3	0.002	0.000	0.000	0.000	0.002	0.000	0.000	0.000	0.000	0.005	0.000	0.000	0.000	0.001	0.000	0.000	0.000	0.000	0.001	0.000	0.000	0.000	0.001	0.000	0.000	0.000	0.000
TiO_2	0.011	0.008	0.028	0.013	0.007	0.007	0.007	0.013	0.016	0.013	0.026	0.009	0.375	0.009	0.006	0.006	0.025	0.003	0.017	0.078	0.005	0.003	0.008	0.012	0.040	0.013	0.007
SnO_2	0.000	0.002	0.003	0.000	0.000	0.000	0.002	0.003	0.004	0.003	0.000	0.005	0.005	0.000	0.000	0.000	0.000	0.000	0.001	0.005	0.003	0.001	0.001	0.000	0.000	0.000	0.001
SiO_2	0.000	0.000	0.000	0.000	0.000	0.000	0.000	0.000	0.000	0.000	0.000	0.000	0.000	0.000	0.000	0.000	0.000	0.000	0.000	0.000	0.000	0.000	0.000	0.000	0.000	0.000	0.000
Y_2O_3	0.003	0.000	0.000	0.004	0.000	0.000	0.000	0.000	0.000	0.000	0.000	0.000	0.000	0.000	0.000	0.000	0.000	0.000	0.000	0.000	0.000	0.000	0.000	0.000	0.000	0.000	0.000
Al_2O_3*	99.008	99.008	99.008	99.008	99.008	99.008	99.008	99.008	99.008	99.008	99.008	99.008	99.008	99.008	99.008	99.008	99.008	99.008	99.008	99.008	99.008	99.008	99.008	99.008	99.008	99.008	99.008
Total*	101.104	100.823	101.218	100.645	100.961	100.403	100.504	101.132	101.016	100.894	100.882	100.849	102.750	100.158	100.757	100.297	100.453	100.274	100.249	100.348	99.749	100.234	100.517	100.069	100.198	100.494	100.506

* The values are not genuine, as Al was not analysed.

Appendix 8-2 (Continued).

Locality/ Date & No. of analyses	Nam Yun, Tue. 1, Jun. 99 (17 analyses).																Nam Yun, 24/5/99		
Colour	Blue												Green				Green		
Sample No	NYEP1	NYEP1	NYEP2	NYEP3	NYEP7	NYEP7	NYEP5	NYEP4	NYEP8	NYEP9	NYEP11	NYEP12	NYEP13	NYEP13	NYEP15	NYEP16	NYEP17	NYEP18	NYEP19
Point	#1	#2	#3	#4	#5	#6	#7	#8	#9	#10	#11	#14	#12	#13	#15	#16	#17	#20	#21
V_2O_5	0.003	0.006	0.006	0.001	0.002	0.006	0.003	0.006	0.003	0.000	0.001	0.002	0.000	0.003	0.002	0.003	0.003	0.001	0.001
NiO	0.000	0.000	0.000	0.000	0.000	0.000	0.000	0.000	0.000	0.000	0.000	0.000	0.000	0.000	0.000	0.000	0.000	0.000	0.000
Ga_2O_3	0.025	0.026	0.026	0.022	0.021	0.026	0.020	0.020	0.025	0.023	0.022	0.037	0.022	0.024	0.022	0.022	0.022	0.024	0.047
Fe_2O_3	1.348	1.545	1.551	1.367	1.315	1.383	1.484	1.190	1.570	1.253	1.025	1.361	1.669	1.684	1.097	1.280	1.399	1.273	0.795
MnO	0.000	0.000	0.000	0.000	0.000	0.000	0.000	0.000	0.000	0.000	0.000	0.000	0.000	0.000	0.000	0.000	0.000	0.000	0.000
Cr_2O_3	0.001	0.000	0.000	0.002	0.000	0.000	0.010	0.000	0.000	0.000	0.002	0.002	0.001	0.005	0.001	0.000	0.002	0.008	0.000
La_2O_3	0.001	0.003	0.003	0.000	0.000	0.000	0.000	0.000	0.002	0.000	0.000	0.000	0.000	0.000	0.000	0.000	0.002	0.000	0.000
TiO_2	0.010	0.027	0.037	0.014	0.025	0.019	0.010	0.014	0.018	0.030	0.030	0.020	0.008	0.019	0.004	0.008	0.006	0.010	0.004
SnO_2	0.000	0.001	0.003	0.002	0.001	0.000	0.001	0.000	0.000	0.002	0.001	0.000	0.002	0.000	0.000	0.002	0.000	0.000	0.000
SiO_2	0.000	0.000	0.000	0.000	0.000	0.000	0.000	0.000	0.007	0.001	0.000	0.000	0.005	0.000	0.000	0.000	0.002	0.000	0.000
Y_2O_3	0.000	0.004	0.001	0.000	0.000	0.000	0.004	0.002	0.000	0.000	0.003	0.004	0.001	0.000	0.000	0.000	0.000	0.000	0.003
Al_2O_3*	99.008	99.008	99.008	99.008	99.008	99.008	99.008	99.008	99.008	99.008	99.008	99.008	99.008	99.008	99.008	99.008	99.008	99.008	99.008
Total*	100.396	100.619	100.635	100.416	100.372	100.442	100.538	100.240	100.634	100.318	100.093	100.435	100.716	100.743	100.134	100.323	100.443	100.324	99.856

* The values are not genuine, as Al was not analysed.

Appendix 8-2 (Continued).

Locality/ Date & No. of analyses	Bo Rai, Th. 4, March 99 (47 analyses).																																					
Colour	Purple																	Ruby										Pink											
Sample No	BREP19	BREP20	BREP20	BREP21	BREP19	BREP21	BREP22	BREP22	BREP23	BREP23	BREP23	BREP23	BREP23	BREP23	BREP23	BREP29	BREP29	BREP30	BREP30	BREP30	BREP31	BREP31	BREP32	BREP32	BREP33	BREP33	BREP34	BREP34	BREP35	BREP35	BREP36	BREP36	BREP36	BREP36	BREP36	BREP36	BREP36	BREP36
Point	#1	#2	#3	#4	#5	#6	#7	#8	#9	#10	#10.1	#10.2	#10.3	#10.4	#21	#22	#23	#24	#25	#26	#27	#28	#29	#30	#31	#32	#33	#34	#35	#36	#37	#38	#39	#40	#41	#42	#43	#44
V_2O_5	0.001	0.005	0.004	0.003	0.002	0.002	0.005	0.005	0.007	0.008	0.011	0.009	0.009	0.007	0.001	0.003	0.006	0.004	0.000	0.002	0.004	0.004	0.001	0.002	0.002	0.003	0.004	0.003	0.002	0.003	0.000	0.000	0.000	0.000	0.000	0.000	0.000	0.000
NiO	0.000	0.000	0.000	0.000	0.000	0.000	0.000	0.000	0.000	0.000	0.000	0.000	0.000	0.000	0.000	0.000	0.000	0.000	0.000	0.000	0.000	0.000	0.000	0.000	0.000	0.000	0.000	0.000	0.000	0.000	0.000	0.000	0.000	0.000	0.000	0.000	0.000	0.000
Ga_2O_3	0.006	0.008	0.002	0.003	0.005	0.003	0.003	0.007	0.005	0.007	0.007	0.005	0.009	0.005	0.000	0.001	0.005	0.004	0.003	0.007	0.005	0.007	0.006	0.001	0.001	0.008	0.005	0.005	0.002	0.002	0.000	0.000	0.000	0.000	0.000	0.000	0.000	0.000
Fe_2O_3	0.472	0.755	0.744	0.663	0.492	0.660	0.581	0.619	0.882	0.842	0.864	0.873	0.872	0.870	0.592	0.592	0.387	0.425	0.578	0.580	0.401	0.427	0.357	0.374	0.507	0.512	0.414	0.436	0.562	0.528	0.000	0.000	0.000	0.000	0.000	0.000	0.000	0.000
MnO	0.000	0.000	0.000	0.000	0.000	0.000	0.000	0.004	0.000	0.000	0.000	0.000	0.000	0.000	0.000	0.000	0.000	0.000	0.000	0.000	0.000	0.000	0.000	0.000	0.000	0.000	0.000	0.000	0.000	0.000	0.000	0.000	0.000	0.000	0.000	0.000	0.000	0.000
Cr_2O_3	0.323	0.201	0.216	0.106	0.294	0.120	0.210	0.200	0.331	0.300	0.333	0.326	0.337	0.318	0.555	0.563	0.223	0.228	0.102	0.087	0.348	0.357	0.114	0.124	0.114	0.086	0.241	0.167	0.147	0.147	0.000	0.000	0.000	0.000	0.000	0.000	0.000	0.000
La_2O_3	0.000	0.000	0.000	0.000	0.000	0.000	0.000	0.000	0.000	0.000	0.001	0.001	0.001	0.000	0.000	0.000	0.000	0.002	0.000	0.002	0.001	0.002	0.001	0.000	0.000	0.000	0.000	0.000	0.000	0.000	0.000	0.000	0.000	0.000	0.000	0.000	0.000	0.000
TiO_2	0.014	0.022	0.023	0.037	0.016	0.037	0.057	0.057	0.073	0.067	0.067	0.068	0.068	0.070	0.010	0.013	0.039	0.039	0.007	0.011	0.022	0.022	0.017	0.019	0.023	0.024	0.021	0.023	0.021	0.021	0.000	0.000	0.000	0.000	0.000	0.000	0.000	0.000
SnO_2	0.000	0.001	0.000	0.005	0.000	0.000	0.000	0.000	0.003	0.000	0.001	0.000	0.001	0.001	0.002	0.004	0.000	0.001	0.003	0.001	0.000	0.000	0.000	0.001	0.001	0.000	0.000	0.000	0.001	0.003	0.000	0.000	0.000	0.000	0.000	0.000	0.000	0.000
SiO_2	0.046	0.016	0.012	0.027	0.046	0.016	0.002	0.005	0.013	0.006	0.006	0.004	0.003	0.006	0.032	0.031	0.028	0.025	0.030	0.032	0.036	0.030	0.041	0.038	0.026	0.027	0.021	0.018	0.022	0.027	0.000	0.000	0.000	0.000	0.000	0.000	0.000	0.000
Y_2O_3	0.000	0.000	0.000	0.000	0.000	0.000	0.004	0.000	0.000	0.000	0.000	0.000	0.000	0.007	0.006	0.001	0.000	0.001	0.003	0.000	0.002	0.002	0.001	0.001	0.000	0.000	0.000	0.003	0.000	0.000	0.000	0.000	0.000	0.000	0.000	0.000	0.000	0.000
Al_2O_3*	99.008	99.008	99.008	99.008	99.008	99.008	99.008	99.008	99.008	99.008	99.008	99.008	99.008	99.008	99.008	99.008	99.008	99.008	99.008	99.008	99.008	99.008	99.008	99.008	99.008	99.008	99.008	99.008	99.008	99.008	99.000	99.000	99.000	99.000	99.000	99.000	99.000	99.000
Total*	99.871	100.016	100.007	99.852	99.864	99.846	99.869	99.904	100.322	100.239	100.298	100.294	100.310	100.291	100.206	100.216	99.697	99.737	99.734	99.729	99.828	99.859	99.545	99.567	99.681	99.668	99.715	99.662	99.765	99.738	99.000	99.000	99.000	99.000	99.000	99.000	99.000	99.000

* The values are not genuine, as Al was not analysed.

Appendix 8-2 (Continued).

Locality/ Date & No. of analyses	Bo Rai, Th. 4, March 99 (47 analyses, continued).																			Nong Bon, Wed. 21, April 99 (12 analyses)										
Colour	Pink						Blue													Purple										
Sample No	BREP37	BREP37	BREP38	BREP38	BREP39	BREP39	BREP40	BREP24	BREP24	BREP25	BREP25	BREP25	BREP26	BREP26	BREP27	BREP27	BREP28	BREP28	BREP28	NBEP1	NBEP2	NBEP3	NBEP6	NBEP5	NBEP4	NBEP7	NBEP8	NBEP9	NBEP12	NBEP11	NBEP10
Point	#37	#38	#39	#40	#41	#42	#43	#11	#12	#13	#14	#15	#16	#17	#18	#19	#20			#1	#2	#3	#4	#5	#6	#7	#8	#9	#10	#11	#12
V_2O_5	0.004	0.002	0.000	0.003	0.002	0.001	0.004	0.000	0.003	0.004	0.000	0.000	0.001	0.000	0.003	0.004	0.002			0.007	0.005	0.003	0.004	0.002	0.002	0.003	0.003	0.004	0.006	0.003	0.005
NiO	0.000	0.000	0.000	0.000	0.000	0.000	0.000	0.000	0.000	0.000	0.000	0.000	0.000	0.000	0.000	0.000	0.000			0.000	0.000	0.000	0.000	0.000	0.000	0.000	0.000	0.000	0.000	0.000	0.000
Ga_2O_3	0.003	0.003	0.005	0.004	0.003	0.002	0.005	0.022	0.019	0.018	0.022	0.025	0.026	0.034	0.028	0.024	0.024			0.004	0.006	0.005	0.007	0.004	0.003	0.005	0.002	0.003	0.004	0.004	0.005
Fe_2O_3	0.546	0.544	0.449	0.478	0.544	0.552	0.349	1.160	1.195	0.726	0.709	1.104	0.559	0.983	0.918	0.787	0.818			0.692	0.533	0.507	0.480	0.471	0.646	0.471	0.597	0.409	0.625	0.360	0.672
MnO	0.000	0.000	0.000	0.000	0.000	0.000	0.000	0.000	0.000	0.000	0.000	0.000	0.000	0.000	0.000	0.000	0.000			0.000	0.003	0.000	0.000	0.000	0.000	0.000	0.000	0.000	0.000	0.000	0.000
Cr_2O_3	0.250	0.248	0.134	0.191	0.199	0.191	0.564	0.000	0.000	0.003	0.000	0.001	0.000	0.000	0.001	0.002	0.001			0.273	0.205	0.255	0.052	0.076	0.153	0.058	0.065	0.036	0.355	0.028	0.194
La_2O_3	0.001	0.000	0.000	0.000	0.000	0.000	0.000	0.000	0.000	0.000	0.000	0.000	0.002	0.002	0.000	0.000	0.001			0.000	0.000	0.000	0.000	0.001	0.001	0.003	0.000	0.000	0.004	0.003	0.000
TiO_2	0.018	0.017	0.020	0.019	0.013	0.012	0.020	0.018	0.014	0.089	0.013	0.009	0.009	0.021	0.010	0.009	0.014			0.048	0.029	0.038	0.017	0.017	0.022	0.022	0.023	0.025	0.062	0.028	0.043
SnO_2	0.000	0.000	0.000	0.002	0.002	0.001	0.000	0.001	0.000	0.001	0.000	0.000	0.000	0.000	0.001	0.000	0.000			0.001	0.000	0.001	0.000	0.000	0.001	0.000	0.002	0.001	0.001	0.000	0.003
SiO_2	0.049	0.039	0.031	0.027	0.017	0.042	0.025	0.000	0.000	0.013	0.000	0.010	0.010	0.000	0.004	0.024	0.012			0.009	0.000	0.003	0.004	0.022	0.024	0.016	0.000	0.016	0.000	0.020	0.003
Y_2O_3	0.003	0.003	0.002	0.001	0.000	0.000	0.003	0.001	0.000	0.000	0.000	0.000	0.000	0.000	0.000	0.000	0.000			0.000	0.006	0.000	0.001	0.000	0.003	0.000	0.000	0.000	0.000	0.000	0.000
Al_2O_3*	99.008	99.008	99.008	99.008	99.008	99.008	99.008	99.008	99.008	99.008	99.008	99.008	99.008	99.008	99.008	99.008	99.008			99.008	99.008	99.008	99.008	99.008	99.008	99.008	99.008	99.008	99.008	99.008	99.008
Total*	99.882	99.863	99.648	99.732	99.787	99.809	99.977	100.210	100.240	99.862	99.752	100.157	99.615	100.047	99.973	99.859	99.880			100.043	99.795	99.821	99.573	99.600	99.863	99.586	99.701	99.502	100.065	99.453	99.933

* The values are not genuine, as Al was not analysed.

Appendix 8-3

Appendix 8-3 Weight % oxides of trace elements in the corundum samples from **outside Thailand** obtained by EPMA.

Locality/ Date & No. of analyses	Natal, Wed 17, Mar, 99 (6 analyses).						Mull, Mon.29, Mar, 99 (22 analyses).																					
Colour	Grey						Blue																					
Sample No	Δ 1556-1	Δ 1556-2	Δ 1556-3	Δ 1556-1	Δ 1556-2	Δ 1556-3	SVI/1	SVI/1	SVI/1	SVI/1	SVI/1	SVI/1	SVI/1	SVI/1	SVI/1	SVI/1	SVI/1	SVI/1	SVI/1	SVI/1	SVI/1	SVI/1	SVI/1	SVI/1	SVI/1	SVI/1	SVI/1	SVI/1
Point	#1	#2	#3	#1.1	#2.1	#3.1	#1	#2	#3	#4	#5	#6	#7	#8	#9	#10	#11	#12	#13	#14	#15	#16	#17	#18	#19	#20	#21	#22
V_2O_5	0.000	0.005	0.000	0.002	0.002	0.002	0.053	0.047	0.057	0.054	0.046	0.083	0.081	0.080	0.061	0.059	0.062	0.058	0.057	0.054	0.073	0.052	0.064	0.047	0.054	0.092	0.060	0.089
NiO	0.000	0.000	0.000	0.000	0.000	0.000	0.000	0.000	0.000	0.000	0.000	0.000	0.000	0.000	0.000	0.000	0.000	0.000	0.000	0.000	0.000	0.000	0.000	0.000	0.000	0.000	0.000	0.000
Ga_2O_3	0.019	0.017	0.018	0.024	0.020	0.020	0.011	0.011	0.014	0.015	0.013	0.014	0.012	0.009	0.015	0.011	0.008	0.012	0.012	0.010	0.013	0.009	0.014	0.006	0.013	0.008	0.012	0.012
Fe_2O_3	1.342	1.191	1.367	1.355	1.467	1.311	0.451	0.437	0.427	0.432	0.426	0.373	0.380	0.386	0.415	0.417	0.432	0.403	0.419	0.423	0.393	0.432	0.417	0.425	0.428	0.390	0.372	0.360
MnO	0.000	0.000	0.000	0.000	0.000	0.000	0.000	0.000	0.000	0.000	0.000	0.000	0.000	0.000	0.000	0.000	0.000	0.000	0.000	0.000	0.000	0.000	0.000	0.000	0.000	0.000	0.000	0.000
Cr_2O_3	0.002	0.003	0.002	0.001	0.003	0.001	0.138	0.100	0.100	0.089	0.122	0.128	0.141	0.131	0.107	0.106	0.113	0.113	0.116	0.116	0.125	0.122	0.099	0.111	0.106	0.127	0.121	0.136
La_2O_3	0.000	0.000	0.000	0.000	0.002	0.000	0.000	0.000	0.000	0.001	0.001	0.000	0.000	0.000	0.002	0.000	0.000	0.000	0.002	0.001	0.000	0.000	0.000	0.002	0.000	0.000	0.000	0.000
TiO_2	0.032	0.010	0.043	0.033	0.007	0.035	0.183	0.130	0.155	0.149	0.133	0.153	0.153	0.155	0.143	0.151	0.149	0.150	0.143	0.146	0.166	0.150	0.164	0.142	0.154	0.167	0.131	0.145
SnO_2	0.001	0.000	0.001	0.004	0.000	0.000	0.001	0.000	0.000	0.000	0.001	0.001	0.000	0.000	0.001	0.000	0.000	0.000	0.000	0.002	0.000	0.000	0.001	0.002	0.000	0.001	0.000	0.004
SiO_2	0.097	0.005	0.000	0.000	0.000	0.006	0.000	0.000	0.010	0.000	0.000	0.040	0.004	0.015	0.000	0.000	0.000	0.000	0.000	0.000	0.000	0.000	0.000	0.000	0.000	0.000	0.000	0.000
Y_2O_3	0.000	0.000	0.001	0.000	0.000	0.325	0.000	0.003	0.000	0.000	0.000	0.000	0.000	0.000	0.000	0.000	0.000	0.000	0.006	0.001	0.000	0.000	0.005	0.000	0.000	0.000	0.000	0.000
Al_2O_3*	99.008	99.008	99.008	99.008	99.008	99.008	99.008	99.008	99.008	99.008	99.008	99.008	99.008	99.008	99.008	99.008	99.008	99.008	99.008	99.008	99.008	99.008	99.008	99.008	99.008	99.008	99.008	99.008
Total*	100.501	100.240	100.440	100.428	100.509	100.709	99.844	99.736	99.770	99.748	99.751	99.800	99.781	99.784	99.753	99.752	99.772	99.744	99.764	99.760	99.778	99.773	99.772	99.742	99.763	99.792	99.704	99.754

* The values are not genuine, as Al was not analysed.

Appendix 8-3 (Continued).

Locality/ Date & No. of analyses	Bushveld, Wed 17, Mar, 99 (6 analyses).						S. India, Wed 17, Mar. 99 (5 analyses).					Bancroft, Tue 13, April. 99 (14 analyses).													
Colour	Purple						Purple					Grey													
Sample No	18058-1	18058-2	18058-3	18058-1	18058-2	18058-3	Δ 793	Δ 793	Δ 793	Δ 793	Δ 793	BC21	BC21	BC21	BC21	BC21	BC21	BC21	BC21	BC21	BC21	BC21	BC21	BC21	BC21
Point	#4	#5	#6	#4.1	#5.1	#6.1	#13	#14	#15	#13.1	#14.1	#12	#13	#14	#15	#16	#17	#18	#19	#20	#21	#22	#23	#24	#25
V_2O_5	0.134	0.196	0.112	0.105	0.159	0.116	0.004	0.002	0.002	0.002	0.002	0.002	0.000	0.000	0.001	0.002	0.000	0.000	0.002	0.000	0.000	0.000	0.000	0.000	0.000
NiO	0.000	0.000	0.000	0.000	0.000	0.000	0.000	0.000	0.000	0.000	0.000	0.000	0.000	0.000	0.000	0.000	0.000	0.000	0.000	0.000	0.000	0.000	0.000	0.000	0.000
Ga_2O_3	0.010	0.013	0.011	0.009	0.012	0.011	0.002	0.000	0.004	0.004	0.001	0.010	0.010	0.011	0.006	0.011	0.012	0.011	0.010	0.014	0.010	0.010	0.012	0.011	0.007
Fe_2O_3	0.192	0.178	0.157	0.179	0.216	0.150	0.521	0.499	0.497	0.518	0.519	0.296	0.209	0.285	0.216	0.296	0.305	0.296	0.287	0.287	0.354	0.213	0.347	0.288	0.288
MnO	0.000	0.000	0.000	0.001	0.000	0.000	0.000	0.000	0.001	0.000	0.000	0.000	0.000	0.000	0.000	0.000	0.000	0.000	0.000	0.000	0.000	0.000	0.000	0.000	0.000
Cr_2O_3	0.655	0.669	0.672	0.658	0.639	0.674	1.252	1.450	1.371	1.331	1.466	0.001	0.001	0.000	0.000	0.000	0.002	0.002	0.001	0.001	0.004	0.000	0.001	0.000	0.003
La_2O_3	0.000	0.000	0.001	0.000	0.000	0.000	0.000	0.000	0.000	0.000	0.000	0.000	0.000	0.002	0.004	0.002	0.000	0.000	0.003	0.000	0.001	0.000	0.000	0.002	0.000
TiO_2	0.123	0.600	0.135	0.107	0.095	0.140	0.006	0.005	0.006	0.007	0.005	0.015	0.003	0.035	0.002	0.036	0.060	0.058	0.027	0.022	0.004	0.003	0.004	0.016	0.018
SnO_2	0.000	0.000	0.000	0.000	0.000	0.000	0.000	0.000	0.001	0.000	0.001	0.003	0.000	0.000	0.000	0.000	0.001	0.000	0.000	0.000	0.001	0.002	0.000	0.000	0.000
SiO_2	0.000	0.000	0.000	0.000	0.000	0.000	0.000	0.000	0.000	0.000	0.000	0.000	0.000	0.000	0.000	0.000	0.000	0.000	0.000	0.000	0.000	0.000	0.000	0.000	0.000
Y_2O_3	0.000	0.000	0.000	0.003	0.000	0.004	0.000	0.397	0.000	0.000	0.000	0.001	0.000	0.000	0.000	0.000	0.000	0.000	0.000	0.000	0.000	0.000	0.001	0.000	0.000
Al_2O_3*	99.008	99.008	99.008	99.008	99.008	99.008	99.008	99.008	99.008	99.008	99.008	99.008	99.008	99.008	99.008	99.008	99.008	99.008	99.008	99.008	99.008	99.008	99.008	99.008	99.008
Total*	100.121	100.665	100.094	100.070	100.129	100.103	100.794	101.361	100.891	100.869	101.002	99.335	99.231	99.340	99.238	99.355	99.387	99.376	99.338	99.331	99.381	99.237	99.374	99.324	99.324

* The values are not genuine, as Al was not analysed.

Appendix 8-3 (Continued).

Locality/ Date & No. of analyses	Etive (Loch Awe), Wed 9, Jun. 99 (10 analyses).										Behelvie, Wed 9, Jun. 99 (15 analyses).															
Colour	Blue										Colourless in thin sections															
Sample No	MM12SA	MM12SA	MM12SA	MM12SA	MM12SA	MM12SA	MM12SA	MM12SA	MM12SA	MM12SA	Δ 1192	Δ 1192	Δ 1192	Δ 1192	Δ 1192	Δ 1192	Δ 1192	Δ 1192	Δ 1192	Δ 1192	Δ 1192	Δ 1192	Δ 1192	Δ 1192	Δ 1192	Δ 1192
Point No.	#1	#2	#3	#4	#5	#6	#7	#8	#9	#10	#11	#12	#13	#14	#15	#16	#17	#18	#19	#20	#21	#22	#23	#24	#25	
V_2O_5	0.025	0.046	0.043	0.015	0.012	0.022	0.022	0.019	0.018	0.044	0.008	0.005	0.011	0.027	0.028	0.016	0.021	0.014	0.010	0.015	0.016	0.024	0.023	0.019	0.010	
NiO	0.000	0.000	0.000	0.000	0.000	0.000	0.000	0.000	0.000	0.000	0.000	0.000	0.000	0.000	0.000	0.000	0.000	0.000	0.000	0.000	0.000	0.000	0.000	0.000	0.000	
Ga_2O_3	0.025	0.033	0.031	0.025	0.018	0.024	0.023	0.025	0.018	0.031	0.006	0.004	0.006	0.011	0.021	0.016	0.011	0.016	0.009	0.017	0.016	0.016	0.023	0.014	0.016	
Fe_2O_3	0.117	0.150	0.141	0.119	0.106	0.142	0.172	0.098	0.135	0.143	0.206	0.185	0.240	0.211	0.189	0.206	0.222	0.209	0.257	0.155	0.135	0.227	0.192	0.173	0.142	
MnO	0.000	0.000	0.000	0.000	0.000	0.004	0.000	0.000	0.001	0.000	0.000	0.000	0.000	0.000	0.000	0.000	0.000	0.000	0.003	0.000	0.000	0.000	0.000	0.000	0.000	
Cr_2O_3	0.032	0.089	0.017	0.017	0.087	0.017	0.011	0.132	0.040	0.007	0.085	0.054	0.164	0.132	0.009	0.084	0.083	0.073	0.037	0.085	0.095	0.016	0.090	0.196	0.034	
La_2O_3	0.001	0.000	0.001	0.000	0.000	0.000	0.000	0.000	0.000	0.000	0.001	0.002	0.000	0.000	0.000	0.002	0.000	0.000	0.000	0.000	0.000	0.000	0.000	0.000	0.003	
TiO_2	0.463	0.037	0.756	0.396	0.435	0.719	0.915	0.170	0.492	0.860	0.011	0.010	0.014	0.089	0.528	0.103	0.507	0.057	0.017	0.021	0.012	0.270	0.159	0.016	0.025	
SnO_2	0.001	0.000	0.002	0.000	0.001	0.000	0.000	0.001	0.000	0.001	0.002	0.000	0.001	0.000	0.001	0.002	0.000	0.000	0.000	0.003	0.002	0.000	0.001	0.001	0.000	
SiO_2	0.000	0.006	0.000	0.000	0.000	0.005	0.098	0.000	0.005	0.051	0.042	0.000	0.000	0.000	0.000	0.000	0.000	0.006	0.000	0.000	0.000	0.000	0.000	0.000	0.000	
Y_2O_3	0.000	0.000	0.000	0.000	0.000	0.000	0.001	0.000	0.000	0.000	0.000	0.002	0.000	0.001	0.000	0.000	0.000	0.002	0.000	0.000	0.000	0.000	0.000	0.000	0.006	
Al_2O_3*	99.008	99.008	99.008	99.008	99.008	99.008	99.008	99.008	99.008	99.008	99.008	99.008	99.008	99.008	99.008	99.008	99.008	99.008	99.008	99.008	99.008	99.008	99.008	99.008	99.008	
Total*	99.670	99.368	99.997	99.581	99.667	99.942	100.249	99.452	99.716	100.145	99.369	99.271	99.444	99.478	99.784	99.438	99.851	99.384	99.340	99.305	99.283	99.561	99.497	99.427	99.244	

* The values are not genuine, as Al was not analysed. The shaded cells contain the maximum values.

Appendix 8-3 (Continued).

Locality/ Date & No. of analyses	Baffin Is., Fri 23, Jul. 99 (12 analyses).												Stoer, Wed 14, Jul. 99 (12 analyses).											
Colour	Colourless in thin sections												Pink											
Sample No	Δ 440	Δ 440	Δ 440	Δ 440	Δ 440	Δ 440	Δ 440	Δ 440	Δ 440	Δ 440	Δ 440	Δ 440	Δ 16136	Δ 16136	Δ 16136	Δ 16136	Δ 16136	Δ 16136	Δ 16136	Δ 16136	Δ 16136	Δ 16136	Δ 16136	Δ 16136
Point No.	#13	#14	#15	#16	#17	#18	#19	#20	#21	#22	#23	#24	#1	#2	#3	#4	#5	#6	#7	#8	#9	#10	#11	#12
V_2O_5	0.004	0.002	0.004	0.004	0.002	0.004	0.005	0.005	0.002	0.005	0.007	0.004	0.002	0.003	0.003	0.004	0.002	0.002	0.004	0.001	0.003	0.002	0.002	0.004
NiO	0.000	0.000	0.000	0.000	0.000	0.000	0.000	0.000	0.000	0.000	0.000	0.000	0.000	0.000	0.000	0.000	0.000	0.000	0.000	0.000	0.000	0.000	0.000	0.000
Ga_2O_3	0.007	0.007	0.008	0.005	0.009	0.008	0.009	0.008	0.004	0.009	0.008	0.008	0.006	0.007	0.008	0.007	0.006	0.006	0.006	0.005	0.007	0.005	0.004	0.004
Fe_2O_3	0.350	0.359	0.309	0.350	0.436	0.319	0.503	0.310	0.372	0.302	0.313	0.327	0.135	0.147	0.149	0.130	0.120	0.132	0.132	0.134	0.129	0.128	0.130	0.155
MnO	0.000	0.000	0.000	0.000	0.000	0.001	0.000	0.000	0.000	0.000	0.000	0.000	0.000	0.000	0.000	0.000	0.000	0.000	0.000	0.000	0.000	0.000	0.000	0.000
Cr_2O_3	0.001	0.000	0.006	0.003	0.001	0.006	0.010	0.009	0.004	0.001	0.007	0.006	0.054	0.050	0.074	0.060	0.085	0.077	0.072	0.066	0.078	0.076	0.070	0.063
La_2O_3	0.000	0.002	0.001	0.000	0.000	0.002	0.000	0.000	0.000	0.000	0.000	0.000	0.000	0.001	0.001	0.000	0.000	0.000	0.000	0.001	0.000	0.001	0.000	0.000
TiO_2	0.008	0.008	0.010	0.008	0.010	0.007	0.008	0.010	0.008	0.008	0.008	0.008	0.025	0.043	0.010	0.014	0.009	0.010	0.028	0.020	0.013	0.005	0.007	0.029
SnO_2	0.000	0.000	0.000	0.000	0.001	0.003	0.000	0.000	0.001	0.000	0.000	0.000	0.001	0.000	0.000	0.000	0.000	0.000	0.000	0.001	0.000	0.001	0.000	0.000
SiO_2	0.000	0.000	0.000	0.000	0.000	0.000	0.000	0.000	0.000	0.000	0.000	0.000	0.000	0.029	0.000	0.000	0.030	0.000	0.000	0.000	0.000	0.000	0.000	0.000
Y_2O_3	0.000	0.000	0.000	0.001	0.000	0.000	0.000	0.000	0.003	0.000	0.000	0.000	0.000	0.000	0.000	0.000	0.000	0.000	0.000	0.000	0.000	0.000	0.000	0.000
Al_2O_3*	99.008	99.008	99.008	99.008	99.008	99.008	99.008	99.008	99.008	99.008	99.008	99.008	99.008	99.008	99.008	99.008	99.008	99.008	99.008	99.008	99.008	99.008	99.008	99.008
Total*	99.378	99.386	99.345	99.380	99.468	99.357	99.545	99.350	99.402	99.334	99.352	99.361	99.231	99.289	99.253	99.223	99.260	99.235	99.250	99.236	99.238	99.228	99.221	99.263

* The values are not genuine, as Al was not analysed.

Appendix 8-3 (Continued).

Locality/ Date & No. of analyses	Limpopo belt, Wed 17, Mar. 99 (6 analyses).						Limpopo belt, Fri. 23, Jul. 99 (12 analyses).												Naxos, Fri. 9, July 99, (12 analyses).											
Colour	Purple						Colourless in thin sections												Colourless in thin sections											
Sample No	BB14A-1	BB14A-2	BB14A-3	BB14A-1	BB14A-2	BB14A-3	BB29F	BB29F	BB29F	BB29F	BB29F	BB29F	BB29F	BB29F	BB29F	BB29F	BB29F	BB29F	Δ 577	Δ 577	Δ 577	Δ 577	Δ 577	Δ 577	Δ 577	Δ 577	Δ 577	Δ 577	Δ 577	Δ 577
Point No.	#7	#8	#9	#7.1	#8.1	#9.1	#1	#2	#3	#4	#5	#6	#7	#8	#9	#10	#11	#12	#10	#11	#12	#13	#14	#15	#16	#17	#19	#20	#21	#22
V_2O_5	0.005	0.003	0.002	0.004	0.004	0.004	0.004	0.004	0.009	0.007	0.004	0.005	0.004	0.004	0.005	0.004	0.009	0.002	0.045	0.003	0.000	0.000	0.006	0.012	0.013	0.004	0.000	0.002	0.001	0.000
NiO	0.000	0.000	0.000	0.000	0.000	0.000	0.000	0.000	0.000	0.000	0.000	0.000	0.000	0.000	0.000	0.000	0.000	0.000	0.000	0.000	0.000	0.000	0.000	0.000	0.000	0.000	0.000	0.000	0.000	0.000
Ga_2O_3	0.004	0.002	0.002	0.005	0.005	0.003	0.007	0.013	0.011	0.012	0.007	0.013	0.009	0.008	0.009	0.005	0.012	0.008	0.012	0.007	0.008	0.006	0.016	0.009	0.007	0.009	0.011	0.008	0.008	0.010
Fe_2O_3	0.176	0.129	0.174	0.173	0.130	0.159	0.613	0.575	0.643	0.653	0.648	0.613	0.466	0.542	0.518	0.323	0.602	0.505	0.811	0.450	0.500	0.506	0.815	1.307	0.656	0.517	0.569	0.419	0.538	0.502
MnO	0.000	0.000	0.001	0.000	0.000	0.000	0.000	0.000	0.000	0.000	0.000	0.000	0.000	0.000	0.000	0.000	0.000	0.000	0.000	0.000	0.000	0.000	0.000	0.000	0.000	0.000	0.000	0.000	0.000	0.000
Cr_2O_3	0.031	0.037	0.033	0.026	0.032	0.031	0.001	0.006	0.007	0.003	0.000	0.004	0.007	0.000	0.009	0.006	0.000	0.003	0.002	0.010	0.014	0.016	0.009	0.013	0.019	0.017	0.016	0.011	0.015	0.016
La_2O_3	0.000	0.001	0.000	0.000	0.000	0.000	0.000	0.000	0.002	0.001	0.000	0.000	0.000	0.000	0.000	0.000	0.000	0.000	0.000	0.003	0.000	0.001	0.004	0.000	0.000	0.000	0.000	0.000	0.000	0.000
TiO_2	0.021	0.020	0.023	0.022	0.017	0.030	0.023	0.017	0.025	0.027	0.022	0.020	0.017	0.015	0.020	0.012	0.023	0.017	0.076	0.004	0.004	0.004	0.240	0.469	0.380	0.005	0.009	0.006	0.020	0.004
SnO_2	0.000	0.001	0.000	0.003	0.003	0.001	0.000	0.000	0.003	0.003	0.001	0.000	0.003	0.005	0.000	0.000	0.001	0.000	0.000	0.001	0.000	0.003	0.002	0.000	0.001	0.000	0.000	0.001	0.000	0.000
SiO_2	0.000	0.000	0.000	0.053	0.000	0.000	0.000	0.000	0.000	0.000	0.000	0.000	0.000	0.000	0.000	0.000	0.000	0.000	0.000	0.000	0.000	0.000	0.256	0.031	0.000	0.000	0.000	0.000	0.000	0.000
Y_2O_3	0.000	0.000	0.000	0.003	0.000	0.000	0.000	0.000	0.003	0.000	0.001	0.000	0.001	0.000	0.003	0.000	0.000	0.000	0.000	0.000	0.000	0.000	0.009	0.000	0.000	0.000	0.003	0.000	0.000	0.000
Al_2O_3*	99.008	99.008	99.008	99.008	99.008	99.008	99.008	99.008	99.008	99.008	99.008	99.008	99.008	99.008	99.008	99.008	99.008	99.008	99.008	99.008	99.008	99.008	99.008	99.008	99.008	99.008	99.008	99.008	99.008	99.008
Total*	99.245	99.201	99.243	99.296	99.198	99.235	99.656	99.622	99.711	99.714	99.690	99.664	99.515	99.582	99.572	99.357	99.655	99.542	99.954	99.486	99.533	99.544	100.364	100.848	100.084	99.560	99.616	99.455	99.589	99.540

* The values are not genuine, as Al was not analysed.

Appendix 8-3 (Continued).

Locality/ Date & No. of analyses	Limpopo-belt, Fri. 9, July 99 (9 analyses).									Sithean Sluain, Wed. 14, July 99 (5 analyses).					
Colour	Colourless in thin sections									Colourless in thin sections					
Sample No	BB19	BB19	BB19	BB19	BB19	BB19	BB19	BB19	BB19	Δ 1378	Δ 1378	Δ 1378	Δ 1378	Δ 1378	Δ 1378
Point No.	#1	#2	#3	#4	#5	#6	#7	#8	#9	#13	#14	#15	#16	#17	
V_2O_5	0.003	0.002	0.005	0.004	0.001	0.008	0.002	0.003	0.003	0.005	0.007	0.005	0.003	0.007	
NiO	0.000	0.000	0.000	0.000	0.000	0.000	0.000	0.000	0.000	0.000	0.000	0.000	0.000	0.000	
Ga_2O_3	0.000	0.002	0.002	0.003	0.004	0.001	0.003	0.000	0.000	0.010	0.006	0.008	0.010	0.009	
Fe_2O_3	0.391	0.419	0.391	0.481	0.428	0.517	0.528	0.436	0.383	4.862	4.895	4.777	3.910	3.615	
MnO	0.000	0.000	0.000	0.000	0.000	0.000	0.000	0.000	0.000	0.000	0.000	0.000	0.000	0.000	
Cr_2O_3	0.023	0.021	0.077	0.031	0.072	0.279	0.220	0.055	0.051	0.047	0.041	0.029	0.038	0.037	
La_2O_3	0.000	0.000	0.000	0.000	0.000	0.002	0.000	0.000	0.001	0.000	0.002	0.000	0.000	0.000	
TiO_2	0.012	0.012	0.011	0.010	0.014	0.015	0.025	0.011	0.028	0.225	0.199	0.204	0.154	0.145	
SnO_2	0.000	0.000	0.002	0.002	0.000	0.000	0.000	0.000	0.000	0.001	0.001	0.000	0.000	0.000	
SiO_2	0.000	0.000	0.000	0.000	0.002	0.000	0.000	0.000	0.000	0.000	0.000	0.000	0.000	0.005	
Y_2O_3	0.001	0.000	0.000	0.000	0.000	0.000	0.000	0.000	0.002	0.001	0.000	0.000	0.002	0.000	
Al_2O_3*	99.008	99.008	99.008	99.008	99.008	99.008	99.008	99.008	99.008	99.008	99.008	99.008	99.008	99.008	
Total*	99.439	99.465	99.495	99.538	99.529	99.830	99.785	99.513	99.477	104.159	104.157	104.032	103.126	102.824	

* The values are not genuine, as Al was not analysed.

Appendix 8-3 (Continued).

Locality/ Date & No. of analyses	Mong Hsu, Mon. 24, May 99(6 analyses).						Mong Hsu, Tue. 14, Sept. 99 (13 analyses).												
Colour	Purple						Purple												
Sample No	TYEP1	TYEP1	TYEP2	TYEP2	TYEP3	TYEP3	MSEP1	MSEP2	MSEP2	MSEP3	MSEP4	MSEP4	MSEP5	MSEP6	MSEP6	MSEP6	MSEP6	MSEP7	MSEP8
Point No.	#1	#2	#3	#4	#5	#6	#1	#2	#3	#4	#5	#6	#7	#1	#2	#3	#4	#5	#6
V_2O_5	0.019	0.015	0.028	0.027	0.050	0.054	0.020	0.102	0.046	0.054	0.029	0.043	0.048	0.027	0.032	0.034	0.034	0.039	0.034
NiO	0.000	0.000	0.000	0.000	0.000	0.000	0.000	0.000	0.000	0.000	0.000	0.000	0.000	0.000	0.000	0.000	0.000	0.000	0.000
Ga_2O_3	0.006	0.001	0.011	0.006	0.006	0.005	0.012	0.011	0.007	0.013	0.008	0.007	0.008	0.007	0.009	0.011	0.005	0.015	0.011
Fe_2O_3	0.000	0.000	0.004	0.000	0.004	0.000	0.000	0.000	0.000	0.004	0.000	0.000	0.000	0.000	0.000	0.000	0.000	0.000	0.000
MnO	0.001	0.000	0.000	0.000	0.000	0.000	0.000	0.000	0.000	0.000	0.000	0.000	0.000	0.000	0.000	0.000	0.000	0.000	0.000
Cr_2O_3	1.459	0.929	0.894	0.977	0.355	0.508	0.704	1.051	0.419	0.607	1.700	0.617	0.811	0.592	0.355	0.430	0.332	0.332	0.364
La_2O_3	0.001	0.000	0.000	0.003	0.003	0.000	0.001	0.001	0.000	0.000	0.000	0.001	0.000	0.000	0.000	0.000	0.000	0.001	0.000
TiO_2	0.021	0.003	0.014	0.013	0.135	0.138	0.008	0.072	0.112	0.157	0.013	0.150	0.035	0.043	0.312	0.429	0.502	0.088	0.242
SnO_2	0.000	0.000	0.002	0.001	0.000	0.001	0.000	0.000	0.000	0.000	0.003	0.000	0.000	0.000	0.000	0.000	0.001	0.000	0.001
SiO_2	0.002	0.005	0.043	0.044	0.022	0.028	0.000	0.000	0.000	0.000	0.000	0.000	0.000	0.000	0.000	0.000	0.000	0.000	0.000
Y_2O_3	0.000	0.000	0.000	0.000	0.000	0.000	0.000	0.000	0.000	0.001	0.000	0.000	0.001	0.000	0.000	0.000	0.000	0.003	0.001
Al_2O_3*	99.008	99.008	99.008	99.008	99.008	99.008	99.008	99.008	99.008	99.008	99.008	99.008	99.008	99.008	99.008	99.008	99.008	99.008	99.008
Total*	100.517	99.962	100.004	100.078	99.582	99.743	99.754	100.244	99.592	99.844	100.760	99.826	99.912	99.677	99.717	99.911	99.882	99.486	99.661

* The values are not genuine, as Al was not analysed.

Appendix 8-3 *Weight % oxides of trace elements in the corundum samples from outside Thailand obtained by EPMA.*

Appendix 8-3 *Weight % oxides of trace elements in the corundum samples from outside Thailand obtained by EPMA.*

Appendix 8-3 (Continued).

Locality/ Date & No. of analyses	Tanzania (corundum in zoisite), Wed. 17, Mar. 99 (6 analyses).						Vietnam, Mon. 24, May 99 (4 analyses).				Africa, Mon. 24, May 99 (3 analyses).			Nigeria, Mon. 24, May 99 (3 analyses).			North Vietnam, Mon. 24, May 99 (3 analyses)		
Colour	Purple						Blue				Purple			Blue			Purple		
Sample No	CRM/ZOI-1	CRM/ZOI-2	CRM/ZOI-3	CRM/ZOI-1	CRM/ZOI-2	CRM/ZOI-3	VNEP1	VNEP2	VNEP3	VNEP3	AFEP1	AFEP2	AFEP3	NAEP1	NAEP2	NAEP3	NVEP1	NVEP2	NVEP3
Point No.	#10	#11	#12	#10.1	#11.1	#12.1	#7	#8	#9	#10	#11	#12	#13	#14	#15	#16	#17	#18	#19
V_2O_5	0.000	0.003	0.004	0.000	0.002	0.000	0.001	0.012	0.001	0.005	0.001	0.000	0.001	0.004	0.001	0.003	0.047	0.026	0.011
NiO	0.000	0.000	0.000	0.000	0.000	0.000	0.000	0.000	0.000	0.000	0.000	0.000	0.000	0.000	0.000	0.000	0.000	0.000	0.000
Ga_2O_3	0.006	0.000	0.004	0.000	0.004	0.000	0.027	0.054	0.023	0.029	0.001	0.003	0.004	0.030	0.026	0.038	0.006	0.002	0.004
Fe_2O_3	0.210	0.197	0.175	0.210	0.216	0.193	1.201	0.709	1.150	1.431	0.277	0.258	0.281	0.382	0.445	0.247	0.005	0.001	0.006
MnO	0.000	0.000	0.000	0.000	0.000	0.000	0.000	0.000	0.000	0.000	0.000	0.000	0.000	0.000	0.000	0.000	0.000	0.000	0.000
Cr_2O_3	0.791	0.784	0.739	0.707	0.875	0.941	0.002	0.000	0.002	0.002	1.145	1.218	1.202	0.000	0.004	0.001	0.432	0.404	0.311
La_2O_3	0.001	0.000	0.000	0.000	0.000	0.000	0.002	0.000	0.000	0.000	0.001	0.000	0.001	0.001	0.001	0.000	0.000	0.000	0.000
TiO_2	0.008	0.006	0.007	0.010	0.013	0.005	0.009	0.047	0.017	0.031	0.011	0.014	0.068	0.012	0.030	0.008	0.188	0.110	0.009
SnO_2	0.000	0.001	0.000	0.000	0.001	0.000	0.000	0.000	0.001	0.002	0.001	0.001	0.000	0.000	0.000	0.002	0.000	0.000	0.000
SiO_2	0.001	0.000	0.000	0.000	0.000	0.000	0.002	0.016	0.011	0.000	0.000	0.000	0.000	0.000	0.000	0.000	0.000	0.000	0.000
Y_2O_3	0.000	0.000	0.000	0.000	0.000	0.000	0.002	0.000	0.000	0.000	0.000	0.000	0.000	0.004	0.000	0.000	0.004	0.000	0.002
Al_2O_3*	99.008	99.008	99.008	99.008	99.008	99.008	99.008	99.008	99.008	99.008	99.008	99.008	99.008	99.008	99.008	99.008	99.008	99.008	99.008
Total*	100.023	99.998	99.937	99.935	100.120	100.147	100.25	99.85	100.21	100.51	100.44	100.50	100.56	99.441	99.515	99.306	99.689	99.550	99.351

* The values are not genuine, as Al was not analysed.

Appendix 9-1
Chemical composition of inclusions and coexisting minerals with corundums.

Appendix 9-1 Garnet inclusions in corundum samples from Bo Rai.

Analysis No	CORXXI-BREP45-GRT1	BREP1-GRT1	BREP1-GRT2	BREP1-GRT3	BREP1-GRT4
SiO_2	41.67	41.90	41.88	40.62	41.86
TiO_2	0.00	0.00	0.00	0.00	0.00
Al_2O_3	23.57	23.42	23.40	22.80	23.76
Fe_2O_3	0.95	0.90	0.00	1.11	1.10
FeO	9.04	6.65	6.91	6.31	5.48
MnO	0	0.235	0.191	0.248	0.244
MgO	15.77	18.18	18.05	17.65	18.83
CaO	9.90	8.43	8.42	8.23	8.41
Na_2O*	0	(0.347)	(0.379)	0	(0.399)
Cr_2O_3	0	0	0	0	0.19
Total	100.90	99.71	98.86	96.97	99.87
Numbers of atoms on the basis of 24 O: $[(Mg, Fe^{2+}, Mn, Ca)_3(Al,Fe^{3+},Cr,Ti)_2(Si,Al)_3O_{12}]$*2					
Si	5.962	5.982	6.019	5.966	5.943
Al	0.038	0.018	0	0.034	0.057
Al	3.936	3.922	3.964	3.912	3.918
Cr	0	0	0	0	0.021
Fe^{3+}	0.103	0.096	0	0.122	0.118
Ti	0	0	0	0	0
Mg	3.363	3.870	3.867	3.865	3.984
Fe^{2+}	1.082	0.794	0.831	0.775	0.651
Mn	0	0.028	0.023	0.031	0.029
Ca	1.517	1.290	1.296	1.294	1.279
Na	0	0	0	0	0
Total	16	16	16	16	16
End members (Deer *et al.*, 1996: 684)					
Almandine	18.1	13.3	13.8	13.0	10.9
Andradrite	2.5	2.4	0.0	3.0	2.9
Grossular	22.9	19.2	21.5	18.7	18.1
Pyrope	56.4	64.7	64.3	64.8	67.0
Spessartine	0	0.5	0.4	0.5	0.5
Uvarovite	0	0	0	0	0.5

* Na_2O is not taken into account as assuming that it was not genuine.

Appendix 9-1 Fassaite inclusions and mineral grains coexisting with corundum from Bo Rai.

Occurrence	Inclusion	Inclusion	Inclusion	Coexisting Min	Coexisting Min	Coexisting Min
Analysis No	BREP43 -FS1	BREP43 -FS2	BREP43 -FS3	BRJ-FS1	BRJ-FS2	BRJ-FS3
SiO_2	46.80	47.07	47.32	48.21	47.39	46.77
TiO_2	0.92	0.97	0.86	0.38	0.37	0.23
Al_2O_3	14.23	14.44	14.69	15.67	15.25	15.92
Fe_2O_3	2.70	2.59	2.93	0.00	0.00	0.00
FeO	0.94	1.19	0.73	3.04	2.94	2.98
MnO	0	0	0	0	0	0
MgO	11.55	11.57	11.70	10.76	10.54	10.19
CaO	21.81	21.84	22.26	22.88	22.13	22.29
Na_2O	1.58	1.59	1.56	1.35	1.31	1.32
K_2O	0.00	0.00	0.00	0.00	0.00	0.00
P_2O_5	0	0	0	0	0	0
NiO	0	0	0	0	0	0
Cr_2O_3	0	0	0	0.28	0.51	0.35
ZnO	0	0	0	0	0	0
Total	100.54	101.24	102.08	102.55	100.45	100.05
Ca%(Wo%)	53.8	53.7	54.1	56.9	56.6	57.5
Mg%(En%)	39.7	39.6	39.5	37.2	37.5	36.5
$(Fe^{2+}+Fe^{3+}+Mn)$% or (Fs%)	6.5	6.8	6.4	5.9	5.9	6.0
mg*=100xMg/ $(Mg+Fe^{2+}+Fe^{3+}+Mn)$	85.9	85.4	86.1	86.3	86.5	85.9
$Mg^{2+}/(Mg^{2+}+Fe^{2+})$	0.96	0.9	0.97	0.9	0.9	0.9
Atoms in sites, $M2M1T_2O_6$						
T						
Si^{4+}	1.691	1.689	1.683	1.708	1.716	1.699
Al^{3+}	0.309	0.311	0.317	0.292	0.284	0.301
Fe^{3+}	0	0	0	0	0	0
M1(Regular. Octa.)						
Al^{3+}	0.296	0.299	0.300	0.363	0.367	0.381
Fe^{3+}	0.073	0.070	0.079	0	0	0
Ti^{4+}	0.025	0.026	0.023	0.010	0.010	0.006
Cr^{3+}	0	0	0	0.008	0.015	0.010
Zn^{2+}	0	0	0	0	0	0
Mg^{2+}	0.579	0.572	0.579	0.535	0.526	0.518
Fe^{2+}	0.027	0.033	0.020	0.085	0.082	0.085
Mn^{2+}	0	0	0	0	0	0
M2(Distorted 8-fold site)						
Mg^{2+}	0.043	0.047	0.042	0.033	0.043	0.034
Fe^{2+}	0.002	0.003	0.001	0.005	0.007	0.006
Mn^{2+}	0	0	0	0	0	0
Ca^{2+}	0.844	0.839	0.849	0.869	0.859	0.867
Na^{+}	0.110	0.111	0.108	0.093	0.092	0.093
K^{+}	0	0	0	0	0	0
Total	4.000	4.000	4.000	4.000	4.000	4.000

Appendix 9-1 Sapphirine inclusions in corundum from Bo Nawong.

Analysis No	NWEP9-SPR2	NWEP9-SPR3	NWEP9-SPR4	NWEP9-SPR5	NWEP11-SPR1	NWEP11-SPR2	NWEP11-SPR3
SiO_2	13.47	13.79	14.06	14.07	14.43	14.07	14.10
TiO_2	0	0	0	0	0	0	0
Al_2O_3	61.87	62.91	62.24	62.64	64.43	62.14	63.13
Fe_2O_3	0	0.80	0	0.18	2.60	0	0.43
FeO	2.86	2.27	3.07	3.14	1.04	3.30	2.86
MnO	0	0.21	0	0	0	0	0
MgO	18.22	18.99	18.63	18.94	19.90	18.56	19.19
CaO	0	0.11	0	0	0	0	0
Na_2O	0	0	0	0	0.34	0	0
K_2O	0	0	0	0	0	0	0
NiO	0.44	0.48	0.39	0.33	0.33	0	0.31
Cr_2O_3	0.19	0.24	0.25	0.38	0.2	0	0
Total	97.05	99.79	98.64	99.68	103.27	98.06	100.01
Nunbers of atoms on the basis of 20 O							
Si	1.620	1.614	1.664	1.649	1.630	1.673	1.644
Ti	0	0	0	0	0	0	0
Al	8.766	8.678	8.683	8.652	8.577	8.709	8.675
Fe^{3+}	0	0.071	0	0.016	0.221	0	0.038
Fe^{2+}	0.288	0.222	0.304	0.308	0.098	0.328	0.279
Mn	0	0.020	0	0	0	0	0
Mg	3.266	3.314	3.288	3.310	3.352	3.291	3.336
Ca	0	0.013	0	0	0	0	0
Na	0	0	0	0	0.075	0	0
K	0	0	0	0	0	0	0
Ni	0.043	0.045	0.037	0.031	0.030	0	0.029
Cr	0.018	0.022	0.023	0.035	0.018	0	0
Total	14.000	14.000	14.000	14.000	14.000	14.000	14.000
$Mg/(Mg+Fe^{2+})$	0.92	0.94	0.92	0.91	0.97	0.91	0.92
$Fe^{3+}/(Fe^{2+}+Fe^{3+})$	0	0.24	0	0.05	0.69	0	0.12

Appendix 9-1 Alkali feldspar (sanidine composition) and nepheline inclusions in corundum from Den Chai and Bo Phloi.

Mineral	Sanidine			Nepheline			
Analysis No	DCEP 16-AF1	DCEP 16-AF2	DCEP 16-AF3	BPEP1 -NE1	BPEP1 -NE2	BPEP1 -NE3	BPEP1 -NE4
SiO_2	65.17	65.35	65.38	43.02	42.72	39.92	42.381
TiO_2	0	0	0	0	0	0	0
Al_2O_3	21.58	21.54	21.65	33.48	33.80	40.08	34.16
$Fe_2O_3^*$	0	0	0	0.32	0.32	0.46	0.53
FeO	-	-	-	-	-	-	-
MgO	0.23	0	0	0.40	0.46	0.56	0.57
CaO	2.68	2.63	2.79	0	0.14	0.19	0.30
Na_2O	6.69	6.51	6.38	14.68	14.98	13.63	14.75
K_2O	5.33	5.59	5.69	8.26	8.45	7.91	8.55
P_2O_5	0.39	0.38	0.46	0	0	0.24	0
BaO	0	0	0	0	0	0	0
Total	102.07	102.00	102.34	100.16	100.88	103.00	101.23
Numbers of atoms on the basis of 32 O							
Si	11.432	11.473	11.445	8.310	8.220	7.470	8.138
Ti	0	0	0	0	0	0	0
Al	4.461	4.457	4.467	7.620	7.664	8.838	7.730
Fe^{3+}	0	0	0	0.047	0.047	0.065	0.076
Fe^{2+}	-	-	-	-	-	-	-
Mg	0.061	0	0	0.114	0.133	0.155	0.163
Ca	0.504	0.494	0.522	0	0.029	0.038	0.062
Na	2.276	2.216	2.165	5.498	5.588	4.945	5.489
K	1.192	1.251	1.270	2.035	2.074	1.889	2.095
P	0.058	0.057	0.068	0	0	0.038	0
Ba	0	0	0	0	0	0	0
Total	19.985	19.947	19.937	23.623	23.755	23.438	23.751
An	12.69	12.47	13.20	Ne = 67.9	Ne = 68.9	Ne = 67.9	Ne = 68.6
Ab	57.29	55.94	54.71	Ks = 28.0	Ks = 28.5	Ks = 28.9	Ks = 29.1
Or	30.02	31.59	32.09	Q = 4.1	Q = 2.6	Q = 3.3	Q = 2.3

* Total Fe as Fe_2O_3

Appendix 9-1 Spinel inclusions in corundum.

Locality	Ban Huai Sai near Chiang Khong		Ban Nong		Bo Phloi			Bang Kacha					
Analysis No	CKEP3 0-SP2	CKEP3 0-SP3	BNEP4-SP1	BNEP4-SP2	BPEP13 -SP1	BPEP13 -SP2	BPEP13 -SP3	BKCEP 4-SP1	BKCEP 4-SP2	BKCEP 4-SP4	BKCEP 4-SP1/1	BKCEP 4-SP2/2	BKCEP 4-SP3/3
SiO_2	0.40	0	0	0	0.39	0.39	0.43	0	0	0	0	0	0
TiO_2	0.25	0.24	0.31	0.30	0	0.29	0.35	1.82	1.84	1.78	1.78	1.87	2.20
Al_2O_3	57.75	55.30	53.27	52.10	56.67	56.41	56.39	12.16	30.53	10.62	18.44	10.57	10.81
Fe_2O_3	3.62	5.06	6.92	5.11	4.69	6.04	6.33	51.91	31.21	50.39	44.45	54.87	52.05
FeO	34.40	33.81	27.78	29.14	30.63	29.79	29.44	29.06	33.58	27.81	30.13	27.58	28.23
MnO	0.58	0.66	0.68	0.73	0.86	0.55	0.65	1.94	1.48	1.82	1.53	2.04	2.06
MgO	3.77	4.03	6.20	5.42	6.65	6.70	6.75	0.47	0.45	0.51	0.55	0.67	0.59
CaO	0	0	0	0	0	0	0	0	0	0	0	0	0
Na_2O	0.35	0	0.29	0	0	0.35	0.43	0.57	0.52	0.49	0.61	0.80	0.53
P_2O_5	0	0	0	0	0	0	0	0	0	0	0	0	0
Cr_2O_3	0	0	0	0	0.77	0.81	0.77	0	0	0	0	0	0
ZnO	0	0	0	0	0	0	0	0	0	0	0	0	0.66
Total	101.12	99.09	95.45	92.81	100.66	101.33	101.54	97.93	99.61	93.42	97.49	98.40	97.13
Numbers of atoms on the basis of 32 O													
Si	0.090	0	0	0	0.087	0.087	0.095	0	0	0	0	0	0
Ti	0.042	0.041	0.055	0.055	0	0.048	0.058	0.398	0.362	0.411	0.379	0.408	0.489
Al	15.276	15.040	14.796	14.954	14.902	14.730	14.690	4.168	9.401	3.839	6.136	3.623	3.760
Fe^{3+}	0.611	0.879	1.227	0.937	0.787	1.007	1.053	11.360	6.136	11.627	9.442	12.013	11.563
Fe^{2+}	6.457	6.524	5.475	5.935	5.715	5.519	5.442	7.068	7.336	7.130	7.112	6.711	6.968
Mn	0.111	0.129	0.136	0.151	0.162	0.104	0.122	0.479	0.328	0.473	0.367	0.502	0.516
Mg	1.262	1.388	2.177	1.969	2.211	2.214	2.223	0.203	0.176	0.232	0.229	0.290	0.260
Ca	0	0	0	0	0	0	0	0	0	0	0	0	0
Na	0.151	0	0.133	0	0	0.149	0.183	0.324	0.261	0.288	0.335	0.452	0.301
P	0	0	0	0	0	0	0	0	0	0	0	0	0
Cr	0	0	0	0	0.137	0.142	0.135	0	0	0	0	0	0
Zn	0	0	0	0	0	0	0	0	0	0	0	0	0.143
Total	24	24	24	24	24	24	24	24	24	24	24	24	24
Spinel	16.3	17.3	27.7	24.6	27.9	28.5	28.8	2.6	2.3	3.0	3.0	3.8	3.4
Hercynite	78.0	75.0	62.2	67.0	64.2	62.4	61.5	15.1	50.6	13.1	28.5	9.3	9.7
Gahnite	0.0	0.0	0.0	0.0	0.0	0.0	0.0	0	0	0	0	0	1.9
Galaxite	1.4	1.6	1.7	1.9	2.0	1.3	1.6	6.2	4.2	6.1	4.8	6.7	6.7
Magnetite	3.8	5.5	7.7	5.9	4.9	6.3	6.6	71.0	38.4	72.7	59.0	75.1	72.3
Chromite	0.0	0.0	0.0	0.0	0.9	0.9	0.8	0	0	0	0	0	0
Ulvöspinel	0.5	0.5	0.7	0.7	0.0	0.6	0.7	5.0	4.5	5.1	4.7	5.1	6.1
Total	100.0	100.0	100.0	100.0	100.0	100.0	100.0	100.0	100.0	100.0	100.0	100.0	100.0